Andreas Öchsner
Markus Merkel

One-Dimensional Finite Elements

An Introduction to the FE Method

One-Dimensional Finite Elements

Andreas Öchsner · Markus Merkel

One-Dimensional Finite Elements

An Introduction to the FE Method

Andreas Öchsner
University of Technology Malaysia
Skudai
Malaysia

and

The University of Newcastle
Newcastle
Australia

Markus Merkel
Aalen University
Aalen
Germany

This book is dedicated to our parents

Preface

The title of this book 'One-Dimensional Finite Elements: An Introduction to the FE Method' stands for content and focus. Nowadays, much literature regarding the topic of the finite element method exists. The different works reflect the multi-faceted perceptions and application possibilities. The basic idea of this introduction into the finite element method relies on the concept of explaining the complex method with the help of *one-dimensional* elements. It is the goal to introduce the manifold aspects of the finite element method and to enable the reader to get a methodical understanding of important subject areas. The reader learns to understand the assumptions and derivations at different physical problems in structural mechanics. Furthermore, he/she learns to critically evaluate possibilities and limitations of the finite element method. Additional comprehensive mathematical descriptions, which solely result from advanced illustrations for two- or three-dimensional problems, are omitted. Hence, the mathematical description largely remains simple and clear. The focus on one-dimensional elements, however, is not just a pure limitation on a simpler and clearer formal illustration of the necessary equations. Within structural engineering, there are various structures—for example bridges or high transmission towers—which are usually modeled via one-dimensional elements. Therefore, this work also contains a 'set of tools', which can also be applied in practice.

The concentration on one-dimensional elements is new for a textbook and allows the treatment of various basic and demanding physical questions of structural mechanics within one single textbook. This new concept, therefore, allows a methodical understanding of important subject areas (for example plasticity or composite materials), which occur to a prospective engineer during professional work, which however are seldom treated in this way at universities. Consequently, simple access is possible, also in supplementary areas of application of the finite element method.

This book originates from a collection of lecture notes which were developed as written material for lectures and training documents for specialized courses on the finite element method. Especially, the calculated examples and the supplementary

problems refer to typical questions which are raised by students and course participants.

The prerequisites for a good understanding are the basics in linear algebra, physics, materials science, and strength of materials, the way they are typically communicated in the basic studies of a technical subject in the field of mechanical engineering.

Within the initial chapters the one-dimensional elements will be introduced, by which the basic load cases of tension/compression, torsion, and bending can be illustrated. In each case, the differential equation as well as the basic equations from the strength of materials (this is the kinematic relationship, the constitutive relationship, and the equilibrium equation) are being derived. Subsequently, the finite elements with the usual definitions for force and displacement parameters are introduced. With the help of examples, the general procedure is illustrated. Short solutions for supplementary problems are attached in the appendix.

Chapter 6 deals with questions which are independent of the loading type and the therewith connected element formulation. A general one-dimensional finite element, which can be constructed from the combination of basic elements, the transformation of elements in the general three-dimensional space, and the numerical integration as an important tool for the implementation of the finite element method is dealt with.

The complete analysis of an entire structure is introduced in Chap. 7. The total stiffness relation results from the single stiffness relation of the basic elements under consideration of the relations to each other. A reduced system results due to the boundary conditions. Unknown parameters are derived from the reduced system. The procedure will be introduced as examples on plane and general three-dimensional structures.

Chapters 8–12 deal with topics which are usually not part of a basics book. The beam element with shear consideration is introduced in Chap. 8. The Timoshenko beam serves as a basis for this.

Within Chap. 9 a special class of material—composite materials—are introduced into a finite element formulation. First, various ways of description for direction dependent material behavior are introduced. Fiber composites are addressed briefly. A composite element is demonstrated by examples of a composite bar and a composite beam.

Chapters 10–12 deal with nonlinearities. In Chap. 10, the different types of nonlinear elasticities are introduced. The case of the nonlinear elasticity is dealt with more closeness. The problem is illustrated for bar elements. First, the principal finite element equation is derived under consideration of the strain dependency. The direct iteration as well as the complete and modified Newton–Raphson iteration is derived for the solution of a nonlinear system of equations. In addition, many examples serve as a demonstration of this issue.

Chapter 11 considers elastoplastic behavior, one of the most common forms of material nonlinearities. First, the continuum mechanics basics for plasticity in the case of the one-dimensional continuum bar are composed. The yield condition, the flow rule, the hardening law, and the elastoplastic modulus are introduced for

uniaxial, monotonic load cases. Within the hardening behavior, the description is limited to isotropic hardening. For the integration of the elastoplastic constitutive equations, the incremental predictor–corrector method is generally introduced and derived for the case of the fully implicit and the semi-implicit backward-Euler algorithm. On crucial points, the difference between one- and three-dimensional descriptions will be pointed out, to guarantee a simple transfer of the derived methods to general problems.

Chapter 12 deals with stability, which is an issue that is especially relevant for the designing and dimensioning of lightweight components. Finite elements developed for this type of nonlinearities are used for the solving of the Euler's buckling loads.

Chapter 13 serves to introduce an FE formulation for dynamic problems. Stiffness matrices as well as mass matrices will be established. Different assumptions for the distribution of the masses, whether continuously or concentrated, lead to different formulations. The issue is discussed by example of axial vibrations of the bar.

As an illustration, each chapter is recessed both with precisely calculated and commented examples as well as with supplementary problems—including short solutions. Each chapter concludes with an extensive bibliography.

Skudai, Hüttlingen, May 2012   Andreas Öchsner
                                                                              Markus Merkel

Acknowledgments

Contents

Symbols and Abbreviations

Latin Symbols (Capital Letters)

A	Surface, cross-sectional area
$\boldsymbol{B}$	Matrix with derivatives of the shape functions
$\boldsymbol{C}$	Elasticity matrix, damping matrix
$\boldsymbol{C}^{\mathrm{elpl}}$	Elasto-plastic stiffness matrix
D	Diameter
$\boldsymbol{D}$	Elasticity matrix
E	Modulus of elasticity
E^{elpl}	Elasto-plastic modulus
E^{pl}	Plastic modulus
$\tilde{E}$	Average modulus
F	Yield condition, force
$\boldsymbol{F}$	Column matrix of the external load
G	Shear modulus
I	Second moment of area
K	Bulk modulus
$\boldsymbol{K}$	Total stiffness matrix
$\boldsymbol{K}_{\mathrm{T}}$	Tangent stiffness matrix
L	Element length
$\mathcal{L}_1$	Differential operator of 1st order
$\mathcal{L}_i^n$	LAGRANGE polynomial
L_{crit}	Buckling length
M	Moment
$\boldsymbol{M}$	Mass matrix
N	Shape function
$\boldsymbol{N}$	Row matrix of the shape functions, $\boldsymbol{N} = \{N_1\ N_2\ \dots\ N_n\}$
Q	Plastic potential
$\boldsymbol{Q}$	Elasticity matrix (plane case), shear force

R	Radius
S	Bar force
S	Compliance matrix
T	Torsional moment
T	Transformation matrix
V	Volume
W	Weighting function
X	Global spatial coordinate
Y	Global spatial coordinate
Z	Global spatial coordinate

Latin Symbols (Small Letters)

a	Geometric dimension
b	Geometric dimension, width
c	Integration constant
d	Geometric dimension
h	Geometric dimension, height
e	Unit vector
f	Function
g	Function, gravitational acceleration
h	Function of the stabilization modification
i	Increment number, variable
j	Iteration index, variable
k	Spring stiffness, yield stress
k_s	Shear correction factor
$\boldsymbol{k}^e$	Element stiffness matrix
m	Number of elements, slope, polynomial degree, mass
m_t	Continuously distributed torsional moment per length
m	Column matrix of residual functions
n	Number of nodes, variable, condition
q	Load, integration order, modal coordinates
q	Matrix of the inner variables
r	Function of the flow direction, radius, residual
r	Vector of the flow direction
t	Time, geometric dimension
t_{ij}	Component of the transformation matrix
u_x	Displacement in *x*-direction
u_y	Displacement in *y*-direction
u_z	Displacement in *z*-direction
u	Column matrix of the nodal displacements
v	Argument vector (NEWTON procedure)
x	Spatial coordinate

| y | Spatial coordinate |
| z | Spatial coordinate |

Greek Symbols (Capital Letters)

Γ	Boundary
Λ	Parameter (TIMOSHENKO beam)
Π	Energy
$\bar{\Pi}$	Complementary energy
Π_{ext}	Potential of the external loads
Π_{int}	Elastic strain energy
Φ	Modal matrix
Ω	Domain, volume

Greek Symbols (Small Letters)

α	Thermal expansion coefficient, constant, angle
β	Angle, constant
γ	Shear strain
δ	Virtual
ε	Strain
ε_{ij}	Strain tensor
$\boldsymbol{\varepsilon}$	Column matrix of the strain components
$\varepsilon_{\text{eff}}^{\text{pl}}$	Equivalent plastic strain
κ	Inner variable (plasticity), curvature (beam bending)
λ	Eigenvalue
$d\lambda$	Consistency parameter
ν	Lateral contraction ratio (POISSON's ratio)
ξ	Unit coordinate $(-1 \leq \xi \leq 1)$
π	Volume specific work, volume specific energy
σ	Stress, normal stress
ρ	Density
$\sigma_{n+1}^{\text{trial}}$	Test stress state
σ_{ij}	Stress tensor
$\boldsymbol{\sigma}$	Column matrix of the stress components
τ	Shear stress
η	Coordinate
ζ	Coordinate
ψ	Phase angle
ϕ	Rotation angle, rotation

φ Rotation angle, rotation
ω Eigenfrequency

Indices, Superscript

$\ldots^{\mathrm{v}}$ Composite
$\ldots^{\mathrm{e}}$ Element
$\ldots^{\mathrm{el}}$ Elastic
$\ldots^{\mathrm{ext}}$ External parameter
$\ldots^{\mathrm{geo}}$ Geometric
$\ldots^{\mathrm{glo}}$ Global
$\ldots^{\mathrm{init}}$ Initial (initial yield stress)
$\ldots^{\mathrm{lo}}$ Local
$\ldots^{\mathrm{pl}}$ Plastic
$\ldots^{\mathrm{red}}$ Reduced
$\ldots^{\mathrm{trial}}$ Test condition (back projection)

Indices, Subscript

$\cdots_{\mathrm{Im}}$ Imaginary part of an imaginary number
$\cdots_{\mathrm{Re}}$ Real part of an imaginary number
$\cdots_{\mathrm{b}}$ Bending
$\cdots_{\mathrm{c}}$ Pressure (compression), damping
$\cdots_{\mathrm{eff}}$ Effective value
$\cdots_{\mathrm{f}}$ Fiber in the composite
$\cdots_{\mathrm{krit}}$ Critical
$\cdots_{\mathrm{l}}$ Lamina
$\cdots_{\mathrm{m}}$ Matrix in the composite, inertia
$\cdots_{\mathrm{p}}$ Nodal value
$\cdots_{\mathrm{s}}$ Shear
$\cdots_{\mathrm{t}}$ Torsion, tension
$\cdots_{\mathrm{w}}$ Wall

Mathematical Symbols

$(\ldots)^{\mathrm{T}}$ Transpose
$|\cdots|$ Absolute value
$\|\cdots\|$ Norm

$\otimes$	Dyadic product
sgn	Sign function
$\mathbb{R}$	Set of real numbers

Abbreviations

1D	One-dimensional
2D	Two-dimensional
CAD	Computer aided design
FCM	Fiber composite material
FE	Finite element
FEM	Finite element method
inc	Increment number

Chapter 1
Introduction

Abstract In this first chapter the content as well as the focus will be classified in various aspects. First, the development of the finite element method will be explained and considered from different perspectives.

1.1 The Finite Element Method at a Glance

Seen chronologically, the roots of the finite element method lie in the middle of the last century. Therefore, this method is a relatively young tool in comparison with other tools and aids for the dimensioning and laying of components. The development of the finite element method was configured in the 1950s. Scientists and users have brought in ideas from quite different fields and have therefore turned the method into a universal tool which has nowadays become an indispensable part in research and development and engineering application.

Initially rather basic questions were focused, for example on questions regarding the principle solvability. Regarding the software implementation, only rudimental resources were available—from today's point of view. The postprocessing consisted of punching of cards, which were fed in batches to a calculating machine. Mistakes during the programming were directly displayed with blinking lights. With progressive computer development, the programming environment has become more comfortable and algorithms could be tested and optimized on more challenging examples. From the point of view of engineering application, the problems, which were analyzed via the finite element method, were limited to simple examples. The computer capacities only allowed a quite rough modeling.

Nowadays, many basic questions have been clarified, the central issue of the problem rather lies on the user side. Finite element program packages are available in a large variety and are used in the most different forms. On the one hand there are program packages, which are primarily used in teaching. It is the goal to illustrate the systematic approach. Source codes are available for such programs. On the other

hand, there are commercial program packages which are used to their full capacity regarding program technology as well as the content. Especially the program modules, which have been adapted to a computer platform or computer architecture (parallel computer) are quite efficient and make the processing of very comprehensive problems possible. Regarding the content, the authors venture to say that there is no physical discipline for which no finite element program exists.

In regard to the development of the finite element method, the focus is nowadays on the cooperation and integration with other development tools, as for example the point of intersection with engineering design. Both classical disciplines calculation and design become more and more connected and are partly already fused underneath by a common operation interface. Besides single finite element software packages there are also in a CAD system integrated solutions available on the market. From the view of the user an appropriate finite element preprocessing and postprocessing of *his/her* special problem is in the foreground. The time intensive process steps of the geometry preparation should not involve a considerable extra effort for the application of the finite element method. Calculation results are supposed to be integrated seamlessly in the according process chain.

Regarding the application areas, there are no limits for the application of the finite element method. The dimensioning and configuration of manufacturing elements, subsystems or complete machines surely is the focus in mechanical and plant engineering.

The application of the finite element method or in general of simulation tools in the product development is often seen as a competing tool to the experiment or test. The authors rather see an ideal complement at this point. Therefore, a single test stands test rig or complete test scenarios can be optimized ex ante via finite element simulation. In return, experimental results help to create more precise simulation models.

1.2 Foundations of Modeling

A model of a physical or technical problem represents the initial situation for the application of the finite element method. Part of the complete description of the problem are

- the geometry for the description of the domain,
- the field equations in the domain,
- the boundary conditions, and
- the initial conditions for time dependent problems.

Within this book solely *one-dimensional* elements will be regarded. The general procedure for two- and three-dimensional problems is similar. The mathematical demand, however, is much more complex.

Usually the problems can be described via the differential equation. Here, differential equations of second order are focused on. As an example, the differential equations

of a certain class of physical problems can in general be described as follows:

$$-\frac{d}{dx}\left[a\,\frac{du(x)}{dx}\right] + cu(x) - f = 0. \tag{1.1}$$

Depending on the physical problem a different meaning is assigned to the variables $u(x)$ and the parameters a, c, and f. The following table lists the meaning of the parameters for a few physical problems [1] (Table 1.1).

Table 1.1 Physical problems in the context of the differential equation. Adapted from [1]

	Field parameter	Coefficient		
Problem	$u(x)$	a	c	f
Heat conduction	Temperature	Heat conduction	Convection	Heat sources
	T	kA	$K\,\beta$	q
Pipe flow	Pressure	Pipe resistance		
	p	$1/R$		
Viscous flow	Velocity	Viscosity		Pressure gradient
	v_x	ν		$\frac{dp}{dx}$
Elastic bars	Displacement	Stiffness		Distributed loads
	u	EA		f
Elastic torsion	Rotation	Stiffness		Torsional moments
	φ	GI_p		m
Electrostatics	Electrical potential	Dielectricity		Charge density
	Φ	ϵ		ρ

To describe a problem completely, the statement about the boundary conditions is necessary besides the differential equation. The local boundary conditions can generally be divided into three groups:

- Boundary condition of the 1st kind or DIRICHLET boundary condition (also referred to as essential, fundamental, geometric or kinematic boundary condition):
  A boundary condition of the 1st kind exists, if the boundary condition is being expressed in parameters in which the differential equation is being formulated.
- Boundary condition of the 2nd kind or NEUMANN boundary condition (also referred to as natural or static boundary condition):
  A boundary condition of the 2nd kind exists, if the boundary condition contains the derivation in the direction of the normal of the boundary Γ.
- Boundary condition of the 3rd kind or CAUCHY boundary condition (also referred to as mixed or ROBIN boundary condition):
  Defines a weighted sum of DIRICHLET and NEUMANN condition on the boundary.

These three types of boundary conditions are summarized in Table 1.2, along with their formulas.

Table 1.2 Different
boundary conditions of a
differential equation

Differential equation	Dirichlet	Neumann	Cauchy
$\mathcal{L}\{u(x)\} = b$	u	$\frac{\mathrm{d}u}{\mathrm{d}x}$	$\alpha u + \beta \frac{\mathrm{d}u}{\mathrm{d}x}$

It needs to be considered at this point that one talks about *homogeneous boundary conditions* if the corresponding variables are zero on the boundary.

Within this book, the finite element method will be highlighted from the view of mathematics, physics or the engineering application. From a mathematical view, the finite element method is an appropriate tool to solve partial differential equations. From a physical view a multitude of physical problems can be worked on via the finite element method. The areas go from electrostatics via the diffusion problem all the way to elasticity theory. Engineers make use of the finite element method for the configuration and the dimensioning of products. Regarding the physical problems, at this point solely elastomechanical problems will be discussed. Within statics

- the tension bar,
- the torsion bar, and
- the bending beam with and without shear contribution,

will be covered. Vibrations of bars and beams will be covered as dynamic problems.

Reference

1. Reddy JN (2006) An Introduction to the Finite Element Method. McGraw Hill, Singapore

Chapter 2
Motivation for the Finite Element Method

Abstract The approach to the finite element method can be derived from different motivations. Essentially there are three ways:

- a rather descriptive way, which has its roots in the engineering working method,
- a physical or
- mathematically motivated approach.

Depending on the perspective, different formulations result, which however all result in a common principal equation of the finite element method. The different formulations will be elaborated in detail based on the following descriptions:

- matrix methods,
- physically based working and energy methods and
- weighted residual method.

The finite element method is used to solve different physical problems. Here solely finite element formulations related to structural mechanics are considered [1, 5–7, 9–12].

2.1 From the Engineering Perspective Derived Methods

Matrix methods can be regarded in elastostatics as the initial point for the application of the finite element method to analyze complex structures [2, 3]. As example a plane structure can be given (see Fig. 2.1). This example is adapted from [8].

The structure consists of various substructures I, II, III and IV. The substructures are referred to as elements. The elements are coupled at the nodes 2, 3, 4 and 5. The entire structure is supported on nodes 1 and 6, an external load affects node 4.

Unknown are

- the displacement and reaction forces on every single inner node and
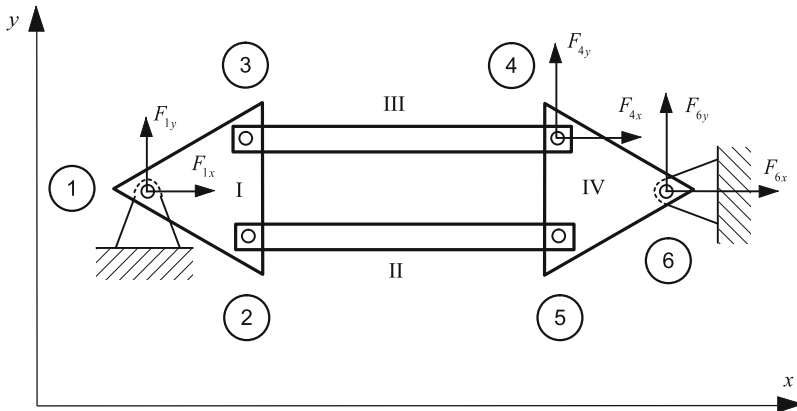
Fig. 2.1 Plane structure, adapted from [8]

• the support reactions

in consequence of the acting load.

To solve the problem, matrix methods can be used. In the matrix methods one distinguishes between the force method (static methods), which is based on a direct determination of the statically indeterminate forces, and the displacement method (kinematic method), which considers the displacements as unknown parameters.

Both methods allow the determination of the unknown parameters. The decisive advantage of the displacement method is that during the application it is not necessary to distinguish between statically determined and statically undeterminate structures. Due to the generality this method is applied in the following.

2.1.1 The Matrix Stiffness Method

It is the primary subgoal to establish the stiffness relation for the entire structure from Fig. 2.1. The following stiffness relation serves as the basis for the matrix displacement method:

$$\boldsymbol{F} = \boldsymbol{K}\,\boldsymbol{u}\,. \tag{2.1}$$

$\boldsymbol{F}$ and $\boldsymbol{u}$ are column matrices, $\boldsymbol{K}$ is a square matrix. $\boldsymbol{F}$ summarizes all nodal forces and $\boldsymbol{u}$ summarizes all nodal displacements. The matrix $\boldsymbol{K}$ represents the stiffness matrix of the entire structure. One single element is identified as the basic unit for the problem and is characterized by the fact that it is coupled with other elements via nodes. Displacements and forces are introduced at every single node.

To solve the entire problem

- the compatibility and
- the equilibrium

have to be fulfilled.

In the matrix displacement method one introduces the nodal displacements as essential unknowns. The displacement vector at a node is defined to be valid for all elements connected at this node. Therewith the compatibility of the entire structure *a priori* is fulfilled.

A Single Element

Forces and displacements are introduced for each node of the single element (see Fig. 2.2).
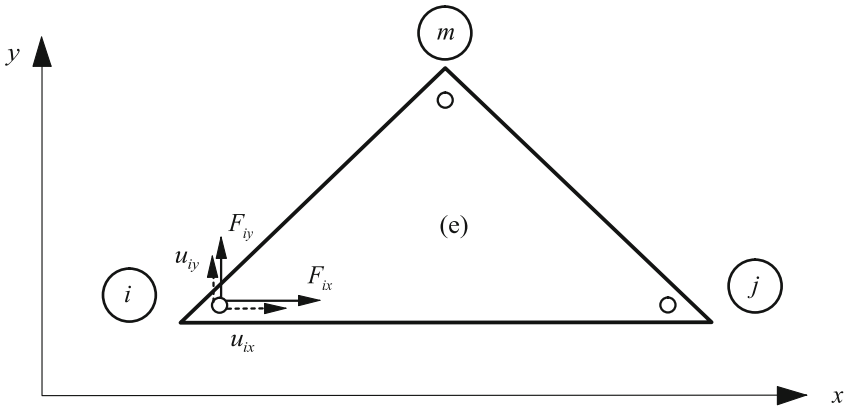
Fig. 2.2 Single element (e) with displacements and forces

For an entirely obvious representation the nodal forces and the nodal displacements are provided with an index 'p' to highlight that these are parameters, which are defined on nodes. The vectors of the nodal displacements u_p or alternatively nodal forces F_p in general consist of various components for the respective coordinates. An additional index 'e' indicates to which element the parameters relate.[1] Therewith the nodal forces result, according to Fig. 2.2, in

---

[1] The additional index 'e' is to be dropped at displacements since the nodal displacement is identical for each linked element in the displacement method.

$$\boldsymbol{F}_i^e = \begin{bmatrix} F_{ix} \\ F_{iy} \end{bmatrix}, \quad \boldsymbol{F}_j^e = \begin{bmatrix} F_{jx} \\ F_{jy} \end{bmatrix}, \quad \boldsymbol{F}_m^e = \begin{bmatrix} F_{mx} \\ F_{my} \end{bmatrix}, \tag{2.2}$$

and the nodal displacements in

$$\boldsymbol{u}_i = \begin{bmatrix} u_{ix} \\ u_{iy} \end{bmatrix}, \quad \boldsymbol{u}_j = \begin{bmatrix} u_{jx} \\ u_{jy} \end{bmatrix}, \quad \boldsymbol{u}_m = \begin{bmatrix} u_{mx} \\ u_{my} \end{bmatrix}. \tag{2.3}$$

If one summarizes all nodal forces and nodal displacements at one element, the

$$\text{entire node force vector } \boldsymbol{F}_{\mathrm{p}}^e = \begin{bmatrix} \boldsymbol{F}_i \\ \boldsymbol{F}_j \\ \boldsymbol{F}_m \end{bmatrix} \tag{2.4}$$

as well as the

$$\text{entire node displacement vector } \boldsymbol{u}_{\mathrm{p}} = \begin{bmatrix} \boldsymbol{u}_i \\ \boldsymbol{u}_j \\ \boldsymbol{u}_m \end{bmatrix} \tag{2.5}$$

for a single element is described. With the vectors for the nodal forces and displacements the stiffness relation for a single element can be defined as follows:

$$\boldsymbol{F}_{\mathrm{p}}^e = \boldsymbol{k}^e \, \boldsymbol{u}_{\mathrm{p}}, \tag{2.6}$$

or alternatively for each node:

$$\boldsymbol{F}_r^e = \boldsymbol{k}_{rs}^e \boldsymbol{u}_s \; (r, s = i, j, m). \tag{2.7}$$

The single stiffness matrix $\boldsymbol{k}^e$ connects the nodal forces . In the present example the single stiffness relation is formally defined as

$$\begin{bmatrix} F_{ix} \\ F_{iy} \\ \hline F_{jx} \\ F_{jy} \\ \hline F_{mx} \\ F_{my} \end{bmatrix} = \begin{bmatrix} k_{ii}^e & k_{ij}^e & k_{im}^e \\ \hline k_{ji}^e & k_{jj}^e & k_{jm}^e \\ \hline k_{mi}^e & k_{mj}^e & k_{mm}^e \end{bmatrix} \begin{bmatrix} u_{ix} \\ u_{iy} \\ \hline u_{jx} \\ u_{jy} \\ \hline u_{mx} \\ u_{my} \end{bmatrix}. \tag{2.8}$$

For further progression it needs to be assumed that the single stiffness matrices of the elements I, II, III and IV are known. The single stiffness relations of one-dimensional

elements will explicitly be derived in the following chapters for different loading types.

The Overall Stiffness

The equilibrium of each single element is fulfilled via the single stiffness relation in Eq. (2.6). The overall equilibrium is satisfied by the fact that each node is set into equilibrium. As an example the equilibrium will be set for node 4 in Fig. 2.3:
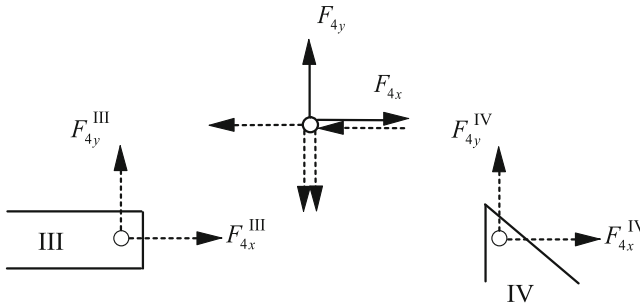
Fig. 2.3 Equilibrium on node 4 for the problem of Fig. 2.1

With

$$F_4 = \begin{bmatrix} F_{4x} \\ F_{4y} \end{bmatrix} \tag{2.9}$$

the following is valid:

$$F_4 = \sum_e F_4^e = F_4^{III} + F_4^{IV}. \tag{2.10}$$

If one substitutes the nodal forces via the single stiffness relations by the nodal displacements, this yields

$$F_4 = k_{43}^{III} u_3 + \left(k_{44}^{III} + k_{44}^{IV} \right) u_4 + k_{45}^{IV} u_5 + k_{46}^{IV} u_6. \tag{2.11}$$

If one sets up the equilibrium on each node accordingly and notes all relations in the form of a matrix equation, the *overall* stiffness relation results

$$F = K\,u \tag{2.12}$$

with

$$K = \sum_e k_{ij}^e, \tag{2.13}$$

or alternatively in detail

$$
\begin{bmatrix}
F_1 \\
0 \\
0 \\
F_4 \\
0 \\
F_6
\end{bmatrix}
=
\begin{bmatrix}
k_{11}^{\mathrm{I}} & k_{12}^{\mathrm{I}} & k_{13}^{\mathrm{I}} & 0 & 0 & 0 \\
k_{21}^{\mathrm{I}} & k_{22}^{\mathrm{I}}+k_{22}^{\mathrm{II}} & k_{23}^{\mathrm{I}} & 0 & k_{25}^{\mathrm{II}} & 0 \\
k_{31}^{\mathrm{I}} & k_{32}^{\mathrm{I}} & k_{33}^{\mathrm{I}}+k_{33}^{\mathrm{III}} & k_{34}^{\mathrm{III}} & 0 & 0 \\
0 & 0 & k_{43}^{\mathrm{III}} & k_{44}^{\mathrm{III}}+k_{44}^{\mathrm{IV}} & k_{45}^{\mathrm{IV}} & k_{46}^{\mathrm{IV}} \\
0 & k_{52}^{\mathrm{II}} & 0 & k_{54}^{\mathrm{IV}} & k_{55}^{\mathrm{II}}+k_{55}^{\mathrm{IV}} & k_{56}^{\mathrm{IV}} \\
0 & 0 & 0 & k_{64}^{\mathrm{IV}} & k_{65}^{\mathrm{IV}} & k_{66}^{\mathrm{IV}}
\end{bmatrix}
\begin{bmatrix}
0 \\
u_2 \\
u_3 \\
u_4 \\
u_5 \\
0
\end{bmatrix}.
$$

(2.14)

This equation is also referred to as the *principal equation of the finite element method*. The vector of the external loads (applied loads or support reactions) is on the left-hand side and the vector of all nodal displacements is on the right-hand side. Both are coupled via the total stiffness matrix K. The elements of the total stiffness matrix result according to Eq. (2.13) by adding the appropriate elements of the single stiffness matrices.

The support conditions $u_1 = 0$ and $u_6 = 0$ are already considered in the displacement vector. From the matrix equations 2 to 5 in (2.14) the unknown nodal displacements u_2, u_3, u_4 and u_5 can be derived. If these are known, one receives, through insertion into the matrix equations 1 and 6 in (2.14), the unknown support reactions F_1 and F_6.

The matrix displacement method is precise as long as the single stiffness matrices can be defined and as long as elements are coupled in well defined nodes. This is the case for example in truss and frame structures within the heretofore valid theories.

With the so far introduced method the nodal displacements and forces in dependency on the external loads can be determined. For the analysis of the strength of a single element the strain and stress state on the inside of the element is of relevance. Usually the displacement field is described via the nodal displacements u_p and shape functions. The strain field can be defined via the kinematic relation and the stress field via the constitutive equation.

2.1.2 Transition to the Continuum

In the previous section, the matrix displacement method was discussed for a joint supporting structure. In contrast to this, in the continuum, the *virtual* discretized finite elements are connected at infinitely many nodal points. However, in a real application of the matrix displacement method, only a finite number of nodes can be considered. Therewith it is not possible to exactly fulfill both demanded conditions for compatibility and for equilibrium at the same time. Either the compatibility or the equilibrium will be fulfilled *on average* (Fig. 2.4).
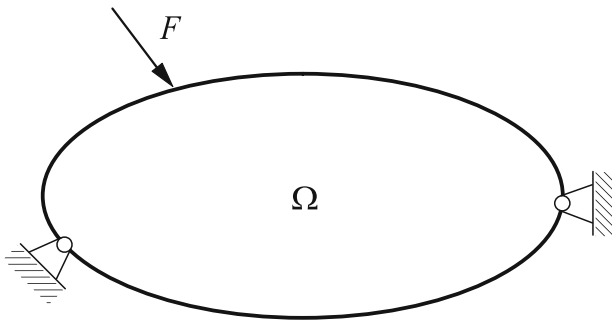
Fig. 2.4   Continuum with load and boundary conditions

In principle, the procedure with the force method or the displacement method can be illustrated. In the following only the *displacement method* will be considered. Here

- the compatibility is *exactly* fulfilled and
- the equilibrium *on average*.

The following approach results:

1. The continuum is discretized, meaning for two-dimensional problems it is divided by virtual lines and for three-dimensional problems through surfaces in subregions, so-called finite elements.

2. The flux of force from element to element occurs in discrete nodes. The displacements of these nodes are introduced as principal unknowns (*displacement method*!).

3. The displacement state within an element is illustrated as a function of the nodal displacement. The displacement formulations are compatible with the adjacent neighboring elements.

4. Through the displacement field the strain state within the element and through the constitutive equation the stress state are known as function of the nodal displacement.

5. Via the *principle of virtual work*, statically equivalent resulting nodal forces are assigned to the stresses along the virtual element boundaries *on average*.

6. To maintain the overall equilibrium all nodal equilibria have to be fulfilled. Via this condition one gets to the total stiffness relation, from which the unknown nodal displacements can be calculated after considering the kinematic boundary conditions.

7. If the nodal displacements are known, one knows the displacement and strain field and therefore also the stress state of each single element.

Comments to the Single Steps

Discretization

Through discretization the entire continuum is divided into elements. An element is in contact with one or various neighboring elements. In the two-dimensional case lines result as contact regions, in the three-dimensional case surfaces occur. Figure 2.5 illustrates a discretization for a plane case.
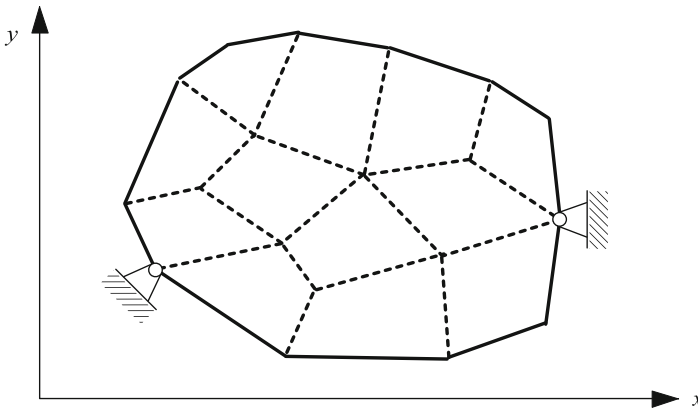
Fig. 2.5 Discretization of a plane area

The discretization can be interpreted as follows: Single points do not change their geometric position within the continuum. The relation to the neighboring points however does change. While each point within the continuum is in interaction with its neighboring point, in the virtual discretized continuum this is only valid within one element. If two points lie within two different elements they are not directly linked.

Nodes and Displacements

The information flow between single elements only occurs via the nodes. In the displacement method, displacements are introduced at the nodes as principal unknowns (see Fig. 2.6).
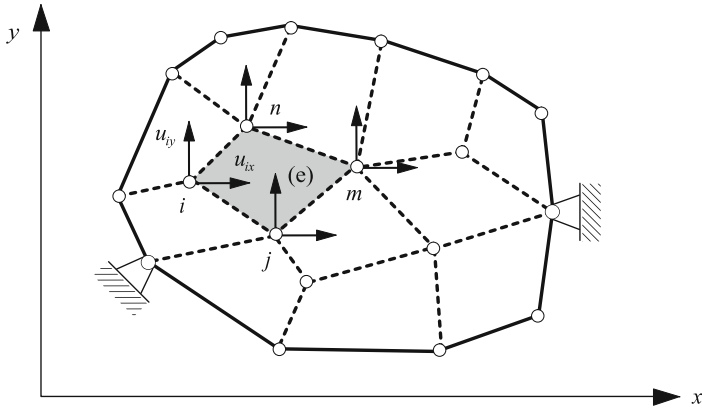
Fig. 2.6 Nodes with displacements

The displacements are identical for each on the node neighboring elements. Forces only flow via the nodes, no forces flow via the element boundaries even though the element boundaries are geometrically identical.

Approximation of the Displacement Field

A typical way to describe the displacement field $\boldsymbol{u}^e(\boldsymbol{x})$ on the inside of an element is to approximate the field through the displacement at the nodes and so-called shape functions (see Fig. 2.7):
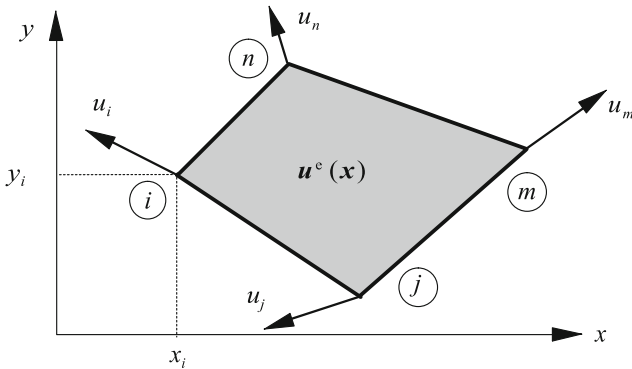
Fig. 2.7 Approximation of the displacement field in the element

$$u^{\mathrm{e}}(x) = N(x)\,u_{\mathrm{p}}\,. \tag{2.15}$$

The discretization must not lead to holes in the continuum. To ensure the compatibility between single elements a suitable description of the displacement field has to be chosen. The choice of the shape functions has a significant influence on the quality of the approximation and will be discussed in detail in Sect. 6.4.

Strain and Stress Fields

From the displacement field $u^{\mathrm{e}}(x)$ one can get to the strain field

$$\varepsilon^{\mathrm{e}}(x) = \mathcal{L}_1 u^{\mathrm{e}}(x) \tag{2.16}$$

via the above kinematic relation. Thereby $\mathcal{L}_1$ is a differential operator of first order.[2] The stress within an element can be determined via the constitutive equation (Fig. 2.8):

$$\sigma^{\mathrm{e}}(x) = D\varepsilon^{\mathrm{e}}(x) = D\mathcal{L}_1 N(x)\,u_{\mathrm{p}} = DB(x)\,u_{\mathrm{p}}\,. \tag{2.17}$$
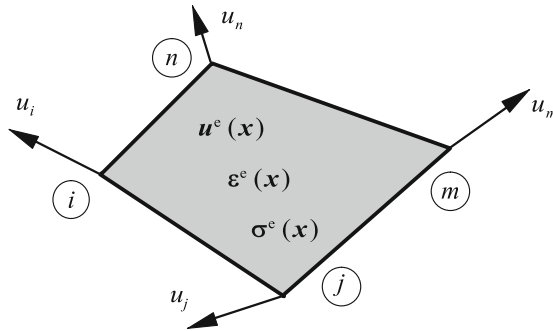
Fig. 2.8 Displacement, strain and stress in the element

The expression $\mathcal{L}_1 N(x)$ contains the derivatives of the shape functions. Usually a new matrix entitled B is introduced.

Principle of Virtual Work, Single Stiffness Matrices

While any point can interact with a neighboring point within the continuum, this is only possible within an element in the discretized structure. A direct exchange beyond the element boundaries is not foreseen. The principle of virtual work represents an

---

[2] In the one-dimensional case the differential operator simplifies to the derivative $\frac{\mathrm{d}}{\mathrm{d}x}$.

appropriate tool to assign statically equivalent nodal forces to the stress along the virtual element boundaries (Fig. 2.9).
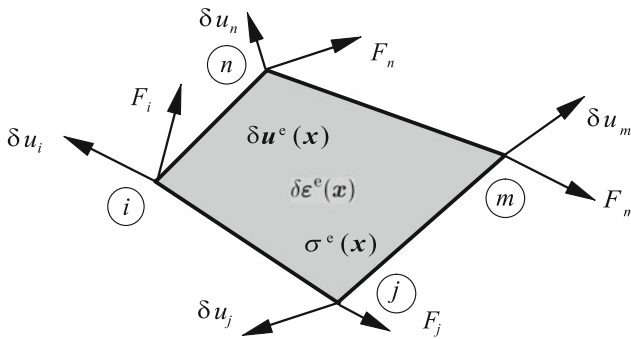
Fig. 2.9 Principle of virtual work at one element

For this, one summarizes the nodal forces to a vector F_p^e. The virtual displacements δu_p do the external virtual work $\delta \Pi_{ext}$ with the nodal forces, the virtual strains $\delta \varepsilon$ do the inner work $\delta \Pi_{int}$ with the stresses σ^e inside:

$$\delta \Pi_{ext} = (F_p^e)^T \delta u_p,$$
$$\delta \Pi_{int} = \int_\Omega (\sigma^e)^T \delta \varepsilon^e d\Omega. \tag{2.18}$$

According to the principle of virtual work the following is valid:

$$\delta \Pi_{ext} = \delta \Pi_{int}. \tag{2.19}$$

If one transposes the equation

$$(F_p^e)^T \delta u_p = \int_\Omega (\sigma^e)^T \delta \varepsilon^e d\Omega$$

and if one inserts (2.16) and (2.17) accordingly, this yields

$$(\delta u_p)^T F_p^e = (\delta u_p)^T \int_\Omega B^T D B d\Omega\, u_p. \tag{2.20}$$

From this one receives the single stiffness relation

$$F_p^e = k^e u_p \tag{2.21}$$

with the element stiffness matrix

$$k^e = \int_\Omega B^T D B d\Omega \, . \tag{2.22}$$

Total Stiffness Relation

One receives the total stiffness relation

$$F = K u \tag{2.23}$$

from the overall equilibrium. This can be achieved by setting up the equilibrium on every single node. The unknown parameters cannot be gained from the total stiffness relation yet. In the context of the equation's solution the system matrix is not regular. Only after taking at least the rigid-body motion (displacement and rotation) from the overall system, a reduced system results

$$F^{red} = K^{red} u_p^{red} \, , \tag{2.24}$$

which can be solved. A description of the equation solution can be found in Sect. 7.2 and in the Appendix A.1.5.

Determination of Element Specific Field Parameters

After the equation's solution the nodal displacements are known. Therewith the displacement, strain and stress field on the inside of every single element can be defined. In addition the support reactions can be determined.

2.2 Integral Principles

The derivation of the finite element method often occurs via the so-called energy principles. Therefore this chapter serves as a short summary about a few important principles. The overall potential or the total potential energy of a system can generally be written as

$$\Pi = \Pi_{int} + \Pi_{ext} \tag{2.25}$$

whereupon Π_{int} represents the elastic strain energy and Π_{ext} represents the potential of the external loads. The elastic strain energy—or work of the internal forces—

results in general for linear elastic material behavior via the column matrix of the stresses and strains into:

$$\Pi_{\text{int}} = \frac{1}{2} \int_{\Omega} \boldsymbol{\sigma}^{\mathrm{T}} \boldsymbol{\varepsilon} \mathrm{d}\Omega .$$ (2.26)

The potential of the external loads—which corresponds with the negative work of the external loads—can be written as follows for the column matrix of the external loads $\boldsymbol{F}$ and the displacements $\boldsymbol{u}$:

$$\Pi_{\text{ext}} = -\boldsymbol{F}^{\mathrm{T}} \boldsymbol{u}.$$ (2.27)

- **Principle of Virtual Work**:

The principle of virtual work comprises the principle of virtual displacements and the principle of virtual forces. The principle of virtual displacements states that if an element is in equilibrium, the entire internal virtual work equals the entire external virtual work for arbitrary, compatible, small, virtual displacements, which fulfill the geometric boundary conditions:

$$\int_{\Omega} \boldsymbol{\sigma}^{\mathrm{T}} \delta \boldsymbol{\varepsilon} \mathrm{d}\Omega = \boldsymbol{F}^{\mathrm{T}} \delta \boldsymbol{u} .$$ (2.28)

Accordingly the principle of virtual forces results in:

$$\int_{\Omega} \delta \boldsymbol{\sigma}^{\mathrm{T}} \boldsymbol{\varepsilon} \mathrm{d}\Omega = \delta \boldsymbol{F}^{\mathrm{T}} \boldsymbol{u} .$$ (2.29)

- **Principle of Minimum of Potential Energy**:

According to this principle the overall potential takes an extreme value in the equilibrium position:

$$\Pi = \Pi_{\text{int}} + \Pi_{\text{ext}} = \text{minimum} .$$ (2.30)

- **Castigliano's Theorem:**

CASTIGLIANO's first theorem states that the partial derivative of the complementary strain energy, see Fig. 2.10a with respect to an external force F_i leads to the displacement of the force application point in the direction of this force. Accordingly it results that the partial derivative of the complementary strain energy with respect to an external moment M_i leads to the rotation of the moment application point in the direction of this moment:
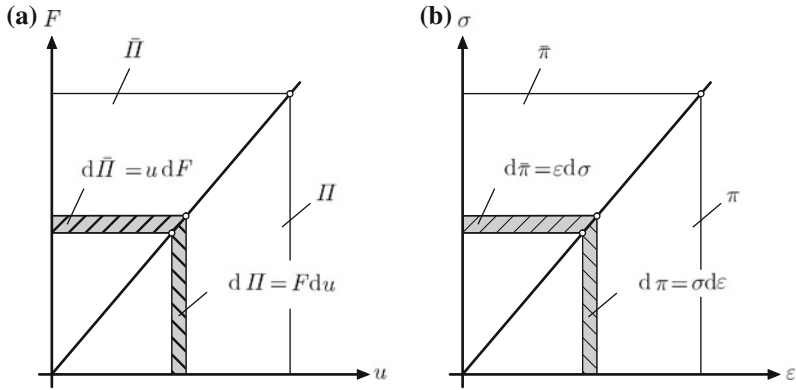
Fig. 2.10   Definition of the strain energy and the complementary strain energy: **a** absolute; **b** volume specific

$$\frac{\partial \bar{\Pi}_{\text{int}}}{\partial F_i} = u_i \,, \tag{2.31}$$

$$\frac{\partial \bar{\Pi}_{\text{int}}}{\partial M_i} = \varphi_i \,. \tag{2.32}$$

CASTIGLIANO's second theorem states that the partial derivative of the strain energy (see Fig. 2.10a) with respect to the displacements u_i leads to the force F_i in direction to the considered displacement u_i. An analogous connection is valid for the rotation and the moment:

$$\frac{\partial \Pi_{\text{int}}}{\partial u_i} = F_i \,, \tag{2.33}$$

$$\frac{\partial \Pi_{\text{int}}}{\partial \varphi_i} = M_i \,. \tag{2.34}$$

2.3 Weighted Residual Method

The initial point of the weighted residual method is the differential equation, which describes the physical problem. In the one-dimensional case such a physical problem within the domain Ω can in general be described via the differential equation

$$\mathcal{L}\{u^0(x)\} = b \quad (x \in \Omega) \tag{2.35}$$

as well as via the boundary conditions, which are prescribed on the boundary Γ. The differential equation is also referred to as a *strong form* of the problem since the

problem is exactly described in every point x of the domain. In Eq. (2.35) $\mathcal{L}\{\ldots\}$ represents an arbitrary differential operator, which can for example take the following forms:

$$\mathcal{L}\{\ldots\} = \frac{d^2}{dx^2}\{\ldots\}, \tag{2.36}$$

$$\mathcal{L}\{\ldots\} = \frac{d^4}{dx^4}\{\ldots\}, \tag{2.37}$$

$$\mathcal{L}\{\ldots\} = \frac{d^4}{dx^4}\{\ldots\} + \frac{d}{dx}\{\ldots\} + \{\ldots\}. \tag{2.38}$$

Furthermore b represents a given function in Eq. (2.35), whereupon one talks about a *homogeneous differential equation* in the case of $b = 0$: $\mathcal{L}\{u^0(x)\} = 0$. The exact or real solution of the problem, $u^0(x)$, fulfills the differential equation in every point of the domain $x \in \Omega$ and the prescribed geometric and static boundary conditions on Γ. Since the exact solution for the most engineering problems cannot be calculated in general, it is the goal of the following derivation to define a best possible approximate solution

$$u(x) \approx u^0(x). \tag{2.39}$$

For the approximate solution in Eq. (2.39) in the following an approach in the form

$$u(x) = \alpha_0 + \sum_{k=1}^{n} \alpha_k \varphi_k(x) \tag{2.40}$$

is chosen, whereupon α_0 needs to fulfill the non-homogeneous boundary conditions, $\varphi_k(x)$ represents a set of linear independent basis functions and α_k are the free parameters of the approximation approach, which are defined via the approximation procedure in a way so that the exact solution u^0 of the approximate solution u is approximated in the best way.

2.3.1 Procedure on Basis of the Inner Product

If one incorporates the approximate formulation for u^0 into the differential equations. (2.35), one receives a local error, the so-called *residual r*:

$$r = \mathcal{L}\{u(x)\} - b \neq 0. \tag{2.41}$$

Within the weighted residual method this error is weighted with a weighting function $W(x)$ and is integrated via the entire domain Ω, so that the error disappears on average:

$$\int\limits_{\Omega} r\,W\mathrm{d}\Omega = \int\limits_{\Omega} (\mathcal{L}\{u(x)\} - b)W\mathrm{d}\Omega \overset{!}{=} 0\,. \tag{2.42}$$

This formulation is also referred to as the *inner product*. One notes that the weighting or test function $W(x)$ allows to weigh the error differently within the domain Ω. However the overall error must on average, meaning integrated over the domain, become zero. The structure of the weighting function is most of the time set in a similar way as with the approximate function $u(x)$

$$W(x) = \sum_{k=1}^{n} \beta_k \psi_k(x)\,, \tag{2.43}$$

whereupon β_k represent *arbitrary* coefficients and $\psi_k(x)$ linear independent shape functions. The approach (2.43) includes—depending on the choice of the amount of the summands k and the functions $\psi_k(x)$—the class of the procedures with equal shape functions for the approximate solution and the weighting function ($\varphi_k(k) = \psi_k(x)$) and the class of the procedures, at which the shape functions are chosen differently ($\varphi_k(k) \neq \psi_k(x)$). Depending on the choice of the weighting function the following classic methods can be differentiated [4, 13]:

• **Point-Collocation Method:** $\psi_k(x) = \delta(x - x_k)$

The point-collocation method takes advantage of the properties of the delta function. The error r disappears exactly on the n freely selectable points $x_1, x_2, \ldots, x_n$, with $x_k \in \Omega$, the so-called collocation points and therefore the approximate solution fulfills the differential equation exactly in the collocation points. The weighting function can therefore be set as

$$W(x) = \beta_1 \underbrace{\delta(x - x_1)}_{\psi_1} + \cdots + \beta_n \underbrace{\delta(x - x_n)}_{\psi_n} = \sum_{k=1}^{n} \beta_k \delta(x - x_k) \tag{2.44}$$

whereupon the delta function is defined as follows:

$$\delta(x - x_k) = \begin{cases} 0 & \text{for } x \neq x_k \\ \infty & \text{for } x = x_k \end{cases}\,. \tag{2.45}$$

If one incorporates this approach into the inner product according to Eq. (2.42) and considers the properties of the delta function,

$$\int\limits_{-\infty}^{\infty} \delta(x - x_k)\,\mathrm{d}x = \int\limits_{x_k - \varepsilon}^{x_k + \varepsilon} \delta(x - x_k)\,\mathrm{d}x = 1\,, \tag{2.46}$$

$$\int\limits_{-\infty}^{\infty} f(x)\delta(x - x_k)\,\mathrm{d}x = \int\limits_{x_k-\varepsilon}^{x_k+\varepsilon} f(x)\delta(x - x_k)\,\mathrm{d}x = f(x_k)\,, \qquad (2.47)$$

n linear independent equations result for the calculation of the free parameters α_k:

$$r(x_1) = \mathcal{L}\{u(x_1)\} - b = 0\,, \qquad\qquad (2.48)$$
$$r(x_2) = \mathcal{L}\{u(x_2)\} - b = 0\,, \qquad\qquad (2.49)$$
$$\vdots$$
$$r(x_n) = \mathcal{L}\{u(x_n)\} - b = 0\,. \qquad\qquad (2.50)$$

One considers that the approximate approach has to fulfill all boundary conditions, meaning the essential and natural boundary conditions. Due to the property of the delta function, $\int_\Omega r\,W(\delta)\mathrm{d}\Omega = r = 0$, no integral has to be calculated within the point-collocation procedure, meaning no integration via the inner product. One therefore does not need to do an integration and receives the approximate solution faster—compared to for example the GALERKIN procedure. A disadvantage is, however, that the collocation points can be chosen freely. These can therefore also be chosen unfavorable.

● **Subdomain-Collocation Procedure:** $\psi_k(x) = 1$ in Ω_k and otherwise zero

This procedure is a collocation method as well, however besides the demand that the error has to disappear on certain points, here it is demanded that the integral of the error becomes zero over the different domains, the subdomains:

$$\int\limits_{\Omega_i} r\,\mathrm{d}\Omega_i = 0 \qquad \text{for a subregion } \Omega_i\,. \qquad (2.51)$$

With this procedure the finite difference method can, for example, be derived.

● **Method of Least Squares:** $\psi_k(x) = \dfrac{\partial r}{\partial \alpha_k}$

The average quadratic error is optimized at the method of least squares

$$\int\limits_{\Omega} (\mathcal{L}\{u(x)\} - b)^2\mathrm{d}\Omega = \text{minimum}\,, \qquad (2.52)$$

or alternatively

$$\frac{\mathrm{d}}{\mathrm{d}\alpha_k} \int\limits_{\Omega} (\mathcal{L}\{u(x)\} - b)^2\mathrm{d}\Omega = 0\,, \qquad (2.53)$$

$$\int\limits_{\Omega} \frac{d(\mathcal{L}\{u(x)\} - b)}{d\alpha_k}(\mathcal{L}\{u(x)\} - b)d\Omega = 0 \,. \tag{2.54}$$

● **Petrov-Galerkin Procedure:** $\psi_k(x) \neq \varphi_k(x)$

This term summarizes all procedures, at which the shape functions of the weighting function and the approximate solution are different. Therefore, for example, the subdomain-collocation method can be allocated to this group.

● **Galerkin Procedure:** $\psi_k(x) = \varphi_k(x)$

The basic idea of the GALERKIN or BUBNOV- GALERKIN method is to choose the *same* shape function for the approximate approach and the weighting function approach. Therefore, the weighting function results in the following for this method:

$$W(x) = \sum_{k=1}^{n} \beta_k \varphi_k(x) \,. \tag{2.55}$$

Since the same shape functions $\varphi_k(x)$ were chosen for $u(x)$ and $W(x)$ and the coefficients β_k are arbitrary, the function $W(x)$ can be written as a variation of $u(x)$ (with $\delta\alpha_0 = 0$):

$$W(x) = \delta u(x) = \delta\alpha_1\varphi_1(x) + \cdots + \delta\alpha_n\varphi_n(x) = \sum_{k=1}^{n} \delta\alpha_k \times \varphi_k(x) \,. \tag{2.56}$$

The variations can be virtual parameters, as for example virtual displacements or velocities. The incorporation of this approach into the inner product according to Eq. (2.42) yields a set of n linear independent equations for a linear operator for the definition of n unknown free parameters α_k:

$$\int\limits_{\Omega} (\mathcal{L}\{u(x)\} - b) \cdot \varphi_1(x) \, d\Omega = 0 \,, \tag{2.57}$$

$$\int\limits_{\Omega} (\mathcal{L}\{u(x)\} - b) \cdot \varphi_2(x) \, d\Omega = 0 \,, \tag{2.58}$$

$$\vdots$$

$$\int\limits_{\Omega} (\mathcal{L}\{u(x)\} - b) \cdot \varphi_n(x) \, d\Omega = 0 \,. \tag{2.59}$$

Conclusion regarding the procedure based on the inner products:

These formulations demand that the shape functions—which have been assumed to be defined over the entire domain Ω—fulfill all boundary conditions, meaning the essential and natural boundary conditions. This demand, as well as the demanded differentiation of the shape functions ($\mathcal{L}$ operator) often lead to a difficulty finding appropriate functions in the practical application. Furthermore, in general, unsymmetric coefficient matrices occur (if the $\mathcal{L}$ operator is symmetric the coefficient matrix of the GALERKIN method is also symmetric).

2.3.2 Procedure on Basis of the Weak Formulation

For the derivation of another class of approximate procedures the inner product is partially integrated again and again until the derivative of $u(x)$ and $W(x)$ has the same order and one reaches the so-called *weak formulation*. Within this formulations the demand regarding the differentiability for the approximate function is diminished, the demand regarding the weighting function however increased. If one uses the idea of the GALERKIN method, meaning equal shape functions for the approximate approach and the weighting function, the demand regarding the differentiability of the shape functions is reduced in total.

For a differential operator of second or fourth order, meaning

$$\int_{\Omega} \mathcal{L}_2\{u(x)\}W(x)\mathrm{d}\Omega , \tag{2.60}$$

$$\int_{\Omega} \mathcal{L}_4\{u(x)\}W(x)\mathrm{d}\Omega , \tag{2.61}$$

a one-time partial integration of Eq. (2.60) yields the weak form

$$\int_{\Omega} \mathcal{L}_1\{u(x)\}\mathcal{L}_1\{W(x)\}\mathrm{d}\Omega = [\mathcal{L}_1\{u(x)\}W(x)]_{\Gamma} , \tag{2.62}$$

or alternatively two-times partial integration the weak form of Eq. (2.61):

$$\int_{\Omega} \mathcal{L}_2\{u(x)\}\mathcal{L}_2\{W(x)\}\mathrm{d}\Omega = [\mathcal{L}_2\{u(x)\}\mathcal{L}_1\{W(x)\} - \mathcal{L}_3\{u(x)\}W(x)]_{\Gamma} . \tag{2.63}$$

For the derivation of the finite element method one switched to domain-wise defined shape functions. For such a domain, meaning a finite element with $\Omega^{\mathrm{e}} < \Omega$ and a local element coordinate x^{e} the weak formulation of (2.62), for example, results in:

$$\int_{\Omega^e} \mathcal{L}_2\{u(x^e)\}\mathcal{L}_2\{W(x^e)\}\mathrm{d}\Omega^e = \left[\mathcal{L}_2\{u(x^e)\}\mathcal{L}_1\{W(x^e)\} - \mathcal{L}_3\{u(x^e)\}W(x^e)\right]_{\Gamma^e}.$$

(2.64)

Since the weak formulation contains the natural boundary conditions—for this also see sample problem 2.2—, it can be demanded in the following that the approach[3] for $u(x)$ only has to fulfill the essential boundary conditions. According to the GALERKIN method it is demanded for the derivation of the principal finite element equation that the same shape functions for the approximate and weighting function are chosen. Within the framework of the finite element method the nodal values u_k are chosen for the free values α_k and the shape functions $\varphi_k(x)$ are referred to as form or shape functions $N_k(x)$. Therefore, the following illustrations result for the approximate solution and the weighting function:

$$u(x) = N_1(x)u_1 + N_2(x)u_2 + \cdots N_n(x)u_n = \sum_{k=1}^{n} N_k(x)u_k,$$

(2.65)

$$W(x) = \delta u_1 N_1(x) + \delta u_2 N_2(x) + \cdots \delta u_n N_n(x) = \sum_{k=1}^{n} \delta u_k N_k(x),$$

(2.66)

whereupon n represents the number of nodes per element. It is important for this procedure that the error on the nodes, whose position has to be defined by the user, is minimized. This is a significant difference to the classic GALERKIN method on the basis of the inner product, which has found the points with $r = 0$ itself. For the further derivation of the principal finite element equation the approaches (2.65) and (2.66) have to be written in matrix form and inserted into the weak form. For further details of the derivation refer to the explanations in Chaps. 3 and 5 at this point.

Within the framework of the finite element method the so-called RITZ method is often mentioned. The classic procedure takes into account the overall potential Π of a system. Within this overall potential an approximate approach in the form of (2.40) is used, which is, however, defined for the entire domain Ω in the RITZ method. The shape functions φ_k have to fulfill the geometric, however not the static boundary conditions.[4] Via the derivative of the potential with respect to the unknown free parameters α_k, meaning definition of the extremum of Π, a system of equations results for the definition of k free parameters, the so-called RITZ coefficients. In general, however, it is difficult to find shape functions with unknown free values, which fulfill *all* geometric boundary conditions of the problem. However, if one modifies the classic RITZ method in a way so that only the domain Ω^e of a finite

---

[3] The index 'e' of the element coordinate is neglected in the following—in the case it does not affect the understanding.

[4] Since the static boundary conditions are implicitly integrated in the overall potential, the shape functions do not have to fulfill those. However, if the shape functions fulfill the static boundary conditions additionally, an even more precise approximation can be achieved.

element is considered and one makes use of an approximate approach according to Eq. (2.65) one also achieves the finite element method at this point.

2.3.3 Procedure on Basis of the Inverse Formulation

Finally it needs to be remarked that the inner product can be partially integrated again and again for the derivation of another class of approximate procedures until the derivative of $u(x)$ can be completely shifted onto $W(x)$. Therewith one achieves the so-called *inverse formulation*. Depending on the choice of the weighting function one receives the following methods:

- Choice of W so that $\mathcal{L}(W) = 0$ or $\mathcal{L}(u) \neq 0$.

  Procedure: *Boundary element method (Boundary integral equation of the first kind)*.

- Use of a so-called fundamental solution $W = W^*$, meaning a solution, which fulfills the equation $\mathcal{L}(W^*) = (-)\delta(\xi)$.

  Procedure: *Boundary element method (Boundary integral equation of the second kind)*.

  The coefficient matrix of the corresponding system of equations is fully occupied and not symmetric. What is decisive for the application of the method is the knowledge about a fundamental solution for the $\mathcal{L}$ operator (in elasticity theory such an analytical solution is known through the KELVIN solution—concentrated load at a point of an infinite elastic medium).

- Equal shape functions for approximation approach and weighting function approach. Procedure: TREFFTZ *method*.

- Equal shape functions for approximate approach and weighting function and $\mathcal{L}(u) = \mathcal{L}(W) = 0$ is valid. Procedure: *Variation of the* TREFFTZ *method*.

2.4 Sample Problems

2.1. Example: Galerkin Method on Basis of the Inner Product

Since the term GALERKIN method is an often used term within the finite element method, the original GALERKIN method needs to be explained in the following within

the framework of this example. For this the differential equation, which is defined in the domain $0 < x < 1$ is considered

$$\mathcal{L}\{u(x)\} - b = \frac{d^2 u^0}{dx^2} + x^2 = 0 \quad (0 < x < 1) \tag{2.67}$$

with the homogeneous boundary conditions $u^0(0) = u^0(1) = 0$. For this problem the exact solution

$$u^0(x) = \frac{x}{12}\left(-x^3 + 1\right) \tag{2.68}$$

can be defined via integration and subsequent consideration of the boundary conditions. Define the approximate solution for an approach with two free values.

2.1 Solution

For the construction of the approximate solution $u(x)$ according to the GALERKIN method the following approach with two free parameters can be made use of:

$$u^0(x) \approx u(x) = \alpha_1 \varphi_1(x) + \alpha_2 \varphi_2(x), \tag{2.69}$$
$$= \alpha_1 x(1 - x) + \alpha_2 x^2(1 - x), \tag{2.70}$$
$$= \alpha_1 x + (\alpha_2 - \alpha_1)x^2 - \alpha_2 x^3. \tag{2.71}$$

One needs to consider that the functions $\varphi_1(x)$ and $\varphi_2(x)$ are chosen in a way so that the boundary conditions, meaning $u(0) = u(1) = 0$, are fulfilled. Therefore, polynomials of first order are eliminated since a linear slope could only connect the two zero points as a horizontal line. Furthermore, both functions are chosen in a way so that they are linearly independent. The first derivatives of the approximation approach result in

$$\frac{du(x)}{dx} = \alpha_1 + 2(\alpha_2 - \alpha_1)x - 3\alpha_2 x^2, \tag{2.72}$$

$$\frac{d^2 u(x)}{dx^2} = 2(\alpha_2 - \alpha_1) - 6\alpha_2 x, \tag{2.73}$$

and the error function results in the following via the second derivative from Eq. (2.41):

$$r(x) = \frac{d^2 u}{dx^2} + x^2 = 2(\alpha_2 - \alpha_1) - 6\alpha_2 x + x^2. \tag{2.74}$$

The insertion of the weighting function, meaning

$$W(x) = \delta u(x) = \delta\alpha_1 x(1 - x) + \delta\alpha_2 x^2(1 - x), \tag{2.75}$$

into the residual equation yields

$$\underbrace{\int\limits_0^1 \left(2(\alpha_2 - \alpha_1) - 6\alpha_2 x + x^2\right)}_{r(x)} \times \underbrace{\left(\delta\alpha_1 x(1-x) + \delta\alpha_2 x^2(1-x)\right)}_{W(x)} dx = 0 \quad (2.76)$$

or generally split into two integrals:

$$\delta\alpha_1 \int\limits_0^1 r(x)\varphi_1(x)dx + \delta\alpha_2 \int\limits_0^1 r(x)\varphi_2(x)dx = 0. \quad (2.77)$$

Since the $\delta\alpha_i$ are arbitrary coefficients and the shape functions $\varphi_i(x)$ are linearly independent, the following system of equations results herefrom:

$$\delta\alpha_1 \int\limits_0^1 \left(2(\alpha_2 - \alpha_1) - 6\alpha_2 x + x^2\right) \times (x(1-x))\, dx = 0, \quad (2.78)$$

$$\delta\alpha_2 \int\limits_0^1 \left(2(\alpha_2 - \alpha_1) - 6\alpha_2 x + x^2\right) \times \left(x^2(1-x)\right) dx = 0. \quad (2.79)$$

After the integration, a system of equations results for the definition of the two unknown free parameters α_1 and α_2

$$\frac{1}{20} - \frac{1}{6}\alpha_2 - \frac{1}{3}\alpha_1 = 0, \quad (2.80)$$

$$\frac{1}{30} - \frac{2}{15}\alpha_2 - \frac{1}{6}\alpha_1 = 0, \quad (2.81)$$

or alternatively in matrix notation:

$$\begin{bmatrix} \frac{1}{3} & \frac{1}{6} \\ \frac{1}{6} & \frac{2}{15} \end{bmatrix} \begin{bmatrix} \alpha_1 \\ \alpha_2 \end{bmatrix} = \begin{bmatrix} \frac{1}{20} \\ \frac{1}{30} \end{bmatrix}. \quad (2.82)$$

From this system of equations the free parameters result in $\alpha_1 = \frac{1}{15}$ and $\alpha_2 = \frac{1}{6}$. Therefore, the approximate solution and the error function finally result in:

$$u(x) = x\left(-\frac{1}{6}x^2 + \frac{1}{10}x + \frac{1}{15}\right), \quad (2.83)$$

(a)

(b)
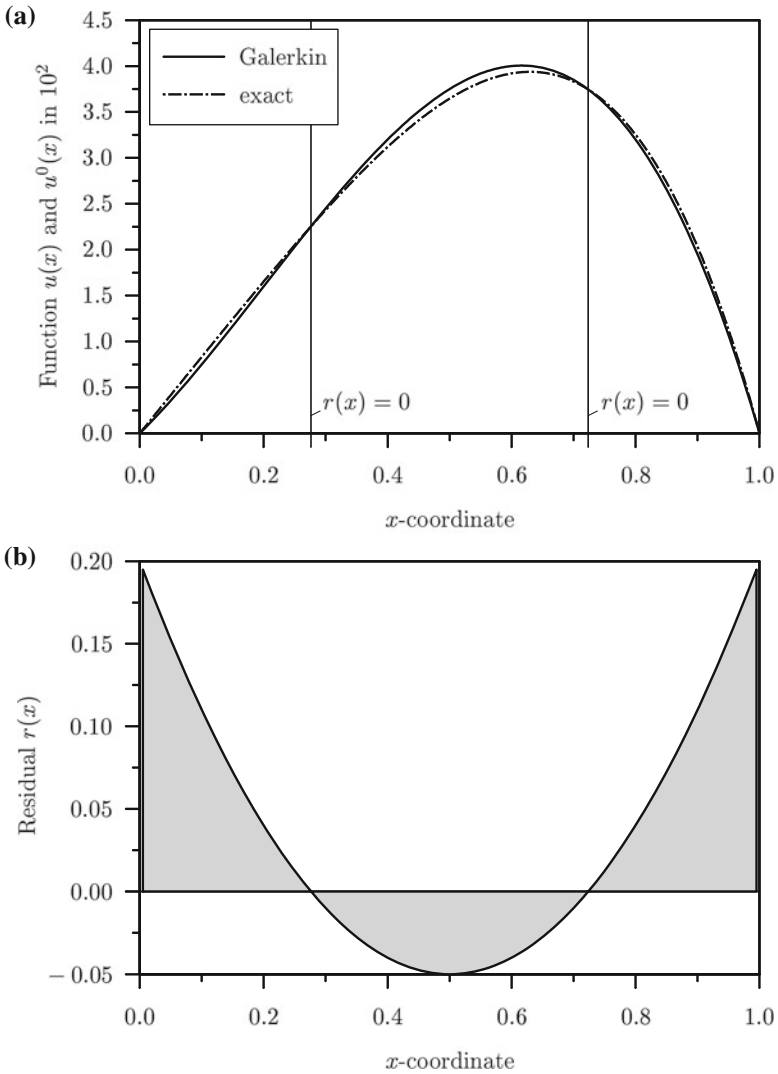
Fig. 2.11 Approximate solution according to the GALERKIN method, **a** exact solution and **b** residual as a function of the coordinate

$$r(x) = x^2 - x + \frac{1}{5}. \tag{2.84}$$

The comparison between the approximate solution and exact solution is illustrated in Fig. 2.11a. One can see that the two solutions coincide on the boundaries—one needs to consider that the approximate approach has to fulfill the boundary conditions—as well as on two other locations.
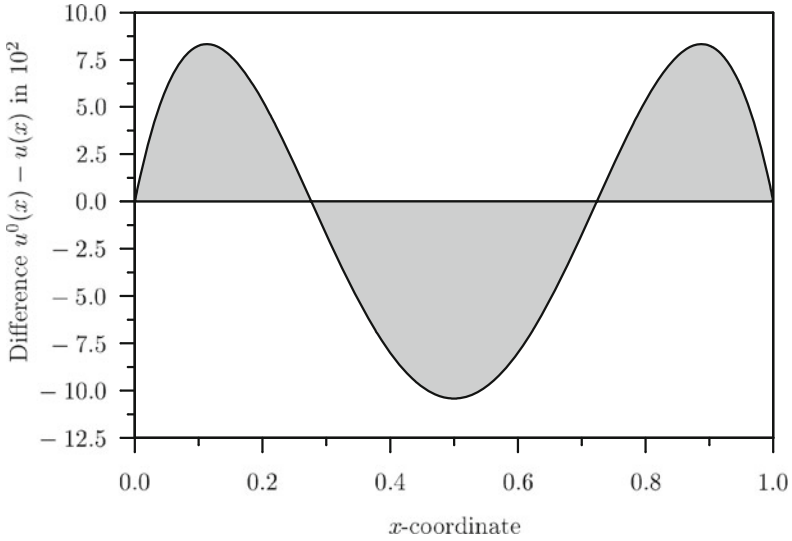
Fig. 2.12 Absolute difference between exact solution and approximate solution as function of the coordinate

It needs to be remarked at this point that the error function—see Fig. 2.11b—does not illustrate the difference between the exact solution and the approximate solution. Rather it is about the error, which results from inserting the approximate solution into the differential equation. To illustrate this, Fig. 2.12 shows the absolute difference between exact solution and approximate solution.

Finally it can be summarized that the advantage of the GALERKIN method is that the procedure itself is in search of the points with $r = 0$. This is quite an advantage in comparison to the collocation method. However within the GALERKIN method the integration needs to be performed and therefore this method is in comparison to the collocation more complex and slower.

2.2 Example: Finite Element Method

For the differential equations (2.67) and the given boundary conditions one needs to calculate, based on the weak formulation, a finite element solution, based on two equidistant elements with linear shape functions.

Solution

The partial integration of the inner product yields the following formulation:

$$\int_0^1 \left(\frac{\mathrm{d}^2 u(x)}{\mathrm{d}x^2} + x^2 \right) W(x)\, \mathrm{d}x = 0 \,, \tag{2.85}$$

$$\int_0^1 \frac{\mathrm{d}^2 u(x)}{\mathrm{d}x^2} W(x)\, \mathrm{d}x + \int_0^1 x^2 W(x)\, \mathrm{d}x = 0 \,, \tag{2.86}$$

$$\left[\frac{\mathrm{d}u(x)}{\mathrm{d}x} W(x) \right]_0^1 - \int_0^1 \frac{\mathrm{d}u(x)}{\mathrm{d}x} \frac{\mathrm{d}W(x)}{\mathrm{d}x}\, \mathrm{d}x + \int_0^1 x^2 W(x)\, \mathrm{d}x = 0 \,, \tag{2.87}$$

or alternatively the weak form in its final form:

$$\int_0^1 \frac{\mathrm{d}u(x)}{\mathrm{d}x} \frac{\mathrm{d}W(x)}{\mathrm{d}x}\, \mathrm{d}x = \left[\frac{\mathrm{d}u(x)}{\mathrm{d}x} W(x) \right]_0^1 + \int_0^1 x^2 W(x)\, \mathrm{d}x \,. \tag{2.88}$$

For the derivation of the finite element method one merges into domain-wise defined shape functions. For such a domain $\Omega^e < \Omega$, namely a finite element[5] of the length L^e, the weak formulation results in:

$$\int_0^{L^e} \frac{\mathrm{d}u(x^e)}{\mathrm{d}x^e} \frac{\mathrm{d}W(x^e)}{\mathrm{d}x^e}\, \mathrm{d}x^e = \left[\frac{\mathrm{d}u(x^e)}{\mathrm{d}x^e} W(x^e) \right]_0^{L^e} + \int_0^{L^e} (x^e + c^e)^2 W(x^e)\, \mathrm{d}x^e \,. \tag{2.89}$$
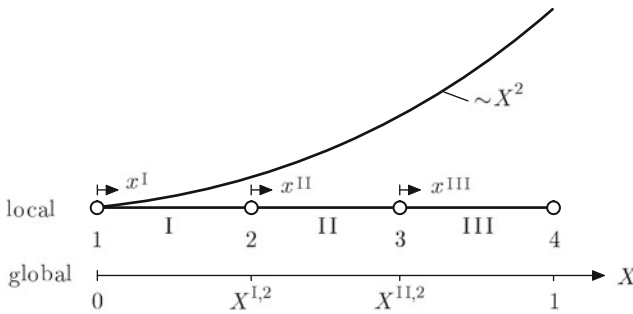
Fig. 2.13 Global coordinate system X and local coordinate system x_i for every element

In the transition from Eqs. (2.88) to (2.89), meaning from the global formulation to the consideration on the element level, in particular the quadratic expression on the right-hand side of Eq. (2.88) needs to be considered. To ensure that the in the

---

[5] Usually a separate *local* coordinate system $0 \le x^e \le L^e$ is introduced for each element 'e'. The coordinate in Eq. (2.88) is then referred to as global coordinate and receives the symbol X.

(a)

(b)
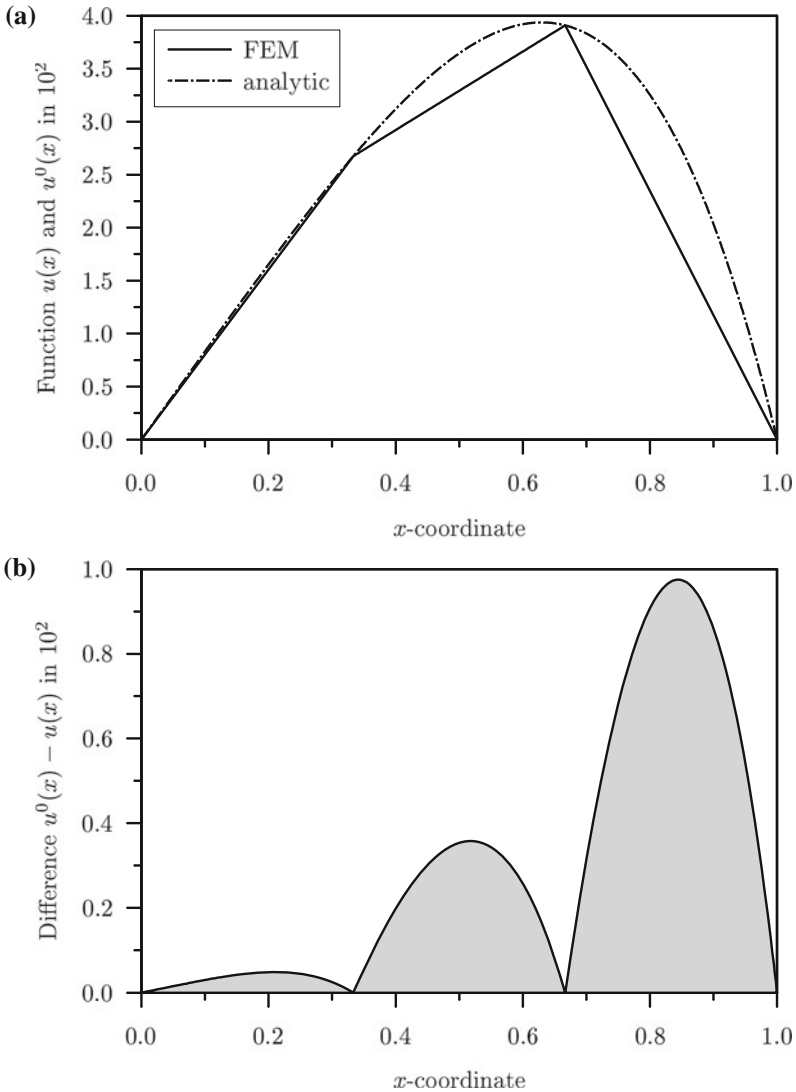
Fig. 2.14 **a** Exact solution and approximate solution and **b** absolute difference between exact solution and finite element solution as a function of the coordinate

global coordinate system defined expression X^2 is considered appropriately in the description on the element level, a coordinate transformation has to be performed for every element 'e' via a term c^e. From Fig. 2.13 it can be seen that the term c turns zero for the first element (I) since global and local coordinate system coincide. For the second element (II) $c^{II} = X^{I,2} = \frac{1}{3}$ results with an equidistant division and $c^{III} = X^{II,2} = \frac{2}{3}$ results accordingly for the third element (III).

Since the weak formulation contains the natural boundary conditions—for this see the boundary expression in Eq. (2.89)—it can be demanded in the following that the approach for $u(x)$ has to fulfill the essential boundary conditions only. According to the GALERKIN method it is demanded for the derivation of the principal finite element equation that the same shape functions for the approximate and weighting function are chosen. Within the framework of the finite element method the nodal values u_k are chosen for the free parameters α_k and the shape functions $\varphi_k(x)$ are referred to as form or shape functions $N_k(x)$. For linear shape functions the following illustrations result for the approximate solution and the weighting function:

$$u(x) = N_1(x)u_1 + N_2(x)u_2 \,, \tag{2.90}$$

$$W(x) = \delta u_1 N_1(x) + \delta u_2 N_2(x) \,. \tag{2.91}$$

For the chosen linear shape functions, an element-wise linear course of the approximate function and a difference between the exact solution and the approximate approach as shown in Fig. 2.14 are obtained. It is obvious that the error is minimal on the nodes, at the best identical with the exact solution.

References

1. Betten J (2001) Kontinuumsmechanik: Elastisches und inelastisches Verhalten isotroper und anisotroper Stoffe. Springer-Verlag, Berlin
2. Betten J (2004) Finite Elemente für Ingenieure 1: Grundlagen. Matrixmethoden, Elastisches Kontinuum, Springer-Verlag, Berlin
3. Betten J (2004) Finite Elemente für Ingenieure 2: Variationsrechnung, Energiemethoden. Näherungsverfahren, Nichtlinearitäten, Numerische Integrationen, Springer-Verlag, Berlin
4. Brebbia CA, Telles JCF, Wrobel LC (1984) Boundary Element Techniques: Theory and Applications. Springer-Verlag, Berlin
5. Gross D, Hauger W, Schröder J, Wall WA (2009) Technische Mechanik 2: Elastostatik. Springer-Verlag, Berlin
6. Gross D, Hauger W, Schröder J, Werner EA (2008) Hydromechanik. Elemente der Höheren Mechanik, Numerische Methoden, Springer-Verlag, Berlin
7. Klein B (2000) FEM. Grundlagen und Anwendungen der Finite-Elemente-Methode, Vieweg-Verlag, Wiesbaden
8. Kuhn G, Winter W (1993) Skriptum Festigkeitslehre Universität Erlangen-Nürnberg.
9. Kwon YW, Bang H (2000) The Finite Element Method Using MATLAB. CRC Press, Boca Raton
10. Oden JT, Reddy JN (1976) Variational methods in theoretical mechanics. Springer-Verlag, Berlin
11. Steinbuch R (1998) Finite Elemente - Ein Einstieg. Springer-Verlag, Berlin
12. Szabó I (1996) Geschichte der mechanischen Prinzipien und ihrer wichtigsten Anwendungen. Birkhäuser Verlag, Basel
13. Zienkiewicz OC, Taylor RL (2000) The Finite Element Method Volume 1: The Basis. Butterworth-Heinemann, Oxford

Chapter 3
Bar Element

Abstract On the basis of the bar element, tension and compression as types of basic load cases will be described. First, the basic equations known from the strength of materials will be introduced. Subsequently the bar element will be introduced, according to the common definitions for load and deformation quantities, which are used in the handling of the FE method. The derivation of the stiffness matrix will be described in detail. Apart from the simple prismatic bar with constant cross-section and material properties also more general bars, where the size varies along the body axis will be analyzed in examples [1–9] and exercises.

3.1 Basic Description of the Bar Element

In the simplest case, the bar element can be defined as a prismatic body with constant cross-sectional area A and constant modulus of elasticity E, which is loaded with a concentrated force F in the direction of the body axis (see Fig. 3.1).
The unknown quantities are

- the extension ΔL and
- the strain ε and stress σ of the bar

dependent on the external load.
The following three basic equations are known from the strength of materials: By

$$\varepsilon(x) = \frac{\mathrm{d}u(x)}{\mathrm{d}x} = \frac{\Delta L}{L} \tag{3.1}$$

kinematics describes the relation between the strains $\varepsilon(x)$ and the deformations $u(x)$.
By

$$\sigma(x) = E\,\varepsilon(x) \tag{3.2}$$
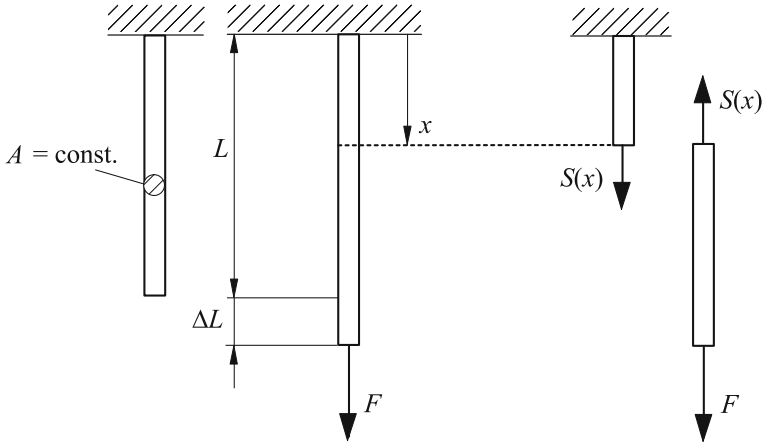
Fig. 3.1 Tensile bar loaded by single force

the constitutive equation describes the relation between the stresses $\sigma(x)$ and the strains $\varepsilon(x)$ and the equilibrium condition results in

$$\sigma(x) = \frac{S(x)}{A(x)} = \frac{S(x)}{A} = \frac{F}{A}. \tag{3.3}$$

The connection between the force F and the length variation ΔL of the bar can easily be described with these three equations:

$$\frac{F}{A} = \sigma = E\varepsilon = E\frac{\Delta L}{L} \tag{3.4}$$

or with

$$F = \frac{EA}{L}\Delta L. \tag{3.5}$$

The relation between force and length variation is described as axial stiffness. Hence, the following occurs for the bar regarding the tensile loading[1]:

$$\frac{F}{\Delta L} = \frac{EA}{L}. \tag{3.6}$$

For the derivation of the differential equation the force equilibrium at an infinitesimal small bar element has to be regarded (see Fig. 3.2). A continuously distributed line load $q(x)$ acts as the load in the unit force per unit length.

---

[1] The parlance tension bar includes the load case compression.
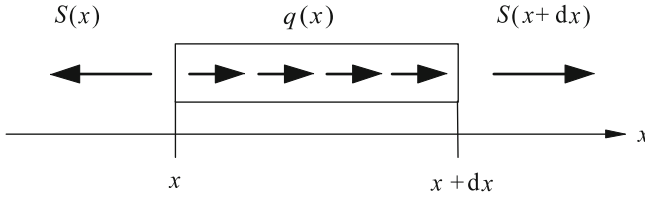
Fig. 3.2 Force equilibrium at an infinitesimal small bar element

The force equilibrium in the direction of the body axis delivers:

$$- S(x) + q(x)\mathrm{d}x + S(x + \mathrm{d}x) = 0. \tag{3.7}$$

After a series expansion of $S(x + \mathrm{d}x) = S(x) + \mathrm{d}S(x)$ the following occurs

$$- S(x) + q(x)\mathrm{d}x + S(x) + \mathrm{d}S(x) = 0 \tag{3.8}$$

or in short:

$$\frac{\mathrm{d}S(x)}{\mathrm{d}x} = -q(x). \tag{3.9}$$

Equations (3.1), (3.2) and (3.3) for kinematics, the constitutive equation and the equilibrium continue to apply. If the Eqs. (3.1) and (3.3) are inserted in (3.2), one obtains

$$EA(x)\frac{\mathrm{d}u(x)}{\mathrm{d}x} = S(x). \tag{3.10}$$

After the differentiation and insertion of Eq. (3.9) one obtains

$$\frac{\mathrm{d}}{\mathrm{d}x}\left[EA(x)\frac{\mathrm{d}u(x)}{\mathrm{d}x}\right] + q(x) = 0 \tag{3.11}$$

as the differential equation for a bar with continuously distributed load. This is a differential equation of 2nd order within the displacements. Under constant cross-section A and constant modulus of elasticity E the term simplifies to

$$EA\frac{\mathrm{d}^2u(x)}{\mathrm{d}x^2} + q(x) = 0. \tag{3.12}$$

3.2 The Finite Element Tension Bar

The tension bar is defined as a prismatic body with a single body axis. Nodes are introduced at both ends of the tension bar, where forces and displacements, as sketched in Fig. 3.3 are positively defined. The main objective is to achieve a stiffness relation for this element in the form
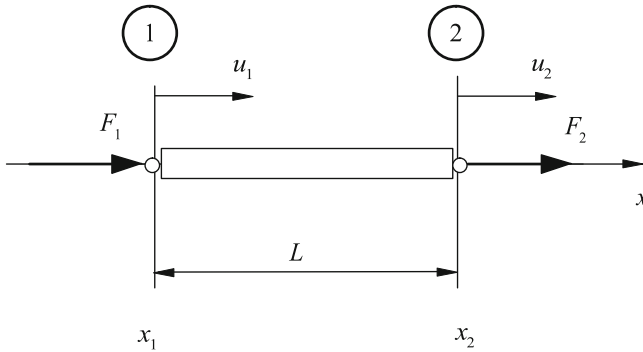
Fig. 3.3 Definition of the finite element tension bar

$$F^e = k^e \cdot u_p$$

or

$$\begin{bmatrix} F_1 \\ F_2 \end{bmatrix}^e = \begin{bmatrix} \cdot & \cdot \\ \cdot & \cdot \end{bmatrix} \begin{bmatrix} u_1 \\ u_2 \end{bmatrix}. \tag{3.13}$$

With this stiffness relation the bar element can be integrated in a structure. Furthermore the displacements, the strains and the stresses *inside* the element are unknown. At first, an easy approach is introduced, in which the bar is modeled as a linear spring (Fig. 3.4).

Fig. 3.4 Tension bar modeled as a linear spring
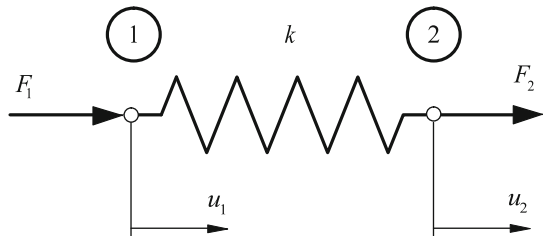
This is possible when

- the cross-sectional area A and
- the modulus of elasticity E

are constant along the body axis. The previously derived axial rigidity of the tension bar can then be interpreted as a spring constant or spring stiffness of a linear spring through

$$\frac{F}{\Delta L} = \frac{EA}{L} = k. \tag{3.14}$$

For the derivation of the stiffness relation, which is requested for the finite element method, a thought experiment is conducted. If, within the spring model at first only

the spring force F_2 is in effect and the spring force F_1 is being faded out, the equation

$$F_2 = k\Delta u = k(u_2 - u_1) \tag{3.15}$$

then describes the relation between the spring force and the length variation of the spring. If subsequently only the spring force F_1 is in effect and the spring force F_2 is being faded out, the equation

$$F_1 = k\Delta u = k(u_1 - u_2) \tag{3.16}$$

then describes the relation between the spring force and the length variation of the spring. Both situations can be superimposed and summarized compactly in matrix-form as

$$\begin{bmatrix} F_1 \\ F_2 \end{bmatrix}^e = \begin{bmatrix} k & -k \\ -k & k \end{bmatrix} \begin{bmatrix} u_1 \\ u_2 \end{bmatrix}. \tag{3.17}$$

With that the desired stiffness relation between the forces and deformations on the nodal points is derived.

The efficiency of this simple model however is limited. Thus no statements regarding the displacement, strain and stress distribution on the inside can be made. Therefore, a more elaborated model is necessary. This will be introduced in the following.

At first the displacement distribution $u^e(x)$ inside a bar will be described through shape functions $N(x)$ and the displacements u_p at the nodes:

$$u^e(x) = N(x)\,u_p. \tag{3.18}$$

In the simplest case, the displacement distribution is approximated linearly for the tension bar (see Fig. 3.5). With the following approach
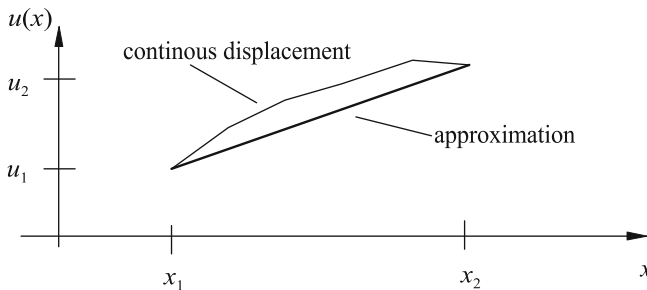
Fig. 3.5 Linear approximation of the displacement distribution in the tension bar

$$u^e(x) = \alpha_1 + \alpha_2 x \tag{3.19}$$

the displacements at the nodes

$$
\begin{bmatrix} u_1 \\ u_2 \end{bmatrix} = \begin{bmatrix} 1 & x_1 \\ 1 & x_2 \end{bmatrix} \begin{bmatrix} \alpha_1 \\ \alpha_2 \end{bmatrix}
\tag{3.20}
$$

can be described. After the elimination of α_i the following results for the displacement distribution:

$$
u^e(x) = \frac{x_2 - x}{x_2 - x_1} u_1 + \frac{x - x_1}{x_2 - x_1} u_2
\tag{3.21}
$$

or summarized

$$
u^e(x) = \frac{1}{L}(x_2 - x)u_1 + \frac{1}{L}(x - x_1)u_2.
\tag{3.22}
$$

By this the shape functions $N_1(x)$ and $N_2(x)$ can be described with

$$
N_1(x) = \frac{1}{L}(x_2 - x) \quad \text{and} \quad N_2(x) = \frac{1}{L}(x - x_1).
\tag{3.23}
$$

The displacement distribution results in a compact form in:

$$
u^e(x) = N_1(x)u_1 + N_2(x)u_2 = [N_1 \; N_2] \begin{bmatrix} u_1 \\ u_2 \end{bmatrix} = N(x)\, u_p.
\tag{3.24}
$$

Through the kinematics relation the strain distribution results

$$
\varepsilon^e(x) = \frac{\mathrm{d}}{\mathrm{d}x} u^e(x) = \frac{\mathrm{d}}{\mathrm{d}x} N(x)\, u_p = B\, u_p
\tag{3.25}
$$

and because of the constitutive equation the stress distribution results in

$$
\sigma^e(x) = E\varepsilon^e(x) = E B u_p,
\tag{3.26}
$$

where the matrix B for the derivation of the shape functions is introduced. For the linear approximation of the displacement distribution the derivatives of the shape functions result in:

$$
\frac{\mathrm{d}}{\mathrm{d}x} N_1(x) = -\frac{1}{L}, \quad \frac{\mathrm{d}}{\mathrm{d}x} N_2(x) = \frac{1}{L}
\tag{3.27}
$$

and therefore the matrix B results in

$$
B = \frac{1}{L}[-1 \;\; 1].
\tag{3.28}
$$

For the derivation of the element stiffness matrix the following integral has to be evaluated

$$k^{\mathrm{e}} = \int_{\Omega} \boldsymbol{B}^{\mathrm{T}} \boldsymbol{D} \boldsymbol{B}\, \mathrm{d}\Omega. \tag{3.29}$$

The elasticity matrix $\boldsymbol{D}$ is represented only through the modulus of elasticity E. For the tension bar, the stiffness matrix therefore results in:

$$k^{\mathrm{e}} = AE \int_{L} \frac{1}{L} \begin{bmatrix} 1 \\ -1 \end{bmatrix} \frac{1}{L} [-1 \ \ 1]\, \mathrm{d}x = \frac{EA}{L^2} L \begin{bmatrix} 1 & -1 \\ -1 & 1 \end{bmatrix}. \tag{3.30}$$

In a compact form, the element stiffness matrix is called:

$$k^{\mathrm{e}} = \frac{EA}{L} \begin{bmatrix} 1 & -1 \\ -1 & 1 \end{bmatrix}. \tag{3.31}$$

There are also other ways to derive the stiffness matrix, which are introduced in the following sections.

3.2.1 Derivation Through Potential

The elastic potential energy[2] of a one-dimensional problem according to Fig. 3.1 with linear-elastic material behavior results in:

$$\Pi_{\mathrm{int}} = \frac{1}{2} \int_{\Omega} \varepsilon_x \sigma_x \mathrm{d}\Omega. \tag{3.32}$$

If stress and strain are substituted by use of the formulations according to Eqs. (3.26) and (3.25) and if $\mathrm{d}\Omega = A\mathrm{d}x$ is taken into consideration, the following applies:

$$\Pi_{\mathrm{int}} = \frac{1}{2} \int_{0}^{L} EA \left(\boldsymbol{B} \boldsymbol{u}_{\mathrm{p}} \right)^{\mathrm{T}} \boldsymbol{B} \boldsymbol{u}_{\mathrm{p}} \mathrm{d}x. \tag{3.33}$$

If the relation for the transpose of a product of two matrices[3] is taken into account the following results

$$\Pi_{\mathrm{int}} = \frac{1}{2} \int_{0}^{L} EA \boldsymbol{u}_{\mathrm{p}}^{\mathrm{T}} \boldsymbol{B}^{\mathrm{T}} \boldsymbol{B} \boldsymbol{u}_{\mathrm{p}} \mathrm{d}x. \tag{3.34}$$

---

[2] The form $\Pi_{\mathrm{int}} = \frac{1}{2} \int_{\Omega} \boldsymbol{\varepsilon}^{\mathrm{T}} \boldsymbol{\sigma} \mathrm{d}\Omega$ can be used in the general three-dimensional case, where $\boldsymbol{\sigma}$ and $\boldsymbol{\varepsilon}$ represents the column matrix with the stress and strain components.

[3] $(\boldsymbol{AB})^{\mathrm{T}} = \boldsymbol{B}^{\mathrm{T}} \boldsymbol{A}^{\mathrm{T}}$

Since the nodal values do not represent a function of x, both column matrices can be eliminated from the integral:

$$\Pi_{\text{int}} = \frac{1}{2} \, \boldsymbol{u}_{\text{p}}^{\text{T}} \left[\int_0^L E A \boldsymbol{B}^{\text{T}} \boldsymbol{B} \mathrm{d}x \right] \boldsymbol{u}_{\text{p}}. \tag{3.35}$$

Under consideration of the $\boldsymbol{B}$ matrix definition according to Eq. (3.28) the following results for constant axial rigidity EA:

$$\Pi_{\text{int}} = \frac{1}{2} \, \boldsymbol{u}_{\text{p}}^{\text{T}} \underbrace{\left[\frac{EA}{L^2} \int_0^L \begin{bmatrix} 1 & -1 \\ -1 & 1 \end{bmatrix} \mathrm{d}x \right]}_{\boldsymbol{k}^{\text{e}}} \boldsymbol{u}_{\text{p}}. \tag{3.36}$$

The last equation is equivalent to the general formulation of the potential energy of a finite element

$$\Pi_{\text{int}} = \frac{1}{2} \, \boldsymbol{u}_{\text{p}}^{\text{T}} \boldsymbol{k}^{\text{e}} \boldsymbol{u}_{\text{p}} \tag{3.37}$$

and allows the identification of the element stiffness matrix $\boldsymbol{k}^{\text{e}}$.

3.2.2 Derivation Through Castigliano's Theorem

If the stress in the formulation for the elastic potential energy according to Eq. (3.32) is substituted by use of HOOKE's law according to Eq. (3.2) and if $\mathrm{d}\Omega = A\mathrm{d}x$ is taken into consideration, the following results:

$$\Pi_{\text{int}} = \frac{1}{2} \int_L E A \varepsilon_x^2 \mathrm{d}x. \tag{3.38}$$

If now the strain is substituted using the kinematic relation according to Eq. (3.1) and introduces the approach for the displacement distribution according to Eq. (3.24), the elastic potential energy for constant axial rigidity EA finally results in:

$$\Pi_{\text{int}} = \frac{EA}{2} \int_0^L \left(\frac{\mathrm{d}N_1(x)}{\mathrm{d}x} u_1 + \frac{\mathrm{d}N_2(x)}{\mathrm{d}x} u_2 \right)^2 \mathrm{d}x. \tag{3.39}$$

The application of CASTIGLIANO's theorem on the potential energy with reference to the nodal displacement u_1 leads to the external force F_1 on the node 1:

$$\frac{\mathrm{d}\Pi_{\text{int}}}{\mathrm{d}u_1} = F_1 = EA \int_0^L \left(\frac{\mathrm{d}N_1(x)}{\mathrm{d}x} u_1 + \frac{\mathrm{d}N_2(x)}{\mathrm{d}x} u_2 \right) \frac{\mathrm{d}N_1(x)}{\mathrm{d}x} \, \mathrm{d}x. \tag{3.40}$$

From the differentiation regarding the other deformation parameter the following arises accordingly:

$$\frac{\mathrm{d}\Pi_{\text{int}}}{\mathrm{d}u_2} = F_2 = EA \int_0^L \left(\frac{\mathrm{d}N_1(x)}{\mathrm{d}x} u_1 + \frac{\mathrm{d}N_2(x)}{\mathrm{d}x} u_2 \right) \frac{\mathrm{d}N_2(x)}{\mathrm{d}x} \, \mathrm{d}x. \tag{3.41}$$

Equations (3.40) and (3.41) can be summarized as the following formulation:

$$EA \int_0^L \begin{bmatrix} \frac{\mathrm{d}N_1(x)}{\mathrm{d}x} \frac{\mathrm{d}N_1(x)}{\mathrm{d}x} & \frac{\mathrm{d}N_2(x)}{\mathrm{d}x} \frac{\mathrm{d}N_1(x)}{\mathrm{d}x} \\ \frac{\mathrm{d}N_1(x)}{\mathrm{d}x} \frac{\mathrm{d}N_2(x)}{\mathrm{d}x} & \frac{\mathrm{d}N_2(x)}{\mathrm{d}x} \frac{\mathrm{d}N_2(x)}{\mathrm{d}x} \end{bmatrix} \mathrm{d}x \begin{bmatrix} u_1 \\ u_2 \end{bmatrix} = \begin{bmatrix} F_1 \\ F_2 \end{bmatrix}. \tag{3.42}$$

After introducing the shape functions according to Eq. (3.23) and executing the integration the element stiffness matrix, which is given in Eq. (3.31), results.

3.2.3 Derivation Through the Weighted Residual Method

In the following, the differential equation for the displacement field according to Eq. (3.13) is being considered. This formulation assumes that the axial rigidity EA is constant and it results in

$$EA \frac{\mathrm{d}^2 u^0(x)}{\mathrm{d}x^2} + q(x) = 0, \tag{3.43}$$

whereupon $u^0(x)$ represents the exact solution of the problem. The last equation with the exact solution is exactly fulfilled at every position x on the bar and is also referred to as the *strong formulation* of the problem. If the exact solution in Eq. (3.43) is substituted through an approximate solution $u(x)$, a residual or remainder r results:

$$r = EA \frac{\mathrm{d}^2 u(x)}{\mathrm{d}x^2} + q(x) \neq 0. \tag{3.44}$$

Due to the introduction of the approximate solution $u(x)$ it is in general not possible anymore to fulfill the differential equation at every position x of the bar. As an alternative, it is demanded in the following that the differential equation is fulfilled over a certain length (and not at every position x anymore) and therefore ends up with the following integral demand

$$\int_0^L W(x)\left(EA\frac{d^2u(x)}{dx^2} + q(x)\right)dx \overset{!}{=} 0, \qquad (3.45)$$

which is also referred to as the *inner product*. $W(x)$ as part of Eq. (3.45) represents the so-called weighting function, which distributes the error or the residual over the regarded length.

The following results through partial integration[4] of the first expression in the parentheses of Eq. (3.45)

$$\int_0^L \underbrace{W}_{f}\, EA\underbrace{\frac{d^2u(x)}{dx^2}}_{g'}\, dx = EA\left[W(x)\frac{du(x)}{dx}\right]_0^L - EA\int_0^L \frac{dW(x)}{dx}\frac{du(x)}{dx}\, dx. \quad (3.46)$$

Under consideration of Eq. (3.45) the so-called *weak formulation* of the problem results in:

$$EA\int_0^L \frac{dW(x)}{dx}\frac{du(x)}{dx}\, dx = EA\left[W\frac{du(x)}{dx}\right]_0^L + \int_0^L W(x)q(x)dx. \qquad (3.47)$$

When considering the weak form it becomes obvious that one derivative of the approximate solution was shifted to the weighting function through the partial integration and that now with reference to the derivation a symmetric form arose. This symmetry with reference to the derivation of the approximate solution and the weighting function will subsequently guarantee that a symmetric element stiffness matrix for the bar element results.

In the following, first the left-hand side of Eq. (3.47) needs to be considered to derive the element stiffness matrix for a linear bar element.

The basic idea of the finite element method now is to no longer approximate the unknown displacement distribution $u(x)$ in the total domain, but to approximately describe the displacement distribution through

$$u^e(x) = N(x)u_p = \begin{bmatrix} N_1 & N_2 \end{bmatrix} \times \begin{bmatrix} u_1 \\ u_2 \end{bmatrix} \qquad (3.48)$$

for a subdomain, the so-called finite element. Within the context of the finite element method the same approach as for the displacement is chosen for the weighting function:

---

[4] A usual representation of the partial integration of two functions $f(x)$ and $g(x)$ is: $\int fg'dx = fg - \int f'gdx$.

$$W(x) = \left[\boldsymbol{N}(x)\, \delta \boldsymbol{u}_{\mathrm{p}} \right]^{\mathrm{T}} = \delta \boldsymbol{u}_{\mathrm{p}}^{\mathrm{T}} \boldsymbol{N}^{\mathrm{T}}(x) = [\delta u_1\ \delta u_2] \times \begin{bmatrix} N_1 \\ N_2 \end{bmatrix}, \qquad (3.49)$$

whereupon δu_i represent the so-called arbitrary or virtual displacements. The derivative of the weighting function results in

$$\frac{\mathrm{d} W(x)}{\mathrm{d} x} = \frac{\mathrm{d}}{\mathrm{d} x} \left(\boldsymbol{N} \delta \boldsymbol{u}_{\mathrm{p}} \right)^{\mathrm{T}} = \left(\boldsymbol{B} \delta \boldsymbol{u}_{\mathrm{p}} \right)^{\mathrm{T}} = \delta \boldsymbol{u}_{\mathrm{p}}^{\mathrm{T}} \boldsymbol{B}^{\mathrm{T}}. \qquad (3.50)$$

In the following it remains to be seen that the virtual displacements can be canceled with an identical expression on the right-hand side of Eq. (3.47) and no further consideration will be necessary at this point. When considering the approaches for the displacement and the weighting function on the left-hand side of Eq. (3.47), the following results for constant axial rigidity EA:

$$EA \int_0^L \left(\delta \boldsymbol{u}_{\mathrm{p}}^{\mathrm{T}} \boldsymbol{B}^{\mathrm{T}} \right) \left(\boldsymbol{B} \boldsymbol{u}_{\mathrm{p}} \right) \mathrm{d} x \qquad (3.51)$$

or under consideration that the vector of the nodal displacement can be regarded as constant:

$$\delta \boldsymbol{u}_{\mathrm{p}}^{\mathrm{T}} EA \underbrace{\int_0^L \boldsymbol{B}^{\mathrm{T}} \boldsymbol{B} \, \mathrm{d} x}_{\boldsymbol{k}^{\mathrm{e}}} \boldsymbol{u}_{\mathrm{p}}. \qquad (3.52)$$

The expression $\delta \boldsymbol{u}_{\mathrm{p}}^{\mathrm{T}}$ can be canceled with an identical expression on the right-hand side of Eq. (3.47) and $\boldsymbol{u}_{\mathrm{p}}$ represents the column matrix of the unknown nodal displacement. Therefore, the stiffness matrix can be calculated due to the derivative of the shape function according to Eq. (3.28) and finally the formulation according to Eq. (3.31) for the element stiffness matrix results.

In the following, the right-hand side of Eq. (3.47) is considered to derive the total load vector for a linear bar element. The first part of the right half is

$$EA \left[W \frac{\mathrm{d} u(x)}{\mathrm{d} x} \right]_0^L \qquad (3.53)$$

with the definition of the weighting function according to Eq. (3.49)

$$EA \left[\left(\boldsymbol{N} \, \delta \boldsymbol{u}_{\mathrm{p}} \right)^{\mathrm{T}} \frac{\mathrm{d} u(x)}{\mathrm{d} x} \right]_0^L = EA \left[\delta \boldsymbol{u}_{\mathrm{p}}^{\mathrm{T}} \boldsymbol{N}^{\mathrm{T}} \frac{\mathrm{d} u(x)}{\mathrm{d} x} \right]_0^L \qquad (3.54)$$

results, or in components

$$\delta u_{\mathrm{p}}^{\mathrm{T}} E A \left[\begin{bmatrix} N_1 \\ N_2 \end{bmatrix} \frac{\mathrm{d}u(x)}{\mathrm{d}x} \right]_0^L . \tag{3.55}$$

The virtual displacements $\delta u_{\mathrm{p}}^{\mathrm{T}}$ in the last equation can be canceled with the corresponding expression in Eq. (3.52). Furthermore, the last equation represents a system of two equations, which have to be evaluated on the boundary of integration at $x = 0$ and $x = L$. The first line results in:

$$\left(N_1 E A \frac{\mathrm{d}u}{\mathrm{d}x} \right)_{x=0} - \left(N_1 E A \frac{\mathrm{d}u}{\mathrm{d}x} \right)_{x=0} . \tag{3.56}$$

Under consideration of the shape functions boundary values, meaning $N_1(L) = 0$ and $N_1(0) = 1$, the following results:

$$-E A \frac{\mathrm{d}u}{\mathrm{d}x} \bigg|_{x=0} \overset{(3.10)}{=} -S(x = 0). \tag{3.57}$$

The value of the second line can be calculated accordingly:

$$E A \frac{\mathrm{d}u}{\mathrm{d}x} \bigg|_{x=0} \overset{(3.10)}{=} S(x = L). \tag{3.58}$$

It must be noted that the forces S represent the internal reactions according to Fig. 3.2, hence the external loads with the positive direction according to Fig. 3.3 result from the internal reactions by reversing the positive direction on the left section and by maintaining the positive direction of the internal reaction on the right section.
The second part of the right-hand side of Eq. (3.47), meaning after canceling of δu^{T}

$$\int_0^L N(x)^{\mathrm{T}} q(x) \mathrm{d}x \tag{3.59}$$

represents the general calculation rule for the definition of the equivalent nodal loads in the case of arbitrarily distributed loads. It should be noted at this point that the evaluation of Eq. (3.59) for a constant distributed load q results in the following load vector:

$$F_q = \frac{qL}{2} \begin{bmatrix} 1 \\ 1 \end{bmatrix} . \tag{3.60}$$

3.3 Sample Problems and Supplementary Problems

3.3.1 Sample Problems

3.1. Tension Bar with Variable Cross-Section

So far the cross-section $A(x)$ was assumed to be constant along the body axis. As an enhancement to that the cross-section needs to be variable. The cross-section $A(x)$ should change linearly along the body axis. The modulus of elasticity is still regarded to be constant. Unknown is the stiffness matrix (Fig. 3.6).
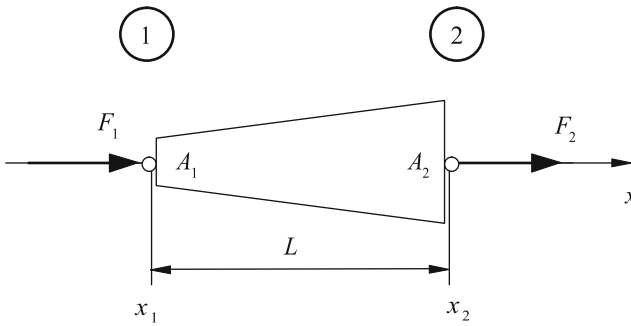
Fig. 3.6 Tension bar with variable cross-section

3.1 Solution

The integral

$$k^{\mathrm{e}} = \int_{\Omega} \boldsymbol{B}^{\mathrm{T}} \boldsymbol{D} \boldsymbol{B} \, \mathrm{d}\Omega \tag{3.61}$$

has to be evaluated to derive the element stiffness matrix. The displacement distribution should be approximated linearly, as in the derivation above. Nothing changes for the shape functions or their derivatives. The following results for matrix $\boldsymbol{B}$

$$\boldsymbol{B} = \frac{1}{L}[-1 \quad 1]. \tag{3.62}$$

In contrast to the prismatic bar with constant cross-section, the area $A(x)$ remains under the integral. The constant modulus of elasticity E in

$$k^{\mathrm{e}} = \int_{L} \frac{1}{L}\begin{bmatrix} 1 \\ -1 \end{bmatrix} E \frac{1}{L}[-1 \quad 1] A(x) \, \mathrm{d}x \tag{3.63}$$

can be drawn in front of the integral. It remains:

$$k^{\text{e}} = \frac{E}{L^2} \begin{bmatrix} 1 & -1 \\ -1 & 1 \end{bmatrix} \int_L A(x)\, \mathrm{d}x. \tag{3.64}$$

The linear course of the cross-section can be described through the following:

$$A(x) = A_1 + \frac{A_2 - A_1}{L}\, x. \tag{3.65}$$

After the execution of the integration

$$\int_L A(x)\, \mathrm{d}x = \int_L \left[A_1 + \frac{A_2 - A_1}{L}\, x \right] \mathrm{d}x = \frac{1}{2}(A_1 + A_2)\, L \tag{3.66}$$

the stiffness matrix

$$k^{\text{e}} = \frac{E}{L}\frac{1}{2}(A_1 + A_2) \begin{bmatrix} 1 & -1 \\ -1 & 1 \end{bmatrix} \tag{3.67}$$

for a tension bar with linear changeable cross-section results.

3.2. Tension Bar Under Dead Weight

Given is a bar with length L with constant cross-section A, constant modulus of elasticity E and constant density ρ along the bar axis. The bar is now loaded through its dead weight (see Fig. 3.7).

Fig. 3.7 Tension bar under dead weight
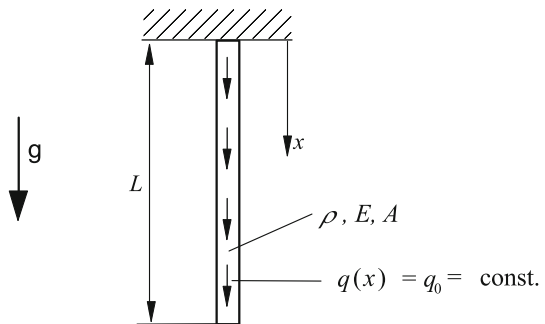
Unknown are:

1. The analytical solution and
2. the finite element solution for a single bar element with linear approximation of the displacement distribution.

3.2 Solution

Analytical Solution for the Tension Bar Under Dead Weight

Equation (3.13) is the basis for the solution. The dead weight force needs to be interpreted as a continuously distributed load $q(x)$, which is constant throughout the length of the bar:

$$q(x) = q_0 = \rho g A. \tag{3.68}$$

Starting from the differential equation of 2nd order

$$EA\frac{d^2 u(x)}{dx^2} = EAu''(x) = -q_0, \tag{3.69}$$

one receives the first derivative of the displacement through a one-time integration

$$EA\frac{du(x)}{dx} = EAu'(x) = -q_0 x + c_1, \tag{3.70}$$

and due to a further integration one receives the function of the displacement:

$$EAu(x) = -\frac{1}{2} q_0 x^2 + c_1 x + c_2. \tag{3.71}$$

The constants of integration c_1 and c_2 are adjusted through the boundary conditions. The displacement is zero at the fixed support and the following applies:

$$u(x = 0) = 0 \Rightarrow c_2 = 0. \tag{3.72}$$

The end of the bar is without force and the following results from Eq. (3.70):

$$EAu'(x = L) = 0 \Rightarrow -q_0 L + c_1 = 0 \Rightarrow c_1 = q_0 L. \tag{3.73}$$

If the constants of integration c_1 and c_2 are inserted with the term for the distributed load, the following results for the displacement field along the bar axis

$$u(x) = \frac{1}{EA}\left[-\frac{1}{2}q_0 x^2 + q_0 L x\right] = \frac{\rho g L^2}{E}\left[-\frac{1}{2}\left(\frac{x}{L}\right)^2 + \left(\frac{x}{L}\right)\right] \tag{3.74}$$

and the strain field

$$\varepsilon(x) = \frac{du(x)}{dx} = \frac{\rho g L}{E}\left[1 - \frac{x}{L}\right] \tag{3.75}$$

and the stress field

$$\sigma(x) = E\varepsilon(x) = \rho g L\left[1 - \frac{x}{L}\right]. \tag{3.76}$$

FE Solution for the Tension Bar Under Dead Weight

The basis for the finite element solution is the stiffness relation

$$\begin{bmatrix} k & -k \\ -k & k \end{bmatrix} \begin{bmatrix} u_1 \\ u_2 \end{bmatrix} = \frac{1}{2} q_0 L \begin{bmatrix} 1 \\ 1 \end{bmatrix} \qquad (3.77)$$

with a linear approximation of the displacement distribution. If the formulations

$$k = \frac{EA}{L}, \quad q_0 = \rho g A \qquad (3.78)$$

are inserted for the stiffness k and the distributed load q_0, the following compact form results

$$\begin{bmatrix} 1 & -1 \\ -1 & 1 \end{bmatrix} \begin{bmatrix} u_1 \\ u_2 \end{bmatrix} = \frac{1}{2} \frac{\rho g L^2}{E} \begin{bmatrix} 1 \\ 1 \end{bmatrix}, \qquad (3.79)$$

from which, the displacement at the lower end of the bar

$$u_2 = \frac{1}{2} \frac{\rho g L^2}{E} \qquad (3.80)$$

can be read off, after introducing the boundary condition ($u_1 = 0$). The displacement at the lower end of the bar matches with the analytical solution. The displacement is linearly distributed on the inside of the bar. The error towards the analytical solution with a quadratic distribution can be minimized or eliminated through the use of more elements or elements with quadratic shape functions.

3.3. Tension Bar Under Dead Weight, Two Elements

Given is the tension bar with length L under dead weight, as in Exercise 3.2. For the determination of the solution on the basis of the FE method, *two* elements with linear shape functions should be used.

3.3 Solution

The basis for the solution is the single stiffness relation for the bar under consideration of a distributed load. One receives the total stiffness relation with two elements through the development of two single stiffness relations.[5] With the formulations for the stiffness k and the distributed load q_0

$$k = \frac{EA}{L}, \quad q_0 = \rho g A \qquad (3.81)$$

---

[5] Here the FE solution is shown in brief. A detailed derivation for the development of a total stiffness matrix, for the introduction of boundary conditions and for the identification of the unknown is introduced in Chap. 7.

a compact form results

$$\frac{EA}{\frac{1}{2}L}\begin{bmatrix} 1 & -1 & 0 \\ -1 & 1+1 & -1 \\ 0 & -1 & 1 \end{bmatrix}\begin{bmatrix} u_1 \\ u_2 \\ u_3 \end{bmatrix} = \frac{1}{2}\rho g A \frac{1}{2}L\begin{bmatrix} 1 \\ 1+1 \\ 1 \end{bmatrix}. \tag{3.82}$$

The first line and column can be eliminated due to the boundary conditions ($u_1 = 0$). It remains a system of equations with two unknowns

$$\begin{bmatrix} 2 & -1 \\ -1 & 1 \end{bmatrix}\begin{bmatrix} u_2 \\ u_3 \end{bmatrix} = \frac{1}{8}\frac{\rho g L^2}{E}\begin{bmatrix} 2 \\ 1 \end{bmatrix}, \tag{3.83}$$

after a short transformation

$$\begin{bmatrix} 2 & -1 \\ 0 & 1 \end{bmatrix}\begin{bmatrix} u_2 \\ u_3 \end{bmatrix} = \frac{1}{8}\frac{\rho g L^2}{E}\begin{bmatrix} 2 \\ 4 \end{bmatrix} \tag{3.84}$$

the displacement at the end node

$$u_3 = \frac{1}{2}\frac{\rho g L^2}{E} \tag{3.85}$$

and through insertion into Eq. (3.84) the displacement at the mid-node

$$u_2 = \frac{1}{2}\left[\frac{1}{2}+\frac{1}{8}\right]\frac{\rho g L^2}{E} = \frac{3}{8}\frac{\rho g L^2}{E} \tag{3.86}$$

can be identified.

3.3.2 Supplementary Problems

3.4. Tension Bar with Quadratic Approximation

Given is a prismatic tension bar with length L, with constant cross-section AL, and modulus of elasticity E. In contrast to the derivation above, the displacement distribution on the inside of the bar element needs to be approximated through a quadratic shape function. Unknown is the stiffness matrix.

3.5. Tension Bar with variable Cross-Section and Quadratic Approximation

The cross-section $A(x)$ changes linearly along the body axis. The modulus of elasticity is constant further on. The displacement distribution on the inside of the bar element needs to be approximated through quadratic shape functions.

References

1. Betten J (2001) Kontinuumsmechanik: Elastisches und inelastisches Verhalten isotroper und anisotroper Stoffe. Springer-Verlag, Berlin
2. Betten J (2004) Finite Elemente für Ingenieure 1: Grundlagen. Matrixmethoden, Elastisches Kontinuum, Springer-Verlag, Berlin
3. Betten J (2004) Finite Elemente für Ingenieure 2: Variationsrechnung, Energiemethoden, Näherungsverfahren. Nichtlinearitäten, Numerische Integrationen, Springer-Verlag, Berlin
4. Gross D, Hauger W, Schröder J, Wall WA (2009) Technische Mechanik 2: Elastostatik. Springer-Verlag, Berlin
5. Gross D, Hauger W, Schröder J, Werner EA (2008) Hydromechanik. Elemente der Höheren Mechanik, Numerische Methoden, Springer-Verlag, Berlin
6. Klein B (2000) FEM. Grundlagen und Anwendungen der Finite-Elemente-Methode, Vieweg-Verlag, Wiesbaden
7. Kwon YW, Bang H (2000) The Finite Element Method Using MATLAB. CRC Press, Boca Raton
8. Oden JT, Reddy JN (1976) Variational methods in theoretical mechanics. Springer-Verlag, Berlin
9. Steinbuch R (1998) Finite Elemente - Ein Einstieg. Springer-Verlag, Berlin

Chapter 4
Torsion Bar

Abstract The basic load type torsion for a prismatic bar is described with the help of a torsion bar. First, the basic equations known from the strength of materials will be introduced. Subsequently, the torsion bar will be introduced, according to the common definitions for the torque and angle variables, which are used in the handling of the FE method. The explanations are limited to torsion bars with circular cross-section. The stiffness matrix will be derived according to the procedure for the tension bar [1–6].

4.1 Basic Description of the Torsion Bar

In the simplest case, the torsion bar can be defined as a prismatic body with constant circular cross-section (outside radius R) and constant shear modulus G, which is loaded with a torsional moment M in the direction of the body axis. Figure 4.1a illustrates the torsion bar with applied load and Fig. 4.1b shows the free body diagram.
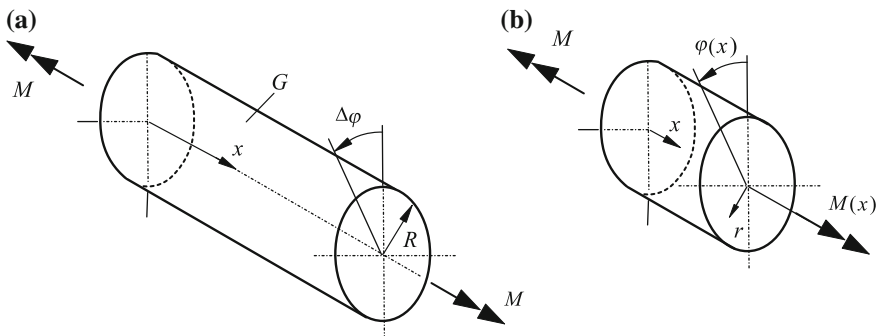
Fig. 4.1 Torsion bar **a** with applied load and **b** free body diagram

The unknown quantities are

- the rotation $\Delta\varphi$ of the end cross-sections,
- the rotation $\varphi(x)$, the shear strain $\gamma(x)$ and the shear stress $\tau(x)$ on a cross-section on the inside of the bar in dependence of the external load.

The following three basic equations are known from strength of materials. The interrelationships of the kinematic state variables are shown in Fig. 4.2 under consideration of a cylindrical coordinate system (x, r, φ).[1]

Fig. 4.2 Torsion bar with state variables
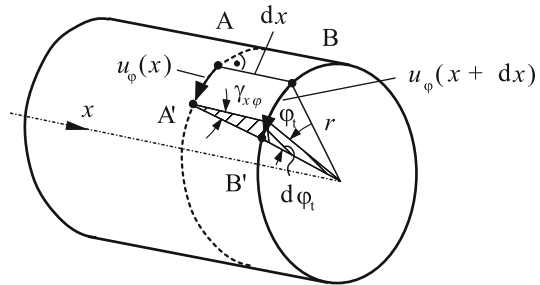
Kinematics describes the relation between the shear strain and the change of angle:

$$\gamma(x) = \frac{\mathrm{d}u_\varphi}{\mathrm{d}x} = r\,\frac{\mathrm{d}\varphi(x)}{\mathrm{d}x}\,. \tag{4.1}$$

The constitutive equation describes the relation between the shear stress and the shear strain with

$$\tau(x) = G\gamma(x)\,. \tag{4.2}$$

The internal moment $M(x)$ is calculated through

$$M(x) = \int_A r\,\tau(x)\mathrm{d}A\,, \tag{4.3}$$

and with the kinematic relation from Eq. (4.1) and the constitutive equation from Eq. (4.2) the following results

$$M(x) = G\frac{\mathrm{d}\varphi}{\mathrm{d}x}\int_A r^2\mathrm{d}A = GI_\mathrm{p}\frac{\mathrm{d}\varphi}{\mathrm{d}x}\,. \tag{4.4}$$

Hereby the elastic behavior regarding the torsion can be described through

---

[1] Besides the shear strain $\gamma_{x\varphi}(r, x)$ and the deformation $u_\varphi(x, r)$ no further deformation parameters occur during the torsion of circular cross-sections. For clarity reasons the indexing for clear dimensions is omitted.

$$\frac{\mathrm{d}\varphi(x)}{\mathrm{d}x} = \frac{M(x)}{G\,I_\mathrm{p}}.$$

(4.5)

On the basis of this equation the interrelation between the rotation $\Delta\varphi$ of the two end cross-sections and the torsional moment M can be described easily:

$$\Delta\varphi = \frac{M}{G\,I_\mathrm{p}}\,L\,.$$

(4.6)

The expression GI_p is called the torsional stiffness. The stiffness for the torsion bar results from the relation between the moment and the rotation of the end cross-section:

$$\frac{M}{\Delta\varphi} = \frac{G\,I_\mathrm{p}}{L}\,.$$

(4.7)

For the derivation of the differential equation the equilibrium at the infinitesimal small torsion bar element has to be regarded (see Fig. 4.3). A continuously distributed load $m_\mathrm{t}(x)$ in the unit moment per unit length serves as the load.
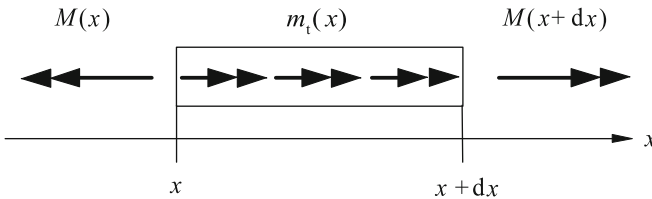
Fig. 4.3 Equilibrium at the infinitesimal small torsion bar element

The moment equilibrium in the direction of the body axis provides the following:

$$-M(x) + m_\mathrm{t}(x)\mathrm{d}x + M(x + \mathrm{d}x) = 0\,.$$

(4.8)

After a series expansion of $M(x + dx) = M(x) + \mathrm{d}M(x)$ the following results

$$-M(x) + m_\mathrm{t}(x)\mathrm{d}x + M(x) + \mathrm{d}M(x) = 0$$

(4.9)

or in short:

$$\frac{\mathrm{d}M(x)}{\mathrm{d}x} + m_\mathrm{t}(x) = 0.$$

(4.10)

Equations (4.1), (4.2) and (4.3) for kinematics, the constitutive equation and the equilibrium furthermore apply. If Eqs. (4.1) and (4.2) are inserted in (4.3), one receives

$$GI_\mathrm{p}(x)\,\frac{\mathrm{d}\varphi(x)}{\mathrm{d}x} = M(x)\,.$$

(4.11)

After differentiating and inserting of Eq. (4.10) one obtains

$$\frac{\mathrm{d}}{\mathrm{d}x}\left[GI_{\mathrm{p}}(x)\,\frac{\mathrm{d}\varphi(x)}{\mathrm{d}x}\right] + m_{\mathrm{t}}(x) = 0 \qquad (4.12)$$

as the differential equation for a torsion bar with continuously distributed load. This is a differential equation of 2nd order in the rotations. At constant torsional rigidity GI_{p} the term simplifies to

$$GI_{\mathrm{p}}\,\frac{\mathrm{d}^2\varphi(x)}{\mathrm{d}x^2} + m_{\mathrm{t}}(x) = 0\,. \qquad (4.13)$$

4.2 The Finite Element Torsion Bar

The handling of the torsion bar occurs analogous to the handling of the tension bar. The procedure is identical. The vectors and matrices, occurring within the frame of the FE method are similar.

The torsion bar is defined as a prismatic body with constant circular cross-section (outside radius R) along the body axis. Nodes are introduced at both ends of the torsion bar, at which moments and angles, as drafted in Fig. 4.4 are positively defined. It is the objective to achieve a stiffness relation in the form

$$\boldsymbol{T}^{\mathrm{e}} = \boldsymbol{k}^{\mathrm{e}}\,\boldsymbol{\varphi}_{\mathrm{p}} \qquad (4.14)$$

Fig. 4.4 Definition for the finite element torsion bar
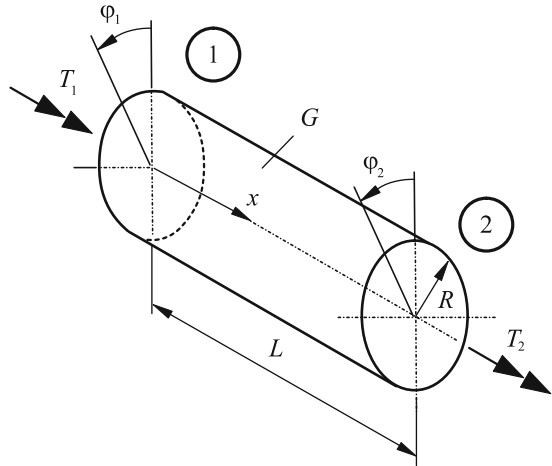
or

$$\begin{bmatrix} T_1 \\ T_2 \end{bmatrix} = \begin{bmatrix} \cdot & \cdot \\ \cdot & \cdot \end{bmatrix} \begin{bmatrix} \varphi_1 \\ \varphi_2 \end{bmatrix} \tag{4.15}$$

for this element. The torsion bar element can be integrated in a structure through this stiffness relation.

First, an easy approach will be introduced, at which the torsion bar is modeled as a linear torsion spring (Fig. 4.5).

Fig. 4.5 Torsion bar modeled as a linear torsion spring
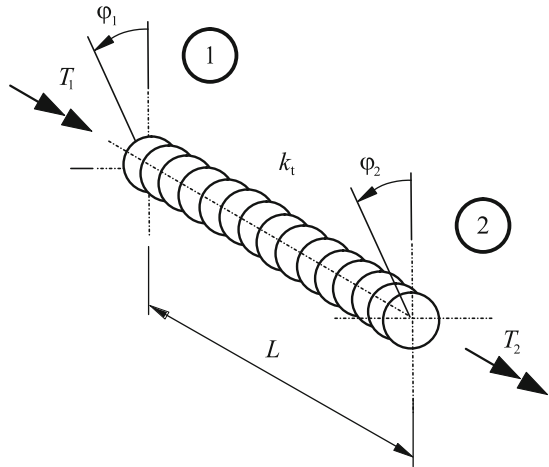
This is possible, when the torsional rigidity GI_p is constant along the body axis. The previously derived stiffness of the torsion bar can then be interpreted with

$$\frac{G\,I_p}{L} = k_t \tag{4.16}$$

as spring constant or spring stiffness of a linear torsion spring. To avoid confusion with the stiffness of the tension bar, the torsional rigidity is exposed with the index 't'.

For the derivation of the stiffness relation, which is requested for the finite element method, a thought experiment is conducted. If, within the spring model at first only the torsional moment T_2 is in effect and the moment T_1 is faded out, the equation

$$T_2 = k_t \Delta \varphi = k_t (\varphi_2 - \varphi_1) \tag{4.17}$$

then describes the relation between the spring moment and the torsion angle of the end cross-sections. If subsequently only the torsional moment T_1 is in effect and the moment T_2 is faded out, the equation

$$T_1 = k_t \Delta \varphi = k_t (\varphi_1 - \varphi_2) \tag{4.18}$$

then describes the relation between the spring moment and the torsion angle of the end cross-sections. Both situations can be superimposed and summarized compactly in matrix form as

$$\begin{bmatrix} T_1 \\ T_2 \end{bmatrix}^{\mathrm{e}} = \begin{bmatrix} k_{\mathrm{t}} & -k_{\mathrm{t}} \\ -k_{\mathrm{t}} & k_{\mathrm{t}} \end{bmatrix} \begin{bmatrix} \varphi_1 \\ \varphi_2 \end{bmatrix}. \tag{4.19}$$

With that the desired stiffness relation between the torsional moments and the rotations on the nodal points is derived.

The element stiffness matrix for the finite element torsion bar is called

$$\boldsymbol{k}^e = k_{\mathrm{t}} \begin{bmatrix} 1 & -1 \\ -1 & 1 \end{bmatrix} = \frac{GI_{\mathrm{p}}}{L} \begin{bmatrix} 1 & -1 \\ -1 & 1 \end{bmatrix} \tag{4.20}$$

and is similar to the stiffness matrix of the tension bar.

The field variables on the inside of the elements are approximated through the nodal values and shape functions. The derivation of this description as well as the derivation of the stiffness relation through other ways are omitted. The proceeding is identical to that for the tension bar.

References

1. Betten J (2004) Finite Elemente für Ingenieure 1: Grundlagen. Matrixmethoden, Elastisches Kontinuum, Springer-Verlag, Berlin
2. Betten J (2004) Finite Elemente für Ingenieure 2: Variationsrechnung, Energiemethoden, Näherungsverfahren. Nichtlinearitäten, Numerische Integrationen, Springer-Verlag, Berlin
3. Gross D, Hauger W, Schröder J, Wall WA (2009) Technische Mechanik 2: Elastostatik. Springer-Verlag, Berlin
4. Gross D, Hauger W, Schröder J, Werner EA (2008) Hydromechanik. Elemente der Höheren Mechanik, Numerische Methoden, Springer-Verlag, Berlin
5. Klein B (2000) FEM. Grundlagen und Anwendungen der Finite-Elemente-Methode, Vieweg-Verlag, Wiesbaden
6. Kuhn G, Winter W (1993) Skriptum Festigkeitslehre Universität Erlangen-Nürnberg.

Chapter 5
Bending Element

Abstract By this element the basic deformation bending will be described. First, several elementary assumptions for modeling will be introduced and the element used in this chapter will be outlined towards other formulations. The basic equations from the strength of materials, meaning kinematics, equilibrium and constitutive equation will be introduced and used for the derivation of the differential equation of the bending line. Analytical solutions will conclude the section of the basic principles. Subsequently, the bending element will be introduced, according to the common definitions for load and deformation parameters, which are used in the handling of the FE method. The derivation of the stiffness matrix is carried out through various methods and will be described in detail. Besides the simple, prismatic bar with constant cross-section and load on the nodes also variable cross-sections, generalized loads between the nodes and orientation in the plane and the space will be analyzed.

5.1 Introductory Remarks

In the following, a prismatic body will be examined, at which the load occurs perpendicular to the center line and therefore bends. Perpendicular to the center line means that either the line of action of a force or the direction of a momental vector are oriented orthogonally to the center line of the element. Consequently a different type of deformation can be modeled with this prismatic body compared to a bar (see Chaps. 3 and 4), see Table 5.1. A general element, which includes all these deformation mechanisms will be introduced in Chap. 6.

Table 5.1 Differentiation between bar and beam element; center line parallel to the x-axis

	Bar	Beam
Force	Along the bar axis	Perpendicular to the beam axis
Unknown	Displacement in or rotation around bar axis	Displacement perpendicular to and rotation perpendicular to the beam axis

Generally in beam statics one distinguishes between shear rigid and shear flexible models. The classic, shear rigid beam, also called BERNOULLI beam, disregards the shear deformation from the shear force. With this modeling one assumes that a cross-section, which was at the right angle to the beam axis before the deformation is also at right angles to the beam axis after the deformation, see Fig. 5.1a. Furthermore it is assumed that a plane cross-section stays plane and unwarped. These two assumptions are also called the BERNOULLI's hypothesis. Altogether one imagines the cross-sections fixed on the center line of the beam,[1] so that a change of the center line affects the entire deformation. Consequently, it is also assumed that the geometric dimensions of the cross-sections[2] do not change. Regarding a shear flexible beam, also referred to as TIMOSHENKO beam besides the bending deformation also the shear deformation is considered, and the cross-sections will be distorted by an angle γ compared to the perpendicular position, see Fig. 5.1b. In general the shear part for beams, which length is 10–20 times bigger than a characteristic dimension of the cross-section[3] is disregarded in the first approximation.

(a)   **(b)**

$\gamma = 0°$ $\gamma \neq 0°$
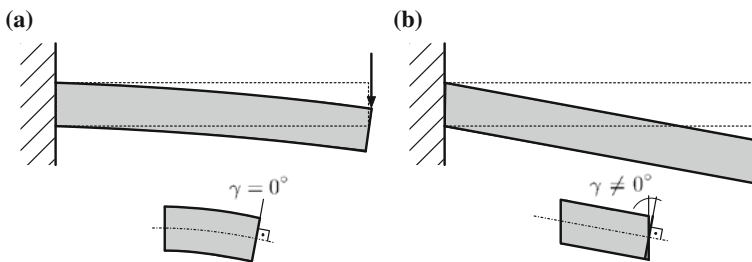
Fig. 5.1 Different deformation of a bending beam: **a** shear rigid and **b** shear flexible. Adapted from [1]

The different load types, meaning pure bending moment or shear as a consequence of shear force, lead to different stress fractions within a bending beam. For a BERNOULLI beam solely loading occurs through normal forces, which rise linearly over the cross-section. Hence, a tension—alternatively compression maximum on the upper—alternatively lower side of the beam occurs, see Fig. 5.2a.

(a)   **(b)**

$+\sigma_x$ τ_{xy}

$-\sigma_x$
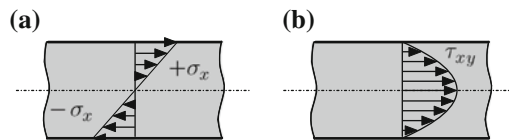
Fig. 5.2 Different stress distribution at the bending beam using the example of a rectangular cross-section for linear-elastic material behavior: **a** normal stress (shear rigid); **b** shear stress (shear flexible)

---

[1] More precisely this is the neutral fiber or the bending line.

[2] Consequently the width b and the height h of a, for example, rectangular cross-section remain the same.

[3] For this see the explanations in Chap. 8.

At symmetric cross-sections the zero crossing[4] occurs in the middle of the cross-section. The shear stress exhibits, for example, with a rectangular cross-section a parabolic course and features zero at the beam boundaries.

Finally, it needs to be noted that the one-dimensional beam theory has a counterpart in the two-dimensional, see Table 5.2. In plate theories the BERNOULLI beam is equal to the shear rigid KIRCHHOFF plate and the TIMOSHENKO beam is equal to the shear flexible REISSNER–MINDLIN plate, [2–4].

Table 5.2 Analogy within the beam and plate theory

	Beam theory	Plate theory
Dimensionality	1D	2D
Shear rigid	BERNOULLI beam	KIRCHHOFF plate
Shear flexible	TIMOSHENKO beam	REISSNER–MINDLIN plate

Further details regarding the beam theory and the corresponding basic definitions and assumptions can be found in Refs. [5–8]. In the following part of the chapter solely the BERNOULLI beam is considered. The consideration of the shear part takes place in Chap. 8.

5.2 Basic Description of the Beam

5.2.1 Kinematics

For the derivation of the kinematic relation a beam with length L under constant moment loading $M_z(x) = $ constant, meaning under *pure* bending, is considered, see Fig. 5.3. One can see that both external single moments at the left and right beam border lead to a positive bending moment distribution M_z within the beam. The vertical position of a point in matters of the center line of the beam *without action* of an external load is described through the y-coordinate. The vertical *displacement* of a point on the center line of the beam, meaning for a point with $y = 0$, under action of the external load is indicated with u_y. The deformed center line is represented by the sum of these points with $y = 0$ and is referred to as the bending line $u_y(x)$.

In the following, the center line of the deformed beam is considered. Through the relation for an arbitrary point (x, u_y) on a circle with radius R around the central point (x_0, y_0), meaning

$$(x - x_0)^2 + (u_y(x) - y_0)^2 = R^2 \,, \tag{5.1}$$

---

[4] The sum of all points with $\sigma = 0$ along the beam axis is called neutral fiber.

(a)

(b)
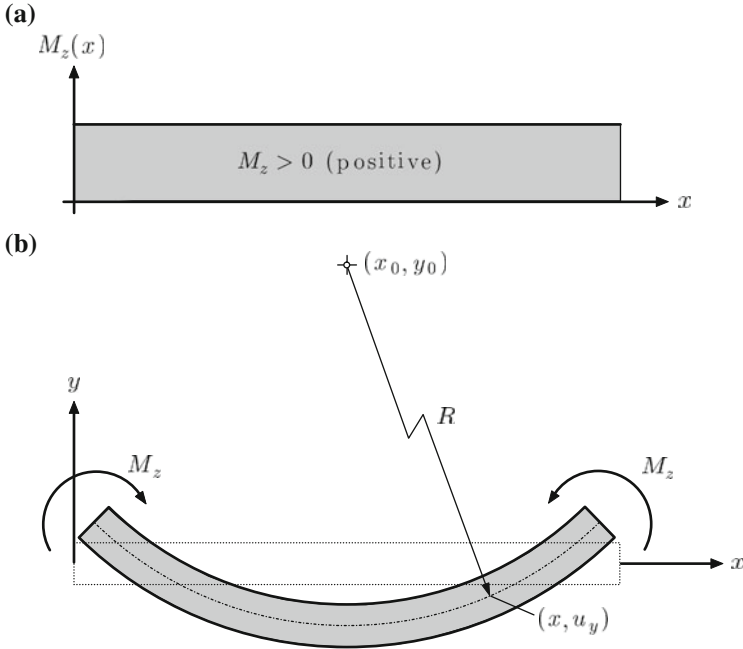
Fig. 5.3 Bending beam under pure bending: **a** moment distribution; **b** deformed beam. Note that the deformation is an overdrawn illustration. For the deformations considered in this chapter the following applies: $R \gg L$

through differentiation regarding the x-coordinate, one obtains

$$2(x - x_0) + 2(u_y(x) - y_0)\frac{\mathrm{d}u_y}{\mathrm{d}x} = 0 \tag{5.2}$$

alternatively after another differentiation:

$$2 + 2\frac{\mathrm{d}u_y}{\mathrm{d}x}\frac{\mathrm{d}u_y}{\mathrm{d}x} + 2(u_y(x) - y_0)\frac{\mathrm{d}^2 u_y}{\mathrm{d}x^2} . \tag{5.3}$$

Equation (5.3) provides the vertical distance of the regarded point on the center line of the beam in matters of the center of a circle to

$$(u_y - y_0) = -\frac{1 + \left(\frac{\mathrm{d}u_y}{\mathrm{d}x}\right)^2}{\frac{\mathrm{d}^2 u_y}{\mathrm{d}x^2}} , \tag{5.4}$$

while the difference of the x-coordinate from Eq. (5.2) results:

$$(x - x_0) = -(u_y - y_0)\frac{\mathrm{d}u_y}{\mathrm{d}x}. \tag{5.5}$$

If the expression according to Eq. (5.4) is used in (5.5) the following results:

$$(x - x_0) = \frac{\mathrm{d}u_y}{\mathrm{d}x} \frac{1 + \left(\frac{\mathrm{d}u_y}{\mathrm{d}x}\right)^2}{\frac{\mathrm{d}^2 u_y}{\mathrm{d}x^2}}. \tag{5.6}$$

Inserting both expressions for the coordinate difference according to Eqs. (5.6) and (5.4) in the circle relation according to (5.1) leads to:

$$R^2 = (x - x_0)^2 + (u_y - y_0)^2 \tag{5.7}$$

$$= \left(\frac{\mathrm{d}u_y}{\mathrm{d}x}\right)^2 \frac{\left(1 + \left(\frac{\mathrm{d}u_y}{\mathrm{d}x}\right)^2\right)^2}{\left(\frac{\mathrm{d}^2 u_y}{\mathrm{d}x^2}\right)^2} + \frac{\left(1 + \left(\frac{\mathrm{d}u_y}{\mathrm{d}x}\right)^2\right)^2}{\left(\frac{\mathrm{d}^2 u_y}{\mathrm{d}x^2}\right)^2}$$

$$= \left(\left(\frac{\mathrm{d}^2 u_y}{\mathrm{d}x^2}\right)^2 + 1\right) \frac{\left(1 + \left(\frac{\mathrm{d}u_y}{\mathrm{d}x}\right)^2\right)^2}{\left(\frac{\mathrm{d}^2 u_y}{\mathrm{d}x^2}\right)^2}$$

$$= \frac{\left(1 + \left(\frac{\mathrm{d}u_y}{\mathrm{d}x}\right)^2\right)^3}{\left(\frac{\mathrm{d}^2 u_y}{\mathrm{d}x^2}\right)^2}. \tag{5.8}$$

Since the circle configuration, shown in Fig. 5.3 is a 'left-handed curve' $\left(\frac{\mathrm{d}u_y^2}{\mathrm{d}x^2} > 0\right)$, the radius of curvature R results in:

$$R = \frac{+}{(-)} \frac{\left(1 + \left(\frac{\mathrm{d}u_y}{\mathrm{d}x}\right)^2\right)^{3/2}}{\left(\frac{\mathrm{d}^2 u_y}{\mathrm{d}x^2}\right)}. \tag{5.9}$$

Note that the expression curvature, which results as a reciprocal value from the curvature radius, $\kappa = \frac{1}{R}$, is used here as well.

For small bending deflections, meaning $u_y \ll L$, $\frac{\mathrm{d}u_y}{\mathrm{d}x} \ll 1$ results and Eq. (5.9) simplifies to:

$$R = \frac{1}{\frac{\mathrm{d}^2 u_y}{\mathrm{d}x^2}} \quad \text{or} \quad \kappa = \frac{\mathrm{d}^2 u_y}{\mathrm{d}x^2}. \tag{5.10}$$

For the determination of the strain one goes back to the general definitions, meaning extension referred to initial length. With the expression from Fig. 5.4 the longitudinal extension for a fibre with the distance y to the neutral fibre results in:

$$\varepsilon_x = \frac{\mathrm{d}s - \mathrm{d}x}{\mathrm{d}x} . \tag{5.11}$$

Fig. 5.4 Segment of a bending beam under pure bending. Note that the deformation is overdrawn for better illustration
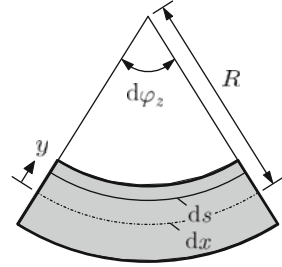
The lengths of the circular arcs $\mathrm{d}s$ and $\mathrm{d}x$ result from the corresponding radii and the central angle in the radian measure for both sectors to:

$$\mathrm{d}x = R\mathrm{d}\varphi_z , \tag{5.12}$$
$$\mathrm{d}s = (R - y)\mathrm{d}\varphi_z . \tag{5.13}$$

If these relations are used for the circular arcs in Eq. (5.11), the following results:

$$\varepsilon_x = \frac{(R - y)\mathrm{d}\varphi_z - R\mathrm{d}\varphi_z}{\mathrm{d}x} = -y\frac{\mathrm{d}\varphi_z}{\mathrm{d}x} . \tag{5.14}$$

From Eq. (5.12) $\frac{\mathrm{d}\varphi_z}{\mathrm{d}x} = \frac{1}{R}$ results and together with relation (5.10) the strain can finally be expressed as follows:

$$\varepsilon_x = -y\frac{\mathrm{d}^2 u_y(x)}{\mathrm{d}x^2} . \tag{5.15}$$

An alternative derivation of the kinematic relation results from consideration of Fig. 5.5.
From the relation for the rectangular triangle $0'1'2'$, meaning $\sin\varphi_z = \frac{u_x}{-y}$, the following[5] results for small angles ($\sin\varphi_z \approx \varphi_z$):

$$u_x = -y\varphi_z . \tag{5.16}$$

---

[5] Note that according to the precondition regarding the BERNOULLI beam the length 01 and $0'1'$ remain unchanged.
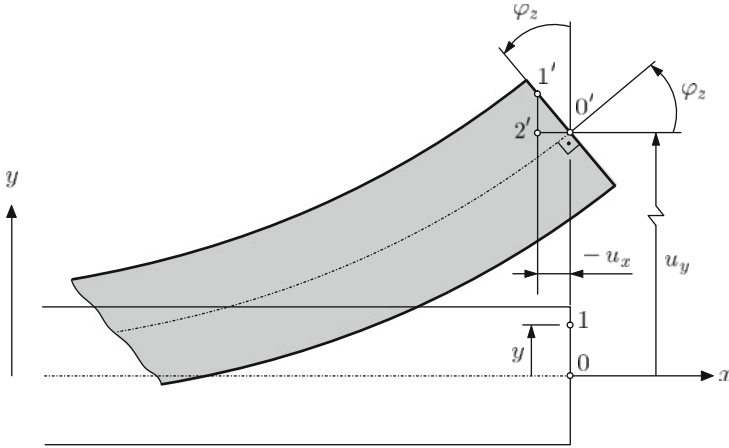
Fig. 5.5 Alternative consideration for the derivation of the kinematic relation. Note that the deformation is overdrawn for better illustration

Furthermore, it continues to apply that the rotation angle of the slope equals the center line for small angles:

$$\tan \varphi_z = \frac{\mathrm{d}u_y(x)}{\mathrm{d}x} \approx \varphi_z \,. \tag{5.17}$$

The definition of the positive and negative rotation angle is illustrated in Fig. 5.6. If Eqs. (5.17) and (5.16) are summarized, the following results
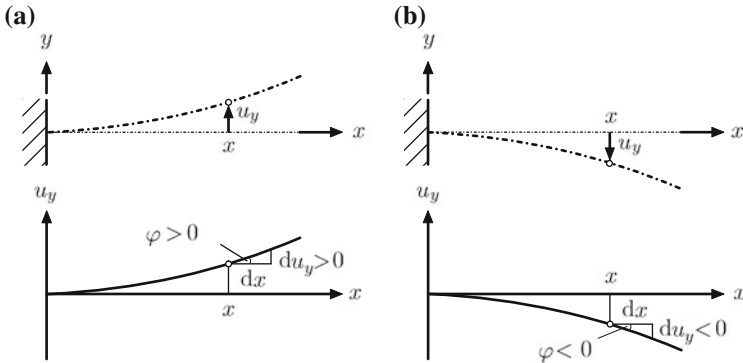
Fig. 5.6 For the definition of the rotation angle: **a** $\varphi_z = \frac{\mathrm{d}u_y}{\mathrm{d}x}$ positive; **b** $\varphi_z = \frac{\mathrm{d}u_y}{\mathrm{d}x}$ negative

$$u_x = -y\frac{\mathrm{d}u_y(x)}{\mathrm{d}x} \,. \tag{5.18}$$

The last relation equals $(\mathrm{d}s - \mathrm{d}x)$ in Eq. (5.11) and differentiation with respect to the x-coordinate leads directly to Eq. (5.15).

5.2.2 Equilibrium

The equilibrium conditions are derived from an infinitesimal beam element with the length dx, which is loaded by a constant distributed load q_y, see Fig. 5.7. The internal reactions are marked at both cutting surfaces, meaning the location x and $x + dx$. One can see that the shear force in the direction of the positive y-axis at the positive[6] cutting surface is positive and that the positive bending moment features the same rotational direction as the positive z-axis (right-hand grip rule[7]). The positive orientation of the shear force and the bending moment are reversed at the negative cutting surface to neutralize the effect of these internal reactions in sum. This convention for the direction of the internal reactions is maintained in the following. Furthermore from Fig. 5.7 it can be derived that an upwards directed *external* force or alternatively a, in a mathematically sense positively rotating *external* moment on the right-hand boundary of a beam lead to a positive shear force or alternatively a positive internal moment. Accordingly it results that on the left-hand boundary of a beam a downwards directed *external* force or alternatively a, in a mathematically sense negatively rotating *external* moment, leads to a positive shear force or alternatively positive internal moment.
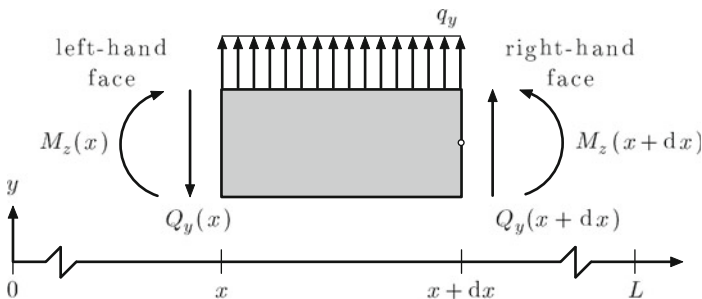
Fig. 5.7 Infinitesimal beam element with internal reactions and load through constant distributed load at deformation in the $x-y$ plane

In the following, the equilibrium will be observed regarding the vertical forces. Assuming that forces in the direction of the positive y-axis are applied positively, the following results:

$$- Q(x) + Q(x + dx) + q_y dx = 0 . \tag{5.19}$$

---

[6] The *positive* cutting surface is defined by the surface normal on the cutting plane which features the same orientation as the positive x-axis. It should be regarded that the surface normal is always directed outwardly. Regarding the *negative* cutting surface the surface normal and the positive x-axis are oriented antiparallel.

[7] If the axis is grasped with the right-hand in a way so that the spread out thumb points in the direction of the positive axis, the bent fingers then show the direction of the positive rotational direction.

If the shear force on the right-hand face is expanded in a TAYLOR's series of first order, meaning

$$Q(x + \mathrm{d}x) \approx Q(x) + \frac{\mathrm{d}Q(x)}{\mathrm{d}x}\,\mathrm{d}x\,, \tag{5.20}$$

Eq. (5.19) results in

$$- Q(x) + Q(x) + \frac{\mathrm{d}Q(x)}{\mathrm{d}x}\,\mathrm{d}x + q_y\mathrm{d}x = 0\,, \tag{5.21}$$

or alternatively after simplification finally to:

$$\frac{\mathrm{d}Q(x)}{\mathrm{d}x} = -q_y\,. \tag{5.22}$$

For the special case that no distributed load occurs ($q_y = 0$), Eq. (5.22) simplifies to:

$$\frac{\mathrm{d}Q(x)}{\mathrm{d}x} = 0\,. \tag{5.23}$$

The equilibrium of moments around the point of reference at $x + \mathrm{d}x$ delivers:

$$M_z(x + \mathrm{d}x) - M_z(x) + Q_y(x)\mathrm{d}x - \frac{1}{2}\,q_y\mathrm{d}x^2 = 0\,. \tag{5.24}$$

If the bending moment on the right-hand face is expanded into a TAYLOR's series of first order according to Eq. (5.20) and consideration that the term $\frac{1}{2}\,q_y\mathrm{d}x^2$ as infinitesimal small size of higher order can be disregarded, finally the following results:

$$\frac{\mathrm{d}M_z(x)}{\mathrm{d}x} = -Q_y(x)\,. \tag{5.25}$$

The combination of Eqs. (5.22) and (5.26) leads to the relation between bending moment and distributed load to:

$$\frac{\mathrm{d}^2 M_z(x)}{\mathrm{d}x^2} = -\frac{\mathrm{d}Q_y(x)}{\mathrm{d}x} = q_y\,. \tag{5.26}$$

5.2.3 Constitutive Equation

The one-dimensional HOOKE's law according to Eq. (3.2) can also be used in the case of the bending beam, since according to the requirements only normal stress is regarded in this chapter:

$$\sigma_x = E\varepsilon_x\,. \tag{5.27}$$

Through the kinematic relation according to Eq. (5.15) stress results as a function of deflection to:

$$\sigma_x(x, y) = -Ey\frac{d^2u_y(x)}{dx^2} .$$ (5.28)
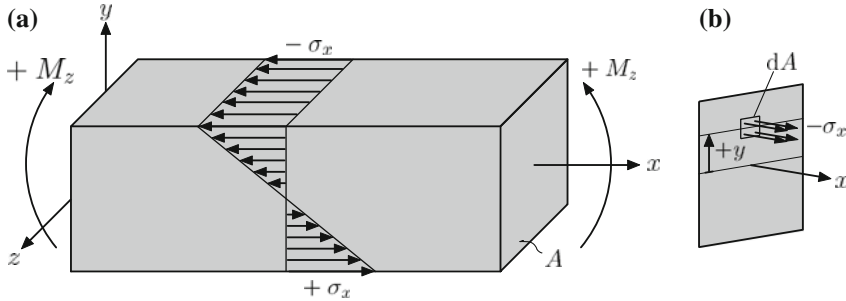
Fig. 5.8 **a** Schematic representation of the normal stress distribution $\sigma_x = \sigma_x(y)$ of a bending beam; **b** definition and position of an infinitesimal surface element for the derivation of the resulting effect of moments of the normal stress distribution

In Fig. 5.8a the shown stress distribution generates the internal moment, which acts at this point. To calculate the effect of the moment, the stress is multiplied with a surface, so that the resulting force is obtained. Multiplication with the corresponding lever arm then delivers the internal moment. Since this is a matter of a changeable stress the consideration takes place on an infinitesimal small surface element:

$$dM_z = (+y)(-\sigma_x)dA = -y\sigma_x dA .$$ (5.29)

Therefore, the entire moment results via integration over the entire surface in:
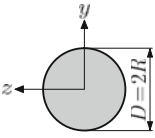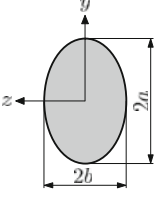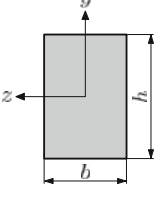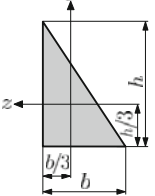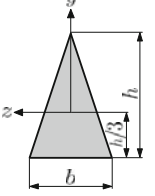
$$M_z = -\int_A y\sigma_x dA \overset{(5.28)}{=} +\int_A yEy\frac{d^2u_y}{dx^2} dA .$$ (5.30)

Assuming that the modulus of elasticity is constant and under the consideration of Eq. (5.10) the internal moment around the z-axis results in:

$$M_z = E\frac{d^2u_y}{dx^2} \underbrace{\int_A y^2 dA}_{I_z} .$$ (5.31)

The integral in Eq. (5.31) is the so-called axial second moment of area or axial surface moment of 2nd order in the SI unit m^4. This factor is only dependent on the geometry of the cross-section and is also a measure for the stiffness of a plane cross-section

Table 5.3 Axial second moment of area around the z- and y-axis

Cross-section	I_z	I_y
	$\dfrac{\pi D^4}{64} = \dfrac{\pi R^4}{4}$	$\dfrac{\pi D^4}{64} = \dfrac{\pi R^4}{4}$
	$\dfrac{\pi ba^3}{4}$	$\dfrac{\pi ab^3}{4}$
	$\dfrac{bh^3}{12}$	$\dfrac{hb^3}{12}$
	$\dfrac{bh^3}{36}$	$\dfrac{hb^3}{36}$
	$\dfrac{bh^3}{36}$	$\dfrac{ah^3}{48}$

against bending. The values of the axial second moment of area for simple geometric cross-sections are collected in Table 5.3.

Consequently, the internal moment can also be shown as

$$M_z = EI_z \frac{d^2 u_y}{dx^2} \stackrel{(5.10)}{=} \frac{EI_z}{R} = EI_z \kappa. \tag{5.32}$$

Equation (5.32) describes the bending line $u_y(x)$ as a function of the bending moment and is therefore also referred to as the bending line–moment relation. The product EI_z in Eq. (5.32) is also called the bending stiffness. If the result from Eq. (5.32) is

used in the relation for the bending stress according to Eq. (5.28), the distribution of stress across the cross-section results in:

$$\sigma_x(y) = -\frac{M_z}{I_z}\, y\,.\tag{5.33}$$

The minus sign causes, that after the introduced sign convention for deformations in the $x-y$ plane, a positive bending moment (see Fig. 5.3) in the upper beam half, meaning for $y > 0$, leads to a compressive stress. The corresponding equations for a deformation in the $x-z$ plane are collected at the end of Sect. 5.2.5.
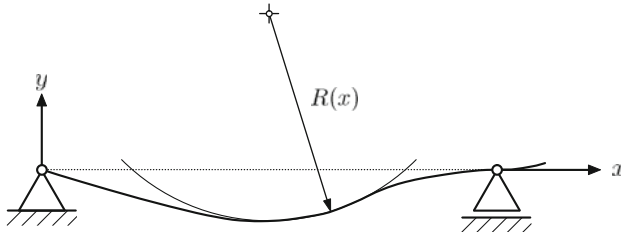
Fig. 5.9 Deformation of a bending beam at plane bending, meaning for $M_z(x) \neq$ const

In the case of plane bending with $M_z(x) \neq$ const. the bending line can be approached in each case locally through a circle of curvature, see Fig. 5.9. Therefore the result of the pure bending according to Eq. (5.32) can be transferred on the result of the plane bending:

$$E I_z \frac{d^2 u_y(x)}{dx^2} = M_z(x)\,.\tag{5.34}$$

Finally, the three elementary basic equations for the bending beam for arbitrary moment loading $M_z(x)$ at bending in the $x-y$ plane are summarized in Table 5.4.

Table 5.4 Elementary basic equations for the bending beam at deformation in the $x-y$ plane

Relation	Equation
Kinematics	$\varepsilon_x(x, y) = -y\frac{d^2 u_y(x)}{dx^2}$
Equilibrium	$\frac{dQ_y(x)}{dx} = -q_y(x);\ \frac{dM_z(x)}{dx} = -Q_y(x)$
Constitutive equation	$\sigma_x(x, y) = E\varepsilon_x(x, y)$
Stress	$\sigma_x(x, y) = -\frac{M_z(x)}{I_z}\, y(x)$
Diff. equation	$E I_z \frac{d^2 u_y(x)}{dx^2} = M_z(x)$
	$E I_z \frac{d^3 u_y(x)}{dx^3} = -Q_y(x)$
	$E I_z \frac{d^4 u_y(x)}{dx^4} = q_y(x)$

5.2.4 Differential Equation of the Bending Line

Two-time differentiation of Eq. (5.32) and consideration of the relation between bending moment and distributed load according to Eq. (5.26) leads to the classic type of differential equation of the bending line,

$$\frac{d^2}{dx^2}\left(EI_z \frac{d^2 u_y}{dx^2}\right) = q_y,\tag{5.35}$$

which is also referred to as the bending line–distributed load relation. For a beam with constant bending stiffness EI_z along the beam axis, the following results:

$$EI_z \frac{d^4 u_y}{dx^4} = q_y.\tag{5.36}$$

The differential equation of the bending line can of course also be applied through the bending moment or the shear force as

$$EI_z \frac{d^2 u_y}{dx^2} = M_z \quad \text{or}\tag{5.37}$$

$$EI_z \frac{d^3 u_y}{dx^3} = -Q_y.\tag{5.38}$$

Finally, the three different formulations for the differential equation for the bending beam at bending in the $x-y$ plane are summarized in Table 5.4.

5.2.5 Analytical Solutions

In the following, the analytical calculation of the bending line for simple statically determinate load cases will be considered. The differential equation of the bending line has to be integrated analytically according to Eqs. (5.36), (5.37) or (5.38). The constants of integration occurring in this integration can be determined with the help of the boundary conditions, see Table 5.5.
If the distributed load (or moment or shear force distribution) cannot be represented in a closed form for the entire bending beam because supports, pin-joints, effects of jumps or kinks in the load function occur, the integration has to be done in sections. The additional constants of integration then have to be defined through the transition conditions. The following transition conditions (conditions of continuity) for the illustrated beam divisions in Fig. 5.10 can for example be named:

$$u_y^{\mathrm{I}}(a) = u_y^{\mathrm{II}}(a),\tag{5.39}$$

$$\frac{du_y^{\mathrm{I}}(a)}{dx} = \frac{du_y^{\mathrm{II}}(a)}{dx}.\tag{5.40}$$

Table 5.5 Boundary conditions at bending in the $x-y$ plane

Symbol	Type of bearing	u_y	$\dfrac{du_y}{dx}$	M_z	Q_y
	Simply supported	0	–	0	–
	Roller support	0	–	0	–
	Free end	–	–	0	0
	Fixed support	0	0	–	–
	Support with shear force link	–	0	–	0
	Spring support	$\dfrac{F}{c}$	–	0	–

Fig. 5.10 For the definition of the transition condition between different sections of a beam
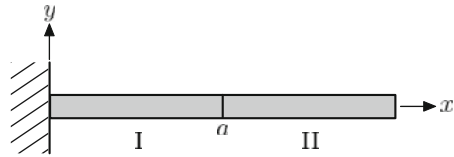
The analytical calculation of the bending line is executed in the following, for example, for a bending beam subjected to a single force, see Fig. 5.11. The differential equation of the bending line in the form with the fourth order derivative according to Eq. (5.36) is chosen as an initial point. A four-time integration gradually leads to the following equations:

$$EI_z \frac{d^3 u_y}{dx^3} = c_1 \ (= -Q_y), \tag{5.41}$$

$$EI_z \frac{d^2 u_y}{dx^2} = c_1 x + c_2 \ (= M_z), \tag{5.42}$$

$$EI_z \frac{d u_y}{dx} = \frac{1}{2} c_1 x^2 + c_2 x + c_3, \tag{5.43}$$

$$EI_z u_y = \frac{1}{6} c_1 x^3 + \frac{1}{2} c_2 x^2 + c_3 x + c_4. \tag{5.44}$$

Consequently, the general solution via the constants of integration $c_1, \ldots, c_4$ has to be adapted to the particular problem according to Fig. 5.11a.

$u_y(0) = 0$ and $\frac{du_y(0)}{dx} = 0$ apply for the fixed support on the left-hand boundary ($x = 0$), see Table 5.5. From Eqs. (5.43) and (5.44) with these boundary conditions $c_3 = c_4 = 0$ results immediately. For the determination of the remaining constants of integration one cannot use Table 5.5. In fact the external load has to be put in relation to the internal reactions. Herefore the infinitesimal element shown in Fig. 5.11b, at

Fig. 5.11 Calculation of the bending line for the bending beam under single force: **a** General configuration and **b** internal reactions at free boundary
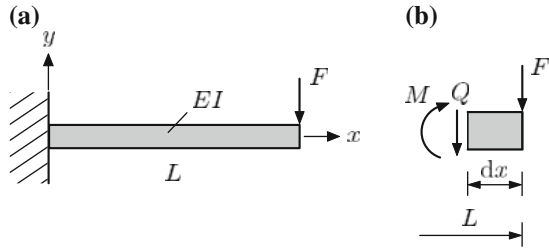
Fig. 5.12 Calculation of the bending line for a beam under single force on the basis of moment distribution
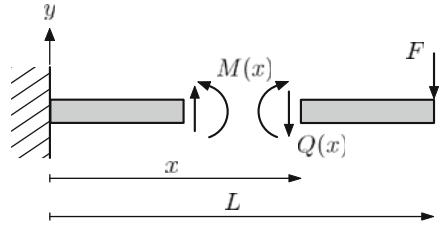
which the external force F acts has to be regarded. The equilibrium between the external loads and the internal reactions has to be formulated at position $x = L$, thus at the point of application of the external force. Therefore the external force does not create a moment action since the case $dx \to 0$ or in other words the position $x = L$ is considered. The equilibrium of moments,[8] meaning $M_z(x = L) = 0$, together with Eq. (5.42) leads to the relation $c_2 = -c_1 L$. The vertical equilibrium of forces according to Fig. 5.11b leads to $Q_y(x = L) = -F$. Through Eq. (5.41) it results therefrom that $c_1 = F$. Consequently the equation of the bending line can be formulated as

$$u_y(x) = \frac{1}{EI_z} \left(\frac{1}{6} F x^3 - \frac{1}{2} F L x^2 \right). \tag{5.45}$$

In particular the maximal bending on the right-hand boundary results in:

$$u_y(L) = -\frac{F L^3}{3 E I_z}. \tag{5.46}$$

The calculation of the bending line can alternatively also start for example from the moment distribution $M_z(x)$. To do so, the beam has to be 'cut' in two parts at an arbitrary position x, see Fig. 5.12. Subsequently it is enough to consider only one of the two parts for the composition of the equilibrium condition.

---

[8] Just for the case that an external moment M^{ext} would act at position $x = L$, the internal moment would result in: $M_z(x = L) = M^{\text{ext}}$. Hereby it was assumed that the external moment M^{ext} would be positive in a mathematical sense.

The equilibrium of moments on the right-hand part around the reference point at position x delivers $+M_z(x) + (L - x)F = 0$, or alternatively solved for the moment distribution:

$$M_z(x) = (x - L)F . \tag{5.47}$$

The differential equation of the bending line in the form with the 2nd order derivative according to Eq. (5.37) is chosen as the initial point. Two-time integration gradually leads to the following equations:

$$EI_z \frac{d^2 u_y}{dx^2} = M_z(x) = (x - L)F , \tag{5.48}$$

$$EI_z \frac{du_y}{dx} = \left(\frac{1}{2} x^2 - Lx\right) F + c_1 , \tag{5.49}$$

$$EI_z u_y(x) = \frac{1}{6} x^3 F - \frac{1}{2} Lx^2 F + c_1 x + c_2 . \tag{5.50}$$

The consideration of the boundary conditions on the fixed support, meaning $u_y(0) = 0$ and $\frac{du_y(0)}{dx} = 0$, finally leads to Eq. (5.45) and the maximal bending deflection according to Eq. (5.46).
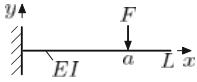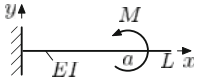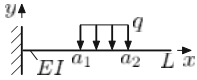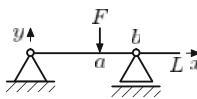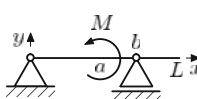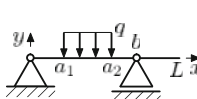
At this point it needs to be noted that regarding the bending in the $x-z$ plane, the basic equations have to be slightly modified at some points since the positive orientation of the angles or rather moments are defined around the positive y-axis. The corresponding basic equations are summarized in Table 5.6 and apply irrespective of the orientation—either positive upwards or positive downwards—of the vertical z-axis.

Table 5.6 Elementary basic equations for the bending beam at deformation in the $x-z$ plane

Name	Equation
Kinematics	$\varepsilon_x(x, z) = -z \frac{d^2 u_z(x)}{dx^2}$
Equilibrium	$\frac{dQ_z(x)}{dx} = -q_z(x) \, ; \, \frac{dM_y(x)}{dx} = Q_z(x)$
Constitutive equation	$\sigma_x(x, z) = E\varepsilon_x(x, z)$
Stress	$\sigma_x(x, z) = \frac{M_y(x)}{I_y} z(x)$
Diff. equation	$EI_y \frac{d^2 u_z(x)}{dx^2} = -M_y(x)$
	$EI_y \frac{d^3 u_z(x)}{dx^3} = -Q_z(x)$
	$EI_y \frac{d^4 u_z(x)}{dx^4} = q_z(x)$

Closed-form solutions for further loading cases will be concluded at the end of this chapter, see Table 5.7 [9, 10]. To be able to realize a closed-form presentation with discontinuities, the so-called FÖPPL bracket was used for the equations of the bending

Table 5.7 Closed-form solutions of the bending line at simple loading cases for statically determinate beams at bending in the $x-y$ plane

Load	Bending line
	$$u_y(x) = \frac{-F}{6EI_z} \times [3ax^2 - x^3 + \langle x - a \rangle^3]$$
	$$u_y(x) = \frac{-M}{2EI_z} \times [-x^2 + \langle x - a \rangle^2]$$
	$$u_y(x) = \frac{-q}{24EI_z} \times [6(a_2^2 - a_1^2)x^2 - 4(a_2 - a_1)x^3 + \langle x - a_1 \rangle^4 - \langle x - a_2 \rangle^4]$$
	$$u_y(x) = \frac{-F}{6bEI_z} \times [(b - a)(b^2x - x^3) - x\langle b - a \rangle^3 + b\langle x - a \rangle^3 - a\langle x - b \rangle^3]$$
	$$u_y(x) = \frac{-M}{6bEI_z} \times [b^2x - x^3 - 3x\langle b - a \rangle^2 + 3b\langle x - a \rangle^2 + \langle x - b \rangle^3]$$
	$$u_y(x) = \frac{-q}{24bEI_z} \times [2(a_2^2 - a_1^2 - 2b(a_2 - a_1)) \times (x^3 - b^2x) - x\langle b - a_1 \rangle^4 + x\langle b - a_2 \rangle^4 \times {} + b\langle x - a_1 \rangle^4 - b\langle x - a_2 \rangle^4 - 2(a_2^2 - a_1^2)\langle x - b \rangle^3]$$

line in Table 5.7. This mathematical notation, which was introduced by August Otto
FÖPPL (1854–1942)[9] has the following meaning:

$$\langle x - a \rangle^n = \begin{cases} 0 & \text{for } x < a \\ (x - a)^n & \text{for } x \geq a . \end{cases} \tag{5.51}$$

In particular with the case $n = 0$

$$\langle x - a \rangle^0 = \begin{cases} 0 \text{ for } x < a \\ 1 \text{ for } x \geq a \end{cases} \tag{5.52}$$

the closed-form presentation of jumps can be realized. Furthermore, derivations and
integrals are defined by regarding the triangular bracket symbol as classical round
brackets:

---

[9] In English-speaking countries this mathematical notation is mostly named after the British mathematician and engineer W.H. MACAULAY (1853–1936)[11]. However this notation was originally proposed by the German mathematician Rudolf Friedrich Alfred CLEBSCH (1833–1872) [12].

$$\frac{d}{dx} \langle x - a \rangle^n = n \langle x - a \rangle^{n-1}, \tag{5.53}$$

$$\int \langle x - a \rangle^n dx = \frac{1}{n+1} \langle x - a \rangle^{n+1} + c. \tag{5.54}$$

5.3 The Finite Element Method of Plane Bending Beams

The bending element is defined as a prismatic body with the center line x and the y-axis orthogonally to the center line. Nodes are introduced at both ends of the bending element, at which displacements and rotations or alternatively forces and moments are defined, as drafted in Fig. 5.13. The deformation and loading parameters are assumed to be positive in the drafted direction.

Fig. 5.13 Definition of the positive direction for the bending element at deformation in the $x-y$ plane: **a** deformation parameters; **b** load parameters
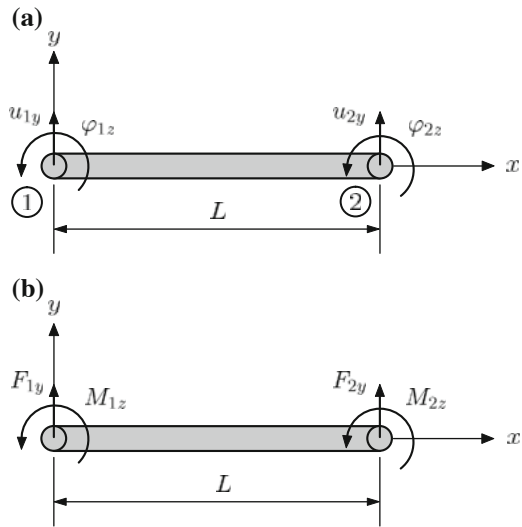
Since deformation parameters are present at both nodes, meaning u_y and $\varphi_z = \frac{du_y}{dx}$, a polynomial with four unknown parameters will be assessed in the following for the displacement field:

$$u_y(x) = \alpha_0 + \alpha_1 x + \alpha_2 x^2 + \alpha_3 x^3 = \begin{bmatrix} 1 & x & x^2 & x^3 \end{bmatrix} \begin{bmatrix} \alpha_0 \\ \alpha_1 \\ \alpha_2 \\ \alpha_3 \end{bmatrix} = \chi^T \alpha. \tag{5.55}$$

Due to differentiation with regard to the x-coordinate the course of the rotation results in:

$$\varphi_z(x) = \frac{\mathrm{d}u_y(x)}{\mathrm{d}x} = \alpha_1 + 2\alpha_2 x + 3\alpha_3 x^2 . \tag{5.56}$$

Evaluation of the deformation distributions $u_y(x)$ and $\varphi_z(x)$ at both nodes, meaning for $x = 0$ and $x = L$, delivers:

$$\text{Node 1:} \quad u_{1y}(0) = \alpha_0 , \tag{5.57}$$
$$\varphi_{1z}(0) = \alpha_1 , \tag{5.58}$$
$$\text{Node 2:} \quad u_{2y}(L) = \alpha_0 + \alpha_1 L + \alpha_2 L^2 + \alpha_3 L^3 , \tag{5.59}$$
$$\varphi_{2z}(L) = \alpha_1 + 2\alpha_2 L + 3\alpha_3 L^2 , \tag{5.60}$$

and in matrix notation:

$$\begin{bmatrix} u_{1y} \\ \varphi_{1z} \\ u_{2y} \\ \varphi_{2z} \end{bmatrix} = \underbrace{\begin{bmatrix} 1 & 0 & 0 & 0 \\ 0 & 1 & 0 & 0 \\ 1 & L & L^2 & L^3 \\ 0 & 1 & 2L & 3L^2 \end{bmatrix}}_{X} \begin{bmatrix} \alpha_0 \\ \alpha_1 \\ \alpha_2 \\ \alpha_3 \end{bmatrix} . \tag{5.61}$$

Solving for the unknown coefficients $\alpha_1, \ldots, \alpha_4$ yields:

$$\begin{bmatrix} \alpha_0 \\ \alpha_1 \\ \alpha_2 \\ \alpha_3 \end{bmatrix} = \begin{bmatrix} 1 & 0 & 0 & 0 \\ 0 & 1 & 0 & 0 \\ -\frac{3}{L^2} & -\frac{2}{L} & \frac{3}{L^2} & -\frac{1}{L} \\ \frac{2}{L^3} & \frac{1}{L^2} & -\frac{2}{L^3} & \frac{1}{L^2} \end{bmatrix} \begin{bmatrix} u_{1y} \\ \varphi_{1z} \\ u_{2y} \\ \varphi_{2z} \end{bmatrix} \tag{5.62}$$

or in matrix notation:

$$\boldsymbol{\alpha} = \boldsymbol{A}\boldsymbol{u}_\mathrm{p} = \boldsymbol{X}^{-1}\boldsymbol{u}_\mathrm{p} . \tag{5.63}$$

The row matrix of the shape functions[10] results from $\boldsymbol{N} = \boldsymbol{\chi}^\mathrm{T}\boldsymbol{A}$ and includes the following components:

$$N_{1u}(x) = 1 - 3\left(\frac{x}{L}\right)^2 + 2\left(\frac{x}{L}\right)^3 , \tag{5.64}$$

$$N_{1\varphi}(x) = x - 2\frac{x^2}{L} + \frac{x^3}{L^2} , \tag{5.65}$$

$$N_{2u}(x) = 3\left(\frac{x}{L}\right)^2 - 2\left(\frac{x}{L}\right)^3 , \tag{5.66}$$

$$N_{2\varphi}(x) = -\frac{x^2}{L} + \frac{x^3}{L^2} . \tag{5.67}$$

---

[10] Alternatively the expression interpolation or form function is used.
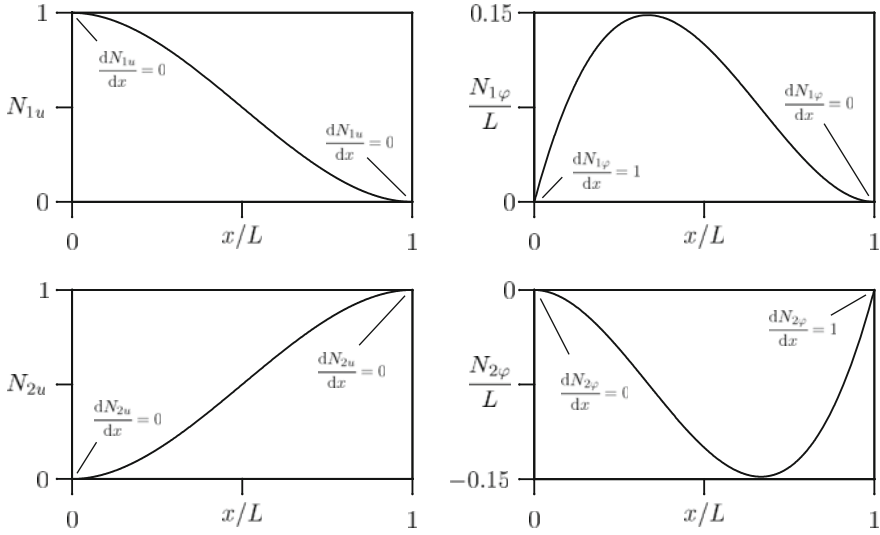
Fig. 5.14 Shape functions for the bending element at bending in the $x-y$ plane

A graphical illustration of the shape functions is given in Fig. 5.14.
In compact form the displacement distribution herewith results in:

$$u_y^e(x) = N_{1u}u_{1y} + N_{1\varphi}\varphi_{1z} + N_{2u}u_{2y} + N_{2\varphi}\varphi_{2z} \tag{5.68}$$

$$= \begin{bmatrix} N_{1u}u_{1y} & N_{1\varphi} & N_{2u}u_{2y} & N_{2\varphi} \end{bmatrix} \begin{bmatrix} u_{1y} \\ \varphi_{1z} \\ u_{2y} \\ \varphi_{2z} \end{bmatrix} = N(x)u_p . \tag{5.69}$$

Through the kinematic relation according to Eq. (5.15) the strain distribution results in:

$$\varepsilon_x^e(x, y) = -y\frac{d^2 u_y^e(x)}{dx^2} = -y\frac{d^2}{dx^2}\left(N(x)u_p\right) = -y\frac{d^2 N(x)}{dx^2} u_p . \tag{5.70}$$

According to the procedure for the bar element in Chap. 3, a generalized B-matrix can be introduced at this point for the bending element. Thus, one obtains an equivalent formulation as in Eq. (3.25), meaning $\varepsilon_x^e = Bu_p$, with

$$B = -y\frac{d^2 N(x)}{dx^2} . \tag{5.71}$$

Through the constitutive law according to Eq. (5.27) the stress distribution results in:

$$\sigma_x^e(x, y) = E\varepsilon_x^e(x, y) = EBu_p . \tag{5.72}$$

The general approach for the derivation of the element stiffness matrix, meaning

$$k^e = \int_{\Omega} B^T D B \, d\Omega \tag{5.73}$$

simplifies itself, since the elasticity matrix D in the regarded one-dimensional case is only represented through the modulus of elasticity E. Consequently the following results:

$$k^e = \int_{\Omega} \left(-y \frac{d^2 N^T(x)}{dx^2} \right) E \left(-y \frac{d^2 N(x)}{dx^2} \right) d\Omega . \tag{5.74}$$

If the cross-section of the beam along the x-axis is constant, the following results:

$$k^e = E \int_L \left(\int_A y^2 \, dA \right) \frac{d^2 N^T(x)}{dx^2} \frac{d^2 N(x)}{dx^2} \, dx = E I_z \int_L \frac{d^2 N^T(x)}{dx^2} \frac{d^2 N(x)}{dx^2} \, dx . \tag{5.75}$$

The conditional equation for the stiffness matrix can be written as follows

$$k^e = E I_z \int_0^L \begin{bmatrix} \dfrac{dN_{1u}^2}{dx^2} \\[2mm] \dfrac{dN_{1\varphi}^2}{dx^2} \\[2mm] \dfrac{dN_{2u}^2}{dx^2} \\[2mm] \dfrac{dN_{2\varphi}^2}{dx^2} \end{bmatrix} \begin{bmatrix} \dfrac{dN_{1u}^2}{dx^2} & \dfrac{dN_{1\varphi}^2}{dx^2} & \dfrac{dN_{2u}^2}{dx^2} & \dfrac{dN_{2\varphi}^2}{dx^2} \end{bmatrix} dx \tag{5.76}$$

due to the single shape functions. After all multiplications are done the following then results:

$$k^e = E I_z \int_0^L \begin{bmatrix} \dfrac{dN_{1u}^2}{dx^2}\dfrac{dN_{1u}^2}{dx^2} & \dfrac{dN_{1u}^2}{dx^2}\dfrac{dN_{1\varphi}^2}{dx^2} & \dfrac{dN_{1u}^2}{dx^2}\dfrac{dN_{2u}^2}{dx^2} & \dfrac{dN_{1u}^2}{dx^2}\dfrac{dN_{2\varphi}^2}{dx^2} \\[3mm] \dfrac{dN_{1\varphi}^2}{dx^2}\dfrac{dN_{1u}^2}{dx^2} & \dfrac{dN_{1\varphi}^2}{dx^2}\dfrac{dN_{1\varphi}^2}{dx^2} & \dfrac{dN_{1\varphi}^2}{dx^2}\dfrac{dN_{2u}^2}{dx^2} & \dfrac{dN_{1\varphi}^2}{dx^2}\dfrac{dN_{2\varphi}^2}{dx^2} \\[3mm] \dfrac{dN_{2u}^2}{dx^2}\dfrac{dN_{1u}^2}{dx^2} & \dfrac{dN_{2u}^2}{dx^2}\dfrac{dN_{1\varphi}^2}{dx^2} & \dfrac{dN_{2u}^2}{dx^2}\dfrac{dN_{2u}^2}{dx^2} & \dfrac{dN_{2u}^2}{dx^2}\dfrac{dN_{2\varphi}^2}{dx^2} \\[3mm] \dfrac{dN_{2\varphi}^2}{dx^2}\dfrac{dN_{1u}^2}{dx^2} & \dfrac{dN_{2\varphi}^2}{dx^2}\dfrac{dN_{1\varphi}^2}{dx^2} & \dfrac{dN_{2\varphi}^2}{dx^2}\dfrac{dN_{2u}^2}{dx^2} & \dfrac{dN_{2\varphi}^2}{dx^2}\dfrac{dN_{2\varphi}^2}{dx^2} \end{bmatrix} dx . \tag{5.77}$$

The derivatives of the single shape functions in Eq. (5.77) result from the Eqs. (5.64)–(5.67):

$$\frac{\mathrm{d}N_{1u}(x)}{\mathrm{d}x} = -\frac{6x}{L^2} + \frac{6x^2}{L^3}, \tag{5.78}$$

$$\frac{\mathrm{d}N_{1\varphi}(x)}{\mathrm{d}x} = 1 - \frac{4x}{L} + \frac{3x^2}{L^2}, \tag{5.79}$$

$$\frac{\mathrm{d}N_{2u}(x)}{\mathrm{d}x} = \frac{6x}{L^2} - \frac{6x^2}{L^3}, \tag{5.80}$$

$$\frac{\mathrm{d}N_{2\varphi}(x)}{\mathrm{d}x} = -\frac{2x}{L} + \frac{3x^2}{L^2}, \tag{5.81}$$

or alternatively the second order derivatives:

$$\frac{\mathrm{d}^2 N_{1u}(x)}{\mathrm{d}x^2} = -\frac{6}{L^2} + \frac{12x}{L^3}, \tag{5.82}$$

$$\frac{\mathrm{d}^2 N_{1\varphi}(x)}{\mathrm{d}x^2} = -\frac{4}{L} + \frac{6x}{L^2}, \tag{5.83}$$

$$\frac{\mathrm{d}^2 N_{2u}(x)}{\mathrm{d}x^2} = \frac{6}{L^2} - \frac{12x}{L^3}, \tag{5.84}$$

$$\frac{\mathrm{d}^2 N_{2\varphi}(x)}{\mathrm{d}x^2} = -\frac{2}{L} + \frac{6x}{L^2}. \tag{5.85}$$

The integration in Eq. (5.77) can be carried out analytically and, after a short calculation, the element stiffness matrix of the bending beam in compact form results:

$$k^{\mathrm{e}} = \frac{EI_z}{L^3} \begin{bmatrix} 12 & 6L & -12 & 6L \\ 6L & 4L^2 & -6L & 2L^2 \\ -12 & -6L & 12 & -6L \\ 6L & 2L^2 & -6L & 4L^2 \end{bmatrix}. \tag{5.86}$$

Taking into account the external loads and deformations shown in Fig. 5.13, the principal finite element equation on element level yields:

$$\frac{EI_z}{L^3} \begin{bmatrix} 12 & 6L & -12 & 6L \\ 6L & 4L^2 & -6L & 2L^2 \\ -12 & -6L & 12 & -6L \\ 6L & 2L^2 & -6L & 4L^2 \end{bmatrix} \begin{bmatrix} u_{1y} \\ \varphi_{1z} \\ u_{2y} \\ \varphi_{2z} \end{bmatrix} = \begin{bmatrix} F_{1y} \\ M_{1z} \\ F_{2y} \\ M_{2z} \end{bmatrix}. \tag{5.87}$$

5.3.1 Derivation Through Potential

The elastic potential energy at an one-dimensional problem[11] with linear-elastic material behavior yields the following:

$$\Pi_{\text{int}} = \frac{1}{2} \int_{\Omega} \sigma_x \varepsilon_x \mathrm{d}\Omega \,. \tag{5.88}$$

If stress and strain are formulated via the shape functions and the node deformations according to Eq. (5.72), the following results:

$$\Pi_{\text{int}} = \frac{1}{2} \int_{\Omega} E \left(\boldsymbol{B} \boldsymbol{u}_{\text{p}} \right)^{\text{T}} \boldsymbol{B} \boldsymbol{u}_{\text{p}} \mathrm{d}\Omega \,. \tag{5.89}$$

If the relation for the transpose of the product of two matrices, meaning $(\boldsymbol{A} \boldsymbol{B})^{\text{T}} = \boldsymbol{B}^{\text{T}} \boldsymbol{A}^{\text{T}}$, is considered, the following results:

$$\Pi_{\text{int}} = \frac{1}{2} \int_{\Omega} E \boldsymbol{u}_{\text{p}}^{\text{T}} \boldsymbol{B}^{\text{T}} \boldsymbol{B} \boldsymbol{u}_{\text{p}} \mathrm{d}\Omega \,. \tag{5.90}$$

Since the nodal values do not represent a function, the following column matrix can be taken out from the integral:

$$\Pi_{\text{int}} = \frac{1}{2} \boldsymbol{u}_{\text{p}}^{\text{T}} \left[\int_{\Omega} E \boldsymbol{B}^{\text{T}} \boldsymbol{B} \mathrm{d}\Omega \right] \boldsymbol{u}_{\text{p}} \,. \tag{5.91}$$

Through the definition for the generalized $\boldsymbol{B}$-matrix according to Eq. (5.71) the following results herefrom:

$$\Pi_{\text{int}} = \frac{1}{2} \boldsymbol{u}_{\text{p}}^{\text{T}} \left[\int_{\Omega} E(-y) \frac{\mathrm{d}^2 \boldsymbol{N}^{\text{T}}(x)}{\mathrm{d}x^2} (-y) \frac{\mathrm{d}^2 \boldsymbol{N}(x)}{\mathrm{d}x^2} \mathrm{d}\Omega \right] \boldsymbol{u}_{\text{p}} \,. \tag{5.92}$$

The axial second moment of area can also be identified at this point, so that the last equation displays as follows:

$$\Pi_{\text{int}} = \frac{1}{2} \boldsymbol{u}_{\text{p}}^{\text{T}} \left[\int_{0}^{L} \left(\int_{A} y^2 \mathrm{d}A \right) E \frac{\mathrm{d}^2 \boldsymbol{N}^{\text{T}}(x)}{\mathrm{d}x^2} \frac{\mathrm{d}^2 \boldsymbol{N}(x)}{\mathrm{d}x^2} \mathrm{d}x \right] \boldsymbol{u}_{\text{p}} \,. \tag{5.93}$$

---

[11] In the general three-dimensional case the form $\Pi_{\text{int}} = \frac{1}{2} \int_{\Omega} \boldsymbol{\varepsilon}^{\text{T}} \boldsymbol{\sigma} \mathrm{d}\Omega$ can be applied, whereat $\boldsymbol{\sigma}$ and $\boldsymbol{\varepsilon}$ represent the column matrix with the stress and strain components.

Hence the elastic potential energy for constant material and cross-section values yields:

$$\Pi_{\text{int}} = \frac{1}{2}\, \boldsymbol{u}_{\text{p}}^{\text{T}} \underbrace{\left[EI_z \int_0^L \frac{\mathrm{d}^2 \boldsymbol{N}^{\text{T}}(x)}{\mathrm{d}x^2} \frac{\mathrm{d}^2 \boldsymbol{N}(x)}{\mathrm{d}x^2}\, \mathrm{d}x \right]}_{\boldsymbol{k}^{\text{e}}} \boldsymbol{u}_{\text{p}}. \tag{5.94}$$

The last equation complies with the general formulation of the potential energy of a finite element

$$\Pi_{\text{int}} = \frac{1}{2}\, \boldsymbol{u}_{\text{p}}^{\text{T}} \boldsymbol{k}^{\text{e}} \boldsymbol{u}_{\text{p}} \tag{5.95}$$

and therefore allows the identification of the element stiffness matrix.

The derivation of the principal finite element equation including the stiffness matrix often takes place through extremal or variational principles as for example the principle of virtual work[12] or the HELLINGER–REISSNER principle, [14–16]. In the following the principal finite element equation will be derived by means of CASTIGLIANO's theorem,[13] see [17, 18]. The elastic potential energy will be regarded as the initial point, which represents itself from Eq. (5.88) through the kinematic relation (5.15) and the constitutive law (5.27) as follows:

$$\Pi_{\text{int}} = \frac{1}{2} \int_{\Omega} E \varepsilon_x^2 \mathrm{d}\Omega = \frac{1}{2} \int_{\Omega} E \left(-y \frac{\mathrm{d}^2 u_y(x)}{\mathrm{d}x^2} \right)^2 \mathrm{d}\Omega \tag{5.96}$$

$$= \frac{1}{2} \int_L E \left(\int_A y^2 \mathrm{d}A \right) \left(\frac{\mathrm{d}^2 u_y(x)}{\mathrm{d}x^2} \right)^2 \mathrm{d}x \tag{5.97}$$

$$= \frac{EI_z}{2} \int_0^L \left(\frac{\mathrm{d}^2 u_y(x)}{\mathrm{d}x^2} \right)^2 \mathrm{d}x . \tag{5.98}$$

Through the approach for the displacement distribution according to Eq. (5.68) the following results here from:

---

[12] The principle of virtual work encompasses the principle of the virtual displacements and the principle of the virtual forces [13].

[13] CASTIGLIANO's theorems were formulated by the Italian builder, engineer and scientist Carl Alberto CASTIGLIANO (1847–1884). The second theorem signifies: the partial derivative of the stored potential energy in a linear-elastic body with regards to the displacement u_i yields the force F_i in the direction of the displacement at the considered point. An analog coherence also applies for the rotation and the moment.

$$\Pi_{\text{int}} = \frac{EI_z}{2} \int\limits_0^L \left(\frac{\mathrm{d}^2 N_{1u}}{\mathrm{d}x^2} u_{1y} + \frac{\mathrm{d}^2 N_{1\varphi}}{\mathrm{d}x^2} \varphi_{1z} + \frac{\mathrm{d}^2 N_{2u}}{\mathrm{d}x^2} u_{2y} + \frac{\mathrm{d}^2 N_{2\varphi}}{\mathrm{d}x^2} \varphi_{2z} \right)^2 \mathrm{d}x \ .$$

(5.99)

The application of the second CASTIGLIANO's theorem on the potential energy regarding the nodal distribution u_{1y} leads to the external force F_{1y} at node 1:

$$\frac{\mathrm{d}\Pi_{\text{int}}}{\mathrm{d}u_{1y}} = F_{1y} = EI_z \int\limits_0^L \left(\frac{\mathrm{d}^2 N_{1u}}{\mathrm{d}x^2} u_{1y} + \frac{\mathrm{d}^2 N_{1\varphi}}{\mathrm{d}x^2} \varphi_{1z} + \right.$$
$$\left. + \frac{\mathrm{d}^2 N_{2u}}{\mathrm{d}x^2} u_{2y} + \frac{\mathrm{d}^2 N_{2\varphi}}{\mathrm{d}x^2} \varphi_{2z} \right) \frac{\mathrm{d}^2 N_{1y}}{\mathrm{d}x^2} \mathrm{d}x \ .$$

(5.100)

Accordingly, the following results from the differentiation with regard to the other deformation parameters on the nodes:

$$\frac{\mathrm{d}\Pi_{\text{int}}}{\mathrm{d}\varphi_{1z}} = M_{1z} = EI_z \int\limits_0^L \left(\frac{\mathrm{d}^2 N_{1u}}{\mathrm{d}x^2} u_{1y} + \frac{\mathrm{d}^2 N_{1\varphi}}{\mathrm{d}x^2} \varphi_{1z} + \right.$$
$$\left. + \frac{\mathrm{d}^2 N_{2u}}{\mathrm{d}x^2} u_{2y} + \frac{\mathrm{d}^2 N_{2\varphi}}{\mathrm{d}x^2} \varphi_{2z} \right) \frac{\mathrm{d}^2 N_{1\varphi}}{\mathrm{d}x^2} \mathrm{d}x \ ,$$

(5.101)

$$\frac{\mathrm{d}\Pi_{\text{int}}}{\mathrm{d}u_{2y}} = F_{2y} = EI_z \int\limits_0^L \left(\frac{\mathrm{d}^2 N_{1u}}{\mathrm{d}x^2} u_{1y} + \frac{\mathrm{d}^2 N_{1\varphi}}{\mathrm{d}x^2} \varphi_{1z} + \right.$$
$$\left. + \frac{\mathrm{d}^2 N_{2u}}{\mathrm{d}x^2} u_{2y} + \frac{\mathrm{d}^2 N_{2\varphi}}{\mathrm{d}x^2} \varphi_{2z} \right) \frac{\mathrm{d}^2 N_{2y}}{\mathrm{d}x^2} \mathrm{d}x \ ,$$

(5.102)

$$\frac{\mathrm{d}\Pi_{\text{int}}}{\mathrm{d}u_{2\varphi}} = M_{2y} = EI_z \int\limits_0^L \left(\frac{\mathrm{d}^2 N_{1u}}{\mathrm{d}x^2} u_{1y} + \frac{\mathrm{d}^2 N_{1\varphi}}{\mathrm{d}x^2} \varphi_{1z} + \right.$$
$$\left. + \frac{\mathrm{d}^2 N_{2u}}{\mathrm{d}x^2} u_{2y} + \frac{\mathrm{d}^2 N_{2\varphi}}{\mathrm{d}x^2} \varphi_{2z} \right) \frac{\mathrm{d}^2 N_{2\varphi}}{\mathrm{d}x^2} \mathrm{d}x \ .$$

(5.103)

After carrying out the integration, Eqs. (5.100)–(5.103) can be summarized in the principal finite element equation in matrix form, see (5.87).

For the derivation of the principal finite element equation often the total potential is used. The total potential or the entire potential energy of a bending beam in general results in

$$\Pi = \Pi_{\text{int}} + \Pi_{\text{ext}} \ ,$$

(5.104)

whereby Π_{int} represents the elastic strain energy (energy of elastic deformation) and Π_{ext} the potential of the external load. The entire potential energy under influence

of the external loading can be stated as follows

$$\Pi = \frac{1}{2} \int_{\Omega} \sigma_x \varepsilon_x \mathrm{d}\Omega - \sum_{i=1}^{m} F_{iy} u_{iy} - \sum_{i=1}^{m'} M_{iz} \varphi_{iz} \,, \tag{5.105}$$

where F_{iy} and M_{iz} represent the external forces and moments acting on the nodes.

5.3.2 Weighted Residual Method

In the following, the partial differential equation of the displacement field $u_y(x)$ according to Eq. (5.35) will be considered. Hereby the easiest case—at which the bending stiffness EI_z is constant and at which no distributed load ($q_y = 0$) occurs— will be considered. Thus, the partial differential equation of the displacement field yields:

$$EI_z \frac{\mathrm{d}^4 u_y^0(x)}{\mathrm{d}x^4} = 0 \,, \tag{5.106}$$

where $u_y^0(x)$ represents the exact solution of the problem. Equation (5.106) is exactly fulfilled at every position x on the beam and is also referred to as the *strong form* of the problem. If the exact solution in Eq. (5.106) is substituted through an approximate solution $u_y(x)$ a residual or remainder r results in:

$$r(x) = EI_z \frac{\mathrm{d}^4 u_y(x)}{\mathrm{d}x^4} \neq 0 \,. \tag{5.107}$$

Due to the introduction of the approximate solution $u_y(x)$ it is in general not possible to fulfill the partial differential equation at every position x of the beam anymore. Alternatively it is demanded in the following that the differential equation is fulfilled throughout a certain domain (and not at every position x) and one receives the following integral requirement

$$\int_0^L W(x) \underbrace{EI_z \frac{\mathrm{d}^4 u_y(x)}{\mathrm{d}x^4}}_{r} \, \mathrm{d}x \overset{!}{=} 0 \,, \tag{5.108}$$

which is also called the *inner product*. $W(x)$ in Eq. (5.108) represents the so-called weighting function, which distributes the error or the residual throughout the regarded domain.
Partial integration[14] of Eq. (5.108) yields:

---

[14] A common representation of the partial integration of two functions $f(x)$ and $g(x)$ is: $\int f'g \, \mathrm{d}x = fg - \int fg' \mathrm{d}x$.

$$\int_0^L EI_z \underbrace{\frac{\mathrm{d}^4 u_y}{\mathrm{d}x^4}}_{f'} \underbrace{W}_{g} \, \mathrm{d}x = EI_z \left[\frac{\mathrm{d}^3 u_y}{\mathrm{d}x^3} W \right]_0^L - \int_0^L EI_z \frac{\mathrm{d}^3 u_y}{\mathrm{d}x^3} \frac{\mathrm{d}W}{\mathrm{d}x} \, \mathrm{d}x = 0 \, . \quad (5.109)$$

Partial integration of the integral on the right-hand side of Eq. (5.109) results in:

$$\int_0^L EI_z \underbrace{\frac{\mathrm{d}^3 u_y}{\mathrm{d}x^3}}_{f'} \underbrace{\frac{\mathrm{d}W}{\mathrm{d}x}}_{g} \, \mathrm{d}x = EI_z \left[\frac{\mathrm{d}^2 u_y}{\mathrm{d}x^2} \frac{\mathrm{d}W}{\mathrm{d}x} \right]_0^L - \int_0^L EI_z \frac{\mathrm{d}^2 u_y}{\mathrm{d}x^2} \frac{\mathrm{d}^2 W}{\mathrm{d}x^2} \, \mathrm{d}x \, . \quad (5.110)$$

The combination of Eqs. (5.109) and (5.110) yields the *weak form* of the problem to:

$$\int_0^L EI_z \frac{\mathrm{d}^2 u_y}{\mathrm{d}x^2} \frac{\mathrm{d}^2 W}{\mathrm{d}x^2} \, \mathrm{d}x = EI_z \left[-W \frac{\mathrm{d}^3 u_y}{\mathrm{d}x^3} + \frac{\mathrm{d}W}{\mathrm{d}x} \frac{\mathrm{d}^2 u_y}{\mathrm{d}x^2} \right]_0^L \, . \quad (5.111)$$

Regarding the weak form it becomes obvious that due to the partial integration, two derivatives (differential operators) are shifted from the approximate solution to the weighting function and regarding the derivatives, a symmetric form results. This symmetry concerning the derivatives of the weighting function and the approximate solution will guarantee in the following that a symmetric stiffness matrix results for the bending element.

First the left-hand side of Eq. (5.111) will be considered to derive the stiffness matrix for a bending element with two nodes.

The basic idea of the finite element method now is not to approximate the unknown displacement u_y for the entire domain but to describe the displacement distribution for a subsection, the so called finite element through

$$u_y^{\mathrm{e}}(x) = N(x)u_{\mathrm{p}} = \begin{bmatrix} N_{1u} & N_{1\varphi} & N_{2u} & N_{2\varphi} \end{bmatrix} \times \begin{bmatrix} u_{1y} \\ \varphi_{1z} \\ u_{2y} \\ \varphi_{2z} \end{bmatrix} \quad (5.112)$$

approximately. Within the framework of the finite element method the same approach is chosen for the weighting function as for the displacement:

$$W(x) = \delta u_{\mathrm{p}}^{\mathrm{T}} N^{\mathrm{T}}(x) = \begin{bmatrix} \delta u_{1y} & \delta \varphi_{1z} & \delta u_{2y} & \delta \varphi_{2z} \end{bmatrix} \times \begin{bmatrix} N_{1u} \\ N_{1\varphi} \\ N_{2u} \\ N_{2\varphi} \end{bmatrix} \, , \quad (5.113)$$

in which δu_i represent arbitrary displacements or alternatively rotation values. The following will show that these arbitrary or so-called virtual values can be canceled

with an identical expression on the right-hand side of Eq. (5.111) and no further considerations are required.

If Eqs. (5.112) and (5.113) in the left-hand side of Eq. (5.111) are considered the following results for constant bending stiffness:

$$E I_z \int_0^L \frac{\mathrm{d}^2}{\mathrm{d}x^2} \left(\delta \boldsymbol{u}_\mathrm{p}^\mathrm{T} \boldsymbol{N}^\mathrm{T}(x) \right) \frac{\mathrm{d}^2}{\mathrm{d}x^2} \left(\boldsymbol{N}(x) \boldsymbol{u}_\mathrm{p} \right) \mathrm{d}x \tag{5.114}$$

or

$$\delta \boldsymbol{u}_\mathrm{p}^\mathrm{T} \ \underbrace{E I_z \int_0^L \frac{\mathrm{d}^2}{\mathrm{d}x^2} \left(\boldsymbol{N}^\mathrm{T}(x) \right) \frac{\mathrm{d}^2}{\mathrm{d}x^2} \left(\boldsymbol{N}(x) \right) \mathrm{d}x}_{k^\mathrm{e}} \ \boldsymbol{u}_\mathrm{p} \ . \tag{5.115}$$

The expression $\delta \boldsymbol{u}_\mathrm{p}^\mathrm{T}$ can be canceled with a corresponding expression on the right-hand side of Eq. (5.111) and $\boldsymbol{u}_\mathrm{p}$ represents the vector of the unknown nodal deformation. Consequently the stiffness matrix can be illustrated through the single shape functions according to Eq. (5.76).

In the following, the right-hand side of Eq. (5.111) is considered in order to derive the column matrix of the external loads for a bending element with two nodes. Considering in

$$E I_z \left[-W \frac{\mathrm{d}^3 u_y}{\mathrm{d}x^3} + \frac{\mathrm{d}W}{\mathrm{d}x} \frac{\mathrm{d}^2 u_y}{\mathrm{d}x^2} \right]_0^L \tag{5.116}$$

the definition of the weighting function according to Eq. (5.113), the following results

$$E I_z \left[-\delta \boldsymbol{u}_\mathrm{p}^\mathrm{T} \boldsymbol{N}^\mathrm{T}(x) \frac{\mathrm{d}^3 u_y}{\mathrm{d}x^3} + \frac{\mathrm{d}}{\mathrm{d}x} \left(\delta \boldsymbol{u}_\mathrm{p}^\mathrm{T} \boldsymbol{N}^\mathrm{T}(x) \right) \frac{\mathrm{d}^2 u_y}{\mathrm{d}x^2} \right]_0^L \tag{5.117}$$

or in components:

$$\delta \boldsymbol{u}_\mathrm{p}^\mathrm{T} E I_z \left[- \begin{bmatrix} N_{1u} \\ N_{1\varphi} \\ N_{2u} \\ N_{2\varphi} \end{bmatrix} \frac{\mathrm{d}^3 u_y}{\mathrm{d}x^3} + \frac{\mathrm{d}}{\mathrm{d}x} \begin{bmatrix} N_{1u} \\ N_{1\varphi} \\ N_{2u} \\ N_{2\varphi} \end{bmatrix} \frac{\mathrm{d}^2 u_y}{\mathrm{d}x^2} \right]_0^L . \tag{5.118}$$

$\delta \boldsymbol{u}_\mathrm{p}^\mathrm{T}$ from the last equation can be canceled with the corresponding expression in Eq. (5.115). Furthermore (5.118) represents a system of four equations, which needs to be evaluated on the integration boundaries, meaning on the borders $x = 0$ and $x = L$. The first line of Eq. (5.118) results in:

$$\left(-N_{1u}EI_z\frac{\mathrm{d}^3u_y}{\mathrm{d}x^3}+\frac{\mathrm{d}N_{1u}}{\mathrm{d}x}\frac{\mathrm{d}^2u_y}{\mathrm{d}x^2}\right)_{x=L}-\left(-N_{1u}EI_z\frac{\mathrm{d}^3u_y}{\mathrm{d}x^3}+\frac{\mathrm{d}N_{1u}}{\mathrm{d}x}\frac{\mathrm{d}^2u_y}{\mathrm{d}x^2}\right)_{x=0}.$$

$$(5.119)$$

Under consideration of the boundary values of the shape functions or alternatively their derivatives according to Fig. 5.14, meaning $N_{1u}(L) = 0$, $\frac{\mathrm{d}N_{1u}}{\mathrm{d}x}(L) = \frac{\mathrm{d}N_{1u}}{\mathrm{d}x}(0) = 0$ and $N_{1u}(0) = 1$, the following results:

$$+EI_z\frac{\mathrm{d}^3u_y}{\mathrm{d}x^3}\bigg|_{x=0} \overset{(5.38)}{=} -Q_y(0)\,. \qquad (5.120)$$

Accordingly the values of the three other lines in Eq. (5.118) can be calculated:

$$\text{Line 2}: \quad -EI_z\frac{\mathrm{d}^2u_y}{\mathrm{d}x^2}\bigg|_{x=0} \overset{(5.37)}{=} -M_z(0)\,, \qquad (5.121)$$

$$\text{Line 3}: \quad -EI_z\frac{\mathrm{d}^3u_y}{\mathrm{d}x^3}\bigg|_{x=L} \overset{(5.38)}{=} +Q_y(L)\,, \qquad (5.122)$$

$$\text{Line 4}: \quad +EI_z\frac{\mathrm{d}^2u_y}{\mathrm{d}x^2}\bigg|_{x=L} \overset{(5.37)}{=} +M_z(L)\,. \qquad (5.123)$$

It needs to be considered that the results in Eqs. (5.120)–(5.123) are the internal reactions according to Fig. 5.7. The external loads with the positive direction according to Fig. 5.13b therefore result from the internal reactions[15] through reversing the positive direction on the left-hand border and through maintaining the positive direction of the internal reaction on the right-hand border.

5.3.3 Comments on the Derivation of the Shape Functions

In Sect. 5.3 the shape functions were derived via a polynomial with four unknown parameters, see Eq. (5.55). The derivation of the shape function can also be achieved through a clearer method. The general feature of a shape function N_i adopting the value 1 on the node i and turning zero on all other nodes has to be considered herefore. In the case of the bending beam it furthermore needs to be considered that the displacement and rotation field on the nodes should be decoupled. Consequently, a shape function for the displacement field has to adopt the value 1 on 'its' node as well as the slope zero. On all other nodes j the value of the function as well as the slope turn zero:

---

[15] See Sect. 5.2.2 with the executions for the internal reactions and external loads.
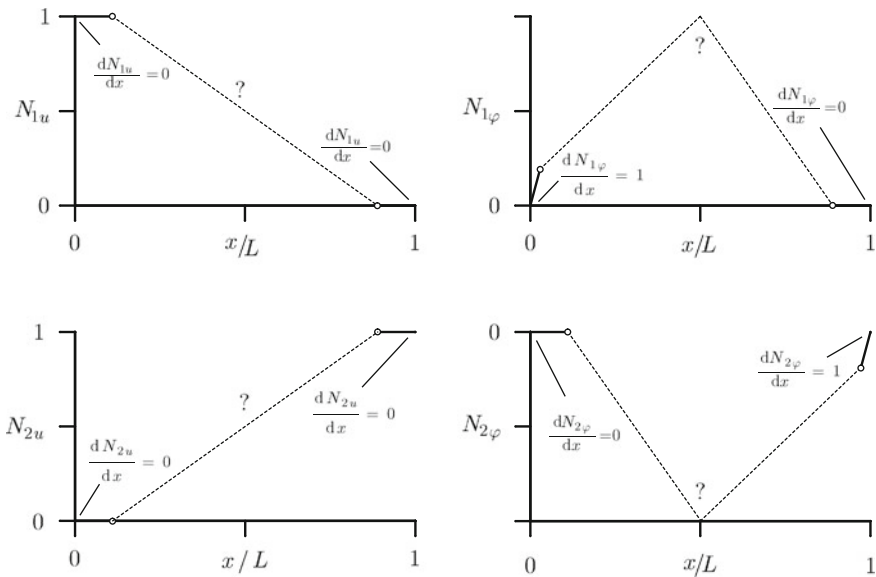
Fig. 5.15 Boundary conditions for the shape functions for the bending element at bending in the $x-y$ plane. Note that the sections for the given slopes are overdrawn for better illustration

$$N_{iu}(x_i) = 1, \tag{5.124}$$

$$N_{iu}(x_j) = 0, \tag{5.125}$$

$$\frac{\mathrm{d}N_{iu}(x_i)}{\mathrm{d}x} = 0, \tag{5.126}$$

$$\frac{\mathrm{d}N_{iu}(x_j)}{\mathrm{d}x} = 0. \tag{5.127}$$

Accordingly it results that a shape function for the rotation field reaches the slope 1 at 'its' node but the function value zero. At all other nodes the function value and the slope are equally zero. Therefore, the boundary conditions shown in Fig. 5.15 result for the four shape functions.

If the course of the shape functions should be without discontinuities, meaning kinks, then every shape function has to change its curvature. Therefore, at least a polynomial of 3rd order has to be applied, so that a linear function results for the curvature, meaning the second order derivative:

$$N(x) = \alpha_0 + \alpha_1 x + \alpha_2 x^2 + \alpha_3 x^3. \tag{5.128}$$

Since a polynomial of 3rd order usually exhibits four unknowns, $\alpha_0, \ldots, \alpha_3$, all unknowns can be defined due to this approach via the four boundary conditions—two for the function values and two for the slope.

In the following, the first shape function is regarded as an example. The boundary conditions in this case result in:

$$N_{1u}(0) = 1 , \tag{5.129}$$

$$\frac{\mathrm{d}N_{1u}}{\mathrm{d}x}(0) = \frac{\mathrm{d}N_{1u}}{\mathrm{d}x}(L) = 0 , \tag{5.130}$$

$$N_{1u}(L) = 0 . \tag{5.131}$$

If the boundary conditions are evaluated according to the approach by Eq. (5.128), the following results:

$$1 = \alpha_0 , \tag{5.132}$$

$$0 = \alpha_1 , \tag{5.133}$$

$$0 = \alpha_0 + \alpha_1 L + \alpha_2 L^2 + \alpha_3 L^3 , \tag{5.134}$$

$$0 = \alpha_1 + 2\alpha_2 L + 3\alpha_3 L^2 , \tag{5.135}$$

or alternatively in matrix notation:

$$\begin{bmatrix} 1 \\ 0 \\ 0 \\ 0 \end{bmatrix} = \begin{bmatrix} 1 & 0 & 0 & 0 \\ 0 & 1 & 0 & 0 \\ 1 & L & L^2 & L^3 \\ 0 & 1 & 2L & 3L^2 \end{bmatrix} \begin{bmatrix} \alpha_0 \\ \alpha_1 \\ \alpha_2 \\ \alpha_3 \end{bmatrix} . \tag{5.136}$$

Solving for the unknowns leads to $\boldsymbol{\alpha} = \begin{bmatrix} 1 & 0 & -\frac{3}{L^2} & \frac{2}{L^3} \end{bmatrix}^{\mathrm{T}}$. With these constants exactly the shape function according to Eq. (5.64) results. Another requirement for the shape function results from Eq. (5.77). Here the second order derivative of the shape functions are contained. Therefore a reasonable formulation of the shape function for a bending element has to at least be a polynomial of 2nd order, so that derivatives different from zero result. To conclude it needs to be remarked that the shape functions for the bending beam are so-called HERMITE's polynomials. A continuous displacement and rotation on the nodes occurs since at this HERMITE's interpolation the nodal value as well as the slope in the considered nodes are examined.

5.4 The Finite Element Bending Beam with two Deformation Planes

In the following, it will be shown that a bending beam can deform in two mutually orthogonal planes. The stiffness matrix according to Eq. (5.86) is given for the bending in the $x - y$ plane:

$$k_{xy}^{e} = \frac{EI_z}{L^3} \begin{bmatrix} 12 & 6L & -12 & 6L \\ 6L & 4L^2 & -6L & 2L^2 \\ -12 & -6L & 12 & -6L \\ 6L & 2L^2 & -6L & 4L^2 \end{bmatrix}. \tag{5.137}$$

In the orthogonal plane, meaning for bending in the $x-z$ plane a slightly modified stiffness matrix results, since the positive orientation of the angles around the y-axis is now in the clockwise direction, see Fig. 5.16. Under consideration of the definition of the positive rotation angle according to $\varphi_y(x) = -\frac{du_z(x)}{dx}$ the stiffness matrix for the bending in the $x-z$ plane results in[16]:

$$k_{xz}^{e} = \frac{EI_y}{L^3} \begin{bmatrix} 12 & -6L & -12 & -6L \\ -6L & 4L^2 & 6L & 2L^2 \\ -12 & 6L & 12 & 6L \\ -6L & 2L^2 & 6L & 4L^2 \end{bmatrix}. \tag{5.138}$$
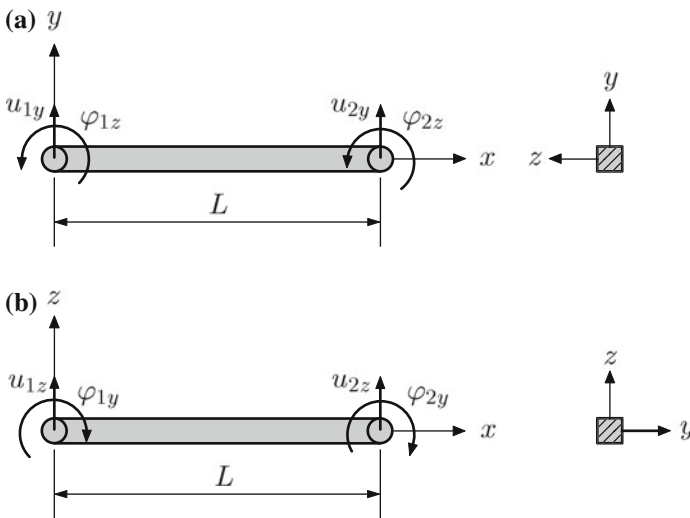
Fig. 5.16 Definition of the positive deformation parameters at bending in the **a** $x-y$ plane and **b** $x-z$ plane

Both stiffness matrices for the deformation in the $x-y$ and $x-z$ plane can easily be superposed, so that the following form for an element with two orthogonal deformation planes results

---

[16] Also see Table 5.6 and supplementary problems 5.6.

$$
k^{\mathrm{e}} = \frac{E}{L^3}
\begin{bmatrix}
12I_z & 0 & 0 & 6I_zL & -12I_z & 0 & 0 & 6I_zL \\
0 & 12I_y & -6I_yL & 0 & 0 & -12I_y & -6I_yL & 0 \\
0 & -6I_yL & 4I_yL^2 & 0 & 0 & 6I_yL & 2I_yL^2 & 0 \\
6I_zL & 0 & 0 & 4I_zL^2 & -6I_zL & 0 & 0 & 2I_zL^2 \\
-12I_z & 0 & 0 & -6I_zL & 12I_z & 0 & 0 & -6I_zL \\
0 & -12I_y & 6I_yL & 0 & 0 & 12I_y & 6I_yL & 0 \\
0 & -6I_yL & 2I_yL^2 & 0 & 0 & 6I_yL & 4I_yL^2 & 0 \\
6I_zL & 0 & 0 & 2I_zL^2 & -6I_zL & 0 & 0 & 4I_zL^2
\end{bmatrix},
$$

$$(5.139)$$

whereupon the deformation and load matrices represent as follows:

$$
\boldsymbol{u}_{\mathrm{p}} = \begin{bmatrix} u_{1y} \; u_{1z} \; \varphi_{1y} \; \varphi_{1z} \; u_{2y} \; u_{2z} \; \varphi_{2y} \; \varphi_{2z} \end{bmatrix}^{\mathrm{T}}, \tag{5.140}
$$

$$
\boldsymbol{F}^{\mathrm{e}} = \begin{bmatrix} F_{1y} \; F_{1z} \; M_{1y} \; M_{1z} \; F_{2y} \; F_{2z} \; M_{2y} \; M_{2z} \end{bmatrix}^{\mathrm{T}}. \tag{5.141}
$$

5.5 Transformation Within the Plane

In the following, a beam, which can deform in the $x - y$ plane will be rotated compared to a global coordinate system in a way that an angle α results between the global (X, Y) and the local (x, y) coordinate system. For this see Fig. 5.17.

Fig. 5.17 Rotatory transformation of a beam element in the plane
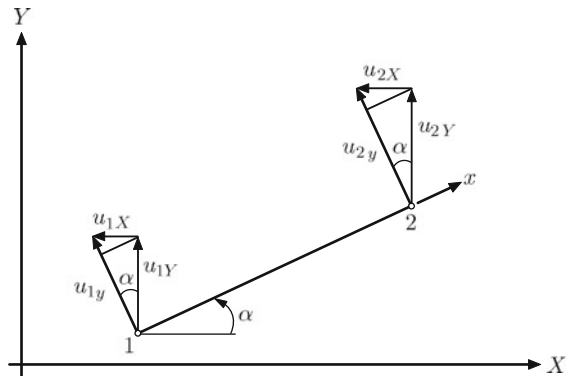
Every node in the global coordinate system now has two degrees of freedom, that means a displacement in the X- and a displacement in the Y-direction. These two displacements at one node can on the other hand be used to determine the displacement perpendicular to the beam axis, meaning in the direction of the local y-axis.

By means of the right-angled triangles illustrated in Fig. 5.17 the displacement in the local coordinate system from the global displacement values results in

$$u_{1y} = - \underbrace{\sin \alpha}_{>0} \underbrace{u_{1X}}_{<0} + \underbrace{\cos \alpha}_{>0} \underbrace{u_{1Y}}_{>0} , \tag{5.142}$$

$$u_{2y} = - \sin \alpha \underbrace{u_{2X}}_{<0} + \cos \alpha \underbrace{u_{2Y}}_{>0} . \tag{5.143}$$

Accordingly, the global displacements can be calculated from the local displacements:

$$u_{1X} = -u_{1y} \sin \alpha , \qquad\qquad u_{2X} = -u_{2y} \sin \alpha , \tag{5.144}$$

$$u_{1Y} = u_{1y} \cos \alpha , \qquad\qquad u_{2Y} = u_{2y} \cos \alpha . \tag{5.145}$$

The last relations between global and local displacements can be written in matrix form:

$$\begin{bmatrix} u_{1X} \\ u_{1Y} \\ u_{2X} \\ u_{2Y} \end{bmatrix} = \begin{bmatrix} -\sin \alpha & 0 \\ \cos \alpha & 0 \\ 0 & -\sin \alpha \\ 0 & \cos \alpha \end{bmatrix} \begin{bmatrix} u_{1y} \\ u_{2y} \end{bmatrix} . \tag{5.146}$$

The rotations of the nodes do not need a transformation and the general transformation rule for the calculation of the global parameters from the local deformations results in abbreviated notation in

$$u_{XY} = T^{\mathrm{T}} u_{xy} , \tag{5.147}$$

or alternatively in components:

$$\begin{bmatrix} u_{1X} \\ u_{1Y} \\ \varphi_{1Z} \\ u_{2X} \\ u_{2Y} \\ \varphi_{1Z} \end{bmatrix} = \begin{bmatrix} -\sin \alpha & 0 & 0 & 0 \\ \cos \alpha & 0 & 0 & 0 \\ 0 & 1 & 0 & 0 \\ 0 & 0 & -\sin \alpha & 0 \\ 0 & 0 & \cos \alpha & 0 \\ 0 & 0 & 0 & 1 \end{bmatrix} \begin{bmatrix} u_{1y} \\ \varphi_{1z} \\ u_{2y} \\ \varphi_{2z} \end{bmatrix} . \tag{5.148}$$

The last equation can also be solved for the deformations in the local coordinate system and through inversion[17] the transformation matrix results

$$u_{xy} = T u_{XY} \tag{5.149}$$

or alternatively in components:

---

[17] Since the transformation matrix T is an orthogonal matrix, the following applies: $T^{\mathrm{T}} = T^{-1}$.

$$\begin{bmatrix} u_{1y} \\ \varphi_{1z} \\ u_{2y} \\ \varphi_{2z} \end{bmatrix} = \begin{bmatrix} -\sin\alpha & \cos\alpha & 0 & 0 & 0 & 0 \\ 0 & 0 & 1 & 0 & 0 & 0 \\ 0 & 0 & 0 & -\sin\alpha & \cos\alpha & 0 \\ 0 & 0 & 0 & 0 & 0 & 1 \end{bmatrix} \begin{bmatrix} u_{1X} \\ u_{1Y} \\ \varphi_{1Z} \\ u_{2X} \\ u_{2Y} \\ \varphi_{1Z} \end{bmatrix}. \tag{5.150}$$

The vector of the external load can be transformed in the same way:

$$\boldsymbol{F}_{XY} = \boldsymbol{T}^{\mathrm{T}} \boldsymbol{F}_{xy}, \tag{5.151}$$

$$\boldsymbol{F}_{xy} = \boldsymbol{T} \boldsymbol{F}_{XY}. \tag{5.152}$$

If the transformation of the local deformation into the global coordinate system is considered in the expression for the elastic potential energy according to Eq. (5.95), the transformation of the stiffness matrix into the global coordinate system results in

$$\boldsymbol{k}^{\mathrm{e}}_{XY} = \boldsymbol{T}^{\mathrm{T}} \boldsymbol{k}^{\mathrm{e}}_{xy} \boldsymbol{T}, \tag{5.153}$$

or alternatively in components:

$$\boldsymbol{k}^{\mathrm{e}}_{XYZ} = \frac{EI_z}{L^3} \begin{bmatrix} 12\mathrm{s}^2\alpha & -12\mathrm{s}\alpha\mathrm{c}\alpha & -6L\mathrm{s}\alpha & -12\mathrm{s}^2\alpha & 12\mathrm{s}\alpha\mathrm{c}\alpha & -6L\mathrm{s}\alpha \\ -12\mathrm{s}\alpha\mathrm{c}\alpha & 12\mathrm{c}^2\alpha & 6L\mathrm{c}\alpha & 12\mathrm{s}\alpha\mathrm{c}\alpha & -12\mathrm{c}^2\alpha & 6L\mathrm{c}\alpha \\ -6L\mathrm{s}\alpha & 6L\mathrm{c}\alpha & 4L^2 & 6L\mathrm{s}\alpha & -6L\mathrm{c}\alpha & 2L^2 \\ -12\mathrm{s}^2\alpha & 12\mathrm{s}\alpha\mathrm{c}\alpha & 6L\mathrm{s}\alpha & -12\mathrm{s}^2\alpha & -12\mathrm{s}\alpha\mathrm{c}\alpha & 6L\mathrm{s}\alpha \\ 12\mathrm{s}\alpha\mathrm{c}\alpha & -12\mathrm{c}^2\alpha & -6L\mathrm{c}\alpha & -12\mathrm{s}\alpha\mathrm{c}\alpha & 12\mathrm{c}^2\alpha & -6L\mathrm{c}\alpha \\ -6L\mathrm{s}\alpha & 6L\mathrm{c}\alpha & 2L^2 & 6L\mathrm{s}\alpha & -6L\mathrm{c}\alpha & 4L^2 \end{bmatrix}. \tag{5.154}$$

The sines and cosines values of the rotation angle α can be calculated through the global node coordinates via

$$\mathrm{s}\alpha \stackrel{\wedge}{=} \sin\alpha = \frac{Y_2 - Y_1}{L} \quad \text{or} \quad \mathrm{c}\alpha \stackrel{\wedge}{=} \cos\alpha = \frac{X_2 - X_1}{L} \tag{5.155}$$

and

$$L = \sqrt{(X_2 - X_1)^2 + (Y_2 - Y_1)^2}. \tag{5.156}$$

It needs to be remarked at this point, that in a mathematical positive sense the angle α always should be plotted from the global to the local coordinate system. The mathematical positive direction of rotation and therefore the algebraic sign of α is illustrated in Fig. 5.18. However, independent from the algebraic sign of α the calculation can always occur according to Eq. (5.155).
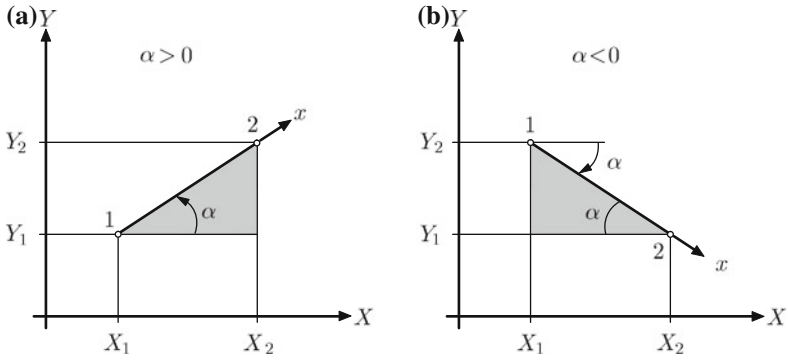
Fig. 5.18 Rotation angle: **a** α positive; **b** α negative

5.6 Transformation Within the Space

For the derivation of the transformation relation within the space, the global (X, Y, Z) and local (x, y, z) coordinate system, illustrated in Fig. 5.19 will be considered.
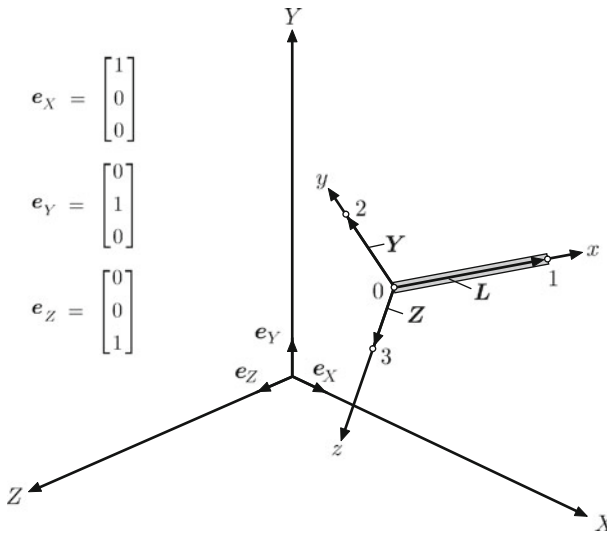
Fig. 5.19 Rotatory transformation of a beam element within the space. The unit vectors in the direction of the global X-, Y- and Z-axis are referred to as $\boldsymbol{e}_i$. Adapted from [7]

The bending beam 0-1 is represented through the following vector $\boldsymbol{L}$, which is oriented in the direction of the local x-axis:

$$\boldsymbol{L} = (X_1 - X_0)\boldsymbol{e}_X + (Y_1 - Y_0)\boldsymbol{e}_Y + (Z_1 - Z_0)\boldsymbol{e}_Z . \qquad (5.157)$$

A vector in the direction of the local y-axis can, according to Fig. 5.19, be represented as

$$\boldsymbol{Y} = (X_2 - X_0)\boldsymbol{e}_X + (Y_2 - Y_0)\boldsymbol{e}_Y + (Z_2 - Z_0)\boldsymbol{e}_Z. \tag{5.158}$$

The direction cosines between the local y-axis and the global coordinate axes result through the global node coordinates to

$$l_y = \cos(y, X) = \frac{X_2 - X_0}{|\boldsymbol{Y}|}, \tag{5.159}$$

$$m_y = \cos(y, Y) = \frac{Y_2 - Y_0}{|\boldsymbol{Y}|}, \tag{5.160}$$

$$n_y = \cos(y, Z) = \frac{Z_2 - Z_0}{|\boldsymbol{Y}|} \tag{5.161}$$

at which the length of the vector $\boldsymbol{Y}$ results as follows:

$$|\boldsymbol{Y}| = \sqrt{(X_2 - X_0)^2 + (Y_2 - Y_0)^2 + (Z_2 - Z_0)^2}. \tag{5.162}$$

Accordingly, a vector in the direction of the local z-axis results in:

$$\boldsymbol{Z} = (X_3 - X_0)\boldsymbol{e}_X + (Y_3 - Y_0)\boldsymbol{e}_Y + (Z_3 - Z_0)\boldsymbol{e}_Z \tag{5.163}$$

and the direction cosines as

$$l_z = \cos(z, X) = \frac{X_3 - X_0}{|\boldsymbol{Z}|}, \tag{5.164}$$

$$m_z = \cos(z, Y) = \frac{Y_3 - Y_0}{|\boldsymbol{Z}|}, \tag{5.165}$$

$$n_z = \cos(z, Z) = \frac{Z_3 - Z_0}{|\boldsymbol{Z}|} \tag{5.166}$$

whereupon the length of the vector $\boldsymbol{Z}$ results as follows:

$$|\boldsymbol{Z}| = \sqrt{(X_3 - X_0)^2 + (Y_3 - Y_0)^2 + (Z_3 - Z_0)^2}. \tag{5.167}$$

An arbitrary vector $\boldsymbol{v}$ can be transformed via the following relation between the local (x, y, z) and the global (X, Y, Z) coordinate system:

$$\boldsymbol{v}_{xyz} = \boldsymbol{T}\boldsymbol{v}_{XYZ}, \tag{5.168}$$

$$\boldsymbol{v}_{XYZ} = \boldsymbol{T}^{\mathrm{T}}\boldsymbol{v}_{xyz}, \tag{5.169}$$

whereupon the transformation matrix can be represented as follows through the direction cosines:

$$
\boldsymbol{T} = \begin{bmatrix} l_x & m_x & n_x \\ l_y & m_y & n_y \\ l_z & m_z & n_z \end{bmatrix} = \begin{bmatrix} \cos(x,X) & \cos(x,Y) & \cos(x,Z) \\ \cos(y,X) & \cos(y,Y) & \cos(y,Z) \\ \cos(z,X) & \cos(z,Y) & \cos(z,Z) \end{bmatrix} . \tag{5.170}
$$

This bending beam does not exhibit an axial deformation, meaning in the direction of the local x-axis, and the first line in the matrix according to Eq. (5.170) can be eliminated.

For small angles the rotation angle can be summarized in one vector and also be transformed according to Eqs. (5.168) and (5.169) between the coordinate systems. Since no torsion around the length axis is designated for this element, the first line of Eq. (5.170) can also be eliminated here. Consequently the total transformation from global to local deformations results in:

$$
\begin{bmatrix} u_{1y} \\ u_{1z} \\ \varphi_{1y} \\ \varphi_{1z} \\ u_{2y} \\ u_{2z} \\ \varphi_{2y} \\ \varphi_{2z} \end{bmatrix} = \underbrace{\begin{bmatrix} l_y\ m_y\ n_y & 0\ 0\ 0 & 0\ 0\ 0 & 0\ 0\ 0 \\ l_z\ m_z\ n_z & 0\ 0\ 0 & 0\ 0\ 0 & 0\ 0\ 0 \\ 0\ 0\ 0 & l_y\ m_y\ n_y & 0\ 0\ 0 & 0\ 0\ 0 \\ 0\ 0\ 0 & l_z\ m_z\ n_z & 0\ 0\ 0 & 0\ 0\ 0 \\ 0\ 0\ 0 & 0\ 0\ 0 & l_y\ m_y\ n_y & 0\ 0\ 0 \\ 0\ 0\ 0 & 0\ 0\ 0 & l_z\ m_z\ n_z & 0\ 0\ 0 \\ 0\ 0\ 0 & 0\ 0\ 0 & 0\ 0\ 0 & l_y\ m_y\ n_y \\ 0\ 0\ 0 & 0\ 0\ 0 & 0\ 0\ 0 & l_z\ m_z\ n_z \end{bmatrix}}_{\boldsymbol{T}} \begin{bmatrix} u_{1X} \\ u_{1Y} \\ u_{1Z} \\ \varphi_{1X} \\ \varphi_{1Y} \\ \varphi_{1Z} \\ u_{2X} \\ u_{2Y} \\ u_{2Z} \\ \varphi_{2X} \\ \varphi_{2Y} \\ \varphi_{2Z} \end{bmatrix} . \tag{5.171}
$$

If the transformation from local to global deformations is considered, the following transpose can be used:

$$
\boldsymbol{T}^{\mathrm{T}} = \begin{bmatrix} l_y & l_z & 0\ 0 & 0\ 0 & 0\ 0 \\ m_y & m_z & 0\ 0 & 0\ 0 & 0\ 0 \\ n_y & n_z & 0\ 0 & 0\ 0 & 0\ 0 \\ 0\ 0 & l_y & l_z & 0\ 0 & 0\ 0 \\ 0\ 0 & m_y & m_z & 0\ 0 & 0\ 0 \\ 0\ 0 & n_y & n_z & 0\ 0 & 0\ 0 \\ 0\ 0 & 0\ 0 & l_y & l_z & 0\ 0 \\ 0\ 0 & 0\ 0 & m_y & m_z & 0\ 0 \\ 0\ 0 & 0\ 0 & n_y & n_z & 0\ 0 \\ 0\ 0 & 0\ 0 & 0\ 0 & l_y & l_z \\ 0\ 0 & 0\ 0 & 0\ 0 & m_y & m_z \\ 0\ 0 & 0\ 0 & 0\ 0 & n_y & n_z \end{bmatrix} . \tag{5.172}
$$

According to the executions in Sect. 5.5, the transformation of the stiffness matrix results in:

$$k_{XYZ}^e = T^T k^e T \,. \tag{5.173}$$

5.7 Determination of Equivalent Nodal Loads

Within the finite element method, external loads can only take effect on the nodes. If distributed loads or point loads[18] appear between the nodes, those have to be converted into equivalent nodal loads. The procedure can be demonstrated in the following for the example of a both-way clamped beam, see Fig. 5.20. First a pragmatic approach will be shown, for which the in Fig. 5.20b the illustrated equivalent statical system forms the basis. Support reactions, consisting of vertical forces and moments occur on the fixed supports, whereby the goal is at this point to determine the inner reactions, which are in effect on the beam borders.

As a starting point the differential equation of the bending line according to Eq. (5.36) in the form according to our problem, meaning with negative load, is chosen:

$$E I_z \frac{d^4 u_y}{dx^4} = -q_y \,. \tag{5.174}$$

Four-time integration yields the general approach for the bending line:

$$E I_z \frac{d^3 u_y}{dx^3} = -q_y x + c_1 \overset{!}{=} -Q_y(x) \,, \tag{5.175}$$

$$E I_z \frac{d^2 u_y}{dx^2} = -\frac{1}{2} q_y x^2 + c_1 x + c_2 \overset{!}{=} M_z(x) \,, \tag{5.176}$$

$$E I_z \frac{d^1 u_y}{dx^1} = -\frac{1}{6} q_y x^3 + \frac{1}{2} c_1 x^2 + c_2 x + c_3 \,, \tag{5.177}$$

$$E I_z u_y(x) = -\frac{1}{24} q_y x^4 + \frac{1}{6} c_1 x^3 + \frac{1}{2} c_2 x^2 + c_3 x + c_4 \,. \tag{5.178}$$

If the boundary conditions are taken into consideration, meaning $u_y(0) = u_y(L) = 0$ and $\varphi_z(0) = \varphi_z(L) = 0$, the four integration constants result in:

$$c_3 = c_4 = 0 \,, \tag{5.179}$$

$$c_2 = -\frac{1}{12} q_y L^2 \,, \tag{5.180}$$

$$c_1 = \frac{1}{2} q_y L \,. \tag{5.181}$$

---

[18] If point loads appear between nodes, the discretization can of course be further sub-divided, so that a new node is positioned on the location of the loading point. However within this chapter the case of no further subdivision of the mesh ought to be regarded.

Fig. 5.20 Calculation of equivalent nodal loads: **a** example configuration; **b** equivalent statical system; **c** free body diagram with support reactions
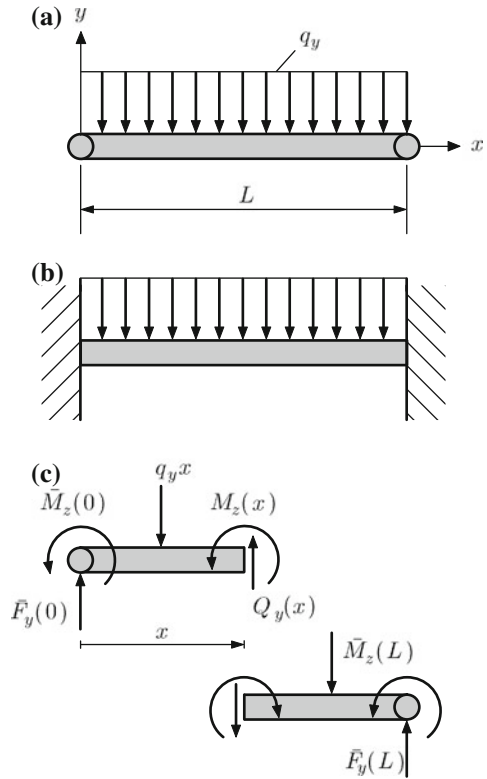
Through these integration constants and the relations in Eqs. (5.175) and (5.176), one obtains the shear force and bending moment distribution within the element:

$$Q_y(x) = -\frac{1}{2} q_y L + q_y x \,, \tag{5.182}$$

$$M_z(x) = -\frac{1}{12} q_y L^2 + \frac{1}{2} q_y L x - \frac{1}{2} q_y x^2 \,. \tag{5.183}$$

Evaluation on the boundaries, meaning for $x = 0$ and $x = L$ leads to the following values of the internal reactions:

$$Q_y(0) = -\frac{1}{2} q_y L \,, \qquad\qquad M_z(0) = -\frac{1}{12} q_y L^2 \,, \tag{5.184}$$

$$Q_y(L) = +\frac{1}{2} q_y L \,, \qquad\qquad M_z(L) = -\frac{1}{12} q_y L^2 \,. \tag{5.185}$$

The support reactions can be defined through the load and moment equilibrium according to Fig. 5.21. Thus the vertical equilibrium of forces yields
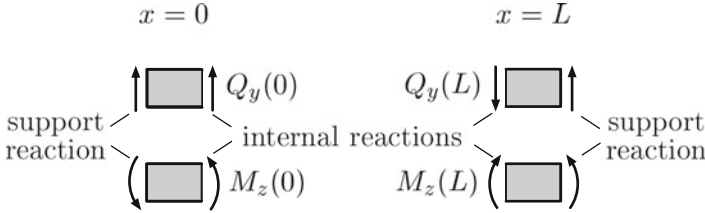
Fig. 5.21 Support and internal reactions at the boundaries of the beam from Fig. 5.20. The support reactions have the direction, which is defined in Fig. 5.20; the internal reactions are according to Fig. 5.7 positive oriented on the corresponding cutting planes

$$+\bar{F}_y(0) + Q_y(0) = 0\,, \tag{5.186}$$

and accordingly all support reactions $\bar{F}_y$ and $\bar{M}_z$ result:

$$\bar{F}_y(0) = -\frac{1}{2}q_y L\,, \qquad\qquad \bar{M}_z(0) = -\frac{1}{12}q_y L^2\,, \tag{5.187}$$

$$\bar{F}_y(L) = +\frac{1}{2}q_y L\,, \qquad\qquad \bar{M}_z(L) = -\frac{1}{12}q_y L^2\,. \tag{5.188}$$

Taking into consideration the definition of the positive direction of the external loads of a beam element according to Fig. 5.13, the equivalent loads on nodes F_{iy} and M_{iz} result through evaluation of the internal reactions Q_y and M_z to:

$$F_{1y} = -\frac{1}{2}q_y L\,, \qquad\qquad M_{1z} = -\frac{1}{12}q_y L^2\,, \tag{5.189}$$

$$F_{2y} = -\frac{1}{2}q_y L\,, \qquad\qquad M_{2z} = +\frac{1}{12}q_y L^2\,. \tag{5.190}$$

It should to be remarked at this point that the equivalent nodal loads are *not* the support reactions. The equivalent nodal loads have to cause the support reactions. At the end of this derivation it is appropriate to point out that at this point it was distinguished between the following parameters:

- internal reactions $Q_y(x)$, $M_z(x)$,
- support reactions $\bar{F}_y$, $\bar{M}_z$ and
- equivalent nodal loads F_{iy}, M_{iz}.

Alternatively, the derivation of the equivalent nodal loads can also take place through the equivalence of the potential of the external loads, meaning the distributed load and the equivalent nodal loads:

$$\Pi_{\text{ext}} = - \int_0^L q_y(x) u_y(x) \mathrm{d}x \overset{!}{=} - \left(F_{1y} u_{1y} + M_{1z} \varphi_{1z} + F_{2y} u_{2y} + M_{2z} \varphi_{2z} \right) .$$

(5.191)

Through application of the approach for the displacement $u_y(x)$ according to Eq. (5.68) the potential of a distributed load can be illustrated as

$$\Pi_{\text{ext}} = - \int_0^L q_y(x) \left(N_{1u} u_{1y} + N_{1\varphi} \varphi_{1z} + N_{2u} u_{2y} + N_{2\varphi} \varphi_{2z} \right) \mathrm{d}x \qquad (5.192)$$

or under consideration that the nodal values of the deformation can be considered as constant for the integration, as

$$\Pi_{\text{ext}} = - \left(\int_0^L q_y(x) N_{1u}(x) \mathrm{d}x \, u_{1y} + \int_0^L q_y(x) N_{1\varphi}(x) \mathrm{d}x \, \varphi_{1z} + \qquad (5.193) \right.$$

$$\left. \int_0^L q_y(x) N_{2u}(x) \mathrm{d}x \, u_{2y} + \int_0^L q_y(x) N_{2\varphi}(x) \mathrm{d}x \, \varphi_{2z} \right) . \qquad (5.194)$$

A comparison of the two potentials finally delivers equivalent nodal loads to

$$F_{1y} = \int_0^L q_y(x) N_{1u}(x) \, \mathrm{d}x , \qquad (5.195)$$

$$M_{1z} = \int_0^L q_y(x) N_{1\varphi}(x) \, \mathrm{d}x , \qquad (5.196)$$
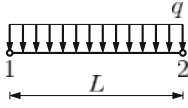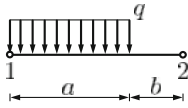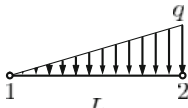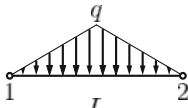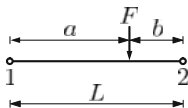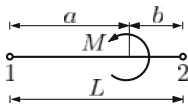
$$F_{2y} = \int_0^L q_y(x) N_{2u}(x) \, \mathrm{d}x , \qquad (5.197)$$

$$M_{2z} = \int_0^L q_y(x) N_{2\varphi}(x) \, \mathrm{d}x , \qquad (5.198)$$

whereas the shape functions according to Eqs. (5.64)–(5.67) have to be used.
If, for example, on a point $x = a$ an external force F acts on the beam, the external potential results in

$$\Pi_{\text{ext}} = -F u_y(a) . \qquad (5.199)$$

Table 5.8 Equivalent nodal loads for bending elements. Adapted from [19]

Load	Shear force	Bending moment
(uniform load q over L)	$F_{1y} = -\dfrac{qL}{2}$ $F_{2y} = -\dfrac{qL}{2}$	$M_{1z} = -\dfrac{qL^2}{12}$ $M_{2z} = +\dfrac{qL^2}{12}$
(partial uniform load q over a, b)	$F_{1y} = -\dfrac{qa}{2L^3}(a^3 - 2a^2L + 2L^3)$ $F_{2y} = -\dfrac{qa^3}{2L^3}(2L - a)$	$M_{1z} = -\dfrac{qa^2}{12L^2}(3a^2 - 8aL + 6L^2)$ $M_{2z} = +\dfrac{qa^3}{12L^2}(4L - 3a)$
(triangular load q over L)	$F_{1y} = -\dfrac{3}{20}qL$ $F_{2y} = -\dfrac{7}{20}qL$	$M_{1z} = -\dfrac{qL^2}{30}$ $M_{2z} = +\dfrac{qL^2}{20}$
(triangular peak load q over L)	$F_{1y} = -\dfrac{1}{4}qL$ $F_{2y} = -\dfrac{1}{4}qL$	$M_{1z} = -\dfrac{5qL^2}{96}$ $M_{2z} = +\dfrac{5qL^2}{96}$
(point force F at a, b)	$F_{1y} = -\dfrac{Fb^2(3a + b)}{L^3}$ $F_{2y} = -\dfrac{Fa^2(a + 3b)}{L^3}$	$M_{1z} = -\dfrac{Fb^2a}{L^2}$ $M_{2z} = +\dfrac{Fa^2b}{L^2}$
(moment M at a, b)	$F_{1y} = -6M\dfrac{ab}{L^3}$ $F_{2y} = +6M\dfrac{ab}{L^3}$	$M_{1z} = -M\dfrac{b(2a - b)}{L^2}$ $M_{2z} = -M\dfrac{a(2b - a)}{L^2}$

A comparison of the two potentials delivers for this case the equivalent nodal loads to:

$$F_{1y} = F N_{1u}(a), \tag{5.200}$$

$$M_{1z} = F N_{1\varphi}(a), \tag{5.201}$$

$$F_{2y} = F N_{2u}(a), \tag{5.202}$$

$$M_{2z} = F N_{2\varphi}(a). \tag{5.203}$$

Equivalent nodal loads for simple loading cases are summarized in Table 5.8. It needs to be remarked at the end of this chapter, that the column matrix of the equivalent nodal loads can be reached in an easier way, if during the application of the weighted residual method the differential equation (5.36) under consideration of the distributed load is used. Under consideration of an arbitrary distributed load the inner product results in:

Fig. 5.22 Sample problem
bending beam: **a** point load; **b**
single moment
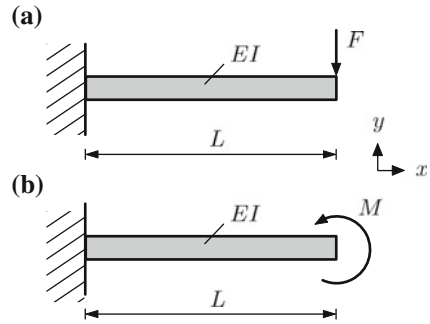
$$\int\limits_0^L W(x)\left(EI_z\frac{\mathrm{d}^4 u_y(x)}{\mathrm{d}x^4} - q_y(x)\right)\mathrm{d}x \stackrel{!}{=} 0. \tag{5.204}$$

After the introduction of the approach for the weighting function, meaning $W(x) = \delta u_\mathrm{p}^\mathrm{T} N^\mathrm{T}(x)$, the expression with the distributed load can be brought on the right-hand side and after cancelling down of $\delta u_\mathrm{p}^\mathrm{T}$ the additional load matrix results:

$$\cdots = \cdots + \int\limits_0^L q_y(x)\begin{bmatrix} N_{1u} \\ N_{1\varphi} \\ N_{2u} \\ N_{2\varphi} \end{bmatrix}\mathrm{d}x. \tag{5.205}$$

This expression equals exactly the Eqs. (5.195)–(5.198).

5.8 Sample Problems and Supplementary Problems

5.8.1 Sample Problems

5.1. Sample: Bending of beam under point load or moment—approximation through a single finite element
The displacement and the rotation of the right-hand end of the beam, which is illustrated in Fig. 5.22 have to be determined through a single finite element. Subsequently the course of the bending line $u_y = u_y(x)$ has to be determined and the finite element solution has to be compared with the analytical solution.
5.1 Solution
(a) The finite element equation on element level according to Eq. (5.87) reduces for the illustrated loading case to:

$$\frac{EI_z}{L^3}\begin{bmatrix} 12 & 6L & -12 & 6L \\ 6L & 4L^2 & -6L & 2L^2 \\ -12 & -6L & 12 & -6L \\ 6L & 2L^2 & -6L & 4L^2 \end{bmatrix}\begin{bmatrix} u_{1y} \\ \varphi_{1z} \\ u_{2y} \\ \varphi_{2z} \end{bmatrix} = \begin{bmatrix} 0 \\ 0 \\ -F \\ 0 \end{bmatrix}. \tag{5.206}$$

Since the displacement and the rotation are zero on the left-hand boundary due to the fixed support, the first two lines and columns of the system of equations can be eliminated:

$$\frac{EI_z}{L^3}\begin{bmatrix} 12 & -6L \\ -6L & 4L^2 \end{bmatrix}\begin{bmatrix} u_{2y} \\ \varphi_{2z} \end{bmatrix} = \begin{bmatrix} -F \\ 0 \end{bmatrix}. \tag{5.207}$$

Solving for the unknown deformations yields:

$$\begin{bmatrix} u_{2y} \\ \varphi_{2z} \end{bmatrix} = \frac{L^3}{EI_z}\begin{bmatrix} 12 & -6L \\ -6L & 4L^2 \end{bmatrix}^{-1}\begin{bmatrix} -F \\ 0 \end{bmatrix} \tag{5.208}$$

$$= \frac{L^3}{EI_z(48L^2 - 36L^2)}\begin{bmatrix} 4L^2 & 6L \\ 6L & 12 \end{bmatrix}\begin{bmatrix} -F \\ 0 \end{bmatrix} = \begin{bmatrix} -\frac{FL^3}{3EI_z} \\ -\frac{FL^2}{2EI_z} \end{bmatrix}. \tag{5.209}$$

According to Table 5.7, the analytical displacement results in:

$$u_y(x = L) = -\frac{F}{6EI_z}\left(3L^3 - L^3\right) = -\frac{FL^3}{3EI_z}. \tag{5.210}$$

The analytical solution for the rotation results from differentiation of the general displacement distribution according to Table 5.7 for $a = L$ to:

$$\varphi_z(x) = \frac{\mathrm{d}u_y(x)}{\mathrm{d}x} = -\frac{F}{6EI_z} \times \left[6Lx - 3x^2\right], \tag{5.211}$$

or alternatively on the right-hand boundary:

$$\varphi_z(x = L) = -\frac{F}{6EI_z} \times \left[6L^2 - 3L^2\right] = -\frac{FL^2}{2EI_z}. \tag{5.212}$$

The course of the bending line $u_y = u_y(x)$ results from the finite element solution through Eq. (5.68) and the shape functions (5.66) and (5.67) to:

$$\begin{aligned} u_y(x) &= N_{2u}(x)u_{2y} + N_{2\varphi}(x)\varphi_{2z} \\ &= \left[3\left(\frac{x}{L}\right)^2 - 2\left(\frac{x}{L}\right)^3\right]\left(-\frac{FL^3}{3EI_z}\right) + \left[-\frac{x^2}{L} + \frac{x^3}{L^2}\right]\left(-\frac{FL^2}{2EI_z}\right) \\ &= \frac{F}{6EI_z}\left(x^3 - 3Lx^2\right). \end{aligned} \tag{5.213}$$

According to Table 5.7 this course matches with the analytical solution.
Conclusion: Finite element solution and analytical solution are identical!

(b) The reduced system of equations in this case results in:

$$\frac{EI_z}{L^3}\begin{bmatrix} 12 & -6L \\ -6L & 4L^2 \end{bmatrix}\begin{bmatrix} u_{2y} \\ \varphi_{2z} \end{bmatrix} = \begin{bmatrix} 0 \\ M \end{bmatrix}.$$ (5.214)

Solving for the unknown deformations yields:

$$\begin{bmatrix} u_{2y} \\ \varphi_{2z} \end{bmatrix} = \frac{L^3}{12EI_zL^2}\begin{bmatrix} 4L^2 & 6L \\ 6L & 12 \end{bmatrix}\begin{bmatrix} 0 \\ M \end{bmatrix} = \begin{bmatrix} \frac{ML^2}{2EI_z} \\ \frac{ML}{EI_z} \end{bmatrix}.$$ (5.215)

The analytical solution according to Table 5.7 delivers

$$u_y(x = L) = -\frac{M}{2EI_z}\left(-L^2\right) = \frac{ML^2}{2EI_z},$$ (5.216)

or alternatively the rotation in general for $a = L$ to:

$$\varphi_z(x) = \frac{\mathrm{d}u_y(x)}{\mathrm{d}x} = -\frac{M}{2EI_z}(-2x)$$ (5.217)

or only on the right-hand boundary:

$$\varphi_z(x = L) = -\frac{M}{2EI_z}(-L) = \frac{ML}{EI_z}.$$ (5.218)

The course of the bending line $u_y = u_y(x)$ results from the finite element solution
through Eq. (5.68) and the shape functions (5.66) and (5.67) to:

$$\begin{aligned} u_y(x) &= N_{2u}(x)u_{2y} + N_{2\varphi}(x)\varphi_{2z} \\ &= \left[3\left(\frac{x}{L}\right)^2 - 2\left(\frac{x}{L}\right)^3\right]\left(\frac{ML^2}{2EI_z}\right) + \left[-\frac{x^2}{L} + \frac{x^3}{L^2}\right]\left(\frac{ML}{EI_z}\right) \\ &= \frac{Mx^2}{2EI_z}. \end{aligned}$$ (5.219)

According to Table 5.7 this course matches with the analytical solution.
Conclusion: Finite element solution and analytical solution are identical!

5.2. Sample: Bending beam under constant distributed load—approximation through a single finite element

The displacement and the rotation (a) of the right-hand boundary and (b) in the
middle of the beam have to be determined for the beam under constant distributed

load, which is illustrated in Fig. 5.23 through a single finite element. Subsequently the course of the bending line $u_y = u_y(x)$ has to be determined and the finite element solution has to be compared with the analytical solution.

(a)   **(b)**
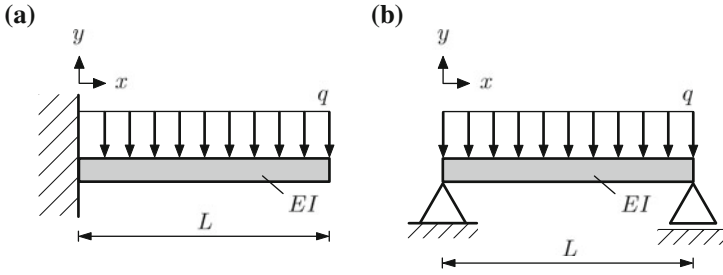
Fig. 5.23 Sample problem bending beam under constant distributed load at different supports: **a** cantilever beam and **b** simply supported beam

5.2 Solution

To solve the problem at first the constant distributed load has to be converted into equivalent nodal loads. These equivalent nodal loads can be extracted from Table 5.8 for the considered case, and the finite element equation results to:

$$\frac{EI_z}{L^3}\begin{bmatrix} 12 & 6L & -12 & 6L \\ 6L & 4L^2 & -6L & 2L^2 \\ -12 & -6L & 12 & -6L \\ 6L & 2L^2 & -6L & 4L^2 \end{bmatrix}\begin{bmatrix} u_{1y} \\ \varphi_{1z} \\ u_{2y} \\ \varphi_{2z} \end{bmatrix} = \begin{bmatrix} -\frac{qL}{2} \\ -\frac{qL^2}{12} \\ -\frac{qL}{2} \\ +\frac{qL^2}{12} \end{bmatrix}. \tag{5.220}$$

(a) Consideration of the support conditions from Fig. 5.23a, meaning the fixed support on the left-hand boundary, and solving for the unknowns yields:

$$\begin{bmatrix} u_{2y} \\ \varphi_{2z} \end{bmatrix} = \frac{L}{12EI_z}\begin{bmatrix} 4L^2 & 6L \\ 6L & 12 \end{bmatrix}\begin{bmatrix} -\frac{qL}{2} \\ +\frac{qL^2}{12} \end{bmatrix} = \begin{bmatrix} -\frac{qL^4}{8EI_z} \\ -\frac{qL^3}{6EI_z} \end{bmatrix}. \tag{5.221}$$

The analytical solution according to Table 5.7 yields

$$u_y(x = L) = -\frac{q}{24EI_z}\left(6L^4 - 4L^4 + L^4\right) = -\frac{qL^4}{8EI_z}, \tag{5.222}$$

or alternatively the rotation in general for $a_1 = 0$ and $a_2 = L$ to:

$$\varphi_z(x) = \frac{du_y(x)}{dx} = -\frac{q}{24EI_z}\left(12L^2x - 12Lx^2 + 4x^3\right) \tag{5.223}$$
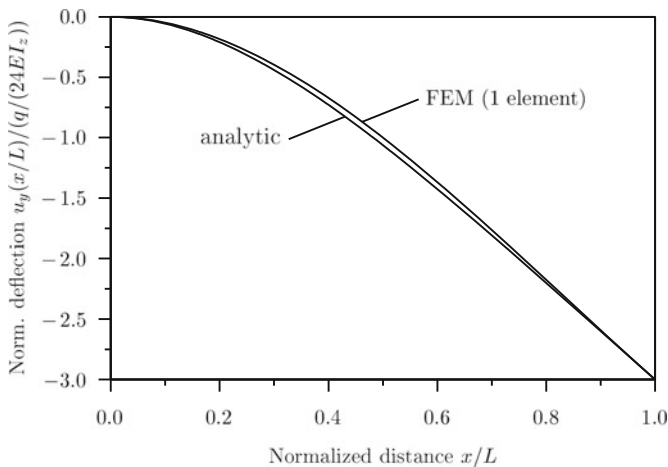
Fig. 5.24 Comparison of the analytical and the finite element solution for the beam according to Fig. 5.23a

or only on the right-hand boundary:

$$\varphi_z(x = L) = -\frac{q}{24EI_z}\left(12L^3 - 12L^3 + 4L^3\right) = -\frac{qL^3}{6EI_z}. \tag{5.224}$$

The course of the bending line $u_y = u_y(x)$ results from the finite element solution through Eq. (5.68) and the shape functions (5.66) and (5.67) to:

$$\begin{aligned}
u_y(x) &= N_{2u}(x)u_{2y} + N_{2\varphi}(x)\varphi_{2z}\\
&= \left[3\left(\frac{x}{L}\right)^2 - 2\left(\frac{x}{L}\right)^3\right]\left(-\frac{qL^4}{8EI_z}\right) + \left[-\frac{x^2}{L} + \frac{x^3}{L^2}\right]\left(-\frac{qL^3}{6EI_z}\right)\\
&= -\frac{q}{24EI_z}\left(-2Lx^3 + 5L^2x^2\right),
\end{aligned} \tag{5.225}$$

however the analytical course according to Table 5.7 results in $u_y(x) = -\frac{q}{24EI_z}$ $(x^4 - 4Lx^3 + 6L^2x^2)$, meaning the analytical and therefore the exact course is not identical with the numerical solution between the nodes $(0 < x < L)$, see Fig. 5.24. One can see that between the nodes a small difference between the two solutions arises. If a higher accuracy is demanded between those two nodes, the beam has to be divided into more elements.

Conclusion: Finite element solution and the analytical solution are only identical on the nodes!

(b) Consideration of the support conditions from Fig. 5.23b, meaning the simple support and the roller support, yields through the elimination of the first and third line and column of the system of equations (5.220):
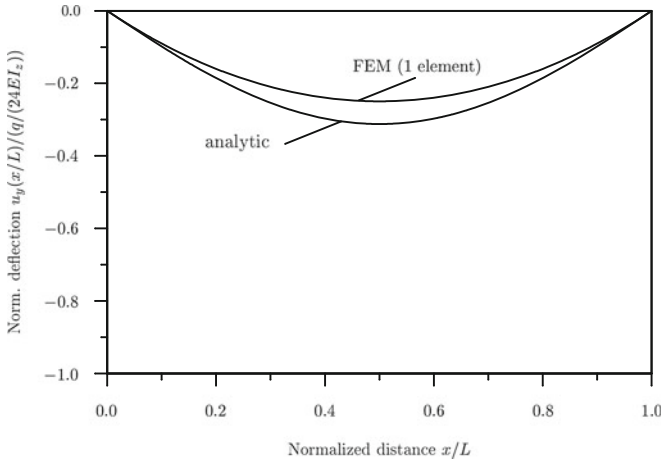
Fig. 5.25 Comparison of the analytical and the finite element solution for the beam according to Fig. 5.23b

$$\frac{EI_z}{L^3} \begin{bmatrix} 4L^2 & 2L^2 \\ 2L^2 & 4L^2 \end{bmatrix} \begin{bmatrix} \varphi_{1z} \\ \varphi_{2z} \end{bmatrix} = \begin{bmatrix} -\frac{qL^2}{12} \\ +\frac{qL^2}{12} \end{bmatrix}. \tag{5.226}$$

Solving for the unknowns yields:

$$\begin{bmatrix} \varphi_{1z} \\ \varphi_{2z} \end{bmatrix} = \frac{1}{12EI_zL} \begin{bmatrix} 4L^2 & -2L^2 \\ -2L^2 & 4L^2 \end{bmatrix} \begin{bmatrix} -\frac{qL^2}{12} \\ +\frac{qL^2}{12} \end{bmatrix} = \begin{bmatrix} -\frac{qL^3}{24EI_z} \\ +\frac{qL^3}{24EI_z} \end{bmatrix}. \tag{5.227}$$

The course of the bending line $u_y = u_y(x)$ results from the finite element solution through Eq. (5.68) and the shape functions (5.65) and (5.67) to:

$$\begin{aligned} u_y(x) &= N_{1\varphi}(x)\varphi_{1z} + N_{2\varphi}(x)\varphi_{2z} \\ &= \left[x - 2\frac{x^2}{L} + \frac{x^3}{L^2} \right] \left(-\frac{qL^3}{24EI_z} \right) + \left[-\frac{x^2}{L} + \frac{x^3}{L^2} \right] \left(+\frac{qL^3}{24EI_z} \right) \\ &= -\frac{q}{24EI_z} \left(-L^2x^2 + L^3x \right), \end{aligned} \tag{5.228}$$

however the analytical course according to Table 5.7 results in $u_y(x) = -\frac{q}{24EI_z}$ $(x^4 - 2Lx^3 + L^3x)$, meaning the analytical and therefore exact course is also at this point not identical with the numerical solution between the nodes ($0 < x < L$), see Fig. 5.25.

The numerical solution for the deflection in the middle of the beam yields $u_y(x = \frac{1}{2}L) = \frac{-4qL^4}{384EI_z}$, however the exact solution is $u_y(x = \frac{1}{2}L) = \frac{-5qL^4}{384EI_z}$.

Conclusion: Finite element solution and analytical solution are only identical on the nodes!

5.3. Sample: Bending beam with variable cross-section

The beam, which is illustrated in Fig. 5.26, has along the x-axis a variable cross-section. One derives for

(a) a circular cross-section,
(b) a square cross-section

the element stiffness matrix for the case $d_1 = 2h$ and $d_2 = h$.

Fig. 5.26 Sample problem
bending beam with variable
cross-section: **a** change along
the x-axis; **b** *circular* cross-
section; **c** *square* cross-section
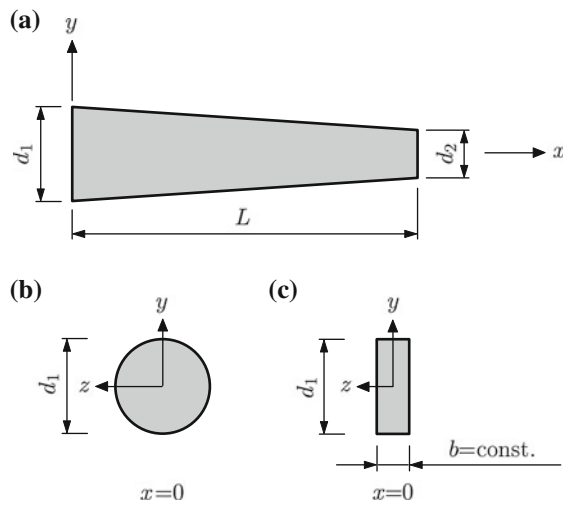
5.3 Solution
(a) Square cross-section:
Equation (5.75) can be used as an initial point for the derivation of the stiffness matrix:

$$k^e = E \int_x \left(\underbrace{\int_A y^2 dA}_{I_z} \right) \frac{d^2 N^T(x)}{dx^2} \frac{d^2 N(x)}{dx^2} dx . \qquad (5.229)$$

Since the axial second moment of area changes along the x-axis, a corresponding function has to be derived at first. An elegant method would be to use the polar second moment of area of the circle, since in this case the function equation of the radius along the x-axis can be used. Hereby the relation, that the polar second moment of area consists of the two axial second moments of area I_y and I_z additively, is used:

$$I_p = \int_A r^2 dA = I_y + I_z . \qquad (5.230)$$

Since the axial second moments of area of a circle are identical, the following expression can be derived for I_z:

$$I_z(x) = \frac{1}{2} I_p(x) = \frac{1}{2} \int_A r^2 dA = \frac{1}{2} \int_{\alpha=0}^{2\pi} \int_0^{r(x)} \hat{r}^2 \underbrace{\hat{r} d\hat{r} d\alpha}_{dA} \tag{5.231}$$

$$= \pi \int_0^{r(x)} \hat{r}^3 d\hat{r} = \pi \left[\frac{1}{4} \hat{r}^4 \right]_0^{r(x)} = \frac{\pi}{4} r(x)^4 . \tag{5.232}$$

The change of the radius along the x-axis can be easily derived from Fig. 5.26a:

$$r(x) = h \left(1 - \frac{x}{2L} \right) = \frac{h}{2} \left(2 - \frac{x}{L} \right) . \tag{5.233}$$

Therefore the axial second moment of area results in

$$I_z(x) = \frac{\pi h^4}{64} \left(2 - \frac{x}{L} \right)^4 \tag{5.234}$$

and can be used in Eq. (5.229):

$$k^e = E \frac{\pi h^4}{64} \int_L \left(2 - \frac{x}{L} \right)^4 \frac{d^2 N^T(x)}{dx^2} \frac{d^2 N(x)}{dx^2} dx . \tag{5.235}$$

The integration can be carried out through the second order derivatives of the shape function according to Eqs. (5.82)–(5.85). As an example for the first component of the stiffness matrix

$$k_{11} = E \frac{\pi h^4}{64} \int_L \left(2 - \frac{x}{L} \right)^4 \left(-\frac{6}{L^2} + \frac{12x}{L^3} \right)^2 dx , \tag{5.236}$$

is used and the entire stiffness matrix finally results after a short calculation:

$$k_{circle}^e = \frac{E}{L^3} \frac{\pi h^4}{64} \begin{bmatrix} \frac{2988}{35} & \frac{1998}{35} L & -\frac{2988}{35} & \frac{198}{7} L \\ \frac{1998}{35} L & \frac{1468}{35} L^2 & -\frac{1998}{35} L & \frac{106}{7} L^2 \\ -\frac{2988}{35} & -\frac{1998}{35} L & \frac{2988}{35} & -\frac{198}{7} L \\ \frac{198}{7} L & \frac{106}{7} L^2 & -\frac{198}{7} L & \frac{92}{7} L^2 \end{bmatrix} . \tag{5.237}$$

(b) Square cross-section:
Regarding the square cross-section, Eq. (5.229) serves as a basis as well. However in this case it seems to be a good idea to go back to the definition of I_z immediately:

$$I_z(x) = \int\limits_A y^2 \mathrm{d}A = \int\limits_{-y(x)}^{y(x)} \hat{y}^2 \underbrace{b\mathrm{d}\hat{y}}_{\mathrm{d}A} = b\left[\frac{1}{3}\hat{y}^3\right]_{-y(x)}^{y(x)} = \frac{2b}{3}y(x)^3 . \qquad (5.238)$$

The course of the function $y(x)$ of the cross-section is identical with the radius of the task part 1 (a) meaning $y(x) = h(1 - \frac{x}{2L})$ and the second moment of area in this case results in:

$$I_z(x) = \frac{2bh^3}{3}\left(1 - \frac{x}{2L}\right)^3 = \frac{bh^3}{12}\left(2 - \frac{x}{L}\right)^3 . \qquad (5.239)$$

Due to the special form of the second moment of area, the stiffness matrix therefore results in

$$k^e = E\frac{bh^3}{12}\int\limits_L \left(2 - \frac{x}{L}\right)^3 \frac{\mathrm{d}^2 N^\mathrm{T}(x)}{\mathrm{d}x^2}\frac{\mathrm{d}^2 N(x)}{\mathrm{d}x^2}\mathrm{d}x \qquad (5.240)$$

or after the integration finally as:

$$k^e_{\mathrm{square}} = \frac{E}{L^3}\frac{bh^3}{12}\begin{bmatrix} \frac{243}{5} & \frac{156}{5}L & -\frac{243}{5} & \frac{87}{5}L \\ \frac{156}{5}L & \frac{114}{5}L^2 & -\frac{156}{5}L & \frac{42}{5}L^2 \\ -\frac{243}{5} & -\frac{156}{5}L & \frac{243}{5} & -\frac{87}{5}L \\ \frac{87}{5}L & \frac{42}{5}L^2 & -\frac{87}{5}L & 9L^2 \end{bmatrix} . \qquad (5.241)$$

5.8.2 Supplementary Problems

5.4. Equilibrium relation for infinitesimal beam element with variable load
The vertical balance of forces and the equilibrium of moments has to be determined for the beam element, which is illustrated in Fig. 5.27.
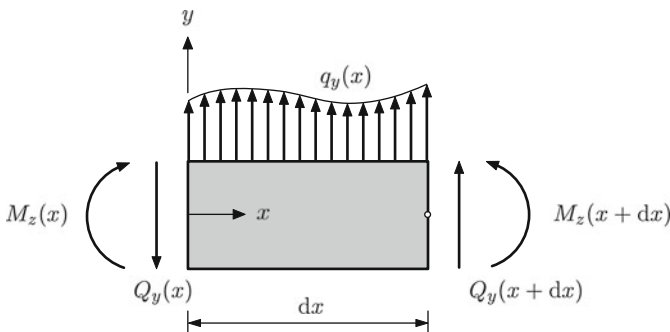
Fig. 5.27 Infinitesimal beam element with internal reactions and loading through variable distributed load

5.5. Weighted residual method with variable distributed load

One derives the finite element equation through the weighted residual method. The initial point therefore should be the bending differential equation *with* an arbitrary distributed load $q_y(x)$. Furthermore it should to be assumed, that the bending stiffness EI_z is constant.

5.6. Stiffness matrix at bending in $x-z$ plane

One derives the stiffness matrix for a beam element at bending in the $x-z$ plane. For this see Eq. (5.138) and Fig. 5.16b.

5.7. Bending beam with variable cross-section

Solve problem 5.3 for arbitrary values of D_1 and D_2!

5.8. Equivalent nodal loads for quadratic distributed load

Calculate the equivalent nodal loads for the bending beam, which is illustrated in Fig. 5.28 in the case of:

(a) $q(x) = q_0 x^2$,
(b) $q(x) = q_0 \left(\frac{x}{L}\right)^2$.
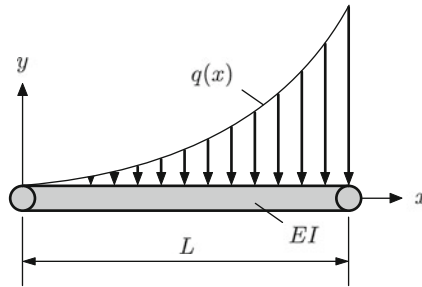
Fig. 5.28 Quadratic distributed load

5.9. Bending beam with variable cross-section under point load

For the beam with variable cross-section, which is illustrated in Fig. 5.29, calculate for $d_1 = 2h$ and $d_2 = h$ the vertical displacement of the right-hand boundary. For this purpose, a single finite element has to be used and the numerical solution has to be compared with the exact solution. Advice: the stiffness matrix can be taken from Example 5.3.
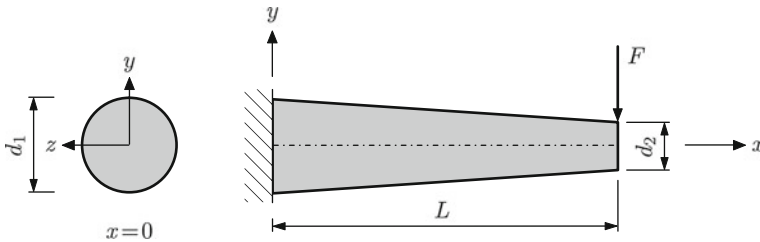
Fig. 5.29 Bending beam with variable cross-section at loading through point load

References

1. Hartman F, Katz C (2007) Structural analysis with finite elements. Springer, Berlin
2. Timoshenko S, Woinowsky-Krieger S (1959) Theory of plates and shells. McGraw-Hill Book Company, New York
3. Gould PL (1988) Analysis of shells and plates. Springer, New York
4. Altenbach H, Altenbach J, Naumenko K (1998) Ebene Flächentragwerke: Grundlagen der Modellierung und Berechnung von Scheiben und Platten. Springer, Berlin
5. Szabó I (2003) Einführung in die Technische Mechanik: Nach Vorlesungen István Szabó. Springer, Berlin
6. Gross D, Hauger W, Schröder J, Wall WA (2009) Technische Mechanik 2: Elastostatik. Springer, Berlin
7. Budynas RG (1999) Advanced strength and applied stress analysis. McGraw-Hill Book, Singapore.
8. Hibbeler RC (2008) Mechanics of materials. Prentice Hall, Singapore
9. Dubbel H, Grote K-H, Feldhusen J (eds) (2004) Dubbel. Taschenbuch für den Maschinenbau. Springer, Berlin
10. Czichos H, Hennecke M (eds) (2007) Hütte. Das Ingenieurwissen. Springer, Berlin
11. Macaulay WH (1919) A note on the deflections of beams. Messenger Math 48:129–130
12. Clebsch RFA (1862) Theorie der Elasticität fester Körper. B.G, Teubner, Leipzig
13. Szabó I (1996) Geschichte der mechanischen Prinzipien und ihrer wichtigsten Anwendungen. Birkhäuser Verlag, Basel
14. Szabó I (2001) Höhere Technische Mechanik: Nach Vorlesungen István Szabó. Springer, Berlin
15. Betten J (2004) Finite Elemente für Ingenieure 2: Variationsrechnung, Energiemethoden, Näherungsverfahren, Nichtlinearitäten, Numerische Integrationen, Springer, Berlin
16. Oden JT, Reddy JN (1976) Variational methods in theoretical mechanics. Springer, Berlin
17. Betten J (2001) Kontinuumsmechanik: Elastisches und inelastisches Verhalten isotroper und anisotroper Stoffe. Springer, Berlin
18. Hutton DV (2004) Fundamentals of finite element analysis. McGraw-Hill Book, Singapore
19. Buchanan GR (1995) Schaum's outline of theory and problems of finite element analysis. McGraw-Hill Book, New York

Chapter 6
General 1D Element

Abstract Within the application the three basic types tension, torsion and bending can occur in an arbitrary combination. This chapter serves to introduce how the stiffness relation for a general 1D element can be gained. The stiffness relation of the basic types build the foundation. For 'simple' loadings the three basic types can be regarded separately and can easily be superposed. A mutual dependency is nonexistent. The generality of the 1D element also relates to the arbitrary orientation within space. Transformation rules from local to global coordinates are provided. As an example, structures in the plane as well as in three-dimensional space will be discussed. Furthermore there will be a short introduction in the subject of numerical integration.

6.1 Superposition to a General 1D Element

A general 1D element can be derived from the basic types of tension, bending and torsion without mutual dependency. For an arbitrary point, the three forces and three moments can be represented as

- normal force $N(x)$,
- respectively a shear force and a bending moment around an axis of the cross-section: $Q_z(x)$, $M_{yb}(x)$, $Q_y(x)$, $M_{zb}(x)$ and
- torsional moment $M_t(x)$ around the body axis.

The six kinematic parameters are described as follows:

- the three displacements $u_x(x)$, $u_y(x)$ and $u_z(x)$. Usually the displacement in the body axis equals the displacement $u_x(x)$.
- the three rotations $\varphi_x(x)$, $\varphi_y(x)$, $\varphi_z(x)$.

Figure 6.1 shows the kinematic parameters, the forces and the moments.
The arrangement of the single parameters in the vectors defines the structure of the total stiffness matrix. If the kinematic parameters are arranged in the order that follows
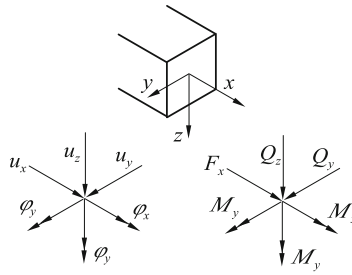
Fig. 6.1 State variables for the general three-dimensional case

$$\boldsymbol{u} = [u_x, u_y, u_z, \varphi_x, \varphi_y, \varphi_z]^{\mathrm{T}}, \tag{6.1}$$

the order of entries for the vector of *generalizes forces* in the stiffness relation results in:

$$\boldsymbol{F} = [N_x, Q_y, Q_z, M_x, M_y, M_z]^{\mathrm{T}}. \tag{6.2}$$

An alternative order results, if the vector of *generalized forces* is established in the following order

- normal force (in the direction of the x-axis),
- bending (around the y-axis and around the z-axis) and
- torsion (around the x-axis),

meaning

$$\boldsymbol{F} = [N_x, Q_z, M_y, Q_y, M_z, M_x]^{\mathrm{T}}. \tag{6.3}$$

For this order, the single stiffness relation in Eq. (6.4) is illustrated. Under the assumption of a two-node element the stiffness matrix consists of the 6 respective entries on both nodes. The dimension of the stiffness matrix results in 12×12.

$$
\begin{bmatrix}
N_{1x} \\
Q_{1z} \\
M_{1y} \\
Q_{1y} \\
M_{1z} \\
M_{1x} \\
\hline
N_{2x} \\
Q_{2z} \\
M_{2y} \\
Q_{2y} \\
M_{2z} \\
M_{2x}
\end{bmatrix}
=
\left[
\begin{array}{cccccc|cccccc}
Z & 0 & 0 & 0 & 0 & 0 & Z & 0 & 0 & 0 & 0 & 0 \\
0 & B_y & B_y & 0 & 0 & 0 & 0 & B_y & B_y & 0 & 0 & 0 \\
0 & B_y & B_y & 0 & 0 & 0 & 0 & B_y & B_y & 0 & 0 & 0 \\
0 & 0 & 0 & B_z & B_z & 0 & 0 & 0 & 0 & B_z & B_z & 0 \\
0 & 0 & 0 & B_z & B_z & 0 & 0 & 0 & 0 & B_z & B_z & 0 \\
0 & 0 & 0 & 0 & 0 & T & 0 & 0 & 0 & 0 & 0 & T \\
\hline
Z & 0 & 0 & 0 & 0 & 0 & Z & 0 & 0 & 0 & 0 & 0 \\
0 & B_y & B_y & 0 & 0 & 0 & 0 & B_y & B_y & 0 & 0 & 0 \\
0 & B_y & B_y & 0 & 0 & 0 & 0 & B_y & B_y & 0 & 0 & 0 \\
0 & 0 & 0 & B_z & B_z & 0 & 0 & 0 & 0 & B_z & B_z & 0 \\
0 & 0 & 0 & B_z & B_z & 0 & 0 & 0 & 0 & B_z & B_z & 0 \\
0 & 0 & 0 & 0 & 0 & T & 0 & 0 & 0 & 0 & 0 & T
\end{array}
\right]
\begin{bmatrix}
u_{1x} \\
u_{1z} \\
\varphi_{1y} \\
u_{1y} \\
\varphi_{1z} \\
\varphi_{1x} \\
\hline
u_{2x} \\
u_{2z} \\
\varphi_{2y} \\
u_{2y} \\
\varphi_{2z} \\
\varphi_{2x}
\end{bmatrix}
\tag{6.4}
$$

The stiffness matrix contains entries,

- which are marked with Z, for entries of the single stiffness matrix of the tension bar,
- which are marked with B_y and B_z, for the entries of the single stiffness matrix of beams bending around the y- and z-axis and
- which are marked with T, for the entries of the single stiffness matrix of the torsion bar.

The stiffness matrix contains 0-entries on many spots. This documents the decoupling of the basic types. To analyze a general three-dimensional problem, a user can choose between various ways for the choice of the elements. Generally the general stiffness matrix can be allocated to each 1D element. This however leads to an increased storage effort and lengthens computing times, since for many elements 'unnecessary' ballast is dragged along. Undoubtedly a preselection by the user makes sense. Commercial program packages mostly contain the basic types within their element library as well as several special cases.

6.1.1 Sample 1: Bar Under Tension and Torsion

In principle, a total stiffness matrix can be established through an arbitrary combination of basic types. Within this example the stiffness relation needs to be established through the basic types *tension bar* and *torsion bar*. Figure 6.2 illustrates the state variables, 6.2a the force parameter and 6.2b the deformation parameters.
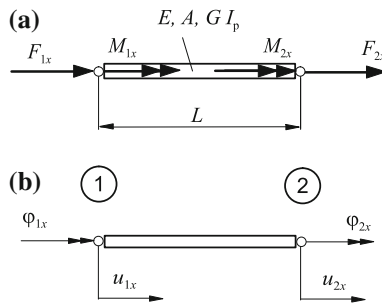
Fig. 6.2 Finite element for tension and torsion: **a** load parameters and **b** deformation parameters

The total stiffness relation for the 1D element

$$\begin{bmatrix} N_{1x} \\ M_{1x} \\ N_{2x} \\ M_{2x} \end{bmatrix} = \begin{bmatrix} Z & 0 & Z & 0 \\ 0 & T & 0 & T \\ Z & 0 & Z & 0 \\ 0 & T & 0 & T \end{bmatrix} \begin{bmatrix} u_{1x} \\ \varphi_{1x} \\ u_{2x} \\ \varphi_{2x} \end{bmatrix} \tag{6.5}$$

consists of the basic types *tension bar* and *torsion bar*: in the matrix, the positions,

- which are marked with Z, state entries of the single stiffness matrix of the tension bar,
- which are marked with T, state entries of the single stiffness matrix of the torsion bar.

In detail, the total stiffness relation via the geometrical and material parameters is:

$$
\begin{bmatrix} N_{1x} \\ M_{1x} \\ N_{2x} \\ M_{2x} \end{bmatrix} = \begin{bmatrix} \frac{EA}{L} & 0 & -\frac{EA}{L} & 0 \\ 0 & \frac{GI_t}{L} & 0 & -\frac{GI_t}{L} \\ -\frac{EA}{L} & 0 & \frac{EA}{L} & 0 \\ 0 & -\frac{GI_t}{L} & 0 & \frac{GI_t}{L} \end{bmatrix} \begin{bmatrix} u_{1x} \\ \varphi_{1x} \\ u_{2x} \\ \varphi_{2x} \end{bmatrix}.
\tag{6.6}
$$

6.1.2 Sample 2: Beam in the Plane with Tension Part

For the bending beam with a normal force part the two basic load types bending and tension have to be combined. First the bending in the $x-y$ plane needs to be described. The state variables of the combined load types are illustrated in Fig. 6.3.
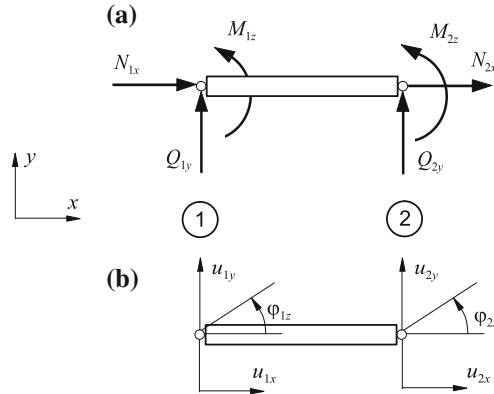
Fig. 6.3 Bending in the $x-y$ plane with normal force: **a** load parameters and **b** deformation parameters

The single stiffness relation is:

$$
\begin{bmatrix} N_{1x} \\ Q_{1y} \\ M_{1z} \\ N_{2x} \\ Q_{2y} \\ M_{2z} \end{bmatrix} = \begin{bmatrix} \frac{EA}{L} & 0 & 0 & -\frac{EA}{L} & 0 & 0 \\ 0 & 12\frac{EI_z}{L^3} & 6\frac{EI_z}{L^2} & 0 & -12\frac{EI_z}{L^3} & 6\frac{EI_z}{L^2} \\ 0 & 6\frac{EI_z}{L^2} & 4\frac{EI_z}{L} & 0 & -6\frac{EI_z}{L^3} & 2\frac{EI_z}{L^2} \\ \frac{EA}{L} & 0 & 0 & -\frac{EA}{L} & 0 & 0 \\ 0 & -12\frac{EI_z}{L^3} & -6\frac{EI_z}{L^2} & 0 & 12\frac{EI_z}{L^3} & -6\frac{EI_z}{L^2} \\ 0 & 6\frac{EI_z}{L^2} & 2\frac{EI_z}{L} & 0 & -6\frac{EI_z}{L^2} & 4\frac{EI_z}{L} \end{bmatrix} \begin{bmatrix} u_{1x} \\ u_{1y} \\ \varphi_{1z} \\ u_{2x} \\ u_{2y} \\ \varphi_{2z} \end{bmatrix}. \tag{6.7}
$$

For the bending in the x–z plane the description of the combined load occurs similarly. The state variables are illustrated in Fig. 6.4.
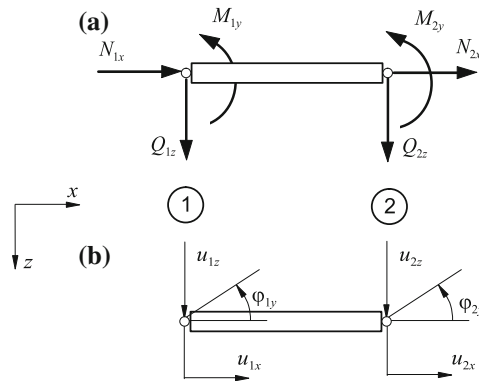
Fig. 6.4 Bending in the x–z plane with normal force: **a** load parameters and **b** deformation parameters

The single stiffness relation is:

$$
\begin{bmatrix} N_{1x} \\ Q_{1z} \\ M_{1y} \\ N_{2x} \\ Q_{2z} \\ M_{2y} \end{bmatrix} = \begin{bmatrix} \frac{EA}{L} & 0 & 0 & -\frac{EA}{L} & 0 & 0 \\ 0 & 12\frac{EI_y}{L^3} & -6\frac{EI_y}{L^2} & 0 & -12\frac{EI_y}{L^3} & -6\frac{EI_y}{L^2} \\ 0 & -6\frac{EI_y}{L^2} & 4\frac{EI_y}{L} & 0 & 6\frac{EI_y}{L^3} & 2\frac{EI_y}{L^2} \\ \frac{EA}{L} & 0 & 0 & -\frac{EA}{L} & 0 & 0 \\ 0 & -12\frac{EI_y}{L^3} & 6\frac{EI_y}{L^2} & 0 & 12\frac{EI_y}{L^3} & 6\frac{EI_y}{L^2} \\ 0 & -6\frac{EI_y}{L^2} & 2\frac{EI_y}{L} & 0 & 6\frac{EI_y}{L^2} & 4\frac{EI_y}{L} \end{bmatrix} \begin{bmatrix} u_{1x} \\ u_{1z} \\ \varphi_{1y} \\ u_{2x} \\ u_{2z} \\ \varphi_{2y} \end{bmatrix}. \tag{6.8}
$$

6.2 Coordinate Transformation

So far, the stiffness relation was formulated for a single element. The basis was the local (lo) coordinate system related to one element. For the simple tension bar the stiffness relation is called:

$$F^{\text{lo}} = k^{\text{lo}}\, u^{\text{lo}} \, . \tag{6.9}$$

However within a plane or general three-dimensional structure the single elements can be oriented arbitrarily within space. Usually a fixed, global coordinate system will be defined. The transformation rule for a vector between the local (lo) and global (glo) coordinate system is generally referred to as:

$$[\,\cdot\,]^{\text{lo}} = T\,[\,\cdot\,]^{\text{glo}} \, . \tag{6.10}$$

T is referred to as a transformation matrix. The mathematical characteristics are described in detail in the appendix. For the following derivation the relation

$$T^{-1} = T^{\text{T}} \tag{6.11}$$

is relevant. This transformation matrix is used for the conversion of all parameters. For the transformation of the displacements and forces from global to local coordinates, the following results

$$\begin{aligned} u^{\text{lo}} &= T\,u^{\text{glo}}\,, \\ F^{\text{lo}} &= T\,F^{\text{glo}}\,, \end{aligned} \tag{6.12}$$

and for the transformation from local to global coordinates

$$\begin{aligned} u^{\text{glo}} &= T^{\text{T}}\,u^{\text{lo}}\,, \\ F^{\text{glo}} &= T^{\text{T}}\,F^{\text{lo}} \, . \end{aligned} \tag{6.13}$$

The stiffness relation, after the transformation

$$\begin{aligned} F^{\text{lo}} &= K^{\text{lo}}\,u^{\text{lo}} \\ T^{-1}\,T\,F^{\text{glo}} &= T^{-1}\,K^{\text{lo}}\,T\,u^{\text{glo}} \\ F^{\text{glo}} &= T^{\text{T}}\,K^{\text{lo}}\,T\,u^{\text{glo}} \end{aligned}$$

can be written in global coordinates:

$$F^{\text{glo}} = K^{\text{glo}}\,u^{\text{glo}} \tag{6.14}$$

with

$$K^{\text{glo}} = T^{\text{T}}\,K^{\text{lo}}\,T. \tag{6.15}$$

Within the following sections the transformation will be introduced with the help of examples for the rotation in the plane and in the general three-dimensional space.

6.2.1 Plane Structures

The transformation for plane structures can be shown graphically. The local x–y coordinate system is rotated with the angle α compared to the X–Y global coordinate system (Fig. 6.5).

Fig. 6.5 Coordinate transformation in the plane
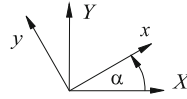
The transformation relation between the local and the global coordinate system for a vector is called:

$$\begin{bmatrix} \cdot \\ \cdot \end{bmatrix}^{\text{lo}} = \begin{bmatrix} \cos\alpha & \sin\alpha \\ -\sin\alpha & \cos\alpha \end{bmatrix} \begin{bmatrix} \cdot \\ \cdot \end{bmatrix}^{\text{glo}}. \tag{6.16}$$

First, the transformation for the element tension bar will be shown. To guarantee a better overview, Fig. 6.6 only illustrates the forces. For the displacement, an equal procedure applies.

Fig. 6.6 Coordinate transformation for the tension bar in the plane
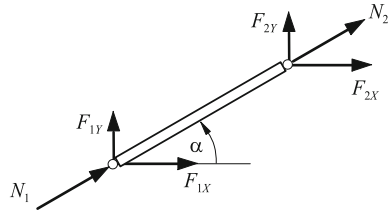
With two nodes the transformation matrix is:

$$\boldsymbol{T} = \begin{bmatrix} \cos\alpha & \sin\alpha & 0 & 0 \\ -\sin\alpha & \cos\alpha & 0 & 0 \\ 0 & 0 & \cos\alpha & \sin\alpha \\ 0 & 0 & -\sin\alpha & \cos\alpha \end{bmatrix}. \tag{6.17}$$

Based on the description in local coordinates, the state vectors are brought into the same dimension (4 components)

$$\boldsymbol{F}^{\text{lo}} = \begin{bmatrix} N_1 \\ 0 \\ N_2 \\ 0 \end{bmatrix}, \quad \boldsymbol{F}^{\text{glo}} = \begin{bmatrix} F_{1X} \\ F_{1Y} \\ F_{2X} \\ F_{2Y} \end{bmatrix} \tag{6.18}$$

and

$$
\boldsymbol{u}^{\mathrm{lo}} = \begin{bmatrix} u_1 \\ 0 \\ u_2 \\ 0 \end{bmatrix}, \quad \boldsymbol{u}^{\mathrm{glo}} = \begin{bmatrix} u_{1X} \\ u_{1Y} \\ u_{2X} \\ u_{2Y} \end{bmatrix}. \tag{6.19}
$$

For the transformation of the single stiffness matrix, one has to conduct the transformation rule of Eq. (6.15) and finally obtains

$$
\boldsymbol{k} = \boldsymbol{k}^{\mathrm{T}} = \frac{EA}{L} \begin{bmatrix} \cos^2\alpha & \cos\alpha\sin\alpha & -\cos^2\alpha & -\cos\alpha\sin\alpha \\ & \sin^2\alpha & -\cos\alpha\sin\alpha & -\sin^2\alpha \\ & & \cos^2\alpha & \cos\alpha\sin\alpha \\ \text{sym.} & & & \sin^2\alpha \end{bmatrix}. \tag{6.20}
$$

For the rotation of the bending beam in the plane, normal force, shear force and the momental vector are already considered in the local coordinate system (see Fig. 6.7). This one is at a right angle and also remains so during a rotation.

Fig. 6.7 Coordinate transformation for the bending beam in the X–Y plane
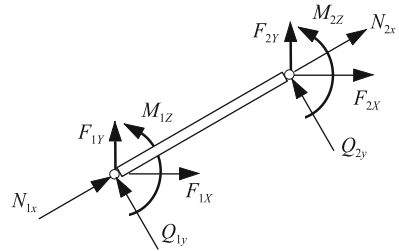
The following transformation matrix results for the bending in the X–Y plane

$$
\boldsymbol{T}^{\mathrm{XY}} = \begin{bmatrix} \cos\alpha & \sin\alpha & 0 & 0 & 0 & 0 \\ -\sin\alpha & \cos\alpha & 0 & 0 & 0 & 0 \\ 0 & 0 & 1 & 0 & 0 & 0 \\ 0 & 0 & 0 & \cos\alpha & \sin\alpha & 0 \\ 0 & 0 & 0 & -\sin\alpha & \cos\alpha & 0 \\ 0 & 0 & 0 & 0 & 0 & 1 \end{bmatrix} \tag{6.21}
$$

for the beam element with tensile loading. A corresponding transformation rule can be formulated for the bending in the X–Z plane.

6.2.2 General Three-Dimensional Structures

The transformation for general, three-dimensional structures can formally be also described via Eq. (6.10). Graphically, however, it is not so easy anymore to display the transformation. The local (x, y, z) coordinate system is defined via three coordinate axes. These can be rotated arbitrarily compared to a global (X, Y, Z) coordinate system (see Fig. 6.8).

Fig. 6.8 Rotatory transformation of a 1D element in the space. The unit vectors in the direction of the global X-, Y- and Z-axis are labelled with e_i
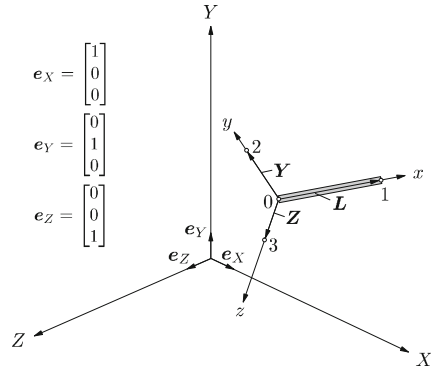
A one-dimensional finite element 0–1 is represented by the vector

$$L = (X_1 - X_0)e_X + (Y_1 - Y_0)e_Y + (Z_1 - Z_0)e_Z, \tag{6.22}$$

which is oriented in the direction of the local x-axis. A vector in the direction of the local y-axis can, according to Fig. 6.8 be illustrated as follows:

$$Y = (X_2 - X_0)e_X + (Y_2 - Y_0)e_Y + (Z_2 - Z_0)e_Z. \tag{6.23}$$

The direction cosines between the local y-axis and the global coordinate axes result via the global nodal coordinates to

$$t_{yX} = \cos(y, X) = \frac{X_2 - X_0}{|Y|}, \tag{6.24}$$

$$t_{yY} = \cos(y, Y) = \frac{Y_2 - Y_0}{|Y|}, \tag{6.25}$$

$$t_{yZ} = \cos(y, Z) = \frac{Z_2 - Z_0}{|Y|}, \tag{6.26}$$

whereupon the length of the vector Y results in

$$|Y| = \sqrt{(X_2 - X_0)^2 + (Y_2 - Y_0)^2 + (Z_2 - Z_0)^2}. \tag{6.27}$$

Accordingly a vector in the direction of the local z-axis results in:

$$Z = (X_3 - X_0)e_X + (Y_3 - Y_0)e_Y + (Z_3 - Z_0)e_Z \tag{6.28}$$

and the direction cosines in

$$t_{zX} = \cos(z, X) = \frac{X_3 - X_0}{|Z|}, \tag{6.29}$$

$$t_{zY} = \cos(z, Y) = \frac{Y_3 - Y_0}{|\mathbf{Z}|}, \tag{6.30}$$

$$t_{zZ} = \cos(z, Z) = \frac{Z_3 - Z_0}{|\mathbf{Z}|}, \tag{6.31}$$

whereupon the length of the vector $\mathbf{Z}$ results in

$$|\mathbf{Z}| = \sqrt{(X_3 - X_0)^2 + (Y_3 - Y_0)^2 + (Z_3 - Z_0)^2}. \tag{6.32}$$

An arbitrary vector $\mathbf{v}$ can be transformed between the local (x, y, z) and global (X, Y, Z) coordinate system with the help of the following relation:

$$\mathbf{v}_{xyz} = \mathbf{T}^{3D}\mathbf{v}_{XYZ}, \tag{6.33}$$

$$\mathbf{v}_{XYZ} = \mathbf{T}^{3D^{\mathrm{T}}}\mathbf{v}_{xyz}, \tag{6.34}$$

whereupon the transformation matrix can be written as follows via the direction cosines:

$$\mathbf{T}^{3D} = \begin{bmatrix} t_{xX} & t_{xY} & t_{xZ} \\ t_{yX} & t_{yY} & t_{yZ} \\ t_{zX} & t_{zY} & t_{zZ} \end{bmatrix} = \begin{bmatrix} \cos(x, X) & \cos(x, Y) & \cos(x, Z) \\ \cos(y, X) & \cos(y, Y) & \cos(y, Z) \\ \cos(z, X) & \cos(z, Y) & \cos(z, Z) \end{bmatrix}. \tag{6.35}$$

A general one-dimensional element bonds six kinematic state variables and six 'force parameters' on one node each. For a two-node element a transformation matrix with the dimension 12×12 results for the transformation of a state variable. With Eq. (6.36) the transformation relation from global to local coordinates for the kinematic state variables is represented here as an example.

$$\begin{bmatrix} u_{1x} \\ u_{1y} \\ u_{1z} \\ \varphi_{1x} \\ \varphi_{1y} \\ \varphi_{1z} \\ u_{2x} \\ u_{2y} \\ u_{2z} \\ \varphi_{2x} \\ \varphi_{2y} \\ \varphi_{2z} \end{bmatrix} = \underbrace{\begin{bmatrix} t_{xX}\ t_{xY}\ t_{xZ} & 0\ 0\ 0 & 0\ 0\ 0 & 0\ 0\ 0 \\ t_{yX}\ t_{yY}\ t_{yZ} & 0\ 0\ 0 & 0\ 0\ 0 & 0\ 0\ 0 \\ t_{zX}\ t_{zY}\ t_{zZ} & 0\ 0\ 0 & 0\ 0\ 0 & 0\ 0\ 0 \\ 0\ 0\ 0 & t_{xX}\ t_{xY}\ t_{xZ} & 0\ 0\ 0 & 0\ 0\ 0 \\ 0\ 0\ 0 & t_{yX}\ t_{yY}\ t_{yZ} & 0\ 0\ 0 & 0\ 0\ 0 \\ 0\ 0\ 0 & t_{zX}\ t_{zY}\ t_{zZ} & 0\ 0\ 0 & 0\ 0\ 0 \\ 0\ 0\ 0 & 0\ 0\ 0 & t_{xX}\ t_{xY}\ t_{xZ} & 0\ 0\ 0 \\ 0\ 0\ 0 & 0\ 0\ 0 & t_{yX}\ t_{yY}\ t_{yZ} & 0\ 0\ 0 \\ 0\ 0\ 0 & 0\ 0\ 0 & t_{zX}\ t_{zY}\ t_{zZ} & 0\ 0\ 0 \\ 0\ 0\ 0 & 0\ 0\ 0 & 0\ 0\ 0 & t_{xX}\ t_{xY}\ t_{xZ} \\ 0\ 0\ 0 & 0\ 0\ 0 & 0\ 0\ 0 & t_{yX}\ t_{yY}\ t_{yZ} \\ 0\ 0\ 0 & 0\ 0\ 0 & 0\ 0\ 0 & t_{zX}\ t_{zY}\ t_{zZ} \end{bmatrix}}_{\mathbf{T}} \begin{bmatrix} u_{1X} \\ u_{1Y} \\ u_{1Z} \\ \varphi_{1X} \\ \varphi_{1Y} \\ \varphi_{1Z} \\ u_{2X} \\ u_{2Y} \\ u_{2Z} \\ \varphi_{2X} \\ \varphi_{2Y} \\ \varphi_{2Z} \end{bmatrix}. \tag{6.36}$$

The transformation of the stiffness matrix results in:

$$k^e_{XYZ} = T^{3D^T} k^e T^{3D} . \tag{6.37}$$

The small letters stand for the axes of the local coordinate system and the capital letters for the axes of the global coordinate system.

6.3 Numerical Integration of a Finite Element

Within this chapter a short introduction into numerical integration is conducted. For a comprehensive overview it is referenced to relevant literature [1–3] at this point. The subject will be introduced with regard to one-dimensional problems.

For the approximate calculation of certain integrals, a number of numerical algorithms or so-called quadrature rules is available. The basic idea is to fractionize the integral

$$\int_a^b f(x)\,dx \approx \sum_{i=1}^q f(x_i)\,\Delta x_i \tag{6.38}$$

into subintervals and to subsequently sum up. Graphically this is shown in Fig. 6.9.

Fig. 6.9 Numerical integration of a function
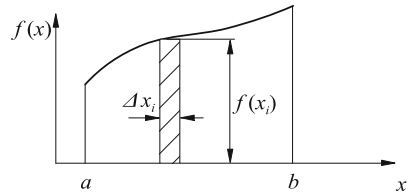
Formulated more generally, the integral consists of partial contributions, which are each calculated through a function value and a weighting coefficient:

$$\int_a^b f(x)\,dx \approx \sum_{i=1}^q f(\xi_i)\,W_i . \tag{6.39}$$

Within the integration formula, the ξ_i are referred to as the integration points, the $f(\xi_i)$ as the discrete function values on these integration points, and W_i as the weighting coefficient. q stands for the integration order.

Numerical integration thus means a multiplication of function values of the integrand on discrete points of support with weights. Subsequently the partial contributions are summed up.

Independent from the boundaries of integration, numerical integration is mostly conducted in the unit domain between -1 and $+1$, which means that the integration interval is transformed on the domain $-1 \leq \xi \leq 1$.

The Gauss quadrature

Within the framework of the finite element method mostly the quadrature formula according to GAUSS is used for the numerical integration. An essential advantage is that a polynomial of the order

$$m = 2q - 1 \tag{6.40}$$

with q integration points can be exactly integrated. Two integration points consequently allow a cubic polynomial to be exactly integrated and with three integration points a polynomial of 5th order can be exactly integrated. The position of the integration points as well as the corresponding weights can be found in tables. Table 6.1 shows the values up to an integration order $q = 3$.

Table 6.1 Points of support and weights for the numerical integration according to GAUSS-LEGENDRE

q	Points of support ξ_i	Weights W_i
1	0.00000	2.00000
2	$\pm \frac{1}{\sqrt{3}} = \pm 0.57735$	1.00000
3	$\pm \sqrt{\frac{3}{5}} = \pm 0.77459$	$\pm \frac{5}{9} = \pm 0.55555$
	0.00000	$+\frac{8}{9} = 0.88888$

The integration illustrated for the one-dimensional case can easily be expanded to integrals with a higher dimension.

Example

The integral

$$\int_{-1}^{+1} (1 + 2x + 3x^2) \, \mathrm{d}x \tag{6.41}$$

is to be evaluated with the help of the quadrature formula according to GAUSS.

Solution

The exact solution results in

$$\int\limits_{-1}^{+1}(1+2x+3x^2)\,dx = \left[x + x^2 + x^3\right]_{-1}^{+1} = (1+1+1)-(-1+1-1) = 4. \quad (6.42)$$

The integrand is a polynomial of second order. From $m = 2 = 2q - 1$ the necessary integration order is calculated to $q = 1.5$. Since this has to be integer, the integration order is appointed with $q = 2$. The positions of the integration points ξ_i with the corresponding weights W_i

$$\xi_{1/2} = \pm\frac{1}{\sqrt{3}}, \quad W_{1/2} = 1.0 \qquad (6.43)$$

for the integration order $q = 2$ are taken from Table 6.1. The numerical integration

$$\int\limits_{-1}^{+1}(1 + 2x + 3x^2)\,dx \approx \sum_{i=1}^{q=2} f(\xi_i)\,W_i = f(\xi_1)\,W_1 + f(\xi_2)\,W_2$$

$$= \left[1 + 2\left(-\frac{1}{\sqrt{3}}\right) + 3\left(-\frac{1}{\sqrt{3}}\right)^2\right]\cdot 1,0$$

$$+ \left[1 + 2\left(+\frac{1}{\sqrt{3}}\right) + 3\left(+\frac{1}{\sqrt{3}}\right)^2\right]\cdot 1,0$$

$$= \left[1 + 2\left(-\frac{1}{\sqrt{3}}\right) + 1\right] + \left[1 + 2\left(+\frac{1}{\sqrt{3}}\right) + 1\right] = 4$$

$$(6.44)$$

delivers the exact result.

6.4 Shape Function

Within the framework of the finite element method, functions have to be approximated. In previous chapters shape functions have already been introduced to approximate the displacement distribution within elements. Now this subject will be introduced in detail. It is the goal to describe the distribution of a physical parameter as easily as possible. As an example, the distribution of the displacement, the strain and the stress along the center line of a bar needs to be named. A common approach is to describe the real distribution of a function through a combination of function values on selected positions, the nodes of a element and functions between those points of support. This approach is also referred to as the nodal approach. The displacement distribution within an element is approximated with

$$\boldsymbol{u}^{\mathrm{e}}(\boldsymbol{x}) = \boldsymbol{N}^{\mathrm{e}}(\boldsymbol{x})\,\boldsymbol{u}_{\mathrm{p}}. \tag{6.45}$$

The parameter $\boldsymbol{u}^{\mathrm{e}}(\boldsymbol{x})$ describes the distribution of the displacement within the element, $\boldsymbol{N}$ stands for the shape function. The index 'e' in the equation stands for the parameter, which is related to an element. The index 'p' labels the node p, at which the nodal point displacement $\boldsymbol{u}_{\mathrm{p}}$ was introduced.

In principle, arbitrary functions can be chosen for the interpolation, however the following conditions have to be fulfilled:

- The shape function has to be consistent on the inside of an element.
- The shape function also has to be constant on the boundaries towards neighboring elements.
- It has to be possible to describe a rigid-body motion with the shape function, so that no strains or stresses in the element are caused as a result.

In general, polynomials fulfill these requirements. In the framework of the FEM such special polynomials are called LAGRANGE polynomials. A LAGRANGE polynomial of the order $n - 1$ is defined through n function values on the coordinates $x_1, x_2, x_3, x_i, ..., x_n$:

$$L_i^n(x) = (x - x_1)\,(x - x_2)\,(x - x_{i-1})(x - x_{i+1}) \cdots (x - x_n). \tag{6.46}$$

Especially it needs to be remarked that the LAGRANGE polynomial

- $L_i^n(x_j)$ takes on the function values $L_i^n(x_j) = 0$ on the locations $x_j = 1, 2, ..., n$, $(j \neq i)$ and
- $L_i^n(x_i)$ takes on the function value $L_i^n(x_i) \neq 0$ at the position x_i.

If the points of support of the LAGRANGE polynomial are put on the nodes of an element and the non-zero function value is used for the scaling, then as a result appropriate shape functions are constructed:

$$N_i(x) = \frac{L_i^n(x)}{L_i^n(x_i)} = \prod_{j=1, j \neq i}^{n} \frac{(x - x_j)}{(x_i - x_j)}. \tag{6.47}$$

For the description of a physical parameter at times it makes sense to define another coordinate system. Element-own coordinates, so-called *natural coordinates* ξ are introduced.

Figure 6.10a shows the local and Fig. 6.10b the natural coordinates. The transformation can be described through

$$\xi = \frac{x - x_{\mathrm{M}}}{L}. \tag{6.48}$$

The central point of the element is described with x_{M} or in natural coordinates with $\xi = 0$. The beginning and the end of the element are described with the natural coordinates $\xi = -1$ and $\xi = +1$. The shape function can also be formulated in natural coordinates

Fig. 6.10 Coordinates **a**
physical and **b** natural
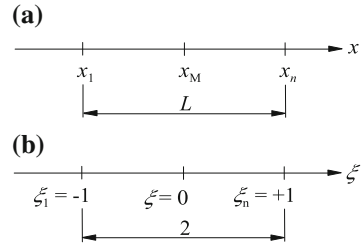
$$N_i(\xi) = L_i(\xi) = \prod_{j=1, j \neq i}^{n} \frac{(\xi - \xi_j)}{(\xi_i - \xi_j)}. \tag{6.49}$$

For a bar element with *linear* shape function, with the two nodes on the coordinates
$\xi_1 = -1$ and $\xi_2 = +1$ the two shape functions result in

$$\begin{aligned}
N_1(\xi) &= \frac{(\xi - \xi_2)}{(\xi_1 - \xi_2)} = \frac{(\xi - 1)}{(-1 - (+1))} = \tfrac{1}{2}(1 - \xi), \\
N_2(\xi) &= \frac{(\xi - \xi_1)}{(\xi_2 - \xi_1)} = \frac{(\xi - (-)1)}{(+1 - (-1))} = \tfrac{1}{2}(1 + \xi).
\end{aligned} \tag{6.50}$$

Fig. 6.11 Shape functions,
linear approach
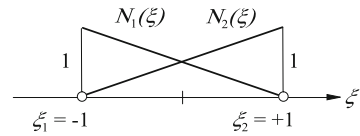
Figure 6.11 shows the two shape functions for the linear approach. For a bar element
with *quadratic* shape functions, with the three nodes on the coordinates $\xi_1 = -1$,
$\xi_2 = 0$ and $\xi_3 = +1$, the three shape functions result in

$$\begin{aligned}
N_1(\xi) &= \frac{(\xi - \xi_2)(\xi - \xi_3)}{(\xi_1 - \xi_2)(\xi_1 - \xi_3)} = \frac{(\xi - 0)(\xi - 1)}{(-1 - 0)(-1 - (+1))} = \tfrac{1}{2}\xi(\xi - 1), \\
N_2(\xi) &= \frac{(\xi - \xi_1)(\xi - \xi_3)}{(\xi_2 - \xi_1)(\xi_2 - \xi_3)} = \frac{(\xi - (-1))(\xi - 1)}{(0 - (-1)(0 - (+1))} = (1 - \xi^2), \\
N_3(\xi) &= \frac{(\xi - \xi_1)(\xi - \xi_2)}{(\xi_3 - \xi_1)(\xi_3 - \xi_2)} = \frac{(\xi - (-1))(\xi - 0)}{(+1 - (-1)(+1 - 0)} = \tfrac{1}{2}\xi(1 + \xi).
\end{aligned} \tag{6.51}$$

Figure 6.12 shows the three shape functions for a quadratic approach.
The definition of the shape functions for a cubic approach represents the content of
Exercise 6.1.

Fig. 6.12 Shape function, quadratic approach

$$N_1(\xi) \qquad N_2(\xi) \qquad N_3(\xi)$$

$$\xi_1 = -1 \qquad \xi_2 = 0 \qquad \xi_2 = +1$$
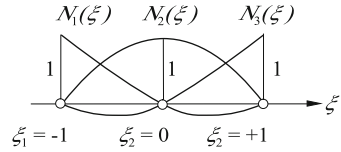
6.5 Unit Domain

Within the process of finite element analysis, numerous vectors and matrices are defined via integration through a state variable X. This is formulated as follows:

$$\int_\Omega X \, \mathrm{d}\Omega \,. \tag{6.52}$$

Hereby X mainly is a parameter, which is dependent on the shape functions N or their derivatives. As an example, the stiffness matrix

$$K = \int_\Omega B^\mathrm{T} D B \, \mathrm{d}\Omega \tag{6.53}$$

needs to be given. Two transformations are necessary for the transaction of the integration. In the first step, a transformation from global to local coordinates is conducted. This step was already discussed in Sect. 6.2. Secondly the integration domain is transformed into a unit domain:

$$\int_\Omega X(x, y, z) \, \mathrm{d}\Omega = \int_{-1}^{+1} \int_{-1}^{+1} \int_{-1}^{+1} \overline{X}(\xi, \eta, \zeta) \, J(\xi, \eta, \zeta) \, \mathrm{d}\xi \, \mathrm{d}\eta \, \mathrm{d}\zeta \tag{6.54}$$

with

$$X(x, y, z) = \overline{X}(x(\xi, \eta, \zeta), y(\xi, \eta, \zeta), z(\xi, \eta, \zeta)) = \overline{X}(\xi, \eta, \zeta). \tag{6.55}$$

In Eq. (6.54) the following expression

$$J(\xi, \eta, \zeta) = \frac{\partial(x, y, z)}{\partial(\xi, \eta, \zeta)} \tag{6.56}$$

stands for the JACOBIan matrix. If the integration is only conducted in one dimension, the transformation rule can be simplified to

$$\int\limits_{L} X(x)\,\mathrm{d}x = \int\limits_{-1}^{+1} \overline{X}(\xi)\, J(\xi)\,\mathrm{d}\xi = \int\limits_{-1}^{+1} \overline{X}(\xi)\, \frac{\partial x}{\partial \xi}\,\mathrm{d}\xi = \qquad (6.57)$$

with

$$X(x) = \overline{X}(x(\xi)) = \overline{X}(\xi). \qquad (6.58)$$

6.6 Supplementary Problems

6.1 Cubic Displacement Distribution Inside the Tension Bar

The displacement distribution for a bar element needs to be approximated through LAGRANGE polynomials. Unknown are the four shape functions in natural coordinates ξ for a cubic approximation of the displacement distribution in the bar element.

6.2 Coordination Transformation for a Tension Bar in the Plane

In a plane the local coordinate system for a bar is rotated by $\alpha = 30°$ compared to the global X–Y coordinate system. The bar is represented by 2 nodes (Fig. 6.13).

Fig. 6.13 Rotated bar in the plane
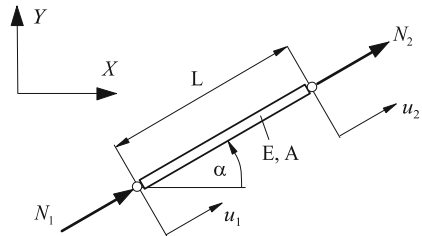
The following has to be defined

1. the transformation matrix and
2. the single stiffness relation in the global X–Y coordinate system.

References

1. Kwon YW, Bang H (2000) The finite element method using MATLAB. CRC Press, Boca Raton
2. Onate E (2009) Structural analysis with the finite element method. Springer, Berlin
3. Stoer J (1989) Numerische Mathematik 1. Springer-Lehrbuch, Berlin

Chapter 7
Plane and Spatial Frame Structures

Abstract Within this chapter the procedure for the analysis of a load-bearing structure will be introduced. Structures will be considered, which consist of multiple elements and are connected with each other on coupling points. The structure is supported properly and subjected with loads. Unknown are the deformations of the structure and the reaction forces on the supports. Furthermore, the internal reactions of the single element are of interest. The stiffness relation of the single elements are already known from the previous chapters. A total stiffness relation forms on the basis of these single stiffness relations. From a mathematical point of view the evaluation of the total stiffness relation equals the solving of a linear system of equations. As examples plane and general three-dimensional structures of bars and beams will be introduced.

7.1 Assembly of the Total Stiffness Relation

It is the goal of this section to formulate the stiffness relation for an entire structure. It is assumed that the stiffness relations for each element are known and can be set up. Each element is connected with the neighboring elements through nodes. One obtains the total stiffness relation by setting up the equilibrium of forces on each node. The structure of the total stiffness relation is therefore predetermined:

$$\boldsymbol{F} = \boldsymbol{K}\boldsymbol{u} \,. \tag{7.1}$$

The dimension of the column matrices $\boldsymbol{F}$ and $\boldsymbol{u}$ equals the sum of the degrees of freedom on all nodes. The assembly of the total matrix $\boldsymbol{K}$ can be illustrated graphically by *sorting* all submatrices $\boldsymbol{k}^{\mathrm{e}}$ in the total stiffness matrix. Formally this can be noted as follows:

$$\boldsymbol{K} = \sum_{e} \boldsymbol{k}^{\mathrm{e}} \,. \tag{7.2}$$

The setup of the total stiffness relation occurs in multiple steps:

1. The single stiffness matrix k^e is known for each element.
2. It is known which nodes are attached to each element. The single stiffness relation can therefore be formulated for each element in local coordinates:

$$F^e = k^e \, u_p.$$

3. The single stiffness relation, formulated in local coordinates has to be formulated in global coordinates.
4. The dimension of the total stiffness matrix is defined via the sum of the degrees of freedom on all nodes.
5. A numeration of the nodes and the degrees of freedom on each node has to be defined.
6. The entries from the single stiffness matrix have to be sorted in the corresponding positions in the total stiffness matrix.

This can be shown with the help of a simple example.

Given is a bar-similar structure with length $2L$ and constant cross-section A. The structure is divided into two parts with length L with differing material (this means different moduli of elasticity). The structure has a fixed support on one side and is loaded with a point load F on the other side (Fig. 7.1).
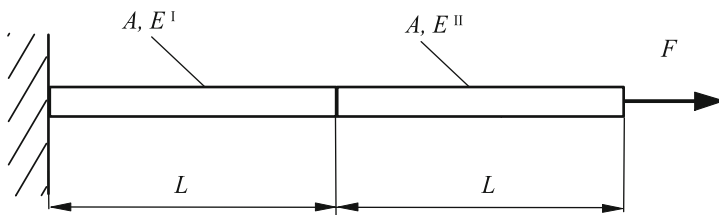
Fig. 7.1 Bar-shaped structure with the length $2L$

For further analysis the structure will be divided into two parts each of length L. The example therefore consists of two finite elements and three nodes, which are numbered in the sequence 1–2–3 (see Fig. 7.2). The nodes 1 and 2 are attached to element I. The single stiffness relation for the element I is:

$$\begin{bmatrix} N_1 \\ N_2 \end{bmatrix}^{\mathrm{I}} = \begin{bmatrix} k & -k \\ -k & k \end{bmatrix}^{\mathrm{I}} \begin{bmatrix} u_1 \\ u_2 \end{bmatrix}^{\mathrm{I}} \tag{7.3}$$

with

$$k^{\mathrm{I}} = \frac{E\,A}{L}. \tag{7.4}$$

Nodes 2 and 3 are attached to element II. The single stiffness relation for the element II is:
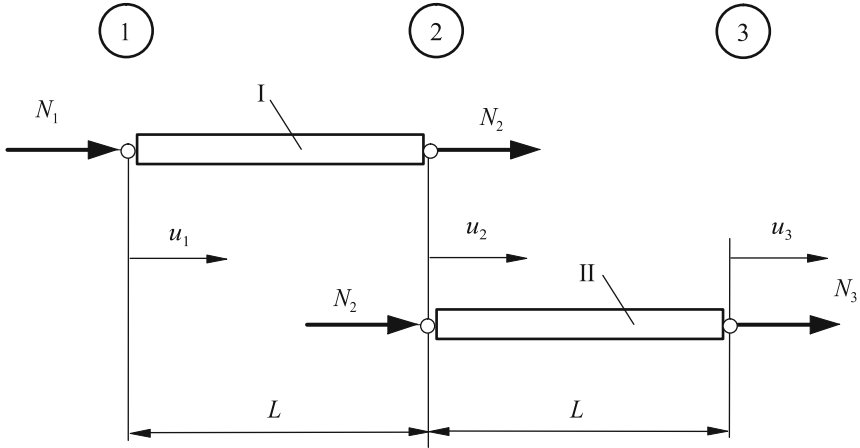
Fig. 7.2   Discretized structure with two finite elements

$$
\left[\begin{array}{c} N_2 \\ N_3 \end{array}\right]^{\mathrm{II}} = \left[\begin{array}{cc} k & -k \\ -k & k \end{array}\right]^{\mathrm{II}} \left[\begin{array}{c} u_2 \\ u_3 \end{array}\right]^{\mathrm{II}} \tag{7.5}
$$

with

$$
k^{\mathrm{II}} = \frac{EA}{L} \,. \tag{7.6}
$$

Since the local and global coordinate systems are identical for the present problem, a coordinate transformation is omitted. The dimension of the total stiffness relation results in 3×3, since one degree of freedom exists on each node. The numbering of the degrees of freedom is defined in the sequence 1–2–3. The total stiffness relation results by assembling all submatrices in the total stiffness matrix:

$$
\left[\begin{array}{c} N_1 \\ N_2 \\ N_3 \end{array}\right] = \left[\begin{array}{ccc} k^{\mathrm{I}} & -k^{\mathrm{I}} & 0 \\ -k^{\mathrm{I}} & k^{\mathrm{I}} + k^{\mathrm{II}} & -k^{\mathrm{II}} \\ 0 & -k^{\mathrm{II}} & k^{\mathrm{II}} \end{array}\right] \left[\begin{array}{c} u_1 \\ u_2 \\ u_3 \end{array}\right] \,. \tag{7.7}
$$

The numbering of the nodes has an influence on the structure of the total stiffness matrix. Instead of numbering the nodes with 1–2–3, the sequence 1–3–2 can be defined (Fig. 7.3).
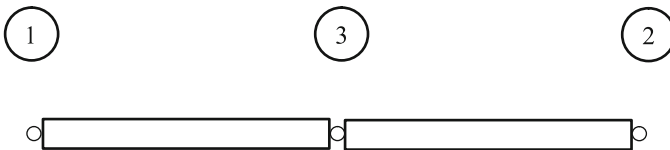
Fig. 7.3   Alternative numbering of nodes for a structure with two bars

Accordingly the total stiffness relation results in:

$$\begin{bmatrix} N_1 \\ N_3 \\ N_2 \end{bmatrix} = \begin{bmatrix} k^{\mathrm{I}} & -k^{\mathrm{I}} & 0 \\ -k^{\mathrm{I}} & k^{\mathrm{I}} + k^{\mathrm{II}} & -k^{\mathrm{II}} \\ 0 & -k^{\mathrm{II}} & k^{\mathrm{II}} \end{bmatrix} \begin{bmatrix} u_1 \\ u_3 \\ u_2 \end{bmatrix} . \tag{7.8}$$

For the case when the numbering is chosen in ascending order (1–2–3), the following results:

$$\begin{bmatrix} N_1 \\ N_2 \\ N_3 \end{bmatrix} = \begin{bmatrix} k^{\mathrm{I}} & 0 & -k^{\mathrm{I}} \\ 0 & k^{\mathrm{II}} & -k^{\mathrm{II}} \\ -k^{\mathrm{I}} & -k^{\mathrm{II}} & k^{\mathrm{I}} + k^{\mathrm{II}} \end{bmatrix} \begin{bmatrix} u_1 \\ u_2 \\ u_3 \end{bmatrix} . \tag{7.9}$$

Compared to Eq. (7.7) the zero entries in the system matrix are in a different position. The numbering of the nodes can influence the result. With an exact number representation and a non-occurring rounding error while conducting mathematical operations the numbering of the nodes would not have an influence on the final result. However in practice, exclusively numerical methods are used. Herewith, for example the sequence of the single mathematical operations and the computer internal number representation have an influence on the subresult as well as the final result. Especially the structure of the system matrix is of importance for the result of the equation. Thus, the assembly process influences speed and quality of the result.

The just now considered example can easily be expanded to multiple elements. Four bar elements are arranged behind each other in Fig. 7.4.
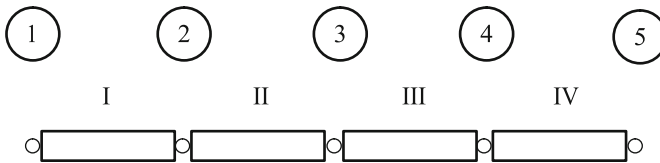
Fig. 7.4 Structure consisting of four bar elements

The total stiffness relation is:

$$\begin{bmatrix} N_1 \\ N_2 \\ N_3 \\ N_4 \\ N_5 \end{bmatrix} = \begin{bmatrix} k^{\mathrm{I}} & -k^{\mathrm{I}} & 0 & 0 & 0 \\ -k^{\mathrm{I}} & k^{\mathrm{I}} + k^{\mathrm{II}} & -k^{\mathrm{II}} & 0 & 0 \\ 0 & -k^{\mathrm{II}} & k^{\mathrm{II}} + k^{\mathrm{III}} & -k^{\mathrm{III}} & 0 \\ 0 & 0 & -k^{\mathrm{III}} & k^{\mathrm{III}} + k^{\mathrm{IV}} & -k^{\mathrm{IV}} \\ 0 & 0 & 0 & -k^{\mathrm{IV}} & k^{\mathrm{IV}} \end{bmatrix} \begin{bmatrix} u_1 \\ u_2 \\ u_3 \\ u_4 \\ u_5 \end{bmatrix} . \tag{7.10}$$

The band structure in the system matrix is clearly visible. Around the main diagonal respectively one secondary diagonal is occupied. Large domains have zero entries. By tendency the domains with zero entries become proportionally bigger with increasing number of finite elements within a structure, the domains with non-zero entries become smaller. The concentration of the non-zero entries around the main diagonal

cannot be enforced at all times. Structures with coupling points, at which multiple elements concur, lead to non-zero entries in the zero domains.

The unknown parameters can be found through the total stiffness relation. Herefore at first proper preconditions have to be established. In a mathematical sense the system matrix is still singular. Degrees of freedom have to be taken from the system. Graphically this means that at least that so many degrees of freedom have to be taken until the rigid-body motion of the remaining system becomes impossible. A reduced system results from the total stiffness relation:

$$\boldsymbol{F}^{\text{red}} = \boldsymbol{K}^{\text{red}}\, \boldsymbol{u}^{\text{red}}\,. \tag{7.11}$$

Herefrom the unknown parameters can be determined. Within the following sequence the solving of the system equation will be elaborated in detail.

7.2 Solving of the System Equation

The solving of a linear system of equations such as system (7.11) is part of the basic tasks in mathematics. A common illustration yields:

$$\boldsymbol{A}\,\boldsymbol{x} = \boldsymbol{b}\,. \tag{7.12}$$

The matrix $\boldsymbol{A}$ is referred to as a system matrix, the vector $\boldsymbol{x}$ contains the unknowns and the vector $\boldsymbol{b}$ represents the right-hand side. The right-hand side represents a load case from the mechanical point of view. Multiple load cases result in a right-hand side matrix, whose number of columns equals the number of load cases. If Eqs. (7.11) and (7.12) are compared,

- the system matrix $\boldsymbol{A}$ with the reduced stiffness matrix $\boldsymbol{K}^{\text{red}}$,
- the vector of the unknown $\boldsymbol{x}$ with $\boldsymbol{u}^{\text{red}}$ and
- the vector of the right-hand side $\boldsymbol{b}$ with $\boldsymbol{F}^{\text{red}}$

can be identified. To solve the linear system of equations basically two methods are possible:

- Direct and
- iterative method.

For an in-depth discussion it can be referred to corresponding literature at this point [1, 2]. From the user's point of view, the following criteria are paramount:

- the reliability of the solvers,
- the accuracy of the solution,
- the time, which is needed for the solving and
- the resources, which are made use of.

The direct methods can be characterized through the following attributes:

- The system is solvable for a well constructed problem.
- The direct solver is implementable as a *black box*.
- Multiple load cases and therefore more right-hand sides can be handled without significant additional expenditure.
- The calculating time is basically defined through the dimension of the system matrix.
- The accuracy of the solution is basically defined through the computer internal number representation.

For iterative methods interim solutions are determined according to a fixed algorithm, based on an initial solution. The essential attributes are:

- The convergence of an iterative method cannot be guaranteed for every application.
- The accuracy of the solution can be influenced and given by the user.
- Multiple right-hand sides demand multiple computing times (n right-hand sides mean n-times solution of the system of equations).

With iterative methods, solutions for many applications can be found very quickly. The computing times for a load case can be a few percent of the computing times of the direct solver. In commercial program packages, mainly direct methods are used for the solution of the equation system. Extended computing times seem to be more reasonable to the user as a possible termination of the iterative solution algorithm.

7.3 Solution Evaluation

After the solving of the linear system of equations, the following displacements $\boldsymbol{u}_\mathrm{p}$ are present on each node for general problems in a global coordinate system. For a further evaluation in the single elements, the displacements are each transformed in the element-own local coordinate system. With the shape functions the displacement field in each element

$$\boldsymbol{u}^\mathrm{e}(x) = \boldsymbol{N}(x)\boldsymbol{u}_\mathrm{p} \tag{7.13}$$

can be defined for each element. Through the kinematic relation furthermore the strain field

$$\boldsymbol{\varepsilon}^\mathrm{e}(x) = \mathcal{L}_1 \, \boldsymbol{u}^\mathrm{e}(x) = \mathcal{L}_1 \, \boldsymbol{N}(x) \, \boldsymbol{u}_\mathrm{p} \tag{7.14}$$

and through the constitutive equation the stress field in the element

$$\boldsymbol{\sigma}^\mathrm{e}(x) = \boldsymbol{D} \, \boldsymbol{\varepsilon}^\mathrm{e}(x) \tag{7.15}$$

can be defined. Furthermore, the unknown support reactions can be determined with the nodal displacement values via a so-called follow-up calculation.

7.4 Examples in the Plane

This section serves to discuss about structures which are positioned in the plane. The first example deals with a structure, which consists of two bars. The second example deals with a beam and a bar.

7.4.1 Plane Structure with Two Bars

As a first and simple example a structure will be discussed which is made of two bars (see Fig. 7.5). Both bars have the same length $\sqrt{2} \times L$ and the same cross-section A, consist of the same material (same modulus of elasticity E), are each simply supported at one end and are pin-jointed at the position C. A single force F acts on position C.
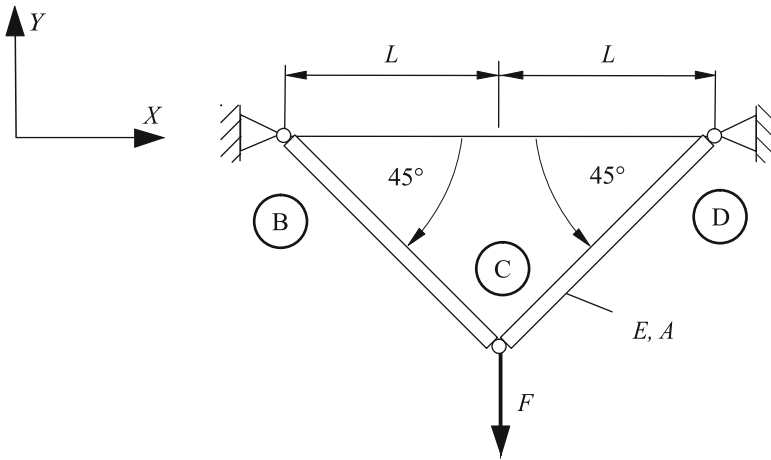
Fig. 7.5 Plane structure made of two bars

Given: E, A, L and F
Unknown are

- the displacement on position C and
- the strain and stress in the elements.

The approach:
The discretization of the structure is obvious. The structure is divided into two elements. The nodes with the numbers 1, 2 and 3 are introduced at the positions B, C and D (see Fig. 7.6).
Nodes 1 and 2 are attached to element I. The single stiffness relation for element I is, in local coordinates:
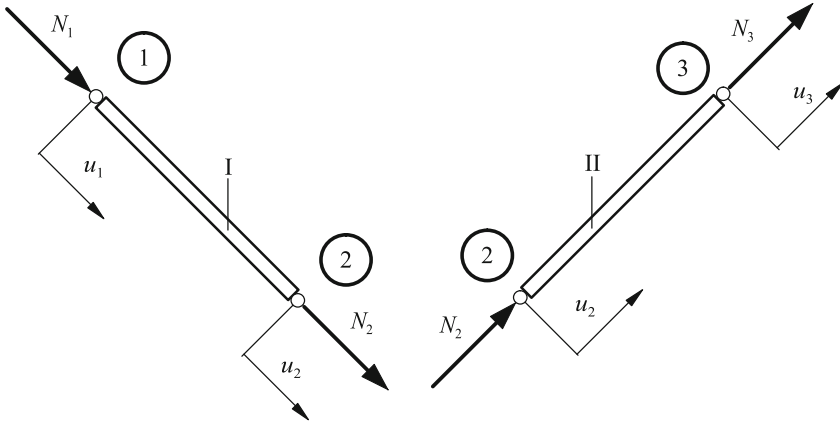
Fig. 7.6 Plane structure with two bar elements

$$\begin{bmatrix} N_1 \\ N_2 \end{bmatrix}^{\mathrm{I}} = \begin{bmatrix} k & -k \\ -k & k \end{bmatrix}^{\mathrm{I}} \begin{bmatrix} u_1 \\ u_2 \end{bmatrix}^{\mathrm{I}} \tag{7.16}$$

with

$$k^{\mathrm{I}} = \frac{EA}{\sqrt{2}L}. \tag{7.17}$$

Nodes 2 and 3 are attached to element II. The single stiffness relation for element II is, in local coordinates:

$$\begin{bmatrix} N_2 \\ N_3 \end{bmatrix}^{\mathrm{II}} = \begin{bmatrix} k & -k \\ -k & k \end{bmatrix}^{\mathrm{II}} \begin{bmatrix} u_2 \\ u_3 \end{bmatrix}^{\mathrm{II}} \tag{7.18}$$

with

$$k^{\mathrm{II}} = \frac{EA}{\sqrt{2}L}. \tag{7.19}$$

Element I is rotated by $\alpha^{\mathrm{I}} = -45°$ compared to the global coordinate system, element II is rotated by $\alpha^{\mathrm{II}} = +45°$. With the expressions

$$\sin(-45°) = -\frac{1}{2}\sqrt{2} \quad \text{and} \quad \cos(-45°) = \frac{1}{2}\sqrt{2} \tag{7.20}$$

for element I and

$$\sin(+45°) = +\frac{1}{2}\sqrt{2} \quad \text{and} \quad \cos(+45°) = \frac{1}{2}\sqrt{2} \tag{7.21}$$

for element II the single stiffness relations are, in global coordinates for element I:

$$
\begin{bmatrix} F_{1X} \\ F_{1Y} \\ F_{2X} \\ F_{2Y} \end{bmatrix} = \frac{1}{2}k^{\mathrm{I}} \begin{bmatrix} 1 & -1 & -1 & 1 \\ -1 & 1 & 1 & -1 \\ -1 & 1 & 1 & -1 \\ 1 & -1 & -1 & 1 \end{bmatrix} \begin{bmatrix} u_{1X} \\ u_{1Y} \\ u_{2X} \\ u_{2Y} \end{bmatrix} \tag{7.22}
$$

and for element II:

$$
\begin{bmatrix} F_{2X} \\ F_{2Y} \\ F_{3X} \\ F_{3Y} \end{bmatrix} = \frac{1}{2}k^{\mathrm{II}} \begin{bmatrix} 1 & 1 & -1 & -1 \\ 1 & 1 & -1 & -1 \\ -1 & -1 & 1 & 1 \\ -1 & -1 & 1 & 1 \end{bmatrix} \begin{bmatrix} u_{2X} \\ u_{2Y} \\ u_{3X} \\ u_{3Y} \end{bmatrix} . \tag{7.23}
$$

One obtains the total stiffness relation by inserting the single stiffness relations in the corresponding positions:

$$
\begin{bmatrix} F_{1X} \\ F_{1Y} \\ F_{2X} \\ F_{2Y} \\ F_{3X} \\ F_{3Y} \end{bmatrix} = \frac{1}{2} \begin{bmatrix} k^{\mathrm{I}} & -k^{\mathrm{I}} & -k^{\mathrm{I}} & k^{\mathrm{I}} & 0 & 0 \\ -k^{\mathrm{I}} & k^{\mathrm{I}} & k^{\mathrm{I}} & -k^{\mathrm{I}} & 0 & 0 \\ -k^{\mathrm{I}} & k^{\mathrm{I}} & k^{\mathrm{I}}+k^{\mathrm{II}} & -k^{\mathrm{I}}+k^{\mathrm{II}} & -k^{\mathrm{II}} & -k^{\mathrm{II}} \\ k^{\mathrm{I}} & -k^{\mathrm{I}} & -k^{\mathrm{I}}+k^{\mathrm{II}} & k^{\mathrm{I}}+k^{\mathrm{II}} & -k^{\mathrm{II}} & -k^{\mathrm{II}} \\ 0 & 0 & -k^{\mathrm{II}} & -k^{\mathrm{II}} & k^{\mathrm{II}} & k^{\mathrm{II}} \\ 0 & 0 & -k^{\mathrm{II}} & -k^{\mathrm{II}} & k^{\mathrm{II}} & k^{\mathrm{II}} \end{bmatrix} \begin{bmatrix} u_{1X} \\ u_{1Y} \\ u_{2X} \\ u_{2Y} \\ u_{3X} \\ u_{3Y} \end{bmatrix} . \tag{7.24}
$$

In the next step, the boundary conditions will be worked in.

- The displacement on node 1 and on node 3 are zero in each case.
- The external force on node 2 acts in the global Y direction.

Therewith the total stiffness relation is:

$$
\begin{bmatrix} F_{1X} \\ F_{1Y} \\ 0 \\ F_{2Y} \\ F_{3X} \\ F_{3Y} \end{bmatrix} = \frac{1}{2} \begin{bmatrix} k^{\mathrm{I}} & -k^{\mathrm{I}} & -k^{\mathrm{I}} & k^{\mathrm{I}} & 0 & 0 \\ -k^{\mathrm{I}} & k^{\mathrm{I}} & k^{\mathrm{I}} & -k^{\mathrm{I}} & 0 & 0 \\ -k^{\mathrm{I}} & k^{\mathrm{I}} & k^{\mathrm{I}}+k^{\mathrm{II}} & -k^{\mathrm{I}}+k^{\mathrm{II}} & -k^{\mathrm{II}} & -k^{\mathrm{II}} \\ k^{\mathrm{I}} & -k^{\mathrm{I}} & -k^{\mathrm{I}}+k^{\mathrm{II}} & k^{\mathrm{I}}+k^{\mathrm{II}} & -k^{\mathrm{II}} & -k^{\mathrm{II}} \\ 0 & 0 & -k^{\mathrm{II}} & -k^{\mathrm{II}} & k^{\mathrm{II}} & k^{\mathrm{II}} \\ 0 & 0 & -k^{\mathrm{II}} & -k^{\mathrm{II}} & k^{\mathrm{II}} & k^{\mathrm{II}} \end{bmatrix} \begin{bmatrix} 0 \\ 0 \\ u_{2X} \\ u_{2Y} \\ 0 \\ 0 \end{bmatrix} . \tag{7.25}
$$

After the crossing out of the lines and columns 1, 2, 5 and 6, a reduced system

$$
\begin{bmatrix} 0 \\ -F \end{bmatrix} = \frac{1}{2} \begin{bmatrix} k^{\mathrm{I}}+k^{\mathrm{II}} & -k^{\mathrm{I}}+k^{\mathrm{II}} \\ -k^{\mathrm{I}}+k^{\mathrm{II}} & k^{\mathrm{I}}+k^{\mathrm{II}} \end{bmatrix} \begin{bmatrix} u_{2X} \\ u_{2Y} \end{bmatrix} \tag{7.26}
$$

with the lines and columns 3 and 4 remains. So far, the stiffnesses for the elements are labeled with the indexes I and II, even though they are identical. For the further approach the stiffnesses are consistently referred to as $k^{\mathrm{I}} = k^{\mathrm{II}} = k = \frac{EA}{\sqrt{2}L}$. The simplified total stiffness relation is:

$$\begin{bmatrix} 0 \\ -F \end{bmatrix} = \begin{bmatrix} k & 0 \\ 0 & k \end{bmatrix} \begin{bmatrix} u_{2X} \\ u_{2Y} \end{bmatrix}. \tag{7.27}$$

Herefrom the unknown displacements u_{2X} and u_{2Y} can be determined:

$$u_{2X} = 0, \quad u_{2Y} = -\frac{F}{k} = -\frac{F}{EA}\sqrt{2}L. \tag{7.28}$$

Through transformation of the displacements u_{2X} and u_{2Y} in the element-own local coordinate systems the following results:

$$u_2^{\mathrm{I}} = \frac{1}{2}\sqrt{2}u_{2X} - \frac{1}{2}\sqrt{2}u_{2Y} = \frac{1}{2}\sqrt{2}\left(0 - \left(-\frac{F}{k}\right)\right) = +\frac{1}{2}\sqrt{2}\frac{F}{k} = +\frac{F}{EA}L,$$
$$\tag{7.29}$$
$$u_2^{\mathrm{II}} = \frac{1}{2}\sqrt{2}u_{2X} + \frac{1}{2}\sqrt{2}u_{2Y} = \frac{1}{2}\sqrt{2}\left(0 + \left(-\frac{F}{k}\right)\right) = -\frac{1}{2}\sqrt{2}\frac{F}{k} = -\frac{F}{EA}L.$$
$$\tag{7.30}$$

From the local displacements the strain in element I

$$\varepsilon^{\mathrm{I}}(x) = \frac{1}{\sqrt{2}L}(+u_2^{\mathrm{I}} - u_1^{\mathrm{I}}) = \left(\frac{F}{EA}L - 0\right)\frac{1}{\sqrt{2}L} = +\frac{1}{2}\sqrt{2}\frac{F}{EA} \tag{7.31}$$

and in element II

$$\varepsilon^{\mathrm{II}}(x) = \frac{1}{\sqrt{2}L}(+u_3^{\mathrm{II}} - u_2^{\mathrm{II}}) = \left(0 - \left(-\frac{F}{EA}L\right)\right)\frac{1}{\sqrt{2}L} = +\frac{1}{2}\sqrt{2}\frac{F}{EA} \tag{7.32}$$

can be determined.

 After the local displacements in the particular elements are known, the local forces can be determined via the single stiffness relation:

Bar I:

$$N_1^{\mathrm{I}} = k\,(+u_1^{\mathrm{I}} - u_2^{\mathrm{I}}) = k\left(0 - \tfrac{1}{2}\sqrt{2}\tfrac{F}{k}\right) = -\tfrac{1}{2}\sqrt{2}F,$$
$$N_2^{\mathrm{I}} = k\,(-u_1^{\mathrm{I}} + u_2^{\mathrm{I}}) = k\left(0 + \tfrac{1}{2}\sqrt{2}\tfrac{F}{k}\right) = +\tfrac{1}{2}\sqrt{2}F. \tag{7.33}$$

Bar II:

$$N_2^{\mathrm{II}} = k\,(+u_2^{\mathrm{II}} - u_3^{\mathrm{II}}) = k\left(-\tfrac{1}{2}\sqrt{2}\tfrac{F}{k} - 0\right) = -\frac{1}{2}\sqrt{2}F,$$
$$N_3^{\mathrm{II}} = k\,(-u_2^{\mathrm{II}} + u_3^{\mathrm{II}}) = k\left(-\left(-\tfrac{1}{2}\sqrt{2}\tfrac{F}{k}\right) + 0\right) = +\frac{1}{2}\sqrt{2}F. \tag{7.34}$$

From the definition of the bar force it becomes obvious that both bar I and also bar II are tension bars. The normal stress in bar I results in:

$$\sigma^{\mathrm{I}} = \frac{1}{2}\sqrt{2}\frac{F}{A} \tag{7.35}$$

and in bar II:

$$\sigma^{\mathrm{II}} = \frac{1}{2}\sqrt{2}\frac{F}{A} \, . \tag{7.36}$$

Herewith also the loading conditions in the single elements are known.

7.4.2 Plane Structure: Beam and Bar

As a second simple example a structure will be discussed which is made up of a beam and a bar (see Fig. 7.7). The beam has a fixed support on one end (position B). The beam is pin-jointed with the bar at position C, which is simply supported at position D. The entire structure is loaded with a point force F.
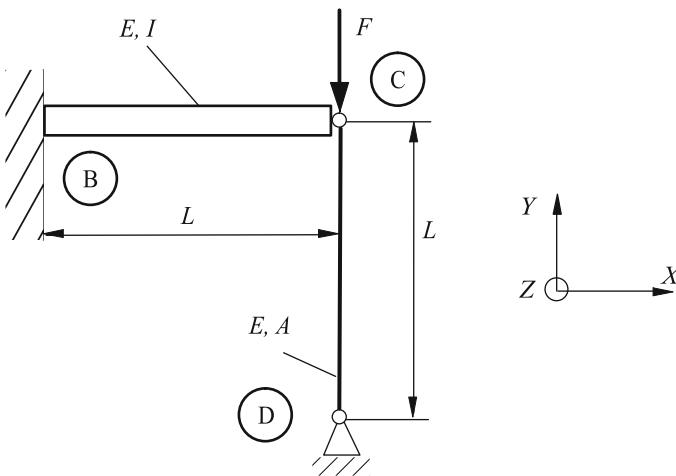
Fig. 7.7 Plane structure composed of a beam and a bar element

Given: E, I, A, L and F
Unknown are

- the displacements and rotations on position C and
- the reaction forces on the fixed supports.

Two ways for solving will be introduced. They can be distinguished in the use of a global coordinate system. First, the approach with the introduction of a global coordinate system will be explained.

The discretization of the structure is obvious. The beam is element I, the bar is element II. The nodes with the numbers 1, 2 and 3 are introduced at the positions B, C and D. For the single elements the kinematic parameters in Fig. 7.8 and the 'load parameters' in Fig. 7.9 are illustrated.
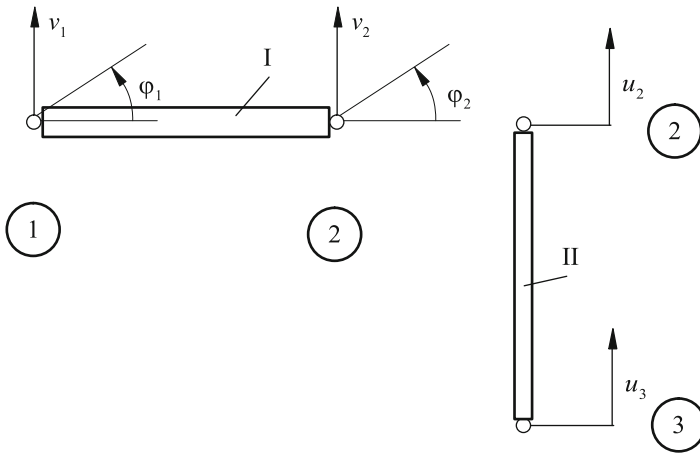
Fig. 7.8 Plane structure with kinematic parameters on the single elements
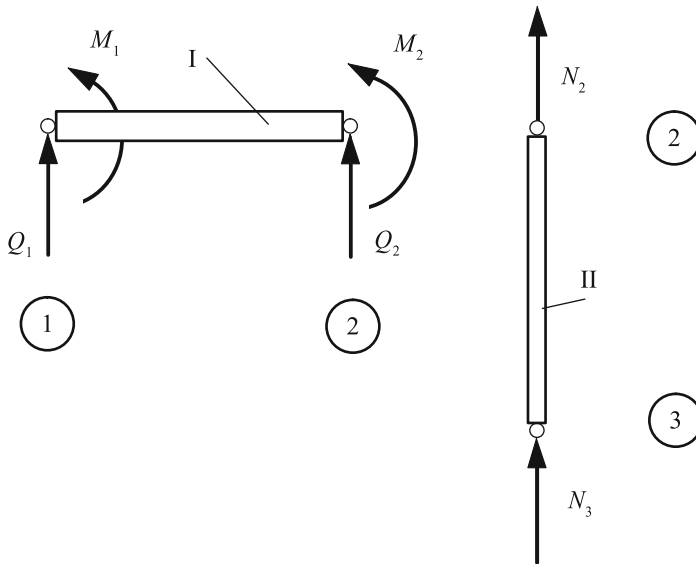
Fig. 7.9 Plane structure with 'load parameters' on the single elements

Nodes 1 and 2 are attached to element I. Herewith the stiffness relation for element I is:

$$\begin{bmatrix} Q_1 \\ M_1 \\ Q_2 \\ M_2 \end{bmatrix} = \frac{EI}{L^3} \begin{bmatrix} 12 & 6L & -12L & 6L \\ 6L & 4L^2 & -6L & 2L^2 \\ -12 & -6L & 12 & -6L \\ 6L & 2L^2 & -6L & 4L^2 \end{bmatrix} \begin{bmatrix} v_1 \\ \varphi_1 \\ v_2 \\ \varphi_2 \end{bmatrix} . \tag{7.37}$$

Nodes 3 and 2 are attached to element II. The element stiffness matrix for element II is:

$$
\begin{bmatrix} N_3 \\ N_2 \end{bmatrix} = \begin{bmatrix} k & -k \\ -k & k \end{bmatrix} \begin{bmatrix} u_3 \\ u_2 \end{bmatrix}. \tag{7.38}
$$

One obtains the total stiffness relation by setting up the overall force equilibrium. This results from the equilibrium on all nodes. The system can be described via the following parameters:

- on position B: displacement v_1 and the rotation φ_1 ,
- on position C: displacement v_2 and the rotation φ_2 ,
- on position D: displacement u_3 .

On the coupling point C

- the displacement v_2 on the beam equals the displacement u_2 on the bar and
- the shear force Q_2 on the beam equals the normal force N_2 on the bar.

The dimension of the total stiffness relation is therewith determined: a 5×5 system. For clarity reasons the entries in the following illustration are not conducted in detail. The abbreviation

- Z stands for the tension and compression bar and
- B stands for the bending beam:

$$
\begin{bmatrix} Q_1 \\ M_1 \\ Q_2 \\ M_2 \\ N_3 \end{bmatrix} = \begin{bmatrix} B & B & B & B & 0 \\ B & B & B & B & 0 \\ B & B & B+Z & B & Z \\ B & B & B & B & 0 \\ 0 & 0 & Z & 0 & Z \end{bmatrix} \begin{bmatrix} v_1 \\ \varphi_1 \\ v_2 \\ \varphi_2 \\ u_3 \end{bmatrix} \tag{7.39}
$$

It is already included in the total stiffness relation

- that the displacement v_2 regarding the bending beam on node 2 is identical with the displacement u_2 on the bar and
- that the shear force Q_2 regarding the bending beam on node 2 is identical with the normal force of the tension bar N_2.

In the next step the boundary conditions will be inserted into the total stiffness relation.

- On node 1 the displacement v_1 and the rotation φ_1 are zero.
- On node 2 there is the external force $-F$, the moment M_2 is zero.
- On node 3 the displacement u_3 is zero.

Herewith the lines and columns 1, 2 and 5 can be removed from the total stiffness relation. A reduced system of equations remains:

$$
\begin{bmatrix} -F \\ 0 \end{bmatrix} = \begin{bmatrix} B+Z & B \\ B & B \end{bmatrix} \begin{bmatrix} v_2 \\ \varphi_2 \end{bmatrix}. \tag{7.40}
$$

The reduced system of equations in detail is:

$$
\begin{bmatrix} -F \\ 0 \end{bmatrix} = \begin{bmatrix} 12\frac{EI}{L^3} + \frac{EA}{L} & -6\frac{EI}{L^2} \\ -6\frac{EI}{L^2} & 4\frac{EI}{L} \end{bmatrix} \begin{bmatrix} v_2 \\ \varphi_2 \end{bmatrix}. \tag{7.41}
$$

Herefrom the unknown displacement v_2 and the rotation φ_2 can be determined:

$$
v_2 = -\frac{F}{3\frac{EI}{L^3} + \frac{EA}{L}}, \quad \varphi_2 = -\frac{3}{2L}\frac{F}{3\frac{EI}{L^3} + \frac{EA}{L}}. \tag{7.42}
$$

Since the parameters v_2 and φ_2 are known now, the support reactions can be defined by inserting those in Eq. (7.39).

In this example, the definition of a global coordinate system and therewith the transformation from local to global coordinates was relinquished. Generally this is not possible. In this example, due to the right-angled position to each other, parameters of one element can be identified with those on the other element.

For the sake of completeness the approach with the coordinate transformation will also be introduced. The single stiffness relations in local coordinates are already known. For both elements the kinematic parameters in Fig. 7.10 as well as the 'load parameters' in Fig. 7.11 are illustrated.
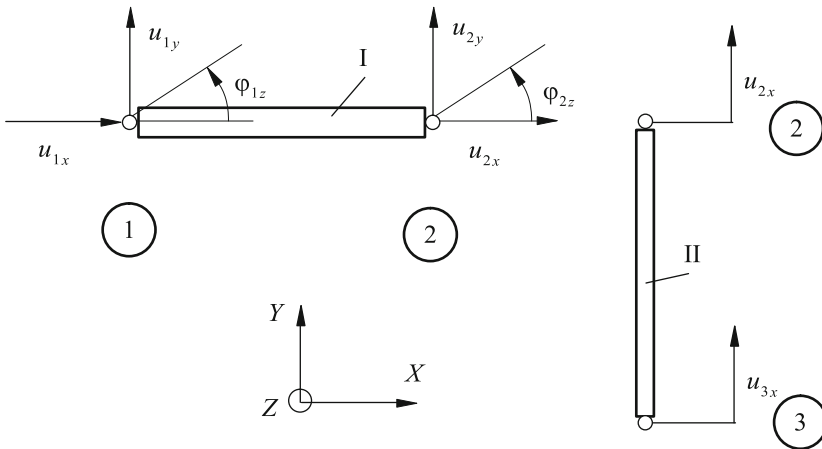
Fig. 7.10 Plane structure with kinematic parameters in local coordinates on the single elements

In the next step, the single stiffness relations will be illustrated in global coordinates. First, a global coordinate system will be defined. The local and global coordinate system are identical for element I. The single stiffness relation for element I is:
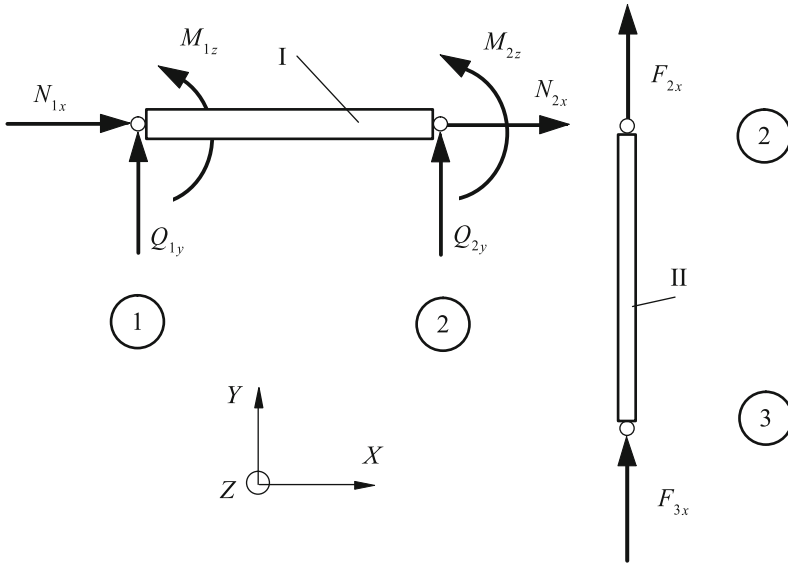
Fig. 7.11 Plane structure with 'load parameters' in local coordinates on the single elements

$$
\begin{bmatrix} F_{1X} \\ F_{1Y} \\ M_{1Z} \\ F_{2X} \\ F_{2Y} \\ M_{2Z} \end{bmatrix} = \frac{EI}{L^3} \begin{bmatrix} 0 & 0 & 0 & 0 & 0 & 0 \\ 0 & 12 & 6L & 0 & -12L & 6L \\ 0 & 6L & 4L^2 & 0 & -6L & 2L^2 \\ 0 & 0 & 0 & 0 & 0 & 0 \\ 0 & -12 & -6L & 0 & 12 & -6L \\ 0 & 6L & 2L^2 & 0 & -6L & 4L^2 \end{bmatrix} \begin{bmatrix} u_{1X} \\ u_{1Y} \\ \varphi_{1Z} \\ u_{2X} \\ u_{2Y} \\ \varphi_{2Z} \end{bmatrix}. \tag{7.43}
$$

The single stiffness relation in local coordinates for element II is:

$$
\begin{bmatrix} F_{3x} \\ F_{3y} \\ F_{2x} \\ F_{2y} \end{bmatrix} = \begin{bmatrix} \frac{EA}{L} & 0 & -\frac{EA}{L} & 0 \\ 0 & 0 & 0 & 0 \\ -\frac{EA}{L} & 0 & \frac{EA}{L} & 0 \\ 0 & 0 & 0 & 0 \end{bmatrix} \begin{bmatrix} u_{3x} \\ u_{3y} \\ u_{2x} \\ u_{2y} \end{bmatrix}. \tag{7.44}
$$

Element II is rotated by $\alpha = 90°$ compared to the global coordinate system. The transformation matrix for a vector is:

$$
T = \begin{bmatrix} 0 & 1 & 0 & 0 \\ 1 & 0 & 0 & 0 \\ 0 & 0 & 0 & 1 \\ 0 & 0 & 1 & 0 \end{bmatrix}. \tag{7.45}
$$

The single stiffness relation therefore results for element II in global coordinates:

$$
\begin{bmatrix} F_{3X} \\ F_{3Y} \\ F_{2X} \\ F_{2Y} \end{bmatrix} = \begin{bmatrix} 0 & 0 & 0 & 0 \\ 0 & \frac{EA}{L} & 0 & -\frac{EA}{L} \\ 0 & 0 & 0 & 0 \\ 0 & -\frac{EA}{L} & 0 & \frac{EA}{L} \end{bmatrix} \begin{bmatrix} u_{3X} \\ u_{3Y} \\ u_{2X} \\ u_{2Y} \end{bmatrix} . \tag{7.46}
$$

The dimension of the total stiffness relation result in 8×8. The kinematic parameters are

- on node 1: $u_{1X}, u_{1Y}, \varphi_{1Z}$,
- on node 2: $u_{2X}, u_{2Y}, \varphi_{2Z}$ and
- on node 3: u_{3X}, u_{3Y}.

The 'load parameter' are

- on node 1: F_{1X}, F_{1Y}, M_{1Z},
- on node 2: F_{2X}, F_{2Y}, M_{2Z} and
- on node 3: F_{3X}, F_{3Y}.

The total stiffness relation therefore results in:

$$
\begin{bmatrix} F_{1X} \\ F_{1Y} \\ M_{1Z} \\ F_{2X} \\ F_{2Y} \\ M_{2Z} \\ F_{3X} \\ F_{3Y} \end{bmatrix} = \begin{bmatrix} 0 & 0 & 0 & 0 & 0 & 0 & 0 & 0 \\ 0 & B & B & 0 & B & B & 0 & 0 \\ 0 & B & B & 0 & B & B & 0 & 0 \\ 0 & 0 & 0 & 0 & 0 & 0 & 0 & 0 \\ 0 & B & B & 0 & B+Z & B & 0 & Z \\ 0 & B & B & 0 & B & B & 0 & 0 \\ 0 & 0 & 0 & 0 & 0 & 0 & 0 & 0 \\ 0 & 0 & 0 & 0 & Z & 0 & 0 & Z \end{bmatrix} \begin{bmatrix} u_{1X} \\ u_{1Y} \\ \varphi_{1Z} \\ u_{2X} \\ u_{2Y} \\ \varphi_{2Z} \\ u_{3X} \\ u_{3Y} \end{bmatrix} . \tag{7.47}
$$

The boundary conditions are inserted into the total stiffness relation.

- On node 1, the fixed support of the beam, the displacement u_{1X}, u_{1Y} and the angle φ_{1Z} are zero.
- On node 2 the external force acts against the Y-direction.
- On node 3 the displacements u_{3X} and u_{3Y} are zero.

Therewith the corresponding lines and columns $(1, 2, 3, 4, 7, 8)$ can be removed from the total stiffness relation. A reduced system of the dimension 2×2 remains:

$$
\begin{bmatrix} -F \\ 0 \end{bmatrix} = \begin{bmatrix} B+Z & B \\ B & B \end{bmatrix} \begin{bmatrix} u_{2Y} \\ \varphi_{2Z} \end{bmatrix} . \tag{7.48}
$$

This system of equations is similar to the system shown above, which resulted from the description in local coordinates. The displacement v_2 equals u_{2Y} and the rotation φ_2 equals φ_{2Z}. The latter approach is identical.

7.5 Examples in the Three-Dimensional Space

The structure consists of three plane sections, which are oriented differently within space. The sections are each arranged mutually right-angled (see Fig. 7.12). The entire structure is fixed supported at position B and is loaded with a point load F at position G.
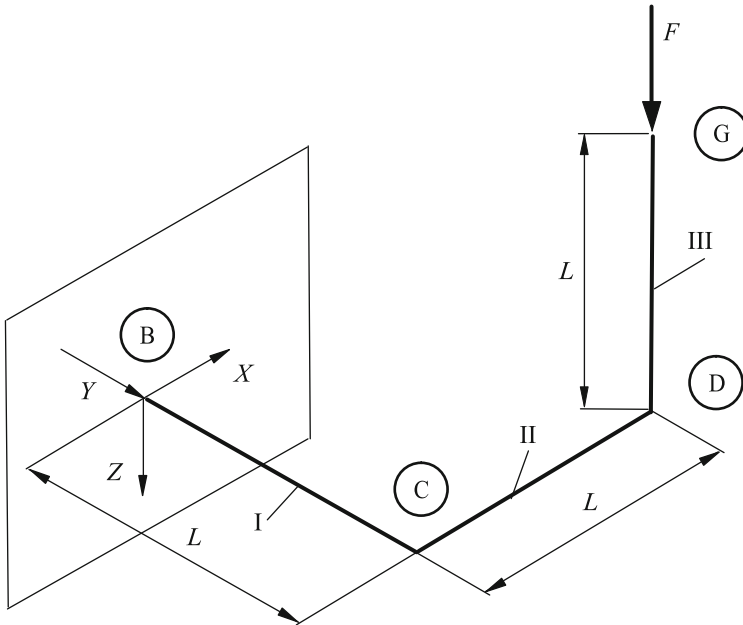
Fig. 7.12 General structure in space

Given: E, v, A, L und F

Unknown are

- the displacement and rotation on each coupling point (these are the positions B, C, D) and
- the reaction force at the fixed support (position B).

Solution :
The sections each equal an 1D element at the modeling as a finite element model. First the elements and nodes are labeled with numbers. For the description of the displacement and rotation a global (X, Y, Z) coordinate system is defined.
In principle, the total stiffness matrix of a general 1D element could be used for any element. This leads to quite extensive descriptions. Alternatively, the corresponding stiffness matrices of the basic load types for each element can be named:

- Element I is loaded by bending and torsion,

- element II by bending and
- element III by compression.

The shear part in element I and II is disregarded.

Figure 7.13 illustrates the state variables for element I in local coordinates. For clarity reasons only the parameters relevant for the description of the bending and compression load are considered.
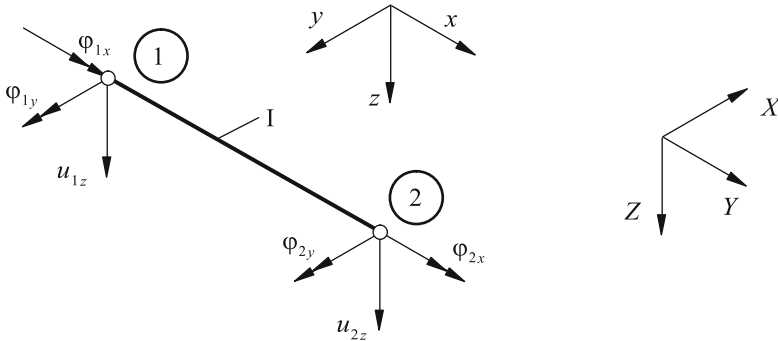
Fig. 7.13 Element I with state variables in local coordinates

In local coordinates the column matrix of the state variables is

$$\left[u_{1x}, u_{1y}, u_{1z}, \varphi_{1x}, \varphi_{1y}, \varphi_{1z}, u_{2x}, u_{2y}, u_{2z}, \varphi_{2x}, \varphi_{2y}, \varphi_{2z}\right]^{\mathrm{T}}, \tag{7.49}$$

$$\left[F_{1x}, F_{1y}, F_{1z}, M_{1x}, M_{1y}, M_{1z}, F_{2x}, F_{2y}, F_{2z}, M_{2x}, M_{2y}, M_{2z}\right]^{\mathrm{T}} \tag{7.50}$$

and the stiffness matrix for element I:

$$\left[\begin{array}{cccccc|cccccc}
0 & 0 & 0 & 0 & 0 & 0 & 0 & 0 & 0 & 0 & 0 & 0 \\
0 & 0 & 0 & 0 & 0 & 0 & 0 & 0 & 0 & 0 & 0 & 0 \\
0 & 0 & 12\frac{EI_y}{L^3} & 0 & -6\frac{EI_y}{L^2} & 0 & 0 & 0 & -12\frac{EI_y}{L^3} & 0 & -6\frac{EI_y}{L^3} & 0 \\
0 & 0 & 0 & \frac{GI_t}{L} & 0 & 0 & 0 & 0 & 0 & -\frac{GI_t}{L} & 0 & 0 \\
0 & 0 & -6\frac{EI_y}{L^2} & 0 & 4\frac{EI_y}{L} & 0 & 0 & 0 & 6\frac{EI_y}{L^2} & 0 & 2\frac{EI_y}{L} & 0 \\
0 & 0 & 0 & 0 & 0 & 0 & 0 & 0 & 0 & 0 & 0 & 0 \\
\hline
0 & 0 & 0 & 0 & 0 & 0 & 0 & 0 & 0 & 0 & 0 & 0 \\
0 & 0 & 0 & 0 & 0 & 0 & 0 & 0 & 0 & 0 & 0 & 0 \\
0 & 0 & -12\frac{EI_y}{L^3} & 0 & 6\frac{EI_y}{L^2} & 0 & 0 & 0 & 12\frac{EI_y}{L^3} & 0 & 6\frac{EI_y}{L^2} & 0 \\
0 & 0 & 0 & -\frac{GI_t}{L} & 0 & 0 & 0 & 0 & 0 & \frac{GI_t}{L} & 0 & 0 \\
0 & 0 & -6\frac{EI_y}{L^2} & 0 & 2\frac{EI_y}{L} & 0 & 0 & 0 & 6\frac{EI_y}{L^2} & 0 & 4\frac{EI_y}{L} & 0 \\
0 & 0 & 0 & 0 & 0 & 0 & 0 & 0 & 0 & 0 & 0 & 0
\end{array}\right]. \tag{7.51}$$

The transformation rule from local to global coordinates for a vector regarding element I is:

$$
\begin{bmatrix}
\cos\left(\frac{\pi}{2}\right) & \cos(0) & \cos\left(\frac{\pi}{2}\right) \\
\cos(\pi) & \cos\left(\frac{\pi}{2}\right) & \cos\left(\frac{\pi}{2}\right) \\
\cos\left(-\frac{\pi}{2}\right) & \cos\left(-\frac{\pi}{2}\right) & \cos(0)
\end{bmatrix} . \tag{7.52}
$$

Element I has two nodes with respectively six scalar parameters. Therefore a 12×12 system results:

$$
\boldsymbol{T}^{\mathrm{I}} =
\begin{bmatrix}
0 & 1 & 0 & 0 & 0 & 0 & 0 & 0 & 0 & 0 & 0 & 0 \\
-1 & 0 & 0 & 0 & 0 & 0 & 0 & 0 & 0 & 0 & 0 & 0 \\
0 & 0 & 1 & 0 & 0 & 0 & 0 & 0 & 0 & 0 & 0 & 0 \\
0 & 0 & 0 & 0 & 1 & 0 & 0 & 0 & 0 & 0 & 0 & 0 \\
0 & 0 & 0 & -1 & 0 & 0 & 0 & 0 & 0 & 0 & 0 & 0 \\
0 & 0 & 0 & 0 & 0 & 1 & 0 & 0 & 0 & 0 & 0 & 0 \\
0 & 0 & 0 & 0 & 0 & 0 & 0 & 1 & 0 & 0 & 0 & 0 \\
0 & 0 & 0 & 0 & 0 & 0 & -1 & 0 & 0 & 0 & 0 & 0 \\
0 & 0 & 0 & 0 & 0 & 0 & 0 & 0 & 1 & 0 & 0 & 0 \\
0 & 0 & 0 & 0 & 0 & 0 & 0 & 0 & 0 & 0 & 1 & 0 \\
0 & 0 & 0 & 0 & 0 & 0 & 0 & 0 & 0 & -1 & 0 & 0 \\
0 & 0 & 0 & 0 & 0 & 0 & 0 & 0 & 0 & 0 & 0 & 1
\end{bmatrix} . \tag{7.53}
$$

After the transformation in global coordinates the single stiffness relation for element I is:

$$
\begin{bmatrix}
0 & 0 & 0 & 0 & 0 & 0 & 0 & 0 & 0 & 0 & 0 & 0 \\
0 & 0 & 0 & 0 & 0 & 0 & 0 & 0 & 0 & 0 & 0 & 0 \\
0 & 0 & 12\frac{EI_y}{L^3} & 6\frac{EI_y}{L^2} & 0 & 0 & 0 & 0 & -12\frac{EI_y}{L^3} & 6\frac{EI_y}{L^2} & 0 & 0 \\
0 & 0 & 6\frac{EI_y}{L^2} & 4\frac{EI_y}{L} & 0 & 0 & 0 & 0 & -6\frac{EI_y}{L^2} & 2\frac{EI_y}{L} & 0 & 0 \\
0 & 0 & 0 & 0 & \frac{GI_t}{L} & 0 & 0 & 0 & 0 & 0 & -\frac{GI_t}{L} & 0 \\
0 & 0 & 0 & 0 & 0 & 0 & 0 & 0 & 0 & 0 & 0 & 0 \\
0 & 0 & 0 & 0 & 0 & 0 & 0 & 0 & 0 & 0 & 0 & 0 \\
0 & 0 & 0 & 0 & 0 & 0 & 0 & 0 & 0 & 0 & 0 & 0 \\
0 & 0 & -12\frac{EI_y}{L^3} & -6\frac{EI_y}{L^2} & 0 & 0 & 0 & 0 & 12\frac{EI_y}{L^3} & -6\frac{EI_y}{L^2} & 0 & 0 \\
0 & 0 & 6\frac{EI_y}{L^2} & 2\frac{EI_y}{L} & 0 & 0 & 0 & 0 & -6\frac{EI_y}{L^2} & 4\frac{EI_y}{L} & 0 & 0 \\
0 & 0 & 0 & 0 & -\frac{GI_t}{L} & 0 & 0 & 0 & 0 & 0 & \frac{GI_t}{L} & 0 \\
0 & 0 & 0 & 0 & 0 & 0 & 0 & 0 & 0 & 0 & 0 & 0
\end{bmatrix}
\begin{bmatrix}
u_{1X} \\ u_{1Y} \\ u_{1Z} \\ \varphi_{1X} \\ \varphi_{1Y} \\ \varphi_{1Z} \\ u_{2X} \\ u_{2Y} \\ u_{2Z} \\ \varphi_{2X} \\ \varphi_{2Y} \\ \varphi_{2Z}
\end{bmatrix} . \tag{7.54}
$$

For element II the local and global coordinates are identical. Figure 7.14 illustrates the state variables for element II in local coordinates. Therewith the single stiffness relation for element II results in:
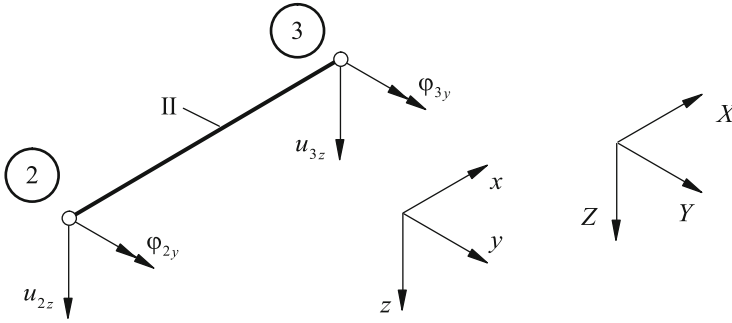
Fig. 7.14 Element II with state variables in local coordinates

$$
\begin{bmatrix}
F_{2X} \\
F_{2Y} \\
F_{2Z} \\
M_{2X} \\
M_{2Y} \\
M_{2Z} \\
\hline
F_{3X} \\
F_{3Y} \\
F_{3Z} \\
M_{3X} \\
M_{3Y} \\
M_{3Z}
\end{bmatrix}
=
\left[
\begin{array}{cccccc|cccccc}
0 & 0 & 0 & 0 & 0 & 0 & 0 & 0 & 0 & 0 & 0 & 0 \\
0 & 0 & 0 & 0 & 0 & 0 & 0 & 0 & 0 & 0 & 0 & 0 \\
0 & 0 & 12\frac{EI_y}{L^3} & 0 & -6\frac{EI_y}{L^2} & 0 & 0 & 0 & -12\frac{EI_y}{L^3} & 0 & -6\frac{EI_y}{L^2} & 0 \\
0 & 0 & 0 & 0 & 0 & 0 & 0 & 0 & 0 & 0 & 0 & 0 \\
0 & 0 & -6\frac{EI_y}{L^2} & 0 & 4\frac{EI_y}{L} & 0 & 0 & 0 & 6\frac{EI_y}{L^2} & 0 & 2\frac{EI_y}{L} & 0 \\
0 & 0 & 0 & 0 & 0 & 0 & 0 & 0 & 0 & 0 & 0 & 0 \\
\hline
0 & 0 & 0 & 0 & 0 & 0 & 0 & 0 & 0 & 0 & 0 & 0 \\
0 & 0 & 0 & 0 & 0 & 0 & 0 & 0 & 0 & 0 & 0 & 0 \\
0 & 0 & -12\frac{EI_y}{L^3} & 0 & 6\frac{EI_y}{L^2} & 0 & 0 & 0 & 12\frac{EI_y}{L^3} & 0 & 6\frac{EI_y}{L^2} & 0 \\
0 & 0 & 0 & 0 & 0 & 0 & 0 & 0 & 0 & 0 & 0 & 0 \\
0 & 0 & -6\frac{EI_y}{L^2} & 0 & 2\frac{EI_y}{L} & 0 & 0 & 0 & 6\frac{EI_y}{L^2} & 0 & 4\frac{EI_y}{L} & 0 \\
0 & 0 & 0 & 0 & 0 & 0 & 0 & 0 & 0 & 0 & 0 & 0
\end{array}
\right]
\begin{bmatrix}
u_{2X} \\
u_{2Y} \\
u_{2Z} \\
\varphi_{2X} \\
\varphi_{2Y} \\
\varphi_{2Z} \\
\hline
u_{3X} \\
u_{3Y} \\
u_{3Z} \\
\varphi_{3X} \\
\varphi_{3Y} \\
\varphi_{3Z}
\end{bmatrix}.
$$

$$(7.55)$$

For element III the local coordinate system is turned compared to the global one. The state variables are illustrated in local coordinates in Fig. 7.15.

The single stiffness relations for element III in local coordinates:

$$
\begin{bmatrix}
F_{3x} \\
F_{3y} \\
F_{3z} \\
M_{3x} \\
M_{3y} \\
M_{3z} \\
\hline
F_{4x} \\
F_{4y} \\
F_{4z} \\
M_{4x} \\
M_{4y} \\
M_{4z}
\end{bmatrix}
=
\left[
\begin{array}{cccccc|cccccc}
\frac{EA}{L} & 0 & 0 & 0 & 0 & 0 & -\frac{EA}{L} & 0 & 0 & 0 & 0 & 0 \\
0 & 0 & 0 & 0 & 0 & 0 & 0 & 0 & 0 & 0 & 0 & 0 \\
0 & 0 & 0 & 0 & 0 & 0 & 0 & 0 & 0 & 0 & 0 & 0 \\
0 & 0 & 0 & 0 & 0 & 0 & 0 & 0 & 0 & 0 & 0 & 0 \\
0 & 0 & 0 & 0 & 0 & 0 & 0 & 0 & 0 & 0 & 0 & 0 \\
0 & 0 & 0 & 0 & 0 & 0 & 0 & 0 & 0 & 0 & 0 & 0 \\
\hline
-\frac{EA}{L} & 0 & 0 & 0 & 0 & 0 & \frac{EA}{L} & 0 & 0 & 0 & 0 & 0 \\
0 & 0 & 0 & 0 & 0 & 0 & 0 & 0 & 0 & 0 & 0 & 0 \\
0 & 0 & 0 & 0 & 0 & 0 & 0 & 0 & 0 & 0 & 0 & 0 \\
0 & 0 & 0 & 0 & 0 & 0 & 0 & 0 & 0 & 0 & 0 & 0 \\
0 & 0 & 0 & 0 & 0 & 0 & 0 & 0 & 0 & 0 & 0 & 0 \\
0 & 0 & 0 & 0 & 0 & 0 & 0 & 0 & 0 & 0 & 0 & 0
\end{array}
\right]
\begin{bmatrix}
u_{3x} \\
u_{3y} \\
u_{3z} \\
\varphi_{3x} \\
\varphi_{3y} \\
\varphi_{3z} \\
\hline
u_{4x} \\
u_{4y} \\
u_{4z} \\
\varphi_{4x} \\
\varphi_{4y} \\
\varphi_{4z}
\end{bmatrix}.
$$

$$(7.56)$$

Fig. 7.15 Element III with state variables in local coordinates

The transformation rule of local to global coordinates for a vector regarding element III is called:

$$
\begin{bmatrix}
\cos\left(-\frac{\pi}{2}\right) & \cos\left(\frac{\pi}{2}\right) & \cos(\pi) \\
\cos\left(\frac{\pi}{2}\right) & \cos(0) & \cos\left(\frac{\pi}{2}\right) \\
\cos(0) & \cos\left(-\frac{\pi}{2}\right) & \cos\left(-\frac{\pi}{2}\right)
\end{bmatrix}.
\tag{7.57}
$$

The total transformation matrix T^{III} therefore results in:

$$
T^{\mathrm{III}} =
\left[
\begin{array}{ccc|ccc|ccc|ccc}
0 & 0 & -1 & 0 & 0 & 0 & 0 & 0 & 0 & 0 & 0 & 0 \\
0 & 1 & 0 & 0 & 0 & 0 & 0 & 0 & 0 & 0 & 0 & 0 \\
1 & 0 & 0 & 0 & 0 & 0 & 0 & 0 & 0 & 0 & 0 & 0 \\
\hline
0 & 0 & 0 & 0 & 0 & -1 & 0 & 0 & 0 & 0 & 0 & 0 \\
0 & 0 & 0 & 0 & 1 & 0 & 0 & 0 & 0 & 0 & 0 & 0 \\
0 & 0 & 0 & 1 & 0 & 0 & 0 & 0 & 0 & 0 & 0 & 0 \\
\hline
0 & 0 & 0 & 0 & 0 & 0 & 0 & 0 & -1 & 0 & 0 & 0 \\
0 & 0 & 0 & 0 & 0 & 0 & 0 & 1 & 0 & 0 & 0 & 0 \\
0 & 0 & 0 & 0 & 0 & 0 & 1 & 0 & 0 & 0 & 0 & 0 \\
\hline
0 & 0 & 0 & 0 & 0 & 0 & 0 & 0 & 0 & 0 & 0 & -1 \\
0 & 0 & 0 & 0 & 0 & 0 & 0 & 0 & 0 & 0 & 1 & 0 \\
0 & 0 & 0 & 0 & 0 & 0 & 0 & 0 & 0 & 1 & 0 & 0
\end{array}
\right].
\tag{7.58}
$$

The single stiffness relation for element III in global coordinates:

$$
\begin{bmatrix}
F_{3X} \\
F_{3Y} \\
F_{3Z} \\
M_{3X} \\
M_{3Y} \\
M_{3Z} \\
\hline
F_{4X} \\
F_{4Y} \\
F_{4Z} \\
M_{4X} \\
M_{4Y} \\
M_{4Z}
\end{bmatrix}
=
\left[\begin{array}{cccccc|cccccc}
0 & 0 & 0 & 0 & 0 & 0 & 0 & 0 & 0 & 0 & 0 & 0 \\
0 & 0 & 0 & 0 & 0 & 0 & 0 & 0 & 0 & 0 & 0 & 0 \\
0 & 0 & \frac{EA}{L} & 0 & 0 & 0 & 0 & 0 & -\frac{EA}{L} & 0 & 0 & 0 \\
0 & 0 & 0 & 0 & 0 & 0 & 0 & 0 & 0 & 0 & 0 & 0 \\
0 & 0 & 0 & 0 & 0 & 0 & 0 & 0 & 0 & 0 & 0 & 0 \\
0 & 0 & 0 & 0 & 0 & 0 & 0 & 0 & 0 & 0 & 0 & 0 \\
\hline
0 & 0 & 0 & 0 & 0 & 0 & 0 & 0 & 0 & 0 & 0 & 0 \\
0 & 0 & 0 & 0 & 0 & 0 & 0 & 0 & 0 & 0 & 0 & 0 \\
0 & 0 & -\frac{EA}{L} & 0 & 0 & 0 & 0 & 0 & \frac{EA}{L} & 0 & 0 & 0 \\
0 & 0 & 0 & 0 & 0 & 0 & 0 & 0 & 0 & 0 & 0 & 0 \\
0 & 0 & 0 & 0 & 0 & 0 & 0 & 0 & 0 & 0 & 0 & 0 \\
0 & 0 & 0 & 0 & 0 & 0 & 0 & 0 & 0 & 0 & 0 & 0
\end{array}\right]
\begin{bmatrix}
u_{3X} \\
u_{3Y} \\
u_{3Z} \\
\varphi_{3X} \\
\varphi_{3Y} \\
\varphi_{3Z} \\
u_{4X} \\
u_{4Y} \\
u_{4Z} \\
\varphi_{4X} \\
\varphi_{4Y} \\
\varphi_{4Z}
\end{bmatrix} . \tag{7.59}
$$

Now all single stiffness relations in global coordinates are known. The total stiffness relation can be established by arranging the single stiffness relations adequately. The dimension of the total stiffness relation results in 24×24, respectively six parameters are considered on the four nodes.

Only the lines and columns with non-zero entries are considered in the illustration of the total stiffness relation. The column matrices of the state variables in global coordinates are called:

$$
[u_{1Z}, \varphi_{1X}, \varphi_{1Y}, u_{2Z}, \varphi_{2X}, \varphi_{2Y}, u_{3Z}, \varphi_{3Y}, u_{4Z}]^{\mathrm{T}} \tag{7.60}
$$

and

$$
[F_{1Z}, M_{1X}, M_{1Y}, F_{2Z}, M_{2X}, M_{2Y}, F_{3Z}, M_{3Y}, F_{4Z}]^{\mathrm{T}} \tag{7.61}
$$

and the total stiffness matrix:

$$
\begin{bmatrix}
12\frac{EI_y}{L^3} & 6\frac{EI_y}{L^2} & 0 & -12\frac{EI_y}{L^3} & 6\frac{EI_y}{L^2} & 0 & 0 & 0 & 0 \\
6\frac{EI_y}{L^2} & 4\frac{EI_y}{L} & 0 & -6\frac{EI_y}{L^2} & 2\frac{EI_y}{L} & 0 & 0 & 0 & 0 \\
0 & 0 & k_{\mathrm{T}} & 0 & 0 & -k_{\mathrm{T}} & 0 & 0 & 0 \\
-12\frac{EI_y}{L^3} & -6\frac{EI_y}{L^2} & 0 & 24\frac{EI_y}{L^3} & -6\frac{EI_y}{L^2} & -6\frac{EI_y}{L^3} & -12\frac{EI_y}{L^3} & -6\frac{EI_y}{L^2} & 0 \\
6\frac{EI_y}{L^2} & 2\frac{EI_y}{L} & 0 & -6\frac{EI_y}{L^2} & 4\frac{EI_y}{L} & 0 & 0 & 0 & 0 \\
0 & 0 & -k_{\mathrm{T}} & -6\frac{EI_y}{L^2} & 0 & k_{\mathrm{T}}+4\frac{EI_y}{L} & 6\frac{EI_y}{L^2} & 2\frac{EI_y}{L} & 0 \\
0 & 0 & 0 & -12\frac{EI_y}{L^3} & 0 & 6\frac{EI_y}{L^2} & 12\frac{EI_y}{L^3}+k_{\mathrm{Z}} & 6\frac{EI_y}{L^2} & -k_{\mathrm{Z}} \\
0 & 0 & 0 & -6\frac{EI_y}{L^2} & 0 & 2\frac{EI_y}{L} & 6\frac{EI_y}{L} & 4\frac{EI_y}{L} & 0 \\
0 & 0 & 0 & 0 & 0 & 0 & -k_{\mathrm{Z}} & 0 & k_{\mathrm{Z}}
\end{bmatrix} \tag{7.62}
$$

with

$$k_{\mathrm{T}} = \frac{GI_{\mathrm{t}}}{L}, \quad k_{\mathrm{Z}} = \frac{EA}{L}. \tag{7.63}$$

The boundary conditions are included in the total stiffness relation. The displacement u_{1Z} and the angles φ_{1X} and φ_{2Y} are zero at the fixed support. Therewith the according lines and columns can be removed from the total stiffness relation. A reduced system remains.

$$\begin{bmatrix} 0 \\ 0 \\ 0 \\ 0 \\ 0 \\ F \end{bmatrix} = \begin{bmatrix} 24\dfrac{EI_y}{L^3} & -6\dfrac{EI_y}{L^2} & -6\dfrac{EI_y}{L^3} & -12\dfrac{EI_y}{L^3} & -6\dfrac{EI_y}{L^2} & 0 \\[2.5ex] -6\dfrac{EI_y}{L^2} & 4\dfrac{EI_y}{L} & 0 & 0 & 0 & 0 \\[2.5ex] -6\dfrac{EI_y}{L^2} & 0 & \dfrac{GI_{\mathrm{t}}}{L}+4\dfrac{EI_y}{L} & 6\dfrac{EI_y}{L^2} & 2\dfrac{EI_y}{L} & 0 \\[2.5ex] -12\dfrac{EI_y}{L^3} & 0 & 6\dfrac{EI_y}{L^2} & 12\dfrac{EI_y}{L^3}+k & 6\dfrac{EI_y}{L^2} & -k \\[2.5ex] -6\dfrac{EI_y}{L^2} & 0 & 2\dfrac{EI_y}{L} & 6\dfrac{EI_y}{L} & 4\dfrac{EI_y}{L} & 0 \\[2.5ex] 0 & 0 & 0 & -k & 0 & k \end{bmatrix} \begin{bmatrix} u_{2Z} \\ \varphi_{2X} \\ \varphi_{2Y} \\ u_{3Z} \\ \varphi_{3Y} \\ u_{4Z} \end{bmatrix}$$

$$\tag{7.64}$$

with

$$k = \frac{EA}{L}. \tag{7.65}$$

Herefrom the unknown parameters can be determined:

$$\begin{bmatrix} u_{2Z} \\ \varphi_{2X} \\ \varphi_{2Y} \\ u_{3Z} \\ \varphi_{3Y} \\ u_{4Z} \end{bmatrix} = \begin{bmatrix} +\dfrac{F}{3\frac{EI_y}{L^3}} \\[3ex] +\dfrac{F}{2\frac{EI_y}{L^2}} \\[3ex] -\dfrac{F}{2\frac{GI_{\mathrm{t}}}{L}} \\[3ex] +\dfrac{2GI_{\mathrm{t}}+3EI_y)L^3F}{3EI_yGI_{\mathrm{t}}} \\[3ex] -\dfrac{L^2(GI_{\mathrm{t}}+2EI_y)F}{2EI_yGI_{\mathrm{t}}} \\[3ex] +\dfrac{(3GI_{\mathrm{t}}I_y+2GI_{\mathrm{t}}AL^2)LF}{3EI_yAGI_{\mathrm{t}}} \end{bmatrix}. \tag{7.66}$$

By inserting the now known kinematic parameters into the total stiffness relation the clamping forces F_{1X} and fixed-end moments M_{1X} and M_{1Y} can be determined.

7.6 Supplementary Problems

7.1. Structure of Beams in the Three-Dimensional Space

For the above executed example, the displacements and rotations needs to be determined for concrete numerical values: $E = 210000\,\text{MPa}$, $G = 80707\,\text{MPa}$, $a = 20\,\text{mm}$, $I_t = 0.141a^4$, $F = 100\,N$.

7.2. Structure of Beams in the Three-Dimensional Space, Alternative Coordinate System

For the above executed example a second global coordinate system needs be defined. Figure 7.16 shows the definition of the coordinate axes. The global Z-coordinate remained the same, the X- and Y-coordinate have changed positions.
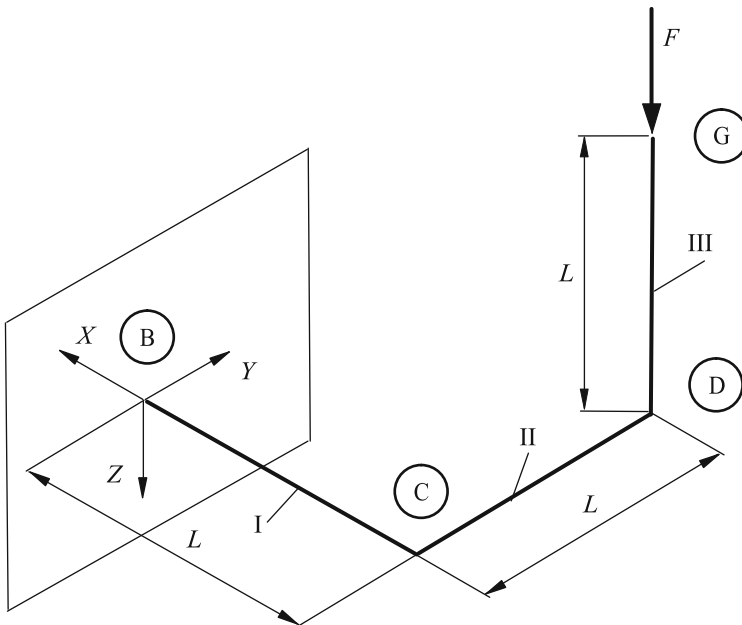
Fig. 7.16   General structure in the space with alternative global coordinate system

The kinematic parameters on the nodal points need to be determined.

References

1. Kwon YW, Bang H (2000) The finite element method using MATLAB. CRC Press, Boca Raton
2. Stoer J (1989) Numerische Mathematik 1. Springer-Lehrbuch, Berlin

Chapter 8
Beam with Shear Contribution

Abstract By this element the basic deformation bending under consideration of the shear influence will be described. First, several basic assumptions for the modeling of the TIMOSHENKO beam will be introduced and the element used in this chapter will be distinguished from other formulations. The basic equations from the strength of materials, meaning kinematics, the equilibrium as well as the constitutive equation will be introduced and used for the derivation of a system of coupled differential equations. The section about the basics is ended with analytical solutions. Subsequently the TIMOSHENKO bending element will be introduced with the definitions for load and deformation parameters which are commonly accepted at the handling via the FE method. The derivation of the stiffness matrix at this point also takes place via various methods and will be described in detail. Besides linear shape functions a general concept for an arbitrary arrangement of the shape functions will be introduced.

8.1 Introductory Remarks

The general differences regarding the deformation and stress distribution of a bending beam with and without shear influence have already been discussed in Chap. 5. In this chapter the shear influence needs to be considered with the help of the TIMOSHENKO beam theory. Within the framework of the following introductive remarks, first the definition of the shear strain and the connection between shear force and shear stress needs to be covered.

For the derivation of the equation for the shear strain in the $x - y$ plane, the infinitesimal rectangular beam element $ABCD$, shown in Fig. 8.1 will be considered, which deforms under exposure of shear stress. Here, a change of the angle of the original right angles as well as a change in the lengths of the edges occurs.

The deformation of the point A can be described via the displacement fields $u_x(x, y)$ and $u_y(x, y)$. These two functions of *two* variables can be expanded in TAYLOR's
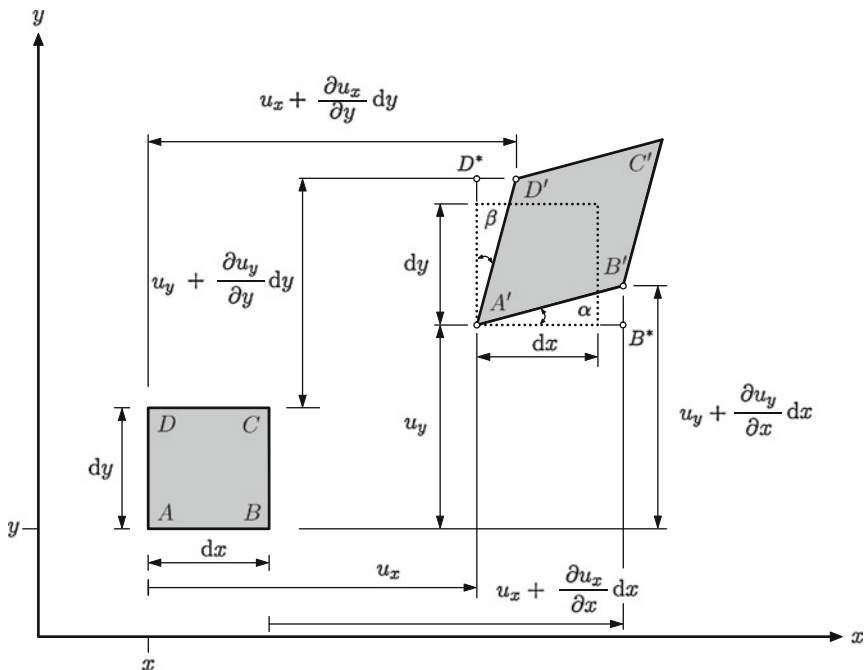
Fig. 8.1 Definition of the shear strain γ_{xy} in the $x - y$ plane at an infinitesimal beam element

series[1] of first order around point A to calculate the deformations of the points B and D approximatively:

$$u_{x,B} = u_x(x + \mathrm{d}x, y) = u_x(x, y) + \frac{\partial u_x}{\partial x} \, \mathrm{d}x + \frac{\partial u_x}{\partial y} \, \mathrm{d}y, \tag{8.1}$$

$$u_{y,B} = u_y(x + \mathrm{d}x, y) = u_y(x, y) + \frac{\partial u_y}{\partial x} \, \mathrm{d}x + \frac{\partial u_y}{\partial y} \, \mathrm{d}y, \tag{8.2}$$

or alternatively

$$u_{x,D} = u_x(x, y + \mathrm{d}y) = u_x(x, y) + \frac{\partial u_x}{\partial x} \, \mathrm{d}x + \frac{\partial u_x}{\partial y} \, \mathrm{d}y, \tag{8.3}$$

$$u_{y,D} = u_y(x, y + \mathrm{d}y) = u_y(x, y) + \frac{\partial u_y}{\partial x} \, \mathrm{d}x + \frac{\partial u_y}{\partial y} \, \mathrm{d}y. \tag{8.4}$$

In Eqs. (8.1) up to (8.4) $u_x(x, y)$ and $u_y(x, y)$ represent the so-called rigid-body displacement, which does not cause a deformation. If one considers that point B has

---

[1] For a function $f(x, y)$ of two variables usually a TAYLOR's series expansion of first order is assessed around the point (x_0, y_0) as follows: $f(x, y) = f(x_0 + \mathrm{d}x, y_0 + \mathrm{d}x) \approx f(x_0, y_0) + \left(\frac{\partial f}{\partial x}\right)_{x_0, y_0} \times (x - x_0) + \left(\frac{\partial f}{\partial y}\right)_{x_0, y_0} \times (y - y_0)$.

the coordinates $(x + \mathrm{d}x, y)$ and D the coordinates $(x, y + \mathrm{d}y)$, the following results:

$$u_{x,B} = u_x(x, y) + \frac{\partial u_x}{\partial x}\, \mathrm{d}x, \tag{8.5}$$

$$u_{y,B} = u_y(x, y) + \frac{\partial u_y}{\partial x}\, \mathrm{d}x, \tag{8.6}$$

or alternatively

$$u_{x,D} = u_x(x, y) + \frac{\partial u_x}{\partial y}\, \mathrm{d}y, \tag{8.7}$$

$$u_{y,D} = u_y(x, y) + \frac{\partial u_y}{\partial y}\, \mathrm{d}y. \tag{8.8}$$

The total shear strain γ_{xy} of the deformed beam element $A'B'C'D'$ results, according to Fig. 8.1 from the sum of the angles α and β, which can be identified at the rectangle, which is deformed as a rhombus. Under consideration of the two right-angled triangles $A'D^*D'$ and $A'B^*B'$ these two angles can be expressed via

$$\tan \alpha = \frac{\dfrac{\partial u_y}{\partial x}\, \mathrm{d}x}{\mathrm{d}x + \dfrac{\partial u_x}{\partial x}\, \mathrm{d}x} \quad \text{and} \quad \tan \beta = \frac{\dfrac{\partial u_x}{\partial y}\, \mathrm{d}y}{\mathrm{d}y + \dfrac{\partial u_y}{\partial y}\, \mathrm{d}y}. \tag{8.9}$$

It holds approximately for small deformations that $\tan \alpha \approx \alpha$ and $\tan \beta \approx \beta$ or alternatively $\frac{\partial u_x}{\partial x} \ll 1$ and $\frac{\partial u_y}{\partial y} \ll 1$, so that the following expression results for the shear strain:

$$\gamma_{xy} = \frac{\partial u_y}{\partial x} + \frac{\partial u_x}{\partial y} . \tag{8.10}$$

This total change of the angle is also called the engineering definition. In contrast the expression $\varepsilon_{xy} = \frac{1}{2}\, \gamma_{xy} = \frac{1}{2}\left(\frac{\partial u_y}{\partial x} + \frac{\partial u_x}{\partial y}\right)$ is enlisted as tensorial definition in the literature. Due to the symmetry of the strain tensor, in general $\gamma_{ij} = \gamma_{ji}$ applies.

The algebraic sign of the shear strain needs to be explained in the following with the help of Fig. 8.2 for the special case that only one shear force acts in parallel to the y-axis. If a shear force acts in direction of the positive y-axis at the right-hand face— hence a positive shear force distribution is assumed at this point—, according to Fig. 8.2a under consideration of Eq. (8.10) a positive shear strain results. Accordingly, a negative shear force distribution, according to Fig. 8.2b leads to a negative shear strain.

It has already been mentioned in Chap. 5 that the shear stress distribution is alterable through the cross-section. As an example, the parabolic shear stress distribution was illustrated through a rectangular cross-section in Fig. 5.2. Via HOOKE's law for a one-dimensional shear stress state (for this see Sect. 4.1), it can be derived that the
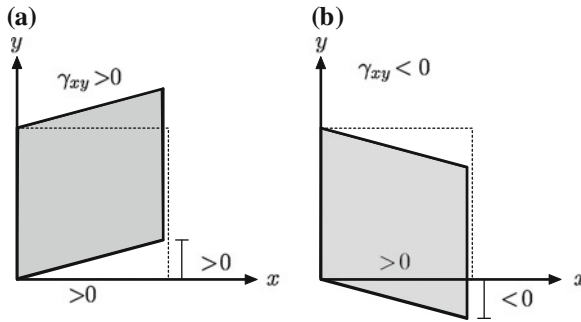
Fig. 8.2 Definition of a **a** positive and **b** negative shear strain in the $x-y$ plane

shear stress has to exhibit a corresponding parabolic course. From the shear stress distribution in the cross-sectional area at the location x of the beam[2] generally through integration, meaning

$$Q_y = \int_A \tau_{xy}(y, z)\mathrm{d}A, \tag{8.11}$$

the acting shear force results. To simplify it is however assumed for the TIMOSHENKO beam that an equivalent *constant* shear stress and strain act:

$$\tau_{xy}(y, z) \rightarrow \tau_{xy}. \tag{8.12}$$

This constant shear stress results from the shear force, which acts in an equivalent cross-sectional area, the so-called shear area A_s:

$$\tau_{xy} = \frac{Q_y}{A_\mathrm{s}}, \tag{8.13}$$
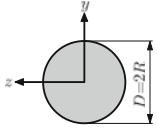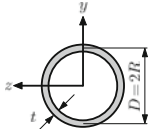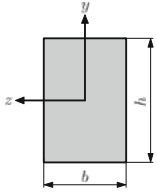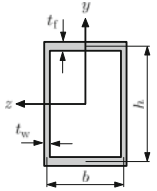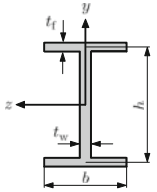
whereupon the relation between the shear area A_s and the actual cross-sectional area A is referred to as the shear correction factor k_s:

$$k_\mathrm{s} = \frac{A_\mathrm{s}}{A}. \tag{8.14}$$

For the calculation of the shear correction factor different assumptions can be made [3]. As an example, it can be demanded [4] that the elastic strain energy of the equivalent shear stress has to be identical with the energy, which results from the acting

---

[2] A closer analysis of the shear stress distribution in the cross-sectional area shows that the shear stress does not just alter through the height of the beam but also through the width of the beam. If the width of the beam is small compared to the height, only a small change along the width occurs and one can assume in the first approximation a constant shear stress throughout the width: $\tau_{xy}(y, z) \rightarrow \tau_{xy}(y)$. See for example [1, 2].

Table 8.1 Characteristics of different cross-sections in the $y-z$ plane

Cross-section	I_z	I_y	A	k_s
	$\dfrac{\pi R^4}{4}$	$\dfrac{\pi R^4}{4}$	πR^2	$\dfrac{9}{10}$
	$\pi R^3 t$	$\pi R^3 t$	$2\pi R t$	0.5
	$\dfrac{bh^3}{12}$	$\dfrac{hb^3}{12}$	hb	$\dfrac{5}{6}$
	$\dfrac{h^2}{6}(ht_{\mathrm{w}} + 3bt_{\mathrm{f}})$	$\dfrac{b^2}{6}(bt_{\mathrm{f}} + 3ht_{\mathrm{w}})$	$2(bt_{\mathrm{f}} + ht_{\mathrm{w}})$	$\dfrac{2ht_{\mathrm{w}}}{A}$
	$\dfrac{h^2}{12}(ht_{\mathrm{w}} + 6bt_{\mathrm{f}})$	$\dfrac{b^3 t_{\mathrm{f}}}{6}$	$ht_{\mathrm{w}} + 2bt_{\mathrm{f}}$	$\dfrac{ht_{\mathrm{w}}}{A}$

I_z and I_y axial second moment of area; A cross-sectional area; k_s shear correction factor. Adapted from [5]

shear stress distribution in the actual cross-sectional-area. Different characteristics of simple geometric cross-sections — including the shear correction factor[3] — are composed in Table 8.1 [5, 6]. Further details regarding the shear correction factor for arbitrary cross-sections can be taken from [7].

Of course the equivalent constant shear stress can alter along the center line of the beam, in case the shear force along the center line of the beam changes. The

---

[3] One notes that in the English literature often the so-called form factor for shear is stated. This results as the reciprocal of the shear correction factor.

attribute 'constant' thus just refers to the cross-sectional area at the location x and the equivalent constant shear stress is therefore in general a function of the coordinate of length for the TIMOSHENKO beam:

$$\tau_{xy} = \tau_{xy}(x). \tag{8.15}$$

8.2 Basic Description of the Beam with Shear Contribution

The so-called TIMOSHENKO beam can be generated by superposing a shear deformation on a BERNOULLI beam according to Fig. 8.3.

One can see that the BERNOULLI hypothesis is partly no longer fulfilled at the TIMO-SHENKO beam: plane cross-sections also remain plane after the deformation, however a cross-section, which stood at the right angle on the beam axis before the deformation is not at a right angle on the beam axis any longer after the deformation. If the demand for planeness of the cross-sections is also given up, one reaches theories of third-order [8–10], at which a parabolic course of the shear strain and stress in the displacement field are considered, see Fig. 8.4. Therefore a shear correction factor is unnecessary for these theories of third-order.

8.2.1 Kinematics

According to the alternative derivation in Sect. 5.2.1, the kinematic relation can also be derived for the beam with shear action, by considering the angle ϕ_z instead of the angle φ_z, see Fig. 8.3c. Following an equivalent procedure as in Sect. 5.2.1, the following relationships are obtained:

$$\sin \phi_z = \frac{u_x}{y} \approx \phi_z \ \text{ or } \ u_x = -y\phi_z, \tag{8.16}$$

wherefrom, via the general relation for the strain, meaning $\varepsilon_x = \mathrm{d}u_x/\mathrm{d}x$, the kinematic relation results through differentiation:

$$\varepsilon_x = -y\frac{\mathrm{d}\phi_z}{\mathrm{d}x}. \tag{8.17}$$

Note that $\phi_z \rightarrow \varphi_z = \dfrac{\mathrm{d}u_y}{\mathrm{d}x}$ results from neglecting of shear deformation and the relation according to Eq. (5.15) results as a special case. Furthermore, the following connection between the angles can be derived from Fig. 8.3c

$$\phi_z = \frac{\mathrm{d}u_y}{\mathrm{d}x} - \gamma_{xy}, \tag{8.18}$$
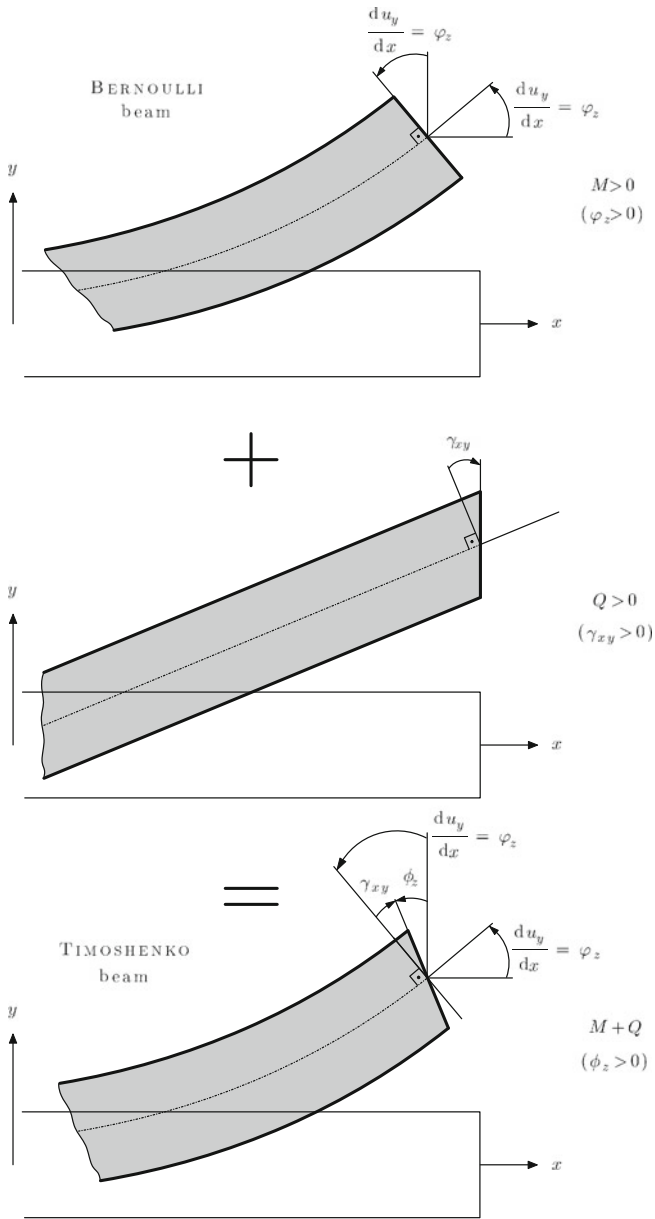
Fig. 8.3 Superposition of the BERNOULLI beam **a** and the shear deformation **b** to the TIMOSHENKO beam **c** in the $x-y$ plane. The marked orientations of the angles equal the positive definitions

TIMOSHENKO   third-order
theory
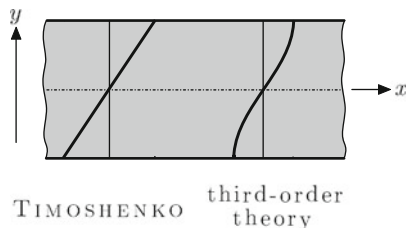
which complements the set of the kinematic relations. It needs to be remarked that at
this point the so-called bending line was considered and therefore the displacement
field u_y is just a function of *one* variable: $u_y = u_y(x)$.

8.2.2 Equilibrium

The derivation of the equilibrium condition for the TIMOSHENKO beam is identical
with the derivation for the BERNOULLI beam according to Sect. 5.2.2:

$$\frac{dQ_y(x)}{dx} = -q_y(x), \tag{8.19}$$

$$\frac{dM_z(x)}{dx} = -Q_y(x). \tag{8.20}$$

8.2.3 Constitutive Equation

For the consideration of the constitutive relation HOOKE's law for a one-dimensional
normal stress state and for a shear stress state is used:

$$\sigma_x = E\varepsilon_x, \tag{8.21}$$

$$\tau_{xy} = G\gamma_{xy}, \tag{8.22}$$

whereupon the shear modulus G can be calculated through the elasticity modulus E
and the POISSON's ratio ν via

$$G = \frac{E}{2(1+\nu)}. \tag{8.23}$$

According to the equilibrium of Fig. 5.8 and Eq. (5.29) the connection between the
internal moment and the bending stress can be used for the TIMOSHENKO beam as
follows:

$$dM_z = (+y)(-\sigma_x)dA, \tag{8.24}$$

or alternatively after integration under the use of the constitutive Eq. (8.21) and the kinematic relation (8.17):

$$M_z(x) = EI_z \frac{\mathrm{d}\phi_z(x)}{\mathrm{d}x}.$$ (8.25)

The connection between shear force and cross-section rotation results via the equilibrium relation (8.20) in:

$$Q_y(x) = -\frac{\mathrm{d}M_z(x)}{\mathrm{d}x} = -EI_z \frac{\mathrm{d}^2\phi_z(x)}{\mathrm{d}x^2}.$$ (8.26)

Before passing over to the differential equations of the bending line, the basic equations for the TIMOSHENKO beam are summarized in Table 8.2. Note that the normal stress and strain are functions of both coordinates of space x and y, however the shear stress and strain is only dependent on x, since an equivalent *constant* shear stress has been introduced via the cross-section as an approximation of the TIMOSHENKO beam approach.

Table 8.2 Elementary basic equations for the bending beam with shear contribution at the deformation in the x–y plane

Description	Equation
Kinematics	$\varepsilon_x(x, y) = -y\dfrac{\mathrm{d}\phi_z(x)}{\mathrm{d}x}$ and $\phi_z(x) = \dfrac{\mathrm{d}u_y(x)}{\mathrm{d}x} - \gamma_{xy}(x)$
Equilibrium	$\dfrac{\mathrm{d}Q_y(x)}{\mathrm{d}x} = -q_y(x)$; $\dfrac{\mathrm{d}M_z(x)}{\mathrm{d}x} = -Q_y(x)$
Constitutive Equation	$\sigma_x(x, y) = E\varepsilon_x(x, y)$ and $\tau_{xy}(x) = G\gamma_{xy}(x)$

8.2.4 Differential Equation of the Bending Line

Within the previous section the relation between the internal moment and the cross-section rotation was derived for the normal stress with the help of HOOKE's law. Differentiation of this relation according to Eq. (8.25) leads to the following connection

$$\frac{\mathrm{d}M_z}{\mathrm{d}x} = \frac{\mathrm{d}}{\mathrm{d}x}\left(EI_z \frac{\mathrm{d}\phi_z}{\mathrm{d}x}\right),$$ (8.27)

which can be transformed with the help of the equilibrium relation (8.20) and the relation for the shear stress according to (8.13) and (8.14) to

$$\frac{\mathrm{d}}{\mathrm{d}x}\left(EI_z\frac{\mathrm{d}\phi_z}{\mathrm{d}x}\right) = -k_\mathrm{s}GA\gamma_{xy}. \tag{8.28}$$

If the kinematic relation (8.18) is considered in the last equation, the so-called bending differential equation results in:

$$\frac{\mathrm{d}}{\mathrm{d}x}\left(EI_z\frac{\mathrm{d}\phi_z}{\mathrm{d}x}\right) + k_\mathrm{s}GA\left(\frac{\mathrm{d}u_y}{\mathrm{d}x} - \phi_z\right) = 0. \tag{8.29}$$

If now for the shear stress according to (8.22) the relation for the shear stress according to (8.13) and (8.14) is considered in HOOKE's law, one obtains

$$Q_y = k_\mathrm{s}AG\gamma_{xy}. \tag{8.30}$$

Via the equilibrium relation (8.20) and the kinematic relation (8.18) the following results herefrom:

$$\frac{\mathrm{d}M_z}{\mathrm{d}x} = -k_\mathrm{s}AG\left(\frac{\mathrm{d}u_y}{\mathrm{d}x} - \phi_z\right). \tag{8.31}$$

After differentiation and the consideration of the equilibrium relation according to (8.19) and (8.20) finally the so-called shear differential equation results in:

$$\frac{\mathrm{d}}{\mathrm{d}x}\left[k_\mathrm{s}AG\left(\frac{\mathrm{d}u_y}{\mathrm{d}x} - \phi_z\right)\right] = -q_y(x). \tag{8.32}$$

Therefore the shear flexible TIMOSHENKO beam will be described through the following two coupled differential equations of second order:

$$\frac{\mathrm{d}}{\mathrm{d}x}\left(EI_z\frac{\mathrm{d}\phi_z}{\mathrm{d}x}\right) + k_\mathrm{s}AG\left(\frac{\mathrm{d}u_y}{\mathrm{d}x} - \phi_z\right) = 0, \tag{8.33}$$

$$\frac{\mathrm{d}}{\mathrm{d}x}\left[k_\mathrm{s}AG\left(\frac{\mathrm{d}u_y}{\mathrm{d}x} - \phi_z\right)\right] = -q_y(x). \tag{8.34}$$

This system contains two unknown functions, namely the deflection $u_y(x)$ and the cross-sectional rotation $\phi_z(x)$. Boundary conditions can be formulated for both functions to be able to solve the system of differential equations.

8.2.5 Analytical Solutions

For the definition of analytical solutions, the system of coupled differential equations according to (8.33) and (8.34) has to be solved. Through the use of a computer algebra

system (CAS) for the symbolic calculation of mathematical expressions,[4] the general solution of the system results in:

$$u_y(x) = \frac{1}{EI_z}\left(\frac{q_y(x)x^4}{24} + c_1\frac{x^3}{6} + c_2\frac{x^2}{2} + c_3 x + c_4\right), \tag{8.35}$$

$$\phi_z(x) = \frac{1}{EI_z}\left(\frac{q_y(x)x^3}{6} + c_1\frac{x^2}{2} + c_2 x + c_3\right) + \frac{q_y(x)x}{k_s AG} + \frac{c_1}{k_s AG}. \tag{8.36}$$

The constants of integration $c_1, \ldots, c_4$ are to be defined through appropriate boundary conditions to calculate the special solution of a concrete problem, meaning under consideration of the support and the load of the beam.

Fig. 8.5 For the calculation of the analytical solution of a Timoshenko beam under distributed line load
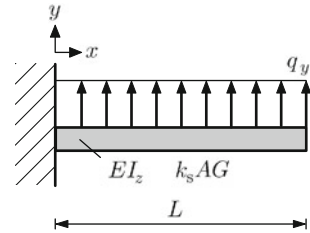
As an example, the beam, which is illustrated in Fig. 8.5, needs to be considered in the following. The loading occurs due to a distributed load q_y and the boundary conditions are given as follows for this example:

$$u_y(x = 0) = 0, \quad \phi_z(x = 0) = 0, \tag{8.37}$$

$$M_z(x = 0) = \frac{q_y L^2}{2}, \quad M_z(x = L) = 0. \tag{8.38}$$

The application of the boundary condition $(8.37)_1$ in the general analytical solution for the deflection according to Eq. (8.35) immediately yields $c_4 = 0$. With the second boundary condition in Eq. (8.37) the relation $c_3 = -c_1\frac{EI_z}{k_s AG}$ results with the general analytical solution for the rotation according to Eq. (8.36). The further definition of the constants of integration demands that the bending moment is expressed with the help of the deformation. Via Eq. (8.25) the moment distribution results in

$$M_z(x) = EI_z\frac{d\phi_z}{dx} = \left(c_1 x + c_2 + \frac{3q_y x^2}{6}\right) + \frac{q_y EI_z}{k_s AG}, \tag{8.39}$$

and the consideration of boundary conditions $(8.38)_1$ yields $c_2 = \frac{q_y L^2}{2} - \frac{q_y EI_z}{k_s AG}$. Accordingly, consideration of the second boundary condition in Eq. (8.38) yields the

---

[4] Maple®, Mathematica® and Matlab® can be listed at this point as commercial examples.

first constant of integration to $c_1 = -q_y L$ and finally $c_3 = \frac{q_y L E I_z}{k_s A G}$. Therefore the deflection distribution results in

$$u_y(x) = \frac{1}{EI_z} \left(\frac{q_y x^4}{24} - q_y L \frac{x^3}{6} + \left[\frac{q_y L^2}{2} - \frac{q_y EI_z}{k_s A G} \right] \frac{x^2}{2} + \frac{q_y L E I_z}{k_s A G} x \right), \quad (8.40)$$

or alternatively the maximal deflection on the right-hand end of the beam, meaning for $x = L$, to:

$$u_y(x = L) = \frac{q_y L^4}{8EI_z} + \frac{q_y L^2}{2k_s A G}. \tag{8.41}$$

Further analytical equations for the maximal deflection of a TIMOSHENKO beam are summarized in Table 8.3. Through comparison with the analytical solutions in Sect. 5.2.5 it becomes obvious that the analytical solutions for the maximal deflection compose additively from the classical solution for the BERNOULLI beam and an additional shear part.

Table 8.3 Maximal deflection of TIMOSHENKO beams at simple load cases for bending in the x-y plane

Load	Maximal deflection
y F $EIk_s AG$ L x	$u_{y,\mathrm{max}} = u_y(L) = \dfrac{FL^3}{3EI_z} + \dfrac{FL}{k_s A G}$
y q $EIk_s AG$ L x	$u_{y,\mathrm{max}} = u_y(L) = \dfrac{q_y L^4}{8EI_z} + \dfrac{q_y L^2}{2k_s A G}$
y F L $EIk_s AG$ x	$u_{y,\mathrm{max}} = u_y\left(\dfrac{L}{2}\right) = \dfrac{FL^3}{48EI_z} + \dfrac{FL}{4k_s A G}$

To highlight the influence of the shear part the maximal deflection needs to be presented in the following over the relation of beam height to beam length. As an example three different loading and support cases for a rectangular cross-section with the width b and the height h are presented in Fig. 8.6. It becomes obvious that the difference between the BERNOULLI and the TIMOSHENKO beam becomes smaller and smaller for a decreasing slenderness ratio, meaning for beams at which the length L is significantly bigger compared to the height h.

The relative difference between the BERNOULLI and the TIMOSHENKO solution results, for example for a POISSON's ratio of 0.3 and a slenderness ratio of 0.1 —
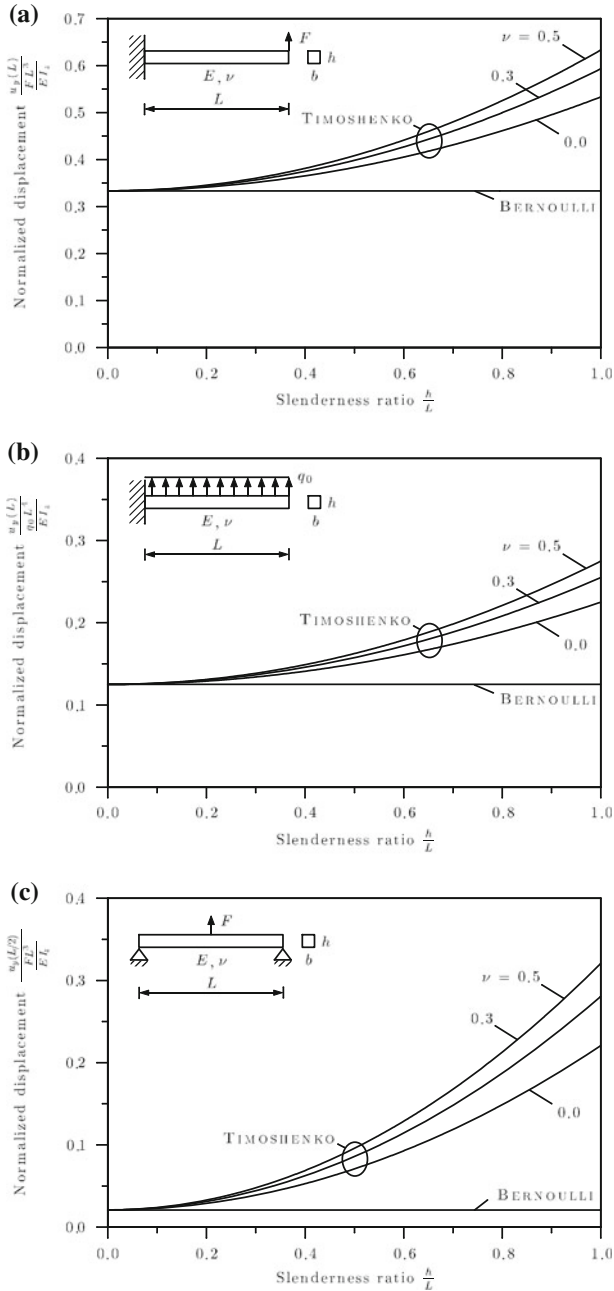
Fig. 8.6 Comparison of the analytical solutions for the BERNOULLI and TIMOSHENKO beam for different boundary conditions

meaning for a beam, at which the length is ten times bigger than the height — depending on the support and load in: 0.77 % for the cantilever with point load, 1.03 % for the cantilever with distributed load and 11.10 % for the simply supported beam. Further analytical solutions for the TIMOSHENKO beam can be withdrawn for example from [12].

Conclusively it needs to be pointed out at this point that for considerations in the $x - z$ plane slightly modified equations occur compared to Table 8.2. The corresponding equations for bending in the x–z plane with shear part are summarized in Table 8.4.

Table 8.4 Elementary basic equations for the bending beam with shear contribution at deformations in the $x - z$ plane

Notation	Equation
Kinematics	$\varepsilon_x(x, z) = -z \dfrac{\mathrm{d}\phi_y(x)}{\mathrm{d}x}$ and $\phi_y(x) = -\dfrac{\mathrm{d}u_z(x)}{\mathrm{d}x} + \gamma_{xz}(x)$
Equilibrium	$\dfrac{\mathrm{d}Q_z(x)}{\mathrm{d}x} = -q_z(x)\,;\; \dfrac{\mathrm{d}M_y(x)}{\mathrm{d}x} = +Q_z(x)$
Constitutive Equation	$\sigma_x(x, z) = E\varepsilon_x(x, z)$ and $\tau_{xz}(x) = G\gamma_{xz}(x)$
Differential Equation	$-\dfrac{\mathrm{d}}{\mathrm{d}x}\left(EI_y \dfrac{\mathrm{d}\phi_y}{\mathrm{d}x}\right) + k_s AG\left(\dfrac{\mathrm{d}u_z}{\mathrm{d}x} + \phi_y\right) = 0$
	$\dfrac{\mathrm{d}}{\mathrm{d}x}\left[k_s AG\left(\dfrac{\mathrm{d}u_z}{\mathrm{d}x} + \phi_y\right)\right] = -q_z(x)$

8.3 The Finite Element of Plane Bending Beams with Shear Contribution

According to Sect. 5.3 the bending element is defined as a prismatic body with the center line x and the y-axis orthogonally to the center line. Also at this point nodes, at which displacements and rotations or alternatively forces and moments, as drafted in Fig. 8.7, are defined, will be introduced at both ends of the bending element. The deformation and load parameters are as positive in the drafted direction.

The two unknowns, meaning the deflection $u_y(x)$ and the herefrom independent cross-sectional rotation $\phi_z(x)$ will be approximated with the help of the following nodal approach:

$$u_y(x) = N_{1u}(x)u_{1y} + N_{2u}(x)u_{2y}, \tag{8.42}$$

$$\phi_z(x) = N_{1\phi}(x)\phi_{1z} + N_{2\phi}(x)\phi_{2z}, \tag{8.43}$$

or alternatively in matrix notation as

Fig. 8.7 Definition of the positive direction for the bending element with shear contribution at deformation in the $x-y$ plane: **a** deformation parameters; **b** load parameters
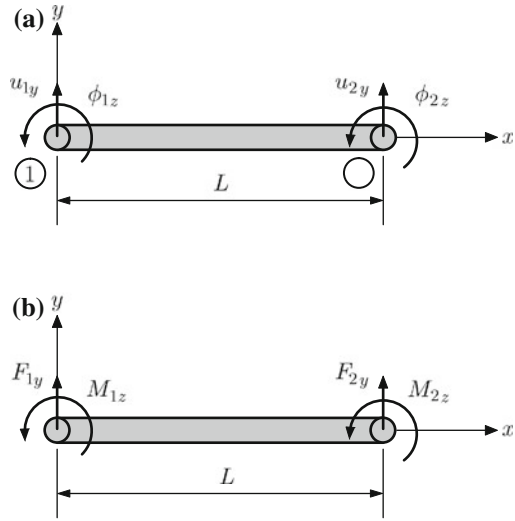
$$u_y(x) = \begin{bmatrix} N_{1u}(x) & 0 & N_{2u}(x) & 0 \end{bmatrix} \begin{bmatrix} u_{1y} \\ \phi_{1z} \\ u_{2y} \\ \phi_{2z} \end{bmatrix} = \boldsymbol{N}_u \boldsymbol{u}_{\mathrm{p}}, \qquad (8.44)$$

$$\phi_z(x) = \begin{bmatrix} 0 & N_{1\phi} & 0 & N_{2\phi}(x) \end{bmatrix} \begin{bmatrix} u_{1y} \\ \phi_{1z} \\ u_{2y} \\ \phi_{2z} \end{bmatrix} = \boldsymbol{N}_\phi \boldsymbol{u}_{\mathrm{p}}. \qquad (8.45)$$

With these relations the derivative of the cross-sectional rotation in the coupled differential equations (8.33) and (8.34) results in

$$\frac{\mathrm{d}\phi_z(x)}{\mathrm{d}x} = \frac{\mathrm{d}N_{1\phi}(x)}{\mathrm{d}x}\phi_{1z} + \frac{\mathrm{d}N_{2\phi}(x)}{\mathrm{d}x}\phi_{2z} = \frac{\mathrm{d}N_\phi}{\mathrm{d}x}\boldsymbol{u}_{\mathrm{p}}. \qquad (8.46)$$

8.3.1 Derivation Through Potential

The elastic strain energy for a TIMOSHENKO beam at linear elastic material behavior results in:

$$\Pi_{\text{int}} = \frac{1}{2} \int_{\Omega} \boldsymbol{\varepsilon}^{\text{T}} \boldsymbol{\sigma} \text{d}\Omega = \frac{1}{2} \int_{\Omega} \left[\varepsilon_x \ \gamma_{xy} \right] \begin{bmatrix} \sigma_x \\ \tau_{xy} \end{bmatrix} \text{d}\Omega \tag{8.47}$$

$$= \frac{1}{2} \int_{\Omega} \varepsilon_x \sigma_x \text{d}\Omega + \frac{1}{2} \int_{\Omega} \gamma_{xy} \tau_{xy} \text{d}\Omega = \Pi_{\text{int,b}} + \Pi_{\text{int,s}}. \tag{8.48}$$

The bending and shear part of the elastic strain energy will be regarded separately in the following and subsequently be superposed.

The bending part of the elastic strain energy results through HOOKE's law according to Eq. (8.21) in:

$$\Pi_{\text{int,b}} = \frac{1}{2} \int_{\Omega} \varepsilon_x \sigma_x \text{d}\Omega = \frac{1}{2} \int_{\Omega} \varepsilon_x E \varepsilon_x \text{d}\Omega. \tag{8.49}$$

The kinematic relation (8.17) can be written as follows via Eq. (8.46)

$$\varepsilon_x = -y \frac{\text{d}\phi}{\text{d}x} = -y \left(\frac{\text{d}N_{1\phi}(x)}{\text{d}x} \phi_{1z} + \frac{\text{d}N_{2\phi}(x)}{\text{d}x} \phi_{2z} \right) \tag{8.50}$$

$$= -y \left[0 \ \frac{\text{d}N_{1\phi}(x)}{\text{d}x} \ 0 \ \frac{\text{d}N_{2\phi}(x)}{\text{d}x} \right] \begin{bmatrix} u_{1y} \\ \phi_{1z} \\ u_{2y} \\ \phi_{2z} \end{bmatrix} = \boldsymbol{B}_{\text{b}} \boldsymbol{u}_{\text{p}} \tag{8.51}$$

whereupon a generalized $\boldsymbol{B}_{\text{b}}$ matrix as

$$\boldsymbol{B}_{\text{b}} = -y \frac{\text{d}\boldsymbol{N}_{\phi}}{\text{d}x} \tag{8.52}$$

has been introduced. With this result therefore the bending part of the elastic strain energy according to Eq. (8.49) results in:

$$\Pi_{\text{int,b}} = \frac{1}{2} \int_{\Omega} \left(\boldsymbol{B}_{\text{b}} \boldsymbol{u}_{\text{p}} \right)^{\text{T}} E \left(\boldsymbol{B}_{\text{b}} \boldsymbol{u}_{\text{p}} \right) \text{d}\Omega = \frac{1}{2} \int_{\Omega} \boldsymbol{u}_{\text{p}}^{\text{T}} \boldsymbol{B}_{\text{b}}^{\text{T}} E \boldsymbol{B}_{\text{b}} \boldsymbol{u}_{\text{p}} \text{d}\Omega$$

$$= \frac{1}{2} \boldsymbol{u}_{\text{p}}^{\text{T}} \left[\int_{\Omega} \boldsymbol{B}_{\text{b}}^{\text{T}} E \boldsymbol{B}_{\text{b}} \text{d}\Omega \right] \boldsymbol{u}_{\text{p}} = \frac{1}{2} \boldsymbol{u}_{\text{p}}^{\text{T}} \left[\int_{\Omega} (-y) \frac{\text{d}\boldsymbol{N}_{\phi}^{\text{T}}}{\text{d}x} E(-y) \frac{\text{d}\boldsymbol{N}_{\phi}}{\text{d}x} \text{d}\Omega \right] \boldsymbol{u}_{\text{p}}$$

$$= \frac{1}{2} \boldsymbol{u}_{\text{p}}^{\text{T}} \left[\int_{0}^{L} \underbrace{\left(\int_{A} y^2 \text{d}A \right)}_{I_z} E \frac{\text{d}\boldsymbol{N}_{\phi}^{\text{T}}}{\text{d}x} \frac{\text{d}\boldsymbol{N}_{\phi}}{\text{d}x} \text{d}x \right] \boldsymbol{u}_{\text{p}}.$$

$$= \frac{1}{2} \boldsymbol{u}_{\mathrm{p}}^{\mathrm{T}} \underbrace{\left[\int_0^L EI_z \frac{\mathrm{d}\boldsymbol{N}_\phi^{\mathrm{T}}}{\mathrm{d}x} \frac{\mathrm{d}\boldsymbol{N}_\phi}{\mathrm{d}x} \, \mathrm{d}x \right]}_{\boldsymbol{k}_{\mathrm{b}}^{\mathrm{e}}} \boldsymbol{u}_{\mathrm{p}}. \tag{8.53}$$

The element stiffness matrix was identified in the last equation with the help of the general formulation of the strain energy according to Eq. (5.95). Herefrom the element stiffness matrix for constant bending stiffness EI_z in components results in:

$$\boldsymbol{k}_{\mathrm{b}}^{\mathrm{e}} = EI_z \int_0^L \begin{bmatrix} 0 & 0 & 0 & 0 \\ 0 & \dfrac{\mathrm{d}N_{1\phi}}{\mathrm{d}x}\dfrac{\mathrm{d}N_{1\phi}}{\mathrm{d}x} & 0 & \dfrac{\mathrm{d}N_{1\phi}}{\mathrm{d}x}\dfrac{\mathrm{d}N_{2\phi}}{\mathrm{d}x} \\ 0 & 0 & 0 & 0 \\ 0 & \dfrac{\mathrm{d}N_{2\phi}}{\mathrm{d}x}\dfrac{\mathrm{d}N_{1\phi}}{\mathrm{d}x} & 0 & \dfrac{\mathrm{d}N_{2\phi}}{\mathrm{d}x}\dfrac{\mathrm{d}N_{2\phi}}{\mathrm{d}x} \end{bmatrix} \mathrm{d}x. \tag{8.54}$$

A further evaluation of Eq. (8.54) demands the introduction of the shape functions N_i.

The shear part of the elastic strain energy results in the following with the help of Eqs. (8.11) up to (8.14):

$$\Pi_{\mathrm{int,s}} = \frac{1}{2} \int_\Omega \gamma_{xy} \tau_{xy} \mathrm{d}\Omega = \frac{1}{2} \int_0^L \gamma_{xy}(x, y) \left(\int_A \tau_{xy}(x, y) \mathrm{d}A \right) \mathrm{d}x \tag{8.55}$$

$$= \frac{1}{2} \int_0^L \gamma_{xy} k_{\mathrm{s}} G A \gamma_{xy} \mathrm{d}x. \tag{8.56}$$

Via Eqs. (8.42) and (8.43) the kinematic relation can be written as follows

$$\gamma_{xy} = \frac{\mathrm{d}u_y}{\mathrm{d}x} - \phi = \frac{\mathrm{d}N_{1u}}{\mathrm{d}x} u_{1y} + \frac{\mathrm{d}N_{2u}}{\mathrm{d}x} u_{2y} - N_{1\phi}\phi_{1z} - N_{2\phi}\phi_{2z} \tag{8.57}$$

$$= \begin{bmatrix} \dfrac{\mathrm{d}N_{1u}}{\mathrm{d}x} & -N_{1\phi} & \dfrac{\mathrm{d}N_{2u}}{\mathrm{d}x} & -N_{2\phi} \end{bmatrix} \begin{bmatrix} u_{1y} \\ \phi_{1z} \\ u_{2y} \\ \phi_{2z} \end{bmatrix} = \boldsymbol{B}_{\mathrm{s}}\boldsymbol{u}_{\mathrm{p}}, \tag{8.58}$$

whereupon at this point a generalized $\boldsymbol{B}_{\mathrm{s}}$ matrix for the shear part has been introduced. With this result the shear part of the elastic strain energy according to Eq. (8.55) therefore results in:

$$\Pi_{\text{int,s}} = \frac{1}{2} \int_0^L \left(\boldsymbol{B}_{\text{s}} \boldsymbol{u}_{\text{p}} \right)^{\text{T}} k_{\text{s}} GA \left(\boldsymbol{B}_{\text{s}} \boldsymbol{u}_{\text{p}} \right) \text{d}x \qquad (8.59)$$

$$= \frac{1}{2} \boldsymbol{u}_{\text{p}}^{\text{T}} \underbrace{\left[\int_0^L k_{\text{s}} GA \boldsymbol{B}_{\text{s}}^{\text{T}} \boldsymbol{B}_{\text{s}} \text{d}x \right]}_{\boldsymbol{k}_{\text{s}}^{\text{e}}} \boldsymbol{u}_{\text{p}}. \qquad (8.60)$$

The element stiffness matrix for constant shear stiffness *GA* results herefrom in components to:

$$\boldsymbol{k}_{\text{s}}^{\text{e}} = k_{\text{s}} GA \int_0^L \begin{bmatrix} \dfrac{\text{d}N_{1u}}{\text{d}x}\dfrac{\text{d}N_{1u}}{\text{d}x} & \dfrac{\text{d}N_{1u}}{\text{d}x}(-N_{1\phi}) & \dfrac{\text{d}N_{1u}}{\text{d}x}\dfrac{\text{d}N_{2u}}{\text{d}x} & \dfrac{\text{d}N_{1u}}{\text{d}x}(-N_{2\phi}) \\[2ex] (-N_{1\phi})\dfrac{\text{d}N_{1u}}{\text{d}x} & (-N_{1\phi})(-N_{1\phi}) & (-N_{1\phi})\dfrac{\text{d}N_{2u}}{\text{d}x} & (-N_{1\phi})(-N_{2\phi}) \\[2ex] \dfrac{\text{d}N_{2u}}{\text{d}x}\dfrac{\text{d}N_{1u}}{\text{d}x} & \dfrac{\text{d}N_{2u}}{\text{d}x}(-N_{1\phi}) & \dfrac{\text{d}N_{2u}}{\text{d}x}\dfrac{\text{d}N_{2u}}{\text{d}x} & \dfrac{\text{d}N_{2u}}{\text{d}x}(-N_{2\phi}) \\[2ex] (-N_{2\phi})\dfrac{\text{d}N_{1u}}{\text{d}x} & (-N_{2\phi})(-N_{1\phi}) & (-N_{2\phi})\dfrac{\text{d}N_{2u}}{\text{d}x} & (-N_{2\phi})(-N_{2\phi}) \end{bmatrix} \text{d}x.$$

$$(8.61)$$

The two expressions for the bending and shear parts of the element stiffness matrix according to Eqs. (8.54) and (8.61) can be superposed for the principal finite element equation of the TIMOSHENKO beam on the element level

$$\boldsymbol{k}^{\text{e}} \boldsymbol{u}_{\text{p}} = \boldsymbol{F}^{\text{e}}, \qquad (8.62)$$

whereupon the total stiffness matrix according to Eq. (8.63) is given.

$$k^e = \begin{bmatrix} k_sGA \int_0^L \dfrac{dN_{1u}}{dx}\dfrac{dN_{1u}}{dx}\,dx & k_sGA \int_0^L \dfrac{dN_{1u}}{dx}(-N_{1\phi})\,dx & k_sGA \int_0^L \dfrac{dN_{1u}}{dx}\dfrac{dN_{2u}}{dx}\,dx & k_sGA \int_0^L \dfrac{dN_{1u}}{dx}(-N_{2\phi})\,dx \\[2em] k_sGA \int_0^L (-N_{1\phi})\dfrac{dN_{1u}}{dx}\,dx & k_sGA \int_0^L (-N_{1\phi})(-N_{1\phi})\,dx \\ + EI_z \int_0^L \dfrac{dN_{1\phi}}{dx}\dfrac{dN_{1\phi}}{dx}\,dx & k_sGA \int_0^L (-N_{1\phi})\dfrac{dN_{2u}}{dx}\,dx & k_sGA \int_0^L (-N_{1\phi})(-N_{2\phi})\,dx \\ + EI_z \int_0^L \dfrac{dN_{2\phi}}{dx}\dfrac{dN_{1\phi}}{dx}\,dx \\[2em] k_sGA \int_0^L \dfrac{dN_{2u}}{dx}\dfrac{dN_{1u}}{dx}\,dx & k_sGA \int_0^L \dfrac{dN_{2u}}{dx}(-N_{1\phi})\,dx & k_sGA \int_0^L \dfrac{dN_{2u}}{dx}\dfrac{dN_{2u}}{dx}\,dx & k_sGA \int_0^L \dfrac{dN_{2u}}{dx}(-N_{2\phi})\,dx \\[2em] k_sGA \int_0^L (-N_{2\phi})\dfrac{dN_{1u}}{dx}\,dx & k_sGA \int_0^L (-N_{2\phi})(-N_{1\phi})\,dx \\ + EI_z \int_0^L \dfrac{dN_{1\phi}}{dx}\dfrac{dN_{2\phi}}{dx}\,dx & k_sGA \int_0^L (-N_{2\phi})\dfrac{dN_{2u}}{dx}\,dx & k_sGA \int_0^L (-N_{2\phi})(-N_{2\phi})\,dx \\ + EI_z \int_0^L \dfrac{dN_{2\phi}}{dx}\dfrac{dN_{2\phi}}{dx}\,dx \end{bmatrix}$$

$$(8.63)$$

8.3.2 Derivation Through the Castigliano's Theorem

The elastic strain energy for a TIMOSHENKO beam according to Eq. (8.48) results via HOOKE's law (8.21) and the kinematic relation (8.17) or alternatively via the equation for the equivalent shear stress according to (8.11) up to (8.14) in:

$$
\begin{aligned}
\Pi_{\text{int}} &= \frac{1}{2} \int_{\Omega} \varepsilon_x \sigma_x \mathrm{d}\Omega + \frac{1}{2} \int_{\Omega} \gamma_{xy}(x, y)\, \tau_{xy}(x, y) \mathrm{d}\Omega \\
&= \frac{1}{2} \int_{\Omega} E\varepsilon_x^2 \mathrm{d}\Omega + \frac{1}{2} \int_0^L \gamma_{xy}(x, y) \left(\int_A \tau_{xy}(x, y) \mathrm{d}A \right) \mathrm{d}x \\
&= \frac{1}{2} \int_{\Omega} E \left(\frac{\mathrm{d}\phi}{\mathrm{d}x} \right)^2 y^2 \mathrm{d}\Omega + \frac{1}{2} \int_0^L \gamma_{xy} Q_y \mathrm{d}x \\
&= \frac{1}{2} \int_0^L E \left(\frac{\mathrm{d}\phi}{\mathrm{d}x} \right)^2 \left(\int_A y^2 \mathrm{d}A \right) \mathrm{d}x + \frac{1}{2} \int_0^L \gamma_{xy} \tau_{xy} k_{\mathrm{s}} A \mathrm{d}x \\
&= \frac{1}{2} \int_0^L EI_z \left(\frac{\mathrm{d}\phi}{\mathrm{d}x} \right)^2 \mathrm{d}x + \frac{1}{2} \int_0^L k_{\mathrm{s}} G A \gamma_{xy}^2 \mathrm{d}x.
\end{aligned}
\tag{8.64}
$$

Herefrom the elastic strain energy for a TIMOSHENKO beam with constant bending and shear stiffness results, via the approaches for the derivation of the cross-sectional rotation $\phi_z(x)$ according to Eq. (8.46) and the shear strain (8.57), in:

$$
\Pi_{\text{int}} = \frac{1}{2} EI_z \int_0^L \left(\frac{\mathrm{d}N_{1\phi}(x)}{\mathrm{d}x} \phi_{1z} + \frac{\mathrm{d}N_{2\phi}(x)}{\mathrm{d}x} \phi_{2z} \right)^2 \mathrm{d}x
$$
$$
+ \frac{1}{2} k_{\mathrm{s}} G A \int_0^L \left(\frac{\mathrm{d}N_{1u}}{\mathrm{d}x} u_{1y} + \frac{\mathrm{d}N_{2u}}{\mathrm{d}x} u_{2y} - N_{1\phi}\phi_{1z} - N_{2\phi}\phi_{2z} \right)^2 \mathrm{d}x.
\tag{8.65}
$$

Application of CASTIGLIANO's theorem on the strain energy in regards to the nodal displacement u_{1y} yields the external force F_{1y} on node 1:

$$
\frac{\mathrm{d}\Pi_{\text{int}}}{\mathrm{d}u_{1y}} = F_{1y} = k_{\mathrm{s}} G A \int_0^L \left(\frac{\mathrm{d}N_{1u}}{\mathrm{d}x} u_{1y} + \frac{\mathrm{d}N_{2u}}{\mathrm{d}x} u_{2y} - N_{1\phi}\phi_{1z} - N_{2\phi}\phi_{2z} \right) \frac{\mathrm{d}N_{1u}}{\mathrm{d}x} \mathrm{d}x.
$$
$$
\tag{8.66}
$$

Accordingly the following results from the differentiation according to other deformation parameters on the nodes:

$$\frac{\mathrm{d}\Pi_{\mathrm{int}}}{\mathrm{d}\phi_{1z}} = M_{1z} = EI_z \int\limits_0^L \left(\frac{\mathrm{d}N_{1\phi}(x)}{\mathrm{d}x} \phi_{1z} + \frac{\mathrm{d}N_{2\phi}(x)}{\mathrm{d}x} \phi_{2z} \right) \frac{\mathrm{d}N_{1\phi}(x)}{\mathrm{d}x} \mathrm{d}x$$

$$+ k_s GA \int\limits_0^L \left(\frac{\mathrm{d}N_{1u}}{\mathrm{d}x} u_{1y} + \frac{\mathrm{d}N_{2u}}{\mathrm{d}x} u_{2y} - N_{1\phi}\phi_{1z} - N_{2\phi}\phi_{2z} \right) (-N_{1\phi}) \mathrm{d}x.$$

(8.67)

$$\frac{\mathrm{d}\Pi_{\mathrm{int}}}{\mathrm{d}u_{2y}} = F_{2y} = k_s GA \int\limits_0^L \left(\frac{\mathrm{d}N_{1u}}{\mathrm{d}x} u_{1y} + \frac{\mathrm{d}N_{2u}}{\mathrm{d}x} u_{2y} - N_{1\phi}\phi_{1z} - N_{2\phi}\phi_{2z} \right) \frac{\mathrm{d}N_{2u}}{\mathrm{d}x} \mathrm{d}x.$$

(8.68)

$$\frac{\mathrm{d}\Pi_{\mathrm{int}}}{\mathrm{d}\phi_{2z}} = M_{2z} = EI_z \int\limits_0^L \left(\frac{\mathrm{d}N_{1\phi}(x)}{\mathrm{d}x} \phi_{1z} + \frac{\mathrm{d}N_{2\phi}(x)}{\mathrm{d}x} \phi_{2z} \right) \frac{\mathrm{d}N_{2\phi}(x)}{\mathrm{d}x} \mathrm{d}x$$

$$+ k_s GA \int\limits_0^L \left(\frac{\mathrm{d}N_{1u}}{\mathrm{d}x} u_{1y} + \frac{\mathrm{d}N_{2u}}{\mathrm{d}x} u_{2y} - N_{1\phi}\phi_{1z} - N_{2\phi}\phi_{2z} \right) (-N_{2\phi}) \mathrm{d}x.$$

(8.69)

The last four equations can be summarized as the principal finite element equation in matrix form, see Eqs. (8.62) and (8.63).

8.3.3 Derivation Through the Weighted Residual Method

According to the procedure in Sect. 5.3.2 one introduces approximate solutions into the differential equations (8.33) and (8.34) and demands that equations have to be fulfilled over a certain domain.

In the following first of all the shear differential equation is considered, which is multiplied with a deflection weighting function $W_u(x)$ to attain the following inner product:

$$\int\limits_0^L \left\{ k_s AG \left(\frac{\mathrm{d}^2 u_y}{\mathrm{d}x^2} - \frac{\mathrm{d}\phi_z}{\mathrm{d}x} \right) + q_y(x) \right\} W_u(x) \mathrm{d}x \overset{!}{=} 0. \qquad (8.70)$$

Partial integration of both expressions in the round brackets yields:

$$\int_0^L k_s AG \frac{d^2 u_y}{dx^2} W_u dx = \left[k_s AG \frac{du_y}{dx} W_u \right]_0^L - \int_0^L k_s AG \frac{du_y}{dx} \frac{dW_u}{dx} dx, \qquad (8.71)$$

$$-\int_0^L k_s AG \frac{d\phi_z}{dx} W_u dx = -\left[k_s AG \phi_z W_u \right]_0^L + \int_0^L k_s AG \phi_z \frac{dW_u}{dx} dx. \qquad (8.72)$$

Next, the bending differential equation (8.33) is multiplied with a rotation weighting function $W_\phi(x)$ and is transformed in the inner product:

$$\int_0^L \left\{ \frac{d}{dx} \left(EI_z \frac{d\phi_z}{dx} \right) + k_s AG \left(\frac{du_y}{dx} - \phi_z \right) \right\} W_\phi(x) dx \overset{!}{=} 0 \qquad (8.73)$$

Partial integration of the first expression yields

$$\int_0^L EI_z \frac{d^2 \phi_z}{dx^2} W_\phi dx = \left[EI_z \frac{d\phi_z}{dx} W_\phi \right]_0^L - \int_0^L EI_z \frac{d\phi_z}{dx} \frac{dW_\phi}{dx} dx \qquad (8.74)$$

and the bending differential equations results in:

$$\left[EI_z \frac{d\phi_z}{dx} W_\phi \right]_0^L - \int_0^L EI_z \frac{d\phi_z}{dx} \frac{dW_\phi}{dx} dx + \int_0^L k_s AG \left(\frac{du_y}{dx} - \phi_z \right) W_\phi(x) dx = 0. \qquad (8.75)$$

Adding of the two converted differential equations yields

$$\left[k_s AG \frac{du_y}{dx} W_u \right]_0^L - \int_0^L k_s AG \frac{du_y}{dx} \frac{dW_u}{dx} dx - \left[k_s AG \phi_z W_u \right]_0^L$$

$$+ \int_0^L k_s AG \phi_z \frac{dW_u}{dx} dx + \int_0^L q_y W_u dx + \int_0^L k_s AG \left(\frac{du_y}{dx} - \phi_z \right) W_\phi(x) dx$$

$$- \int_0^L EI_z \frac{d\phi_z}{dx} \frac{dW_\phi}{dx} dx + \left[EI_z \frac{d\phi_z}{dx} W_\phi \right]_0^L = 0, \qquad (8.76)$$

or alternatively after a short conversion the weak form of the shear flexible bending beam:

$$\int\limits_0^L EI_z \frac{\mathrm{d}\phi_z}{\mathrm{d}x} \frac{\mathrm{d}W_\phi}{\mathrm{d}x}\, \mathrm{d}x + \int\limits_0^L k_s A G \underbrace{\left(\frac{\mathrm{d}u_y}{\mathrm{d}x} - \phi_z\right)}_{\gamma_{xy}} \underbrace{\left(\frac{\mathrm{d}W_u}{\mathrm{d}x} - W_\phi\right)}_{\delta\gamma_{xy}}\, \mathrm{d}x$$

$$= \int\limits_0^L q_y W_u \mathrm{d}x + \left[k_s A G \left(\frac{\mathrm{d}u_y}{\mathrm{d}x} - \phi_z\right) W_u\right]_0^L + \left[EI_z \frac{\mathrm{d}\phi_z}{\mathrm{d}x} W_\phi\right]_0^L. \qquad (8.77)$$

One can see that the first part of the left-hand half represents the bending part and the second half the shear part. The right-hand side results from the external loads of the beam. In the following, first of all the left-hand half of the weak form will be considered to derive the stiffness matrix:

$$\int\limits_0^L EI_z \frac{\mathrm{d}\phi_z}{\mathrm{d}x} \frac{\mathrm{d}W_\phi}{\mathrm{d}x}\, \mathrm{d}x + \int\limits_0^L k_s A G \left(\frac{\mathrm{d}W_u}{\mathrm{d}x} - W_\phi\right)\left(\frac{\mathrm{d}u_y}{\mathrm{d}x} - \phi_z\right) \mathrm{d}x. \qquad (8.78)$$

In the next step the approaches for the deflection and rotation of the nodes or alternatively their derivatives according to Eqs. (8.44) and (8.45), meaning

$$u_y(x) = N_u(x)u_p, \quad \frac{\mathrm{d}u_y(x)}{\mathrm{d}x} = \frac{\mathrm{d}N_u(x)}{\mathrm{d}x} u_p, \qquad (8.79)$$

$$\phi_z(x) = N_\phi(x)u_p, \quad \frac{\mathrm{d}\phi_z(x)}{\mathrm{d}x} = \frac{\mathrm{d}N_\phi(x)}{\mathrm{d}x} u_p, \qquad (8.80)$$

have to be considered. The approaches for the weighting functions are chosen analogous to the approaches for the unknowns:

$$W_u(x) = \delta u_p^T N_u^T(x), \qquad (8.81)$$

$$W_\phi(x) = \delta u_p^T N_\phi^T(x), \qquad (8.82)$$

or alternatively for the derivatives:

$$\frac{W_u(x)}{\mathrm{d}x} = \delta u_p^T \frac{N_u^T(x)}{\mathrm{d}x}, \qquad (8.83)$$

$$\frac{W_\phi(x)}{\mathrm{d}x} = \delta u_p^T \frac{N_\phi^T(x)}{\mathrm{d}x}. \qquad (8.84)$$

Therefore the left-hand half of Eq. (8.78) — under consideration that the rotation or alternatively the virtual rotation can be considered as constant respective to the integration — results in:

$$\delta \boldsymbol{u}_{\mathrm{p}}^{\mathrm{T}} \int_0^L E I_z \frac{\mathrm{d} \boldsymbol{N}_\phi^{\mathrm{T}}}{\mathrm{d} x} \frac{\mathrm{d} \boldsymbol{N}_\phi}{\mathrm{d} x} \, \mathrm{d} x \, \boldsymbol{u}_{\mathrm{p}}$$

$$+ \delta \boldsymbol{u}_{\mathrm{p}}^{\mathrm{T}} \int_0^L k_{\mathrm{s}} A G \left(\frac{\mathrm{d} \boldsymbol{N}_u^{\mathrm{T}}}{\mathrm{d} x} - \boldsymbol{N}_\phi^{\mathrm{T}} \right) \left(\frac{\mathrm{d} \boldsymbol{N}_u}{\mathrm{d} x} - \boldsymbol{N}_\phi \right) \mathrm{d} x \, \boldsymbol{u}_{\mathrm{p}}. \tag{8.85}$$

In the following, it remains to be seen that the virtual deformations $\delta \boldsymbol{u}^{\mathrm{T}}$ can be canceled with a corresponding expression on the right-hand side of Eq. (8.77). Therefore, on the left-hand side there remains

$$\underbrace{\int_0^L E I_z \frac{\mathrm{d} \boldsymbol{N}_\phi^{\mathrm{T}}}{\mathrm{d} x} \frac{\mathrm{d} \boldsymbol{N}_\phi}{\mathrm{d} x} \, \mathrm{d} x \, \boldsymbol{u}_{\mathrm{p}}}_{\boldsymbol{k}_{\mathrm{b}}^{\mathrm{e}}} + \underbrace{\int_0^L k_{\mathrm{s}} A G \left(\frac{\mathrm{d} \boldsymbol{N}_u^{\mathrm{T}}}{\mathrm{d} x} - \boldsymbol{N}_\phi^{\mathrm{T}} \right) \left(\frac{\mathrm{d} \boldsymbol{N}_u}{\mathrm{d} x} - \boldsymbol{N}_\phi \right) \mathrm{d} x \, \boldsymbol{u}_{\mathrm{p}}}_{\boldsymbol{k}_{\mathrm{s}}^{\mathrm{e}}} \tag{8.86}$$

and the bending or alternatively the shear stiffness matrix can be identified, see Eqs. (8.54) and (8.61).

Finally, the right-hand side of the weak form according to Eq. (8.77) is considered:

$$\int_0^L q_y W_u \mathrm{d} x + \left[k_{\mathrm{s}} A G \left(\frac{\mathrm{d} u_y}{\mathrm{d} x} - \phi_z \right) W_u \right]_0^L + \left[E I_z \frac{\mathrm{d} \phi_z}{\mathrm{d} x} W_\phi \right]_0^L. \tag{8.87}$$

Consideration of the relations for the shear force and the internal moment according to Eqs. (8.30) and (8.25) in the right-hand side of the weak form yields

$$\int_0^L q_y W_u \mathrm{d} x + \left[Q_y(x) W_u(x) \right]_0^L + \left[M_z(x) W_\phi(x) \right]_0^L, \tag{8.88}$$

or alternatively after the introduction of the approaches for the deflection and rotation of the nodes according to Eqs. (8.44) and (8.45):

$$\delta \boldsymbol{u}_{\mathrm{p}}^{\mathrm{T}} \int_0^L q_y \boldsymbol{N}_u^{\mathrm{T}} \mathrm{d} x + \delta \boldsymbol{u}_{\mathrm{p}}^{\mathrm{T}} \left[Q_y(x) \boldsymbol{N}_u^{\mathrm{T}}(x) \right]_0^L + \delta \boldsymbol{u}_{\mathrm{p}}^{\mathrm{T}} \left[M_z(x) \boldsymbol{N}_\phi^{\mathrm{T}}(x) \right]_0^L. \tag{8.89}$$

$\delta \boldsymbol{u}_{\mathrm{p}}^{\mathrm{T}}$ can be canceled with the corresponding expression in Eq. (8.85) and the following remains

$$\int\limits_0^L q_y \boldsymbol{N}_u^{\mathrm{T}} \mathrm{d}x + \left[Q_y(x) \boldsymbol{N}_u^{\mathrm{T}}(x) \right]_0^L + \left[M_z(x) \boldsymbol{N}_\phi^{\mathrm{T}}(x) \right]_0^L, \tag{8.90}$$

or alternatively in components:

$$\int\limits_0^L q_y(x) \begin{bmatrix} N_{1u} \\ 0 \\ N_{2u} \\ 0 \end{bmatrix} \mathrm{d}x + \begin{bmatrix} -Q_{y(0)} \\ 0 \\ +Q_{y(L)} \\ 0 \end{bmatrix} + \begin{bmatrix} 0 \\ -M_{z(0)} \\ 0 \\ +M_{z(L)} \end{bmatrix}. \tag{8.91}$$

One notes that the general characteristics of the shape function have been used during the evaluation of the boundary integrals:

$$1^{\mathrm{st}} \text{ row}: \quad Q_y(L) \underbrace{N_{1u}(L)}_{0} - Q_y(0) \underbrace{N_{1u}(0)}_{1}, \tag{8.92}$$

$$2^{\mathrm{nd}} \text{ row}: \quad M_z(L) \underbrace{N_{1\phi}(L)}_{0} - M_z(0) \underbrace{N_{1\phi}(0)}_{1}, \tag{8.93}$$

$$3^{\mathrm{rd}} \text{ row}: \quad Q_y(L) \underbrace{N_{2u}(L)}_{1} - Q_y(0) \underbrace{N_{2u}(0)}_{0}, \tag{8.94}$$

$$4^{\mathrm{th}} \text{ row}: \quad M_z(L) \underbrace{N_{2\phi}(L)}_{1} - M_z(0) \underbrace{N_{2\phi}(0)}_{0}. \tag{8.95}$$

8.3.4 Linear Shape Functions for the Deflection and Displacement Field

Only the first order derivatives of the shape functions appear in the element stiffness matrices $\boldsymbol{k}_{\mathrm{b}}^{\mathrm{e}}$ and $\boldsymbol{k}_{\mathrm{s}}^{\mathrm{e}}$ according to Eqs. (8.54) and (8.61). This demand on the differentiability of the shape functions leads to polynomials of minimum first order (linear functions) for the deflection and displacement field, so that in the approaches according to Eqs. (8.42) and (8.43) the following linear shape functions can be used:

$$N_{1u}(x) = N_{1\phi}(x) = 1 - \frac{x}{L}, \tag{8.96}$$

$$N_{2u}(x) = N_{2\phi}(x) = \frac{x}{L}. \tag{8.97}$$

The necessary derivatives result in:

$$\frac{dN_{1u}}{dx} = \frac{dN_{1\phi}}{dx} = -\frac{1}{L}, \tag{8.98}$$

$$\frac{dN_{2u}}{dx} = \frac{dN_{2\phi}}{dx} = \frac{1}{L}. \tag{8.99}$$

A graphical illustration of the shape function is given in Fig. 8.8. Additionally the shape functions in the natural coordinate $\xi \in [-1, 1]$ are given. This formulation is more beneficial for the numerical integration of the stiffness matrices.
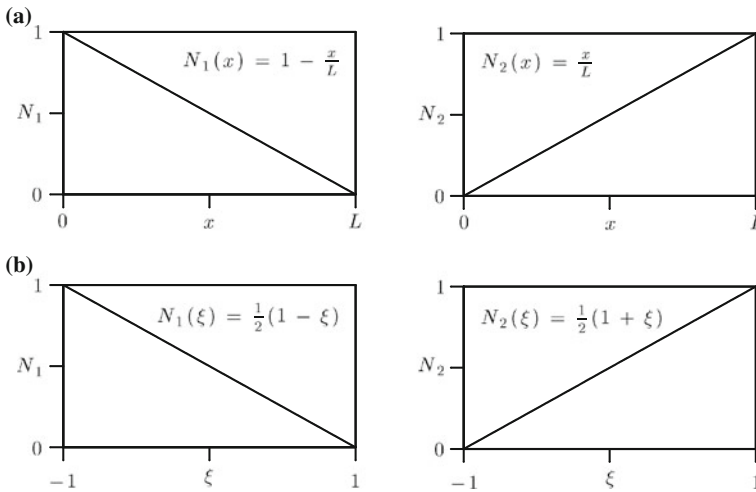
Fig. 8.8 Linear shape functions $N_1 = N_{1u}(x) = N_{1\phi}(x)$ and $N_2 = N_{2u}(x) = N_{2\phi}(x)$ for the TIMOSHENKO element in **a** physical (x) and **b** natural coordinates (ξ)

The integrals of the element stiffness matrices k_b^e and k_s^e according to Eqs. (8.54) and (8.61) need to be calculated analytically in the following. For the bending stiffness matrix the following results, using the linear approaches for the shape functions:

$$k_b^e = EI_z \int_0^L \begin{bmatrix} 0 & 0 & 0 & 0 \\ 0 & \dfrac{1}{L^2} & 0 & -\dfrac{1}{L^2} \\ 0 & 0 & 0 & 0 \\ 0 & -\dfrac{1}{L^2} & 0 & \dfrac{1}{L^2} \end{bmatrix} dx = EI_z \begin{bmatrix} 0 & 0 & 0 & 0 \\ 0 & \dfrac{x}{L^2} & 0 & -\dfrac{x}{L^2} \\ 0 & 0 & 0 & 0 \\ 0 & -\dfrac{x}{L^2} & 0 & \dfrac{x}{L^2} \end{bmatrix}_0^L, \tag{8.100}$$

or alternatively under consideration of the integration boundaries:

$$
k_{\mathrm{b}}^{\mathrm{e}} = EI_z
\begin{bmatrix}
0 & 0 & 0 & 0 \\
0 & \dfrac{1}{L} & 0 & -\dfrac{1}{L} \\
0 & 0 & 0 & 0 \\
0 & -\dfrac{1}{L} & 0 & \dfrac{1}{L}
\end{bmatrix}.
\tag{8.101}
$$

For the shear stiffness matrix the following results, using the linear approaches for the shape functions:

$$
k_{\mathrm{s}}^{\mathrm{e}} = k_{\mathrm{s}} A G \int_0^L
\begin{bmatrix}
\dfrac{1}{L^2} & \left(1-\dfrac{x}{L}\right)\dfrac{1}{L} & -\dfrac{1}{L^2} & \dfrac{x}{L^2} \\
\left(1-\dfrac{x}{L}\right)\dfrac{1}{L} & \left(1-\dfrac{x}{L}\right)^2 & -\left(1-\dfrac{x}{L}\right)\dfrac{1}{L} & \left(1-\dfrac{x}{L}\right)\dfrac{x}{L} \\
-\dfrac{1}{L^2} & -\left(1-\dfrac{x}{L}\right)\dfrac{1}{L} & \dfrac{1}{L^2} & -\dfrac{x}{L^2} \\
\dfrac{x}{L^2} & \left(1-\dfrac{x}{L}\right)\dfrac{x}{L} & -\dfrac{x}{L^2} & \dfrac{x^2}{L^2}
\end{bmatrix} \mathrm{d}x
\tag{8.102}
$$

$$
= k_{\mathrm{s}} A G
\begin{bmatrix}
\dfrac{x}{L^2} & \dfrac{x(-2L+x)}{2L^2} & -\dfrac{x}{L^2} & \dfrac{x^2}{2L^2} \\
\dfrac{x(-2L+x)}{2L^2} & \dfrac{(-L+x)^3}{3L^2} & \dfrac{x(-2L+x)}{2L^2} & \dfrac{x^2(2x-3L)}{6L^2} \\
-\dfrac{x}{L^2} & \dfrac{x(-2L+x)}{2L^2} & \dfrac{x}{L^2} & -\dfrac{x^2}{2L^2} \\
\dfrac{x^2}{2L^2} & \dfrac{x^2(2x-3L)}{6L^2} & -\dfrac{x^2}{2L^2} & \dfrac{x^3}{3L^2}
\end{bmatrix}_0^L
\tag{8.103}
$$

and finally after considering the constants of integration:

$$
k_{\mathrm{s}}^{\mathrm{e}} = k_{\mathrm{s}} A G
\begin{bmatrix}
+\dfrac{1}{L} & +\dfrac{1}{2} & -\dfrac{1}{L} & +\dfrac{1}{2} \\
+\dfrac{1}{2} & +\dfrac{L}{3} & -\dfrac{1}{2} & +\dfrac{L}{6} \\
-\dfrac{1}{L} & -\dfrac{1}{2} & +\dfrac{1}{L} & -\dfrac{1}{2} \\
+\dfrac{1}{2} & +\dfrac{L}{6} & -\dfrac{1}{2} & +\dfrac{L}{3}
\end{bmatrix}.
\tag{8.104}
$$

The two stiffness matrices according to Eqs. (8.101) and (8.104) can be summarized additively to the total stiffness matrix of the TIMOSHENKO beam:

$$
\boldsymbol{k}^{e} =
\begin{bmatrix}
\dfrac{k_{s}AG}{L} & \dfrac{k_{s}AG}{2} & -\dfrac{k_{s}AG}{L} & \dfrac{k_{s}AG}{2} \\[2mm]
\dfrac{k_{s}AG}{2} & \dfrac{k_{s}AGL}{3}+\dfrac{EI_{z}}{L} & -\dfrac{k_{s}AG}{2} & \dfrac{k_{s}AGL}{6}-\dfrac{EI_{z}}{L} \\[2mm]
-\dfrac{k_{s}AG}{L} & -\dfrac{k_{s}AG}{2} & \dfrac{k_{s}AG}{L} & -\dfrac{k_{s}AG}{2} \\[2mm]
\dfrac{k_{s}AG}{2} & \dfrac{k_{s}AGL}{6}-\dfrac{EI_{z}}{L} & -\dfrac{k_{s}AG}{2} & \dfrac{k_{s}AGL}{3}+\dfrac{EI_{z}}{L}
\end{bmatrix}
\tag{8.105}
$$

or alternatively via the abbreviation $\alpha = \frac{4EI_{z}}{k_{s}AG}$

$$
\boldsymbol{k}^{e} = \frac{k_{s}AG}{4L}
\begin{bmatrix}
4 & 2L & -4 & 2L \\[2mm]
2L & \dfrac{4}{3}L^{2}+\alpha & -2L & \dfrac{4}{6}L^{2}-\alpha \\[2mm]
-4 & -2L & 4 & -2L \\[2mm]
2L & \dfrac{4}{6}L^{2}-\alpha & -2L & \dfrac{4}{3}L^{2}+\alpha
\end{bmatrix}
\tag{8.106}
$$

or alternatively via the abbreviation $\varLambda = \dfrac{EI_{z}}{k_{s}AGL^{2}}$

$$
\boldsymbol{k}^{e} = \frac{EI_{z}}{6\varLambda L^{3}}
\begin{bmatrix}
6 & 3L & -6 & 3L \\
3L & L^{2}(2+6\varLambda) & -3L & L^{2}(1-6\varLambda) \\
-6 & -3L & 6 & -3L \\
3L & L^{2}(1-6\varLambda) & -3L & L^{2}(2+6\varLambda)
\end{bmatrix} .
\tag{8.107}
$$

In the following, the deformation behavior of this analytically integrated[5] TIMO-
SHENKO element needs to be analyzed. For this, the configuration in Fig. 8.9 needs
to be considered for which a beam has a fixed support on the left-hand side and a
point load on the right-hand side. The displacement of the loading point has to be
analyzed.

Fig. 8.9 Analysis of a TIMO-
SHENKO element under point
load
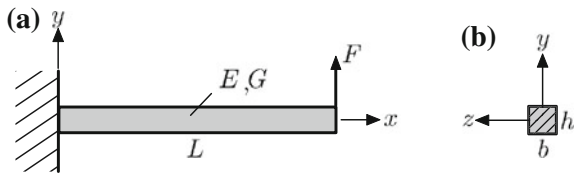
Through the stiffness matrix according to Eq. (8.106), the principal finite element
equation for a single element results in

---

[5] A numerical GAUSS integration with two integration points yields the same results as the exact
analytical integration.

$$\frac{k_s AG}{4L}\begin{bmatrix} 4 & 2L & -4 & 2L \\ 2L & \frac{4}{3}L^2+\alpha & -2L & \frac{4}{6}L^2-\alpha \\ -4 & -2L & 4 & -2L \\ 2L & \frac{4}{6}L^2-\alpha & -2L & \frac{4}{3}L^2+\alpha \end{bmatrix}\begin{bmatrix} u_{1y} \\ \phi_{1z} \\ u_{2y} \\ \phi_{2z} \end{bmatrix}=\begin{bmatrix} \cdots \\ \cdots \\ F \\ 0 \end{bmatrix}, \tag{8.108}$$

or alternatively after considering the fixed support ($u_{1y}=0$, $\phi_{1z}=0$) of the left-hand side:

$$\frac{k_s AG}{4L}\begin{bmatrix} 4 & -2L \\ -2L & \frac{4}{3}L^2+\alpha \end{bmatrix}\begin{bmatrix} u_{2y} \\ \phi_{2z} \end{bmatrix}=\begin{bmatrix} F \\ 0 \end{bmatrix}. \tag{8.109}$$

Solving this 2×2 system of equations for the unknown parameters on the right-hand end yields:

$$\begin{bmatrix} u_{2y} \\ \phi_{2z} \end{bmatrix}=\frac{4L}{k_s AG}\times\frac{1}{4\left(\frac{4}{3}L^2+\alpha\right)-(-2L)(-2L)}\begin{bmatrix} \frac{4}{3}L^2+\alpha & 2L \\ 2L & 4 \end{bmatrix}\begin{bmatrix} F \\ 0 \end{bmatrix}, \tag{8.110}$$

or alternatively solved for the unknown displacement on the right-hand end:

$$u_{2y}(L)=\frac{12EI_z+4k_s AGL^2}{12EI_z+k_s AGL^2}\times\left(\frac{FL}{k_s AG}\right). \tag{8.111}$$

Considering the rectangular cross-section, illustrated in Fig. 8.9, meaning $A=hb$ and $k_s=\frac{5}{6}$ and furthermore the relation for the shear modulus according to Eq. (8.23), after a short calculation the displacement on the right-hand end results:

$$u_{2y}(L)=\frac{12(1+\nu)\left(\frac{h}{L}\right)^2+20}{60+25\left(\frac{L}{h}\right)^2\frac{1}{1+\nu}}\times\left(\frac{FL^3}{EI_z}\right). \tag{8.112}$$

For very compact beams, meaning $h\gg L$, $\frac{L}{h}\to 0$ results and Eq. (8.112) converges against the analytical solution.[6] For very slender beams however, meaning $h\ll L$, a boundary value[7] of $\frac{4FL}{k_s AG}$ results from Eq. (8.111).

This boundary value only contains the shear part without bending and runs against a wrong solution. This phenomenon is called *shear locking*. A graphical illustration of this behavior is given in Fig. 8.10 via the normalized deflection with the BERNOULLI solution. One can clearly see the different convergence behaviors for different domains of the slenderness ratio, meaning for slender and compact beams.

---

[6] For this see Fig. 8.6 and the supplementary problem 8.6.

[7] One considers the definition of I_z and A in Eq. (8.111) and divides the fraction by h^3.
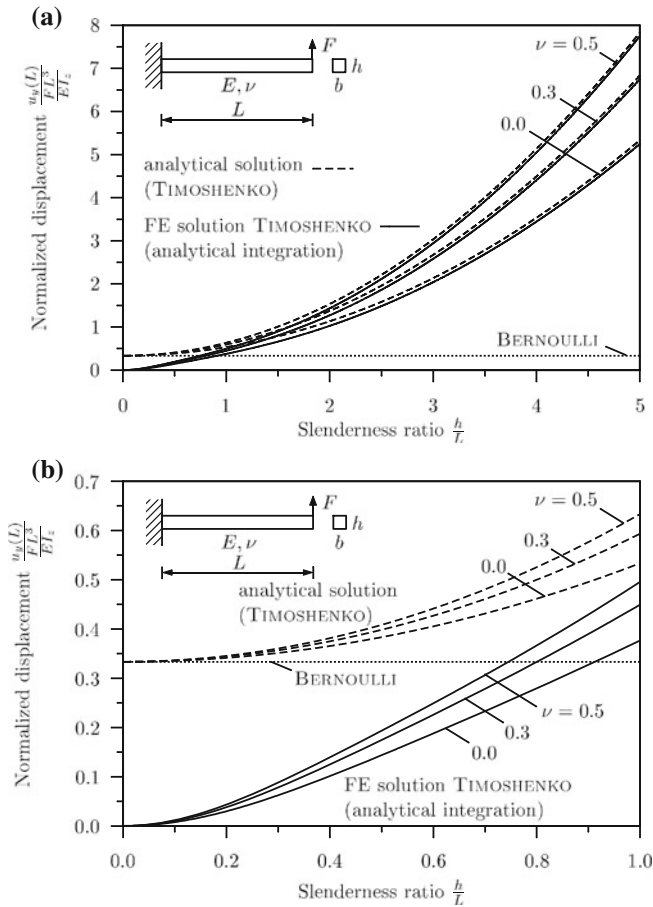
Fig. 8.10 Comparison of the analytical solution for a TIMOSHENKO beam and the corresponding discretization via one single finite element at analytical integration of the stiffness matrix

For the improvement of the convergence behavior, the literature suggests [13, 14] to conduct the integration via numerical GAUSS integration with only one integration point. Therefore the arguments and the integration boundaries in the formulations of the element stiffness matrices for k_b^e and k_s^e according to Eqs. (8.54) and (8.61) have to be transformed into the natural coordinate $-1 \leq \xi \leq 1$. Furthermore the shape functions need to be used according to Fig. 8.8. Via the transformation of the derivative to the new coordinate, meaning $\frac{dN}{dx} = \frac{dN}{d\xi}\frac{d\xi}{dx}$ and the transformation of the coordinate $\xi = -1 + 2\frac{x}{L}$ or alternatively $d\xi = \frac{2}{L}dx$, the bending stiffness matrix results in:

$$
k_{\mathrm{b}}^{\mathrm{e}} = EI_z \int_0^L \frac{4}{L^2}
\begin{bmatrix}
0 & 0 & 0 & 0 \\[4pt]
0 & \dfrac{\mathrm{d}N_{1\phi}}{\mathrm{d}\xi}\dfrac{\mathrm{d}N_{1\phi}}{\mathrm{d}\xi} & 0 & \dfrac{\mathrm{d}N_{1\phi}}{\mathrm{d}\xi}\dfrac{\mathrm{d}N_{2\phi}}{\mathrm{d}\xi} \\[10pt]
0 & 0 & 0 & 0 \\[4pt]
0 & \dfrac{\mathrm{d}N_{2\phi}}{\mathrm{d}\xi}\dfrac{\mathrm{d}N_{1\phi}}{\mathrm{d}\xi} & 0 & \dfrac{\mathrm{d}N_{2\phi}}{\mathrm{d}\xi}\dfrac{\mathrm{d}N_{2\phi}}{\mathrm{d}\xi}
\end{bmatrix}
\frac{L}{2}\,\mathrm{d}\xi,
\tag{8.113}
$$

$$
k_{\mathrm{b}}^{\mathrm{e}} = \frac{2EI_z}{L}\int_0^L \frac{4}{L^2}
\begin{bmatrix}
0 & 0 & 0 & 0 \\[2pt]
0 & \dfrac{1}{4} & 0 & -\dfrac{1}{4} \\[6pt]
0 & 0 & 0 & 0 \\[2pt]
0 & -\dfrac{1}{4} & 0 & \dfrac{1}{4}
\end{bmatrix}
\mathrm{d}\xi
= \frac{EI_z}{2L}\sum_{i=1}^{1}
\begin{bmatrix}
0 & 0 & 0 & 0 \\
0 & 1 & 0 & -1 \\
0 & 0 & 0 & 0 \\
0 & -1 & 0 & 1
\end{bmatrix} \times 2
\tag{8.114}
$$

and after all in the final formulation in:

$$
k_{\mathrm{b}}^{\mathrm{e}} = EI_z
\begin{bmatrix}
0 & 0 & 0 & 0 \\[2pt]
0 & \dfrac{1}{L} & 0 & -\dfrac{1}{L} \\[8pt]
0 & 0 & 0 & 0 \\[2pt]
0 & -\dfrac{1}{L} & 0 & \dfrac{1}{L}
\end{bmatrix}.
\tag{8.115}
$$

One can see that the same result for the bending stiffness matrix results as for the analytical integration. In the case of the bending stiffness matrix therefore the GAUSS integration with just one integration point is accurate.

The following expression results for the shear stiffness matrix under the use of the natural coordinate:

$$
\frac{2k_sGA}{L}\int_0^L
\begin{bmatrix}
\dfrac{\mathrm{d}N_{1u}}{\mathrm{d}\xi}\dfrac{\mathrm{d}N_{1u}}{\mathrm{d}\xi} & \dfrac{L}{2}\dfrac{\mathrm{d}N_{1u}}{\mathrm{d}\xi}(-N_{1\phi}) & \dfrac{\mathrm{d}N_{1u}}{\mathrm{d}\xi}\dfrac{\mathrm{d}N_{2u}}{\mathrm{d}\xi} & \dfrac{L}{2}\dfrac{\mathrm{d}N_{1u}}{\mathrm{d}\xi}(-N_{2\phi}) \\[10pt]
\dfrac{L}{2}(-N_{1\phi})\dfrac{\mathrm{d}N_{1u}}{\mathrm{d}\xi} & \dfrac{L^2}{4}(N_{1\phi})(N_{1\phi}) & \dfrac{L}{2}(-N_{1\phi})\dfrac{\mathrm{d}N_{2u}}{\mathrm{d}\xi} & \dfrac{L^2}{4}(N_{1\phi})(N_{2\phi}) \\[10pt]
\dfrac{\mathrm{d}N_{2u}}{\mathrm{d}\xi}\dfrac{\mathrm{d}N_{1u}}{\mathrm{d}\xi} & \dfrac{L}{2}\dfrac{\mathrm{d}N_{2u}}{\mathrm{d}\xi}(-N_{1\phi}) & \dfrac{\mathrm{d}N_{2u}}{\mathrm{d}\xi}\dfrac{\mathrm{d}N_{2u}}{\mathrm{d}\xi} & \dfrac{L}{2}\dfrac{\mathrm{d}N_{2u}}{\mathrm{d}\xi}(-N_{2\phi}) \\[10pt]
\dfrac{L}{2}(-N_{2\phi})\dfrac{\mathrm{d}N_{1u}}{\mathrm{d}\xi} & \dfrac{L^2}{4}(N_{2\phi})(N_{1\phi}) & \dfrac{L}{2}(-N_{2\phi})\dfrac{\mathrm{d}N_{2u}}{\mathrm{d}\xi} & \dfrac{L^2}{4}(N_{2\phi})(N_{2\phi})
\end{bmatrix}
\mathrm{d}\xi,
\tag{8.116}
$$

or alternatively after the introduction of the shape functions

$$
\frac{2k_{\mathrm{s}}GA}{L} \int_0^L
\begin{bmatrix}
\dfrac{1}{4} & \dfrac{L}{2}\left(\dfrac{1}{4}-\dfrac{x}{4}\right) & -\dfrac{1}{4} & \dfrac{L}{2}\left(\dfrac{1}{4}+\dfrac{x}{4}\right) \\[2mm]
\dfrac{L}{2}\left(\dfrac{1}{4}-\dfrac{x}{4}\right) & \dfrac{L^2}{4}\left(\dfrac{(-1+x)^2}{4}\right) & \dfrac{L}{2}\left(-\dfrac{1}{4}+\dfrac{x}{4}\right) & \dfrac{L^2}{4}\left(\dfrac{1}{4}-\dfrac{x^2}{4}\right) \\[2mm]
-\dfrac{1}{4} & \dfrac{L}{2}\left(-\dfrac{1}{4}+\dfrac{x}{4}\right) & \dfrac{1}{4} & \dfrac{L}{2}\left(-\dfrac{1}{4}-\dfrac{x}{4}\right) \\[2mm]
\dfrac{L}{2}\left(\dfrac{1}{4}+\dfrac{x}{4}\right) & \dfrac{L^2}{4}\left(\dfrac{1}{4}-\dfrac{x^2}{4}\right) & \dfrac{L}{2}\left(-\dfrac{1}{4}-\dfrac{x}{4}\right) & \dfrac{L^2}{4}\left(\dfrac{(1+x)^2}{4}\right)
\end{bmatrix}
\,\mathrm{d}\xi
$$

$$(8.117)$$

or after the transition to the numerical integration

$$
\frac{2k_{\mathrm{s}}GA}{L}
\begin{bmatrix}
\dfrac{1}{4} & \dfrac{L}{2}\dfrac{1}{4} & -\dfrac{1}{4} & \dfrac{L}{2}\dfrac{1}{4} \\[2mm]
\dfrac{L}{2}\dfrac{1}{4} & \dfrac{L^2}{4}\dfrac{1}{4} & \dfrac{L}{2}\left(-\dfrac{1}{4}\right) & \dfrac{L^2}{4}\dfrac{1}{4} \\[2mm]
-\dfrac{1}{4} & \dfrac{L}{2}\left(-\dfrac{1}{4}\right) & \dfrac{1}{4} & \dfrac{L}{2}\left(-\dfrac{1}{4}\right) \\[2mm]
\dfrac{L}{2}\dfrac{1}{4} & \dfrac{L^2}{4}\dfrac{1}{4} & \dfrac{L}{2}\left(-\dfrac{1}{4}\right) & \dfrac{L^2}{4}\dfrac{1}{4}
\end{bmatrix}_{\xi_i=0} \times 2
$$

$$(8.118)$$

and after all in the final formulation in:

$$
k_{\mathrm{s}}^{\mathrm{e}} = k_{\mathrm{s}}AG
\begin{bmatrix}
\dfrac{1}{L} & \dfrac{1}{2} & -\dfrac{1}{L} & \dfrac{1}{2} \\[2mm]
\dfrac{1}{2} & \dfrac{L}{4} & -\dfrac{1}{2} & \dfrac{L}{4} \\[2mm]
-\dfrac{1}{L} & -\dfrac{1}{2} & \dfrac{1}{L} & -\dfrac{1}{2} \\[2mm]
\dfrac{1}{2} & \dfrac{L}{4} & -\dfrac{1}{2} & \dfrac{L}{4}
\end{bmatrix}.
$$

$$(8.119)$$

The two stiffness matrices according to Eqs. (8.115) and (8.119) can be summarized additively to the total stiffness matrix of the TIMOSHENKO beam and with the abbreviation $\alpha = \frac{4EI_z}{k_{\mathrm{s}}AG}$ the following results:

$$
k^{\mathrm{e}} = \frac{k_{\mathrm{s}}AG}{4L}
\begin{bmatrix}
4 & 2L & -4 & 2L \\
2L & L^2+\alpha & -2L & L^2-\alpha \\
-4 & -2L & 4 & -2L \\
2L & L^2-\alpha & -2L & L^2+\alpha
\end{bmatrix}
$$

$$(8.120)$$

or alternatively via the abbreviation $\Lambda = \frac{EI_z}{k_s AGL^2}$:

$$k^e = \frac{EI_z}{6\Lambda L^3} \begin{bmatrix} 6 & 3L & -6 & 3L \\ 3L & L^2(1,5+6\Lambda) & -3L & L^2(1,5-6\Lambda) \\ -6 & -3L & 6 & -3L \\ 3L & L^2(1,5-6\Lambda) & -3L & L^2(2+6\Lambda) \end{bmatrix}. \qquad (8.121)$$

With the help of this formulation for the stiffness matrix the example according to Fig. 8.9 needs to be analyzed once again in the following to analyze the differences to the analytical integration. Via the stiffness matrix according to Eq. (8.120), the principal finite element equation for a single element under consideration of the fixed support ($u_{1y} = 0$, $\phi_{1z} = 0$) on the left-hand side results in:

$$\frac{k_s AG}{4L} \begin{bmatrix} 4 & -2L \\ -2L & L^2 + \alpha \end{bmatrix} \begin{bmatrix} u_{2y} \\ \phi_{2z} \end{bmatrix} = \begin{bmatrix} F \\ 0 \end{bmatrix}. \qquad (8.122)$$

Solving of this 2×2 system of equations for the unknown displacement on the right-hand side yields:

$$u_{2y}(L) = \left(1 + \frac{4EI_z}{k_s AGL^2}\right) \times \frac{FL^3}{4EI_z}. \qquad (8.123)$$

If the illustrated rectangular cross-section in Fig. 8.9 is considered at this point as well, after a short calculation the displacement on the right-hand side, via $A = hb$, $k_s = \frac{5}{6}$ and the relation for the shear modulus according to Eq. (8.23) results in:

$$u_{2y}(L) = \left(\frac{1}{4} + \frac{1}{5}(1+\nu)\left(\frac{h}{L}\right)^2\right) \times \left(\frac{FL^3}{EI_z}\right). \qquad (8.124)$$

For very compact beams, meaning $h \gg L$, the solution converges against the analytical solution.[8] For very slender beams however, meaning $h \ll L$, a boundary value of $\frac{FL^3}{4EI_z}$ results from Eq. (8.124), whereupon the analytical solution yields a value of $\frac{FL^3}{3EI_z}$. However, the phenomenon of shear locking does not occur and therefore, compared to the stiffness matrix based on the analytical integration, an improvement of the element formulation has been achieved.

A graphical illustration of this behavior via the normalized deflection is given in Fig. 8.11. One can clearly see the improved convergence behavior for small slenderness ratios. For big slenderness ratios the behavior remains according to the result of the analytical integration, since both approaches converge against the analytical solution.

---

[8] For this see Fig. 8.6 and the supplementary problem 8.6.

(a)

(b)
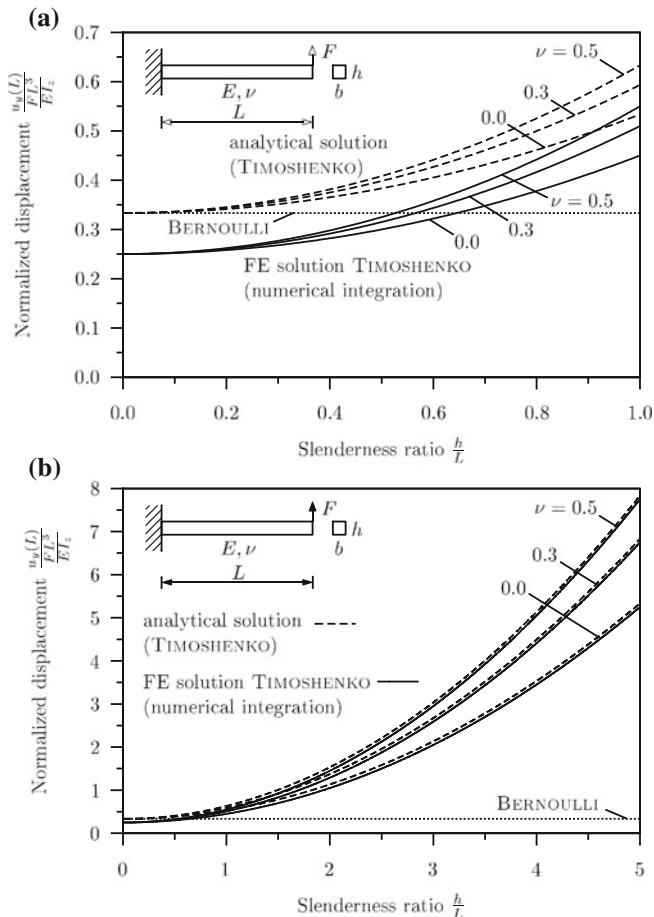
Fig. 8.11 Comparison of the analytical solution for a TIMOSHENKO beam and the appropriate discretization via one single finite element at numerical integration of the corresponding matrix with the help of one integration point

When the differential equations according to (8.33) and (8.34) are considered, it becomes obvious that the derivative $\frac{du_y}{dx}$ and the function ϕ_z itself are contained there. If linear shape functions are used for u_y and ϕ_z, the degree for polynomials for $\frac{du_y}{dx}$ and ϕ_z is different. In the limiting case of slender beams however the relation $\phi \approx \frac{du_y}{dx}$ has to be fulfilled and the consistency of the polynomials for $\frac{du_y}{dx}$ and ϕ_z is of importance. The linear approach for u_y yields for $\frac{du_y}{dx}$ a constant function and therefore also for ϕ_z a constant would be desirable. However, at this point it needs to be considered that the demand for the differentiability of ϕ_z at least results

in a linear function. The one-point integration[9] in the case of the shear stiffness matrix with the expressions $N_{i\phi}N_{j\phi}$ causes however that the linear approach for ϕ_z is treated as a constant term, since two integration points would have to be used for an exact integration. A one-point integration can at most integrate a polynomial of first order exactly, meaning proportional to x^1, and therefore the following point of view results $(N_{i\phi}N_{j\phi}) \sim x^1$. This however means that at most $N_{i\phi} \sim x^{0.5}$ or alternatively $N_{j\phi} \sim x^{0.5}$ holds. Since the polynomial approach solely allows integer values for the exponent of x, $N_{i\phi} \sim x^0$ or alternatively $N_{j\phi} \sim x^0$ results and the rotation needs to be seen as a constant term. This is consistent with the demand that the shear strain $\gamma_{xy} = \frac{du_y}{dx} - \phi_z$ has to be constant in an element for constant bending stiffness EI_z. Therefore in this case *shear locking* does not occur.

As another option for the improvement of the convergence behavior of linear TIMO-SHENKO elements with numerical one-point integrations [13, 15] suggests to correct the shear stiffness $k_s AG$ according to the analytical correct solution.[10] To this the elastic strain energy is regarded, which results from Eqs. (8.49) and (8.56) for the energies and the kinematic relations (8.17) and (8.18) as follows:

$$\Pi_{\text{int}} = \frac{1}{2} \int_0^L EI_z \left(\frac{d\phi_z(x)}{dx} \right)^2 dx + \frac{1}{2} \int_0^L k_s AG \left(\frac{du_y(x)}{dx} - \phi_z(x) \right)^2 dx. \quad (8.125)$$

It is now demanded that the strain energy for the analytical solution and the finite element solution under the use of the corrected shear stiffness $(k_s AG)^*$ are identical. The analytical solution[11] for the problem in Fig. 8.9 results in

$$u_y(x) = \frac{1}{EI_z} \left(-F\frac{x^3}{6} + FL\frac{x^2}{2} + \frac{EI_z F}{k_s AG} x \right), \quad (8.126)$$

$$\phi_z(x) = \frac{1}{EI_z} \left(-F\frac{x^2}{2} + FLx \right), \quad (8.127)$$

and the elastic strain energy for the analytical solution therefore results in:

$$\Pi_{\text{int}} = \frac{F^2}{2EI_z} \int_0^L (L-x)^2 dx + \frac{F^2(EI_z)^2}{2k_s AG} \int_0^L dx = \frac{F^2 L^3}{6EI_z} + \frac{F^2 L}{2k_s AG}. \quad (8.128)$$

Via Eq. (8.122) the finite element solution of the elastic strain energy results in:

---

[9] The numerical integration according to the GAUSS–LEGENDRE method with n integration points integrates a polynomial, which degree is at most $2n - 1$, exactly.

[10] MACNEAL hereford uses the expression 'residual bending flexibility' [16, 17].

[11] For this see the supplementary problem 8.5.

$$\Pi_{\text{int}} = \frac{EI_z}{2} \int\limits_0^L \left(\frac{FL}{2EI_z} \right)^2 \mathrm{d}x$$

$$+ \frac{(k_s AG)^*}{2} \int\limits_0^L \left(\left(1 + \frac{4EI_z}{(k_s AG)^* L^2} \right) \frac{FL^2}{4EI_z} - \frac{FLx}{2EI_z} \right)^2 \mathrm{d}x. \qquad (8.129)$$

This integral has to be evaluated numerically with a one-point integration rule and it is therefore necessary to introduce the natural coordinate via the transformation $x = \frac{L}{2}(\xi + 1)$:

$$\Pi_{\text{int}} = \frac{F^2 L^3}{8EI_z}$$

$$+ \frac{(k_s AG)^*}{2} \int\limits_0^L \left(\left(1 + \frac{4EI_z}{(k_s AG)^* L^2} \right) \frac{FL^2}{4EI_z} - \frac{FL}{2EI_z}(\xi + 1)\frac{L}{2} \right)^2 \frac{L}{2} \, \mathrm{d}\xi$$

$$= \frac{F^2 L^3}{8EI_z} + \frac{(k_s AG)^*}{2} \left(\frac{4EI_z}{(k_s AG)^* L^2} \times \frac{FL^2}{4EI_z} \right)^2 \frac{L}{2} \, 2 \qquad (8.130)$$

and finally

$$\Pi_{\text{int}} = \frac{F^2 L^3}{8EI_z} + \frac{F^2 L}{2(k_s AG)^*}. \qquad (8.131)$$

Equalizing of the two energy expressions according to Eqs. (8.128) and (8.131) finally yields the corrected shear stiffness:

$$(k_s AG)^* = \left(\frac{L^2}{12EI_z} + \frac{1}{k_s AG} \right)^{-1}. \qquad (8.132)$$

By inserting these with the 'residual bending flexibility' $\frac{L^2}{12EI_z}$ corrected shear stiffness into the finite element solution according to Eq. (8.123), the analytically exact solution results. The same result is derived in [15], starting from the general — meaning without considering a certain support of the beam — solution for the beam deflection, and in [13] the derivation for the equality of the deflection on the loading point according to the analytical and the corrected finite element solution takes place. It is to be considered that the derived corrected shear stiffness is not just valid for the cantilevered beam under point load, but yields the same value for arbitrary support and load on the ends of the beam. However, the derivation of the corrected shear stiffness for nonhomogeneous, anisotropic and non-linear materials appears problematic [13].

8.3.5 *Higher-Order Shape Functions for the Beam with Shear Contribution*

Within the framework of this subsection, first a general approach for a TIMOSHENKO element with an arbitrary amount of nodes will be derived [14]. Furthermore the number of nodes, at which the deflection and the rotation are evaluated, can be different here. Therefore in the generalization of Eqs. (8.42) and (8.43) the following approach for the unknowns on the nodes results:

$$u_y(x) = \sum_{i=1}^{m} N_{iu}(x)u_{iy}, \tag{8.133}$$

$$\phi_z(x) = \sum_{i=1}^{n} N_{i\phi}(x)\phi_{iz}, \tag{8.134}$$

or alternatively in matrix notation as

$$u_y(x) = \begin{bmatrix} N_{1u} \ \dots \ N_{mu} \ 0 \ \dots \ 0 \end{bmatrix} \begin{bmatrix} u_{1y} \\ \vdots \\ u_{my} \\ \phi_{1z} \\ \vdots \\ \phi_{nz} \end{bmatrix} = N_u u_p, \tag{8.135}$$

$$\phi_z(x) = \begin{bmatrix} 0 \ \dots \ 0 \ N_{1\phi} \ \dots \ N_{n\phi} \end{bmatrix} \begin{bmatrix} u_{1y} \\ \vdots \\ u_{my} \\ \phi_{1z} \\ \vdots \\ \phi_{nz} \end{bmatrix} = N_\phi u_p. \tag{8.136}$$

With this generalized approach the deflection can be evaluated on m nodes and the rotation on n nodes. For the shape functions N_i usually LAGRANGE polynomials[12] are used, which in general are calculated as follows in the case of deflection:

---

[12] At the so-called LAGRANGE interpolation, m points are approximated via the ordinate values with the help of a polynomial of the order $m - 1$. In the case of the HERMITE interpolation the slope of the regarded points is considered in addition to the ordinate value. For this see Chap. 6.

$$N_i = \prod_{j=0 \wedge j \neq i}^{m} \frac{x_j - x}{x_j - x_i}$$

$$= \frac{(x_1 - x)(x_2 - x) \cdots [x_i - x] \cdots (x_m - x)}{(x_1 - x_i)(x_2 - x_i) \cdots [x_i - x_i] \cdots (x_m - x_i)}, \tag{8.137}$$

whereupon the expressions in the square brackets for the ith shape function remains unconsidered. The abscissa values $x_1, \ldots, x_m$ represent the x-coordinates of the m nodes. In the case of rotation the variable m has to be replaced by n in Eq. (8.137). For the derivation of the general stiffness matrix we revert at this point to different methods. If, for example, the weighted residual method is considered, one can use the new approaches (8.135) and (8.136) in Eq. (8.86). Execution of the multiplication for the bending stiffness matrix yields

$$\boldsymbol{k}_b^e = \int_0^L EI_z \begin{bmatrix} 0 & \cdots & 0 & 0 & \cdots & 0 \\ \vdots & (m \times m) & \vdots & \vdots & (m \times n) & \vdots \\ 0 & \cdots & 0 & 0 & \cdots & 0 \\ \hline 0 & \cdots & 0 & \dfrac{\mathrm{d}N_{1\phi}}{\mathrm{d}x}\dfrac{\mathrm{d}N_{1\phi}}{\mathrm{d}x} & \cdots & \dfrac{\mathrm{d}N_{1\phi}}{\mathrm{d}x}\dfrac{\mathrm{d}N_{n\phi}}{\mathrm{d}x} \\ \vdots & (n \times m) & \vdots & \vdots & (n \times n) & \vdots \\ 0 & \cdots & 0 & \dfrac{\mathrm{d}N_{n\phi}}{\mathrm{d}x}\dfrac{\mathrm{d}N_{1\phi}}{\mathrm{d}x} & \cdots & \dfrac{\mathrm{d}N_{n\phi}}{\mathrm{d}x}\dfrac{\mathrm{d}N_{n\phi}}{\mathrm{d}x} \end{bmatrix} \mathrm{d}x \tag{8.138}$$

and accordingly the execution of the multiplication for the shear stiffness matrix $\boldsymbol{k}_s^e$ yields

$$\int_0^L k_s AG \begin{bmatrix} \dfrac{\mathrm{d}N_{1u}}{\mathrm{d}x}\dfrac{\mathrm{d}N_{1u}}{\mathrm{d}x} & \cdots & \dfrac{\mathrm{d}N_{1u}}{\mathrm{d}x}\dfrac{\mathrm{d}N_{mu}}{\mathrm{d}x} & \dfrac{\mathrm{d}N_{1u}}{\mathrm{d}x}(-N_{1\phi}) & \cdots & \dfrac{\mathrm{d}N_{1u}}{\mathrm{d}x}(-N_{n\phi}) \\ \vdots & (m \times m) & \vdots & \vdots & (m \times n) & \vdots \\ \dfrac{\mathrm{d}N_{mu}}{\mathrm{d}x}\dfrac{\mathrm{d}N_{1u}}{\mathrm{d}x} & \cdots & \dfrac{\mathrm{d}N_{mu}}{\mathrm{d}x}\dfrac{\mathrm{d}N_{mu}}{\mathrm{d}x} & \dfrac{\mathrm{d}N_{mu}}{\mathrm{d}x}(-N_{1\phi}) & \cdots & \dfrac{\mathrm{d}N_{mu}}{\mathrm{d}x}(-N_{m\phi}) \\ \hline -N_{1\phi}\dfrac{\mathrm{d}N_{1u}}{\mathrm{d}x} & \cdots & -N_{1\phi}\dfrac{\mathrm{d}N_{mu}}{\mathrm{d}x} & N_{1\phi}N_{1\phi} & \cdots & N_{1\phi}N_{n\phi} \\ \vdots & (n \times m) & \vdots & \vdots & (n \times n) & \vdots \\ -N_{n\phi}\dfrac{\mathrm{d}N_{1u}}{\mathrm{d}x} & \cdots & -N_{n\phi}\dfrac{\mathrm{d}N_{mu}}{\mathrm{d}x} & N_{n\phi}N_{1\phi} & \cdots & N_{n\phi}N_{n\phi} \end{bmatrix} \mathrm{d}x. \tag{8.139}$$

These two stiffness matrices can be superposed additively at this point and the following general structure for the total stiffness matrix yields:

$$k^e = \begin{bmatrix} k^{11} & k^{12} \\ k^{21} & k^{22} \end{bmatrix},$$

(8.140)

with

$$k_{kl}^{11} = \int_0^L k_s AG \frac{dN_{ku}}{dx} \frac{dN_{lu}}{dx} \, dx,$$

(8.141)

$$k_{kl}^{12} = \int_0^L k_s AG \frac{dN_{ku}}{dx} (-N_{l\phi}) dx,$$

(8.142)

$$k_{kl}^{21} = k_{kl}^{12,T} = \int_0^L k_s AG (-N_{k\phi}) \frac{dN_{lu}}{dx} \, dx,$$

(8.143)

$$k_{kl}^{22} = \int_0^L \left(k_s AG N_{k\phi} N_{l\phi} + EI_z \frac{dN_{k\phi}}{dx} \frac{dN_{l\phi}}{dx} \right) dx.$$

(8.144)

The derivation of the right-hand side can occur according to Eq. (8.91) and the following load vector results:

$$F^e = \int_0^L q_y(x) \begin{bmatrix} N_{1u} \\ \vdots \\ N_{mu} \\ 0 \\ \vdots \\ 0 \end{bmatrix} dx + \begin{bmatrix} F_{1y} \\ \vdots \\ F_{my} \\ M_{1z} \\ \vdots \\ M_{nz} \end{bmatrix}.$$

(8.145)

In the following, a quadratic interpolation for $u_y(x)$ as well as a linear interpolation for $\phi_z(x)$ are chosen [14]. Therefore for $\frac{du_y(x)}{dx}$ and $\phi_z(x)$ functions of the same order result and the phenomenon of *shear locking* can be avoided. Quadratic interpolation for the deflection means that the deflection will be evaluated on three nodes. The linear approach for the rotation means that the unknowns will be evaluated on only two nodes. Therefore the illustrated configuration in Fig. 8.12 for this TIMOSHENKO element results.

(a) y

u_{1y} ϕ_{1z} u_{2y} u_{3y} ϕ_{3z}

x

L

(b) y

F_{1y} M_{1z} F_{2y} F_{3y} M_{3z}

x

L
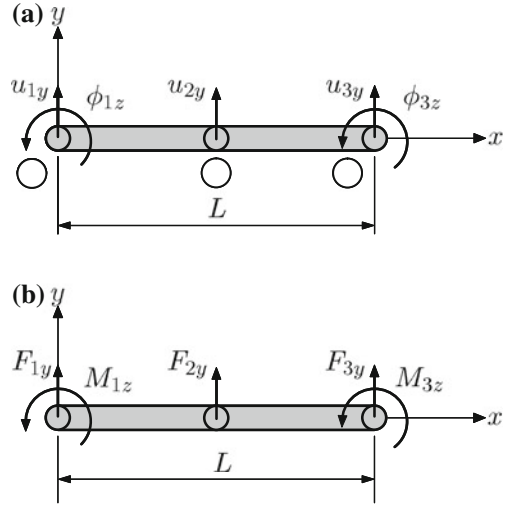
Evaluation of the general LAGRANGE polynomial according to Eq. (8.137) for the
deflection, meaning under consideration of three nodes, yields

$$N_{1u} = \frac{(x_2 - x)(x_3 - x)}{(x_2 - x_1)(x_3 - x_1)} = 1 - 3\frac{x}{L} + 2\left(\frac{x}{L}\right)^2, \tag{8.146}$$

$$N_{2u} = \frac{(x_1 - x)(x_3 - x)}{(x_1 - x_2)(x_3 - x_2)} = 4\frac{x}{L} - 4\left(\frac{x}{L}\right)^2, \tag{8.147}$$

$$N_{3u} = \frac{(x_1 - x)(x_2 - x)}{(x_1 - x_3)(x_2 - x_3)} = -\frac{x}{L} + 2\left(\frac{x}{L}\right)^2, \tag{8.148}$$

or alternatively for both nodes for the rotation:

$$N_{1\phi} = \frac{(x_2 - x)}{(x_2 - x_1)} = 1 - \frac{x}{L}, \tag{8.149}$$

$$N_{2\phi} = \frac{(x_1 - x)}{(x_1 - x_2)} = \frac{x}{L}. \tag{8.150}$$

A graphical illustration of the shape functions is given in Fig. 8.13. One can see that
the typical characteristics for shape functions, meaning $N_i(x_i) = 1 \wedge N_i(x_j) = 0$
and $\sum_i N_i = 1$ are fulfilled.
With these shape functions the submatrices $k^{11}, \ldots, k^{22}$ in Eq. (8.140) result in the
following via the analytical integration:
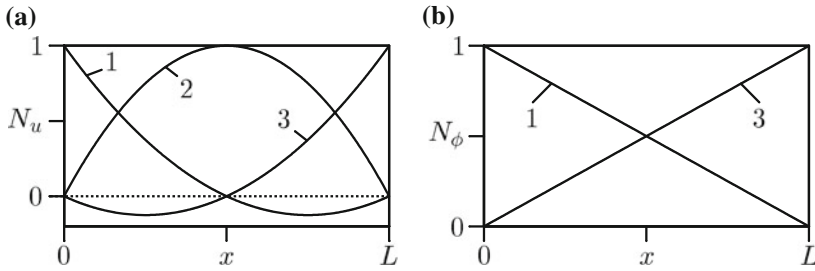
Fig. 8.13 Shape functions for a TIMOSHENKO element with **a** quadratic approach for the deflection and **b** linear approach for the rotation

$$k^{11} = \frac{k_s AG}{3L} \begin{bmatrix} 7 & -8 & 1 \\ -8 & 16 & -8 \\ 1 & -8 & 7 \end{bmatrix}, \tag{8.151}$$

$$k^{12} = \frac{k_s AG}{6} \begin{bmatrix} 5 & 1 \\ -4 & 4 \\ -1 & -5 \end{bmatrix} = (k^{21})^{\mathrm{T}}, \tag{8.152}$$

$$k^{22} = \frac{k_s AGL}{6} \begin{bmatrix} 2 & 1 \\ 1 & 2 \end{bmatrix} + \frac{EI_z}{L} \begin{bmatrix} 1 & -1 \\ -1 & 1 \end{bmatrix}, \tag{8.153}$$

which can be put together for the principal finite element equation by making use of the abbreviation $\Lambda = \frac{EI_z}{k_s AGL^2}$:

$$\frac{k_s AG}{6L} \begin{bmatrix} 14 & -16 & 2 & 5L & 1L \\ -16 & 32 & -16 & -4L & 4L \\ 2 & -16 & 14 & -1L & -5L \\ 5L & -4L & -1L & 2L^2(1+3\Lambda) & L^2(1-6\Lambda) \\ 1L & 4L & -5L & L^2(1-6\Lambda) & 2L^2(1+3\Lambda) \end{bmatrix} \begin{bmatrix} u_{1y} \\ u_{2y} \\ u_{3y} \\ \phi_{1z} \\ \phi_{3z} \end{bmatrix} = \begin{bmatrix} F_{1y} \\ F_{2y} \\ F_{3y} \\ M_{1z} \\ M_{3z} \end{bmatrix}. \tag{8.154}$$

Since only one displacement is evaluated on the middle node, the number of unknowns is not the same on each node. This circumstance complicates the creation of the global system of equations for several of these elements. The degree of freedom u_{2y}, however, can be expressed via the remaining unknowns and therefore the possibility exists to eliminate this node from the system of equations. For this, the second Eq. (8.154)[13] has to be evaluated:

---

[13] It needs to be remarked that the influence of distributed loads is disregarded in the derivation. If distributed loads occur, the equivalent nodal loads have to be distributed on the remaining nodes.

$$\frac{k_s AG}{6L} \left(-16u_{1y} + 32u_{2y} - 16u_{3y} - 4L\phi_{1z} + 4L\phi_{3z} \right) = F_{2y}, \qquad (8.155)$$

$$u_{2y} = \frac{6L}{32k_s AG} F_{2y} + \frac{u_{1y} + u_{3y}}{2} + \frac{\phi_{1z} - \phi_{3z}}{8} L. \qquad (8.156)$$

Furthermore, it can be demanded that no external force should have an effect on the middle node, so that the relation between the deflection on the middle node and the other unknowns yields as follows:

$$u_{2y} = \frac{u_{1y} + u_{3y}}{2} + \frac{\phi_{1z} - \phi_{3z}}{8} L. \qquad (8.157)$$

This relation can be introduced into the system of Eq. (8.154) to eliminate the degree of freedom u_{2u}. Finally, after a new arrangement of the unknowns, the following principal finite element equation results, which is reduced by one column and one row:

$$\frac{EI_z}{6\Lambda L^3} \begin{bmatrix} 6 & 3L & -6 & 3L \\ 3L & L^2(1,5+6\Lambda) & -3L & L^2(1,5-6\Lambda) \\ -6 & -3L & 6 & -3L \\ 3L & L^2(1,5-6\Lambda) & -3L & L^2(1,5+6\Lambda) \end{bmatrix} \begin{bmatrix} u_{1y} \\ \phi_{1z} \\ u_{3y} \\ \phi_{3z} \end{bmatrix} = \begin{bmatrix} F_{1y} \\ M_{1z} \\ F_{3y} \\ M_{3z} \end{bmatrix}.$$
$$(8.158)$$

This element formulation is identical with Eq. (8.121), which was derived with linear shape functions and numerical one-point integration. However, it is to be considered that the interpolation between the nodes during the use of (8.158) takes place with quadratic functions.

Further details and formulations regarding the TIMOSHENKO element can be found in the scientific papers [11, 18].

8.4 Sample Problems and Supplementary Problems

8.4.1 Sample Problems

8.1. Discretization of a Beam with five Linear Elements with Shear Contribution
The beam,[14] which is illustrated in Fig. 8.14 needs to be discretized equally with five linear TIMOSHENKO elements and the displacement of the loading point needs to be discussed as dependent on the slenderness ratio and the POISSON's ratio. One considers the case of the (a) analytical and (b) the numerical (one integration point) integrated stiffness matrix.

8.1 Solution
(a) Stiffness matrix via analytical integration:

---

[14] A similar example is presented in [19].

Fig. 8.14 Discretization of a beam structure with elements under consideration of the shear contribution

discretization:
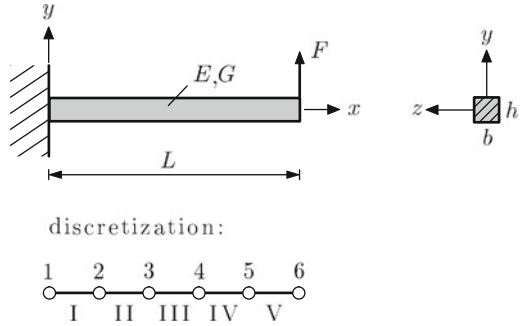
The element stiffness matrix according to Eq. (8.106) can be used for each of the five elements, whereupon it has to be considered that the single element length results in $\frac{L}{5}$. The resulting total stiffness matrix has the dimension 12×12, which reduces to a 10×10 matrix due to the consideration of the fixed support on the left-hand boundary ($u_{1y} = 0$, $\phi_{1z} = 0$). Through inversion of the stiffness matrix, the reduced system of equations can be solved via $\boldsymbol{u} = \boldsymbol{K}^{-1}\boldsymbol{F}$. The following extract shows the most important entries in this system of equations:

$$
\begin{bmatrix} u_{2y} \\ \vdots \\ u_{6y} \\ \phi_{6z} \end{bmatrix} = \frac{\frac{4}{5}L}{k_{\mathrm{s}}AG} \underbrace{\begin{bmatrix} \mathsf{x} \cdots & \mathsf{x} & \mathsf{x} \\ \vdots & \vdots & \vdots \\ \mathsf{x} \cdots & \dfrac{125(3\alpha + 4L^2)}{4(75\alpha + L^2)} & \mathsf{x} \\ \mathsf{x} \cdots & \mathsf{x} & \mathsf{x} \end{bmatrix}}_{10 \times 10 \text{ matrix}} \begin{bmatrix} 0 \\ \vdots \\ F \\ 0 \end{bmatrix}.
\tag{8.159}
$$

Multiplication of the 9th row of the matrix with the load vector yields the displacement of the loading point to:

$$
u_{6y} = \frac{25(3\alpha + 4L^2)}{75\alpha + L^2} \times \frac{FL}{k_{\mathrm{s}}AG},
\tag{8.160}
$$

or alternatively via $A = hb$, $k_{\mathrm{s}} = \frac{5}{6}$ and the relation for the shear modulus according to Eq. (8.23) after a short calculation:

$$
u_{6y} = \frac{12(1 + \nu)\left(\frac{h}{L}\right)^2 + 20}{60 + \left(\frac{L}{h}\right)^2 \frac{1}{1+\nu}} \times \frac{FL^3}{EI_z}.
\tag{8.161}
$$

A graphical illustration of the displacement dependent on the slenderness ratio can be seen in Fig. 8.15. A comparison with Fig. 8.10 shows that the convergence behavior
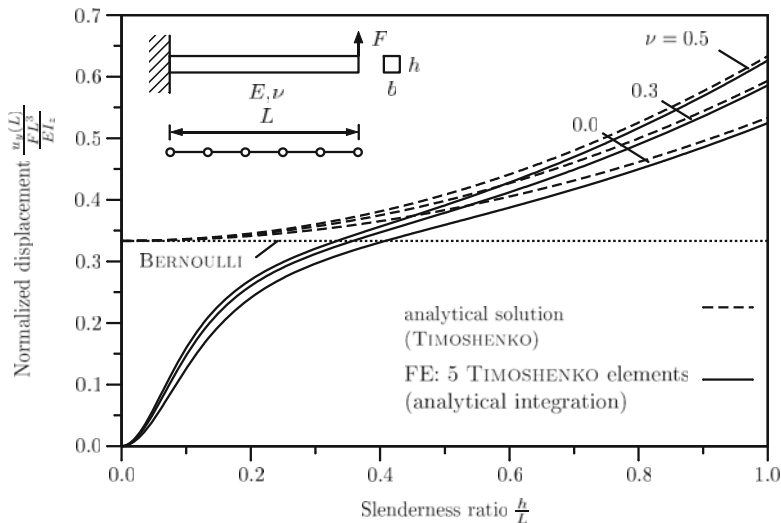
Fig. 8.15 Discretization of a beam via five linear TIMOSHENKO elements at analytical integration of the stiffness matrix

in the lower domain of the slenderness ratio for $0.2 < \frac{h}{L} < 1.0$ has significantly improved through the fine discretization, the phenomenon of the *shear lockings* for $\frac{h}{L} \to 0$ however still occurs.

(b) Stiffness matrix via numerical integration with one integration point:

According to the procedure in part (a) of this problem, the following 10×10 system of equations results at this point via the stiffness matrix according to Eq. (8.120)

$$
\begin{bmatrix} u_{2y} \\ \vdots \\ u_{6y} \\ \phi_{6z} \end{bmatrix} = \frac{\frac{4}{5}L}{k_s AG} \underbrace{\begin{bmatrix} \times \cdots & \times & \times \\ \vdots & \vdots & \vdots \\ \times \cdots & \dfrac{25\alpha + 33L^2}{20\alpha} & \times \\ \times \cdots & \times & \times \end{bmatrix}}_{10 \times 10 \text{ matrix}} \begin{bmatrix} 0 \\ \vdots \\ F \\ 0 \end{bmatrix}, \tag{8.162}
$$

from which the displacement on the right-hand boundary can be defined as the following

$$
u_{6y} = \frac{4}{5}\left(\frac{5}{4} + \frac{33L^2}{20\alpha}\right) \times \frac{FL}{k_s AG}. \tag{8.163}
$$

With the use of $A = hb$, $k_s = \frac{5}{6}$ and the relation for the shear modulus according to Eq. (8.23) results in the following after a short calculation:
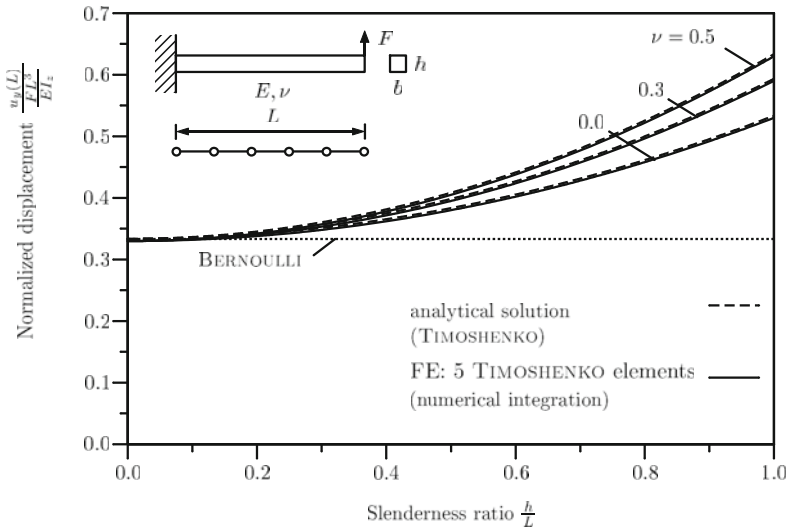
Fig. 8.16 Discretization of a beam via five linear TIMOSHENKO elements at numerical integration of the stiffness matrix with one integration point

$$u_{6y} = \left(\frac{33}{100} + \frac{1}{5}\,(1 + \nu)\left(\frac{h}{L}\right)^2 \right) \times \frac{FL^3}{EI_z}. \tag{8.164}$$

The graphical illustration of the displacement in Fig. 8.16 shows that an excellent conformity with the analytical solution throughout the entire domain of the slenderness ratio results through the mesh refinement. Therefore the accuracy at a TIMOSHENKO element with linear shape functions and reduced numerical integration can be increased considerably through mesh refinement.

8.2. TIMOSHENKO Bending Element with Quadratic Shape Functions for the Deflection and the Rotation
The stiffness matrix and the principal finite element equation $k^e u_p = F^e$ are to be derived for the illustrated TIMOSHENKO bending element in Fig. 8.17 with quadratic shape functions. One distinguishes in the derivation between the analytical and numerical integration. Subsequently the convergence behavior of an element needs to be analyzed for the illustrated configuration in Fig. 8.9.

8.2. Solution
Evaluation of the general LAGRANGE polynomial according to Eq. (8.137) under consideration of 3 nodes yields the following shape functions for the deflection and the rotation:

Fig. 8.17 TIMOSHENKO bending element with quadratic shape functions for the deflection and the rotation: **a** deformation parameters; **b** load parameters
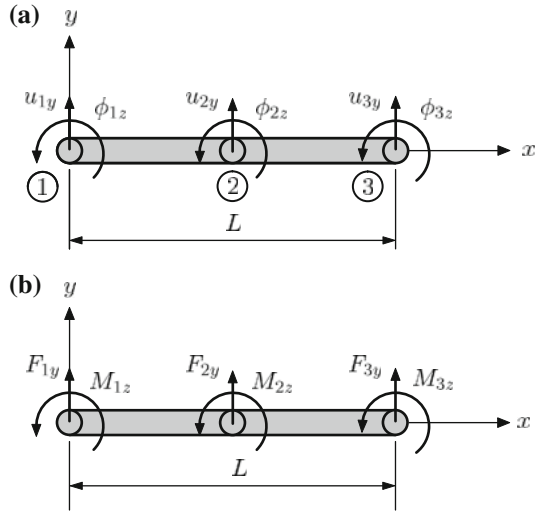
$$N_{1u} = N_{1\phi} = \frac{(x_2 - x)(x_3 - x)}{(x_2 - x_1)(x_3 - x_1)} = 1 - 3\frac{x}{L} + 2\left(\frac{x}{L}\right)^2, \tag{8.165}$$

$$N_{2u} = N_{2\phi} = \frac{(x_1 - x)(x_3 - x)}{(x_1 - x_2)(x_3 - x_2)} = 4\frac{x}{L} - 4\left(\frac{x}{L}\right)^2, \tag{8.166}$$

$$N_{3u} = N_{3\phi} = \frac{(x_1 - x)(x_2 - x)}{(x_1 - x_3)(x_2 - x_3)} = -\frac{x}{L} + 2\left(\frac{x}{L}\right)^2. \tag{8.167}$$

With these shape functions the submatrices $k^{11}, \ldots, k^{22}$ in Eq. (8.140) result as follows through *analytical* integration:

$$k^{11} = \frac{k_s AG}{6L} \begin{bmatrix} 14 & -16 & 2 \\ -16 & 32 & -16 \\ 2 & -16 & 14 \end{bmatrix}, \tag{8.168}$$

$$k^{12} = \frac{k_s AG}{6L} \begin{bmatrix} 3L & 4L & -1L \\ -4L & 0 & 4L \\ 1L & -4L & -3L \end{bmatrix} = (k^{21})^{\mathrm{T}}, \tag{8.169}$$

$$k^{22} = \frac{k_s AGL}{30} \begin{bmatrix} 4 & 2 & -1 \\ 2 & 16 & 2 \\ -1 & 2 & 4 \end{bmatrix} + \frac{EI_z}{3L} \begin{bmatrix} 7 & -8 & 1 \\ -8 & 16 & -8 \\ 1 & -8 & 7 \end{bmatrix}, \tag{8.170}$$

which can be composed to the stiffness matrix k^e via the use of the abbreviation $\Lambda = \frac{EI_z}{k_s AGL^2}$:

$$\frac{k_s AG}{6L} \begin{bmatrix} 14 & -16 & 2 & 3L & 4L & -1L \\ -16 & 32 & -16 & -4L & 0 & 4L \\ 2 & -16 & 14 & 1L & -4L & -3L \\ 3L & -4L & 1L & L^2\left(\frac{4}{5}+14\Lambda\right) & L^2\left(\frac{2}{5}-16\Lambda\right) & L^2\left(-\frac{1}{5}+2\Lambda\right) \\ 4L & 0 & -4L & L^2\left(\frac{2}{5}-16\Lambda\right) & L^2\left(\frac{16}{5}+32\Lambda\right) & L^2\left(\frac{2}{5}-16\Lambda\right) \\ -1L & 4L & -3L & L^2\left(-\frac{1}{5}+2\Lambda\right) & L^2\left(\frac{2}{5}-16\Lambda\right) & L^2\left(\frac{4}{5}+14\Lambda\right) \end{bmatrix}.$$

$$(8.171)$$

With this stiffness matrix the principal finite element equation results in $k^e u_p = F^e$, at which the deformation and load vector contains the following components:

$$u_p = \begin{bmatrix} u_{1y} & u_{2y} & u_{3y} & \phi_{1z} & \phi_{2z} & \phi_{3z} \end{bmatrix}^T, \tag{8.172}$$

$$F^e = \begin{bmatrix} F_{1y} & F_{2y} & F_{3y} & M_{1z} & M_{2z} & M_{3z} \end{bmatrix}^T. \tag{8.173}$$

For the analysis of the convergence behavior of an element for the illustrated beam in Fig. 8.9 with point load, the columns and rows for the entries u_{1y} and ϕ_{1z} in Eq. (8.171) can be canceled due to the fixed support on this node. This reduced 4×4 stiffness matrix can be inverted and the following system of equations for the definition of the unknown degrees of freedom results:

$$\begin{bmatrix} u_{2y} \\ u_{3y} \\ \vdots \\ \phi_{3z} \end{bmatrix} = \frac{6L}{k_s AG} \underbrace{\begin{bmatrix} \mathsf{x} & \cdots & & \cdots & \mathsf{x} \\ \mathsf{x} & \frac{-3+340\Lambda+1200\Lambda^2}{8(-1-45\Lambda+900\Lambda^2)} & \cdots & \mathsf{x} \\ \vdots & & & & \vdots \\ \mathsf{x} & & & \cdots & \mathsf{x} \end{bmatrix}}_{4\times 4 \text{ matrix}} \begin{bmatrix} 0 \\ F \\ \vdots \\ 0 \end{bmatrix}, \tag{8.174}$$

from which, through evaluation of the second row, the displacement on the right-hand boundary can be defined as:

$$u_{3y} = \underbrace{\frac{6L}{k_s AG}}_{\dfrac{6\Lambda L^3}{EI_z}} \times \frac{-3+340\Lambda+1200\Lambda^2}{8(-1-45\Lambda+900\Lambda^2)} \times F. \tag{8.175}$$

For a rectangular cross-section $\Lambda = \frac{1}{5}(1+\nu)\left(\frac{h}{L}\right)^2$ results, and one can see that *shear locking* occurs also at this point for slender beams with $L \gg h$, since in the limit case $u_{3y} \to 0$ occurs.

In the following, the reduced numerical integration of the stiffness matrix needs to be analyzed. For the definition of a reasonable amount of integration points one takes into account the following consideration:

If quadratic shape functions are used for u_y and ϕ_z, the degree of the polynomials for $\frac{du_y}{dx}$ and ϕ_z differs. The quadratic approach for u_y yields for $\frac{du_y}{dx}$ a linear function and thus a linear function would also be desirable for ϕ_z. The two-point integration however determines that the quadratic approach for ϕ_z is treated as a linear function. A two-point integration can exactly integrate a polynomial of third order, meaning proportional to x^3, at most and therefore the following view results: $(N_{i\phi}N_{j\phi}) \sim x^3$. This however means that $N_{i\phi} \sim x^{1.5}$ or alternatively $N_{j\phi} \sim x^{1.5}$ applies at most. Since the polynomial approach only allows integer values for the exponent, $N_{i\phi} \sim x^1$ or alternatively $N_{j\phi} \sim x^1$ results and the rotation needs to be regarded as a linear function.

The integration via numerical GAUSS integration with two integration points demands that the arguments and the integration boundaries in the formulations of the submatrices $k^{11}, \ldots, k^{22}$ in Eq. (8.140) have to be transformed to the natural coordinate $-1 \leq \xi \leq 1$. Via the transformation of the derivative onto the new coordinate, meaning $\frac{dN}{dx} = \frac{dN}{d\xi}\frac{d\xi}{dx}$ and the transformation of the coordinate $\xi = -1 + 2\frac{x}{L}$ or alternatively $d\xi = \frac{2}{L}dx$, the numerical approximation of the submatrices for two integration points $\xi_{1,2} = \pm\frac{1}{\sqrt{3}}$ results in:

$$k^{11} = \sum_{i=1}^{2}\frac{2k_s AG}{L}\begin{bmatrix} \dfrac{dN_{1u}}{d\xi}\dfrac{dN_{1u}}{d\xi} & \dfrac{dN_{1u}}{d\xi}\dfrac{dN_{2u}}{d\xi} & \dfrac{dN_{1u}}{d\xi}\dfrac{dN_{3u}}{d\xi} \\[2mm] \dfrac{dN_{2u}}{d\xi}\dfrac{dN_{1u}}{d\xi} & \dfrac{dN_{2u}}{d\xi}\dfrac{dN_{2u}}{d\xi} & \dfrac{dN_{2u}}{d\xi}\dfrac{dN_{3u}}{d\xi} \\[2mm] \dfrac{dN_{3u}}{d\xi}\dfrac{dN_{1u}}{d\xi} & \dfrac{dN_{3u}}{d\xi}\dfrac{dN_{2u}}{d\xi} & \dfrac{dN_{3u}}{d\xi}\dfrac{dN_{3u}}{d\xi} \end{bmatrix} \times 1, \qquad (8.176)$$

$$k^{12} = \sum_{i=1}^{2}k_s AG\begin{bmatrix} \dfrac{dN_{1u}}{d\xi}(-N_{1\phi}) & \dfrac{dN_{1u}}{d\xi}(-N_{2\phi}) & \dfrac{dN_{1u}}{d\xi}(-N_{3\phi}) \\[2mm] \dfrac{dN_{2u}}{d\xi}(-N_{1\phi}) & \dfrac{dN_{2u}}{d\xi}(-N_{2\phi}) & \dfrac{dN_{2u}}{d\xi}(-N_{3\phi}) \\[2mm] \dfrac{dN_{3u}}{d\xi}(-N_{1\phi}) & \dfrac{dN_{3u}}{d\xi}(-N_{2\phi}) & \dfrac{dN_{3u}}{d\xi}(-N_{3\phi}) \end{bmatrix} \times 1, \qquad (8.177)$$

$$k^{22} = \sum_{i=1}^{2} \frac{k_s AGL}{2} \begin{bmatrix} N_{1\phi}N_{1\phi} & N_{1\phi}N_{2\phi} & N_{1\phi}N_{3\phi} \\ N_{2\phi}N_{1\phi} & N_{2\phi}N_{2\phi} & N_{2\phi}N_{3\phi} \\ N_{3\phi}N_{1\phi} & N_{3\phi}N_{2\phi} & N_{3\phi}N_{3\phi} \end{bmatrix} \times 1 \tag{8.178}$$

$$+ \sum_{i=1}^{2} \frac{2EI_z}{L} \begin{bmatrix} \dfrac{dN_{1\phi}}{d\xi}\dfrac{dN_{1\phi}}{d\xi} & \dfrac{dN_{1\phi}}{d\xi}\dfrac{dN_{2\phi}}{d\xi} & \dfrac{dN_{1\phi}}{d\xi}\dfrac{dN_{3\phi}}{d\xi} \\[2mm] \dfrac{dN_{2\phi}}{d\xi}\dfrac{dN_{1\phi}}{d\xi} & \dfrac{dN_{2\phi}}{d\xi}\dfrac{dN_{2\phi}}{d\xi} & \dfrac{dN_{2\phi}}{d\xi}\dfrac{dN_{3\phi}}{d\xi} \\[2mm] \dfrac{dN_{3\phi}}{d\xi}\dfrac{dN_{1\phi}}{d\xi} & \dfrac{dN_{3\phi}}{d\xi}\dfrac{dN_{2\phi}}{d\xi} & \dfrac{dN_{3\phi}}{d\xi}\dfrac{dN_{3\phi}}{d\xi} \end{bmatrix} \times 1. \tag{8.179}$$

The quadratic shape functions, which have already been introduced in Eqs. (8.146) up to (8.148), still have to be transformed onto the new coordinates via the transformation $x = (\xi + 1)\frac{L}{2}$. Therefore for the shape functions or alternatively their derivatives the following results:

$$N_1(\xi) = -\frac{1}{2}(\xi - \xi^2), \quad \frac{dN_1}{d\xi} = -\frac{1}{2}(1 - 2\xi), \tag{8.180}$$

$$N_2(\xi) = 1 - \xi^2, \quad \frac{dN_2}{d\xi} = -2\xi, \tag{8.181}$$

$$N_3(\xi) = \frac{1}{2}(\xi + \xi^2), \quad \frac{dN_3}{d\xi} = \frac{1}{2}(1 + 2\xi). \tag{8.182}$$

The use of these shape functions or alternatively their derivatives finally leads to the following submatrices

$$k^{11} = \frac{k_s AG}{6L} \begin{bmatrix} 14 & -16 & 2 \\ -16 & 32 & -16 \\ 2 & -16 & 14 \end{bmatrix}, \tag{8.183}$$

$$k^{12} = \frac{k_s AG}{6L} \begin{bmatrix} 3L & 4L & -L \\ -4L & 0 & 4L \\ +L & -4L & -3L \end{bmatrix}, \tag{8.184}$$

$$k^{22} = \frac{k_s AG}{6L} \begin{bmatrix} \dfrac{2}{3}L^2 & \dfrac{2}{3}L^2 & -\dfrac{1}{3}L^2 \\[2mm] \dfrac{2}{3}L^2 & \dfrac{8}{3}L^2 & \dfrac{2}{3}L^2 \\[2mm] -\dfrac{1}{3}L^2 & \dfrac{2}{3}L^2 & \dfrac{2}{3}L^2 \end{bmatrix} + \frac{EI_z}{L^3} \begin{bmatrix} \dfrac{7}{3}L^2 & -\dfrac{8}{3}L^2 & \dfrac{1}{3}L^2 \\[2mm] -\dfrac{8}{3}L^2 & \dfrac{16}{3}L^2 & -\dfrac{8}{3}L^2 \\[2mm] \dfrac{1}{3}L^2 & -\dfrac{8}{3}L^2 & \dfrac{7}{3}L^2 \end{bmatrix}, \tag{8.185}$$

which can be put together to the stiffness matrix k^e under the use of the abbreviation $\Lambda = \frac{EI_z}{k_s AGL^2}$:

$$\frac{k_s AG}{6L} \begin{bmatrix} 14 & -16 & 2 & 3L & 4L & -1L \\ -16 & 32 & -16 & -4L & 0 & 4L \\ 2 & -16 & 14 & 1L & -4L & -3L \\ 3L & -4L & 1L & L^2\left(\frac{2}{3}+14\Lambda\right) & L^2\left(\frac{2}{3}-16\Lambda\right) & L^2\left(-\frac{1}{3}+2\Lambda\right) \\ 4L & 0 & -4L & L^2\left(\frac{2}{3}-16\Lambda\right) & L^2\left(\frac{8}{3}+32\Lambda\right) & L^2\left(\frac{2}{3}-16\Lambda\right) \\ -1L & 4L & -3L & L^2\left(-\frac{1}{3}+2\Lambda\right) & L^2\left(\frac{2}{3}-16\Lambda\right) & L^2\left(\frac{2}{3}+14\Lambda\right) \end{bmatrix},$$

$$(8.186)$$

whereupon the deformation and load vector also contains the following components at this point:

$$\boldsymbol{u}_p = \begin{bmatrix} u_{1y} & u_{2y} & u_{3y} & \phi_{1z} & \phi_{2z} & \phi_{3z} \end{bmatrix}^T, \tag{8.187}$$

$$\boldsymbol{F}^e = \begin{bmatrix} F_{1y} & F_{2y} & F_{3y} & M_{1z} & M_{2z} & M_{3z} \end{bmatrix}^T. \tag{8.188}$$

For the analysis of the convergence behavior for the beam according to Fig. 8.9 the columns and rows for the entries u_{1y} and ϕ_{1z} in the present system of equations can be canceled. The inverted 4×4 stiffness matrix can be used for the definition of the unknown degrees of freedom:

$$\begin{bmatrix} u_{2y} \\ u_{3y} \\ \vdots \\ \phi_{3z} \end{bmatrix} = \frac{6L}{k_s AG} \underbrace{\begin{bmatrix} \times & \cdots & & \cdots & \times \\ \times & \frac{1+3\Lambda}{18\Lambda} & & \cdots & \times \\ \vdots & & & & \vdots \\ \times & & & \cdots & \times \end{bmatrix}}_{4\times4 \text{ matrix}} \begin{bmatrix} 0 \\ F \\ \vdots \\ 0 \end{bmatrix}, \tag{8.189}$$

from which, through evaluation of the second row, the deformation on the right-hand boundary can be defined as:

$$u_{3y} = \underbrace{\frac{6L}{k_s AG}}_{\frac{6\Lambda L^3}{EI_z}} \times \frac{1+3\Lambda}{18\Lambda} \times F = \left(\frac{1}{3}+\Lambda\right)\frac{FL^3}{EI_z}. \tag{8.190}$$

For a rectangular cross-section $\Lambda = \frac{1}{5}(1+\nu)\left(\frac{h}{L}\right)^2$ results and one receives the exact solution[15] of the problem as:

---

[15] For this see the supplementary problem 8.6.

$$u_{3y} = \left(\frac{1}{3} + \frac{1+\nu}{5} \left(\frac{h}{L} \right)^2 \right) \times \frac{FL^3}{EI_z}. \tag{8.191}$$

According to the procedure for the TIMOSHENKO element with quadratic-linear shape functions in the Sect. 8.3.5, the middle node can be eliminated. Under the assumption that no forces or moments should have an effect on the middle node, the 2nd and 5th row of Eq. (8.186) yields the following relation for the unknowns on the middle node:

$$u_{2y} = \frac{1}{2} u_{1y} + \frac{1}{2} u_{3y} + \frac{1}{8} L\phi_{1z} - \frac{1}{8} L\phi_{3z}, \tag{8.192}$$

$$\phi_{2z} = \frac{-4u_{1y}}{L \left(\frac{8}{3} + 32\Lambda \right)} + \frac{4u_{3y}}{L \left(\frac{8}{3} + 32\Lambda \right)} - \frac{\left(\frac{2}{3} - 16\lambda \right)\phi_{1z}}{\left(\frac{8}{3} + 32\Lambda \right)} - \frac{\left(\frac{2}{3} - 16\lambda \right)\phi_{3z}}{\left(\frac{8}{3} + 32\Lambda \right)}. \tag{8.193}$$

These two relations can be considered in Eq. (8.186) so that the following principal finite element equation results after a short conversion:

$$\frac{2EI_z}{L^3(1+12\Lambda)} \begin{bmatrix} 6 & 3L & -6 & 3L \\ 3L & 2L^2(1+3\Lambda) & -3L & L^2(1-6\Lambda) \\ -6 & -3L & 6 & -3L \\ 3L & L^2(1-6\Lambda) & -3L & 2L^2(1+3\Lambda) \end{bmatrix} \begin{bmatrix} u_{1y} \\ \phi_{1z} \\ u_{3y} \\ \phi_{3z} \end{bmatrix} = \begin{bmatrix} F_{1y} \\ M_{1z} \\ F_{3y} \\ M_{3z} \end{bmatrix}. \tag{8.194}$$

With this formulation the one-beam problem according to Fig. 8.9 can be solved a little bit faster since after the consideration of the boundary conditions only a 2×2 matrix needs to be inverted. In this case, for the definition of the unknown the following results:

$$\frac{L^3(1+12\Lambda)}{2EI_z} \begin{bmatrix} \frac{2(1+3\Lambda)}{3(1+12\Lambda)} & \frac{1}{L(1+12\Lambda)} \\ \frac{1}{L(1+12\Lambda)} & \frac{2}{L^2(1+12\Lambda)} \end{bmatrix} \begin{bmatrix} F \\ 0 \end{bmatrix} = \begin{bmatrix} u_{3y} \\ \phi_{3z} \end{bmatrix}, \tag{8.195}$$

which results from the exact solution for the deflection according to Eq. (8.191).

8.4.2 Supplementary Problems

8.3. Calculation of the Shear Correction Factor for Rectangular Cross-Section
For a rectangular cross-section with width b and height h, the shear stress distribution is given as follows [20]:

$$\tau_{xy}(y) = \frac{6Q_y}{bh^3} \left(\frac{h^2}{4} - y^2 \right) \quad \text{with} \quad -\frac{h}{2} \le y \le \frac{h}{2}. \tag{8.196}$$

Compute the shear correction factor k_s under the assumption that the constant — in the surface A_s acting — equivalent shear stress $\tau_{xy} = Q_y/A_s$ yields the same shear strain energy as the actual shear stress distribution $\tau_{xy}(y)$, which acts in the actual cross-sectional area A of the beam.

8.4. Differential Equation Under Consideration of Distributed Moment

For the derivation of the equilibrium condition, the infinitesimal beam element, illustrated in Fig. 8.18 needs to be considered, which is additionally loaded with a constant 'distributed moment' $m_z = \frac{\text{moment}}{\text{length}}$. Subsequently one needs to derive the differential equation for the TIMOSHENKO beam under consideration of a general moment distribution $m_z(x)$.
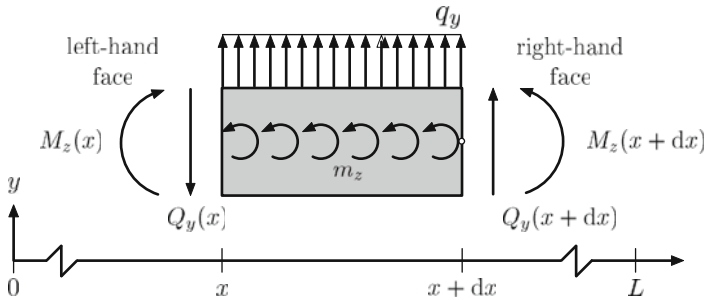
Fig. 8.18 Infinitesimal beam element with internal reactions and distributed loads

8.5. Analytical Calculation of the Distribution of the Deflection and Rotation for a Cantilever Under Point Load

For the illustrated cantilever in Table 8.3, which is loaded with a point load F at the right-hand end, calculate the distribution of the deflection $u_y(x)$ and the rotation $\phi_z(x)$ under consideration of the shear influence. Subsequently, the maximal deflection and the rotation at the loading point needs to be determined. Furthermore, the boundary value of the deflection at the loading point for slender ($h \ll L$) and compact ($h \gg L$) beams has to be determined.

8.6. Analytical Calculation of the Normalized Deflection for Beams with Shear Contribution

For the illustrated courses of the maximal normalized deflection $u_{y,\text{norm}}$ in Fig. 8.6 as a function of the slenderness ratio, the corresponding equations have to be derived.

8.7. Timoshenko Bending Element with Quadratic Shape Functions for the Deflection and Linear Shape Functions for the Rotation

For a TIMOSHENKO bending element with quadratic shape functions for the deflection and linear shape functions for the rotation, the stiffness matrix, after elimination of the middle node according to Eq. (8.158), is given. One has to derive the additional load vector on the right-hand side of the principal finite element equation which

results from a distributed load $q_y(x)$. Subsequently the result for a constant load has to be simplified.

8.8. Timoshenko Bending Element with Cubic Shape Functions for the Deflection and Quadratic Shape Functions for the Rotation

For a TIMOSHENKO bending element with cubic shape functions for the deflection and quadratic shape functions for the rotation, the stiffness matrix and the principal finite element equation $\boldsymbol{k}^{\mathrm{e}}\boldsymbol{u}_{\mathrm{p}} = \boldsymbol{F}^{\mathrm{e}}$ have to be derived. The exact solution has to be used for the integration. Subsequently the convergence behavior of an element configuration, which is illustrated in Fig. 8.9, has to be analyzed. The element deforms in the $x-y$ plane. How does the principal finite element equation change, when the deformation in the $x-z$ plane occurs?

References

1. Timoshenko SP, Goodier JN (1970) Theory of elasticity. McGraw-Hill, New York
2. Beer FP, Johnston ER Jr, DeWolf JT, Mazurek DF (2009) Mechanics of materials. McGraw-Hill, Singapore
3. Cowper GR (1966) The shear coefficient in Timoshenko's beam theory. J Appl Mech 33:335–340
4. Bathe K-J (2002) Finite-Elemente-Methoden. Springer, Berlin
5. Weaver W Jr, Gere JM (1980) Matrix analysis of framed structures. Van Nostrand Reinhold Company, New York
6. Gere JM, Timoshenko SP (1991) Mechanics of materials. PWS-KENT Publishing Company, Boston
7. Gruttmann F, Wagner W (2001) Shear correction factors in Timoshenko's beam theory for arbitrary shaped cross-sections. Comput Mech 27:199–207
8. Levinson M (1981) A new rectangular beam theory. J Sound Vib 74:81–87
9. Reddy JN (1984) A simple higher-order theory for laminated composite plate. J Appl Mech 51:745–752
10. Reddy JN (1997) Mechanics of laminated composite plates: theory and analysis. CRC Press, Boca Raton
11. Reddy JN (1997) On locking-free shear deformable beam finite elements. Comput Method Appl Mech Eng 149:113–132
12. Wang CM (1995) Timoshenko beam-bending solutions in terms of Euler-Bernoulli solutions. J Eng Mech-ASCE 121:763–765
13. Cook RD, Malkus DS, Plesha ME, Witt RJ (2002) Concepts and applications of finite element analysis. Wiley, New York
14. Reddy JN (2006) An introduction to the finite element method. McGraw Hill, Singapore
15. MacNeal RH (1994) Finite elements: their design and performance. Marcel Dekker, New York
16. Russel WT, MacNeal RH (1953) An improved electrical analogy for the analysis of beams in bending. J Appl Mech 20:349–355
17. MacNeal RH (1978) A simple quadrilateral shell element. Comput Struct 8:175–183
18. Reddy JN (1999) On the dynamic behaviour of the Timoshenko beam finite elements. Sadhana-Acad Proc Eng Sci 24:175–198
19. Steinke P (2010) Finite-Elemente-Methode–Rechnergestützte Einführung. Springer, Berlin
20. Hibbeler RC (2008) Mechanics of materials. Prentice Hall, Singapore

Chapter 9
Beams of Composite Materials

Abstract The beam elements discussed so far consist of homogeneous, isotropic material. Within this chapter a finite element formulation for a special material type — composite materials — will be introduced. On the basis of plane layers the behavior for the one-dimensional situation on the beam will be developed. First, different description types for direction dependent material behavior will be introduced. Shortly a special type of composite material, the fiber reinforced materials, will be considered.

9.1 Composite Materials

In the previous chapters, homogeneous, isotropic material has been assumed. However, in practice, elements or components are made of different materials to fulfill the multiple operational demands through the combination of different materials with their specific characteristics. At this point, the treatment of these materials will be shown for bars and beams within the framework of the finite element formulation [1–4].

Figure 9.1a illustrates the assembly of a beam of composite material in the longitudinal cross-section. The single layers represent different materials with different material characteristics and can be variably thick. Figure 9.1b illustrates a quite simple composite beam. It consists of only two different materials. Figure 9.1c illustrates an often occurring special case. The assembly is symmetric. Figure 9.1d illustrates the assembly for a sandwich structure. The relatively thick core material and the relatively thin cover layers are typical. The fiber reinforced materials stand for a composite material, at which the direction dependent behavior is predetermined via the structural assembly. Figure 9.2a illustrates a layer with fibers, which are embedded into a matrix.

In general, the fiber direction can be different for each layer (see Fig. 9.2b). In practice, one can often find a symmetric assembly.

(a)

(b)

(c)

(d)
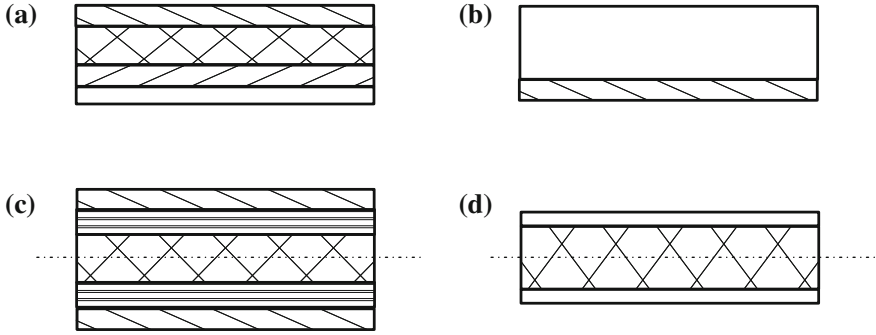
Fig. 9.1 Beams of composite materials: **a** general, **b** two materials, **c** symmetric assembly and **d** sandwich with thick core material and thin cover layers

(a)

(b)
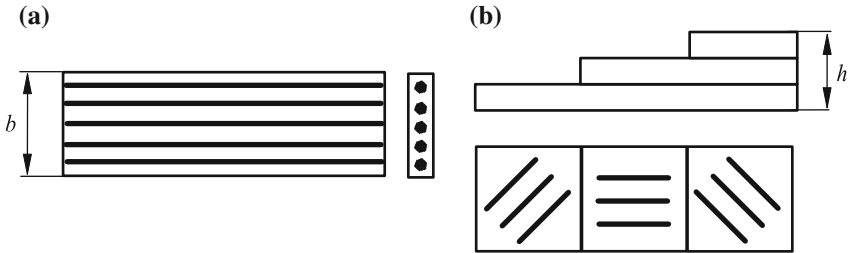
Fig. 9.2 **a** Composite layer with fibers and **b** composite with layers of different fiber directions

9.2 Anisotropic Material Behavior

Direction dependent behavior is a typical behavior of composite materials. As an extension to an isotropic material, other description forms for the relation between the strains and stress result. These will be introduced in the following. Regardless of this, within this chapter a linear elastic behavior is assumed for each material.
The general material description (constitutive description) for anisotropic bodies, connects with

$$\sigma_{ij} = C_{ijpq}\,\varepsilon_{pq} \tag{9.1}$$

the strain tensor (2nd order) via a so-called elasticity tensor (4th order tensor) with the stress tensor (2nd order tensor). Due to the symmetries of the stress and strain tensor the first as well as the second index groups in the elasticity tensor

$$C_{jipq} = C_{ijpq}; \quad C_{ijqp} = C_{ijpq} \tag{9.2}$$

are invariant against permutation. Therewith only 36 from the originally 81 compo-
nents of the elasticity tensor remain. Usually column matrices are introduced for the
symmetric stress tensor

$$
\begin{bmatrix}
\sigma_{xx} & \sigma_{xy} & \sigma_{xz} \\
\sigma_{xy} & \sigma_{yy} & \sigma_{yz} \\
\sigma_{xz} & \sigma_{yz} & \sigma_{zz}
\end{bmatrix}
\Rightarrow
\begin{bmatrix}
\sigma_{xx} \\
\sigma_{yy} \\
\sigma_{zz} \\
\sigma_{yz} \\
\sigma_{zx} \\
\sigma_{xy}
\end{bmatrix}
\Rightarrow
\begin{bmatrix}
\sigma_1 \\
\sigma_2 \\
\sigma_3 \\
\sigma_4 \\
\sigma_5 \\
\sigma_6
\end{bmatrix}
\tag{9.3}
$$

and the symmetric strain tensor

$$
\begin{bmatrix}
\varepsilon_{xx} & \varepsilon_{xy} & \varepsilon_{xz} \\
\varepsilon_{xy} & \varepsilon_{yy} & \varepsilon_{yz} \\
\varepsilon_{xz} & \varepsilon_{yz} & \varepsilon_{zz}
\end{bmatrix}
\Rightarrow
\begin{bmatrix}
\varepsilon_{xx} \\
\varepsilon_{yy} \\
\varepsilon_{zz} \\
\varepsilon_{yz} \\
\varepsilon_{zx} \\
\varepsilon_{xy}
\end{bmatrix}
\Rightarrow
\begin{bmatrix}
\varepsilon_1 \\
\varepsilon_2 \\
\varepsilon_3 \\
\varepsilon_4 \\
\varepsilon_5 \\
\varepsilon_6
\end{bmatrix}.
\tag{9.4}
$$

Therewith the stress strain relation (9.1) can be formulated in matrix notation as

$$
\begin{bmatrix}
\sigma_1 \\
\sigma_2 \\
\sigma_3 \\
\sigma_4 \\
\sigma_5 \\
\sigma_6
\end{bmatrix}
=
\begin{bmatrix}
C_{11} & C_{12} & C_{13} & C_{14} & C_{15} & C_{16} \\
C_{21} & C_{22} & C_{23} & C_{24} & C_{25} & C_{26} \\
C_{31} & C_{31} & C_{33} & C_{34} & C_{35} & C_{36} \\
C_{41} & C_{42} & C_{43} & C_{44} & C_{45} & C_{46} \\
C_{51} & C_{52} & C_{53} & C_{54} & C_{55} & C_{56} \\
C_{61} & C_{62} & C_{63} & C_{64} & C_{65} & C_{66}
\end{bmatrix}
\begin{bmatrix}
\varepsilon_1 \\
\varepsilon_2 \\
\varepsilon_3 \\
\varepsilon_4 \\
\varepsilon_5 \\
\varepsilon_6
\end{bmatrix}
\tag{9.5}
$$

or in compact form as

$$
\boldsymbol{\sigma} = \boldsymbol{C}\,\boldsymbol{\varepsilon}.
\tag{9.6}
$$

The specific elastic strain energy (related to the volume element) in matrix form

$$
\pi = \frac{1}{2}\,\boldsymbol{\varepsilon}^\mathrm{T}\,\boldsymbol{\sigma} ,
\tag{9.7}
$$

looks like this, which leads to the following, together with the constitutive equation
according to Eq. (9.1)

$$
\pi = \frac{1}{2}\,\boldsymbol{\varepsilon}^\mathrm{T}\,\boldsymbol{C}\,\boldsymbol{\varepsilon}.
\tag{9.8}
$$

Due to its energetic character this form has to be defined positively ($\pi \geq 0$). This
however requires $\boldsymbol{C}^\mathrm{T} = \boldsymbol{C}$, thus the symmetry of the $\boldsymbol{C}$ matrix. Because of this, only
21 components from the 36 components of the stiffness matrix are independent from
each other ($C_{ij} = C_{ji}$). This material is also referred to as *triclinic* material.

In the strain-stress relation

$$\boldsymbol{\varepsilon} = \boldsymbol{S}\,\boldsymbol{\sigma} \tag{9.9}$$

the compliance matrix $\boldsymbol{S}$ connects the stress with the strains. The valid relation for the general three-dimensional case

$$
\begin{bmatrix}
\varepsilon_1 \\
\varepsilon_2 \\
\varepsilon_3 \\
\varepsilon_4 \\
\varepsilon_5 \\
\varepsilon_6
\end{bmatrix}
=
\begin{bmatrix}
S_{11} & S_{12} & S_{13} & S_{14} & S_{15} & S_{16} \\
S_{21} & S_{22} & S_{23} & S_{24} & S_{25} & S_{26} \\
S_{31} & S_{31} & S_{33} & S_{34} & S_{35} & S_{36} \\
S_{41} & S_{42} & S_{43} & S_{44} & S_{45} & S_{46} \\
S_{51} & S_{52} & S_{53} & S_{54} & S_{55} & S_{56} \\
S_{61} & S_{62} & S_{63} & S_{64} & S_{65} & S_{66}
\end{bmatrix}
\begin{bmatrix}
\sigma_1 \\
\sigma_2 \\
\sigma_3 \\
\sigma_4 \\
\sigma_5 \\
\sigma_6
\end{bmatrix}
\tag{9.10}
$$

can be simplified for various special cases. This will be introduced in the following section.

9.2.1 Special Symmetries

For further simplifications special symmetries will be considered. The following system can be regarded as an important selection. The stress–strain relation is represented in detail with the stiffness matrix $\boldsymbol{C}$. The same derivation is valid for the strain-stress relation with the compliance matrix $\boldsymbol{S}$.

Monoclinic Systems

Plane $z = 0$, for example, is a plane of symmetry, then all components of the $\boldsymbol{C}$ matrix, which are related with the z-axis

$$
\begin{bmatrix}
\sigma_1 \\
\sigma_2 \\
\sigma_3 \\
\sigma_4 \\
\sigma_5 \\
\sigma_6
\end{bmatrix}
=
\begin{bmatrix}
C_{11} & C_{12} & C_{13} & 0 & 0 & C_{16} \\
C_{12} & C_{22} & C_{23} & 0 & 0 & C_{26} \\
C_{13} & C_{23} & C_{33} & 0 & 0 & C_{36} \\
0 & 0 & 0 & C_{44} & C_{45} & 0 \\
0 & 0 & 0 & C_{45} & C_{55} & 0 \\
C_{16} & C_{26} & C_{36} & 0 & 0 & C_{66}
\end{bmatrix}
\begin{bmatrix}
\varepsilon_1 \\
\varepsilon_2 \\
\varepsilon_3 \\
\varepsilon_4 \\
\varepsilon_5 \\
\varepsilon_6
\end{bmatrix}
\tag{9.11}
$$

are invariant against change of signs. Therewith 13 independent material constants remain.

Orthotropic Systems

Here, 3 mutually perpendicular planes of symmetry in the material exist. The corresponding invariancy against the change of signs yields for orthotropic systems in

$$
\begin{bmatrix} \sigma_1 \\ \sigma_2 \\ \sigma_3 \\ \sigma_4 \\ \sigma_5 \\ \sigma_6 \end{bmatrix}
=
\begin{bmatrix}
C_{11} & C_{12} & C_{13} & & & \\
C_{12} & C_{22} & C_{23} & & 0 & \\
C_{13} & C_{23} & C_{33} & & & \\
 & & & C_{44} & & \\
 & 0 & & & C_{55} & \\
 & & & & & C_{66}
\end{bmatrix}
\begin{bmatrix} \varepsilon_1 \\ \varepsilon_2 \\ \varepsilon_3 \\ \varepsilon_4 \\ \varepsilon_5 \\ \varepsilon_6 \end{bmatrix}
\tag{9.12}
$$

just nine independent material constants.

Transversely Isotropic Systems

This, for the fiber reinforced material important group, is characterized through an isotropic behavior in one plane (for example in the y–z plane). Therewith just five independent material constants are necessary for the description of the stress–strain relation

$$
\begin{bmatrix} \sigma_1 \\ \sigma_2 \\ \sigma_3 \\ \sigma_4 \\ \sigma_5 \\ \sigma_6 \end{bmatrix}
=
\begin{bmatrix}
C_{11} & C_{12} & C_{12} & & & \\
C_{12} & C_{22} & C_{23} & & 0 & \\
C_{12} & C_{23} & C_{22} & & & \\
 & & & \frac{(C_{22}-C_{23})}{2} & & \\
 & 0 & & & C_{66} & \\
 & & & & & C_{66}
\end{bmatrix}
\begin{bmatrix} \varepsilon_1 \\ \varepsilon_2 \\ \varepsilon_3 \\ \varepsilon_4 \\ \varepsilon_5 \\ \varepsilon_6 \end{bmatrix}
\tag{9.13}
$$

for transversely isotropic systems. The relation for the constant C_{44} comes from the equivalence of pure shear and a combined tension and compression load.

Isotropic Systems

If two material is isotropic, meaning invariant under all orthogonal transformations, just two independent material constants are needed for the stress–strain relation

$$
\begin{bmatrix} \sigma_1 \\ \sigma_2 \\ \sigma_3 \\ \sigma_4 \\ \sigma_5 \\ \sigma_6 \end{bmatrix}
=
\begin{bmatrix}
C_{11} & C_{12} & C_{12} & & & \\
C_{12} & C_{11} & C_{12} & & 0 & \\
C_{12} & C_{12} & C_{11} & & & \\
 & & & \frac{(C_{11}-C_{12})}{2} & & \\
 & 0 & & & \frac{(C_{11}-C_{12})}{2} & \\
 & & & & & \frac{(C_{11}-C_{12})}{2}
\end{bmatrix}
\begin{bmatrix} \varepsilon_1 \\ \varepsilon_2 \\ \varepsilon_3 \\ \varepsilon_4 \\ \varepsilon_5 \\ \varepsilon_6 \end{bmatrix}
\tag{9.14}
$$

(HOOKE's material).

9.2.2 Engineering Constants

In the theory of isotropic continua usually the two material properties E (modulus of elasticity) and v (lateral contraction number, POISSON's ratio) are used, which are easily defined experimentally. Likewise, based on the differential equation, the LAMÉ's coefficients λ and μ are used or the bulk modulus K, the shear modulus G. The single parameters are dependent on each other and can be converted with

$$\lambda = \frac{Ev}{(1+v)(1-2v)} \quad , \quad \mu = \frac{E}{2(1+v)} = G \quad , \quad K = \frac{E}{2(1-2v)} \quad (9.15)$$

$$v = \frac{\lambda}{2(\lambda+\mu)} \quad , \quad E = \frac{\mu(3\lambda+2\mu)}{\lambda+\mu} \quad , \quad K = \lambda + \frac{2}{3}\mu.$$

The meaning of these parameters can be read functionally from the compliance matrix.

Isotropic Systems

For isotropic materials the strain-stress relation looks as follows

$$
\begin{bmatrix} \varepsilon_1 \\ \varepsilon_2 \\ \varepsilon_3 \\ \varepsilon_4 \\ \varepsilon_5 \\ \varepsilon_6 \end{bmatrix}
=
\begin{bmatrix}
\frac{1}{E} & \frac{-v}{E} & \frac{-v}{E} & & & \\
& \frac{1}{E} & \frac{-v}{E} & & 0 & \\
& & \frac{1}{E} & & & \\
& & & \frac{1}{G} & & \\
& \text{sym.} & & & \frac{1}{G} & \\
& & & & & \frac{1}{G}
\end{bmatrix}
\begin{bmatrix} \sigma_1 \\ \sigma_2 \\ \sigma_3 \\ \sigma_4 \\ \sigma_5 \\ \sigma_6 \end{bmatrix}.
\qquad (9.16)
$$

Through inversion of the so-called compliance matrix the stiffness matrix follows. The components of the stiffness matrix

$$C_{11} = (1-v)\overline{E} \qquad\qquad (9.17)$$
$$C_{12} = v\overline{E}$$
$$\frac{(C_{11}-C_{12})}{2} = \frac{E}{2(1+v)} = G$$

with

$$\overline{E} = E\frac{1}{(1+v)(1-2v)} \qquad\qquad (9.18)$$

result from comparison with Eq. (9.14).

Transversely Isotropic Systems

As an example, the transversely isotropic behavior for the x-plane is assumed. Of course the considerations can also be adopted to other directions in space. The compliance matrix for transversely isotropic system looks as follows

$$
\begin{bmatrix} \varepsilon_1 \\ \varepsilon_2 \\ \varepsilon_3 \\ \varepsilon_4 \\ \varepsilon_5 \\ \varepsilon_6 \end{bmatrix} =
\begin{bmatrix}
\frac{1}{E_1} & \frac{-v_{12}}{E_2} & \frac{-v_{12}}{E_2} & & & \\
 & \frac{1}{E_2} & \frac{-v_{23}}{E_2} & & 0 & \\
 & & \frac{1}{E_2} & & & \\
 & & & \frac{1}{2G_{23}} & & \\
 & \text{sym.} & & & \frac{1}{2G_{12}} & \\
 & & & & & \frac{1}{2G_{12}}
\end{bmatrix}
\begin{bmatrix} \sigma_1 \\ \sigma_2 \\ \sigma_3 \\ \sigma_4 \\ \sigma_5 \\ \sigma_6 \end{bmatrix} .
\tag{9.19}
$$

The shear modulus G_{23} can be calculated as with isotropic media from E_2 and v_{23}. The indexing of the lateral contraction ratio is carried out according to the following scheme:

- 1st index = direction of the contraction,
- 2nd index = direction of the load, which elicits this contraction.

Through inversion of the compliance matrix and comparison one obtains

$$C_{11} = (1 - v_{23}^2)\, \overline{v}\, E_1 \tag{9.20}$$

$$C_{22} = (1 - v_{12}v_{21})\, \overline{v}\, E_2 \tag{9.21}$$

$$C_{12} = v_{12}(1 + v_{23})\, \overline{v}\, E_1 = v_{21}\,(1 + v_1)\, \overline{v}\, E_2 \tag{9.22}$$

$$C_{23} = (v_{23} + v_{21}v_{12})\, \overline{v}\, E_2 \tag{9.23}$$

$$C_{22} - C_{23} = (1 - v_{22} - 2v_{21}v_{12})\, \overline{v}\, E_2 \tag{9.24}$$

$$C_{66} = G_{12} \tag{9.25}$$

with

$$\overline{v} = \frac{1}{(1 + v_{23})\,(1 - v_{23} - 2v_{21}v_{12})} \tag{9.26}$$

the relation between the engineering constants and the components C_{ij} of the stiffness matrix. With the relation

$$v_{12}\, E_1 = v_{21}\, E_2 \tag{9.27}$$

the single material values are connected.

9.2.3 Transformation Behavior

In a composite material, materials for the single layers are used, which behave directionally dependent due to their structural configuration. This preferential direction — mostly it is one — is characteristic for one layer. The preferential directions can be defined variably in layers when consolidating in the network. For the macroscopic description of the composite material, transformation instructions are therefore necessary to consider the preferential direction of a single layer in the network. An instruction has to be given on how the material equations transform in case of a change of the coordinate system. This instruction can be gained from the transformation behavior of tensors. Thereby however only against each other rotated Cartesian coordinate systems are necessary (so-called orthogonal transformations).

For an arbitrary tensor of 2nd order A_{ij} the following transformation is applicable in the case of a change from a Cartesian (ij) into another (kl') Cartesian system (herein are the c_{ij} the so-called direction cosines):

$$A'_{kl} = c_{ki} \, c_{lj} \, A_{ij} \tag{9.28}$$

and therefore especially for the strain and for the stress tensor

$$\varepsilon'_{kl} = c_{ki} \, c_{lj} \, \varepsilon_{ij} \,, \tag{9.29}$$
$$\sigma'_{kl} = c_{ki} \, c_{lj} \, \sigma_{ij} \,. \tag{9.30}$$

If the stresses and strains are each expressed as column matrices, the transformation can then be written as

$$\boldsymbol{\varepsilon}' = \boldsymbol{T}_\varepsilon \, \boldsymbol{\varepsilon} \tag{9.31}$$
$$\boldsymbol{\sigma}' = \boldsymbol{T}_\sigma \, \boldsymbol{\sigma} \tag{9.32}$$

or

$$\boldsymbol{\varepsilon} = \boldsymbol{T}_\varepsilon^{-1} \, \boldsymbol{\varepsilon}' \tag{9.33}$$
$$\boldsymbol{\sigma} = \boldsymbol{T}_\sigma^{-1} \, \boldsymbol{\sigma}'. \tag{9.34}$$

With the properties for these transformation matrices

$$\boldsymbol{T}_\varepsilon^{-1} = \boldsymbol{T}_\sigma^{\mathrm{T}} \quad , \quad \boldsymbol{T}_\sigma^{-1} = \boldsymbol{T}_\varepsilon^{\mathrm{T}} \tag{9.35}$$

the relations for the transformations of the stiffness matrix follow based on

$$\boldsymbol{\sigma}' = \boldsymbol{C}' \, \boldsymbol{\varepsilon}' \tag{9.36}$$

with the conversions

$$T_\sigma \, \sigma = C' \, T_\varepsilon \, \varepsilon \tag{9.37}$$
$$(T_\sigma)^{-1} \, T_\sigma \, \sigma = (T_\sigma)^{-1} \, C' \, T_\varepsilon \, \varepsilon$$
$$\sigma = (T_\sigma)^{\mathrm{T}} \, C' \, T_\varepsilon \, \varepsilon$$

or based on

$$\sigma = C \, \varepsilon \tag{9.38}$$

with the conversions

$$(T_\sigma)^{-1} \, \sigma' = C'(T_\sigma)^{-1} \, C' \tag{9.39}$$
$$(T_\sigma) \, (T_\sigma)^{-1} \, \sigma' = (T_\sigma) \, C(T_\sigma)^{-1} \, \varepsilon'$$
$$\sigma' = (T_\sigma) \, C(T_\varepsilon)^{\mathrm{T}} \, \varepsilon'$$

finally in

$$C' = T_\sigma \, C \, T_\sigma^{\mathrm{T}} \tag{9.40}$$
$$C = T_\varepsilon^{\mathrm{T}} \, C' \, T_\varepsilon. \tag{9.41}$$

On the lines of this one obtains the following for the transformation of the compliance matrix

$$S' = T_\varepsilon \, S \, (T_\varepsilon)^{\mathrm{T}} \tag{9.42}$$
$$S = T_\sigma^{\mathrm{T}} \, S' \, T_\sigma \,. \tag{9.43}$$

For the important group of transversal isotropic materials the following transformation matrices

$$T_\sigma = \begin{bmatrix} c^2 & s^2 & 0 & 0 & 0 & 2cs \\ s^2 & c^2 & 0 & 0 & 0 & -2cs \\ 0 & 0 & 1 & 0 & 0 & 0 \\ 0 & 0 & 0 & c & -s & 0 \\ 0 & 0 & 0 & s & c & 0 \\ -sc & -sc & 0 & 0 & 0 & c^2 - s^2 \end{bmatrix} \tag{9.44}$$

and

$$T_\varepsilon = \begin{bmatrix} c^2 & s^2 & 0 & 0 & 0 & cs \\ s^2 & c^2 & 0 & 0 & 0 & -ss \\ 0 & 0 & 1 & 0 & 0 & 0 \\ 0 & 0 & 0 & c & -s & 0 \\ 0 & 0 & 0 & s & c & 0 \\ -2cs & -2cs & 0 & 0 & 0 & c^2 - s^2 \end{bmatrix} \tag{9.45}$$

for a rotation around the z-axis with $s = \sin \alpha$ and $c = \cos \alpha$ result.

9.2.4 Plane Stress States

A crucial simplification of the stress–strain relation results from the reduction to two-dimensional, instead of spatial stress states. A *thin* layer in the composite can be regarded under the assumption of the plane stress state. Stress components, which are not in the considered plane, are set equal to zero. It should be remarked that the plane stress state is only valid by approximation. Here the plane stress state for the x–y plane will be considered. For the stress states in the x–z or y–z plane similar formulations result.

The assumption of the plane stress states simplifies the stress–strain relation. Only three equations remain

$$\sigma_1 = C_{11}\varepsilon_1 + C_{12}\varepsilon_2 + C_{13}\varepsilon_3 + C_{16}\varepsilon_6 \tag{9.46}$$
$$\sigma_2 = C_{12}\varepsilon_1 + C_{22}\varepsilon_2 + C_{23}\varepsilon_3 + C_{26}\varepsilon_6 \tag{9.47}$$
$$\sigma_6 = C_{16}\varepsilon_1 + C_{26}\varepsilon_2 + C_{33}\varepsilon_3 + C_{66}\varepsilon_6 \tag{9.48}$$

for the three stress components σ_1, σ_2 and σ_6. The strain ε_3 at the right angle to the considered plane can be determined from the relation

$$\varepsilon_3 = -\frac{1}{C_{33}}(C_{13}\varepsilon_1 + C_{23}\varepsilon_2 + C_{36}\varepsilon_3). \tag{9.49}$$

If ε_3 is replaced in the above three equations, a modified form results

$$\sigma_i = \left(C_{ij} - \frac{C_{i3}\,C_{j3}}{C_{33}}\right)\varepsilon_j, \qquad i,j = 1, 2, 6 \tag{9.50}$$

which is usually described with
$$\sigma_i = Q_{ij}\,\varepsilon_j \tag{9.51}$$

or in matrix notation with
$$\boldsymbol{\sigma} = \boldsymbol{Q}\boldsymbol{\varepsilon}. \tag{9.52}$$

For the plane stress state the components of the compliance matrix S_{ij} in the strain-stress relation
$$\boldsymbol{\varepsilon} = \boldsymbol{S}\boldsymbol{\sigma} \tag{9.53}$$

remain the same. In further considerations the stress–strain relations and the strain-stress relations for the different lamina will be specified under a plane stress state. In a practical application three different layers occur:

1. Layers, which are treated as quasi homogeneous and quasi isotropic. The elastic behavior does not show a preferential direction. A typical example are layers, whose matrix is supported with short fibers, whose direction is however arbitrary.

2. Layers, at which long fibers with preferential direction are embedded in a matrix, so-called *unidirectional lamina*. The load also occurs in this preferential direction. From a macroscopic point of view the material is regarded as quasi-homogeneous and orthotropic.
3. Layers as in (2). The load however can occur in any direction.

Isotropic Lamina

For isotropic lamina only two independent from each other material components are needed in the stress–strain relation

$$
\begin{bmatrix} \sigma_1 \\ \sigma_2 \\ \sigma_6 \end{bmatrix} = \begin{bmatrix} Q_{11} & Q_{12} & 0 \\ Q_{12} & Q_{11} & 0 \\ 0 & 0 & Q_{66} \end{bmatrix} \begin{bmatrix} \varepsilon_1 \\ \varepsilon_2 \\ \varepsilon_6 \end{bmatrix} \tag{9.54}
$$

with

$$
Q_{11} = E/(1 - v^2) \tag{9.55}
$$
$$
Q_{12} = Ev/(1 - v^2) \tag{9.56}
$$
$$
C_{66} = E/2(1 + v) \tag{9.57}
$$

and in the strain-stress relation

$$
\begin{bmatrix} \varepsilon_1 \\ \varepsilon_2 \\ \varepsilon_6 \end{bmatrix} = \begin{bmatrix} S_{11} & S_{12} & 0 \\ S_{12} & S_{11} & 0 \\ 0 & 0 & S_{66} \end{bmatrix} \begin{bmatrix} \sigma_1 \\ \sigma_2 \\ \sigma_6 \end{bmatrix} \tag{9.58}
$$

with

$$
S_{11} = 1/E \tag{9.59}
$$
$$
S_{12} = -v/E \tag{9.60}
$$
$$
S_{66} = 1/G = 2(1 + v)/E. \tag{9.61}
$$

The equations show that no coupling exists between the normal stress and the shear stress.

Unidirectional Lamina, Load in Direction of the Fiber

Usually a lamina related coordinate system $(1', 2')$ is introduced for the description of the unidirectional lamina. The direction $1'$ equals the fiber direction (L), the direction $2'$ equals the direction perpendicular to the fiber direction (T). In the stress–strain

relation

$$
\begin{bmatrix} \sigma_1' \\ \sigma_2' \\ \sigma_6' \end{bmatrix}
\begin{bmatrix} Q_{11}' & Q_{12}' & 0 \\ Q_{12}' & Q_{22}' & 0 \\ 0 & 0 & Q_{66}' \end{bmatrix}
\begin{bmatrix} \varepsilon_1' \\ \varepsilon_2' \\ \varepsilon_6' \end{bmatrix}
\tag{9.62}
$$

with

$$
Q_{11}' = E_1'/(1 - \nu_{12}'\nu_{21}')
\tag{9.63}
$$
$$
Q_{22}' = E_2'/(1 - \nu_{12}'\nu_{21}')
\tag{9.64}
$$
$$
Q_{12}' = E_2'\nu_{12}'/(1 - \nu_{12}'\nu_{21}')
\tag{9.65}
$$
$$
Q_{66}' = G_{12}'
\tag{9.66}
$$

and in the strain-stress relation

$$
\begin{bmatrix} \varepsilon_1' \\ \varepsilon_2' \\ \varepsilon_6' \end{bmatrix} =
\begin{bmatrix} S_{11}' & S_{12}' & 0 \\ S_{12}' & S_{22}' & 0 \\ 0 & 0 & S_{66}' \end{bmatrix}
\begin{bmatrix} \sigma_1' \\ \sigma_2' \\ \sigma_6' \end{bmatrix}
\tag{9.67}
$$

with

$$
S_{11}' = 1/E_1'
\tag{9.68}
$$
$$
S_{22}' = 1/E_2'
\tag{9.69}
$$
$$
S_{12}' = -\nu_{12}'/E_1' = -\nu_{21}'/E_2'
\tag{9.70}
$$
$$
S_{66}' = G_{12}'
\tag{9.71}
$$

Four independent from each other material parameters are necessary. The valid parameters in the lamina own coordinate system can be formulated with the following

$$
E_1' = E_L \quad , \quad E_2' = E_T \quad , \quad G_{12}' = G_{LT} \quad , \quad \nu_{12}' = \nu_{LT}
\tag{9.72}
$$

in the engineering constants.

Unidirectional Lamina, Arbitrary Load Direction in the Plane

In contrast to the above considerations the load cannot just occur in the preferential direction of the lamina, but in every direction of the plane. However, to be able to use the material values of the $(1', 2')$ coordinate system, a transformation of the stiffness and compliance matrix from the $(1', 2')$ system into the $(1, 2)$ system is necessary. The material equation for the plane stress state in the $(1', 2')$ system appears as follows:

$$
\begin{bmatrix} \varepsilon'_1 \\ \varepsilon'_2 \\ \varepsilon'_6 \end{bmatrix} = \begin{bmatrix} \frac{1}{E'_1} & \frac{-\nu_{12}}{E'_1} & 0 \\ \frac{-\nu_{12}}{E'_1} & \frac{1}{E'_2} & 0 \\ 0 & 0 & \frac{1}{2G_{12}} \end{bmatrix} \begin{bmatrix} \sigma'_1 \\ \sigma'_2 \\ \sigma'_6 \end{bmatrix}.
\tag{9.73}
$$

Through the application of the transformation relation of the transversal isotropic body with the 'plane' transformation matrix one obtains for the compliance matrix

$$
\begin{bmatrix} S_{11} \\ S_{12} \\ S_{16} \\ S_{22} \\ S_{26} \\ S_{66} \end{bmatrix} = \begin{bmatrix} c^4 & 2c^2s^2 & s^4 & c^2s^2 \\ c^2s^2 & c^4 + s^4 & c^2s^2 & -c^2s^2 \\ 2c^3s & -2cs(c^2 - s^2) & -2cs^3 & -cs(c^2 - s^2) \\ s^4 & 2c^2s^2 & c^4 & c^2s^2 \\ 2cs^3 & 2cs(c^2 - s^2) & -2c^3s & cs(c^2 - s^2) \\ 4c^2s^2 & -8c^2s^2 & 4c^2s^2 & (c^2 - s^2)^2 \end{bmatrix} \begin{bmatrix} S'_{11} \\ S'_{12} \\ S'_{22} \\ S'_{66} \end{bmatrix}
\tag{9.74}
$$

and for the stiffness matrix

$$
\begin{bmatrix} Q_{11} \\ Q_{12} \\ Q_{16} \\ Q_{22} \\ Q_{26} \\ Q_{66} \end{bmatrix} = \begin{bmatrix} c^4 & 2c^2s^2 & s^4 & 4c^2s^2 \\ c^2s^2 & c^4 + s^4 & c^2s^2 & -4c^2s^2 \\ c^3s & -cs(c^2 - s^2) & -cs^3 & -2cs(c^2 - s^2) \\ s^4 & 2c^2s^2 & c^4 & 4c^2s^2 \\ cs^3 & cs(c^2 - s^2) & -c^3s & 2cs(c^2 - s^2) \\ c^2s^2 & -2c^2s^2 & c^2s^2 & (c^2 - s^2)^2 \end{bmatrix} \begin{bmatrix} Q'_{11} \\ Q'_{12} \\ Q'_{22} \\ Q'_{66} \end{bmatrix}
\tag{9.75}
$$

with

$$
s = \sin\alpha, \, c = \cos\alpha.
\tag{9.76}
$$

Therewith the stiffness and compliance matrix for transversely isotropic lamina in arbitrary (in the plane rotated) Cartesian coordinate systems can be illustrated (Assumption here: the rotation occurs in the plane around the z-axis, which is at right angles to the lamina plane) (Fig. 9.3).

Fig. 9.3 Lamina with angular misalignment between preferential and load direction
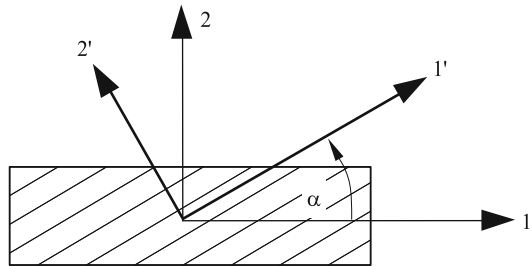
Table 9.1 Material models
with the amount of none-zero
entries and independent
parameters

Material model	Three-dimensional		Two-dimensional	
	$\neq 0$	Independent parameter	$\neq 0$	Independent parameter
Isotropic	12	2	5	2
Transversely isotropic	12	5	-	-
Orthotropic	12	9	5	4
Monoclinic	20	13	-	-
Anisotropic	36	21	9	6

In the following Table 9.1, the number of non-zero entries and the number of independent parameters are summarized for different material models. One distinguishes between the general three-dimensional and the plane stress state.

9.3 Introduction to the Micromechanics of the Fiber Composite Materials

Micromechanics serves to determine the properties of a composite from the properties of the single components. For the description of the fiber composite materials (FCM) so-called *unidirectional lamina* are used as the model, which belongs to the group of transversely isotropic materials. The model is based on the following assumptions:

1. the fibers are distributed equally in the matrix,
2. between the fibers and the matrix there are ideal contact conditions (consistency of the tangential component of the displacement)
3. the matrix does not contain any cavities,
4. the external load acts in the direction of the fibers or perpendicular to that,
5. no eigenstress exists in the lamina,
6. the fiber as well as the matrix material are linear elastic and
7. the fibers are infinitely long.

At the load of fiber composite materials one needs to distinguish between the load in and perpendicular to the fiber direction. Figure 9.4 illustrates the occurrent parameters for the load in the fiber direction.

Fig. 9.4 Stress–strain relation at load in fiber direction
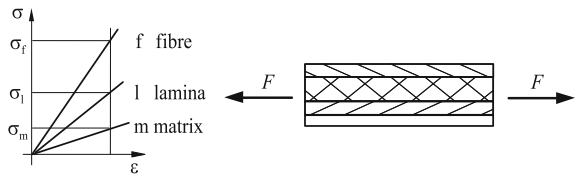
Due to precondition (2) the following occurs

$$\varepsilon_f = \varepsilon_m = \varepsilon_l \tag{9.77}$$

and according to precondition (6) the following is valid

$$\begin{aligned}
\sigma_f &= E_f\,\varepsilon_f = E_f\,\varepsilon_l \\
\sigma_m &= E_m\,\varepsilon_m = E_m\,\varepsilon_l.
\end{aligned} \tag{9.78}$$

Since in general $E_f \geq E_m$ applies, $\sigma_f \geq \sigma_m$ follows.
From the equilibrium of forces

$$F = F_f + F_m \tag{9.79}$$

with A_f as the cross-section of the fibre and A_m as the cross-section of the matrix

$$\sigma_l A_l = \sigma_f A_f + \sigma_m A_m \tag{9.80}$$

the stress in the lamina results in

$$\sigma_l = \sigma_f \frac{A_f}{A_l} + \sigma_m \frac{A_m}{A_l}\;. \tag{9.81}$$

Due to

$$A_l = A_f + A_m \tag{9.82}$$

and the abbreviations

$$v_f = \frac{A_f}{A_l} \quad \text{and} \quad v_m = \frac{A_m}{A_l} \tag{9.83}$$

the following results

$$\frac{A_m}{A_l} = 1 - v_f = v_m \tag{9.84}$$

and therewith

$$\sigma_l = \sigma_f v_f + \sigma_m (1 - v_f)\,. \tag{9.85}$$

The division of this relation by ε_l leads to the so-called *rule of mixtures*

$$E_l = E_f\,v_f + E_m\,v_m = E_f\,v_f + E_m\,(1 - v_f). \tag{9.86}$$

With the relation

$$\frac{F_f}{F_l} = \frac{\sigma_f v_f}{\sigma_f v_f + \sigma_m(1 - v_f)} = \frac{E_f v_f}{E_f v_f + E_m(1 - v_f)} \tag{9.87}$$

the load fraction, which is transferred from the fibers from the total load is described.

9.4 Multilayer Composite

A composite material usually consists of various layers. These layers can differ in the geometric dimensions as well as in the material properties. In the following, a single layer will be analyzed at first, subsequently the entire composite. For the finite element formulation, the often occurring cases in practice will be introduced. The macromechanical behavior is described under the following assumptions:

- The single layers of the composite are perfectly connected with each other. There is *no intermediate layer*.
- Each layer can be regarded as quasi-homogeneous.
- The displacements and strains are continuously throughout the entire composite. Within one layer the displacements and strains can be described with a linear course.

9.4.1 One Layer in the Composite

For a single layer (lamina) it should be assumed that the thickness of the layer is much smaller than the length dimension. Therewith a plane stress state can be used for the description.
Furthermore two situations need to be distinguished. The stresses are

- constant or
- not constant

within a composite layer. In the first case a, from the stress resulting force vector for the kth layer in the composite results in

$$N^k = [N_1^k, N_2^k, N_6^k]^\mathrm{T} , \tag{9.88}$$

which is defined through

$$N^k = \int_h \sigma \, \mathrm{d}z. \tag{9.89}$$

N_i^k are forces, which are related to a unit width, the real normal forces one receives through multiplication with the width b^k of a composite layer. N_1^k, N_2^k are resulting normal forces, N_6^k stands for a shear force in the plane. For a constant stress over the cross-section the following results:

$$N^k = \sigma^k \, h^k . \tag{9.90}$$

In the reduced stiffness matrix Q the components are constant, too. With

$$\sigma^k = Q^k \, \varepsilon^0 \tag{9.91}$$

the following results

$$N^k = Q^k \, \varepsilon^0 \, h^k = A^k \varepsilon^0 \,. \tag{9.92}$$

For the case when the stresses are not constant over the layer thickness, a resulting momental vector occurs

$$M^k = [M_1^k, \, M_2^k, \, M_6^k]^{\mathrm{T}} \,, \tag{9.93}$$

which is defined via

$$M^k = \int_h \sigma^k(z) \, z \, \mathrm{d}z. \tag{9.94}$$

M_i^k are moments, which are related to a unit width, whereupon M_1^k, M_2^k stand for bending moments and M_6^k for the torsional moment. According to the deformation model the strains run linearly over the cross-section and can be expressed via

$$\varepsilon^k(z) = z\,\kappa \,. \tag{9.95}$$

For the resulting momental vector therefore the following results

$$M^k = \int_h Q^k \, \varepsilon^k \, z \, \mathrm{d}z = Q^k \kappa \int_{-h/2}^{+h/2} z^2 \mathrm{d}z = Q^k \kappa \, \frac{(h^k)^3}{12} = D^k \kappa \,. \tag{9.96}$$

If, for a layer, a constant as well as a linear fraction in the strains occur, the following is valid

$$\varepsilon(z) = \varepsilon^0 + z\,\kappa \tag{9.97}$$

and therefore

$$N^k = \int_h \sigma^k(z) \, \mathrm{d}z = \int_h Q^k(\varepsilon^0 + z\kappa) \mathrm{d}z \tag{9.98}$$

and

$$M^k = \int_h \sigma^k(z) \, z \, \mathrm{d}z = \int_h Q^k(\varepsilon^0 + z\kappa) \, z \, \mathrm{d}z \,. \tag{9.99}$$

Both a resulting force and momental vector occur. Both derived formulations can be combined as

$$N^k = A^k \varepsilon_0 + B^k \kappa \tag{9.100}$$

$$M^k = B^k \varepsilon_0 + D^k \kappa \tag{9.101}$$

and compactly summarized as

$$\begin{bmatrix} N^k \\ M^k \end{bmatrix} = \begin{bmatrix} A^k & B^k \\ B^k & D^k \end{bmatrix} \begin{bmatrix} \varepsilon^0 \\ \kappa \end{bmatrix}. \tag{9.102}$$

For layers, which are symmetric to the center plane $z = 0$, the coupling matrix B^k disappears and it remains

$$\begin{bmatrix} N^k \\ M^k \end{bmatrix} = \begin{bmatrix} A^k & 0 \\ 0 & D^k \end{bmatrix} \begin{bmatrix} \varepsilon^0 \\ \kappa \end{bmatrix} \tag{9.103}$$

with

$$A^k = Q^k h^k \quad , \quad D^k = Q^k \frac{(h^k)^3}{12}. \tag{9.104}$$

A special case, for which solely one preferential direction is considered with

$$A_{11}^k = Q_{11}^k h^k \quad , \quad D_{11} = Q_{11}^k \frac{(h^k)^3}{12} \tag{9.105}$$

serves for the description of a composite layer in a beam.

9.4.2 The Multilayer Composite

The composite is built by various layers (laminate). In the determination of the resulting forces and moments one needs to integrate throughout the total heights. Since the stiffness matrices per lamina are independent of the z-coordinate, the integration can be substituted through a corresponding summation. Therewith the following results:

$$N = A\varepsilon^0 + Bk, \tag{9.106}$$

$$M = B\varepsilon^0 + Dk, \tag{9.107}$$

or summarized

$$\begin{bmatrix} N \\ M \end{bmatrix} = \begin{bmatrix} A & B \\ B & D \end{bmatrix} \begin{bmatrix} \varepsilon^0 \\ k \end{bmatrix}. \tag{9.108}$$

The matrices A, B and D represent abbreviations for:

$$A = \sum_{k=1}^{N} Q^k (z^k - z^{k-1}), \tag{9.109}$$

$$B = \frac{1}{2} \sum_{k=1}^{N} Q^k \, (z^k - z^{k-1})^2, \tag{9.110}$$

$$D = \frac{1}{3} \sum_{k=1}^{N} Q^k \, (z^k - z^{k-1})^3. \tag{9.111}$$

In the case of a layer construction of the composite, which is symmetric to the center plane ($z = 0$), the coupling matrix B disappears.

The general process to describe a composite is:

1. Calculation of the layer stiffness from the engineering constants for each layer in the corresponding layer coordinate system.
2. Potential transformation of each layer stiffness matrix into the layer coordinate system.
3. Calculation of the layer stiffnesses in the composite.
4. Through inversion of the stiffness matrix one can receive the compliance matrices of the composite from

$$\varepsilon^0 = \alpha N + \beta M, \tag{9.112}$$

$$k = \beta^{\mathrm{T}} N + \delta M, \tag{9.113}$$

whereupon the following matrices are introduced for the abbreviation

$$\alpha = A^{-1} + A^{-1} B \tilde{D}^{-1} B A^{-1}, \tag{9.114}$$

$$\beta = A^{-1} + B \tilde{D}^{-1}, \tag{9.115}$$

$$\beta^{\mathrm{T}} = \tilde{D}^{-1} B A^{-1}, \tag{9.116}$$

$$\delta = \tilde{D}^{-1}, \tag{9.117}$$

$$\tilde{D}^{-1} = D - B A^{-1} B. \tag{9.118}$$

From the above equations, layer deformations can be defined under given external loads. Through reverse transformation the layer deformations result in the according lamina coordinate system and, through the stiffness matrices of the lamina, the *intralaminar* stress results.

9.5 A Finite Element Formulation

Within this chapter, a finite element formulation for a *composite* element is derived. The considerations about the general two-dimensional composite serve as a basis. Here, the derivation concentrates on the one-dimensional situation, whereupon one needs to distinguish between the following two loading cases:

- The loading occurs in the direction of the center line of the beam. The beam can therefore be described as a bar. Tension and compression loads occur.
- The load occurs perpendicular to the center line of the beam. Bending and shear occur.

9.5.1 The Composite Bar

Figure 9.5 illustrates a composite bar under tensile loading. The general procedure for the determination of the stiffness matrix remains the same. The displacement distribution in the element is approximated via the nodal displacements and the shape functions. In the simplest case the approach is described with a linear approach. The stiffness matrix can be derived via various motivations, for example via the principle of virtual work or via the potential. For the tension bar with homogeneous, isotropic material, constant modulus of elasticity E and cross-sectional area A the stiffness matrix results in:

$$k^e = \frac{EA}{L} \begin{bmatrix} 1 & -1 \\ -1 & 1 \end{bmatrix}. \qquad (9.119)$$

Fig. 9.5 Composite bar under tensile loading
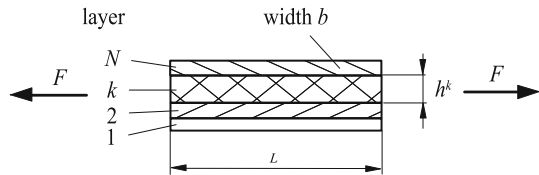
If one also assumes for the derivation of the stiffness matrix for the composite bar that the material properties and the cross-sectional area are constant along the bar axis, a similar formulation results:

$$k^e = \frac{(EA)^V}{L} \begin{bmatrix} 1 & -1 \\ -1 & 1 \end{bmatrix} \qquad (9.120)$$

The expression $(EA)^V$ stands for an axial stiffness, which refers to the unit length. From the comparison with the composite the following results

$$(EA)^V = A_{11} b = b \sum_{k=1}^{N} Q_{11}^k h^k. \qquad (9.121)$$

If the single composite layers each consist of a quasi-homogeneous, quasi-isotropic material, the relation simplifies

$$(EA)^{\mathrm{V}} = A_{11}\,b = b \sum_{k=1}^{N} E_1^k\,h^k\,. \tag{9.122}$$

The context can be simply but precisely interpreted as follows. The macroscopic axial stiffness which is represented of the composite material is composed of the weighted moduli of the elasticity of the single composite layers. At equal width the weights equate to the heights fractions.

Summary:
For a composite bar with a symmetric composition throughout the thickness, the stiffness matrix can be derived similarly to the bar with homogeneous, isotropic material.

9.5.2 The Composite Beam

Figure 9.6 illustrates a composite beam under bending condition.

Fig. 9.6 Symmetric composite beam under bending conditions
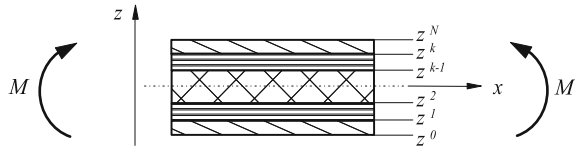
First it needs to be assumed that only bending occurs as the loading condition. Therewith only the matrix D has to be provided in the relation, which reduces to D_{11} for the one-dimensional beam. The connection between bending moment and curvature results as

$$M_1 = D_{11}\,\kappa\,. \tag{9.123}$$

For a beam of homogeneous, isotropic material the relation between bending moment and curvature appears as follows:

$$M = EI\,\kappa\,. \tag{9.124}$$

From the comparison a similar formulation for the composite beam can be gained:

$$(EI)^{\mathrm{V}} = b\,D_{11}\,. \tag{9.125}$$

The expression $(EI)^{\mathrm{V}}$ represents macroscopically the bending stiffness of the composite beam. For a single composite layer the relation is

$$D_{11}^k = Q_{11}^k \frac{h^3}{12} = Q_{11}^k \frac{1}{12}(z^k - z^{k-1})^3 \,, \tag{9.126}$$

whereupon as the absolute layer the $z = 0$ axis was assigned as the center plane. In the composite beam the cross-section dislocates from the 0-layer. Under consideration of the STEINER's fraction (parallel axis theorem)

$$\left(\frac{1}{2}(z^k + z^{k-1})\right)^2 b^k h^k = \frac{1}{4}(z^k + z^{k-1})^2 b^k (z^k - z^{k-1}) \tag{9.127}$$

the following relation results:

$$(EI)^V = D_{11} b = b \frac{1}{3} \sum_{k=1}^N Q_{11}^k \left((z^k)^3 - (z^{k-1})^3\right). \tag{9.128}$$

If the single composite layers each consist of a homogeneous, isotropic material, the relation simplifies to

$$(EI)^V = D_{11} b = b \frac{1}{3} \sum_{k=1}^N E_1^k \left((z^k)^3 - (z^{k-1})^3\right). \tag{9.129}$$

The context can be simply but precisely interpreted as follows. The macroscopic bending stiffness which is representative of the composite material is composed of the weighted moduli of the elasticity of the single composite layers. At equal width the weights equate to the heights fractions under consideration of STEINER's fraction due to the eccentric position of a layer.

Summary:
For a composite beam — designed symmetrically in respect to the thickness — the bending stiffness can be derived similarly to the homogeneous, isotropic beam.

9.6 Sample Problems and Supplementary Problems

9.1. Composite Bar with Three Layers

Given is a composite which is constructed symmetrically in height. The three layers are equally thick, which means the same heights h. Figure 9.7 illustrates the composite in the longitudinal section. Each layer consists of homogeneous, isotropic material. For each layer the modulus of elasticity is given with $E^{(1)}$, $E^{(2)}$ and $E^{(3)} = E^{(1)}$. Furthermore $E^{(2)} = \frac{1}{10} E^{(1)}$ should be valid.

Fig. 9.7 Symmetric composite beam with three layers
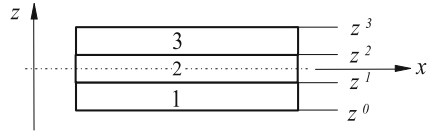
All layers in the composite have the same length L and the same width b.

Unknown are

1. the axial stiffness matrix for a load in the longitudinal direction of the composite and
2. the bending stiffness at a bending load. The bending moment is perpendicular to the x–z plane.

References

1. Altenbach H, Altenbach J, Naumenko K (1998) Ebene Flächentragwerke: Grundlagen der Modellierung und Berechnung von Scheiben und Platten. Springer, Berlin
2. Altenbach H, Altenbach J, Kissing W (2004) Mechanics of Composite Structural Elements. Springer, Berlin
3. Clebsch RFA (1862) Theorie der Elasticität fester Körper. B.G, Teubner, Leipzig
4. Kwon YW, Bang H (2000) The Finite Element Method Using MATLAB. CRC Press, Boca Raton

Chapter 10
Nonlinear Elasticity

Abstract Within this chapter, the case of the nonlinear elasticity, meaning strain-dependent modulus of elasticity, will be considered. The problem will be illustrated with the example of bar elements. First, the stiffness matrix or alternatively the principal finite element equation will be derived under consideration of the strain dependency. For the solving of the nonlinear system of equations three approaches will be derived, namely the direct iteration, the complete NEWTON–RAPHSON iteration and the modified NEWTON–RAPHSON iteration, and will be demonstrated with the help of multiple examples. Within the framework of the complete NEWTON–RAPHSON iteration the derivation of the tangent stiffness matrix will be discussed in detail.

10.1 Introductory Remarks

In the context of the finite element method it is common to distinguish between the following kind of nonlinearities [1]:

- **Physical or material nonlinearities**: This relates to nonlinear material behavior, as, for example, in the elastic area (covered within this chapter) of rubber or elasto-plastic behavior (covered in Chap. 11).
- **Nonlinear boundary conditions**: This is, for example, the case that in the course of the load application, a displacement boundary condition changes. Typical for this case are contact problems. This will not be covered within this book.
- **Geometric or kinematic nonlinearity**: This relates to large displacements and rotations at small strains. As examples structure elements such as wires and beams can be named. This will not be covered within this book.
- **Large deformations**: This relates to large displacements, rotations and large strains. This will not be covered within this book.
- **Stability problems**: Here, one has to distinguish between the geometric instability (as, for example, the buckling of bars and plates) and the material instability (as, for

(a)

(b)
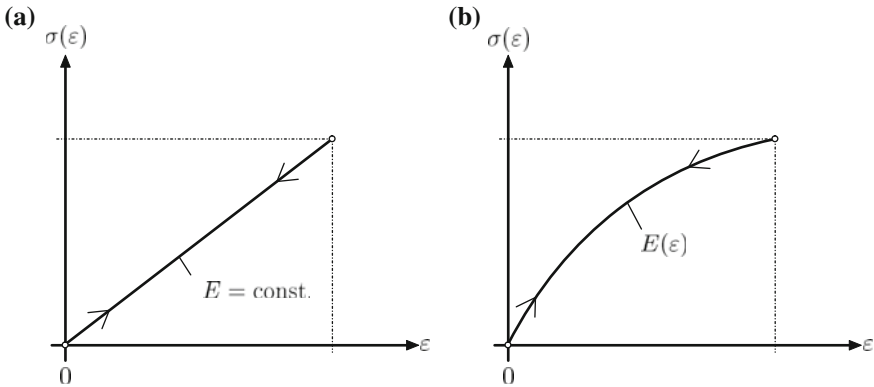
Fig. 10.1 Different behavior in the elastic range: **a** linear ; **b** nonlinear stress–strain diagram

example, the necking of tensile samples or the formation of shear bands). Within
this book only the buckling of bars will be covered in Chap. 12.

The basic characteristic of elastic material behavior is that the strains go back to zero
completely after unloading.[1] In the case of linear elasticity with a constant modulus
of elasticity the loading and unloading takes places in the stress–strain diagram along
a straight line, see Fig. 10.1a. The slope of this straight line equals exactly the constant
modulus of elasticity E, according to HOOKE's law. In generalization of this linear
elastic behavior the loading and unloading can also take place along a nonlinear
curve, and in this case one talks about nonlinear elasticity, see Fig. 10.1b. In this case
HOOKE's law is only valid in an incremental or differential form:

$$\frac{\mathrm{d}\sigma(\varepsilon)}{\mathrm{d}\varepsilon} = E(\varepsilon). \qquad (10.1)$$

One considers here that the denotation 'linear' or alternatively 'nonlinear' elastic-
ity relates to the behavior of the stress–strain curve. Furthermore, the modulus of
elasticity can also be dependent on the coordinate. This is, for example, the case of
functionally graded materials, the so-called gradient materials. Therefore the modu-
lus of elasticity in general, under the consideration of the kinematic relation, can be
indicated as

$$E = E(x, u). \qquad (10.2)$$

However, a dependency from the x-coordinate can be treated as a variable cross-
section[2] and demands no further analysis at this point. Therefore, in the following,
the focus is on dependencies of the form $E = E(u)$ or alternatively $E = E\left(\frac{\mathrm{d}u}{\mathrm{d}x}\right)$.

---

[1] At plastic material behavior remaining strains occur. This case will be covered in Chap. 11.

[2] For this, see the treatment of bar elements with variable cross-sectional areas $A = A(x)$ in Chap. 3.

10.2 Element Stiffness Matrix for Strain Dependent Elasticity

The following derivations will be carried out for the example case that the modulus of elasticity is dependent linearly on the strain, see Fig. 10.2. Under this assumption, the according Fig. 10.2a, a nonlinear stress–strain diagram results. The linear course of the modulus of elasticity can be defined in the following via the two sampling points $E(\varepsilon = 0) = E_0$ and $E(\varepsilon = \varepsilon_1) = E_1$.
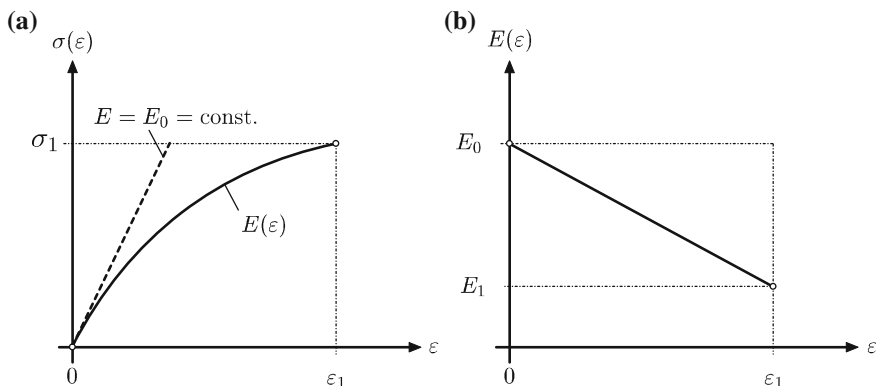
Fig. 10.2 **a** Nonlinear stress–strain diagram; **b** strain dependent modulus of elasticity

Therefore, the following course of the function for the strain dependent modulus of elasticity results for the two sampling points:

$$E(\varepsilon) = E_0 - \frac{\varepsilon}{\varepsilon_1}(E_0 - E_1) = E_0\left(1 - \varepsilon \times \underbrace{\frac{1 - E_1/E_0}{\varepsilon_1}}_{\alpha_{01}}\right) = E_0(1 - \varepsilon\alpha_{01}).$$

$$(10.3)$$

It needs to be remarked at this point that the principal route for the derivation does not change as long as the strain dependency of the modulus of elasticity can be described via a polynomial. This is often the case in practical applications, since experimental values are often approximated through a polynomial regression.

After the introduction of the kinematic relation for a bar, meaning $\varepsilon = \frac{du}{dx}$, herefrom the modulus of elasticity results in dependence of the displacement—or, to be precise, dependence of the derivative of the displacement—in:

$$E(u) = E_0\left(1 - \alpha_{01}\frac{du}{dx}\right). \qquad (10.4)$$

This strain dependent modulus of elasticity can be integrated analytically via the differential HOOKE's law and the following stress distribution results[3]:

$$\sigma(\varepsilon) = E_0\varepsilon - \frac{E_0 - E_1}{2E_0\varepsilon_1}\varepsilon^2 = E_0\varepsilon - \frac{1}{2}\alpha_{01}E_0\varepsilon^2. \tag{10.5}$$

One notes that the classical relations for linear elastic material behavior result for $E_0 = E_1$ or alternatively $\alpha_{01} = 0$.

For the derivation of the element stiffness matrix, the differential equation for a bar has to be considered. For simplification reasons it is assumed at this point that the bar cross-section A is constant and that no distributed loads are acting. Therefore the following formulation for the differential equation results:

$$A\frac{\mathrm{d}}{\mathrm{d}x}\left(E(u)\frac{\mathrm{d}u}{\mathrm{d}x}\right) = 0. \tag{10.6}$$

At first, the case is regarded that $E(u)$ is replaced by the expression according to Eq. (10.4):

$$A\frac{\mathrm{d}}{\mathrm{d}x}\left(E_0\left(1 - \alpha_{01}\frac{\mathrm{d}u}{\mathrm{d}x}\right)\frac{\mathrm{d}u}{\mathrm{d}x}\right) = AE_0\frac{\mathrm{d}}{\mathrm{d}x}\left(\frac{\mathrm{d}u}{\mathrm{d}x} - \alpha_{01}\left(\frac{\mathrm{d}u}{\mathrm{d}x}\right)^2\right) = 0. \tag{10.7}$$

After the completion of the differentiation the following expression results for the differential equation, which describes the problem:

$$AE_0\frac{\mathrm{d}^2u(x)}{\mathrm{d}x^2} - 2AE_0\alpha_{01}\frac{\mathrm{d}u(x)}{\mathrm{d}x}\frac{\mathrm{d}^2u(x)}{\mathrm{d}x^2} = 0. \tag{10.8}$$

Within the framework of the weighted residual method the inner product results herefrom through multiplication with the weighting function $W(x)$ and subsequent integration via the bar length in:

$$\int_0^L W(x)\left(AE_0\frac{\mathrm{d}^2u(x)}{\mathrm{d}x^2} - 2AE_0\alpha_{01}\frac{\mathrm{d}u(x)}{\mathrm{d}x}\frac{\mathrm{d}^2u(x)}{\mathrm{d}x^2}\right)\mathrm{d}x \overset{!}{=} 0. \tag{10.9}$$

Partial integration of the first expression in brackets yields:

$$\int_0^L AE_0\underbrace{W}_{f}\underbrace{\frac{\mathrm{d}^2u}{\mathrm{d}x^2}}_{g'}\mathrm{d}x = AE_0\left[\underbrace{W}_{f}\underbrace{\frac{\mathrm{d}u}{\mathrm{d}x}}_{g}\right]_0^L - \int_0^L AE_0\underbrace{\frac{\mathrm{d}W}{\mathrm{d}x}}_{f'}\underbrace{\frac{\mathrm{d}u}{\mathrm{d}x}}_{g}\mathrm{d}x. \tag{10.10}$$

---

[3] At this point it was assumed that for $\varepsilon = 0$ the stress turns 0. Therefore, for example no residual stress exists.

Accordingly, the second expression in brackets can be reformulated via partial integration:

$$
\int_0^L 2AE_0\alpha_{01} \underbrace{\left(W\frac{du}{dx}\right)}_{f} \underbrace{\frac{d^2u}{dx^2}}_{g'} dx
$$

$$
= 2AE_0\alpha_{01} \left[\underbrace{W\frac{du}{dx}}_{f} \underbrace{\frac{du}{dx}}_{g}\right]_0^L - \int_0^L 2AE_0\alpha_{01} \underbrace{\frac{d}{dx}\left(W\frac{du}{dx}\right)}_{f'} \underbrace{\frac{du}{dx}}_{g} dx
$$

$$
= 2AE_0\alpha_{01} \left[W\left(\frac{du}{dx}\right)^2\right]_0^L - \int_0^L 2AE_0\alpha_{01} \left(\frac{dW}{dx}\frac{du}{dx} + W\frac{d^2u}{dx^2}\right)\frac{du}{dx} dx
$$

$$
= 2AE_0\alpha_{01} \left[W\left(\frac{du}{dx}\right)^2\right]_0^L - \int_0^L 2AE_0\alpha_{01} \frac{dW}{dx}\left(\frac{du}{dx}\right)^2 dx
$$

$$
- \int_0^L 2AE_0\alpha_{01} W\frac{d^2u}{dx^2}\frac{du}{dx} dx. \tag{10.11}
$$

Finally, the following results for the partial integration of the second expression:

$$
\int_0^L 2AE_0\alpha_{01} W\frac{du}{dx}\frac{d^2u}{dx^2} dx = AE_0\alpha_{01}\left[W\left(\frac{du}{dx}\right)^2\right]_0^L
$$

$$
- \int_0^L AE_0\alpha_{01} \frac{dW}{dx}\left(\frac{du}{dx}\right)^2 dx. \tag{10.12}
$$

The following expression results, when the expressions of the partial integrations according to Eqs. (10.10) and (10.12) are inserted into the inner product according to Eq. (10.9) and when the domain and boundary integrals are arranged:

$$
\int_0^L AE_0\frac{dW}{dx}\frac{du}{dx} dx - \int_0^L AE_0\alpha_{01}\frac{dW}{dx}\left(\frac{du}{dx}\right)^2 dx
$$

$$
= AE_0\left[W\frac{du}{dx} - \alpha_{01}W\left(\frac{du}{dx}\right)^2\right]_0^L. \tag{10.13}
$$

The introduction of the approaches for the displacement and the weighting function, meaning $u(x) = N u_\mathrm{p}$ and $W(x) = \delta u_\mathrm{p}^\mathrm{T} N^\mathrm{T}(x)$, leads to the following expression, after canceling of the virtual displacement $\delta u_\mathrm{p}^\mathrm{T}$ and factoring out the displacement vector u_p:

$$
A E_0 \int_0^L \left(\frac{\mathrm{d} N^\mathrm{T}(x)}{\mathrm{d} x} \frac{\mathrm{d} N(x)}{\mathrm{d} x} - \alpha_{01} \frac{\mathrm{d} N^\mathrm{T}(x)}{\mathrm{d} x} \left(\frac{\mathrm{d} N(x)}{\mathrm{d} x} u_\mathrm{p} \right) \frac{\mathrm{d} N(x)}{\mathrm{d} x} \right) \mathrm{d} x \times u_\mathrm{p}
$$

$$
= A E_0 \left[\frac{\mathrm{d} N^\mathrm{T}(x)}{\mathrm{d} x} \left(\frac{\mathrm{d} u}{\mathrm{d} x} - \alpha_{01} \left(\frac{\mathrm{d} u}{\mathrm{d} x} \right)^2 \right) \right]_0^L . \tag{10.14}
$$

Therefore, in dependence of the nodal displacement u_p the element stiffness matrix[4] results in:

$$
k^\mathrm{e} = A E_0 \int_0^L \left(\frac{\mathrm{d} N^\mathrm{T}(x)}{\mathrm{d} x} \frac{\mathrm{d} N(x)}{\mathrm{d} x} - \alpha_{01} \left(\frac{\mathrm{d} N^\mathrm{T}(x)}{\mathrm{d} x} \frac{\mathrm{d} N(x)}{\mathrm{d} x} \right) \left(u_\mathrm{p} \frac{\mathrm{d} N(x)}{\mathrm{d} x} \right) \right) \mathrm{d} x .
$$

$$\tag{10.15}$$

If the shape functions are known, the stiffness matrix can be evaluated. The second expression in the outer brackets yields an additional symmetrical expression, which can be superposed to the classical stiffness matrix for linear elastic material behavior. For a constant modulus of elasticity $\alpha_{01} = 0$ results and one receives the classical solution. The following dimensions of the single matrix products results if the bar element has m nodes and therefore m shape functions:

$$
\frac{\mathrm{d} N^\mathrm{T}(x)}{\mathrm{d} x} \frac{\mathrm{d} N(x)}{\mathrm{d} x} \rightarrow \quad m \times m \text{ matrix,} \tag{10.16}
$$

$$
u_\mathrm{p} \frac{\mathrm{d} N(x)}{\mathrm{d} x} \rightarrow \quad m \times m \text{ matrix,} \tag{10.17}
$$

$$
\left(\frac{\mathrm{d} N^\mathrm{T}(x)}{\mathrm{d} x} \frac{\mathrm{d} N(x)}{\mathrm{d} x} \right) \left(u_\mathrm{p} \frac{\mathrm{d} N(x)}{\mathrm{d} x} \right) \rightarrow \quad m \times m \text{ matrix.} \tag{10.18}
$$

However, in the following an alternative strategy is illustrated, which leads slightly faster to the principal finite element equation. On the basis of the differential equation in the form (10.6), the inner product can be derived without replacing the expression for $E(u)$ *a priori*:

$$
\int_0^L W(x) A \frac{\mathrm{d}}{\mathrm{d} x} \left(E(u(x)) \frac{\mathrm{d} u(x)}{\mathrm{d} x} \right) \mathrm{d} x \stackrel{!}{=} 0 . \tag{10.19}
$$

---

[4] One considers that the associative law applies for matrix multiplications.

Partial integration yields

$$\int\limits_0^L \underbrace{W}_{f}\ A\underbrace{\frac{\mathrm{d}}{\mathrm{d}x}\left(E(u)\frac{\mathrm{d}u}{\mathrm{d}x}\right)}_{g'}\,\mathrm{d}x = \left[\underbrace{W}_{f}\ \underbrace{AE(u)\frac{\mathrm{d}u}{\mathrm{d}x}}_{g}\right]_0^L - \int\limits_0^L \underbrace{\frac{\mathrm{d}W}{\mathrm{d}x}}_{f'}\ \underbrace{AE(u)\frac{\mathrm{d}u}{\mathrm{d}x}}_{g}\,\mathrm{d}x = 0,$$

and the weak form of the problem appears as follows:

$$\int\limits_0^L AE(u)\frac{\mathrm{d}W}{\mathrm{d}x}\frac{\mathrm{d}u}{\mathrm{d}x}\,\mathrm{d}x = \left[AE(u)W\frac{\mathrm{d}u}{\mathrm{d}x}\right]_0^L. \tag{10.20}$$

Via the approaches for the displacement and the weighting function, the following results herefrom:

$$A\underbrace{\int\limits_0^L E(u)\frac{\boldsymbol{N}^{\mathrm{T}}}{\mathrm{d}x}\frac{\boldsymbol{N}}{\mathrm{d}x}\,\mathrm{d}x}_{\boldsymbol{k}^{\mathrm{e}}} \times \boldsymbol{u}_{\mathrm{p}} = \left[AE(u)\frac{\mathrm{d}u}{\mathrm{d}x}\frac{\mathrm{d}\boldsymbol{N}^{\mathrm{T}}}{\mathrm{d}x}\right]_0^L. \tag{10.21}$$

The right-hand side can be handled according to the procedure in Chap. 3 and yields the vector of the external loads. The left-hand side, however, requires that the modulus of elasticity $E(u)$ is considered appropriately. If the approach for the displacement, meaning $u(x) = N(x)\boldsymbol{u}_{\mathrm{p}}$, is considered in the formulation of the modulus of elasticity according to Eq. (10.4), the following results:

$$E(\boldsymbol{u}_{\mathrm{p}}) = E_0\left(1 - \alpha_{01}\frac{\mathrm{d}\boldsymbol{N}}{\mathrm{d}x}\boldsymbol{u}_{\mathrm{p}}\right). \tag{10.22}$$

It can be considered at this point that the expression $\frac{\mathrm{d}\boldsymbol{N}}{\mathrm{d}x}\boldsymbol{u}_{\mathrm{p}}$ yields a scalar parameter. Therefore, the stiffness matrix results in:

$$\boldsymbol{k}^{\mathrm{e}} = AE_0\int\limits_0^L \underbrace{\left(1 - \alpha_{01}\frac{\mathrm{d}\boldsymbol{N}}{\mathrm{d}x}\boldsymbol{u}_{\mathrm{p}}\right)}_{\text{scalar}}\frac{\mathrm{d}\boldsymbol{N}^{\mathrm{T}}}{\mathrm{d}x}\frac{\mathrm{d}\boldsymbol{N}}{\mathrm{d}x}\,\mathrm{d}x. \tag{10.23}$$

This stiffness matrix is—as Eq. (10.15)—symmetric since the symmetric matrix $\frac{\mathrm{d}\boldsymbol{N}^{\mathrm{T}}}{\mathrm{d}x}\frac{\mathrm{d}\boldsymbol{N}}{\mathrm{d}x}$ is multiplied by a scalar.

In the following, a bar element with two nodes, meaning linear shape functions, can be considered. Both shape functions and their derivatives in this case result in:

$$N_1(x) = 1 - \frac{x}{L}, \quad \frac{dN_1(x)}{dx} = -\frac{1}{L}, \tag{10.24}$$

$$N_2(x) = \frac{x}{L}, \quad \frac{dN_2(x)}{dx} = \frac{1}{L}. \tag{10.25}$$

Therefore the stiffness matrix results in:

$$k^e = AE_0 \int_0^L \left(1 - \alpha_{01}\frac{dN_1}{dx}u_1 - \alpha_{01}\frac{dN_2}{dx}u_2\right) \begin{bmatrix} \dfrac{dN_1}{dx}\dfrac{dN_1}{dx} & \dfrac{dN_1}{dx}\dfrac{dN_2}{dx} \\ \dfrac{dN_2}{dx}\dfrac{dN_1}{dx} & \dfrac{dN_2}{dx}\dfrac{dN_2}{dx} \end{bmatrix} dx, \tag{10.26}$$

or alternatively under consideration of the derivatives of the shape functions

$$k^e = \frac{AE_0}{L^2} \int_0^L \left(1 + \frac{\alpha_{01}}{L}u_1 - \frac{\alpha_{01}}{L}u_2\right) \begin{bmatrix} 1 & -1 \\ -1 & 1 \end{bmatrix} dx. \tag{10.27}$$

After completion of the integration herefrom the element stiffness matrix results in

$$k^e = \frac{AE_0}{L^2}(L + \alpha_{01}u_1 - \alpha_{01}u_2)\begin{bmatrix} 1 & -1 \\ -1 & 1 \end{bmatrix} \tag{10.28}$$

or the principal finite element equation as:

$$\frac{AE_0}{L^2}(L + \alpha_{01}u_1 - \alpha_{01}u_2)\begin{bmatrix} 1 & -1 \\ -1 & 1 \end{bmatrix}\begin{bmatrix} u_1 \\ u_2 \end{bmatrix} = \begin{bmatrix} F_1 \\ F_2 \end{bmatrix}. \tag{10.29}$$

One considers that for the constant modulus of elasticity, meaning $\alpha_{01} = 0$, the classical solution from Chap. 3 results. For the variable modulus of elasticity the following system of equations results in matrix notation:

$$k^e(u_p)u_p = F^e, \tag{10.30}$$

or, alternatively, with various elements for the total system

$$K(u)u = F. \tag{10.31}$$

Since the stiffness matrix is dependent on the unknown nodal displacements u, a nonlinear system of equations results, which cannot be solved directly through inverting of the stiffness matrix.

10.3 Solving of the Nonlinear System of Equations

The solving of the nonlinear system of equations can be explained in the following for a bar, which is fixed on one side and loaded by a single force F on the other side, with the help of various methods, see Fig. 10.3. The modulus of elasticity is,
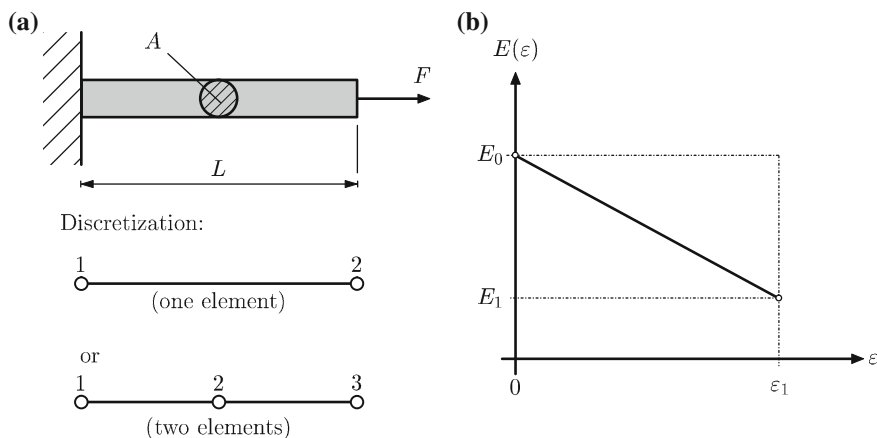
Fig. 10.3 Bar element under point load and strain dependent modulus of elasticity

according to Eq. (10.3), linearly dependent on the strain. First the discretization via one single element takes place, so that, under consideration of the fixed support, a system with one single degree of freedom results. The resulting equations are therefore solely dependent on one variable, the nodal displacement at the loading point. In the following step, one merges to the general case of a system with various degrees of freedom. The illustration takes place via a discretization of the problem according to Fig. 10.3a with two elements and therefore with two degrees of freedom. For the example according to Fig. 10.3, the following values can be assumed: Geometry: $A = 100\,\text{mm}^2$, $L = 400\,\text{mm}$. Material characteristics: $E_0 = 70{,}000$ MPa, $E_1 = 49{,}000\,\text{MPa}$, $\varepsilon_1 = 0.15$. Load: $F = 800\,\text{kN}$.

10.3.1 Direct Iteration

At the direct or PICARD's iteration [2, 3], the system of Eq. (10.31) is solved by evaluating the stiffness matrix in the previous and therefore known step. Through the selection of a reasonable initial value—for example from a linear elastic relation—the solution can be determined via the following formula through gradual inserting:

$$K(u^{(j)})u^{(j+1)} = F. \tag{10.32}$$

The schematic illustration of the direct iteration is shown in Fig. 10.4.

Fig. 10.4 Schematic illustration of the direct iteration
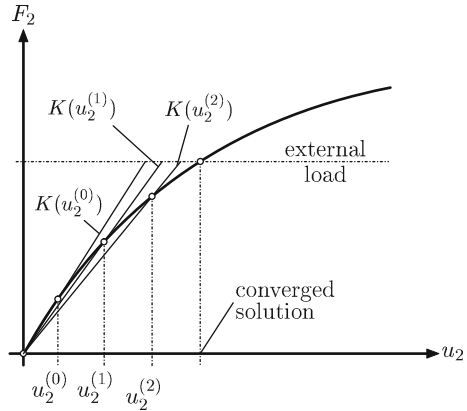
This method converges for modest nonlinearities with linear convergence rate.

10.3.1.1 Direct Iteration for a Finite Element Model with One Unknown

For the example corresponding to Fig. 10.3 and the principal finite element equation according to (10.29), under consideration of the fixed support, the iteration formula results in:

$$\frac{AE_0}{L^2}\left(L - \alpha_{01}u_2^{(j)}\right)u_2^{(j+1)} = F_2, \tag{10.33}$$

or alternatively solved for the new displacement:

$$u_2^{(j+1)} = \frac{F_2 L^2}{AE_0\left(L - \alpha_{01}u_2^{(j)}\right)}. \tag{10.34}$$

The evaluation of Eq. (10.34) for the example corresponding to Fig. 10.3 is summarized in Table 10.1 for an arbitrary initial value of $u_2^{(0)} = 20$ mm. The normalized displacement difference was indicated as convergence criteria, whose fulfillment requires 23 iterations for a value of 10^{-6}. Furthermore, one considers the absolute value of the displacement at the 31st increment, which is also consulted as a reference value in other methods.

10.3.1.2 Direct Iteration for a Finite Element Model with Various Unknowns

For the application of the direct iteration on a model with various unknowns, the bar, according to Fig. 10.3 can be considered in the following. The discretization

Table 10.1 Numerical values for the direct iteration in the case of one element with an external load of $F_2 = 800\,\text{kN}$ and an initial value of $u_2^{(0)} = 20\,\text{mm}$. Geometry: $A = 100\,\text{mm}^2$, $L = 400\,\text{mm}$. Material characteristics: $E_0 = 70{,}000\,\text{MPa}$, $E_1 = 49{,}000\,\text{MPa}$, $\varepsilon_1 = 0.15$

Iteration j	$u_2^{(j)}$ (mm)	$\varepsilon_2^{(j)}$	$\sqrt{\dfrac{\left(u_2^{(j)}-u_2^{(j-1)}\right)^2}{\left(u_2^{(j)}\right)^2}}$
0	20.000000	0.050000	–
1	50.793651	0.126984	0.606250
2	61.276596	0.153191	0.171076
3	65.907099	0.164768	0.070258
4	68.183007	0.170458	0.033379
5	69.360231	0.173401	0.016973
6	69.985252	0.174963	0.008931
7	70.321693	0.175804	0.004784
8	70.504137	0.176260	0.002588
9	70.603469	0.176509	0.001407
10	70.657668	0.176644	0.000767
11	70.687276	0.176718	0.000419
12	70.703461	0.176759	0.000229
13	70.712312	0.176781	0.000125
14	70.717152	0.176793	0.000068
15	70.719800	0.176800	0.000037
16	70.721248	0.176803	0.000020
17	70.722041	0.176805	0.000011
18	70.722474	0.176806	0.000006
19	70.722711	0.176807	0.000003
20	70.722841	0.176807	0.000002
21	70.722912	0.176807	0.000001
22	70.722951	0.176807	0.000001
23	70.722972	0.176807	0.000000
⋮	⋮	⋮	⋮
31	70.722998	0.176807	0.000000

should occur through two bar elements, which have the same length. Therefore, the following element stiffness matrix results for each of the two elements with length $\frac{L}{2}$:

$$\frac{4AE_0}{L^2}\left(\frac{L}{2} + \alpha_{01}u_1 - \alpha_{01}u_2\right)\begin{bmatrix} 1 & -1 \\ -1 & 1 \end{bmatrix}\text{(element I)},\qquad(10.35)$$

$$\frac{4AE_0}{L^2}\left(\frac{L}{2} + \alpha_{01}u_2 - \alpha_{01}u_3\right)\begin{bmatrix} 1 & -1 \\ -1 & 1 \end{bmatrix}\text{(element II)}.\qquad(10.36)$$

The following reduced system of equations results, if the two matrices are summarized to the global principal finite element equation and if the boundary conditions

are considered:

$$\frac{4AE_0}{L^2}\begin{bmatrix} (L - \alpha_{01}u_3) & -\left(\frac{L}{2} + \alpha_{01}u_2 - \alpha_{01}u_3\right) \\ -\left(\frac{L}{2} + \alpha_{01}u_2 - \alpha_{01}u_3\right) & \left(\frac{L}{2} + \alpha_{01}u_2 - \alpha_{01}u_3\right) \end{bmatrix}\begin{bmatrix} u_2 \\ u_3 \end{bmatrix} = \begin{bmatrix} 0 \\ F_3 \end{bmatrix}.$$

(10.37)

Through inversion one obtains the following iteration formula of the direct iteration:

$$\begin{bmatrix} u_2 \\ u_3 \end{bmatrix}_{(j+1)} = \frac{\frac{L^2}{4AE_0}}{DET^{(j)}}\begin{bmatrix} \left(\frac{L}{2} + \alpha_{01}u_2 - \alpha_{01}u_3\right) & \left(\frac{L}{2} + \alpha_{01}u_2 - \alpha_{01}u_3\right) \\ \left(\frac{L}{2} + \alpha_{01}u_2 - \alpha_{01}u_3\right) & (L - \alpha_{01}u_3) \end{bmatrix}_{(j)}\begin{bmatrix} 0 \\ F_3 \end{bmatrix}_{(j)},$$

(10.38)

whereupon the determinant of the reduced stiffness matrix is given through the following equation:

$$DET = (L - \alpha_{01}u_3)\left(\frac{L}{2} + \alpha_{01}u_2 - \alpha_{01}u_3\right) - \left(\frac{L}{2} + \alpha_{01}u_2 - \alpha_{01}u_3\right)^2.$$

(10.39)

In general, the iteration instruction according to Eq. (10.38) can also be written as

$$u^{(j+1)} = \left(K(u^{(j)})\right)^{-1}F.$$

(10.40)

The numerical results of the iteration for the example according to Fig. 10.3 with two elements are summarized in Table 10.2. A comparison with the direct iteration with one element, meaning Table 10.1, yields that the division in two elements has practically no influence on the convergence behavior. One considers that the displacements on node 2 and 3 are listed in Table 10.2 and that only in the converged situation the condition $u_2 = \frac{1}{2}u_3$ results.

10.3.2 Complete Newton–Raphson Method

10.3.2.1 Newton's Method for a Function with One Variable

For the definition of the root of a function $f(x)$, meaning $f(x) = 0$, NEWTON's iteration is often used. For the derivation of the iteration method, one develops the function $f(x)$ around the point x_0 in a TAYLOR's series

Table 10.2 Numerical values for the direct iteration in the case of two elements with an external load of $F_2 = 800\,\text{kN}$ and initial values of $u_2^{(0)} = 10$ and $u_3^{(0)} = 20\,\text{mm}$. Geometry: $A = 100\,\text{mm}^2$, $L_\text{I} = L_\text{II} = 200\,\text{mm}$. Material characteristics: $E_0 = 70{,}000\,\text{MPa}$, $E_1 = 49{,}000\,\text{MPa}$, $\varepsilon_1 = 0.15$

Iteration j	$u_2^{(j)}$ (mm)	$u_3^{(j)}$ (mm)	$\sqrt{\dfrac{\left(u_2^{(j)}-u_2^{(j-1)}\right)^2+\left(u_3^{(j)}-u_3^{(j-1)}\right)^2}{\left(u_2^{(j)}\right)^2+\left(u_3^{(j)}\right)^2}}$
0	10.000000	20.000000	–
1	28.571429	49.350649	0.706244
2	32.000000	60.852459	0.174565
3	33.613445	65.739844	0.069707
4	34.430380	68.106422	0.032806
5	34.859349	69.3222247	0.016616
6	35.088908	69.9655414	0.008727
7	35.213000	70.3112206	0.004671
8	35.280446	70.4984992	0.002525
9	35.317213	70.6004116	0.001372
10	35.337288	70.6560035	0.000748
⋮	⋮	⋮	⋮
23	35.361489	70.7229715	0.000000
⋮	⋮	⋮	⋮
31	35.361499	70.7229976	0.000000

$$f(x) = f(x_0) + \left(\frac{\mathrm{d}f}{\mathrm{d}x}\right)_{x_0} \cdot (x - x_0) + \frac{1}{2!}\left(\frac{\mathrm{d}^2 f}{\mathrm{d}x^2}\right)_{x_0} \cdot (x - x_0)^2$$
$$+ \cdots + \frac{1}{k!}\left(\frac{\mathrm{d}^k f}{\mathrm{d}x^k}\right)_{x_0} \cdot (x - x_0)^k. \tag{10.41}$$

If the expressions of quadratic and higher order are disregarded, the following approximation results:

$$f(x) \approx f(x_0) + \left(\frac{\mathrm{d}f}{\mathrm{d}x}\right)_{x_0} \cdot (x - x_0). \tag{10.42}$$

When considering that the derivative of a function equals the slope of the tangent line in the considered point and that the slope-intercept equation of a straight line is given via $f(x) - f(x_0) = m \cdot (x - x_0)$, one can see that the approximation via a TAYLOR's series of first order is given through the straight line through the point $(x_0, f(x_0))$ with slope $m = (\mathrm{d}f/\mathrm{d}x)_{x_0}$, see Fig. 10.5.

For the derivation of the iteration formula for the definition of the roots, one sets Eq. (10.42) equal 0 and obtains the following calculation instruction via the

$f(x)$
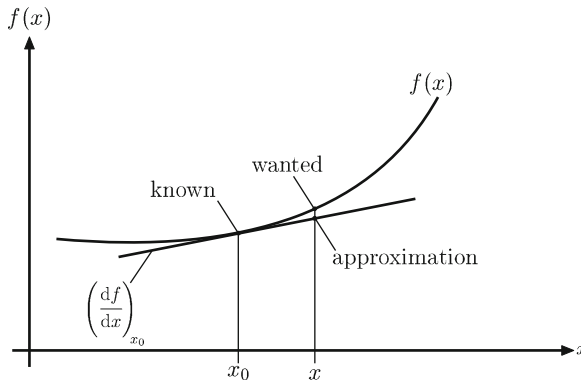
Fig. 10.5 Development of a function into a TAYLOR's series of first order

substitutions $x_0 \to x^{(j)}$ and $x \to x^{(j+1)}$:

$$x^{(j+1)} = x^{(j)} - \frac{f(x^{(j)})}{\left(\dfrac{\mathrm{d}f}{\mathrm{d}x}\right)_{x^{(j)}}}. \tag{10.43}$$

The principle course of action of a NEWTON's iteration is illustrated in Fig. 10.6. At

Fig. 10.6 Definition of the root of a function via NEW-TON's iteration
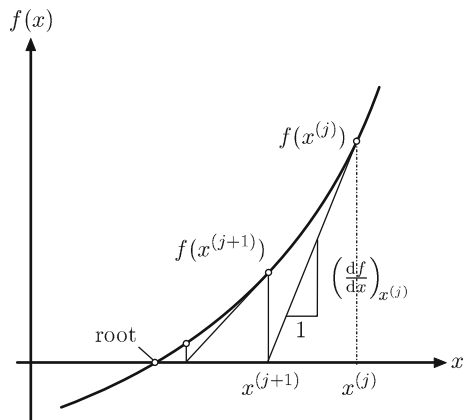
the initial point of the iteration, the tangent is pictured on the graph of the function $f(x)$ and subsequently the root of this tangent will be defined. In the ordinate value of this root, the next tangent will be formed and the procedure will be continued according to the course of action in the initial point. If $f(x)$ is a continuous and monotonic function in the considered interval and if the initial point of the iteration lies 'close enough' to the unknown solution, the method converges quadratically against the root.

10.3.2.2 Newton–Raphson Method for a Finite Element Model with One Unknown

For the example according to Fig. 10.3, the problem reduces to locating the roots of the function, under consideration of the boundary conditions on the left-hand node

$$r(u_2) = \frac{AE_0}{L^2}(L - \alpha_{01}u_2)\, u_2 - F_2 = K(u_2)u_2 - F_2 = 0. \qquad (10.44)$$

When applying the iteration instruction of the previous Sect. 10.3.2.1 on the residual function $r(u_2)$, the following NEWTON–RAPHSON iteration instruction[5] results in

$$u_2^{(j+1)} = u_2^{(j)} - \frac{r(u_2^{(j)})}{\dfrac{\mathrm{d}r(u_2^{(j)})}{\mathrm{d}u_2}} = u_2^{(j)} - \left(K_{\mathrm{T}}^{(j)}\right)^{-1} r(u_2^{(j)}), \qquad (10.45)$$

whereupon the parameter K_{T} is in general referred to as the tangent stiffness matrix.[6] In the example considered at this point, K_{T} however reduces to a scalar function. On the basis of Eq. (10.44) the tangent stiffness matrix for our example results in:

$$K_{\mathrm{T}}(u_2) = \frac{\mathrm{d}r(u_2)}{\mathrm{d}u_2} = K(u_2) + \frac{\mathrm{d}K(u_2)}{\mathrm{d}u_2}u_2 \qquad (10.46)$$

$$= \frac{AE_0}{L^2}(L - \alpha_{01}u_2) - \frac{AE_0}{L^2}\alpha_{01}u_2$$

$$= \frac{AE_0}{L^2}(L - 2\alpha_{01}u_2). \qquad (10.47)$$

When using the last result in the iteration instruction (10.45) and when considering the definition of the residual function according to (10.44), the iteration instruction for the regarded example finally results in:

$$u_2^{(j+1)} = u_2^{(j)} - \frac{\dfrac{AE_0}{L^2}\left(L - \alpha_{01}u_2^{(j)}\right)u_2^{(j)} - F_2^{(j)}}{\dfrac{AE_0}{L^2}\left(L - 2\alpha_{01}u_2^{(j)}\right)}. \qquad (10.48)$$

The application of the iteration instruction according to Eq. (10.48) with $\alpha_{01} = 2$ leads to the summarized results in Table 10.3. One can see that only six iteration steps are necessary for the complete NEWTON–RAPHSON iteration, due to the quadratic convergence behavior, to achieve the convergence criteria ($<10^{-6}$) and the absolute value of $u_2 = 70.722998\,\mathrm{mm}$. In the general case of the method however, the

---

[5] In the context of the finite element method NEWTON's iteration is often referred to as the NEWTON–RAPHSON iteration [4].

[6] Alternative names in literature are HESSIAN, JACOBIAN or tangent matrix [1].

Table 10.3 Numerical values for the complete NEWTON–RAPHSON method at an external load of $F_2 = 800\,\text{kN}$. Geometry: $A = 100\,\text{mm}^2$, $L = 400\,\text{mm}$. Material behavior: $E_0 = 70{,}000\,\text{MPa}$, $E_1 = 49{,}000\,\text{MPa}$, $\varepsilon_1 = 0.15$

Iteration j	$u_2^{(j)}$ (mm)	$\varepsilon_2^{(j)}$	$\sqrt{\dfrac{\left(u_2^{(j)}-u_2^{(j-1)}\right)^2}{\left(u_2^{(j)}\right)^2}}$
0	0	0	–
1	45.714286	0.114286	1
2	64.962406	0.162406	0.296296
3	70.249443	0.175624	0.075261
4	70.719229	0.176798	0.006643
5	70.722998	0.176807	0.000053
6	70.722998	0.176807	0.000000

huge disadvantage arises that the tangent stiffness *matrix* has to be recalculated and inverted for each iteration step. For huge systems of equations this leads to quite calculational intensive operations and can perhaps compensate the advantage of the quadratic convergence.

When increasing the external load F_2, a limit value results, however, from which no convergence can be achieved with the NEWTON–RAPHSON method any longer. A strain dependent modulus of elasticity according to Eq. (10.4) leads through integration to the illustrated parabolic stress distribution in Fig. 10.7. Based on this illustra-
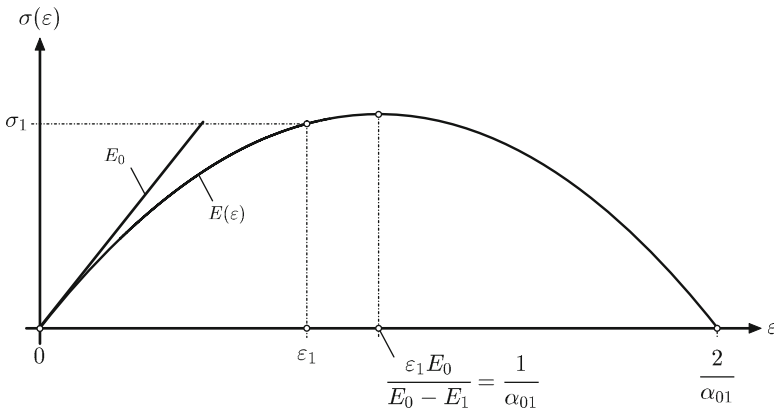
Fig. 10.7 Stress–strain course for a strain dependent modulus of elasticity according to Eq. (10.4)

tion the maximal stress to $\sigma_{\text{max}} = \frac{E_0}{2\alpha_{01}}$ or alternatively the maximal force in a bar to $F_{\text{max}} = \frac{E_0 A}{2\alpha_{01}}$ can be defined.

However, through gradual increasing of the external force F_2 in the regarded example, it results that the convergence limit is achieved clearly lower than the maximal force of $F_{\text{max}} = 1{,}750\,\text{kN}$. Via a few iteration cycles it can be shown that starting with a value of about $900\,\text{kN}$, no convergence can be achieved any longer in the considered

example. One also considers that a reasonable physical choice of the external force always has to meet the condition $F_2 \leq F_{\max}$.

To explain the loss of convergence, the residual function according to Eq. (10.44) has to be considered more closely, whereupon it has to be considered that the iteration method needs to define the roots of this function. The considered residual function is a quadratic function in u_2, which can be changed into the following equation of a parabola by completing the square:

$$\left(u_2 - \frac{L}{2\alpha_{01}}\right)^2 + \left(\frac{F_2}{E_0 A} - \frac{1}{4\alpha_{01}}\right)\frac{L^2}{\alpha_{01}} = 0. \tag{10.49}$$

Therefore Eq. (10.44) represents an upward facing parabola with the vertex $\left(\frac{L}{2\alpha_{01}}, \left(\frac{F_2}{E_0 A} - \frac{1}{4\alpha_{01}}\right)\frac{L^2}{\alpha_{01}}\right)$. Depending on the position of the vertex, a different number of roots results (see Fig. 10.8), so that the boundary value for the convergence of the iteration method is defined through the boundary point of the parabola with the u_2-axis:

$$\frac{F_2}{E_0 A} - \frac{1}{4\alpha_{01}} = 0. \tag{10.50}$$

Therefore, the NEWTON–RAPHSON iteration method for the considered case, that the modulus of elasticity according to Eq. (10.4) is dependent linearly on the strain, converges solely within the following boundaries:

$$F_2 \leq \frac{E_0 A}{4\alpha_{01}}, \quad \text{or alternatively} \quad \varepsilon \leq \frac{1}{2\alpha_{01}}. \tag{10.51}$$

The schematic process of the NEWTON–RAPHSON iteration is illustrated in Fig. 10.9. The tangent stiffness matrix $K_{\mathrm{T}}^{(j)}$ is calculated in every single iteration point $u_2^{(j)}$, to conclude the follow-on value $u_2^{(j+1)}$ via a linearization. It is important at this point that the tangent stiffness matrix can be identified as the derivative in the force displacement diagram, see Fig. 10.9a. To receive the illustration in a stress–strain diagram, one has to divide the residual equation (10.44) through the cross-sectional area and has to scale the displacement with the length, so that one obtains the following form:

$$E_0 \left(1 - \alpha_{01}\frac{u_2}{L}\right)\frac{u_2}{L} - \frac{F_2}{A} = 0, \tag{10.52}$$

or alternatively in the variables stress and strain as

$$r(\varepsilon) = \underbrace{E_0 \left(1 - \alpha_{01}\varepsilon\right)}_{E(\varepsilon)} \varepsilon - \sigma = 0. \tag{10.53}$$

(a)

$r(u_2)$

$$F_2 < \frac{E_0 A}{4\alpha_{01}} \quad \varepsilon < \frac{1}{2\alpha_{01}}$$

initial value

root

0 u_2

(b) $r(u_2)$

$$F_2 > \frac{E_0 A}{4\alpha_{01}}$$

$$\varepsilon > \frac{1}{2\alpha_{01}}$$

0 $\dfrac{L}{2\alpha_{01}}$ u_2

(c) $r(u_2)$

$$F_2 = \frac{E_0 A}{4\alpha_{01}} \quad \varepsilon = \frac{1}{2\alpha_{01}}$$

0 $\dfrac{L}{2\alpha_{01}}$ u_2
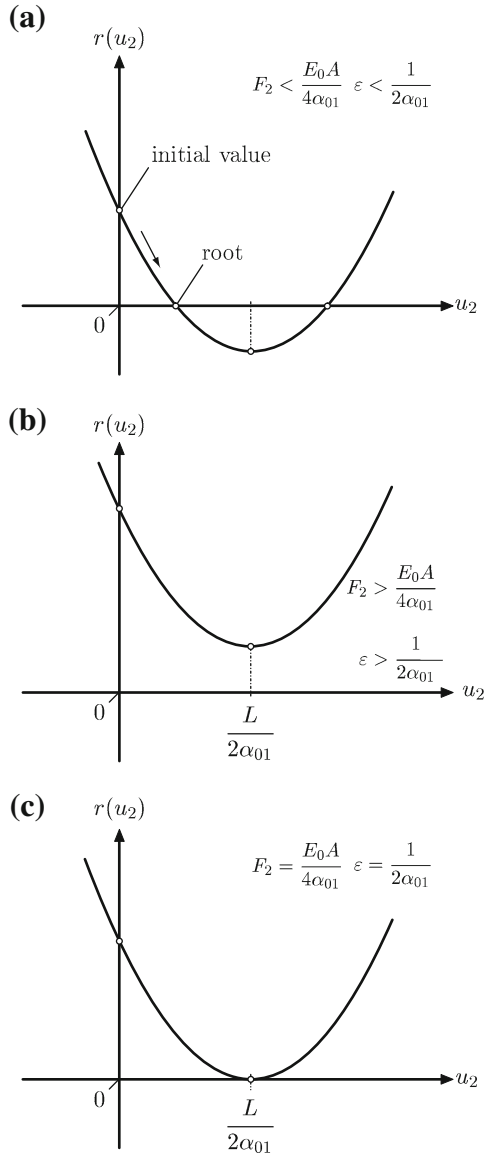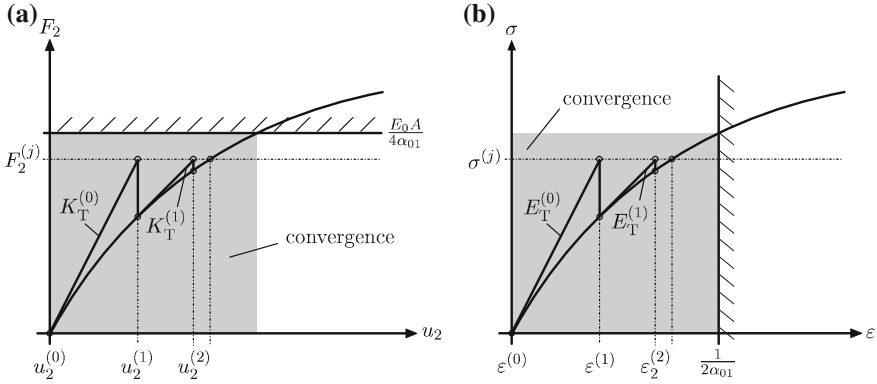
Fig. 10.9 Schematic illustration of the complete NEWTON–RAPHSON iteration

It is important at this point to note that the last equation is not confused with the stress–strain course according to Eq. (10.5), since the last equation deals with the outer and inner forces. Application of the iteration instruction according to Eq. (10.45) leads to the following formula at this juncture

$$\varepsilon^{(j+1)} = \varepsilon^{(j)} - \frac{r(\varepsilon^{(j)})}{\dfrac{dr(\varepsilon^{(j)})}{d\varepsilon}}, \tag{10.54}$$

whereupon

$$\frac{dr(\varepsilon)}{d\varepsilon} = E_{\mathrm{T}} = E(\varepsilon) + \frac{dE}{d\varepsilon}\,\varepsilon, \tag{10.55}$$

$$= E_0(1 - \alpha_{01}\varepsilon) - E_0\alpha_{01}\varepsilon, \tag{10.56}$$

$$= E_0(1 - 2\alpha_{01}\varepsilon) \tag{10.57}$$

is referred to as the consistent modulus E_{T} to the iteration formula. One considers the difference for the continuum mechanical modulus according to Eq. (10.3). Solely in the case of $\alpha_{01} = 0$, meaning for a constant modulus of elasticity, both moduli match.

At this point it needs to be remarked that the residual equation (10.44) can be further generalized by introducing a displacement dependent external load $F_2 = F_2(u_2)$:

$$r(u_2) = K(u_2)u_2 - F_2(u_2) = 0. \tag{10.58}$$

In this generalized case, the tangent stiffness matrix would result as follows:

$$K_{\mathrm{T}}(u_2) = \frac{dr(u_2)}{du_2} = K(u_2) + \frac{dK(u_2)}{du_2}\,u_2 - \frac{dF_2(u_2)}{du_2}. \tag{10.59}$$

10.3.2.3 Newton–Raphson Method for a Finite Element Model with m Unknowns

The complete NEWTON–RAPHSON method [1, 5, 6] for a model with various unknowns is, in general, expressed through the following equation

$$u^{(j+1)} = u^{(j)} - \left(K_T^{(j)}\right)^{-1} r(u^{(j)}), \qquad (10.60)$$

whereupon the tangent stiffness matrix in general is defined as

$$K_T = \frac{\partial r(u)}{\partial u}. \qquad (10.61)$$

The vectorial function of the residuals is generally defined as

$$r(u) = Ku - F \qquad (10.62)$$

and can be illustrated in components for a model with two linear bar elements as follows:

$$\begin{bmatrix} r_1(u) \\ r_2(u) \\ r_3(u) \end{bmatrix} = \begin{bmatrix} K_{11} & K_{12} & K_{13} \\ K_{21} & K_{22} & K_{23} \\ K_{31} & K_{32} & K_{33} \end{bmatrix} \begin{bmatrix} u_1 \\ u_2 \\ u_3 \end{bmatrix} - \begin{bmatrix} F_1 \\ F_2 \\ F_3 \end{bmatrix}. \qquad (10.63)$$

The JACOBIAN matrix $\dfrac{\partial r}{\partial u}$ of the residual function results in general from the partial derivatives r_i to:

$$\frac{\partial r}{\partial u}(u) = K_T(u) = \begin{bmatrix} K_{T,11} & K_{T,12} & K_{T,13} \\ K_{T,21} & K_{T,22} & K_{T,23} \\ K_{T,31} & K_{T,32} & K_{T,33} \end{bmatrix} = \begin{bmatrix} \dfrac{\partial r_1}{\partial u_1} & \dfrac{\partial r_1}{\partial u_2} & \dfrac{\partial r_1}{\partial u_3} \\ \dfrac{\partial r_2}{\partial u_1} & \dfrac{\partial r_2}{\partial u_2} & \dfrac{\partial r_2}{\partial u_3} \\ \dfrac{\partial r_3}{\partial u_1} & \dfrac{\partial r_3}{\partial u_2} & \dfrac{\partial r_3}{\partial u_3} \end{bmatrix}. \qquad (10.64)$$

The partial derivatives in Eq. (10.64) can be calculated the easiest, if the residual equation (10.63) are written in detail:

$$r_1(u_1, u_2, u_3) = K_{11}u_1 + K_{12}u_2 + K_{13}u_3, \qquad (10.65)$$
$$r_2(u_1, u_2, u_3) = K_{21}u_1 + K_{22}u_2 + K_{23}u_3, \qquad (10.66)$$
$$r_3(u_1, u_2, u_3) = K_{31}u_1 + K_{32}u_2 + K_{33}u_3. \qquad (10.67)$$

As an example, two partial derivatives are given in the following:

$$\frac{\partial r_1}{\partial u_1} = \left(\frac{\partial K_{11}}{\partial u_1} u_1 + K_{11}\right) + \frac{\partial K_{12}}{\partial u_1} u_2 + \frac{\partial K_{13}}{\partial u_1} u_3, \tag{10.68}$$

$$\frac{\partial r_1}{\partial u_2} = \frac{\partial K_{11}}{\partial u_2} u_1 + \left(\frac{\partial K_{12}}{\partial u_2} u_2 + K_{12}\right) + \frac{\partial K_{13}}{\partial u_2} u_2. \tag{10.69}$$

Therefore, the tangent stiffness matrix results in the illustrated form in Eq. (10.75), which is composed from the stiffness matrix and a matrix with partial derivatives, which are multiplied with the nodal displacements. In general, the tangent stiffness matrix can therefore be formulated for a model with m degrees of freedom as

$$K_{T,ij} = K_{ij} + \sum_{k=1}^{m} \frac{\partial K_{ik}}{\partial u_j} u_k, \tag{10.70}$$

or alternatively in matrix notation as

$$\boldsymbol{K}_T = \boldsymbol{K} + \frac{\partial \boldsymbol{K}}{\partial \boldsymbol{u}} \boldsymbol{u}. \tag{10.71}$$

As a concluding remark, two important special cases need to be listed at this point:

- Scalar tangent stiffness matrix (see Sect. 10.3.2.2):

$$K_T(u) = K(u) + \frac{\mathrm{d}K}{\mathrm{d}u} u. \tag{10.72}$$

- Two-dimensional tangent stiffness matrix (for example linear bar element without displacement boundary conditions):

$$\boldsymbol{K}_T(\boldsymbol{u}) = \begin{bmatrix} K_{11} & K_{12} \\ K_{21} & K_{22} \end{bmatrix} + \begin{bmatrix} \dfrac{\partial K_{11}}{\partial u_1} u_1 + \dfrac{\partial K_{12}}{\partial u_1} u_2 & \dfrac{\partial K_{11}}{\partial u_2} u_1 + \dfrac{\partial K_{12}}{\partial u_2} u_2 \\[2ex] \dfrac{\partial K_{21}}{\partial u_1} u_1 + \dfrac{\partial K_{22}}{\partial u_1} u_2 & \dfrac{\partial K_{21}}{\partial u_2} u_1 + \dfrac{\partial K_{22}}{\partial u_2} u_2 \end{bmatrix}. \tag{10.73}$$

The general case with $\boldsymbol{u} = [u_1, u_2, \ldots, u_m]^{\mathrm{T}}$ and $\dim(\boldsymbol{K}) = m \times m$ can easily be derived from the above considerations.

$$K_T =
\begin{bmatrix}
\frac{\partial K_{11}}{\partial u_1}u_1 + \frac{\partial K_{12}}{\partial u_1}u_2 + \frac{\partial K_{13}}{\partial u_1}u_3 + K_{11} & \frac{\partial K_{11}}{\partial u_2}u_1 + \frac{\partial K_{12}}{\partial u_2}u_2 + \frac{\partial K_{13}}{\partial u_2}u_3 + K_{12} & \frac{\partial K_{11}}{\partial u_3}u_1 + \frac{\partial K_{12}}{\partial u_3}u_2 + \frac{\partial K_{13}}{\partial u_3}u_3 + K_{13} \\[2mm]
\frac{\partial K_{21}}{\partial u_1}u_1 + \frac{\partial K_{22}}{\partial u_1}u_2 + \frac{\partial K_{23}}{\partial u_1}u_3 + K_{21} & \frac{\partial K_{21}}{\partial u_2}u_1 + \frac{\partial K_{22}}{\partial u_2}u_2 + \frac{\partial K_{23}}{\partial u_2}u_3 + K_{22} & \frac{\partial K_{21}}{\partial u_3}u_1 + \frac{\partial K_{22}}{\partial u_3}u_2 + \frac{\partial K_{23}}{\partial u_3}u_3 + K_{23} \\[2mm]
\frac{\partial K_{31}}{\partial u_1}u_1 + \frac{\partial K_{32}}{\partial u_1}u_2 + \frac{\partial K_{33}}{\partial u_1}u_3 + K_{31} & \frac{\partial K_{31}}{\partial u_2}u_1 + \frac{\partial K_{32}}{\partial u_2}u_2 + \frac{\partial K_{33}}{\partial u_2}u_3 + K_{32} & \frac{\partial K_{31}}{\partial u_3}u_1 + \frac{\partial K_{32}}{\partial u_3}u_2 + \frac{\partial K_{33}}{\partial u_3}u_3 + K_{33}
\end{bmatrix},
\tag{10.74}$$

$$=
\begin{bmatrix}
\frac{\partial K_{11}}{\partial u_1}u_1 + \frac{\partial K_{12}}{\partial u_1}u_2 + \frac{\partial K_{13}}{\partial u_1}u_3 & \frac{\partial K_{11}}{\partial u_2}u_1 + \frac{\partial K_{12}}{\partial u_2}u_2 + \frac{\partial K_{13}}{\partial u_2}u_3 & \frac{\partial K_{11}}{\partial u_3}u_1 + \frac{\partial K_{12}}{\partial u_3}u_2 + \frac{\partial K_{13}}{\partial u_3}u_3 \\[2mm]
\frac{\partial K_{21}}{\partial u_1}u_1 + \frac{\partial K_{22}}{\partial u_1}u_2 + \frac{\partial K_{23}}{\partial u_1}u_3 & \frac{\partial K_{21}}{\partial u_2}u_1 + \frac{\partial K_{22}}{\partial u_2}u_2 + \frac{\partial K_{23}}{\partial u_2}u_3 & \frac{\partial K_{21}}{\partial u_3}u_1 + \frac{\partial K_{22}}{\partial u_3}u_2 + \frac{\partial K_{23}}{\partial u_3}u_3 \\[2mm]
\frac{\partial K_{31}}{\partial u_1}u_1 + \frac{\partial K_{32}}{\partial u_1}u_2 + \frac{\partial K_{33}}{\partial u_1}u_3 & \frac{\partial K_{31}}{\partial u_2}u_1 + \frac{\partial K_{32}}{\partial u_2}u_2 + \frac{\partial K_{33}}{\partial u_2}u_3 & \frac{\partial K_{31}}{\partial u_3}u_1 + \frac{\partial K_{32}}{\partial u_3}u_2 + \frac{\partial K_{33}}{\partial u_3}u_3
\end{bmatrix}
+
\begin{bmatrix}
K_{11} & K_{12} & K_{13} \\
K_{21} & K_{22} & K_{23} \\
K_{31} & K_{32} & K_{33}
\end{bmatrix}.
\tag{10.75}$$
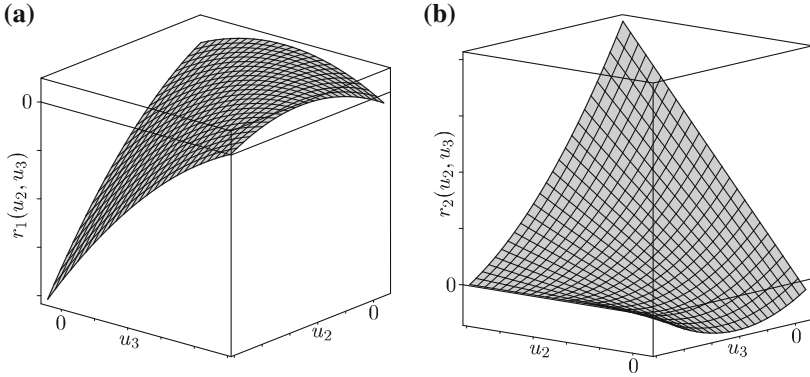
Fig. 10.10 Illustration of the residual functions according to Eq. (10.76)

In the following, the model with two bar elements according to Fig. 10.3 can be considered again. The discretization for two elements with the length $\dfrac{L}{2}$ leads the residual equation to:

$$\begin{bmatrix} r_1 \\ r_2 \end{bmatrix} = \frac{4AE_0}{L^2} \begin{bmatrix} (L - \alpha_{01}u_3) & -\left(\dfrac{L}{2} + \alpha_{01}u_2 - \alpha_{01}u_3\right) \\ -\left(\dfrac{L}{2} + \alpha_{01}u_2 - \alpha_{01}u_3\right) & \left(\dfrac{L}{2} + \alpha_{01}u_2 - \alpha_{01}u_3\right) \end{bmatrix} \begin{bmatrix} u_2 \\ u_3 \end{bmatrix} - \begin{bmatrix} 0 \\ F_3 \end{bmatrix} = 0.$$

(10.76)

A graphical illustration of the residual functions according to Eq. (10.76) is given in Fig. 10.10. Both functions are dependent on two variables, u_2 and u_3, in this case, and therefore at this point, surfaces in the space result, whose intersection curves have to be found via the u_2−u_3 planes. For this purpose, a tangent plane is built on the corresponding surface in every single point within the iteration scheme.

The application of the calculation instruction according to Eq. (10.73) leads to the tangent stiffness matrix as follows in this special case:

$$\begin{aligned} \boldsymbol{K}_{\mathrm{T}} = {} & \frac{4AE_0}{L^2} \begin{bmatrix} (L - \alpha_{01}u_3) & -\left(\dfrac{L}{2} + \alpha_{01}u_2 - \alpha_{01}u_3\right) \\ -\left(\dfrac{L}{2} + \alpha_{01}u_2 - \alpha_{01}u_3\right) & \left(\dfrac{L}{2} + \alpha_{01}u_2 - \alpha_{01}u_3\right) \end{bmatrix} \\ & + \frac{4AE_0}{L^2} \begin{bmatrix} 0 - \alpha_{01}u_3 & -\alpha_{01}u_2 + \alpha_{01}u_3 \\ -\alpha_{01}u_2 + \alpha_{01}u_3 & \alpha_{01}u_2 - \alpha_{01}u_3 \end{bmatrix}. \end{aligned}$$

(10.77)

The two matrices in the last equation can still be summarized and one obtains the following illustration for the tangent stiffness matrix:

$$\boldsymbol{K}_\text{T} = \frac{4AE_0}{L^2} \begin{bmatrix} L - 2\alpha_{01}u_3 & -\dfrac{L}{2} - 2\alpha_{01}u_2 + 2\alpha_{01}u_3 \\ -\dfrac{L}{2} - 2\alpha_{01}u_2 + 2\alpha_{01}u_3 & \dfrac{L}{2} + 2\alpha_{01}u_2 - 2\alpha_{01}u_3 \end{bmatrix}. \quad (10.78)$$

The tangent stiffness matrix still has to be inverted[7] for the iteration scheme according to Eq. (10.85) and after a short calculation one obtains:

$$(\boldsymbol{K}_\text{T})^{-1} = \frac{L^2}{4AE_0\left(\dfrac{L}{2} - 2\alpha_{01}u_2\right)} \left[\begin{array}{c|c} 1 & \dfrac{1}{L - 2\alpha_{01}u_3} \\ \hline 1 & \dfrac{L}{2} + 2\alpha_{01}u_2 - 2\alpha_{01}u_3 \end{array} \right]. \quad (10.79)$$

Therefore, the iteration scheme $\boldsymbol{u}^{(j+1)} = \boldsymbol{u}^{(j)} - \left(\boldsymbol{K}_\text{T}^{(j)}\right)^{-1} \boldsymbol{r}(\boldsymbol{u}^{(j)})$ can be applied as follows for the example according to Fig. 10.3:

$$\begin{bmatrix} u_2 \\ u_3 \end{bmatrix}_{(j+1)} = \begin{bmatrix} u_2 \\ u_3 \end{bmatrix}_{(j)} - \frac{L^2(4AE_0)^{-1}}{\dfrac{L}{2} - 2\alpha_{01}u_2^{(j)}} \left[\begin{array}{c|c} 1 & \dfrac{1}{L - 2\alpha_{01}u_3} \\ 1 & \dfrac{L}{2} + 2\alpha_{01}u_2 - 2\alpha_{01}u_3 \end{array} \right]_{(j)}$$

$$\times \left(\frac{4AE_0}{L^2} \begin{bmatrix} L - \alpha_{01}u_3 & -\dfrac{L}{2} - \alpha_{01}u_2 + \alpha_{01}u_3 \\ -\dfrac{L}{2} - \alpha_{01}u_2 + \alpha_{01}u_3 & \dfrac{L}{2} + \alpha_{01}u_2 - \alpha_{01}u_3 \end{bmatrix}_{(j)} \begin{bmatrix} u_2 \\ u_3 \end{bmatrix}_{(j)} - \begin{bmatrix} 0 \\ F_3 \end{bmatrix} \right). \quad (10.80)$$

The numerical values of the iteration are summarized in Table 10.4. Due to a comparison with the values from Table 10.3 for a model with one single element, one can see that the convergence behavior is identical.

For practical applications however one would not calculate the tangent stiffness matrix of the global total system but the derivatives element by element. Subsequently the tangent stiffness matrices of the single elements—as in the case of the total stiffness matrix—can be put together for the tangent stiffness matrix of the global total system:

$$\boldsymbol{K}_\text{T} = \sum \boldsymbol{K}_\text{T}^\text{e}. \quad (10.81)$$

---

[7] One considers that the calculation of the inverse has to be carried out numerically in commercial programs.

Table 10.4 Numerical values for the complete NEWTON–RAPHSON method in the case of two elements with an external load of $F_2 = 800\,\text{kN}$. Geometry: $A = 100\,\text{mm}^2$, $L_\text{I} = L_\text{II} = 200\,\text{mm}$. Material behavior: $E_0 = 70,000\,\text{MPa}$, $E_1 = 49,000\,\text{MPa}$, $\varepsilon_1 = 0.15$

Iteration j	$u_2^{(j)}$ (mm)	$u_3^{(j)}$ (mm)	$\sqrt{\dfrac{\left(u_2^{(j)}-u_2^{(j-1)}\right)^2+\left(u_3^{(j)}-u_3^{(j-1)}\right)^2}{\left(u_2^{(j)}\right)^2+\left(u_3^{(j)}\right)^2}}$
0	0	0	–
1	22.857143	45.714286	1
2	32.481203	64.962406	0.296296
3	35.124722	70.249443	0.075261
4	35.359614	70.719229	0.006643
5	35.361498	70.722998	0.000053
6	35.361499	70.722998	0.000000

For a linear element with a strain dependent modulus of elasticity according to Eq. (10.3) follows from the stiffness matrix according to Eq. (10.28), meaning

$$k^\text{e} = \frac{AE_0}{L^2}\left(L + \alpha_{01}\,u_1 - \alpha_{01}\,u_2\right)\begin{bmatrix} 1 & -1 \\ -1 & 1 \end{bmatrix}, \tag{10.82}$$

under application of the calculation instruction (10.73), the following tangent stiffness matrix for a single element with two nodes:

$$\begin{aligned} K_\text{T}^\text{e} &= k^\text{e} + \begin{bmatrix} \alpha_{01}u_1 - \alpha_{01}u_2 & -\alpha_{01}u_1 + \alpha_{01}u_2 \\ -\alpha_{01}u_1 + \alpha_{01}u_2 & \alpha_{01}u_1 - \alpha_{01}u_2 \end{bmatrix} \\ &= \frac{AE_0}{L^2}\left(L + 2\alpha_{01}\,u_1 - 2\alpha_{01}\,u_2\right)\begin{bmatrix} 1 & -1 \\ -1 & 1 \end{bmatrix}. \end{aligned} \tag{10.83}$$

10.3.3 Modified Newton–Raphson Method

10.3.3.1 Modified Newton–Raphson Method for a Finite Element Model with One Unknown

The disadvantage of the complete NEWTON–RAPHSON method is that the tangent stiffness matrix has to be calculated and inverted subsequently at each iteration step. If the tangent stiffness matrix is only calculated once at the beginning, one attains the modified NEWTON–RAPHSON method [1, 5, 6]. From Eq. (10.45) the modified iteration scheme results in:

$$u_2^{(j+1)} = u_2^{(j)} - \frac{r(u_2^{(j)})}{\dfrac{\mathrm{d}r(u_2^{(0)})}{\mathrm{d}u_2}} = u_2^{(j)} - \left(K_\text{T}^{(0)}\right)^{-1} r(u_2^{(j)}). \tag{10.84}$$

A schematic illustration is given in Fig. 10.11. One can see that the same initial tangent is used in every iteration step, whereby in comparison with the complete method, more iteration steps result; the method does not converge quadratically anymore but only linearly. However, the calculation intensive inversion of the tangent stiffness matrix in every step drops out and the calculation simplifies significantly.

If the iteration instruction of the modified method according to Eq. (10.84) is applied to the problem according to Fig. 10.3, the summarized results in Table 10.5 are obtained. Thirty-six steps are necessary at this point for the fulfillment of the convergence criteria $(<10^{-6})$ and the reference value of $u_2 = 70.722998$ can only be achieved after 53 iteration steps. A comparison with the two other iteration schemes shows that the modified NEWTON–RAPHSON method—with functions of one variable—converges the slowest. However one considers that this conclusion does not have to be valid for a system of equations anymore.

10.3.3.2 Modified Newton–Raphson Method for a Finite Element Model with Various Unknowns

The modified NEWTON–RAPHSON method for a model with various unknowns is generally given through the following equation

$$\boldsymbol{u}^{(j+1)} = \boldsymbol{u}^{(j)} - \left(\boldsymbol{K}_{\mathrm{T}}^{(0)}\right)^{-1} \boldsymbol{r}(\boldsymbol{u}^{(j)}), \tag{10.85}$$

or alternatively for the example according to Fig. 10.3:

$$\begin{bmatrix} u_2 \\ u_3 \end{bmatrix}_{(j+1)} = \begin{bmatrix} u_2 \\ u_3 \end{bmatrix}_{(j)} - \frac{L^2(4AE_0)^{-1}}{\dfrac{L}{2} - 2\alpha_{01}u_2^{(0)}} \begin{bmatrix} 1 & \dfrac{1}{L - 2\alpha_{01}u_3} \\ 1 & \dfrac{\dfrac{L}{2} + 2\alpha_{01}u_2 - 2\alpha_{01}u_3}{} \end{bmatrix}_{(0)}$$

Table 10.5 Numerical values for a modified NEWTON–RAPHSON method at an external load of $F_2 = 800\,\text{kN}$. Geometry: $A = 100\,\text{mm}^2$, $L = 400\,\text{mm}$. Material behavior: $E_0 = 70,000\,\text{MPa}$, $E_1 = 49,000\,\text{MPa}$, $\varepsilon_1 = 0.15$

Iteration j	$u_2^{(j)}$ (mm)	$\varepsilon_2^{(j)}$	$\sqrt{\dfrac{\left(u_2^{(j)}-u_2^{(j-1)}\right)^2}{\left(u_2^{(j)}\right)^2}}$
0	0	0	–
1	45.714286	0.114286	1
2	56.163265	0.140408	0.186047
3	61.485848	0.153715	0.086566
4	64.616833	0.161542	0.048455
5	66.590961	0.166477	0.029646
6	67.886066	0.169715	0.019078
7	68.756876	0.171892	0.012665
8	69.351825	0.173380	0.008579
9	69.762664	0.174407	0.005889
10	70.048432	0.175121	0.004080
11	70.248200	0.175621	0.002844
12	70.388334	0.175971	0.001991
13	70.486873	0.176217	0.001398
14	70.556282	0.176391	0.000984
15	70.605231	0.176513	0.000693
16	70.639779	0.176599	0.000489
17	70.664177	0.176660	0.000345
18	70.681416	0.176704	0.000244
19	70.693598	0.176734	0.000172
20	70.702210	0.176756	0.000122
⋮	⋮	⋮	⋮
35	70.722883	0.176807	0.000001
36	70.722916	0.176807	0.000000
⋮	⋮	⋮	⋮
53	70.722998	0.176807	0.000000

$$\times \left(\frac{4AE_0}{L^2} \begin{bmatrix} L - \alpha_{01}u_3 & -\dfrac{L}{2} - \alpha_{01}u_2 + \alpha_{01}u_3 \\ -\dfrac{L}{2} - \alpha_{01}u_2 + \alpha_{01}u_3 & \dfrac{L}{2} + \alpha_{01}u_2 - \alpha_{01}u_3 \end{bmatrix}_{(j)} \begin{bmatrix} u_2 \\ u_3 \end{bmatrix}_{(j)} - \begin{bmatrix} 0 \\ F_3 \end{bmatrix} \right).$$

$$(10.86)$$

The numerical values of the iteration are summarized in Table 10.8. Due to a comparison with the values from Table 10.5 for the model with one single element, one can see that the convergence behavior is identical.

10.3.4 Convergence Criteria

For the evaluation, if an iterative scheme converges, the following normalized displacement difference in the form

$$
\sqrt{\frac{\left(u_2^{(j)} - u_2^{(j-1)}\right)^2 + \left(u_3^{(j)} - u_3^{(j-1)}\right)^2 + \cdots + \left(u_m^{(j)} - u_m^{(j)}\right)^2}{\left(u_2^{(j)}\right)^2 + \left(u_3^{(j)}\right)^2 + \cdots + \left(u_m^{(j)}\right)^2}}
\tag{10.87}
$$

was already used in previous chapters, whereupon m represents the number of unknown degrees of freedom. If this value is below a certain limit value, for example the computational accuracy in the program, the iteration can be regarded as converged.

Alternatively, the residual vector $r^{(j)} = K(u^{(j)})u^{(j)} - F^{(j)}$ can be regarded, whose norm can be indicated as follows

$$
\sqrt{\sum_{i=1}^{m} \left(r_i^{(j)}\right)^2}.
\tag{10.88}
$$

If this norm is below a certain limit value, convergence is achieved.

At the end of this chapter, the discussed iteration instructions are summarized in Table 10.6, and those are opposed to the calculation procedure for linear elasticity.

It needs to be remarked at this point that the three listed procedures for linear elasticity simplify as the method of inversion of the stiffness matrix in the case of linear elasticity.

Table 10.6 Calculation procedure in the linear and nonlinear elasticity
(N–R = Newton–Raphson)

Procedure	Calculation instruction
Linear elasticity: $Ku = F$	
• Inversion of the stiffness matrix	$u = (K)^{-1}F$
• $\cdots$	$\cdots$
Nonlinear elasticity: $K(u)u = F$	
• Direct iteration	$u^{(j+1)} = \left(K(u^{(j)})\right)^{-1} F$
• Complete N–R iteration	$u^{(j+1)} = u^{(j)} - \left(K_T^{(j)}\right)^{-1} r(u^{(j)})$
• Modified N–R iteration	$u^{(j+1)} = u^{(j)} - \left(K_T^{(0)}\right)^{-1} r(u^{(j)})$
• $\cdots$	$\cdots$

In the literature, a further series of methods are known, as for example the arc length method, with which the convergence range of the discussed methods here can be expanded significantly [7–9].

Table 10.7 Numerical values for the complete NEWTON–RAPHSON method in the case of one element with quadratic shape function with one external load of $F_2 = 800\,\text{kN}$. Geometry: $A = 100\,\text{mm}^2$, $L = 400\,\text{mm}$. Material behavior: $E_0 = 70,000\,\text{MPa}$, $E_1 = 49,000\,\text{MPa}$, $\varepsilon_1 = 0.15$

Iteration j	$u_2^{(j)}$ (mm)	$u_3^{(j)}$ (mm)	$\sqrt{\dfrac{\left(u_2^{(j)}-u_2^{(j-1)}\right)^2+\left(u_3^{(j)}-u_3^{(j-1)}\right)^2}{\left(u_2^{(j)}\right)^2+\left(u_3^{(j)}\right)^2}}$
0	0	0	–
1	22.857143	45.714286	1
2	32.481203	64.962406	0.296296
3	35.124722	70.249443	0.075261
4	35.359614	70.719229	0.006643
5	35.361498	70.722998	0.000053
6	35.361499	70.722998	0.000000

10.4 Sample Problems and Supplementary Problems

10.4.1 Sample Problems

10.1 Example: Tension Bar with Quadratic Approach and Strain Dependent Modulus of Elasticity

One needs to derive the stiffness matrix for a bar element with quadratic shape functions for a strain dependent modulus of elasticity in the form

$$E(u) = E_0 \left(1 - \alpha_{01} \frac{\mathrm{d}u}{\mathrm{d}x}\right). \tag{10.89}$$

In this, the element has length L and the inner node is placed exactly in the middle of the element. Subsequently one needs to calculate the tangent stiffness matrix $\boldsymbol{K}_\mathrm{T}$ based on the stiffness matrix.

10.1 Solution

Based on Eq. (10.90), meaning

$$\boldsymbol{k}^\mathrm{e} = A E_0 \int_0^L \underbrace{\left(1 - \alpha_{01} \frac{\mathrm{d}\boldsymbol{N}}{\mathrm{d}x} \boldsymbol{u}_\mathrm{p}\right)}_{\text{scalar}} \frac{\mathrm{d}\boldsymbol{N}^\mathrm{T}}{\mathrm{d}x} \frac{\mathrm{d}\boldsymbol{N}}{\mathrm{d}x} \, \mathrm{d}x, \tag{10.90}$$

and the shape functions for a quadratic bar element, or alternatively their derivatives

$$N_1(x) = 1 - 3\frac{x}{L} + 2\left(\frac{x}{L}\right)^2, \quad \frac{\mathrm{d}N_1(x)}{\mathrm{d}x} = -\frac{3}{L} + 4\frac{x}{L^2}, \tag{10.91}$$

$$N_2(x) = 4\frac{x}{L} - 4\left(\frac{x}{L}\right)^2, \quad \frac{\mathrm{d}N_2(x)}{\mathrm{d}x} = \frac{4}{L} - 8\frac{x}{L^2}, \tag{10.92}$$

$$N_3(x) = -\frac{x}{L} + 2\left(\frac{x}{L}\right)^2, \quad \frac{\mathrm{d}N_2(x)}{\mathrm{d}x} = -\frac{1}{L} + 2\frac{x}{L^2}, \tag{10.93}$$

the stiffness matrix in general results in:

$$k^{\mathrm{e}} = AE_0 \int\limits_0^L \left(1 - \alpha_{01}\frac{\mathrm{d}N_1}{\mathrm{d}x}u_1 - \alpha_{01}\frac{\mathrm{d}N_2}{\mathrm{d}x}u_2 - \alpha_{01}\frac{\mathrm{d}N_3}{\mathrm{d}x}u_3\right)$$

$$\times \begin{bmatrix} \dfrac{\mathrm{d}N_1}{\mathrm{d}x}\dfrac{\mathrm{d}N_1}{\mathrm{d}x} & \dfrac{\mathrm{d}N_1}{\mathrm{d}x}\dfrac{\mathrm{d}N_2}{\mathrm{d}x} & \dfrac{\mathrm{d}N_1}{\mathrm{d}x}\dfrac{\mathrm{d}N_3}{\mathrm{d}x} \\[2mm] \dfrac{\mathrm{d}N_2}{\mathrm{d}x}\dfrac{\mathrm{d}N_1}{\mathrm{d}x} & \dfrac{\mathrm{d}N_2}{\mathrm{d}x}\dfrac{\mathrm{d}N_2}{\mathrm{d}x} & \dfrac{\mathrm{d}N_2}{\mathrm{d}x}\dfrac{\mathrm{d}N_3}{\mathrm{d}x} \\[2mm] \dfrac{\mathrm{d}N_3}{\mathrm{d}x}\dfrac{\mathrm{d}N_1}{\mathrm{d}x} & \dfrac{\mathrm{d}N_3}{\mathrm{d}x}\dfrac{\mathrm{d}N_2}{\mathrm{d}x} & \dfrac{\mathrm{d}N_3}{\mathrm{d}x}\dfrac{\mathrm{d}N_3}{\mathrm{d}x} \end{bmatrix} \mathrm{d}x. \tag{10.94}$$

After completion of the integration, the element stiffness matrix results herefrom to:

$$k^{\mathrm{e}} = \frac{AE_0}{3L}\begin{bmatrix} 7 & -8 & 1 \\ -8 & 16 & -8 \\ 1 & -8 & 7 \end{bmatrix}$$

$$+ \frac{AE_0\alpha_{01}}{3L^2}\begin{bmatrix} 15u_1 - 16u_2 + u_3 & -16u_1 + 16u_2 & u_1 - u_3 \\ -16u_1 + 16u_2 & 16u_1 - 16u_3 & -16u_2 + 16u_3 \\ u_1 - u_3 & -16u_2 + 16u_3 & -u_1 + 16u_2 - 15u_3 \end{bmatrix}. \tag{10.95}$$

Application of the calculation instruction for a (3×3) matrix according to Eq. (10.75) leads to the tangent stiffness matrix as:

$$K_{\mathrm{T}} = k^{\mathrm{e}} + \frac{AE_0\alpha_{01}}{3L^2}\begin{bmatrix} 15u_1 - 16u_2 + u_3 & -16u_1 + 16u_2 & u_1 - u_3 \\ -16u_1 + 16u_2 & 16u_1 - 16u_3 & -16u_2 + 16u_3 \\ u_1 - u_3 & -16u_2 + 16u_3 & -u_1 + 16u_2 - 15u_3 \end{bmatrix}, \tag{10.96}$$

or, alternatively, after the summarization of the two matrices with the nodal displacements to:

$$K_{\mathrm{T}}^{\mathrm{e}} = \frac{AE_0}{3L}\begin{bmatrix} 7 & -8 & 1 \\ -8 & 16 & -8 \\ 1 & -8 & 7 \end{bmatrix}$$

$$+ \frac{AE_0\alpha_{01}}{3L^2}\begin{bmatrix} 30u_1 - 32u_2 + 2u_3 & -32u_1 + 32u_2 & 2u_1 - 2u_3 \\ -32u_1 + 32u_2 & 32u_1 - 32u_3 & -32u_2 + 32u_3 \\ 2u_1 - 2u_3 & -32u_2 + 32u_3 & -2u_1 + 32u_2 - 30u_3 \end{bmatrix}. \tag{10.97}$$

10.2 Example: One-Sided Fixed Tension Bar with Quadratic Approach and Strain Dependent Modulus of Elasticity

With the derived bar element in example 10.1 with quadratic shape function and strain dependent modulus of elasticity one can calculate a bar, which is fixed supported on the left-hand end and is loaded through a single force of 800 kN on the right-hand end. The material behavior is assumed as in example 10.1, whereupon the values $E_0 = 70,000$ MPa and $\alpha_{01} = 2$ can be used. The length of the bar accounts $L = 400$ mm and the cross-sectional area is $A = 100$ mm^2. For the solution one can make us of the complete NEWTON–RAPHSON method.

10.2 Solution

Under consideration of the boundary conditions, the principal finite element equation results as follows from Eq. (10.95)

$$\left(\frac{AE_0}{3L} \begin{bmatrix} 16 & -8 \\ -8 & 7 \end{bmatrix} + \frac{AE_0\alpha_{01}}{3L^2} \begin{bmatrix} -16u_3 & -16u_2 + 16u_3 \\ -16u_2 + 16u_3 & 16u_2 - 15u_3 \end{bmatrix} \right) \begin{bmatrix} u_2 \\ u_3 \end{bmatrix} = \begin{bmatrix} 0 \\ F_3 \end{bmatrix}.$$
(10.98)

and from Eq. (10.97) the tangent stiffness matrix follows under consideration of the boundary conditions as

$$\boldsymbol{K}_{\mathrm{T}}^{\mathrm{e}} = \frac{AE_0}{3L} \begin{bmatrix} 16 & -8 \\ -8 & 7 \end{bmatrix} + \frac{AE_0\alpha_{01}}{3L^2} \begin{bmatrix} 32u_1 - 32u_3 & -32u_2 + 32u_3 \\ -32u_2 + 32u_3 & -2u_1 + 32u_2 - 30u_3 \end{bmatrix}.$$
(10.99)

The tangent stiffness matrix still has to be inverted for the iteration scheme according to Eq. (10.85) and one obtains the following representation after a short calculation:

$$(\boldsymbol{K}_{\mathrm{T}})^{-1} = \frac{3L^2}{AE_0(3L^2 - 12\alpha_{01}u_3L + 64\alpha_{01}^2 u_2 u_3 - 4\alpha_{01}^2 u_3^2 - 64\alpha_{01}^2 u_2^2)}$$
$$\times \begin{bmatrix} \dfrac{7}{16}L + 2\alpha_{01}u_2 - \dfrac{15}{8}\alpha_{01}u_3 & \dfrac{1}{2}L + 2\alpha_{01}u_2 - 2\alpha_{01}u_3 \\ \dfrac{1}{2}L + 2\alpha_{01}u_2 - 2\alpha_{01}u_3 & L - 2\alpha_{01}u_3 \end{bmatrix}. \quad (10.100)$$

The numerical results of the iteration are summarized in Table 10.7. A comparison with the results of the discretization with two linear elements in Table 10.4 shows that the results for the regarded case are identical.

10.3 Example: Tension Bar with Three Different Elements for Strain Dependent Modulus of Elasticity and Force Boundary Condition

The illustrated finite element model in Fig. 10.12 of a one-sided fixed bar consists of three elements, which exhibit different characteristics. The bar is loaded with a point load F_0 on the right-hand end.

Table 10.8 Numerical values for a modified NEWTON–RAPHSON method in the case of two elements with an external load of $F_2 = 800$ kN. Geometry: $A = 100$ mm^2, $L = 400$ mm. Material behavior: $E_0 = 70,000$ MPa, $E_1 = 49,000$ MPa, $\varepsilon_1 = 0.15$

Iteration j	$u_2^{(j)}$ (mm)	$u_3^{(j)}$ (mm)	$\sqrt{\dfrac{\left(u_2^{(j)}-u_2^{(j-1)}\right)^2+\left(u_3^{(j)}-u_3^{(j-1)}\right)^2}{\left(u_2^{(j)}\right)^2+\left(u_3^{(j)}\right)^2}}$
0	0	0	–
1	22.857143	45.714286	1
2	28.081633	56.163265	0.186046
3	30.742924	61.485848	0.086566
4	32.308416	64.616833	0.048455
5	33.295481	66.590961	0.029646
6	33.943033	67.886066	0.019078
7	34.378438	68.756876	0.012665
8	34.675913	69.351825	0.008579
9	34.881332	69.762664	0.005889
10	35.024216	70.048432	0.004080
⋮	⋮	⋮	⋮
36	35.361458	70.722916	0.000000
⋮	⋮	⋮	⋮
53	35.361499	70.722998	0.000000
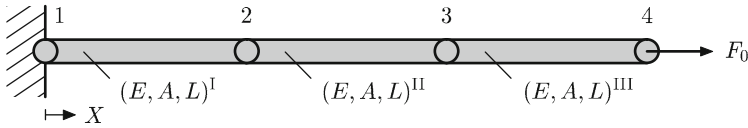
Fig. 10.12 Tension bar with three different elements for strain dependent modulus of elasticity and force boundary condition

One considers the case that all three bars have a linear strain dependent modulus of elasticity according to Eq. (10.3) in the form

$$E^i(\varepsilon) = E_0^i \left(1 - \varepsilon\alpha_{01}\right), \quad i = \text{I, II, III}. \tag{10.101}$$

For the considered problem the following relations for the initial axial rigidity can be assumed:

$$(E_0A)^{\text{I}} = 3E_0A, \tag{10.102}$$

$$(E_0A)^{\text{II}} = 2E_0A, \tag{10.103}$$

$$(E_0A)^{\text{III}} = 1E_0A. \tag{10.104}$$

As a numerical value one can use $F_0 = 800$ kN, $A = 100$ mm^2, $L^{\text{I}} = L^{\text{II}} = L^{\text{III}} = 400/3$ mm, $E_0 = 70,000$ MPa, $E_1 = 49,000$ MPa, $\varepsilon_1 = 0.15$ and one can

define the displacement of the nodes with the complete NEWTON–RAPHSON iteration procedure.

10.3 Solution

The element stiffness matrices according to Eq. (10.28) for the three elements result in

$$k^{\mathrm{I}} = \frac{3E_0 A}{L^2}\,(L + \alpha_{01} u_1 - \alpha_{01} u_2)\begin{bmatrix} 1 & -1 \\ -1 & 1 \end{bmatrix}, \tag{10.105}$$

$$k^{\mathrm{II}} = \frac{2E_0 A}{L^2}\,(L + \alpha_{01} u_2 - \alpha_{01} u_3)\begin{bmatrix} 1 & -1 \\ -1 & 1 \end{bmatrix}, \tag{10.106}$$

$$k^{\mathrm{III}} = \frac{1E_0 A}{L^2}\,(L + \alpha_{01} u_3 - \alpha_{01} u_3)\begin{bmatrix} 1 & -1 \\ -1 & 1 \end{bmatrix}, \tag{10.107}$$

which can be composed to the following reduced system of equations under consideration of the fixed support:

$$\frac{E_0 A}{L^2}\begin{bmatrix} \begin{array}{c} 3L - 3\alpha_{01}u_2 + 2L \\ +2\alpha_{01}u_2 - 2\alpha_{01}u_3 \end{array} & -2L - 2\alpha_{01}u_2 + 2\alpha_{01}u_3 & 0 \\ -2L - 2\alpha_{01}u_2 + 2\alpha_{01}u_3 & \begin{array}{c} 2L + 2\alpha_{01}u_2 - 2\alpha_{01}u_3 \\ +1L + 1\alpha_{01}u_3 - 1\alpha_{01}u_4 \end{array} & -1L - 1\alpha_{01}u_3 + 1\alpha_{01}u_4 \\ 0 & -1L - 1\alpha_{01}u_3 + 1\alpha_{01}u_4 & 1L + 1\alpha_{01}u_3 - 1\alpha_{01}u_4 \end{bmatrix}$$

$$\times \begin{bmatrix} u_2 \\ u_3 \\ u_4 \end{bmatrix} = \begin{bmatrix} 0 \\ 0 \\ F_0 \end{bmatrix}. \tag{10.108}$$

The tangent stiffness matrices for the three elements result in the following according to Eq. (10.83)

$$K_{\mathrm{T}}^{\mathrm{I}} = \frac{3E_0 A}{L^2}\,(L + 2\alpha_{01} u_1 - 2\alpha_{01} u_2)\begin{bmatrix} 1 & -1 \\ -1 & 1 \end{bmatrix}, \tag{10.109}$$

$$K_{\mathrm{T}}^{\mathrm{II}} = \frac{2E_0 A}{L^2}\,(L + 2\alpha_{01} u_2 - 2\alpha_{01} u_3)\begin{bmatrix} 1 & -1 \\ -1 & 1 \end{bmatrix}, \tag{10.110}$$

$$K_{\mathrm{T}}^{\mathrm{III}} = \frac{1E_0 A}{L^2}\,(L + 2\alpha_{01} u_3 - 2\alpha_{01} u_3)\begin{bmatrix} 1 & -1 \\ -1 & 1 \end{bmatrix} \tag{10.111}$$

and can be combined to the following tangent stiffness matrix of the reduced system of equations under consideration of the fixed support:

$$K_{\mathrm{T}} = \frac{E_0 A}{L^2}\begin{bmatrix} \begin{array}{c} 3L - 6\alpha_{01}u_2 + 2L + 4\alpha_{01} \\ u_2 - 4\alpha_{01}u_3 \end{array} & -2L - 4\alpha_{01}u_2 + 4\alpha_{01}u_3 & 0 \\ -2L - 4\alpha_{01}u_2 + 4\alpha_{01}u_3 & \begin{array}{c} 2L + 4\alpha_{01}u_2 - 4\alpha_{01}u_3 \\ +1L + 2\alpha_{01}u_3 - 2\alpha_{01}u_4 \end{array} & -1L - 2\alpha_{01}u_3 + 2\alpha_{01}u_4 \\ 0 & -1L - 2\alpha_{01}u_3 + 2\alpha_{01}u_4 & 1L + 2\alpha_{01}u_3 - 2\alpha_{01}u_4 \end{bmatrix}. \tag{10.112}$$

Table 10.9 Numerical values for the complete NEWTON–RAPHSON method in the case of three elements with an external load of $F_2 = 800\,\text{kN}$. Geometry: $A^i = 100\,\text{mm}^2$, $L^i = 400/3\,\text{mm}$. Material behavior: $E_0 = \beta^i \times 70,000\,\text{MPa}$, $E_1 = 49,000\,\text{MPa}$, $\varepsilon_1 = 0.15$

Iteration j	$u_2^{(j)}$ (mm)	$u_3^{(j)}$ (mm)	$u_4^{(j)}$ (mm)	$\sqrt{\dfrac{\sum_{i=1}^{3}\left(u_i^{(j)}-u_i^{(j-1)}\right)^2}{\sum_{i=1}^{3}\left(u_i^{(j)}\right)^2}}$
0	0	0	0	–
1	5.079365	12.698413	27.936508	1
2	5.535937	14.283733	35.937868	0.209121
3	5.539687	14.313393	37.729874	0.044001
4	5.539687	14.313407	37.886483	0.003831
5	5.539687	14.313407	37.887740	0.000030
6	5.539687	14.313407	37.887740	0.000000

The iteration scheme $\boldsymbol{u}^{(j+1)} = \boldsymbol{u}^{(j)} - (\boldsymbol{K}_{\mathrm{T}}^{(j)})^{-1}\boldsymbol{r}(\boldsymbol{u}^{(j)})$ can be used via the reduced system of equations and the tangent stiffness matrix. The numerical results are summarized in Table 10.9.

10.4 Example: Tension Bar with Three Different Elements for Strain Dependent Modulus of Elasticity and Displacement Boundary Condition

The finite element model of an one-sided fixed bar, which is illustrated in Fig. 10.13, consists of three elements, which exhibit different characteristics. A displacement u_0 is given on the right-hand end of the bar.
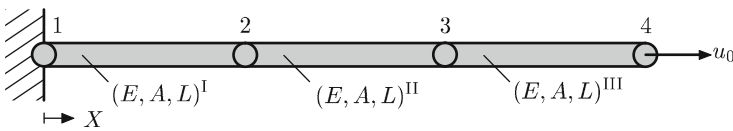
Fig. 10.13 Tension bar with three different elements for strain dependent modulus of elasticity and displacement boundary condition

One can consider the case that all three bars exhibit a linear strain dependent modulus of elasticity according to Eq. (10.3) in the form

$$E^i(\varepsilon) = E_0^i\left(1 - \varepsilon\alpha_{01}\right), \quad i = \mathrm{I, II, III}. \tag{10.113}$$

The following relations for the initial axial rigidity can be assumed for the considered problem:

$$(E_0 A)^{\mathrm{I}} = \beta^{\mathrm{I}} E_0 A, \tag{10.114}$$

$$(E_0 A)^{\mathrm{II}} = \beta^{\mathrm{II}} E_0 A, \tag{10.115}$$

$$(E_0 A)^{\mathrm{III}} = \beta^{\mathrm{III}} E_0 A, \tag{10.116}$$

whereupon two different cases need to be analyzed:

$$
\begin{array}{c|ccc|c}
 & \beta^{\mathrm{I}} & \beta^{\mathrm{II}} & \beta^{\mathrm{III}} & u_o \text{ in mm} \\
\hline
\text{Case a)} & 1 & 1 & 1 & 33 \\
\text{Case b)} & 3 & 2 & 1 & 37.887740 \\
\end{array}
\qquad (10.117)
$$

As further numerical values one can use $A = 100\,\text{mm}^2$, $L^{\mathrm{I}} = L^{\mathrm{II}} = L^{\mathrm{III}} = 400/3\,\text{mm}$, $E_0 = 70,000\,\text{MPa}$, $E_1 = 49,000\,\text{MPa}$, $\varepsilon_1 = 0.15$ and one can define the displacement of the nodes and the reaction force on the right-hand end via the complete NEWTON–RAPHSON iteration method.

10.4 Solution

According to the procedure in example 10.3, the total stiffness matrix results as follows, under consideration of the fixed support on the left-hand end:

$$
\frac{E_0 A}{L^2}
\begin{bmatrix}
\begin{array}{c} \beta^{\mathrm{I}}L - \beta^{\mathrm{I}}\alpha_{01}u_2 + \\ \beta^{\mathrm{II}}L + \beta^{\mathrm{II}}\alpha_{01}u_2 \\ -\beta^{\mathrm{II}}\alpha_{01}u_3 \end{array} &
\begin{array}{c} -\beta^{\mathrm{II}}L - \beta^{\mathrm{II}}\alpha_{01}u_2 \\ +\beta^{\mathrm{II}}\alpha_{01}u_3 \end{array} &
0 \\
\hline
\begin{array}{c} -\beta^{\mathrm{II}}L - \beta^{\mathrm{II}}\alpha_{01}u_2 \\ +\beta^{\mathrm{II}}\alpha_{01}u_3 \end{array} &
\begin{array}{c} \beta^{\mathrm{II}}L + \beta^{\mathrm{II}}\alpha_{01}u_2 \\ -\beta^{\mathrm{II}}\alpha_{01}u_3 + \beta^{\mathrm{III}}L \\ +\beta^{\mathrm{III}}\alpha_{01}u_3 - \beta^{\mathrm{III}}\alpha_{01}u_4 \end{array} &
\begin{array}{c} -\beta^{\mathrm{III}}L - \beta^{\mathrm{III}}\alpha_{01}u_3 \\ +\beta^{\mathrm{III}}\alpha_{01}u_4 \end{array} \\
\hline
0 &
\begin{array}{c} -\beta^{\mathrm{III}}L - \beta^{\mathrm{III}}\alpha_{01}u_3 \\ +\beta^{\mathrm{III}}\alpha_{01}u_4 \end{array} &
\begin{array}{c} \beta^{\mathrm{III}}L + \beta^{\mathrm{III}}\alpha_{01}u_3 \\ -\beta^{\mathrm{III}}\alpha_{01}u_4 \end{array}
\end{bmatrix} .
$$

$$(10.118)$$

If the known displacement is brought to the 'right-hand side' of the system of equations, the following reduced (2×2) system of equations results after canceling of the column and line, which belong to u_4:

$$
\frac{E_0 A}{L^2}
\begin{bmatrix}
\begin{array}{c} \beta^{\mathrm{I}}L - \beta^{\mathrm{I}}\alpha_{01}u_2 + \\ \beta^{\mathrm{II}}L + \beta^{\mathrm{II}}\alpha_{01}u_2 \\ -\beta^{\mathrm{II}}\alpha_{01}u_3 \end{array} &
\begin{array}{c} -\beta^{\mathrm{II}}L - \beta^{\mathrm{II}}\alpha_{01}u_2 \\ +\beta^{\mathrm{II}}\alpha_{01}u_3 \end{array} \\
\hline
\begin{array}{c} -\beta^{\mathrm{II}}L - \beta^{\mathrm{II}}\alpha_{01}u_2 \\ +\beta^{\mathrm{II}}\alpha_{01}u_3 \end{array} &
\begin{array}{c} \beta^{\mathrm{II}}L + \beta^{\mathrm{II}}\alpha_{01}u_2 \\ -\beta^{\mathrm{II}}\alpha_{01}u_3 + \beta^{\mathrm{III}}L \\ +\beta^{\mathrm{III}}\alpha_{01}u_3 - \beta^{\mathrm{III}}\alpha_{01}u_4 \end{array}
\end{bmatrix}
\begin{bmatrix} u_2 \\ u_3 \end{bmatrix}
$$

$$
= \frac{E_0 A}{L^2}
\begin{bmatrix} 0 \\ -(-\beta^{\mathrm{III}}L - \beta^{\mathrm{III}}\alpha_{01}u_3 + \beta^{\mathrm{III}}\alpha_{01}u_4)u_4 \end{bmatrix} .
\qquad (10.119)
$$

According to the procedure in example 10.3 the tangent stiffness matrix results in (2×2) form in:

$$
\boldsymbol{K}_{\mathrm{T}} = \frac{E_0 A}{L^2}
\begin{bmatrix}
\begin{array}{c}
\beta^{\mathrm{I}} L - 2\beta^{\mathrm{I}} \alpha_{01} u_2 + \\
\beta^{\mathrm{II}} L + 2\beta^{\mathrm{II}} \alpha_{01} u_2 \\
-2\beta^{\mathrm{II}} \alpha_{01} u_3
\end{array}
&
\begin{array}{c}
-\beta^{\mathrm{II}} L - 2\beta^{\mathrm{II}} \alpha_{01} u_2 \\
+2\beta^{\mathrm{II}} \alpha_{01} u_3
\end{array} \\
\hline
\begin{array}{c}
-\beta^{\mathrm{II}} L - 2\beta^{\mathrm{II}} \alpha_{01} u_2 \\
+2\beta^{\mathrm{II}} \alpha_{01} u_3
\end{array}
&
\begin{array}{c}
\beta^{\mathrm{II}} L + 2\beta^{\mathrm{II}} \alpha_{01} u_2 - 2\beta^{\mathrm{II}} \alpha_{01} u_3 \\
+\beta^{\mathrm{I}} L + 2\beta^{\mathrm{I}} \alpha_{01} u_3 - 2\beta^{\mathrm{I}} \alpha_{01} u_4
\end{array}
\end{bmatrix} . \quad (10.120)
$$

The iteration scheme $\boldsymbol{u}^{(j+1)} = \boldsymbol{u}^{(j)} - (\boldsymbol{K}_{\mathrm{T}}^{(j)})^{-1} \boldsymbol{r}(\boldsymbol{u}^{(j)})$ can be used due to the reduced system of equations and the tangent stiffness matrix. The reaction force $F_{\mathrm{r}4}$ on the right-hand end can be calculated after each iteration step by evaluating the 4th equation of the total system. The numerical results are summarized in Tables 10.10 and 10.11.

Table 10.10 Numerical values for the complete NEWTON–RAPHSON method in the case of three elements with displacement boundary conditions of $u_0 = 33\,\mathrm{mm}$. Geometry: $A^i = 100\,\mathrm{mm}^2$, $L^i = 400/3\,\mathrm{mm}$. Material behavior: $E_0 = \beta^i \times 70{,}000\,\mathrm{MPa}$, $E_1 = 49{,}000\,\mathrm{MPa}$, $\varepsilon_1 = 0.15$, $\beta^{\mathrm{I}} = \beta^{\mathrm{II}} = \beta^{\mathrm{III}} = 1$

Iteration j	$u_2^{(j)}$ (mm)	$u_3^{(j)}$ (mm)	$F_{\mathrm{r}4}^{(j)}$ (kN)	$\sqrt{\dfrac{\sum_{i=1}^{2}\left(u_i^{(j)} - u_i^{(j-1)}\right)^2}{\sum_{i=1}^{2}\left(u_i^{(j)}\right)^2}}$
0	0	0	0	–
1	16.338235	32.676471	16.902865	1
2	11.514910	23.029821	445.153386	0.418876
3	11.005802	22.011604	481.804221	0.046258
4	11.000001	22.000002	482.212447	0.000527
5	11.000000	22.000000	482.212500	0.000000

Table 10.11 Numerical values for the complete NEWTON–RAPHSON method in the case of three elements with displacement boundary conditions of $u_0 = 37.887740\,\mathrm{mm}$. Geometry: $A^i = 100\,\mathrm{mm}^2$, $L^i = 400/3\,\mathrm{mm}$. Material behavior: $E_0 = \beta^i \times 70{,}000\,\mathrm{MPa}$, $E_1 = 49{,}000\,\mathrm{MPa}$, $\varepsilon_1 = 0.15$, $\beta^{\mathrm{I}} = 3$, $\beta^{\mathrm{II}} = 2$, $\beta^{\mathrm{III}} = 1$

Iteration j	$u_2^{(j)}$ (mm)	$u_3^{(j)}$ (mm)	$F_{\mathrm{r}4}^{(j)}$ (kN)	$\sqrt{\dfrac{\sum_{i=1}^{2}\left(u_i^{(j)} - u_i^{(j-1)}\right)^2}{\sum_{i=1}^{2}\left(u_i^{(j)}\right)^2}}$
0	0	0	0	–
1	6.152350	15.380875	782.695217	1
2	5.539025	14.319014	799.913803	0.079871
3	5.539687	14.313407	800.000003	0.000368
4	5.539687	14.313407	800.000000	0.000000

Case (a) with the results in Table 10.10 can be considered as a test case for the iteration scheme. Due to the displacement boundary condition on the right-hand end and the identical elements, the iteration needs to result in $u_2 = \frac{1}{3} u_0$ and $u_3 = \frac{2}{3} u_0$ at this point. As can be seen from Table 10.10, this is the case after five iterations for the chosen convergence criteria. The case (b) with the results in Table 10.11 represents the

reversion of example 10.3. Since the result for the displacement from example 10.3 has been brought up as a boundary condition, the reaction force in the converged condition has to achieve a value of 800 kN. This is the case after four iteration steps.

10.4.2 Supplementary Problems

10.5 Strain Dependent Modulus of Elasticity with Quadratic Course
The strain dependent modulus of elasticity, which is illustrated in Fig. 10.14 was defined by experiment. Approximate the course with a quadratic function of the form $E(\varepsilon) = a + b\varepsilon + c\varepsilon^2$ and define the constants $a, \ldots, c$. Subsequently, calculate the stress–strain course through integration and illustrate the course graphically. In the next step, derive the element stiffness matrix for a linear bar element under consideration of the strain dependent modulus of elasticity. In the last step, define the tangent stiffness matrix.

**Fig. 10.14** Experimentally determined strain dependent modulus of elasticity
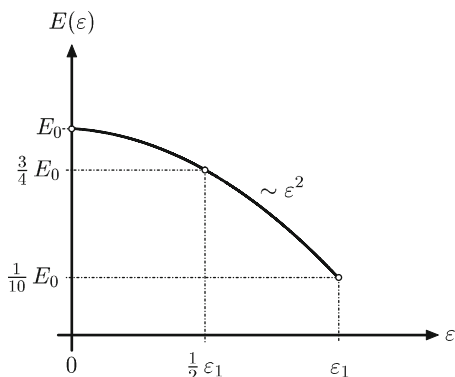
10.6 Direct Iteration with Different Initial Values
Discretize the bar according to Fig. 10.3 with one single linear element and use the direct iteration for the solution at different initial values: $u_2^{(0)} = 0$ or 30 or 220 mm. Further data can be taken from Table 10.1.

10.7 Complete Newton–Raphson Scheme for a Linear Element with Quadratic Modulus of Elasticity
The beam illustrated in Fig. 10.15a can be discretized via one single linear element. The strain dependent modulus of elasticity exhibits a quadratic course according to Fig. 10.15b. Based on the element stiffness matrix from problem 10.5, solve the problem with the complete NEWTON–RAPHSON scheme for an external force of $F = 370$ kN. As convergence criteria use a relative displacement difference of $< 10^{-6}$. Subsequently, analyze the convergence range of the iteration scheme in general. For the geometry the concrete values $A = 100 \, \text{mm}^2$ and $L = 400 \, \text{mm}$ and for

(a)

(b)
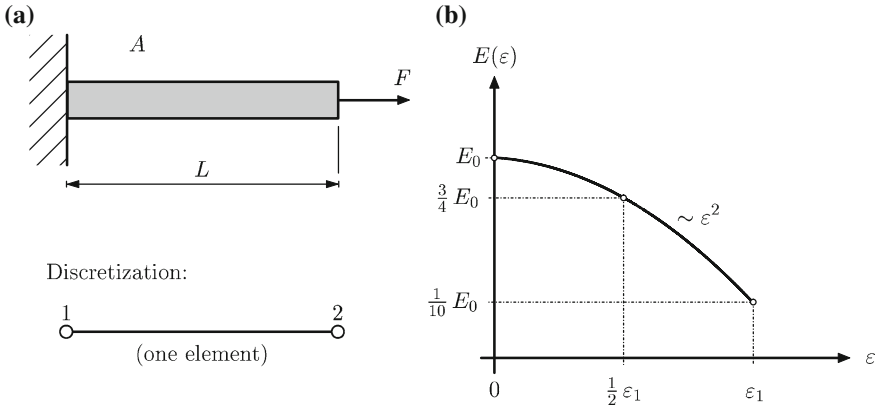
Fig. 10.15 Bar element under point load and quadratic strain dependency of the modulus of elasticity

the material behavior the concrete values $E_0 = 70,000 \, \text{MPa}$ and $\varepsilon_1 = 0.15$ can be used.

10.8 Strain Dependent Modulus of Elasticity with General Quadratic Course

In extension of problem 10.5 one can consider the illustrated course in Fig. 10.16 with the three sampling points $(0, E_0)$, $(\frac{1}{2}\varepsilon_1, \beta_{05} E_0)$ and $(\varepsilon_1, \beta_1 E_0)$. The form of the curve can be adapted more easily to the sampling points with the scale values β_{05} and β_1. The curve course can be approximated through a quadratic course in the form $E(\varepsilon) = a + b\varepsilon + c\varepsilon^2$. Define the constants $a, \ldots, c$ and derive the element stiffness matrix for a linear bar element under consideration of the strain dependent modulus of elasticity.

Fig. 10.16 Experimentally determined strain dependent modulus of elasticity; general quadratic course
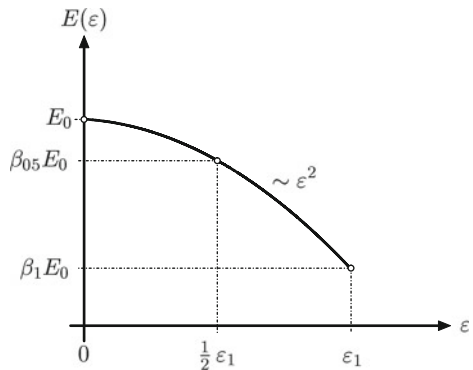
References

1. Wriggers P (2001) Nichtlineare Finite-Element-Methoden. Springer, Berlin
2. Reddy JN (2004) An introduction to nonlinear finite element analysis. Oxford University Press, Oxford
3. Betten J (2004) Finite Elemente für Ingenieure 2: Variationsrechnung, Energiemethoden, Näherungsverfahren, Nichtlinearitäten. Numerische Integrationen, Springer, Berlin
4. Belytschko T, Liu WK, Moran B (2000) Nonlinear finite elements for continua and structures. Wiley, Chichester
5. Cook RD, Malkus DS, Plesha ME, Witt RJ (2002) Concepts and applications of finite element analysis. Wiley, New York
6. Bathe K-J (2002) Finite-Elemente-Methoden. Springer, Berlin
7. Riks E (1972) The application of newtons method to the problem of elastic stabilty. J Appl Mech 39:1060–1066
8. Crisfield MA (1981) A fast encremental/iterative solution procedure that handles snap through. Comput Struct 13:55–62
9. Schweizerhof K, Wriggers P (1986) Consistent linearization for path following methods in nonlinear fe-analysis. Comput Method Appl Mech Eng 59:261–279

Chapter 11
Plasticity

Abstract The continuum mechanics basics for the one-dimensional bar will be compiled at the beginning of this chapter. The yield condition, the flow rule, the hardening law and the elasto-plastic modulus will be introduced for uniaxial, monotonic loading conditions. Within the scope of the hardening law, the description is limited to isotropic hardening, which occurs for example for the uniaxial tensile test with monotonic loading. For the integration of the elasto-plastic constitutive equation, the incremental predictor-corrector method is generally introduced and derived for the fully implicit and semi-implicit backward-Euler algorithm. On crucial points the difference between one- and three-dimensional descriptions will be pointed out, to guarantee a simple transfer of the derived methods to general problems. Calculated examples and supplementary problems with short solutions serve as an introduction for the theoretical description.

11.1 Continuum Mechanics Basics

The characteristic feature of plastic material behavior is that a remaining strain ε^{pl} occurs after complete unloading, see Fig. 11.1a. Solely the elastic strains ε^{el} return to zero at complete unloading. An additive composition of the strains by their elastic and plastic parts

$$\varepsilon = \varepsilon^{\text{el}} + \varepsilon^{\text{pl}} \tag{11.1}$$

is permitted at restrictions to small strains. The elastic strains ε^{el} can hereby be determined via HOOKE's law, whereby ε in Eq. (3.2) has to be substituted by ε^{el}. Furthermore, no explicit correlation is given anymore for plastic material behavior in general between stress and strain, since the strain state is also dependent on the loading history. Due to this, rate equations are necessary and need to be integrated throughout the entire load history. Within the framework of the time-independent
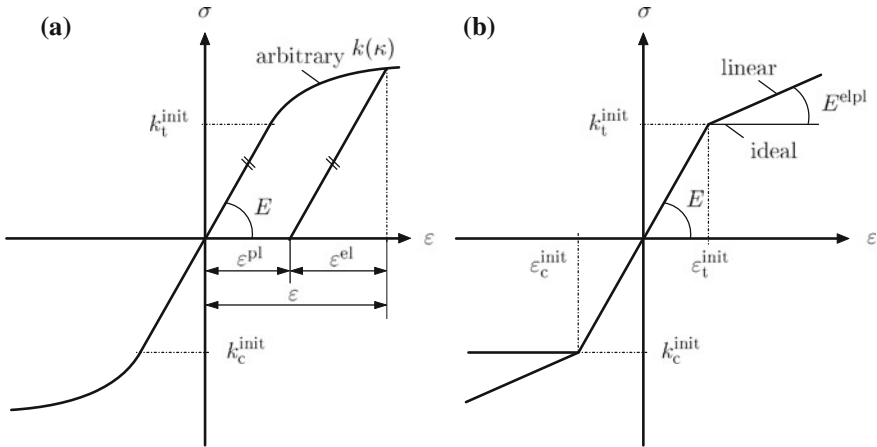
Fig. 11.1 Uniaxial stress–strain diagrams for different isotropic hardening approaches: **a** arbitrary hardening; **b** linear hardening and ideal plasticity

plasticity investigated here, the rate equations can be simplified to incremental relations. From Eq. (11.1) the additive composition of the strain increments results in:

$$d\varepsilon = d\varepsilon^{el} + d\varepsilon^{pl} . \tag{11.2}$$

The constitutive description of plastic material behavior includes

- a yield condition,
- a flow rule and
- a hardening law.

In the following, solely the case of the monotonic loading[1] is considered, so that solely the isotropic hardening is considered in the case of the material hardening. This important case, for example, occurs in the experimental mechanics at the uniaxial tensile test with monotonic loading. Furthermore, it is assumed that the yield stress is identical in the tensile and compressive regime: $k_t = k_c = k$.

11.1.1 Yield Condition

The yield condition enables one to determine whether the relevant material suffers only elastic or also plastic strains at a certain stress state at a point of the relevant body. In the uniaxial tensile test, plastic flow begins when reaching the initial yield

---

[1] The case of unloading or alternatively load reversal will not be regarded at this point due to simplification reasons.
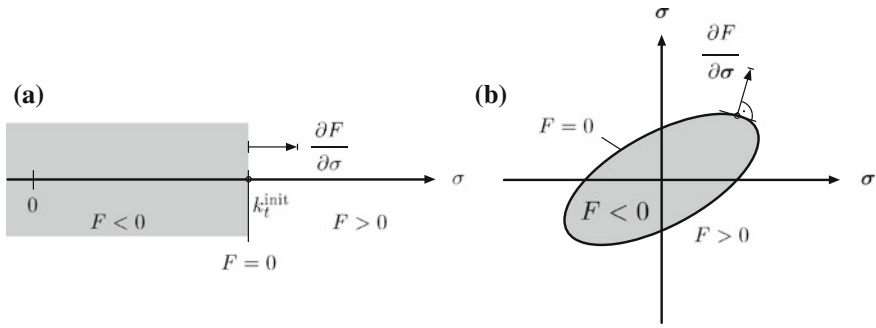
Fig. 11.2 Schematic illustration of the values of the yield condition and the direction of the stress gradient in the **a** one-dimensional and **b** multi-dimensional stress space. Here the σ–σ coordinate system represents a schematic illustration of the n-dimensional stress space

stress k^{init}, see Fig. 11.1. The yield condition in its general one-dimensional form can be set as follows ($\mathbb{R} \times \mathbb{R} \to \mathbb{R}$):

$$F = F(\sigma, \kappa), \tag{11.3}$$

whereupon κ represents the inner variable of the isotropic hardening. In the case of the ideal plasticity, see Fig. 11.1b, the following is valid: $F = F(\sigma)$. The values of F have the following mechanical meaning, see Fig. 11.2:

$$F(\sigma, \kappa) < 0 \quad \to \quad \text{elastic material behavior,} \tag{11.4}$$
$$F(\sigma, \kappa) = 0 \quad \to \quad \text{plastic material behavior,} \tag{11.5}$$
$$F(\sigma, \kappa) > 0 \quad \to \quad \text{invalid.} \tag{11.6}$$

A further simplification results under the assumption that the yield condition can be split into a pure stress fraction $f(\sigma)$, the so-called yield criterion,[2] and into an experimental material parameter $k(\kappa)$, the so-called flow stress:

$$F(\sigma, \kappa) = f(\sigma) - k(\kappa). \tag{11.7}$$

For a uniaxial tensile test (see Fig. 11.1) the yield condition can be noted in the following form:

$$F(\sigma, \kappa) = |\sigma| - k(\kappa) \leq 0. \tag{11.8}$$

---

[2] If the unit of the yield criterion equals the stress, $f(\sigma)$ represents the equivalent stress or effective stress. In the general three-dimensional case the following is valid under consideration of the symmetry of the stress tensor $\sigma_{\text{eff}} : (\mathbb{R}^6 \to \mathbb{R}_+)$.

If one considers the idealized case of the linear hardening (see Fig. 11.1b), Eq. (11.8) can be written as

$$F(\sigma, \kappa) = |\sigma| - (k^{\text{init}} + E^{\text{pl}}\kappa) \leq 0. \tag{11.9}$$

Parameter E^{pl} hereby is the plastic modulus (see Fig. 11.3), which becomes zero in the case of the ideal plasticity:

$$F(\sigma, \kappa) = |\sigma| - k^{\text{init}} \leq 0. \tag{11.10}$$

11.1.2 Flow Rule

The flow rule serves as a mathematical description of the evolution of the infinitesimal increments of the plastic strain $d\varepsilon^{\text{pl}}$ in the course of the load history of the body. In its most general one-dimensional form, the flow rule can be set up as follows [1]:

$$d\varepsilon^{\text{pl}} = d\lambda\, r(\sigma, \kappa), \tag{11.11}$$

whereupon the factor $d\lambda$ is described as the consistency parameter ($d\lambda \geq 0$) and $r : (\mathbb{R} \times \mathbb{R} \to \mathbb{R})$ as the function of the flow direction.[3] One considers that solely for $d\varepsilon^{\text{pl}} = 0\ d\lambda = 0$ results. Based on the stability postulate of DRUCKER [2] the following flow rule can be derived[4]:

$$d\varepsilon^{\text{pl}} = d\lambda\frac{\partial F(\sigma, \kappa)}{\partial \sigma}. \tag{11.12}$$

Such a flow rule is referred to as the normal rule[5] (see Fig. 11.2a) or due to $r = \partial F(\sigma, \kappa)/\partial\sigma$ as the *associated* flow rule.

Experimental results, among other things from the area of the granular materials [4] can however be approximated better if the stress gradient is substituted through a different function, the so-called plastic potential Q. The resulting flow rule is then referred to as the *non-associated* flow rule:

$$d\varepsilon^{\text{pl}} = d\lambda\frac{\partial Q(\sigma, \kappa)}{\partial \sigma}. \tag{11.13}$$

---

[3] In the general three-dimensional case *r* hereby defines the direction of the vector $d\varepsilon^{\text{pl}}$, while the scalar factor defines the absolute value.

[4] A formal alternative derivation of the associated flow rule can occur via the LAGRANGE multiplier method as extreme value with side-conditions from the principle of maximum plastic work [3].

[5] In the general three-dimensional case the image vector of the plastic strain increment has to be positioned upright and outside oriented to the yield surface, see Fig. 11.2b.

In the case of quite complicated yield conditions often the case occurs that a more simple yield condition is used for Q in the first approximation, for which the gradient can easily be determined.

The application of the associated flow rules (11.12) to the yield conditions according to Eqs. (11.8)–(11.10) yields for all three types of yield conditions (meaning arbitrary hardening, linear hardening and ideal plasticity):

$$d\varepsilon^{pl} = d\lambda\,\text{sgn}(\sigma), \tag{11.14}$$

whereupon $\text{sgn}(\sigma)$ represents the so-called sign function,[6] which can adopt the following values:

$$\text{sgn}(\sigma) = \begin{cases} -1 & \text{for } \sigma < 0 \\ 0 & \text{for } \sigma = 0 \\ +1 & \text{for } \sigma > 0 \end{cases}. \tag{11.15}$$

11.1.3 Hardening Law

The hardening law allows the consideration of the influence of material hardening on the yield condition and the flow rule. Within isotropic hardening the yield stress is described as dependent on an inner variable κ:

$$k = k(\kappa). \tag{11.16}$$

If the equivalent plastic strain[7] is used for the hardening variable ($\kappa = |\varepsilon^{pl}|$), then one talks about strain hardening.

Another possibility is to describe the hardening in dependency of the specific[8] plastic work $\left(\kappa = w^{pl} = \int \sigma\,d\varepsilon^{pl}\right)$. Then one talks about work hardening. If Eq. (11.16) is combined with the flow rule according to (11.14), the evolution equation for the isotropic hardening variable results in:

$$d\kappa = d|\varepsilon^{pl}| = d\lambda. \tag{11.17}$$

---

[6] Also signum function; from the Latin 'signum' for 'sign'.

[7] The effective plastic strain is in the general three-dimensional case the function $\varepsilon^{pl}_{eff} : (\mathbb{R}^6 \to \mathbb{R}_+)$. In the here regarded one-dimensional case the following is valid: $\varepsilon^{pl}_{eff} = \sqrt{\varepsilon^{pl}\varepsilon^{pl}} = |\varepsilon^{pl}|$. Attention: Finite element programs optionally use the more general definition for the illustration in the post processor, this means $\varepsilon^{pl}_{eff} = \sqrt{\frac{2}{3}\sum \Delta\varepsilon^{pl}_{ij}\sum \Delta\varepsilon^{pl}_{ij}}$, which considers the lateral contraction at uniaxial stress problems in the plastic area via the factor $\frac{2}{3}$. However in pure one-dimensional problems *without* lateral contraction, this formula leads to an illustration of the effective plastic strain, which is reduced by the factor $\sqrt{\frac{2}{3}} \approx 0.816$.

[8] This is the volume-specific definition, meaning $\left[w^{pl}\right] = \frac{N}{m^2}\frac{m}{m} = \frac{kg\,m}{s^2 m^2}\frac{m}{m} = \frac{kg\,m^2}{s^2 m^3} = \frac{J}{m^3}$.

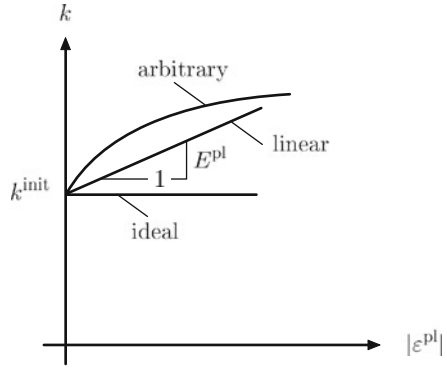**Fig. 11.3** Flow curve for different hardening approaches

Figure 11.3 shows the flow curve, meaning the graphical illustration of the yield stress in dependence on the inner variable for different hardening approaches.

11.1.4 Elasto-Plastic Material Modulus

At plastic material behavior the stiffness of the material changes and the strain state is dependent on the loading history. Therefore, the valid HOOKE's law for the linear-elastic material behavior according to Eq. (3.2) has to be replaced by the following infinitesimal incremental relation:

$$d\sigma = E^{\text{elpl}} d\varepsilon. \tag{11.18}$$

In (11.18) E^{elpl} refers to the elasto-plastic material modulus (see Fig. 11.1b), which is derived in the following.[9] The total differential of the yield condition (11.8) gives:

$$dF = \left(\frac{\partial F}{\partial \sigma}\right) d\sigma + \left(\frac{\partial F}{\partial \kappa}\right) d\kappa = \text{sgn}(\sigma) d\sigma + \left(\frac{\partial F}{\partial \kappa}\right) d\kappa = 0. \tag{11.19}$$

If HOOKE's law (3.2) and the flow rule (11.14) are inserted in Eq. (11.2) for the additive composition of the elastic and plastic strain, one obtains:

$$d\varepsilon = \frac{1}{E} d\sigma + d\lambda \, \text{sgn}(\sigma). \tag{11.20}$$

Multiplication of Eq. (11.20) with $\text{sgn}(\sigma)E$ and integration in Eq. (11.19) yields, under the use of the evolution equation of the hardening variables (11.17), the

---

[9] In the general three-dimensional case one talks about the elasto-plastic stiffness matrix $\boldsymbol{C}^{\text{elpl}}$.

consistency parameter:

$$d\lambda = \frac{\mathrm{sgn}(\sigma)E}{E - \left(\frac{\partial F}{\partial \kappa}\right)}\, d\varepsilon\,.\qquad(11.21)$$

Insertion of the consistency parameters in Eq. (11.20) and solving for $d\sigma$ finally yields the elasto-plastic material modulus:

$$E^{\mathrm{elpl}} = \frac{d\sigma}{d\varepsilon} = \frac{E \times \left(\frac{\partial F}{\partial \kappa}\right)}{\left(\frac{\partial F}{\partial \kappa}\right) - E}\,.\qquad(11.22)$$

For the special case of linear hardening, meaning $\frac{\partial F}{\partial \kappa} = -E^{\mathrm{pl}}$, Eq. (11.22) can be simplified as follows:

$$E^{\mathrm{elpl}} = \frac{E \times E^{\mathrm{pl}}}{E + E^{\mathrm{pl}}}\,.\qquad(11.23)$$

The different general definitions of the moduli are given comparatively in Table 11.1.

Table 11.1 Comparison of the different definitions of the stress–strain characteristics (moduli)

Range	Definition
Elastic	$E = \dfrac{d\sigma}{d\varepsilon^{\mathrm{el}}}$
Plastic	$E^{\mathrm{elpl}} = \dfrac{d\sigma}{d\varepsilon}$ for $\varepsilon > \varepsilon^{\mathrm{init}}$
	$E^{\mathrm{pl}} = \dfrac{d\sigma}{d|\varepsilon^{\mathrm{pl}}|}$

A comparison of the different equations and formulations of the one-dimensional plasticity with the general three-dimensional illustration (see for example [1, 5]) is given in Table 11.2.

Further details regarding plasticity can be taken from, for example, [6–10].

11.2 Integration of the Material Equations

In comparison to a FE calculation with pure linear-elastic material behavior, the calculation at a simulation of plastic material behavior cannot be conducted in one step any longer, since at this point in general no obvious connection between stress and strain exists.[10] The load is instead applied incrementally, whereupon in each increment a nonlinear system of equations has to be solved (for example NEWTON-RAPHSON algorithm). The principal finite element equation therefore has to be set in

---

[10] In the general case with six stress and strain components (under consideration of the symmetry of the stress and strain tensor) an obvious relation only exists between effective stress and effective plastic strain. In the one-dimensional case however these parameters reduce to: $\sigma_{\mathrm{eff}} = |\sigma|$ and $\varepsilon^{\mathrm{pl}}_{\mathrm{eff}} = |\varepsilon^{\mathrm{pl}}|$.

Table 11.2 Comparison between general 3D plasticity and 1D plasticity with isotropic (arbitrary or ideal) strain hardening

| General 3D plasticity	1D plasticity *arbitrary* hardening	1D plasticity *linear* hardening
Yield condition		
$F(\boldsymbol{\sigma}, \boldsymbol{q}) \leq 0$	$F = \lvert\sigma\rvert - k(\kappa) \leq 0$	$F = \lvert\sigma\rvert - (k^{\text{init}} + E^{\text{pl}}\kappa) \leq 0$
Flow rule		
$\varepsilon^{\text{pl}} = \mathrm{d}\lambda \times \boldsymbol{r}(\boldsymbol{\sigma}, \boldsymbol{q})$	$\mathrm{d}\varepsilon^{\text{pl}} = \mathrm{d}\lambda \times \mathrm{sgn}(\sigma)$	$\mathrm{d}\varepsilon^{\text{pl}} = \mathrm{d}\lambda \times \mathrm{sgn}(\sigma)$
Hardening law		
$\boldsymbol{q} = [\kappa, \boldsymbol{\alpha}]^{\text{T}}$	κ	κ
$\mathrm{d}\boldsymbol{q} = \mathrm{d}\lambda \times \boldsymbol{h}(\boldsymbol{\sigma}, \boldsymbol{q})$	$\mathrm{d}\kappa = \mathrm{d}\lambda$	$\mathrm{d}\kappa = \mathrm{d}\lambda$
Elasto-plastic material modulus		
$\boldsymbol{C}^{\text{elpl}} = \left(\boldsymbol{C} - \dfrac{(\boldsymbol{Cr}) \otimes \left(\boldsymbol{C}\frac{\partial F}{\partial \boldsymbol{\sigma}} \right)}{\left(\frac{\partial F}{\partial \boldsymbol{\sigma}} \right)^{\text{T}} \boldsymbol{Cr} - \frac{\partial F}{\partial \boldsymbol{q}} \boldsymbol{h}} \right)$	$E^{\text{elpl}} = \dfrac{E \times \left(\frac{\partial F}{\partial \kappa} \right)}{\left(\frac{\partial F}{\partial \kappa} \right) - E}$	$E^{\text{elpl}} = \dfrac{E \times E^{\text{pl}}}{E + E^{\text{pl}}}$

the following incremental form:

$$\boldsymbol{K}\,\Delta\boldsymbol{u} = \Delta\boldsymbol{F} \,. \tag{11.24}$$

Additionally, the state variables—as for example the stress σ_{n+1}—have to be calculated for each increment $(n + 1)$ in each integration point (GAUSS point), based on the stress state at the end of the previous increment (n) and the given strain increment $(\Delta\varepsilon_n)$ (see Fig. 11.4).
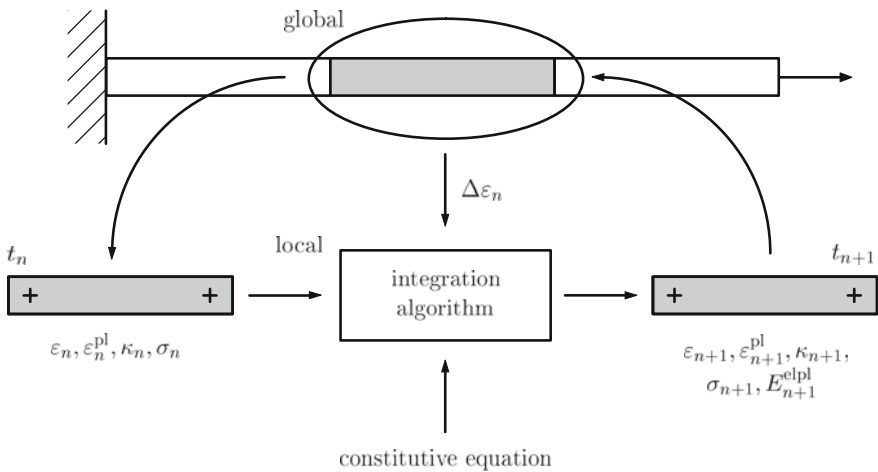
Fig. 11.4 Schematic illustration of the integration algorithm for plastic material behavior in the FEM; adopted from [11]. Integration points are marked schematically through the symbol '+'

To that, the explicit material law in infinitesimal form given has to be integrated numerically according to Eqs. (11.2) and (11.22). Explicit integration methods, as
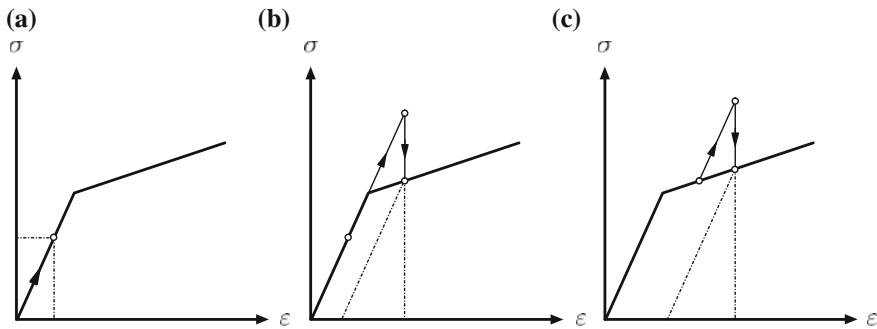
Fig. 11.5 Schematic illustration of the predictor-corrector method in the stress–strain diagram: **a** elastic predictor in the elastic area; **b** and **c** elastic predictor outside the yield surface boundary

for example the EULER procedure[11] however are inaccurate and possibly unstable, since a global error could accumulate [12]. Within the FEM one uses so-called predictor-corrector methods (see Fig. 11.5), in which, first a so-called predictor is explicitly determined and afterwards implicitly corrected instead of explicit integration procedures. In a first step, a test stress state (the so-called trial stress condition) is calculated under the assumption of pure linear-elastic material behavior via an elastic predictor[12]:

$$\sigma_{n+1}^{\text{trial}} = \sigma_n + \underbrace{E \Delta \varepsilon_n}_{\text{predictor } \Delta \sigma_n^{\text{el}}} . \tag{11.25}$$

The given hardening condition in this test stress state equals the condition at the end of the previous increment. Therefore, it is assumed that the load step occurs pure elastically, meaning without plastic deformation and therefore without hardening:

$$\kappa_{n+1}^{\text{trial}} = \kappa_n . \tag{11.26}$$

Based on the location of the test stress state in the stress space two elementary conditions can be distinguished with the help of the yield condition:

(a) The stress state is in the elastic area (see Fig. 11.5a) or on the yield surface boundary (valid stress state):

$$F\left(\sigma_{n+1}^{\text{trial}}, \kappa_{n+1}^{\text{trial}}\right) \leq 0 . \tag{11.27}$$

---

[11] The explicit EULER procedure or polygon method (also EULER-CAUCHY method) is the most simple procedure for the numerical solution of an initial value problem. The new stress state results according to this procedure in $\sigma_{n+1} = \sigma_n + E_n^{\text{elpl}} \Delta \varepsilon$, whereupon the initial value problem can be named as $\frac{d\sigma}{d\varepsilon} = E^{\text{elpl}}(\sigma, \varepsilon)$ with $\sigma(\varepsilon_0) = \sigma_0$.

[12] In the general three-dimensional case the relation is applied on the stress vector and the increment of the strain vector: $\boldsymbol{\sigma}_{n+1}^{\text{trial}} = \boldsymbol{\sigma}_n + \boldsymbol{C} \Delta \boldsymbol{\varepsilon}_n$.

In this case, the test state can be taken on as the new stress/hardening state, since it equals the real state:

$$\sigma_{n+1} = \sigma_{n+1}^{\text{trial}}, \tag{11.28}$$

$$\kappa_{n+1} = \kappa_{n+1}^{\text{trial}}. \tag{11.29}$$

In conclusion, one devolves to the next increment.

(b) The stress state is outside the yield surface boundary (invalid stress state), see Fig. 11.5b, c:

$$F\left(\sigma_{n+1}^{\text{trial}}, \kappa_{n+1}^{\text{trial}}\right) > 0. \tag{11.30}$$

If this case occurs, a valid state $(F(\sigma_{n+1}, \kappa_{n+1}) = 0)$ on the yield surface boundary is calculated in the second part of the procedure from the invalid test state. Therefore, the necessary stress difference

$$\Delta\sigma^{\text{pl}} = \sigma_{n+1}^{\text{trial}} - \sigma_{n+1} \tag{11.31}$$

is referred to as the plastic corrector.

For the calculation of the plastic corrector, the terms back projection, return mapping or catching up are used. Figure 11.6 illustrates the predictor-corrector method schematically in the one- and multi-dimensional stress space in comparison.
In the following the back projection is considered closely. Detailed illustrations can be found in [1, 5, 12–15].
The stress difference between initial and final state (stress increment)

$$\Delta\sigma_n = \sigma_{n+1} - \sigma_n \tag{11.32}$$

results, according to HOOKE's law from the elastic part of the strain increment, which results as the difference from the total strain increment and its plastic part:

$$\Delta\sigma_n = E\Delta\varepsilon_n^{\text{el}} = E\left(\Delta\varepsilon_n - \Delta\varepsilon_n^{\text{pl}}\right). \tag{11.33}$$

Figure 11.7 shows that the total strain increment in dependence on the test stress state can be illustrated as follows:

$$\Delta\varepsilon_n = \varepsilon_{n+1} - \varepsilon_n = \frac{1}{E}\left(\sigma_{n+1}^{\text{trial}} - \sigma_n\right). \tag{11.34}$$

If the last equation as well as the flow rule[13] according to (11.14) are inserted in Eq. (11.33), the final stress state σ_{n+1} in dependence on the test stress state $\sigma_{n+1}^{\text{trial}}$

---

[13] At this point within the notation it is formally switched from $d\lambda$ to $\Delta\lambda$. Therefore the transition from the differential to the incremental notation occurs.
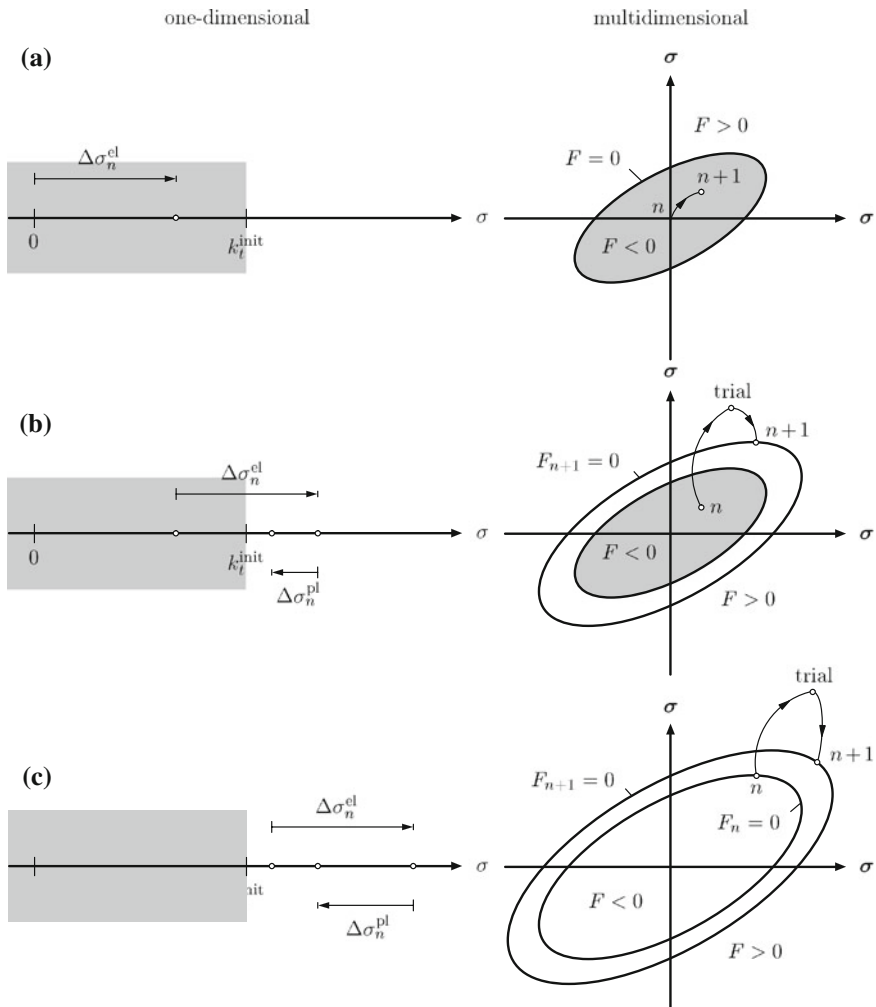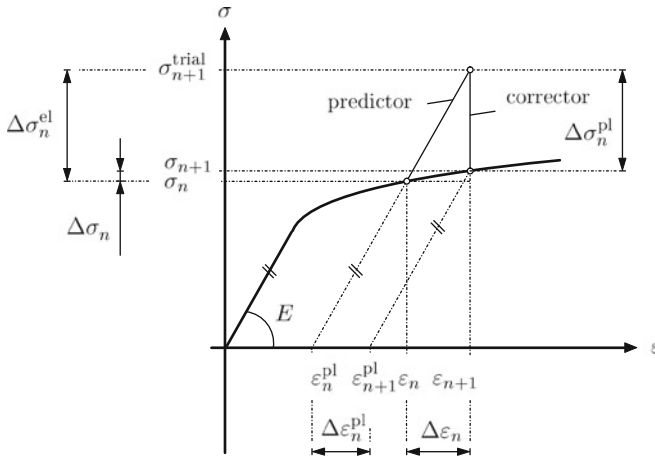
Fig. 11.6 Schematic illustration of the predictor-corrector method in the one-dimensional and multi-dimensional stress space. Here the $\sigma-\sigma$ coordinate system represents a schematic illustration of the n-dimensional stress space. **a** elastic predictor in the elastic area; **b** and **c** elastic predictor outside of the yield surface

results in:

$$\sigma_{n+1} = \sigma_{n+1}^{\text{trial}} - \Delta\lambda_{n+1} E \operatorname{sgn}(\sigma) . \tag{11.35}$$

Dependent on the location of the evaluation of the function $\operatorname{sgn}(\sigma)$ different methods result in the general case (see Table 11.3) to calculate the initial value for the plastic corrector or alternatively to define the final stress state iteratively. To obtain an initial

Fig. 11.7 Schematic illustration of the back projection in the stress–strain diagram. Adapted from [1]

value for the plastic corrector, $\mathrm{sgn}(\sigma)$ can either be evaluated in the test stress state (backward-EULER) or on the yield surface (forward-EULER; at the transition from the elastic to the plastic area this is the initial yield surface, see Fig. 11.5b). If the function $\mathrm{sgn}(\sigma)$ is evaluated in the final state at the iterative calculation, the normal rule (see Sect. 11.1.2) is fulfilled in the final state. For this fully implicit backward-EULER algorithm [also referred to as the closest point projection (CPP)] [1] however in the general three-dimensional case derivatives of higher order must be calculated. In the so-called cutting-plane algorithm [16] the function $\mathrm{sgn}(\sigma)$ is calculated in the stress state of the ith iteration step. The normal rule is not exactly fulfilled in the final state, however no calculations of derivatives of higher order are necessary. At the so-called mid-point rule [17] the function $\mathrm{sgn}(\sigma)$ is evaluated in the final state and on the yield surface as well as weighted in equal parts. If the function $\mathrm{sgn}(\sigma)$ is only evaluated on the yield surface, this leads to the semi-implicit backward-EULER algorithm [18], for which only derivatives of first order are necessary.

If one considers the dependency of the yield condition from the hardening variable, one needs another equation, which describes the hardening. From the evolution equation of the hardening variables (11.17) the following incremental relation results

$$\kappa_{n+1} = \kappa_n + \Delta\lambda_{n+1} \tag{11.36}$$

for the definition of the hardening variable.

Finally, it can be remarked that three of the listed integration rules in Table 11.3 can be summarized via the following equation

$$\sigma_{n+1} = \sigma_{n+1}^{\mathrm{trial}} - \Delta\lambda_{n+1} E\left([1-\eta]\mathrm{sgn}(\sigma_n) + \eta\,\mathrm{sgn}(\sigma_{n+1})\right). \tag{11.37}$$

The parameter η then becomes 1, 0 or $\frac{1}{2}$.

Table 11.3 Overview over the predictor-corrector methods

Location of the evaluation of sgn(n)	Equation (11.35)
Initial value for corrector	
Trial condition	$\sigma_{n+1} = \sigma_{n+1}^{\text{trial}} - \Delta\lambda_{n+1} E \operatorname{sgn}(\sigma_{n+1}^{\text{trial}})$
On the flow curve	$\sigma_{n+1} = \sigma_{n+1}^{\text{trial}} - \Delta\lambda_{n+1} E \operatorname{sgn}(\sigma_n)$
During the iteration	
In the final stress state (fully implicit backward-EULER algorithm) (closest point projection)	$\sigma_{n+1} = \sigma_{n+1}^{\text{trial}} - \Delta\lambda_{n+1} E \operatorname{sgn}(\sigma_{n+1})$
On the flow curve (semi-implicit backward-EULER algorithm)	$\sigma_{n+1} = \sigma_{n+1}^{\text{trial}} - \Delta\lambda_{n+1} E \operatorname{sgn}(\sigma_n)$
In the final state on the flow curve (mid-point rule)	$\sigma_{n+1} = \sigma_{n+1}^{\text{trial}} - \Delta\lambda_{n+1} E \frac{1}{2} \times (\operatorname{sgn}(\sigma_{n+1}) + \operatorname{sgn}(\sigma_n))$
Stress state of ith iteration step (cutting-plane algorithm)	$\sigma_{n+1} = \sigma_{n+1}^{\text{trial}} - \Delta\lambda_{n+1} E \operatorname{sgn}(\sigma^{(i)})$

11.3 Derivation of the Fully Implicit Backward-Euler Algorithm

11.3.1 Mathematical Derivation

In this back projection method, the stress location on the yield surface, which is energetically closest to the test state (see Sect. 11.3.2) is calculated. Therefore this does not involve, as the name suggests, a calculation of the closest geometric point. The assumption that the plastic work takes on a maximum at a given strain serves as a basis for the method. Together with the elementary demand that the calculated stress state has to lie on the flow curve (yield surface), the CPP method can be interpreted in the mathematical sense as a solution of an extremal value problem (maximum of the plastic work) with side-conditions (the unknown stress condition has to be on the yield surface) [1]. The method is hereby implicit in the calculation of the function $\operatorname{sgn}(\sigma)$ since the evaluation occurs in the final state $n + 1$. Because of this, the CPP algorithm is also referred to as the fully implicit backward-EULER algorithm. In the final state the following equations are therefore fulfilled:

$$\sigma_{n+1} = \sigma_{n+1}^{\text{trial}} - \Delta\lambda_{n+1} E \operatorname{sgn}(\sigma_{n+1}), \tag{11.38}$$

$$\kappa_{n+1} = \kappa_n + \Delta\lambda_{n+1}, \tag{11.39}$$

$$F = F(\sigma_{n+1}, \kappa_{n+1}) = 0. \tag{11.40}$$

Outside of the final state, however, at each of these equations a residual[14] r remains:

$$r_\sigma(\sigma, \kappa, \Delta\lambda) = \sigma - \sigma_{n+1}^{\text{trial}} + \Delta\lambda E \operatorname{sgn}(\sigma) \neq 0 \quad \text{or}$$
$$= E^{-1}\sigma - E^{-1}\sigma_{n+1}^{\text{trial}} + \Delta\lambda \operatorname{sgn}(\sigma) \neq 0, \tag{11.41}$$

---

[14] from the Latin 'residuus' for left or remaining.

$$r_\kappa(\kappa, \Delta\lambda) = \kappa - \kappa_n - \Delta\lambda \neq 0 \quad \text{or}$$
$$= -\kappa + \kappa_n + \Delta\lambda \neq 0 \,, \tag{11.42}$$
$$r_F(\sigma, \kappa) = F(\sigma, \kappa) = |\sigma| - k(\kappa) \neq 0 \,. \tag{11.43}$$

The unknown stress/hardening state therefore represents the root of a vector function $\boldsymbol{m}$, which consists of the single residual functions. Furthermore, it seems to make sense to also summarize the arguments for a single vector argument $\boldsymbol{v}$:

$$\boldsymbol{m}(\boldsymbol{v}) \in (\mathbb{R}^3 \to \mathbb{R}^3) = \begin{bmatrix} r_\sigma(\boldsymbol{v}) \\ r_\kappa(\boldsymbol{v}) \\ r_F(\boldsymbol{v}) \end{bmatrix}, \, \boldsymbol{v} = \begin{bmatrix} \sigma \\ \kappa \\ \Delta\lambda \end{bmatrix}. \tag{11.44}$$

The NEWTON method (iteration index: i) is used for the definition of the root[15]:

$$\boldsymbol{v}^{(i+1)} = \boldsymbol{v}^{(i)} - \left(\frac{\mathrm{d}\boldsymbol{m}}{\mathrm{d}\boldsymbol{v}}(\boldsymbol{v}^{(i)}) \right)^{-1} \boldsymbol{m}(\boldsymbol{v}^{(i)}) \,, \tag{11.45}$$

whereupon the following

$$\boldsymbol{v}^{(0)} = \begin{bmatrix} \sigma^{(0)} \\ \kappa^{(0)} \\ \Delta\lambda^{(0)} \end{bmatrix} = \begin{bmatrix} \sigma_{n+1}^{\text{trial}} \\ \kappa_n \\ 0 \end{bmatrix} \tag{11.46}$$

has to be used as the initial value. The JACOBIan matrix $\frac{\partial\boldsymbol{m}}{\partial\boldsymbol{v}}$ of the residual functions results from the partial derivatives of the Eqs. (11.41)–(11.43) to:

$$\frac{\partial\boldsymbol{m}}{\partial\boldsymbol{v}}(\sigma, \kappa, \Delta\lambda) = \begin{bmatrix} \frac{\partial r_\sigma}{\partial\sigma} & \frac{\partial r_\sigma}{\partial\kappa} & \frac{\partial r_\sigma}{\partial\Delta\lambda} \\ \frac{\partial r_\kappa}{\partial\sigma} & \frac{\partial r_\kappa}{\partial\kappa} & \frac{\partial r_\kappa}{\partial\Delta\lambda} \\ \frac{\partial r_F}{\partial\sigma} & \frac{\partial r_F}{\partial\kappa} & \frac{\partial r_F}{\partial\Delta\lambda} \end{bmatrix} = \begin{bmatrix} E^{-1} & 0 & \text{sgn}(\sigma) \\ 0 & -1 & 1 \\ \text{sgn}(\sigma) & -\frac{\partial k(\kappa)}{\partial\kappa} & 0 \end{bmatrix}. \tag{11.47}$$

Next to the fulfillment of Eqs. (11.38)–(11.40), which are given due to plasticity, in each integration point also the global force equilibrium hast to be fulfilled. In order to make use of the NEWTON method, it is even necessary at small strains in the general three-dimensional case to define the elasto-plastic stiffness matrix,[16] which is consistent to the integration algorithm [11]. The consistent elasto-plastic modulus

---

[15] The NEWTON method is usually used as follows for a one-dimensional function: $x^{(i+1)} = x^{(i)} - \left(\frac{\mathrm{d}f}{\mathrm{d}x}(x^{(i)})\right)^{-1} \times f(x^{(i)})$.

[16] Also referred to as consistent elasto-plastic tangent modulus matrix, consistent tangent stiffness matrix or algorithmic stiffness matrix.

results from the following in the one-dimensional case:

$$E_{n+1}^{\text{elpl}} = \frac{\partial \sigma_{n+1}}{\partial \varepsilon_{n+1}} = \frac{\partial \Delta \sigma_n}{\partial \varepsilon_{n+1}}. \tag{11.48}$$

With the inversion of the JACOBIan matrix $\frac{\partial \boldsymbol{m}}{\partial \boldsymbol{v}}$, which has to be evaluated in the converged condition of the above listed NEWTON iteration,

$$\left[\left(\frac{\partial \boldsymbol{m}}{\partial \boldsymbol{v}}\right)_{n+1}\right]^{-1} = \begin{bmatrix} \tilde{m}_{11} & \tilde{m}_{12} & \tilde{m}_{13} \\ \tilde{m}_{21} & \tilde{m}_{22} & \tilde{m}_{23} \\ \tilde{m}_{31} & \tilde{m}_{32} & \tilde{m}_{33} \end{bmatrix}_{n+1} \tag{11.49}$$

$$= \frac{E}{E + \frac{\partial k}{\partial \kappa}} \begin{bmatrix} \frac{\partial k}{\partial \kappa} & -\text{sgn}(\sigma)\frac{\partial k}{\partial \kappa} & \text{sgn}(\sigma) \\ \text{sgn}(\sigma) & -1 & -E^{-1} \\ \text{sgn}(\sigma) & E^{-1}\frac{\partial k}{\partial \kappa} & -E^{-1} \end{bmatrix}_{n+1} \tag{11.50}$$

the elasto-plastic modulus can be defined from

$$E_{n+1}^{\text{elpl}} = \tilde{m}_{11}. \tag{11.51}$$

For this consider Eq. (11.22) and note that under the assumption of Eq. (11.7) the relation $\frac{\partial F}{\partial \kappa} = -\frac{\partial k}{\partial \kappa}$ results. As can be seen from Eq. (11.50), the consistent elasto-plastic modulus in the *one-dimensional* case does not depend on the chosen integration algorithm and equals the continuum form given in Eq. (11.22). However at this point it needs be considered that this identity does not have to exist at higher dimensions any longer.

For the special case of linear hardening, meaning $\frac{\partial k}{\partial \kappa} = E^{\text{pl}} = \text{const.}$, Eq. (11.45) is not to be solved iteratively and the unknown solution vector $\boldsymbol{v}_{n+1}$ results directly with the help of the initial value (11.46) in:

$$\boldsymbol{v}_{n+1} = \boldsymbol{v}^{(0)} - \left(\frac{\mathrm{d}\boldsymbol{m}}{\mathrm{d}\boldsymbol{v}}(\boldsymbol{v}^{(0)})\right)^{-1} \boldsymbol{m}(\boldsymbol{v}^{(0)}), \tag{11.52}$$

or in components as:

$$\begin{bmatrix} \sigma_{n+1} \\ \kappa_{n+1} \\ \Delta\lambda_{n+1} \end{bmatrix} = \begin{bmatrix} \sigma_{n+1}^{\text{trial}} \\ \kappa_n \\ 0 \end{bmatrix} - \frac{E}{E+E^{\text{pl}}}$$

$$\times \begin{bmatrix} E^{\text{pl}} & -\text{sgn}(\sigma_{n+1}^{\text{trial}})E^{\text{pl}} & \text{sgn}(\sigma_{n+1}^{\text{trial}}) \\ \text{sgn}(\sigma_{n+1}^{\text{trial}}) & -1 & -E^{-1} \\ \text{sgn}(\sigma_{n+1}^{\text{trial}}) & E^{-1}E^{\text{pl}} & -E^{-1} \end{bmatrix} \begin{bmatrix} 0 \\ 0 \\ F_{n+1}^{\text{trial}} \end{bmatrix}. \tag{11.53}$$

The third equation of (11.53) yields the consistency parameter in the case of the linear hardening to:

$$\Delta\lambda_{n+1} = \frac{F_{n+1}^{\text{trial}}}{E + E^{\text{pl}}} .$$ (11.54)

The insertion of the consistency parameter into the first equation of (11.53) yields the stress in the final stress state to:

$$\sigma_{n+1} = \left(1 - \frac{F_{n+1}^{\text{trial}}}{E + E^{\text{pl}}} \times \frac{E}{|\sigma_{n+1}^{\text{trial}}|}\right) \sigma_{n+1}^{\text{trial}} .$$ (11.55)

From the second equation of (11.53) the isotropic hardening variable in the final stress state is given in the following with the last two results:

$$\kappa_{n+1} = \kappa_n + \frac{F_{n+1}^{\text{trial}}}{E + E^{\text{pl}}} = \kappa_n + \Delta\lambda_{n+1} .$$ (11.56)

Finally, the plastic strain results into the following via the flow rule

$$\varepsilon_{n+1}^{\text{pl}} = \varepsilon_n^{\text{pl}} + \Delta\lambda_{n+1} \, \text{sgn}(\sigma_{n+1}) ,$$ (11.57)

and the consistent elasto-plastic modulus can be defined according to Eq. (11.23). To conclude, the calculation steps of the CPP algorithm are presented in compact form:

I. Calculation of the Test State

$$\sigma_{n+1}^{\text{trial}} = \sigma_n + E \Delta\varepsilon_n$$
$$\kappa_{n+1}^{\text{trial}} = \kappa_n$$

II. Test of Validity of the Stress State

$F(\sigma_{n+1}^{\text{trial}}, \kappa_{n+1}^{\text{trial}}) \le 0$	
Y ⟍	⟍ N
$\sigma_{n+1} = \sigma_{n+1}^{\text{trial}}$ $\kappa_{n+1} = \kappa_{n+1}^{\text{trial}}$ End CPP	Back Projection necessary ($\Rightarrow$ Step III)

III. Back Projection
Initial Values:

$$\boldsymbol{v}^{(0)} = \begin{bmatrix} \sigma^{(0)} \\ \kappa^{(0)} \\ \Delta\lambda^{(0)} \end{bmatrix} = \begin{bmatrix} \sigma_{n+1}^{\text{trial}} \\ \kappa_n \\ 0 \end{bmatrix}$$

Root Finding with the NEWTON Method:

$$v^{(i+1)} = v^{(i)} - \left(\frac{dm}{dv}(v^{(i)})\right)^{-1} m(v^{(i)})$$

$$\text{As long } \|v^{(i+1)} - v^{(i)}\| < t_{\text{end}}^{v}$$

In the termination criterion the vector norm (or length) of a vector has been used, which results in the following $\|x\| = \left(\sum_{i=1}^{n} x_i^2\right)^{0.5}$ for an arbitrary vector x.

IV. Actualization of the Parameters

$$\sigma_{n+1} = \sigma^{(i+1)}$$
$$\kappa_{n+1} = \kappa^{(n+1)}$$
$$E_{n+1}^{\text{elpl}} = \tilde{m}_{11}$$

The internally used calculation precision in the FE system appears perfect as termination precision t_{end}^{v} in the NEWTON method.

Figure 11.7 shows that the entire strain increment in dependence on the test stress state can be illustrated as

$$\Delta\varepsilon_n = \varepsilon_{n+1} - \varepsilon_n = E^{-1}(\sigma_{n+1}^{\text{trial}} - \sigma_n). \tag{11.58}$$

If one integrates the last equation and the flow rule[17] according to (11.14) in Eq. (11.33), the final stress state σ_{n+1} in dependence on the test stress state $\sigma_{n+1}^{\text{trial}}$ results in:

$$\sigma_{n+1} = \sigma_{n+1}^{\text{trial}} - \Delta\lambda_{n+1} E \, \text{sgn}\left(\sigma_{n+1}^{\text{trial}}\right). \tag{11.59}$$

The general procedure of an elasto-plastic finite element calculation is illustrated in Fig. 11.8.

One can see that the solution of an elasto-plastic problem occurs on two levels. On the global level, meaning for the global system of equations under consideration of the boundary conditions, the NEWTON-RAPHSON iteration scheme is made use of to define the incremental global displacement vector Δu_n. By summing the displacement increments, the total global displacement vector u_{n+1} of the unknown nodal displacement of a structure consisting of finite elements results. Via the strain-displacement relation the strain ε_{n+1} or, alternatively the strain increment $\Delta\varepsilon_n$ per

---

[17] At this point it is switched from $d\lambda$ to $\Delta\lambda$.

state n:	$\boldsymbol{u}_n, \sigma_n, \varepsilon_n, \varepsilon_n^{\mathrm{pl}}, \kappa_n, E_n^{\mathrm{elpl}}$	
global system of equation	- element stiffness matrix k_i^e - global stiffness matrix $\boldsymbol{K}$ - global system of equations $\boldsymbol{K}\Delta\boldsymbol{u} = \Delta\boldsymbol{F}$ - consideration of boundary conditions - NEWTON RAPHSON algorithm $\Delta\boldsymbol{u}_n \to \boldsymbol{u}_{n+1}$ $\quad \to \varepsilon_{n+1} \to \Delta\varepsilon_n$ for each element	NEWTON-RAPHSON algorithm
local: integration point	CPP:$\qquad\qquad \Delta\varepsilon_n$ $\qquad\qquad\quad \Downarrow$ Predictor $\qquad\qquad\quad \sigma_{n+1}^{\mathrm{trial}}$ $\qquad\qquad\quad \Downarrow$ Corrector $\sigma_{n+1}, \varepsilon_{n+1}^{\mathrm{pl}}, \kappa_{n+1}, E_{n+1}^{\mathrm{elpl}}$	Predictor-Corrector algorithm
state $n+1$:	$\boldsymbol{u}_{n+1}, \sigma_{n+1}, \varepsilon_{n+1}, \varepsilon_{n+1}^{\mathrm{pl}}, \kappa_{n+1}, E_{n+1}^{\mathrm{elpl}}$	

Fig. 11.8 General procedure of an elasto-plastic finite element calculation

element, can be determined from the nodal displacement.[18] The strain increment of an element is now used on the level of the integration points, to define the remaining state variables iteratively with the help of a predictor-corrector method.

11.3.2 Interpretation as Convex Optimization Problem

The fully implicit backward-EULER algorithm can also be understood as a solution of a convex optimization problem. A general derivation of the following is given in

---

[18] At this point for the considered linear bar elements a constant strain distribution per element results. In general, the strain results as a function of the element coordinates which is usually evaluated on the integration points. Therefore, one would in the general case normally define a strain *vector* ε per element, which combines the different strain values on the integration points. This however is unnecessary for a linear bar element. A scalar strain or alternative stress value is enough for the description.

[1]. As an objective function the complementary energy has to be minimized hereby under the side-condition that the yield condition is fulfilled.

In the following, the derivation of the optimization problem for the example of isotropic strain hardening is illustrated. The complementary energy[19] between the test stress state and an arbitrary state $(\sigma, |\varepsilon^{pl}|)$ at an increment of the back projection can be split into its elastic and plastic parts according to

$$\bar{\pi}(\sigma, |\varepsilon^{pl}|) = \bar{\pi}^{el}(\sigma, |\varepsilon^{pl}|) + \bar{\pi}^{pl}(\sigma, |\varepsilon^{pl}|). \tag{11.60}$$

At this point in the case of the considered *linear* elasticity, the complementary energy $\bar{\pi}^{el}$ and the potential energy π^{el} are the same. Due to the assumption of the *linear isotropic* hardening accordingly it is valid that $\bar{\pi}^{pl} = \pi^{pl}$ (see Fig. 11.9). Therefore the following occurs for the complementary energy

$$\begin{aligned}
\bar{\pi} &= \pi^{el} + \bar{\pi}^{pl} \\
&= \int \left(\sigma_{n+1}^{trial} - \sigma \right) d\varepsilon^{el} + \int \left(|\varepsilon^{pl}| - |\varepsilon_n^{pl}| \right) d\sigma . \tag{11.61}
\end{aligned}$$

The assumption of linearity in the elastic and plastic area, meaning $d\sigma = E d\varepsilon^{el}$ and $d\sigma = E^{pl} d\varepsilon^{pl}$, can be used in Eq. (11.61) so that the following finally results for the complementary energy

$$\bar{\pi}(\sigma, |\varepsilon^{pl}|) = \frac{1}{2}(\sigma_{n+1}^{trial} - \sigma)\frac{1}{E}(\sigma_{n+1}^{trial} - \sigma) + \frac{1}{2}(|\varepsilon_n^{pl}| - |\varepsilon^{pl}|)E^{pl}(|\varepsilon_n^{pl}| - |\varepsilon^{pl}|). \tag{11.62}$$

The fractions of $\bar{\pi}$ result as triangular areas in Fig. 11.9, which can also be used directly for the definition of the complementary energy. For the case that the flow curve k exhibits a certain course, the plastic energy parts for an arbitrary state $(\sigma, |\varepsilon^{pl}|)$ can be calculated via
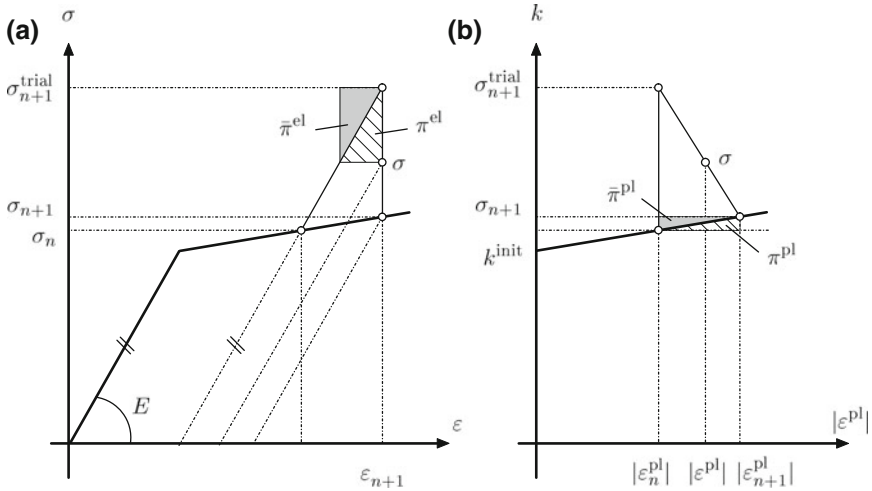
$$\pi^{pl} = \int_{|\varepsilon_n^{pl}|}^{|\varepsilon^{pl}|} \left(k(|\varepsilon^{pl}|) - \sigma_n \right) d|\varepsilon^{pl}|, \tag{11.63}$$

$$\bar{\pi}^{pl} = \int_{|\varepsilon_n^{pl}|}^{|\varepsilon^{pl}|} \left(\sigma - k(|\varepsilon^{pl}|) \right) d|\varepsilon^{pl}|. \tag{11.64}$$

The side-condition of the optimization problem is given through the yield condition and states that the final stress state has to be within or on the boundary of the elastic

---

[19] Hereby the energy per unit volume is considered.

Fig. 11.9 Illustration of the elastic potential and plastic dissipative energy and the corresponding complementary energy between two states of the back projection in the case of the linear hardening

area. From Eq. (11.9) a limiting line results in a $\varepsilon^{\mathrm{pl}} - \sigma$ coordinate system:

$$\varepsilon^{\mathrm{pl}} \geq \frac{1}{E^{\mathrm{pl}}} \left(|\sigma| - k^{\mathrm{init}} \right) \quad \text{and} \quad \varepsilon^{\mathrm{pl}} \geq 0 \,. \tag{11.65}$$

Generally, the side-condition, meaning the elastic area, can also be specified as

$$\mathbb{E}_\sigma := \left\{ (\sigma, |\varepsilon^{\mathrm{pl}}|) \in \mathbb{R} \times \mathbb{R}_+ | F(\sigma, |\varepsilon^{\mathrm{pl}}|) \leq 0 \right\} \tag{11.66}$$

and the convex optimization problem can be formulated as follows:

$$\text{Define}(\sigma_{n+1}, |\varepsilon^{\mathrm{pl}}_{n+1}|) \in \mathbb{E}_\sigma, \text{ so that}$$
$$\bar{\pi}(\sigma_{n+1}, |\varepsilon^{\mathrm{pl}}_{n+1}|) = \min \left\{ \bar{\pi}(\sigma, |\varepsilon^{\mathrm{pl}}|) \right\} \Big|_{(\sigma, |\varepsilon^{\mathrm{pl}}|) \in \mathbb{E}_\sigma} \,.$$

Since $E > 0$—and under the assumption $E^{\mathrm{pl}} > 0$—it results that $\bar{\pi}$ is a convex function. The side-condition, meaning $F \leq 0$, also represents a convex function,[20] and the application of the LAGRANGE multiplier method leads to

$$\mathcal{L}(\sigma, |\varepsilon^{\mathrm{pl}}|, \mathrm{d}\lambda) := \bar{\pi}(\sigma, |\varepsilon^{\mathrm{pl}}|) + \mathrm{d}\lambda F(\sigma, |\varepsilon^{\mathrm{pl}}|) \,. \tag{11.67}$$

---

[20] The convexity of a yield condition can be derived from the DRUCKER's stability postulate [19, 20].
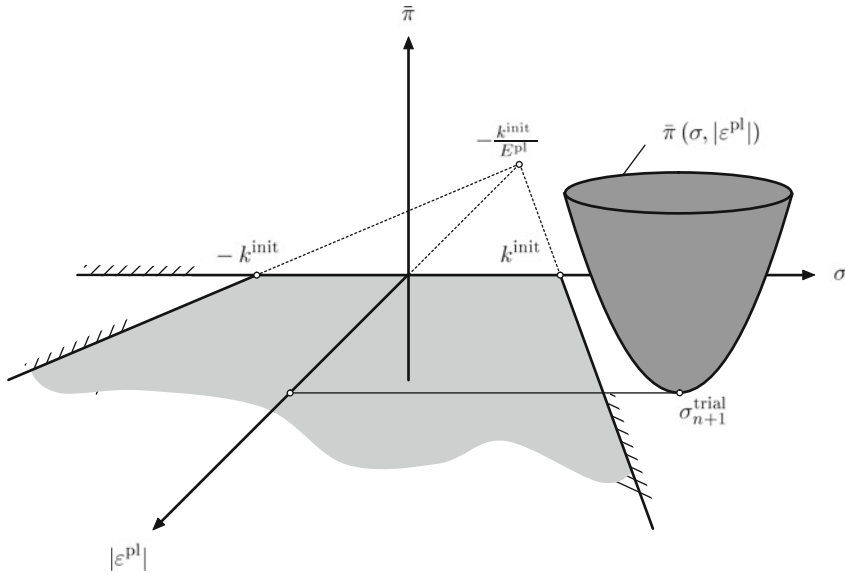
Fig. 11.10 Interpretation of the fully implicit backward-EULER algorithm as a convex optimization problem. Adapted from [1]

The gradients of the LAGRANGE function $\mathcal{L}$ result in:

$$\frac{\partial}{\partial \sigma} \mathcal{L}(\sigma_{n+1}, |\varepsilon^{\mathrm{pl}}_{n+1}|, \mathrm{d}\lambda) = 0, \tag{11.68}$$

$$\frac{\partial}{\partial |\varepsilon^{\mathrm{pl}}|} \mathcal{L}(\sigma_{n+1}, |\varepsilon^{\mathrm{pl}}_{n+1}|, \mathrm{d}\lambda) = 0. \tag{11.69}$$

For Eqs. (11.68) and (11.69) the following results

$$\frac{\partial \mathcal{L}}{\partial \sigma} = (\sigma^{\mathrm{trial}}_{n+1} - \sigma)\left(-\frac{1}{E}\right) + \mathrm{d}\lambda \, \mathrm{sgn}(\sigma) = 0, \tag{11.70}$$

$$\frac{\partial \mathcal{L}}{\partial |\varepsilon^{\mathrm{pl}}|} = (|\varepsilon^{\mathrm{pl}}_n| - |\varepsilon^{\mathrm{pl}}|)(-E^{\mathrm{pl}}) + \mathrm{d}\lambda(-E^{\mathrm{pl}}) = 0. \tag{11.71}$$

The last two equations comply with the rules (11.56) and (11.35) of the previous section. A graphical interpretation of the implicit backward-EULER algorithm in the sense of a convex optimization problem is given in Fig. 11.10. If an invalid test state $(F > 0)$ results, the ellipsoid of the complementary energy lies outside of the valid area of the elastic energy. It needs to be remarked at this point that the absolute minimum (without side-condition) of the complementary energy lies in the $\sigma - |\varepsilon^{\mathrm{pl}}|$ plane and therefore results in $\bar{\pi}\left(\sigma^{\mathrm{trial}}_{n+1}, |\varepsilon^{\mathrm{pl}}_n|\right) = 0$.

The minimum of the complementary energy under consideration of the side-condition, meaning $F \leq 0$, therefore has to be localized on the cutting curve between the ellipsoid of the complementary energy and the plane along the flow curve[21] (see Eq. (11.65)). If Eq. (11.65) in the complementary energy according to (11.62) is considered, the following results

$$\bar{\pi}(\sigma, |\varepsilon^{\mathrm{pl}}|) = \frac{1}{2E}(\sigma_{n+1}^{\mathrm{trial}} - \sigma)^2 + \frac{1}{2}\, E^{\mathrm{pl}}\left(|\varepsilon_n^{\mathrm{pl}}| - \frac{1}{E^{\mathrm{pl}}}\left(\sigma - k^{\mathrm{init}}\right)\right)^2, \quad (11.72)$$

this means a polynomial of 2nd order in the variable σ. The minimum of this function—and therefore the state $n + 1$—results via partial derivative for $\sigma > 0$ (meaning for a tensile test) in:

$$\frac{\partial \bar{\pi}}{\partial \sigma} = -\frac{\sigma_{n+1}^{\mathrm{trial}} - \sigma_{n+1}}{E} - \left(|\varepsilon_n^{\mathrm{pl}}| - \frac{\sigma_{n+1} - k^{\mathrm{init}}}{E^{\mathrm{pl}}}\right) \quad (11.73)$$

or

$$\sigma_{n+1} = \underbrace{\frac{E\, E^{\mathrm{pl}}}{E + E^{\mathrm{pl}}}}_{E^{\mathrm{elpl}}}\left(\frac{k^{\mathrm{init}}}{E^{\mathrm{pl}}} + \frac{\sigma_{n+1}^{\mathrm{trial}}}{E} + |\varepsilon_n^{\mathrm{pl}}|\right). \quad (11.74)$$

Via Eq. (11.65) the plastic strain in the final stress state results in:

$$\varepsilon_{n+1}^{\mathrm{pl}} = \underbrace{\frac{E\, E^{\mathrm{pl}}}{E + E^{\mathrm{pl}}}}_{E^{\mathrm{elpl}}}\left(\frac{k^{\mathrm{init}}}{E\, E^{\mathrm{pl}}} + \frac{\sigma_{n+1}^{\mathrm{trial}}}{E\, E^{\mathrm{pl}}} + \frac{|\varepsilon_n^{\mathrm{pl}}|}{E^{\mathrm{pl}}}\right) - \frac{k^{\mathrm{init}}}{E^{\mathrm{pl}}}. \quad (11.75)$$

A graphical illustration of the cutting curve is given in Fig. 11.11. One can consider at this point that $|\varepsilon_n^{\mathrm{pl}}|$ equals the test stress state.

11.4 Derivation of the Semi-Implicit Backward-Euler Algorithm

To avoid the higher derivatives in the JACOBIan matrix $\frac{\partial m}{\partial v}$ of the residual functions in the general three-dimensional case, the so-called semi-implicit backward-EULER algorithm can be made use of. This procedure is implicit in the consistency parameter (state $n + 1$), however explicit in the function $\mathrm{sgn}(\sigma)$ since the calculation occurs in the initial state n. Because of that, the normal rule in the final state $n + 1$ is not

---

[21] This plane has to stand vertically on the $\sigma - |\varepsilon^{\mathrm{pl}}|$ plane. For a tensile test the plane has to go through the limit curve in the area $\sigma > 0$. For a compression test the according straight line from the area $\sigma < 0$ has to be chosen.

Fig. 11.11 Illustration of the complementary energy in a cutting plane along the flow curve
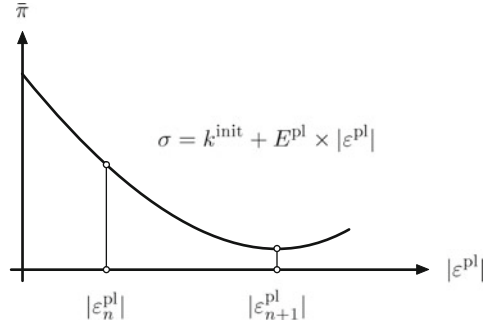
fulfilled exactly. To avoid a drift away from the flow curve, the yield condition in the final state $n + 1$ is fulfilled exactly. Therefore the integration scheme results in:

$$\sigma_{n+1} = \sigma_{n+1}^{\text{trial}} - \Delta\lambda_{n+1} E \, \text{sgn}(\sigma_n), \qquad (11.76)$$

$$\kappa_{n+1} = \kappa_n + \Delta\lambda_{n+1}, \qquad (11.77)$$

$$F = F(\sigma_{n+1}, \kappa_{n+1}) = 0. \qquad (11.78)$$

Outside of the final state also at this point a residual r remains at each of these equations:

$$r_\sigma(\sigma, \kappa, \Delta\lambda) = E^{-1}\sigma - E^{-1}\sigma_{n+1}^{\text{trial}} + \Delta\lambda \, \text{sgn}(\sigma_n) \neq 0,$$
$$r_\kappa(\kappa, \Delta\lambda) = -\kappa + \kappa_n + \Delta\lambda \neq 0,$$
$$r_F(\sigma, \kappa) = F(\sigma, \kappa) = |\sigma| - k(\kappa) \neq 0. \qquad (11.79)$$

The partial derivatives of the residual functions finally lead to the following JACOBIan matrix:

$$\frac{\partial \boldsymbol{m}}{\partial \boldsymbol{v}}(\sigma, \kappa, \Delta\lambda) = \begin{bmatrix} E^{-1} & 0 & \text{sgn}(\sigma_n) \\ 0 & -1 & 1 \\ \text{sgn}(\sigma) & -\frac{\partial k(\kappa)}{\partial \kappa} & 0 \end{bmatrix}. \qquad (11.80)$$

If one compares the JACOBIan matrix according to Eqs.(11.80) and (11.47) one can see that the integration requirements for the fully implicit and semi-implicit algorithm are identical for the considered one-dimensional case at this point, as long as the stress state σ and σ_n lie in the same quadrant, meaning exhibiting the same algebraic sign. Similar conclusions can be drawn for the, in Table 11.3 summarized integration requirements.

To conclude, it can be remarked that the concept of the plastic material behavior, which was originally developed for the permanent deformation of metals, is also applied for other classes of material. Typically the macroscopic stress–strain diagram is regarded at this point, which exhibits a similar course as for classic metals. As an

example, the following materials and disciplines can be listed here for:

- Plastics [21],
- Fibre-reinforced plastics [22],
- Soil mechanics [23, 24],
- Concrete [25].

11.5 Sample Problems and Supplementary Problems

11.5.1 Sample Problems

11.1 Example: Back Projection at Linear Hardening: Continuum Bar

Figure 11.12a shows an idealized stress–strain diagram as it can, for example, be derived experimentally from an uniaxial tensile test. With the help of this material behavior the deformation of a tension bar (see Fig. 11.12b) can be simulated. Thereby the right-hand end is displaced by $u = 8 \times 10^{-3}$ m in total, whereupon the deformation is applied in 10 equal increments. The bar needs to be regarded as a continuum hereby and should not be discretized with finite elements.

(a) Calculate the stress state with the help of the CPP algorithm in each increment and mark all values, which have to be updated.

(b) Graphically illustrate the stress distribution.
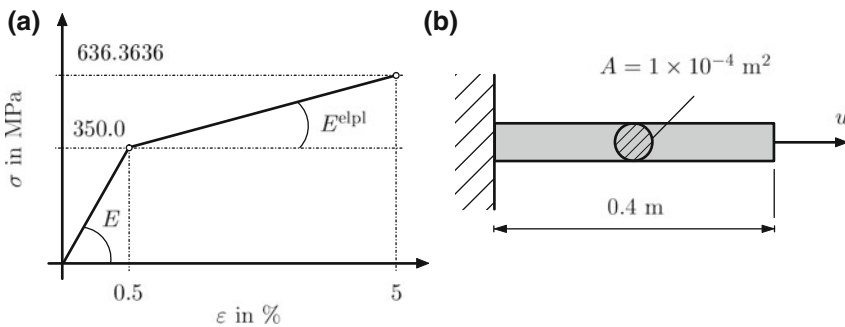
Fig. 11.12 Sample problem back projection at linear hardening: **a** stress–strain distribution; **b** geometry and boundary conditions

11.1 Solution

(a) For the back projection various material properties of the elastic and plastic regime are needed. The modulus of elasticity E results as a quotient from the stress and strain increment in the elastic regime in:

$$E = \frac{\Delta\sigma}{\Delta\varepsilon} = \frac{350 \text{ MPa}}{0.005} = 70000 \text{ MPa}.$$ (11.81)

The plastic modulus E^{pl} results as a quotient from the yield stress and the plastic strain increment in:

$$E^{\text{pl}} = \frac{\Delta k}{\Delta \varepsilon^{\text{pl}}} = \frac{636.3636 \text{ MPa} - 350 \text{ MPa}}{(0.05 - 636.3636 \text{ MPa}/E) - (0.005 - 350 \text{ MPa}/E)}$$
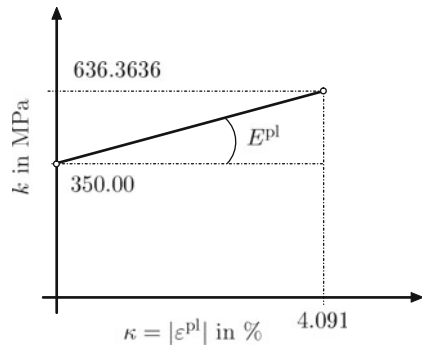$$= 7000 \text{ MPa}. \tag{11.82}$$

Therefore the elasto-plastic material modulus can be calculated via Eq. (11.23) in

$$E^{\text{elpl}} = \frac{E \times E^{\text{pl}}}{E + E^{\text{pl}}} = \frac{70000 \text{ MPa} \times 7000 \text{ MPa}}{70000 \text{ MPa} + 7000 \text{ MPa}} = 6363.636 \text{ MPa}. \tag{11.83}$$

Finally the equation of the flow curve results in the following via the initial yield stress:
$$k(\kappa) = 350 \text{ MPa} + 7000 \text{ MPa} \times \kappa. \tag{11.84}$$

Fig. 11.13 Flow curve for continuum bar

A graphical illustration of the flow curve is given in Fig. 11.13. For the integration algorithm the strain increment is additionally necessary. At a total displacement of 8×10^{-3} m and 10 equidistant steps, the strain increment can be determined via:

$$\Delta \varepsilon = \frac{1}{10} \times \frac{0.008 \text{ m}}{0.4 \text{ m}} = 0.002. \tag{11.85}$$

For the first two increments test stress states in the elastic regime ($F < 0$) result, and the resulting stress can be calculated via Eq. (11.25) via HOOKE's law. From the third increment on an invalid test stress state ($F > 0$) results for the first time and the stress has to be calculated via Eq. (11.53), whereupon the constant matrix expression results in:

$$\begin{bmatrix} 7000 & -7000 & 1 \\ 1 & -1 & -(70000)^{-1} \\ 1 & 0,1 & -(70000)^{-1} \end{bmatrix}. \tag{11.86}$$

Table 11.4 Numerical values of the back projection for a continuum bar with linear hardening (10 increments, $\Delta\varepsilon = 0.002$)

inc	ε	σ^{trial}	σ	κ	$d\lambda$	E^{elpl}
–	–	MPa	MPa	10^{-3}	10^{-3}	MPa
1	0.002	140.0	140.0	0.0	0.0	0.0
2	0.004	280.0	280.0	0.0	0.0	0.0
3	0.006	420.0	356.364	0.909091	0.909091	6363.636
4	0.008	496.364	369.091	2.727273	1.818182	6363.636
5	0.010	509.091	381.818	4.545455	1.818182	6363.636
6	0.012	521.818	394.545	6.363636	1.818182	6363.636
7	0.014	534.545	407.273	8.181818	1.818182	6363.636
8	0.016	547.273	420.000	10.000000	1.818182	6363.636
9	0.018	560.000	432.727	11.818182	1.818182	6363.636
10	0.020	572.727	445.455	13.636364	1.818182	6363.636
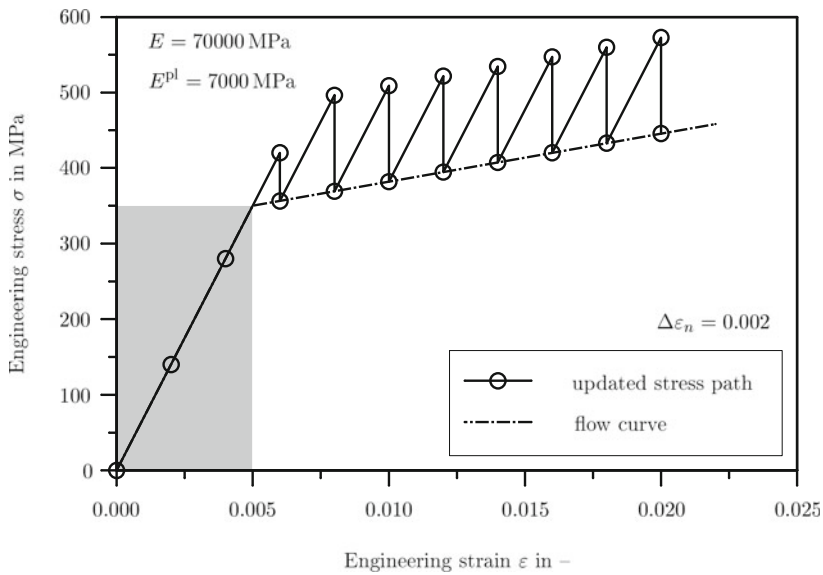
Fig. 11.14 Stress distribution in the case of the back projection for a continuum bar with linear hardening (10 increments, $\Delta\varepsilon = 0.002$)

Table 11.4 summarizes the numerical results for the 10 increments.

(b) A graphical illustration of the stress distribution is given in Fig. 11.14. Due to the linear hardening, the back projection for each increment occurs in one step.

Finally it needs to be remarked at this point that for the special case of *linear* hardening at *uniaxial* stress states, the stress in the plastic area (inc ≥ 3) can directly be calculated

via (see Fig. 11.1b)

$$\sigma(\varepsilon) = k_t^{\text{init}} + E^{\text{elpl}} \times (\varepsilon - \varepsilon_t^{\text{init}})$$
$$= E\varepsilon_t^{\text{init}} + E^{\text{elpl}}\varepsilon - E^{\text{elpl}}\varepsilon_t^{\text{init}}$$
$$\sigma(\varepsilon) = (E - E^{\text{elpl}}) \times \varepsilon_t^{\text{init}} + E^{\text{elpl}} \times \varepsilon. \tag{11.87}$$

The intention of this example however is to illustrate the concept of the back projection and not to define the stress according to the simplest method.

11.2 Example: Back Projection at Linear Hardening: Discretization via one Finite Element, Displacement and Force Boundary Condition

The continuum bar from example 1.1 can be discretized within the frame of this example via one single finite element. The material behavior can be made as shown in Fig. 11.12a. The load on the right-hand end of the bar can be applied in 10 equal increments, whereupon

(a) $u = 8 \times 10^{-3}$ m,
(b) $F = 100$ kN

can be applied. Calculate the stress state in each increment with the help of the CPP algorithm and mark all values, which have to be updated. As convergence criteria an absolute displacement difference of 1×10^{-5} mm can be assigned (Fig. 11.15).
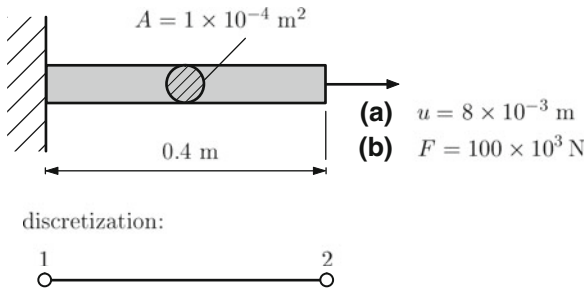
Fig. 11.15 Sample problem back projection in the case of linear hardening: (*a*) displacement boundary condition; (*b*) force boundary condition

11.2 Solution

When using solely one element, the global system of equations results in the following—without the consideration of the boundary conditions:

$$\frac{A\tilde{E}}{L}\begin{bmatrix} 1 & -1 \\ -1 & 1 \end{bmatrix}\begin{bmatrix} \Delta u_1 \\ \Delta u_2 \end{bmatrix} = \begin{bmatrix} \Delta F_1 \\ \Delta F_2 \end{bmatrix}. \tag{11.88}$$

Since in general this is a nonlinear system of equations, an incremental form has been assigned. The modulus $\tilde{E}$ equals the elasticity modulus E in the elastic range and

the elasto-plastic material modulus E^{elpl} in the plastic range. Since a fixed support is given on the left-hand node ($\Delta u_1 = 0$), Eq. (11.88) can be simplified to

$$\frac{A\tilde{E}}{L} \times \Delta u_2 = \Delta F_2. \tag{11.89}$$

Case (a) Displacement boundary condition $u = 8 \times 10^{-3}$ m on the right-hand node: In the case of the displacement boundary condition Eq. (11.89) must not be solved, since for each increment $\Delta u_2 = 8 \times 10^{-3}/10 = 8 \times 10^{-4}$ m is known. Via the equation for the strain in the element, meaning $\varepsilon = \frac{1}{L}(u_2 - u_1)$, the strain increment results in the following in the case of the fixed support on the left-hand node:

$$\Delta\varepsilon = \frac{1}{L} \times \Delta u_2 = \frac{8 \times 10^{-4} \text{ m}}{0.4 \text{ m}} = 0.002 \,. \tag{11.90}$$

The entire displacement or alternatively strain can be calculated through the summation of the incremental displacement or alternatively strain values, see Table 11.5. It can be remarked at this point that for this case of displacement boundary condition at one element, the calculation of the displacement or alternatively the strain for all increments can be done without a stress calculation.

Table 11.5 Numerical values of the displacement and strain for displacement boundary condition (10 increments, $\Delta\varepsilon = 0.002$)

inc	Δu_2	$\Delta\varepsilon$	u_2	ε
–	10^{-4} m	–	10^{-4} m	–
1	8.0	0.002	8.0	0.002
2	8.0	0.002	16.0	0.004
3	8.0	0.002	24.0	0.006
4	8.0	0.002	32.0	0.008
5	8.0	0.002	40.0	0.010
6	8.0	0.002	48.0	0.012
7	8.0	0.002	56.0	0.014
8	8.0	0.002	64.0	0.016
9	8.0	0.002	72.0	0.018
10	8.0	0.002	80.0	0.020

To calculate the stress and plastic strain in each increment, the calculation via the CPP algorithm for each increment has to be conducted via the strain increment $\Delta\varepsilon$ from Table 11.5. This is exactly what is calculated in example 11.1 and the numerical results can be taken from Table 11.4.

Case (b) Force boundary condition $F = 100$ kN on the right-hand node: In the case of the force boundary condition, Eq. (11.89) can be solved via the NEWTON-RAPHSON method. To do so, this equation has to be written in the form of a residual r as

$$r = \frac{A\tilde{E}}{L} \times \Delta u_2 - \Delta F_2 = \tilde{E}(u_2) \times \frac{A}{L} \times \Delta u_2 - \Delta F_2 = 0 \,. \tag{11.91}$$

If one develops the last equation into a TAYLOR's series and neglects the terms of higher order, the following form results

$$r(\Delta u_2^{(i+1)}) = r(\Delta u_2^{(i)}) + \left(\frac{\partial r}{\partial \Delta u_2}\right)^{(i)} \times \delta(\Delta u_2) + \cdots, \tag{11.92}$$

whereupon

$$\delta(\Delta u_2) = \Delta u_2^{(i+1)} - \Delta u_2^{(i)} \tag{11.93}$$

is valid and

$$\left(\frac{\partial r}{\partial \Delta u_2}\right)^{(i)} = K_T^{(i)} \tag{11.94}$$

represents the tangent stiffness matrix[22] in the i-th iteration step. Then Eq. (11.92) can also be written as

$$\delta(\Delta u_2) K_T^{(i)} = -r(\Delta u_2^{(i)}) = \Delta F^{(i)} - \frac{\tilde{E} A}{L} \Delta u_2^{(i)}. \tag{11.95}$$

Multiplication via $\left(K_T^{(i)}\right)^{-1}$ and the use of Eq. (11.93) finally leads to

$$\Delta u_2^{(i+1)} = \Delta F^{(i)} \times \frac{L}{\tilde{E} A}, \tag{11.96}$$

whereupon $\tilde{E} = E$ is valid in the elastic range (increment 1–3) and $\tilde{E} = E^{\text{elpl}}$ in the plastic range (increment 4–10).

Application of Eq. (11.96) leads to a value of $\Delta u_2 = 0.571429$ mm in the elastic range (increment 1–3) and in the plastic range (increment 4–10) a displacement increment of $\Delta u_2 = 6.285715$ mm occurs. It can be remarked at this point that the calculation of the displacement increments (increments 1–3 and 4–10) does not need an iteration and the application of Eq. (11.96) directly yields the desired result. As soon as the displacement increments (Δu_2) are calculated, the entire displacement on node 2 results via summation of the incremental values. Subsequently the strain in the element can be calculated via the relation $\varepsilon = \frac{1}{L}(u_2 - u_1)$, and the strain increments result through subtraction of two consecutive strain values (see Table 11.7).

The calculation of the stress and the plastic strain now requires that the CPP algorithm is used in each increment, based on the strain increment $\Delta\varepsilon$. The graphical illustration of the back projection is given in Fig. 11.16. One can see clearly that the strain increments at a force boundary condition differ in the elastic and plastic range. As

---

[22] In the considered example with linear hardening, $\tilde{E}$ is constant in the elastic range (increment 1–3) and in the plastic range (increment 4–10) and therefore not a function of u_2. In the general case however $\tilde{E}$ has to be differentiated as well.
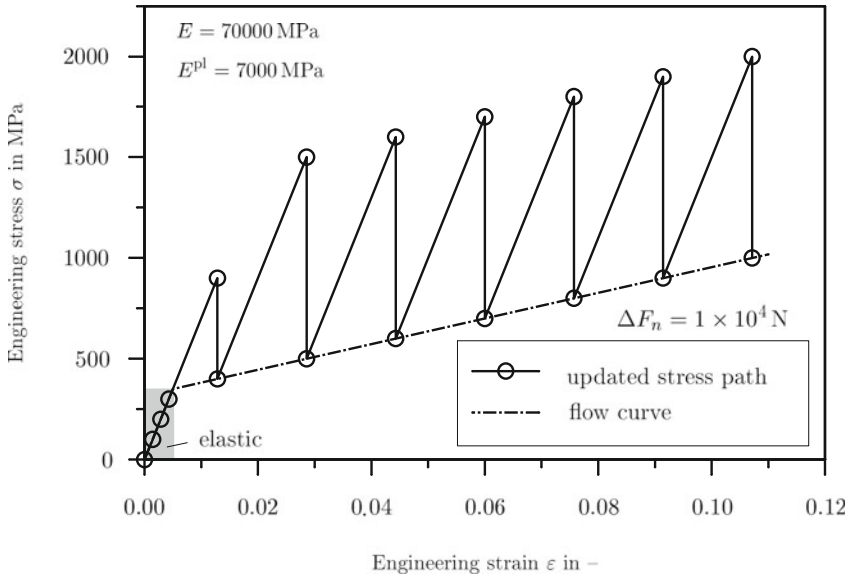
Fig. 11.16 Stress distribution in the case of the back projection for a continuum bar with linear hardening (10 increments, $\Delta F = 1 \times 10^4$)

a consequence, quite high values result for the test stress state in the plastic range. Thus for the increments 5–10 $\sigma_{n+1}^{\text{trial}} = \sigma_{n+1} + 1000$ MPa is valid (Table 11.6).

Table 11.6 Numerical values for one element in the case of linear hardening (10 increments; $\Delta F = 1 \times 10^4$ N)

inc	ex. Force	Δu_2	u_2	ε	$\Delta\varepsilon$	σ	ε^{pl}
–	10^4 N	mm	mm	10^{-2}	10^{-2}	MPa	10^{-2}
1	1.0	0.5714	0.5714	0.1429	0.1429	100.0	0.0
2	2.0	0.5714	1.1427	0.2857	0.1429	200.0	0.0
3	3.0	0.5714	1.7143	0.4286	0.1429	300.0	0.0
4	4.0	4.4286	5.1429	1.2857	0.8571	400.0	0.7143
5	5.0	6.2857	11.4286	2.8571	1.5714	500.0	2.1429
6	6.0	6.2857	17.7143	4.4286	1.5714	600.0	3.5714
7	7.0	6.2857	24.0000	6.0000	1.5714	700.0	5.0000
8	8.0	6.2857	30.2857	7.5714	1.5714	800.0	6.4286
9	9.0	6.2857	36.5714	9.1429	1.5714	900.0	7.8571
10	10.0	6.2857	42.8571	10.7143	1.5714	1000.0	9.2857

Particular attention is required at the transition from the elastic to the plastic regime, meaning from increment 3 to 4. Here the modulus $\tilde{E}$ is not defined clearly and Eq. (11.96) has to be solved iteratively. For the first cycle of the calculation (cycle $j = 0$) the arithmetic mean between the modulus of elasticity E and the elasto-plastic material modulus E^{elpl} can be applied. For the further cycles (cycle $j \geq 1$) $\tilde{E}$ can be approximated via an intermediate modulus (secant modulus, see Fig. 11.17).

Fig. 11.17 Definition of the intermediate modulus $\tilde{E}$ in the case of the transition from the elastic to the plastic range
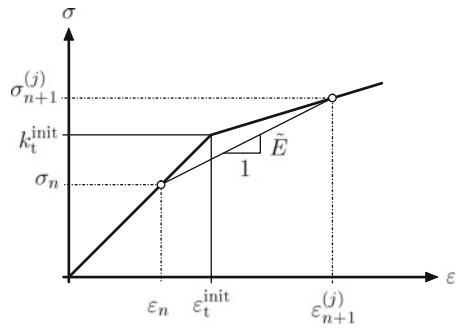
Therefore the following relation results as a calculation requirement for the intermediate modulus $\tilde{E}$ in the elasto-plastic transition regime (at this point in the considered example at the transition from increment 3 to 4):

$$
\tilde{E} = \begin{cases} \frac{E+E^{\text{elpl}}}{2} & \text{for } j = 0 \\[2mm] \frac{\sigma_{n+1}^{(j)} - \sigma_n}{\varepsilon_{n+1}^{(j)} - \varepsilon_n} & \text{for } j > 0 \end{cases}.
\tag{11.97}
$$

The numerical values of the intermediate modulus $\tilde{E}$ at the transition from increment 3 to 4 and the differences of the displacement, which result herefrom on node 2 are summarized in Table 11.7. Since an absolute displacement difference of 1×10^{-5} mm was required as convergence criteria, 18 cycles are necessary to iterate the difference between the new and old displacement on node 2 under these values. It can be considered at this point that the difference between the displacements on node 2 in the first cycle (cycle 0) result in $u_2^{\text{new}} - u_2^{\text{old}} = u_2^{(j=0)} - u_2|_{\text{inc } 3}$ and for the following cycles of the iteration via $u_2^{(j+1)} - u_2^{(j)}$.

The convergence behavior of the iteration rule is illustrated graphically in Fig. 11.18. An equidistant division was chosen in Fig. 11.18a and a logarithmic division (to be base 10) in Fig. 11.18b. One can see that quite a high convergence rate occurs at the beginning of the iteration, which flattens throughout the different cycles. At the chosen convergence criteria here of 10^{-5} the 18 iteration steps are therefore necessary, to finally reach the required absolute displacement difference. If one would require an absolute difference of 10^{-6} as convergence criteria, 21 iteration steps would be necessary.

11.3 Example: Back Projection for Bimaterial Bar

Two different material behaviors (see Fig. 11.19a) can be considered in the following to model a bimaterial bar (see Fig. 11.19 b) via the FE method. The right-hand end is displaced by $u = 8 \times 10^{-3}$ m hereby, whereupon the deformation is applied in 10 equal increments. The bar can be discretized with two finite elements hereby.

**Table 11.7** Numerical values for the transition from increment 3 to 4

cycle	$\tilde{E}^{(i)}$	$u_2^{\text{new}} - u_2^{\text{old}}$
–	MPa	mm
0	38181.84	1.048×10^{-0}
1	23719.00	6.388×10^{-1}
2	17145.00	6.466×10^{-1}
3	14157.16	4.925×10^{-1}
4	12798.56	2.999×10^{-1}
5	12181.16	1.584×10^{-1}
6	11900.52	7.744×10^{-2}
7	11772.96	3.642×10^{-2}
8	11715.00	1.682×10^{-2}
9	11688.64	7.699×10^{-3}
10	11676.64	3.511×10^{-3}
11	11671.20	1.598×10^{-3}
12	11668.72	7.270×10^{-4}
13	11667.60	3.305×10^{-4}
14	11667.08	1.503×10^{-4}
15	11666.88	6.831×10^{-5}
16	11666.76	3.105×10^{-5}
17	11666.72	1.411×10^{-5}
18	11666.68	6.416×10^{-6}
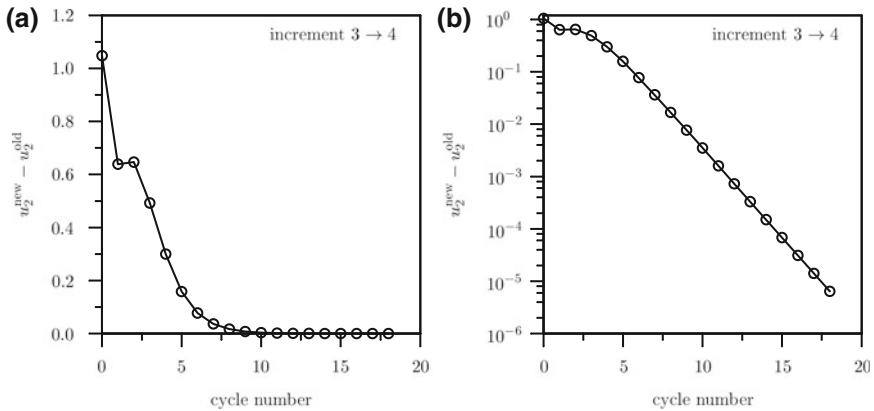
Fig. 11.18 Convergence behavior in the case of the transition from increment 3 to 4: **a** equidistant division; **b** logarithmic division of the absolute displacement difference

Examine the following material combinations:

(a) Material I: pure elastic; Material II: pure elastic,
(b) Material I: elasto-plastic; Material II: elasto-plastic,
(c) Material I: pure elastic; Material II: elasto-plastic,
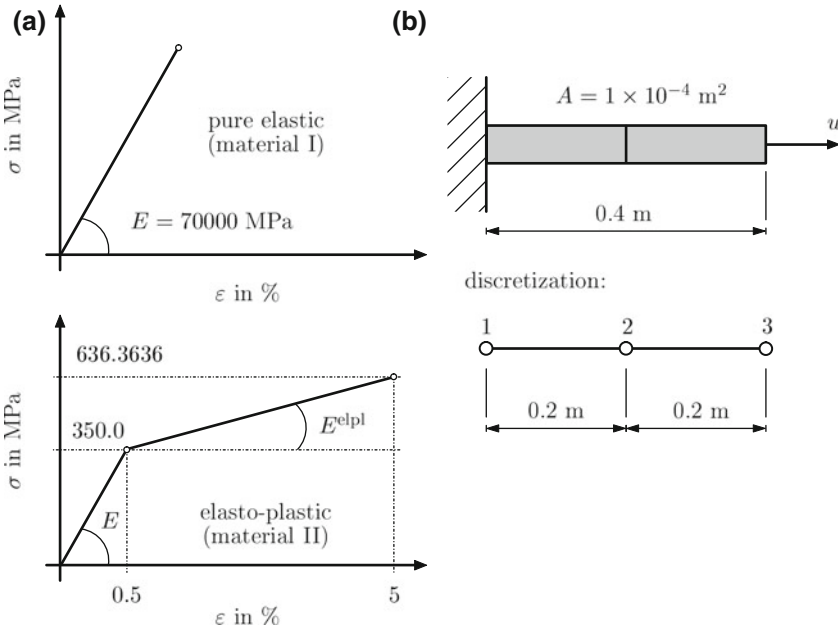
Fig. 11.19 Sample problem back projection in the case of a bar with different materials: **a** stress–strain distributions, **b** geometry and boundary conditions

to calculate the displacement of the middle node. Furthermore, calculate the stress state in each element with the help of the CPP algorithm and mark all values, which have to be updated.

11.3 Solution

When using two finite elements, the global system of equations, without consideration of the boundary conditions, results in the following incremental form for this example:

$$\frac{A}{L} \times \begin{bmatrix} \tilde{E}^{\mathrm{I}} & -\tilde{E}^{\mathrm{I}} & 0 \\ -\tilde{E}^{\mathrm{I}} & \tilde{E}^{\mathrm{I}} + \tilde{E}^{\mathrm{II}} & -\tilde{E}^{\mathrm{II}} \\ 0 & -\tilde{E}^{\mathrm{II}} & \tilde{E}^{\mathrm{II}} \end{bmatrix} \begin{bmatrix} \Delta u_1 \\ \Delta u_2 \\ \Delta u_3 \end{bmatrix} = \begin{bmatrix} \Delta F_1 \\ \Delta F_2 \\ \Delta F_3 \end{bmatrix}. \tag{11.98}$$

The consideration of the boundary condition on the left-hand side, meaning $u_1 = 0$, yields the following reduced global system of equations:

$$\frac{A}{L} \times \begin{bmatrix} \tilde{E}^{\mathrm{I}} + \tilde{E}^{\mathrm{II}} & -\tilde{E}^{\mathrm{II}} \\ -\tilde{E}^{\mathrm{II}} & \tilde{E}^{\mathrm{II}} \end{bmatrix} \begin{bmatrix} \Delta u_2 \\ \Delta u_3 \end{bmatrix} = \begin{bmatrix} \Delta F_2 \\ \Delta F_3 \end{bmatrix}. \tag{11.99}$$

The consideration of the displacement boundary condition on the right-hand side, meaning $u_3 = u(t)$, and that $\Delta F_2 = \Delta F_3 = 0$ is valid, yields:

$$\frac{A}{L} \times (\tilde{E}^{\mathrm{I}} + \tilde{E}^{\mathrm{II}})\Delta u_2 = \frac{\tilde{E}_2 A}{L} \Delta u_3 , \tag{11.100}$$

or

$$\left(\frac{\tilde{E}^{\mathrm{I}}}{\tilde{E}^{\mathrm{II}}} + 1\right)\Delta u_2 = \Delta u_3 . \tag{11.101}$$

For the application of the NEWTON-RAPHSON method, Eq. (11.101) is written as a residual equation:

$$r = \left(\frac{\tilde{E}^{\mathrm{I}}}{\tilde{E}^{\mathrm{II}}} + 1\right)\Delta u_2 - \Delta u_3 = 0 . \tag{11.102}$$

If one develops the last equation into a TAYLOR's series and neglects the terms of higher order according to the procedure in Example 11.2, finally the following iteration rule results for the definition of the displacement of the middle node:

$$\Delta u_2^{(i+1)} = \left(\frac{\tilde{E}^{\mathrm{I}}}{\tilde{E}^{\mathrm{II}}} + 1\right)^{-1} \times \Delta u_3^{(i)} . \tag{11.103}$$

In Eq. (11.103) in the elastic regime the elasticity modulus E has to be used for $\tilde{E}$ and in the plastic regime the elasto-plastic material modulus E^{elpl}.
Case (a) Material I: pure elastic; Material II: pure elastic:
For the case that both sections exhibit pure elastic material behavior with $E^{\mathrm{I}} = E^{\mathrm{II}}$, Eq. (11.103) simplifies in:

$$\Delta u_2^{(i+1)} = (1+1)^{-1} \times \Delta u_3^{(i)} = \frac{1}{2} \times \Delta u_3^{(i)} = 4\,\mathrm{mm} . \tag{11.104}$$

The strain in the left-hand element—which is identical with the strain in the right-hand element—can easily be defined via $\Delta\varepsilon = \frac{1}{200\,\mathrm{mm}} \times \Delta u_2$, and the stress results from the strain through multiplication with the modulus of elasticity. The results of this pure elastic calculation are summarized in Table 11.8.
In addition to the displacement, strain and stress values[23] Table 11.8 also contains the reaction forces on node 3. These reaction forces result due to multiplication of the stiffness matrix with the resultant vector of the displacements and have to be in equilibrium with the resulting forces from the stress: $F_{\mathrm{r},3} = \sigma A$.
Case (b) Material I: elasto-plastic; Material II: elasto-plastic:
For the case that both sections exhibit the same elasto-plastic material behavior, $\tilde{E}^{\mathrm{I}} = \tilde{E}^{\mathrm{II}}$ is always valid, and Eq. (11.103) also at this point yields a displacement

---

[23] One considers that in both sections or alternatively elements, the stress and strain are identical.

Table 11.8 Numerical values for a bimaterial bar in the case of pure linear-elastic behavior (10 increments; $\Delta u_3 = 0.8$ mm; $A = 100$ mm^2)

inc	Δu_2	u_2	$\Delta\varepsilon$	ε	σ	$F_{r,3}$
–	mm	mm	–	–	MPa	10^4 N
1	0.4	0.4	0.002	0.002	140.0	1.4
2	0.4	0.8	0.002	0.004	280.0	2.8
3	0.4	1.2	0.002	0.006	420.0	4.2
4	0.4	1.6	0.002	0.008	560.0	5.6
5	0.4	2.0	0.002	0.010	700.0	7.0
6	0.4	2.4	0.002	0.012	840.0	8.4
7	0.4	2.8	0.002	0.014	980.0	9.8
8	0.4	3.2	0.002	0.016	1120.0	11.2
9	0.4	3.6	0.002	0.018	1260.0	12.6
10	0.4	4.0	0.002	0.020	1400.0	14.0

increment on the middle node from $\Delta u_2^{(i+1)} = \frac{1}{2} \times \Delta u_3^{(i)} = 4$ mm or alternatively a strain increment of $\Delta\varepsilon = 0.002$. For the calculation of the stress and the plastic strain for element II in the non-linear regime, the CPP algorithm has to be made use of, as in Example 11.1. The corresponding values are summarized in Table 11.9.

Table 11.9 Numerical values for a bimaterial bar in the case of elasto-plastic behavior (10 Increments; $\Delta u_3 = 0.8$ mm; $A = 100$ mm^2)

inc	Δu_2	u_2	$\Delta\varepsilon$	ε	σ	ε^{pl}	$F_{r,3}$
–	mm	mm	–	–	MPa	10^{-3}	10^4 N
1	0.4	0.4	0.002	0.002	140.0	0.0	1.4
2	0.4	0.8	0.002	0.004	280.0	0.0	2.8
3	0.4	1.2	0.002	0.006	356.364	0.909091	3.56364
4	0.4	1.6	0.002	0.008	369.091	2.727273	3.69091
5	0.4	2.0	0.002	0.010	381.818	4.545455	3.81818
6	0.4	2.4	0.002	0.012	394.545	6.363636	3.94545
7	0.4	2.8	0.002	0.014	407.273	8.181818	4.07273
8	0.4	3.2	0.002	0.016	420.000	10.000000	4.20000
9	0.4	3.6	0.002	0.018	432.727	11.818182	4.32727
10	0.4	4.0	0.002	0.020	445.455	13.636364	4.45455

Case (c) Material I: pure elastic; Material II: elasto-plastic:
At this point in the elastic regime of both elements also it occurs that the displacement at the middle node amounts to half of the displacement, which occurred on the right-hand node. As soon as the plastic flow occurs in the right-hand half of the bar, $\tilde{E}^{I} \neq \tilde{E}^{II}$ occurs and for the right-hand half of the bar, the elasto-plastic material modulus has to be made use of. Therefore the calculation requirement for the displacement increment can be summarized as follows:

$$\Delta u_2^{(i+1)} = \begin{cases} \frac{1}{2} \times \Delta u_3^{(i)} & \text{in the elastic region} \\ \left(\frac{E^{I}}{E^{elpl,II}} + 1\right)^{-1} \times \Delta u_3^{(i)} & \text{in the plastic region} \end{cases} . \qquad (11.105)$$

Table 11.10 Numerical values for a bimaterial bar in the case of different material behavior (10 Increments; $\Delta u_3 = 0.8$ mm; $A = 100$ mm^2)

inc	Δu_2	u_2	ε^{I}	ε^{II}	σ^{I}	σ^{II}	$\varepsilon^{\text{pl,I}}$	$\varepsilon^{\text{pl,II}}$	$F_{\text{r},3}$
–	mm	mm	10^{-3}	10^{-3}	MPa	MPa	10^{-3}	10^{-3}	10^4 N
1	0.4	0.4	2.0	2.0	140.0	140.0	0.0	0.0	1.4
2	0.4	0.8	4.0	4.0	280.0	280.0	0.0	0.0	2.8
3	0.23333	1.03333	5.16667	6.83333	361.667	361.667	0.0	1.66667	3.61667
4	0.06667	1.10000	5.50000	10.50000	385.000	385.000	0.0	5.00000	3.85000
5	0.06667	1.16667	5.83333	14.16667	408.333	408.333	0.0	8.33333	4.08333
6	0.06667	1.23333	6.16667	17.83333	431.667	431.667	0.0	11.66667	4.31667
7	0.06667	1.30000	6.50000	21.50000	455.000	455.000	0.0	15.00000	4.55000
8	0.06667	1.36667	6.83333	25.16667	478.333	478.333	0.0	18.33333	4.78333
9	0.06667	1.43333	7.16667	28.83333	501.667	501.667	0.0	21.66667	5.01667
10	0.06667	1.50000	7.50000	32.50000	525.000	525.000	0.0	25.00000	5.25000

Table 11.11 Numerical values for transition from increment 2 to 3

cycle	$\tilde{E}^{\text{II},(i)}$	$\Delta u_2^{(i)}$	$u_2^{(i)}$	$|u_2^{\text{new}} - u_2^{\text{old}}|$	$\varepsilon^{\text{II},(i)}$	$\Delta \varepsilon^{\text{II},(i)}$	$\sigma^{\text{II},(i)}$
–	MPa	mm	mm	10^{-2}mm	10^{-3}	10^{-3}	MPa
0	38181.82	0.282353	1.082353	28.235294	6.588235	2.588235	360.1070
1	30950.41	0.245272	1.045272	3.708073	6.773639	2.773639	361.2868
2	29306.91	0.236092	1.036092	0.918059	6.819542	2.819542	361.5789
3	28933.39	0.233962	1.033963	0.212904	6.830187	2.830187	361.6466
4	28848.50	0.233476	1.033476	0.0486115	6.832618	2.832618	361.6621
5	28829.20	0.233366	1.033366	0.0110598	6.833171	2.833171	361.6656
6	28824.82	0.233341	1.033341	0.0025142	6.833296	2.833296	361.6664
7	28823.82	0.233335	1.033335	0.0005714	6.833325	2.833325	361.6666

The total displacement at the middle node results from the displacement increments through summation and the strain for each element can be defined via $\varepsilon = \frac{1}{L}(-u_{\text{l}} + u_{\text{r}})$ (Index 'l' for left-hand and index 'r' for right-hand node of the bar element). As soon as the right-hand part of the bar enters the plastic region, the predictor-corrector method has to be made use of to be able to calculate the state variables. The numerical values of the incremental solution method are summarized in Table 11.10. At this point it can be remarked that in the plastic region a similar relation as in the elastic region can be set to calculate the stress increment from the strain increment (see Eq. 11.106). However thereby it has to be considered that the modulus of elasticity has to be substituted by the elasto-plastic material modulus (Table 11.11):

$$\Delta \sigma = \begin{cases} \Delta \varepsilon \times E & \text{in the elastic region} \\ \Delta \varepsilon \times E^{\text{elpl}} & \text{in the plastic region} \end{cases}. \tag{11.106}$$

The transition from the elastic to the plastic region, meaning from increment 2 to 3, demands a special consideration at this point. The intermediate modulus $\tilde{E}^{\text{II}}$ hereby has to be calculated according to Eq. (11.97), to be able to define the displacement increment subsequently according to Eq. (11.105)$_2$. The absolute displacement on

the middle node results from the summation, meaning $u_2^{(i)} = \Delta u_2^{(i)} + u_2|_{\text{inc 2}}$. The difference of the displacement on the middle node has to be determined in the first cycle (cycle 0) via $|u_2^{(i=0)} - u_2|_{\text{inc 2}}$ and for each further cycle (i) via $|u_2^{(i)} - u_2^{(i-1)}|$. The calculation of the strain in the right-hand half of the bar can occur via the given boundary condition u_3 via $\varepsilon^{\text{II},(i)} = \frac{1}{L}\left(-u_2^{(i)} + u_3\right)$. Finally the stress results via the CPP algorithm, based on the strain increment $\Delta\varepsilon^{\text{II},(i)} = \varepsilon^{\text{II},(i)} - \varepsilon^{\text{II}}|_{\text{inc 2}}$. If the stress and strains are known, the new intermediate modulus can be determined for the next cycle via Eq. (11.97). As convergence criteria for the absolute displacement difference a value of 10^{-5} was given within this example.

11.5.2 Supplementary Problems

11.4 Plastic Modulus and Elasto-Plastic Material Modulus
Discuss the case (a) $E^{\text{pl}} = E$ and (b) $E^{\text{elpl}} = E$.

11.5 Back Projection at Linear Hardening
Calculate Example 11.1 for the following linear flow curve of a steal:
$k(\kappa) = (690 + 21000\kappa)$ MPa. The modulus of elasticity amounts 210000 MPa. The geometric dimensions of Example 11.1 can be assumed.

(a) For 10 increments with $\Delta\varepsilon = 0.001$,
(b) For 20 increments with $\Delta\varepsilon = 0.0005$,
(c) For 20 increments with $\Delta\varepsilon = 0.001$.

Compare and interpret all the results.

11.6 Back Projection at Non-Linear Hardening
Calculate Example 11.1 for the following non-linear flow curve:
$k(\kappa) = (350 + 12900\kappa - 1.25 \times 10^5\kappa^2)$ MPa. All other parameters can be taken as in Example 11.1.

11.7 Back Projection for Bar at Fixed Support at Both Ends
Calculate for the illustrated bar in Fig. 11.20 with fixed support at both ends, the displacement of the point of load application. The bar has an elasto-plastic material behavior ($E = 1 \times 10^5$ MPa; $E^{\text{elpl}} = 1 \times 10^3$ MPa; $k_{\text{t}}^{\text{init}} = 200$ MPa) and a force of $F = 6 \times 10^4$ N is applied in 3 increments equally. It can be assumed that the material behavior is identical under tensile and compression loading. Calculate the displacement of the point of load application and determine the stress and strain in both elements. As convergence criteria an absolute displacement difference on the point of load application of 10^{-5} mm can be given.
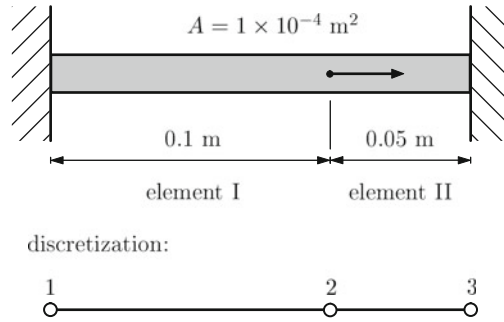
Fig. 11.20 Sample problem back projection for a bar with fixed supports at both ends

11.8 Back Projection for a Finite Element at Ideal-Plastic Material Behavior

Discuss the case of a single finite element with force boundary condition at ideal-plastic material behavior. It can be assumed thereby that the applied force increases linearly starting with zero. The problem and the material behavior are schematically illustrated in Fig. 11.21. Why is no convergence achieved in the plastic region at the force boundary condition? What changes if the force boundary condition is substituted by a displacement boundary condition?
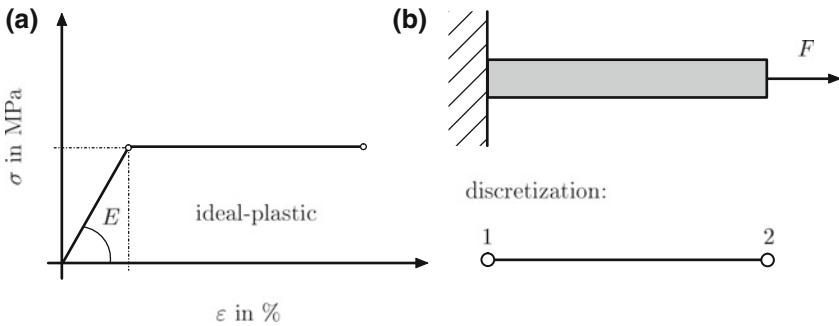
Fig. 11.21 Sample problem back projection for a finite element in the case of ideal-plastic material behavior: **a** material behavior and **b** general configuration

References

1. Simo JC, Hughes TJR (1998) Computational inelasticity. Springer, New York
2. Drucker DC et al (1952) A more fundamental approach to plastic stress–strain relations. In: Sternberg E (ed) Proceedings of the 1st US national congress for applied mechanics. Edward Brothers Inc, Michigan, p 491
3. Betten J (2001) Kontinuumsmechanik. Springer, Berlin
4. de Borst R (1986) Non-linear analysis of frictional materials. Delft University of Technology, Dissertation

5. Belytschko T, Liu WK, Moran B (2000) Nonlinear finite elements for continua and structures. Wiley, Chichester

6. Mang H, Hofstetter G (2008) Festigkeitslehre. Springer, Wien

7. Altenbach H, Altenbach J, Zolochevsky A (1995) Erweiterte Deformationsmodelle und Versagenskriterien der Werkstoffmechanik. Deutscher Verlag für Grundstoffindustrie, Stuttgart

8. Jirásek M, Bazant ZP (2002) Inelastic analysis of structures. Wiley, Chichester

9. Chakrabarty J (2009) Applied plasticity. Springer, New York

10. Yu M-H, Zhang Y-Q, Qiang H-F, Ma G-W (2006) Generalized plasticity. Springer, Berlin

11. Wriggers P (2001) Nichtlineare finite-element-methoden. Springer, Berlin

12. Crisfield MA (2001) Non-linear finite element analysis of solids and structures. Bd. 1: essentials. Wiley, Chichester.

13. Crisfield MA (2000) Non-linear finite element analysis of solids and structures. Bd. 2: advanced topics. Wiley, Chichester.

14. de Souza Neto EA, Perić D, Owen DRJ (2008) Computational methods for plasticity: theory and applications. Wiley, Chichester

15. Dunne F, Petrinic N (2005) Introduction to computational plasticity. Oxford University Press, Oxford

16. Simo JC, Ortiz M (1985) A unified approach to finite deformation elastoplasticity based on the use of hyperelastic constitutive equations. Comput Method Appl M 49:221–245

17. Ortiz M, Popov EP (1985) Accuracy and stability of integration algorithms for elastoplastic constitutive equations. Int J Num Meth Eng 21:1561–1576

18. Moran B, Ortiz M, Shih CF (1990) Formulation of implicit finite element methods for multiplicative finite deformation plasticity. Int J Num Meth Eng 29:483–514

19. Betten J (1979) Über die Konvexität von Fließkörpern isotroper und anisotroper Stoffe. Acta Mech 32:233–247

20. Lubliner J (1990) Plasticity theory. Macmillan Publishing Company, New York

21. Balankin AS, Bugrimov AL (1992) A fractal theory of polymer plasticity. Polym Sci 34:246–248

22. Spencer AJM (1992) Plasticity theory for fibre-reinforced composites. J Eng Math 26:107–118

23. Chen WF, Baladi GY (1985) Soil plasticity. Elsevier, Amsterdam

24. Chen WF, Liu XL (1990) Limit analysis in soil mechanics. Elsevier, Amsterdam

25. Chen WF (1982) Plasticity in reinforced concrete. McGraw-Hill, New York

Chapter 12
Stability (Buckling)

Abstract In common and technical parlance the term stability is used in many ways. Here it is restricted to the static stability of elastic structures. The derivations concentrate on elastic bars and beams. The initial situation is a loaded elastic structure. If the acting load remains under a critical value, the structure reacts 'simple' and one can describe the reaction with the models and equations of the preceding chapters. If the load reaches or exceeds the critical value, bars and beams begin to buckle. The situation becomes ambiguous, beyond the initial situation several equilibrium positions can exist. From the technical application the smallest load is critical for which buckling in either bars or beams appears.

12.1 Stability in Bar/Beam

The initial situation is a structure, which consists of bars and beams. Bars and beams are connected through nodes grids, through which forces and moments are introduced into each single element. As long as the loads lie on an element lower than the critical limit, the element reacts linear elastic. If, however, a critical value is reached or exceeded, buckling occurs. Figure 12.1 illustrates various situations when buckling can occur.

For the analysis of the stability performance several description possibilities are available [1–4]. In the following the energy-approach is used.

The total potential Π of a bar or beam can be generally described as

$$\Pi = \frac{1}{2}\boldsymbol{u}^{\mathrm{T}}\boldsymbol{K}\boldsymbol{u} - \boldsymbol{u}^{\mathrm{T}}\boldsymbol{F}, \tag{12.1}$$

where $\boldsymbol{u}$ stands for the vector of deformation, $\boldsymbol{K}$ for the stiffness matrix and $\boldsymbol{F}$ for the vector of external loads. In an equilibrium state the entire potential energy Π of a system is stationary. For a stationary value of Π the first variation $\delta\Pi$ has to disappear:

(a) **(b)**
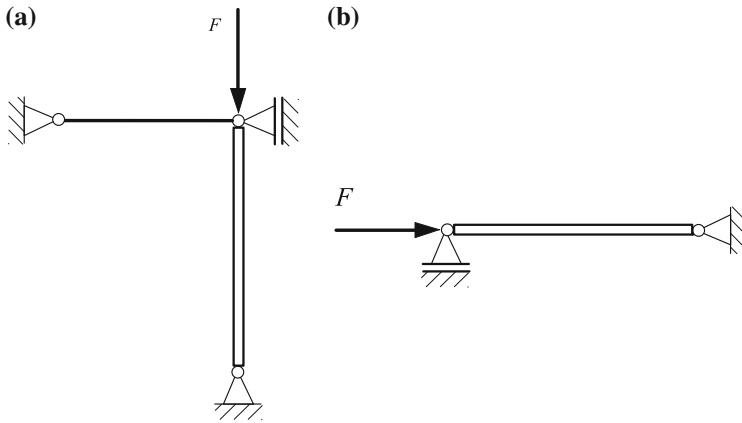
Fig. 12.1 Buckling of structures at **a** two elements **b** one element

$$\delta \Pi = \frac{\partial \Pi}{\partial \boldsymbol{u}} \delta \boldsymbol{u} \overset{!}{=} 0. \tag{12.2}$$

For the clarification of the type of the stationary value the second variation of the potential has to be analyzed. Three states of equilibrium arise, see Fig. 12.2.

| stable | indifferent | unstable |
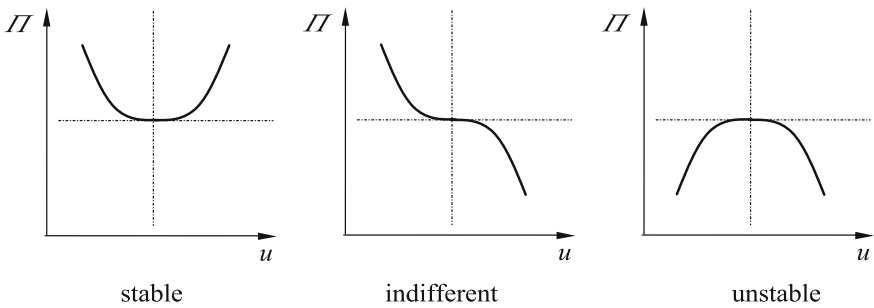
Fig. 12.2 Stability: states of equilibrium

In the case of $\delta^2 \Pi > 0$ a stable equilibrium occurs. If the second variation disappears, one talks about an indifferent or neutral equilibrium. In the case of $\delta^2 \Pi < 0$ an unstable equilibrium exists. When buckling of bars and beams occurs, one assumes an indifferent balance. The second variation is called:

$$\delta^2 \Pi = \frac{\partial^2 \Pi}{\partial \boldsymbol{u}^2} \delta^2 \boldsymbol{u} = 0. \tag{12.3}$$

The demand for the second variation of Π to disappear can solely be fulfilled if the determinant of $\boldsymbol{K}$ becomes 0.

The stiffness matrix K for large deformations consists of an elastic and geometric fraction:

$$K = K^{el} + K^{geo}. \tag{12.4}$$

K^{el} stands for the stiffness matrix, which serves as a basis in the description of the linear elastic reaction. It is already known from the previous paragraphs. The assembly of K^{el} is independent of the axial load. In contrast, K^{geo} contains the axial load F as a prefactor. The detailed derivation of the geometric stiffness matrix K^{geo} follows later on.

If this force is scaled with a factor λ, one obtains:

$$K = K^{el} + \lambda \tilde{K}^{geo}. \tag{12.5}$$

The requirement that the determinant K has to disappear leads to:

$$\det(K) = \det\left[K^{el} + \lambda \tilde{K}^{geo}\right] \overset{!}{=} 0. \tag{12.6}$$

With this equation, an eigenvalue problem is formulated, where λ represents the unknown value. The formation of the determinant leads to a scalar function in λ, which is called the characteristic equation. It is obvious that this equation does not just possess a single eigenvalue. The roots of the characteristic equation correspond with the eigenvalues of the problem. The expression λF stands for the so-called buckling load. From a technical point of view, the smallest eigenvalue and therefore the smallest buckling load are interesting.

12.2 Large Deformations

Thus far, it was assumed that the occurring deformations are small. Equilibrium was established on the undeformed body. Within the discussion of nonlinear problems however, large deformations can occur. Those will now be described in more detail. The linear relation between the deformations and strains will be complemented by the nonlinear term in the strain-deformation relation

$$\varepsilon = \frac{1}{2}(\nabla u^T + u\nabla^T) + \frac{1}{2}(\nabla u^T \times u\nabla^T). \tag{12.7}$$

The second addend expresses the nonlinear term. During large deformations of the considered bars and beams a deformation in axial direction as well as another deformation occur. The complete strain matrix is called:

$$\varepsilon = \begin{bmatrix} \varepsilon_{xx} & \varepsilon_{xy} \\ \varepsilon_{yx} & \varepsilon_{yy} \end{bmatrix} \tag{12.8}$$

and results from:

$$\varepsilon = \frac{1}{2}\left[\left[\begin{array}{c}\frac{\partial}{\partial x}\\\frac{\partial}{\partial y}\end{array}\right](u_x\,u_y) + \begin{pmatrix}u_x\\u_y\end{pmatrix}\left[\begin{array}{cc}\frac{\partial}{\partial x} & \frac{\partial}{\partial y}\end{array}\right]\right] \tag{12.9}$$

$$+ \frac{1}{2}\left[\left[\begin{array}{c}\frac{\partial}{\partial x}\\\frac{\partial}{\partial y}\end{array}\right](u_x\,u_y) \times \begin{pmatrix}u_x\\u_y\end{pmatrix}\left[\begin{array}{cc}\frac{\partial}{\partial x} & \frac{\partial}{\partial y}\end{array}\right]\right]. \tag{12.10}$$

For further considerations only the elongation ε_{xx} towards the bar or beam axis is of relevance. This component can be extracted as

$$\varepsilon_{xx} = \frac{\mathrm{d}u_x}{\mathrm{d}x} + \frac{1}{2}\left[\left(\frac{\mathrm{d}u_x}{\mathrm{d}x}\right)^2 + \left(\frac{\mathrm{d}u_y}{\mathrm{d}x}\right)^2\right] \tag{12.11}$$

from the complete strain matrix. Under the condition $\mathrm{d}u_x/\mathrm{d}x \ll 1$ as well as $(\mathrm{d}u_x/\mathrm{d}x)^2 \ll (\mathrm{d}u_y/\mathrm{d}x)^2$ the entire term simplifies itself to

$$\varepsilon_{xx} = \frac{\mathrm{d}u_x}{\mathrm{d}x} + \frac{1}{2}\left(\frac{\mathrm{d}u_y}{\mathrm{d}x}\right)^2. \tag{12.12}$$

This relation for the strain can be used directly for bars. For beams, the complete deformation results from two parts

$$u_x = u_{xs} + u_{xb}. \tag{12.13}$$

The first term represents the amount of deformation on the neutral axis of the beam. The second term represents the amount of pure bending and can be described as

$$u_{xb} = -y\frac{\mathrm{d}u_y}{\mathrm{d}x}. \tag{12.14}$$

With that said, the entire strain of the beam is represented in the following form:

$$\varepsilon_{xx} = \frac{\mathrm{d}u_{xs}}{\mathrm{d}x} - y\frac{\mathrm{d}^2u_y}{\mathrm{d}x^2} + \frac{1}{2}\left(\frac{\mathrm{d}u_y}{\mathrm{d}x}\right)^2. \tag{12.15}$$

The elastic strain energy of the bar can be formulated as

$$\Pi_{\mathrm{int}} = \frac{1}{2}\int_{\Omega} E\varepsilon_{xx}^2\,\mathrm{d}\Omega = \int_{\Omega} E\left[\frac{\mathrm{d}u_x}{\mathrm{d}x} + \frac{1}{2}\left(\frac{\mathrm{d}u_y}{\mathrm{d}x}\right)^2\right]^2\,\mathrm{d}\Omega \tag{12.16}$$

through the strains. After a few transformations the strain energy converts itself into the following:

$$\Pi_{\text{int}} = \frac{1}{2} A E \int_L \left(\frac{\mathrm{d}u_x}{\mathrm{d}x} \right)^2 \mathrm{d}x + \frac{1}{2} F \int_L \left(\frac{\mathrm{d}u_y}{\mathrm{d}x} \right)^2 \mathrm{d}x. \tag{12.17}$$

The elastic strain energy of the beam can be formulated as

$$\Pi_{\text{int}} = \int_\Omega E \varepsilon_{xx}^2 \mathrm{d}\Omega = \int_\Omega E \left[\frac{\mathrm{d}u_{xs}}{\mathrm{d}x} - y \frac{\mathrm{d}^2 u_y}{\mathrm{d}x^2} + \frac{1}{2} \left(\frac{\mathrm{d}u_y}{\mathrm{d}x} \right)^2 \right]^2 \mathrm{d}\Omega \tag{12.18}$$

through the strains. After a few transformations the strain energy converts itself into the following:

$$\Pi_{\text{int}} = \frac{1}{2} A E \int_L \left(\frac{\mathrm{d}u_{xs}}{\mathrm{d}x} \right)^2 \mathrm{d}x + \frac{1}{2} E I \int_L \left(\frac{\mathrm{d}^2 u_y}{\mathrm{d}x^2} \right)^2 \mathrm{d}x + \frac{1}{2} F \int_L \left(\frac{\mathrm{d}u_y}{\mathrm{d}x} \right)^2 \mathrm{d}x. \tag{12.19}$$

The 1st and 3rd term is equivalent to the strain energy of the bar. The 2nd term is equivalent to the energy fraction of the bending.

12.3 Stiffness Matrices in Large Deformations

As for the small deformations, it should also be assumed that for large deformations the course through the nodal values and form functions can be described. Figure 12.3 shows the kinematical quantities, which are relevant for buckling.

Fig. 12.3 State variables for buckling behavior
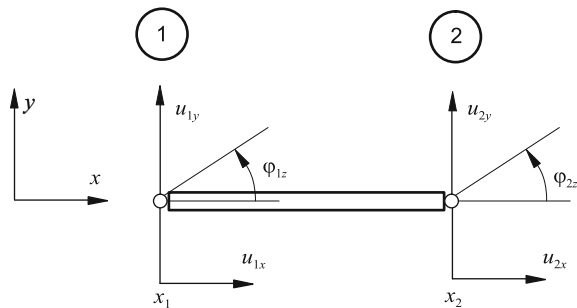
In general, various shape functions can be used for different directions of the displacement:

$$u_x(x) = N_x(x)u_p, \tag{12.20}$$

$$u_y(x) = N_y(x)u_p. \tag{12.21}$$

In the following, the stiffness matrices for large deformations for the bar and the beam will be derived.

12.3.1 Bar with Large Deformations

Within the strains according to the Eq. (12.12) the first derivatives du_x/dx and du_y/dx occur. These lead to

$$\frac{du_x(x)}{dx} = \frac{d}{dx}N_x(x)u_p = N'_x(x)u_p, \tag{12.22}$$

$$\frac{du_y(x)}{dx} = \frac{d}{dx}N_y(x)u_p = N'_y(x)u_p. \tag{12.23}$$

In discretized form the entire potential can be formulated as

$$\Pi = \frac{1}{2}u_p^T \underbrace{A E \int_L N_x'^T N_x' dx}_{K^{\text{el, bar}}} u_p + \frac{1}{2}u_p^T \underbrace{F \int_L N_y'^T N_y' dx}_{K^{\text{geo, bar}}} u_p - u_p^T F. \tag{12.24}$$

The stiffness matrices can be determined from Eq. (12.24). The submatrices result in:

$$K^{\text{el, bar}} = A E \int_L N_x'^T N_x' dx, \tag{12.25}$$

$$K^{\text{geo, bar}} = F \int_L N_y'^T N_y' dx. \tag{12.26}$$

Depending on the type of shape function, different stiffness matrices result. The shape functions for the displacement field $u_x(x)$ are described in Chap. 3. With

$$u_y(x) = N_1(x)u_{1y} + N_2(x)u_{2y} = [0 \quad N_1(x) \quad 0 \quad N_2(x)] \begin{bmatrix} u_{1x} \\ u_{1y} \\ u_{2x} \\ u_{2y} \end{bmatrix} \tag{12.27}$$

an appropriate approach for the displacement field $\boldsymbol{u}_y(x)$ is chosen. First of all, with

$$N_1(x) = \frac{1}{L}(x_2 - x) \quad \text{and} \quad N_2(x) = \frac{1}{L}(x - x_1) \tag{12.28}$$

a simple, linear approach for the deformation perpendicular to the principal bar axis is chosen. The derivatives of the shape functions $\boldsymbol{N}'_y$ is needed in Eq. (12.26). These result in:

$$\frac{\partial \boldsymbol{N}_y(x)}{\partial x} = \begin{bmatrix} 0 & \dfrac{\partial N_1(x)}{\partial x} & 0 & \dfrac{\partial N_2(x)}{\partial x} \end{bmatrix} = \begin{bmatrix} 0 & -\dfrac{1}{L} & 0 & +\dfrac{1}{L} \end{bmatrix}. \tag{12.29}$$

With this, the integration $\int_L \boldsymbol{N}'^{\mathrm{T}}_y \boldsymbol{N}'_y \mathrm{d}x$ can be conducted. The geometric stiffness matrix, in dependence on the external load F results in:

$$\boldsymbol{K}^{\mathrm{geo, bar}} = F \int_L \frac{1}{L^2} \begin{bmatrix} 0 & 0 & 0 & 0 \\ 0 & 1 & 0 & -1 \\ 0 & 0 & 0 & 0 \\ 0 & -1 & 0 & -1 \end{bmatrix} \mathrm{d}x = \frac{F}{L} \begin{bmatrix} 0 & 0 & 0 & 0 \\ 0 & 1 & 0 & -1 \\ 0 & 0 & 0 & 0 \\ 0 & -1 & 0 & -1 \end{bmatrix}. \tag{12.30}$$

With this, the overall stiffness matrix can be assembled through two submatrices

$$\boldsymbol{K}^{\mathrm{bar}} = \frac{EA}{L} \begin{bmatrix} 1 & 0 & -1 & 0 \\ 0 & 0 & 0 & 0 \\ -1 & 0 & 1 & 0 \\ 0 & 0 & 0 & 0 \end{bmatrix} + \frac{F}{L} \begin{bmatrix} 0 & 0 & 0 & 0 \\ 0 & 1 & 0 & -1 \\ 0 & 0 & 0 & 0 \\ 0 & -1 & 0 & 1 \end{bmatrix}. \tag{12.31}$$

12.3.2 Beams with Large Deformations

In the strains according to Eq. (12.15) the first derivatives $\mathrm{d}u_{xs}/\mathrm{d}x$ and $\mathrm{d}u_y/\mathrm{d}x$ as well as the second derivative $\mathrm{d}^2 u_y/\mathrm{d}u_y^2$ occur. These result in

$$\frac{\mathrm{d}u_{xs}(x)}{\mathrm{d}x} = \frac{\mathrm{d}}{\mathrm{d}x} N_x(x) \boldsymbol{u}_{\mathrm{p}} = \boldsymbol{N}'_x(x) \boldsymbol{u}_{\mathrm{p}}, \tag{12.32}$$

$$\frac{\mathrm{d}u_y(x)}{\mathrm{d}x} = \frac{\mathrm{d}}{\mathrm{d}x} N_y(x) \boldsymbol{u}_{\mathrm{p}} = \boldsymbol{N}'_y(x) \boldsymbol{u}_{\mathrm{p}}, \tag{12.33}$$

$$\frac{\mathrm{d}^2 u_y(x)}{\mathrm{d}x^2} = \frac{\mathrm{d}^2}{\mathrm{d}x^2} N_y(x) \boldsymbol{u}_{\mathrm{p}} = \boldsymbol{N}''_y(x) \boldsymbol{u}_{\mathrm{p}}. \tag{12.34}$$

With this, the entire potential can be presented in discretized form as

$$\Pi = \frac{1}{2}\boldsymbol{u}_{\mathrm{p}}^{\mathrm{T}} A E \underbrace{\int_{L} \boldsymbol{N}_{x}'^{\mathrm{T}} \boldsymbol{N}_{x}' \mathrm{d}x}_{\boldsymbol{K}^{\mathrm{el,\,bar}}} \boldsymbol{u}_{\mathrm{p}} + \frac{1}{2}\boldsymbol{u}_{\mathrm{p}}^{\mathrm{T}} E I \underbrace{\int_{L} \boldsymbol{N}_{y}''^{\mathrm{T}} \boldsymbol{N}_{y}'' \mathrm{d}x}_{\boldsymbol{K}^{\mathrm{el,\,bending}}} \boldsymbol{u}_{\mathrm{p}}$$

$$+ \frac{1}{2}\boldsymbol{u}_{\mathrm{p}}^{\mathrm{T}} F \underbrace{\int_{L} \boldsymbol{N}_{y}'^{\mathrm{T}} \boldsymbol{N}_{y}' \mathrm{d}x}_{\boldsymbol{K}^{\mathrm{geo}}} \boldsymbol{u}_{\mathrm{p}} - \boldsymbol{u}_{\mathrm{p}}^{\mathrm{T}} \boldsymbol{F}. \tag{12.35}$$

The elastic stiffness matrix $\boldsymbol{K}^{\mathrm{el}}$ consists of the fractions $\boldsymbol{K}^{\mathrm{el,\,bar}}$ and $\boldsymbol{K}^{\mathrm{el,\,bending}}$. The geometric stiffness matrix $\boldsymbol{K}^{\mathrm{geo}}$ is represented in the third term. The stiffness matrices can be calculated through Eq. (12.35). The submatrices result in:

$$\boldsymbol{K}^{\mathrm{el,\,bar}} = A E \int_{L} \boldsymbol{N}_{x}'^{\mathrm{T}} \boldsymbol{N}_{x}' \mathrm{d}x, \tag{12.36}$$

$$\boldsymbol{K}^{\mathrm{el,\,bending}} = E I \int_{L} \boldsymbol{N}_{y}''^{\mathrm{T}} \boldsymbol{N}_{y}'' \mathrm{d}x, \tag{12.37}$$

$$\boldsymbol{K}^{\mathrm{geo}} = F \int_{L} \boldsymbol{N}_{y}'^{\mathrm{T}} \boldsymbol{N}_{y}' \mathrm{d}x. \tag{12.38}$$

According to the usual procedure the fraction from the elongation of the bar is approximatively disregarded when describing the beam. For further considerations only the fraction from the bending is considered. Depending on the type of shape function different stiffness matrices occur. The general approach was already introduced in Chap. 5 and reads as follows:

$$\boldsymbol{u}_{y}(x) = N_{1}(x)u_{1y} + N_{2}(x)\varphi_{1} + N_{3}(x)u_{2y} + N_{4}(x)\varphi_{2}. \tag{12.39}$$

A cubic approach for the deformation perpendicular to the axial direction is chosen. The following shape functions are already known through Chap. 5

$$N_{1}(x) = 1 - 3\frac{x^{2}}{L^{2}} + 2\frac{x^{3}}{L^{3}},$$
$$N_{2}(x) = x - 2\frac{x^{2}}{L} + \frac{x^{3}}{L^{2}},$$
$$N_{3}(x) = 3\frac{x^{2}}{L^{2}} - 2\frac{x^{3}}{L^{3}},$$
$$N_{4}(x) = -\frac{x^{2}}{L} + \frac{x^{3}}{L^{2}}. \tag{12.40}$$

The derivatives of the shape functions N'_y are needed in Eq. (12.35). These result in:

$$\frac{\partial N_1(x)}{\partial x} = -6\frac{x}{L^2} + 6\frac{x^2}{L^3},$$

$$\frac{\partial N_2(x)}{\partial x} = 1 - 4\frac{x}{L} + 3\frac{x^2}{L^2},$$

$$\frac{\partial N_3(x)}{\partial x} = 6\frac{x}{L^2} - 6\frac{x^2}{L^3},$$

$$\frac{\partial N_4(x)}{\partial x} = -2\frac{x}{L} + 3\frac{x^2}{L^2}. \tag{12.41}$$

With this, the integration $\int_L N'^{T}_y N'_y \, dx$ can be done. The integration is shown as an example using the matrix element $(1,1)$:

$$k_{11} = \int_0^L \left(-\frac{6x}{L^2} + \frac{6x^2}{L^3}\right)^2 dx = \frac{36}{L^2}\int_0^L \left(-x + \frac{x^2}{L}\right)^2 dx$$

$$= \frac{36}{L^2}\left[\frac{1}{3}x^3 - \frac{1}{2L}x^4 + \frac{1}{5L^2}x^5\right]_0^L = \frac{36}{L^2}\frac{L^3}{30} = \frac{36}{30L}. \tag{12.42}$$

The geometric stiffness matrix, depending on the external load F results in:

$$\boldsymbol{K}^{\text{geo}} = \frac{F}{30L}\begin{bmatrix} 36 & 3L & -36 & 3L \\ & 4L^2 & -3L & -L^2 \\ & & 36 & -3L^2 \\ \text{sym.} & & & 4L^2 \end{bmatrix}. \tag{12.43}$$

The entire stiffness matrix therefore consists of the two submatrices

$$\boldsymbol{K} = \frac{EI}{L^3}\begin{bmatrix} 12 & 6L & -12 & 6L \\ 6L & 4L^2 & -6L & 2L^2 \\ -12 & -6L & 12 & -6L \\ 6L & 2L^2 & -6L & 4L^2 \end{bmatrix} + \frac{F}{30L}\begin{bmatrix} 36 & 3L & -36 & 3L \\ 3L & 4L^2 & -3L & -L^2 \\ -36 & -3L & 36 & -3L^2 \\ 3L & -L^2 & -3L^2 & 4L^2 \end{bmatrix}. \tag{12.44}$$

12.4 Examples of Buckling: The Four Euler's Buckling Loads

Given is a prismatic beam, which is loaded with a concentrated force F in axial direction on one end. The beam has a cross-sectional area A, the second moment of area I and the modulus of elasticity E. All factors are constant along the body axis. Required are the critical load F_{crit} and the buckling length L_{crit}, respectively (Fig. 12.4). The four EULER's buckling cases vary according to the boundary conditions on both ends.
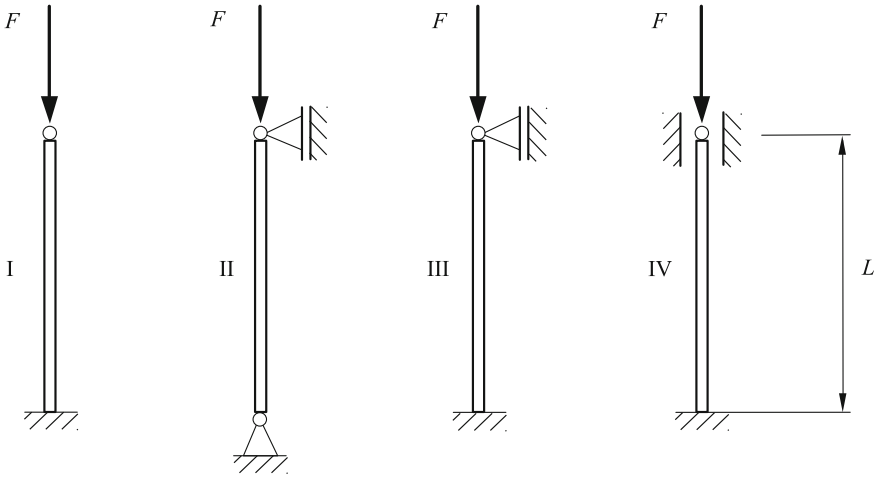
Fig. 12.4 The four EULER's buckling cases

12.4.1 Analytical Solutions for Euler's Buckling Loads

The differential equation of the buckling is [2]:

$$u_y'''' + \lambda^2 u_y'' = 0 \quad \text{with} \quad \lambda^2 = \frac{F}{EI}. \tag{12.45}$$

The general solution of the differential equation

$$u_y(x) = \bar{A}\,\cos(\lambda x) + \bar{B}\,\sin(\lambda x) + \bar{C}\,\lambda x + \bar{D} \tag{12.46}$$

consists of four constant terms.[1] The constant term $\bar{D}$ describes the translational rigid-body motion of the beam, the term $\bar{C}\,\lambda x$ describes the rigid-body rotation of the beam around the origin. The trigonometrical parts describe the deformation of the beam in the deformed position. The constant terms $\bar{A}, \bar{B}, \bar{C}$ and $\bar{D}$ can be determined from the boundary conditions. Required are the derivatives of the deformation from (12.46):

$$u_y'(x) = -\bar{A}\lambda \sin(\lambda x) + \bar{B}\lambda \cos(\lambda x) + \bar{C}\lambda, \tag{12.47}$$

$$u_y''(x) = -\bar{A}\lambda^2 \cos(\lambda x) - \bar{B}\lambda^2 \sin(\lambda x), \tag{12.48}$$

$$u_y'''(x) = +\bar{A}\lambda^3 \sin(\lambda x) - \bar{B}\lambda^3 \cos(\lambda x), \tag{12.49}$$

$$u_y''''(x) = +\bar{A}\lambda^4 \cos(\lambda x) + \bar{B}\lambda^4 \sin(\lambda x). \tag{12.50}$$

Table 12.1 shows the critical loads and buckling lengths for the EULER's buckling cases. Analogous to the critical load, the buckling lengths L_{crit} for EULER's buckling

---

[1] In order to avoid conflicts with other variables the constants are headed by a bar.

Table 12.1 Buckling load and buckling length

EULER case		I	II	III	IV
Buckling load	$F_{crit} = \pi^2 \frac{EI}{L^2} \times$	$\frac{1}{4}$	1	1.43^2	4
Buckling length	$L_{crit} = L \times$	2	1	$\frac{1}{1.43}$	$\frac{1}{2}$

can be introduced. The critical load and the buckling length are, regardless of the boundary conditions, connected through

$$F_{crit} = \pi^2 \frac{EI}{L_{crit}^2}. \qquad (12.51)$$

These values serve as a reference for the established solutions of the finite element method.

12.4.2 The Finite Element Method

The basis for the finite element analysis of the buckling behavior of beams is the stiffness matrix (12.44). With the abbreviations $e = \frac{EI}{L^3}$ and $f = \frac{F}{30L}$ the compact form of the entire stiffness matrix results in:

$$K = \begin{bmatrix} 12e - 36\lambda f & 6eL - 3\lambda fL & -12e + 36\lambda f & 6eL - 3\lambda fL \\ 6eL - 3\lambda fL & 4eL^2 - 4\lambda fL^2 & -6eL + 3\lambda fL & 2eL^2 + \lambda fL^2 \\ -12e + 36\lambda f & -6eL + 3\lambda fL & 12e - 36\lambda f & -6eL + 3\lambda fL^2 \\ 6eL - 3\lambda fL & 2eL^2 + 3\lambda fL^2 & -6eL + 3\lambda fL^2 & 4eL^2 - 4\lambda fL^2 \end{bmatrix}. \qquad (12.52)$$

The four EULER's cases differ due to the boundary conditions. In the following the first EULER's buckling case will be described. Node 1 is clamped firmly. By this, the displacement u_{1x} and the torsion φ_1 vanish. The most simple finite element model consists of exactly one beam. The rows 1 and 2 as well as the columns 1 and 2 will be deleted in the system matrix. What remains is a reduced submatrix:

$$K^{red} = \begin{bmatrix} 12e - 36\lambda fL & -6eL + 3\lambda f \\ -6eL + 3\lambda fL & 4eL^2 - 4\lambda fL \end{bmatrix}. \qquad (12.53)$$

To define the eigenvalue λ_i, the determinant of the reduced system matrix has to be constituted. This leads to the characteristic equation. Two solutions result from the quadratic equation. For statements regarding the stability, the smallest eigenvalue is of relevance. With this, the following emerges for the buckling load:

$$F_{crit} = \lambda_{min} F = \frac{4}{3}(13 - 2\sqrt{31}) \frac{EI}{L^2} = 2.486 \frac{EI}{L^2}. \qquad (12.54)$$

Compared to the precise solution $F = \frac{\pi^2}{4} \frac{EI}{L^2}$ an error of 0.8 % occurs.

12.5 Supplementary Problems

12.1 Entries of the Geometric Stiffness Matrix

In the above descriptions, the integration $\int_L N_y'^{\mathrm{T}} N_y' \mathrm{d}x$ for an assembly of the geometric stiffness matrix of a bending beam has only been shown for the matrix element (1,1).

The geometric stiffness matrix can be defined for a cubic displacement approach perpendicular to the bending axis in all matrix elements.

12.2 Euler's Buckling Cases II, III and IV, One Element

The above descriptions relate to EULER's buckling case I. Unknown are the finite element solution for the buckling load for EULER's buckling cases II, III and IV. Thereby discretization for the buckling can occur with one single beam element.

Problem:

1. Set up of the system matrix consisting of elastic and geometric stiffness matrix.
2. Definition of the eigenvalues.

12.3 Euler's Buckling Cases, Two Elements

Unknown are finite element solutions for the critical buckling load of EULER's buckling cases I, II, III and IV. Thereby the buckling bar can be discretized with *two* beam elements.

12.4 Euler's Buckling Cases, Error in Regard to Analytical Solution

With the help of the finite element method the error from the determined solution of the critical buckling load in regard to the analytical solution can be discussed depending on the number of applied elements. Unknown are the finite element solution for critical buckling load of EULER's buckling cases I, II, III and IV. Thereby the bending bar can be discretized with various beam elements.

References

1. Gross D, Hauger W, Schröder J, Werner EA (2008) Hydromechanik, Elemente der Höheren Mechanik. Numerische Methoden, Springer, Berlin
2. Gross D, Hauger W, Schröder J, Wall WA (2009) Technische Mechanik 2: Elastostatik. Springer, Berlin

3. Klein B (2000) FEM. Grundlagen und Anwendungen der Finite-Elemente-Methode, Vieweg-Verlag, Wiesbaden
4. Kwon YW, Bang H (2000) The finite element method using MATLAB. CRC Press, Boca Raton

Chapter 13
Dynamics

Abstract Within the chapter on dynamics the transient behavior of the acting loads on the structure will be introduced additionally into the analysis. The procedure for the analysis of dynamic problems depends essentially on the character of the time course of the loads. At deterministic loads the vector of the external loads is a given function of the time. The major amount of problems in engineering, plant and vehicle construction can be analyzed under this assumption. In contrast to that, the coincidence is relevant in the case of stochastic loads. Such cases will not be regarded here. For deterministic loads a distinction is drawn between

- periodic and non-periodic,
- slow and fast changing load-time functions (relatively related to the dynamic eigenbehaviour of the structure).

In the following chapter linear dynamic processes will be considered, which can be traced back to an external stimulation. The field of self-excited oscillation will not be covered.

13.1 Principles of Linear Dynamics

The point of origin is an elastic continuum with mass which is, in contrast to previous problems, stressed with time-dependent loads. The mass with density ρ extends itself over the volume Ω (Fig. 13.1). For dealing with dynamic problems in the context of the finite element method various model assumptions can be discussed [1–7]:

1. the distribution of the mass and
2. the treatment of the time dependency of all involved parameters.

Within the framework of the FE method the continuum will be discretized. A first model assumes that the distribution of the masses is not influenced by the discretization. The masses are also distributed continuously in the discretized condition. Figure 13.2a shows the continuously distributed mass for a bar. Another model assumes that
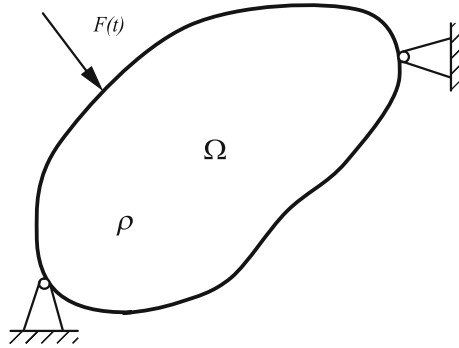
Fig. 13.1 Elastic continuum with mass under time-dependent load
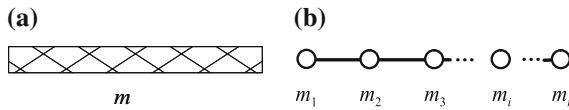
Fig. 13.2 Models of dynamic systems with **a** continuously and **b** discrete distributed masses

the originally continuously distributed mass can be concentrated on discrete points (see Fig. 13.2b).

The total mass

$$m = \sum_{i}^{n} m_i \tag{13.1}$$

of the system remains. The connection between the points with mass will be applied with elements without mass, which may represent further physical properties, for example stiffness.

Regarding the time dependency of the state variables, both the loads and the deformations as response of the system to the external loads are time changeable. Depending on the character of the external load, different problem areas are distinguished in dynamics (see Fig. 13.3) and pursue different strategies for the solution:

- Modal analysis
  Here the vibration behavior is considered without external loads. Eigenfrequency and eigenmodes are determined.
- Forced vibrations
  An external periodic force excites the component to resonate in the excitation frequency.
- Transient analysis
  The external stimulating force $F(t)$ is an arbitrary non-periodic function of time.

Problem definition

In addition to the elastic forces at pure static problems, inertia forces and frictional forces occur. According to the principle of d'ALEMBERT, these forces are
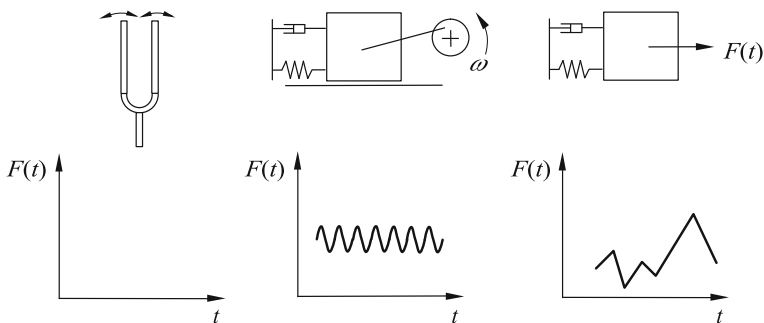
Fig. 13.3 Solution strategies structured according to the time course of the external loads

at equilibrium with the external forces at all times:

$$\boldsymbol{F}_m + \boldsymbol{F}_c + \boldsymbol{F}_k = \boldsymbol{F}(t). \tag{13.2}$$

In Eq. (13.2)

- $\boldsymbol{F}_m$ stands for the vector of the inertia forces,
- $\boldsymbol{F}_c$ stands for the vector of the damping forces, whereas in the following a velocity-related damping is assumed,
- $\boldsymbol{F}_k$ stands for the vector of the elastic reset forces and
- $\boldsymbol{F}$ stands for the vector of the external acting forces.

In static problems the deformation state on the inside of an element

$$\boldsymbol{u}^e(x) = \boldsymbol{N}(x)\,\boldsymbol{u}_p \tag{13.3}$$

is expressed through shape functions and nodal displacements. This assumption also applies for dynamics. With $\ddot{\boldsymbol{u}}$ as acceleration and second derivative of the displacement after the time and $\dot{\boldsymbol{u}}$ as velocity and first derivative of the displacement after the time one obtains a differential equation

$$\boldsymbol{M}\ddot{\boldsymbol{u}} + \boldsymbol{C}\dot{\boldsymbol{u}} + \boldsymbol{K}\boldsymbol{u} = \boldsymbol{F}(t) \tag{13.4}$$

in the displacements $\boldsymbol{u}$ as basic equation of dynamics. Thereby

- $\boldsymbol{M}$ stands for the mass matrix,
- $\boldsymbol{C}$ stands for the damping matrix and
- $\boldsymbol{K}$ stands for the stiffness matrix, which is already known from statics.

In the continuum, this equation stands for a partial differential equation in space and time (wave equation). Resulting from the spatial discretization in the framework of the FE method, Eq. (13.4) only represents a system of common differential equations in time.

13.2 The Mass Matrices

The structure of the mass matrices is essentially defined through the assumption of the distribution of the masses. For an element, with continuously distributed mass, equivalent forces, which are acting in the nodal points can be determined via the principle of virtual work

$$\Delta u_{\mathrm{p}}^{\mathrm{T}} M u_{\mathrm{p}} = \int_{\Omega} \rho (\Delta u)^{\mathrm{T}} u \, \mathrm{d}\Omega. \tag{13.5}$$

With the approaches for the displacements u and the accelerations $\ddot{u}$ one obtains the following as the mass matrix

$$M = \int_{\Omega} \rho N^{\mathrm{T}} N \mathrm{d}\Omega. \tag{13.6}$$

Consideration of the frictional forces F_c leads to the damping matrix

$$C = \int_{\Omega} N^{\mathrm{T}} \mu N \mathrm{d}\Omega. \tag{13.7}$$

For a distribution of the masses in discrete points, the mass matrix can be determined much easier. The proceeding will be shown in Sect. 13.6.2 for the example of the axial vibration of a bar.

13.3 Modal Analysis

An elastic, mass containing structure reacts to a time limited, external stimulation with a response in certain frequencies and modes of oscillation, whose entity is considered as an eigensystem of eigenfrequency and eigenmode. A basic assumption for the solution is that the changeable displacements in space and time are described in a separation approach

$$u(x, t) = \Phi(x) \, q(t), \tag{13.8}$$

whereby with $\Phi(x)$ the dependence of the displacement on space and with $q(t)$ the dependence of the displacement on the time are described.

Development of Eigenmodes and Eigenfrequencies

For low damped systems the eigenmodes can be established from the corresponding undamped system:

$$M\ddot{u} + Ku = 0. \tag{13.9}$$

With the approach for the displacement:

$$\boldsymbol{u}(x, t) = \boldsymbol{\Phi}(x)\, e^{i\omega t} \tag{13.10}$$

this leads to the generalized eigenvalue problem

$$(-\omega^2 \boldsymbol{M} + \boldsymbol{K})\, \boldsymbol{\Phi} = \boldsymbol{0}. \tag{13.11}$$

The nontrivial solutions (standing for the statics) one obtains from

$$\det(-\omega^2 \boldsymbol{M} + \boldsymbol{K}) = 0. \tag{13.12}$$

the ω_i, $i = 1, ..., n$, which fulfill the equation, are referred to as eigenfrequencies, and the corresponding $\boldsymbol{\Phi}_i$ are referred to as eigenmodes of the system with n degrees of freedom.[1] The single eigenmodes $\boldsymbol{\Phi}_i$ can be summarized in the modal matrix $\boldsymbol{\Phi}$

$$\boldsymbol{\Phi} = [\boldsymbol{\Phi}_1\, \boldsymbol{\Phi}_2\, \boldsymbol{\Phi}_3 \ldots\, \boldsymbol{\Phi}_n]. \tag{13.13}$$

The eigenmodes possess essential characteristics:

1. The orthogonality of two eigenmodes:

$$\boldsymbol{\Phi}_i^{\mathrm{T}} \boldsymbol{\Phi}_j = 0 \quad , \quad i \neq j. \tag{13.14}$$

2. The normalization regarding $\boldsymbol{M}$:
   The eigenmodes and therefore the eigenvectors can be $\boldsymbol{M}$-normalized. The eigenvectors can be stretched or bulged, so that an $\boldsymbol{M}$-orthonormality occurs. If the mass matrix $\boldsymbol{M}$ is multiplied with $\boldsymbol{\Phi}^{\mathrm{T}}$ from the left-hand and with $\boldsymbol{\Phi}$ from the right-hand, the modal mass matrix $\tilde{\boldsymbol{M}}$ results, which has entries exclusively on the main diagonal, to be precise a '1':

$$\boldsymbol{\Phi}^{\mathrm{T}} \boldsymbol{M} \boldsymbol{\Phi} = \tilde{\boldsymbol{M}} = \begin{bmatrix} 1 & 0 \\ 0 & 1 \end{bmatrix}. \tag{13.15}$$

   If the stiffness matrix $\boldsymbol{K}$ is multiplied accordingly from the left-hand and the right-hand, the modal stiffness matrix $\tilde{\boldsymbol{K}}$ results, which has entries exclusively on the main diagonal, to be precise the squares of the eigenfrequencies ω_i:

$$\boldsymbol{\Phi}^{\mathrm{T}} \boldsymbol{K} \boldsymbol{\Phi} = \tilde{\boldsymbol{K}} = \begin{bmatrix} \omega_1^2 & 0 \\ 0 & \omega_2^2 \end{bmatrix}. \tag{13.16}$$

---

[1] With the eigenmodes the space dependent displacements are characterized. However, the absolute magnitude of any displacement cannot be determined. The reason is that the system (13.13) has always more unknowns than equations. For the illustration of eigenmodes one assigns a value for an arbitrary eigenmode and relates all other eigenmodes to that.

3. Modal Damping:
   If the damping matrix C is multiplied accordingly from the left-hand and the right-hand, the modal damping matrix $\tilde{C}$ results, which has entries exclusively on the main diagonal, to be precise the eigenfrequencies ω_i and the modal damping coefficients ζ_i:

$$\boldsymbol{\Phi}^{\mathrm{T}} \boldsymbol{C} \boldsymbol{\Phi} = \tilde{\boldsymbol{C}} = \begin{bmatrix} \omega_1 \zeta_1 & 0 \\ 0 & \omega_2 \zeta_2 \end{bmatrix}. \tag{13.17}$$

   The damping approach is known under the name RAYLEIGH's damping and is possible, when the damping matrix is represented in the following form:

$$\boldsymbol{C} = \alpha \boldsymbol{M} + \beta \boldsymbol{K}. \tag{13.18}$$

4. Decoupling:
   In total, one receives an equivalent system of *decoupled* differential equations

$$\boldsymbol{\Phi}^{\mathrm{T}} \boldsymbol{M} \boldsymbol{\Phi} + \boldsymbol{\Phi}^{\mathrm{T}} \boldsymbol{C} \boldsymbol{\Phi} + \boldsymbol{\Phi}^{\mathrm{T}} \boldsymbol{K} \boldsymbol{\Phi} = \boldsymbol{0}, \tag{13.19}$$

   which can be written in generalized displacements q, also called modal coordinates, as

$$q_j + 2\omega_j \dot{q}_j + \omega_j^2 = \tilde{F}_j. \tag{13.20}$$

13.4 Forced Oscillation, Periodic Load

One talks about forced oscillation if a system suffers a periodic stimulation. Any eigenoscillations are decayed due to damping. Since every periodic stimulation can be analyzed via a FOURIER analysis, it is enough to assume single forces of the following kind

$$F(t) = F_0 e^{\mathrm{i}\omega t}, \tag{13.21}$$

which take effect periodically with the frequency ω. In linear systems the total response comes from the superposition of the single responses. It can be assumed that in the equation of motion

$$\boldsymbol{M} \ddot{\boldsymbol{u}} + \boldsymbol{C} \dot{\boldsymbol{u}} + \boldsymbol{K} \boldsymbol{u} = \boldsymbol{F}_0 e^{\mathrm{i}\omega t} \tag{13.22}$$

the deformation, the velocities and the accelerations can be illustrated as vectors of the following type

$$\boldsymbol{u}(t) = \boldsymbol{u}_0 e^{\mathrm{i}(\omega t - \psi)}, \tag{13.23}$$

$$\dot{\boldsymbol{u}}(t) = \mathrm{i}\omega \boldsymbol{u}_0 e^{\mathrm{i}(\omega t - \psi)}, \tag{13.24}$$

$$\ddot{\boldsymbol{u}}(t) = -\omega^2 \boldsymbol{u}_0 e^{\mathrm{i}(\omega t - \psi)}. \tag{13.25}$$

If the splitting of the complex displacement is inserted into the real and imaginary part

$$\mathbf{u}(t) = \mathbf{u}_{\text{Re}}e^{i\omega t} + i\mathbf{u}_{\text{Im}}e^{i\omega t} = \mathbf{u}_0 e^{i\omega t}(\cos\psi + i\sin\psi). \qquad (13.26)$$

one obtains from

$$[-\omega^2 M(\mathbf{u}_{\text{Re}} + i\mathbf{u}_{\text{Im}}) + i\omega C(\mathbf{u}_{\text{Re}} + i\mathbf{u}_{\text{Im}}) + K(\mathbf{u}_{\text{Re}} + i\mathbf{u}_{\text{Im}})]e^{i\omega t} = F_0 e^{i\omega t} \quad (13.27)$$

via

$$[(K - \omega^2 M)\mathbf{u}_{\text{Re}} - \omega C\mathbf{u}_{\text{Im}}] + i[(K - \omega^2 M)\mathbf{u}_{\text{Im}} + \omega C\mathbf{u}_{\text{Re}}] = F_0 \qquad (13.28)$$

after the separation of the products of the real matrix with the complex vectors in the real and imaginary parts $2n$ equations of the following kind

$$(K - \omega^2 M)\mathbf{u}_{\text{Re}} - \omega C\mathbf{u}_{\text{Im}} = F_0, \qquad (13.29)$$

$$(K - \omega^2 M)\mathbf{u}_{\text{Im}} + \omega C\mathbf{u}_{\text{Re}} = 0. \qquad (13.30)$$

With n degrees of freedom this is a solvable linear system of equations with the $2n$ unknowns of the respective n component of the real and imaginary part of the complex displacement $u = u_{\text{Re}} + iu_{\text{Im}}$. For each of the n degrees of freedom the amplitude is defined through

$$u_k = \sqrt{u_{k,\text{Re}}^2 + u_{k,\text{Im}}^2} \qquad (13.31)$$

and the phase shift through

$$\psi_k = \arctan\left(\frac{u_{k,\text{Im}}}{u_{k,\text{Re}}}\right), \qquad (13.32)$$

except the multiples of π.

13.5 Direct Methods of Integration, Transient Analysis

Transient dynamic requires the integration of the equation of motion (13.4), which describes the correlation between acceleration, damping, deformation and the external force throughout the time interval of interest. Needed are integration procedures, which identify the deformation in the regarded time interval from the equation of motion

$$\ddot{u}(t) = M^{-1}[F(t) - [C\dot{u}(t) + Ku(t)]]. \qquad (13.33)$$

An estimation of the displacement regarding time $t + \Delta t$ can be received through the expansion in series up to the 2nd element

$$u\left(t + \Delta t\right) \approx u\left(t\right) + \Delta t \dot{u}\left(t\right) + \frac{\Delta t^2}{2} \ddot{u}\left(t\right) \tag{13.34}$$

and an estimation of the velocity through an expansion of the series

$$\dot{u}\left(t + \Delta t\right) \approx \dot{u}\left(t\right) + \Delta t \ddot{u}\left(t\right), \tag{13.35}$$

which interrupts after the 1st element. To be able to make use of the integration instructions according to Eqs. (13.33) and (13.35), displacement and velocity from the initial moment t_0 have to be known. The necessity of two instructions follows from the fact that the equation of motion (13.4) represents a PDE of 2nd order in time (two time derivatives occur). With a sufficiently small Δt, the thus found displacement approximates the time course of the displacement $u(t)$ satisfactorily. The basic construction of the two mostly used integration procedures, which are ideally similar to the quadratic procedures (or procedures of 2nd order), will be described here.

13.5.1 Integration According to Newmark

In the time interval $[t, t + \Delta t]$ the constant averaged acceleration

$$\ddot{u}_m = \frac{1}{2} \left[\dot{u}\left(t\right) + \ddot{u}\left(t + \Delta t\right)\right] \tag{13.36}$$

is assumed. Therewith a quadratic course results for the displacement

$$u\left(t + \Delta t\right) = u\left(t\right) + \Delta t \dot{u}\left(t\right) + \frac{\Delta t^2}{4} \ddot{u}\left(t\right) + \ddot{u}\left(t + \Delta t\right) \tag{13.37}$$

and a linear course for the velocity $\dot{u}\left(t\right)$

$$\dot{u}\left(t + \Delta t\right) = \dot{u}\left(t\right) + \frac{\Delta t^2}{2} \ddot{u}\left(t\right) + \ddot{u}\left(t + \Delta t\right). \tag{13.38}$$

Together with the equation of motion (13.4) at the point of time $t + \Delta t$

$$M \ddot{u}\left(t + \Delta t\right) + C \dot{u}\left(t + \Delta t\right) + K u\left(t + \Delta t\right) = F\left(t + \Delta t\right) \tag{13.39}$$

three equations for three unknowns are available $u\left(t + \Delta t\right)$, $\dot{u}\left(t + \Delta t\right)$, $\ddot{u}\left(t + \Delta t\right)$. Setting $\Delta u = u\left(t + \Delta t\right) - u\left(t\right)$, for this increase of the displacement the following

results

$$\Delta u = S^{-1} F \left(t + \Delta t \right) - K u \left(t \right) + M \left[\ddot{u} \left(t \right) + \frac{4}{\Delta t} \dot{u} \left(t \right) \right] + C \dot{u} \left(t \right) \qquad (13.40)$$

with

$$S = \frac{4}{\Delta t^2} M + \frac{2}{\Delta t} C + K. \qquad (13.41)$$

The velocity $\dot{u} \left(t + \Delta t \right)$ and the acceleration $\ddot{u} \left(t + \Delta t \right)$ are calculated from Eqs. (13.35) and (13.33). The time integration according to NEWMARK in fact requires the often expensive calculation of these inverses, however allows relatively large time steps, so that this disadvantage is compensated for in many cases. In particular, for linear problems, in which the system matrices are not dependent on the actual displacements, this procedure can be used very effectively since the inverse S^{-1} only has to be calculated once.

13.5.2 Central Difference Method

The velocity $\dot{u} \left(t \right)$, as first derivative of the displacement according to time, can be approximated through the displacement to the times $t - \Delta t$ and $t + \Delta t$ at sufficiently small time step Δt through

$$\dot{u} \left(t \right) \approx \frac{u \left(t + \Delta t \right) - u \left(t - \Delta t \right)}{2 \Delta t}. \qquad (13.42)$$

The acceleration $\ddot{u} \left(t \right)$ as second derivative of the displacement according to time is approximated with

$$\ddot{u} \left(t \right) \approx \frac{u \left(t + \Delta t \right) - 2u \left(t \right) + u \left(t - \Delta t \right)}{\Delta t^2}. \qquad (13.43)$$

If these relations are inserted into the equation of motion (13.4) at the point of time t, one obtains with the abbreviations $u_1 = u \left(t + \Delta t \right)$, $u_0 = u \left(t \right)$ und $u_{-1} = u \left(t - \Delta t \right)$

$$M \frac{u_1 - 2u_0 + u_{-1}}{\Delta t^2} + C \frac{u_1 - u_{-1}}{2 \Delta t} + K u_0 = F \left(t \right) \qquad (13.44)$$

a relation, from which the displacement $u_1 = u \left(t + \Delta t \right)$ can be calculated, if the displacement at the previous points of time t and $t - \Delta t$ are known:

$$u_1 = S^{-1} F \left(t \right) - \left(K - \frac{2M}{\Delta t^2} \right) u_0 - \left(\frac{M}{\Delta t^2} - \frac{C}{2 \Delta t} \right) u_{-1} \qquad (13.45)$$

with

$$S = \frac{1}{\Delta t^2} M + \frac{1}{2\Delta t} C. \tag{13.46}$$

To calculate the new displacement $u_1 = u(t + \Delta t)$, values of the displacement u at two points of time are necessary. Since for a transient problem, initial displacement and velocity and therefore according to Eq. (13.33) also the acceleration at the point of time $t = 0$ have to be known, a virtual displacement at the time $-\Delta t$ from the expansion of series is supplied

$$u_1 = u(t - \Delta t) \approx u(0) - \Delta t \dot{u}(0) + \frac{\Delta t^2}{2} \ddot{u}(0) \tag{13.47}$$

and, in the first time step, the displacement $u_1 = u(\Delta t)$ can be calculated.

The central difference method is *explicitly* named, since the displacement $u(t + \Delta t)$ is calculated from the conditions at the point of time t and not with an analysis of the equation of motion at the point of time $t + \Delta t$, while the *implicit* NEWMARK method considers the equilibrium of forces at the point of time $t + \Delta t$. This explicit method is of great importance for diagonal mass and damping matrices M and C, at which the inverses can easily be defined by

$$S = \begin{bmatrix} S_{1,1} & 0 & \cdots & 0 \\ 0 & S_{2,2} & \cdots & 0 \\ \cdots & \cdots & \cdots & \cdots \\ \cdots & \cdots & \cdots & \cdots \\ 0 & 0 & \cdots & S_{n,n} \end{bmatrix} \tag{13.48}$$

through

$$S^{-1} = \begin{bmatrix} \frac{1}{S_{1,1}} & 0 & \cdots & 0 \\ 0 & \frac{1}{S_{2,2}} & \cdots & 0 \\ \cdots & \cdots & \cdots & \cdots \\ \cdots & \cdots & \cdots & \cdots \\ 0 & 0 & \cdots & \frac{1}{S_{n,n}} \end{bmatrix} \tag{13.49}$$

with

$$S_{i,i} = \frac{M_i}{\Delta t^2} + \frac{C_i}{2\Delta t} \quad , \quad (i = 1 - n). \tag{13.50}$$

The extremely fast, nonlinear crash programs, which conduct hundreds of thousands of integration steps during a calculation and in the process constantly calculate new matrices, make use of this or the herefrom derived methods. The time steps, with which the motion of a component can be calculated satisfactory, are clearly smaller than with the NEWMARK method, in return the calculations are done very easily and are outstandingly parallelizable, meaning very fast on computers with various or many processors. Furthermore only little storage space is needed, since the matrices in Eq. (13.50) never have to be derived completely.

13.6 Examples

So far, the introduced approaches can be discussed with the help of examples:

- Axial vibration in the bar and
- Bending vibration in the bending beam.

Essentially three models will be analysed:

1. The analytical solution, which results from the solution of the differential equation,
2. the solution according to the FE method, whereupon the masses are continuously distributed and
3. the solution according to the FE method, when the masses are concentrated on discrete points.

First of all the necessary mass and stiffness matrices will be given in general.

13.6.1 Provision of Mass and Stiffness Matrices

The general calculation instruction for the mass matrix

$$M^{\mathrm{e}} = \int_{\Omega} \rho N^{\mathrm{T}} N \, \mathrm{d}\Omega \tag{13.51}$$

with continuously distributed mass and for the stiffness matrix

$$K^{\mathrm{e}} = \int_{\Omega} B^{\mathrm{T}} D B \, \mathrm{d}\Omega \tag{13.52}$$

are known from previous chapters. In the following, the issue will be discussed with the help of examples.

Axial Vibration in the Bar

In Fig. 13.4 the bar is drafted with degrees of freedom, which serve as a basis for the analysis of the dynamic behavior. The names are closely connected with the definition of the degrees of freedom in statics.

Fig. 13.4 Bar with degrees of freedom for the dynamic analysis
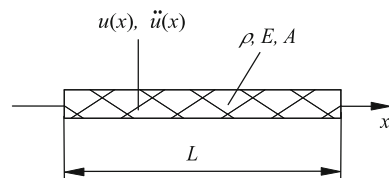
Besides the displacement $u(x)$ also the acceleration $\ddot{u}(x)$ is a state variable within the considered system. Figure 13.5 illustrates the bar element with the degrees of freedom for a linear approach.

Fig. 13.5 Bar with linear approach
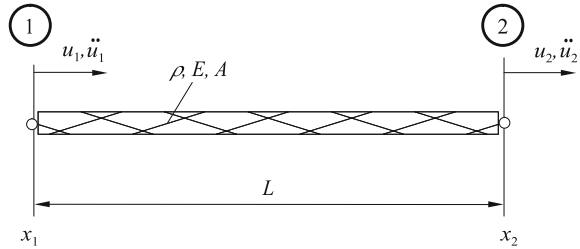
With linear shape functions the following mass matrix results

$$M^{\mathrm{e}} = \frac{\rho A L}{6} \begin{bmatrix} 2 & 1 \\ 1 & 2 \end{bmatrix} \tag{13.53}$$

and the following stiffness matrix results

$$K^{\mathrm{e}} = \frac{E A}{L} \begin{bmatrix} 1 & -1 \\ -1 & 1 \end{bmatrix}. \tag{13.54}$$

The expression

$$M^{\mathrm{e}} \ddot{u}^{\mathrm{e}} + K^{\mathrm{e}} u^{\mathrm{e}} \tag{13.55}$$

can therefore be written as

$$\frac{\rho A L}{6} \begin{bmatrix} 2 & 1 \\ 1 & 2 \end{bmatrix} \begin{bmatrix} \ddot{u}_1 \\ \ddot{u}_2 \end{bmatrix} + \frac{E A}{L} \begin{bmatrix} 1 & -1 \\ -1 & 1 \end{bmatrix} \begin{bmatrix} u_1 \\ u_2 \end{bmatrix}. \tag{13.56}$$

Figure 13.6 shows the bar element with the degrees of freedom for a quadratic approach.
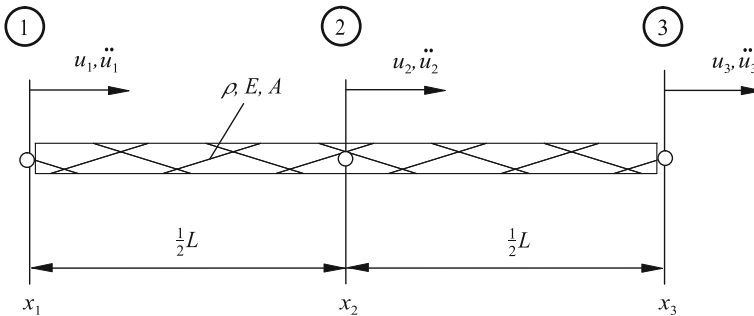
Fig. 13.6 Bar element with quadratic approach

With a quadratic shape function the mass matrix results in

$$\boldsymbol{M}^{\mathrm{e}} = \frac{\rho A L}{30} \begin{bmatrix} 4 & 2 & -1 \\ 2 & 16 & 2 \\ -1 & 2 & 4 \end{bmatrix} \tag{13.57}$$

and the stiffness matrix in:

$$\boldsymbol{K}^{\mathrm{e}} = \frac{E A}{3L} \begin{bmatrix} 7 & -8 & 1 \\ -8 & 16 & -8 \\ 1 & -8 & 7 \end{bmatrix}. \tag{13.58}$$

The expression

$$\boldsymbol{M}^{\mathrm{e}} \ddot{\boldsymbol{u}}^{\mathrm{e}} + \boldsymbol{K}^{\mathrm{e}} \boldsymbol{u}^{\mathrm{e}} \tag{13.59}$$

can therefore be written as

$$\frac{\rho A L}{30} \begin{bmatrix} 4 & 2 & -1 \\ 2 & 16 & 2 \\ -1 & 2 & 4 \end{bmatrix} \begin{bmatrix} \ddot{u}_1 \\ \ddot{u}_2 \\ \ddot{u}_3 \end{bmatrix} + \frac{E A}{3L} \begin{bmatrix} 7 & -8 & 1 \\ -8 & 16 & -8 \\ 1 & -8 & 7 \end{bmatrix} \begin{bmatrix} u_1 \\ u_2 \\ u_3 \end{bmatrix}. \tag{13.60}$$

Bending Vibration in the Beam

In Fig. 13.7 the bending beam with the degrees of freedom is drafted, which serve as a basis for the analysis of the dynamic behavior. The notation is closely connected with the definition of the degrees of freedom in statics. First of all the influence of the inertia in rotation can be disregarded. This issue will be introduced later on. From static analysis the relation, how the deflection $u_z(x)$ at an arbitrary point x is connected with the fixed nodal values u_{1z}, φ_{1y}, u_{2z} and φ_{2y} is already known. The basis for this is an approach for the displacement in the form

$$u_z(x) = \sum_i^4 N_i(x) u_i. \tag{13.61}$$

Fig. 13.7 Bending beam with degrees of freedom for the dynamic analysis
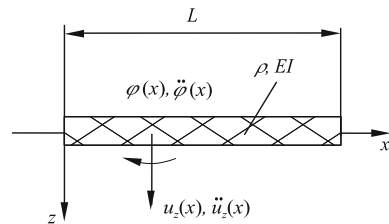
With the four shape functions

$$N_1(x) = 1 - 3\frac{x^2}{L^2} + 2\frac{x^3}{L^3},$$

$$N_2(x) = -x + 2\frac{x^2}{L} - \frac{x^3}{L^2},$$

$$N_3(x) = 3\frac{x^2}{L^2} - 2\frac{x^3}{L^3},$$

$$N_4(x) = \frac{x^2}{L} - \frac{x^3}{L^2} \tag{13.62}$$

one obtains the following description for the deformation

$$u_z(x) = \left(1 - 3\frac{x^2}{L^2} + 2\frac{x^3}{L^3}\right) u_{1z} + \left(-\frac{x}{L} + 2\frac{x^2}{L^2} - \frac{x^3}{L^3}\right) L\,\varphi_{1y}$$

$$+ \left(\frac{3x^2}{L^2} - 2\frac{x^3}{L^3}\right) u_{2z} + \left(\frac{x^2}{L^2} - \frac{x^3}{L^3}\right) L\,\varphi_{2y} \tag{13.63}$$

regarding nodal values and shape functions.

Single entries can be determined with the shape functions from the calculation instruction for the mass matrix (13.51). For the bending beam 16 entries result for the mass matrix. The calculation will be illustrated as an example on the entries m_{11} and m_{12}. From the matrix element m_{11}

$$m_{11} = \rho A \int_0^L \left(1 - \frac{3x^2}{L^2} + \frac{2x^3}{L^3}\right) dx$$

$$= \rho A \int_0^L \left(1 - \frac{6x^2}{L^2} + \frac{4x^3}{L^3} + \frac{9x^4}{L^4} - \frac{12x^5}{L^5} + \frac{4x^6}{L^6}\right) dx$$

$$= \rho A \left[x - \frac{2x^3}{L^2} + \frac{x^4}{L^3} + \frac{9x^5}{5L^4} - \frac{2x^6}{L^5} + \frac{4x^7}{7L^6}\right] \Big|_0^L$$

$$= \frac{156}{420} \rho AL \tag{13.64}$$

the matrix element m_{12}

$$m_{12} = \rho A \int_0^L \left(1 - \frac{3x^2}{L^2} + \frac{2x^3}{L^3}\right) \times \left(-\frac{x}{L} + \frac{2x^2}{L^2} - \frac{x^3}{L^3}\right) L\,dx$$

$$= \frac{22}{420} \rho A L^2, \tag{13.65}$$

up to the matrix element m_{44}

$$m_{44} = \rho A \int\limits_0^L \left(\frac{x^2}{L^2} - \frac{x^3}{L^3}\right)^2 \times L^2 \mathrm{d}x = \frac{4}{420}\rho A L^3 \qquad (13.66)$$

the total mass matrix results

$$M = \frac{\rho\, AL}{420} \begin{bmatrix} 156 & -22L & 54 & 13L \\ & 4L^2 & -13L & -3L \\ & & 156 & 22L \\ \text{sym.} & & & 4L^2 \end{bmatrix} \qquad (13.67)$$

for the description of the bending vibration in the bending beam.

So far, the influence of the cross-sectional rotation is disregarded. Besides the deflection u_z in z-direction the cross-section rotates around the y-axis. For the vibration behavior the inertia in rotation is additionally considered.

The total mass matrix

$$M^{\mathrm{e}} = \frac{\rho\, A\, L}{420} \begin{bmatrix} 156 & -22L & 54 & 13L \\ & 4L^2 & -13L & -3L^2 \\ & & 156 & 22L \\ \text{sym.} & & & 4L^2 \end{bmatrix} \qquad (13.68)$$

$$+ \frac{\rho\, A\, L}{30} \left(\frac{I_y}{A \times L^2}\right) \begin{bmatrix} 36 & -3L & -36 & 3L \\ & 4L^2 & 3L & -L^2 \\ & & 36 & -3L \\ \text{sym.} & & & 4L^2 \end{bmatrix} \qquad (13.69)$$

can be dispersed in a translational and a rotatory part. The expression I_y stands for the axial second moment of area of 2nd order around the y-axis. The first matrix corresponds with the already known matrix from consideration without the rotatory part.

13.6.2 Axial Vibration in the Bar

A prismatic tension bar serves as the point of origin, which is continuously loaded with mass (density ρ) and whose modulus of elasticity E and cross-sectional area A are constant. Unknown are the eigenfrequencies (Fig. 13.8).

From the differential equation for the axial vibration of a bar

$$\frac{\partial^2 u(x, t)}{\partial t^2} = \frac{E}{\rho}\frac{\partial^2 u(x, t)}{\partial x^2} \qquad (13.70)$$
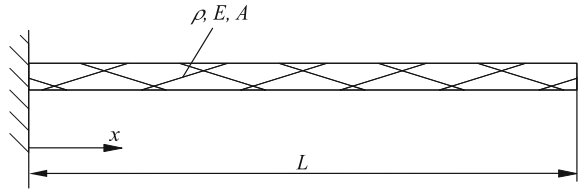
the eigenfrequencies result in:

$$\omega_n = \frac{2n-1}{2}\pi\sqrt{\frac{E}{\rho L^2}}. \tag{13.71}$$

The first eigenfrequencies calculate for $n = 1, 2, 3, 4$ in the following:

$$\omega_1 = \frac{1}{2}\pi = 1.5708\sqrt{E/\rho L^2}, \tag{13.72}$$

$$\omega_2 = \frac{3}{2}\pi = 4.7124\sqrt{E/\rho L^2}, \tag{13.73}$$

$$\omega_3 = \frac{5}{2}\pi = 7.854\sqrt{E/\rho L^2}, \tag{13.74}$$

$$\omega_4 = \frac{7}{2}\pi = 10.99\sqrt{E/\rho L^2}. \tag{13.75}$$

Figure 13.9 shows a finite element discretization with continuously distributed mass. The total mass and stiffness matrix can be established by combining the formulated matrices for a single element properly. Therefore one obtains the general equation of motion:

$$m\begin{bmatrix} 2 & 1 & & & & \\ 1 & 4 & 1 & & & \\ & 1 & 4 & 1 & & \\ & & \ddots & \ddots & \ddots & \\ & & & 1 & 4 & 1 \\ & & & & 1 & 2 \end{bmatrix}\begin{bmatrix} \ddot{u}_0 \\ \ddot{u}_1 \\ \ddot{u}_2 \\ \vdots \\ \ddot{u}_n \end{bmatrix} + k\begin{bmatrix} 1 & -1 & & & & \\ -1 & 2 & -1 & & & \\ & -1 & 2 & & & \\ & & \ddots & \ddots & \ddots & \\ & & & -1 & 2 & -1 \\ & & & & -1 & 2 \end{bmatrix}\begin{bmatrix} u_0 \\ u_1 \\ u_2 \\ \vdots \\ u_n \end{bmatrix} = 0 \tag{13.76}$$

with $m = \frac{\rho A \frac{1}{n} L}{6}$ and $k = \frac{EA}{\frac{1}{n}L}$. On the fixed support the boundary conditions $\ddot{u}_0 = 0$ (no acceleration) and $u_0 = 0$ (no displacement) apply. Hence the first row and the first column of a matrix in each case can be cancelled from the entire system of equations.

$$\frac{\rho A \frac{1}{n} L}{6}\begin{bmatrix} 4 & 1 & & & \\ 1 & 4 & 1 & & \\ & \ddots & \ddots & \ddots & \\ & & 1 & 4 & 1 \\ & & & 1 & 2 \end{bmatrix}\begin{bmatrix} \ddot{u}_1 \\ \ddot{u}_2 \\ \vdots \\ \ddot{u}_N \end{bmatrix} + \frac{EA}{\frac{1}{n}L}\begin{bmatrix} 2 & -1 & & & \\ -1 & 2 & & & \\ & \ddots & \ddots & \ddots & \\ & & -1 & 2 & -1 \\ & & & -1 & 2 \end{bmatrix}\begin{bmatrix} u_1 \\ u_2 \\ \vdots \\ u_n \end{bmatrix} = 0.$$

$$\tag{13.77}$$

Fig. 13.9 FE discretization for axial vibration in the bar

The matrices do not have a diagonal shape. Between two nodes (i) and $(i + 1)$ respectively there is a partial mass. This leads to secondary diagonals. In a nodal point (i) two '*finite masses*' bump against each other, in the endpoint only one. This becomes noticeable on the main diagonal in the last entry. Both matrices have a band structure with a band width of 3.

Lumped Mass Equivalent System

For a Lumped Mass Method (LMM) equivalent system the continuously distributed mass will be concentrated on discrete points. When modeling the bar it needs to be considered that at the bar beginning and at the bar end only $m/2$ needs to be added respectively. One obtains the mass and stiffness matrix according to the above described procedure. The first row and the first column can be canceled in the equation of motion with $n + 1$ nodes since the following values for the displacement $u_0 = 0$ and the acceleration $\ddot{u}_0 = 0$ hold (Fig. 13.10).

Fig. 13.10 FE discretization (concentrated mass) for tension vibration in a bar

$$
\rho A \frac{1}{n} L
\begin{bmatrix}
1 & & & & \\
& 1 & & & 0 \\
& & 1 & & \\
& & & \ddots & \\
0 & & & & 1 \\
& & & & & \frac{1}{2}
\end{bmatrix}
\begin{bmatrix}
\ddot{u}_1 \\
\ddot{u}_2 \\
\vdots \\
\ddot{u}_n
\end{bmatrix}
+
\frac{EA}{\frac{1}{n}L}
\begin{bmatrix}
2 & -1 & & & \\
-1 & 2 & -1 & & 0 \\
& -1 & 2 & -1 & \\
& & \ddots & \ddots & \ddots \\
0 & & -1 & 2 & -1 \\
& & & -1 & 1
\end{bmatrix}
\begin{bmatrix}
u_1 \\
u_2 \\
\vdots \\
u_n
\end{bmatrix}
= 0.
$$

$$(13.78)$$

To be noted:
The mass matrix has a diagonal shape, the stiffness matrix has a band structure with a band width of three.

13.6.2.1 Solutions with Linear Shape Functions

The number of finite elements has a decisive influence on the accuracy of the results. First of all the tension bar will be discretized with linear and later on with quadratic shape functions. The solution with continuously distributed masses as well as the solution with concentrated masses will be introduced.

Continuously Distributed Masses

First of all the entire bar is regarded as a single element (Fig. 13.11).
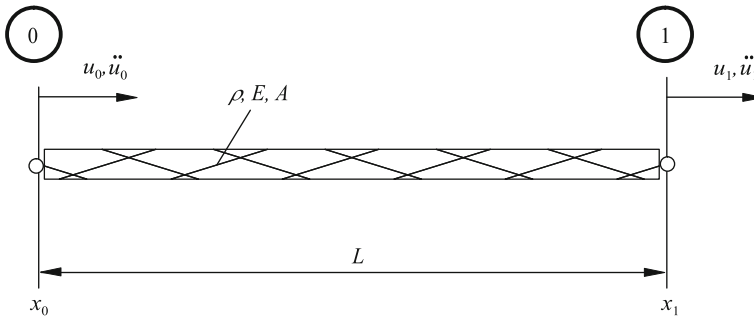
Fig. 13.11 An element with continuously distributed mass

With the mass and stiffness matrix

$$M = \frac{\rho A L}{6} \begin{bmatrix} 2 & 1 \\ 1 & 2 \end{bmatrix} \quad \text{and} \quad K = \frac{E A}{L} \begin{bmatrix} 1 & -1 \\ -1 & 1 \end{bmatrix} \tag{13.79}$$

the equation of motion results as

$$\begin{bmatrix} 2 & 1 \\ 1 & 2 \end{bmatrix} \begin{bmatrix} \ddot{u}_0 \\ \ddot{u}_1 \end{bmatrix} + 6 \frac{E}{\rho L^2} \begin{bmatrix} 1 & -1 \\ -1 & 1 \end{bmatrix} \begin{bmatrix} u_0 \\ u_1 \end{bmatrix} = \begin{bmatrix} 0 \\ 0 \end{bmatrix} . \tag{13.80}$$

No acceleration ($\ddot{u} = 0$) and no displacement ($u = 0$) occur on the node 0 with the coordinate x_0. The first row of the system of equations can therefore be cancelled. Two equations result from the second line:

$$\ddot{u}_1 - 6 \frac{E}{\rho L^2} u_1 = 0, \quad 2 \ddot{u}_1 + 6 \frac{E}{\rho L^2} u_1 = 0. \tag{13.81}$$

With the approach $u_1 = \hat{u}_1 e^{(i\omega t)}$ one obtains the following from the first equation:

$$\left(-\omega^2 - 6\frac{E}{\rho L^2}\right)\hat{u}_1 = 0 \quad \Rightarrow \quad \omega = \sqrt{6\frac{E}{\rho L^2}}i. \tag{13.82}$$

The second equation leads to:

$$\left(-2\omega^2 + 6\frac{E}{\rho L^2}\right)\hat{u}_1 = 0 \quad \Rightarrow \quad \omega = \sqrt{3}\sqrt{\frac{E}{\rho L^2}} \tag{13.83}$$

or alternatively

$$\omega = 1.7321\sqrt{\frac{E}{\rho L^2}} \quad . \tag{13.84}$$

The result deviates significantly from that of the analytical solution. An improvement can be achieved via a discretization with *two* finite elements.

Two Elements

The system now consists of two finite elements with linear shape functions and three nodes 0, 1 and 2 on the coordinates x_0, x_1 and x_2 (Fig. 13.12). No accelerations ($\ddot{u} = 0$) and no displacements $u = 0$ occur on the fixing point. From the above considerations the reduced mass and stiffness matrix can be established
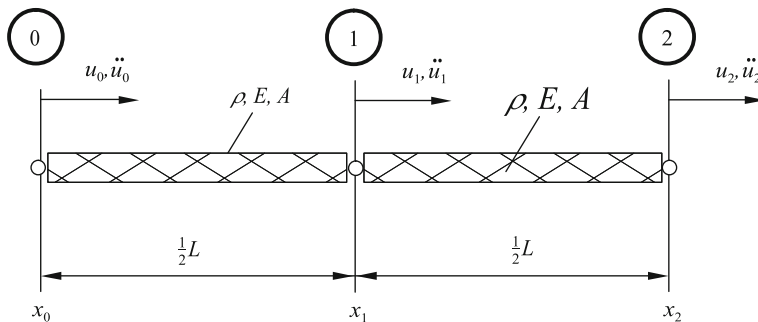
Fig. 13.12 Two elements with continuously distributed masses

$$M^{\text{red}} = \frac{\rho A \frac{1}{2}L}{6}\begin{bmatrix} 4 & 1 \\ 1 & 2 \end{bmatrix} \quad \text{and} \quad K^{\text{red}} = \frac{EA}{\frac{1}{2}L}\begin{bmatrix} 2 & -1 \\ -1 & 1 \end{bmatrix} \tag{13.85}$$

so that the following characteristic equation

$$\begin{vmatrix} -4\lambda^2 + 2 & -1\lambda^2 - 1 \\ -1\lambda^2 - 1 & -2\lambda^2 + 1 \end{vmatrix} \overset{!}{=} 0 \quad \Rightarrow \quad 2(1 - 2\lambda^2)^2 = (1 + \lambda^2)^2 \tag{13.86}$$

with the abbreviations

$$\lambda^2 = \frac{1}{6} \frac{\rho \frac{1}{4} L^2}{E} \omega^2 \tag{13.87}$$

results. Two solutions result

$$\lambda_1^2 = \frac{\sqrt{2} - 1}{1 + 2\sqrt{2}} \quad \text{and} \quad \lambda_2^2 = \frac{1 + \sqrt{2}}{2\sqrt{2} - 1}, \tag{13.88}$$

which look as follows, written in detail:

$$\omega_1^2 = \frac{24\left(\sqrt{2} - 1\right)}{1 + 2\sqrt{2}} \frac{E}{\rho L^2} \quad \Rightarrow \quad \omega_1 = 1.61 \sqrt{\frac{E}{\rho L^2}}, \tag{13.89}$$

$$\omega_2^2 = \frac{24\left(1 + \sqrt{2}\right)}{2\sqrt{2} - 1} \frac{E}{\rho L^2} \quad \Rightarrow \quad \omega_2 = 5.63 \sqrt{\frac{E}{\rho L^2}}. \tag{13.90}$$

The values for the eigenfrequencies so far deviate significantly from the analytical solutions. The next simplification equals a division of the bar into *three* finite elements.

Three Elements

The system now consists of three finite elements with linear shape functions and four nodes 0, 1, 2 and 3 on the coordinates x_0, x_1, x_2 and x_3. No accelerations ($\ddot{u}_0 = 0$) and no displacements ($u_0 = 0$) occur at the fixing point. Therefore the first row and the first column can be cancelled from the system of equations (Fig. 13.13). The reduced mass and stiffness matrix remains

$$M^{\text{red}} = \frac{\rho A \frac{1}{3} L}{6} \begin{bmatrix} 4 & 1 & 0 \\ 1 & 4 & 1 \\ 0 & 1 & 2 \end{bmatrix} \quad \text{and} \quad K^{\text{red}} = \frac{EA}{\frac{1}{3} L} \begin{bmatrix} 2 & -1 & 0 \\ -1 & 2 & -1 \\ 0 & -1 & 1 \end{bmatrix}, \tag{13.91}$$

with which the following characteristic equation

$$\begin{vmatrix} -4\lambda^2 + 2 & -1\lambda^2 - 1 & 0 \\ -1\lambda^2 - 1 & -2\lambda^2 + 1 & -1\lambda - 1 \\ 0 & -1\lambda & 1 \end{vmatrix} \overset{!}{=} 0 \tag{13.92}$$
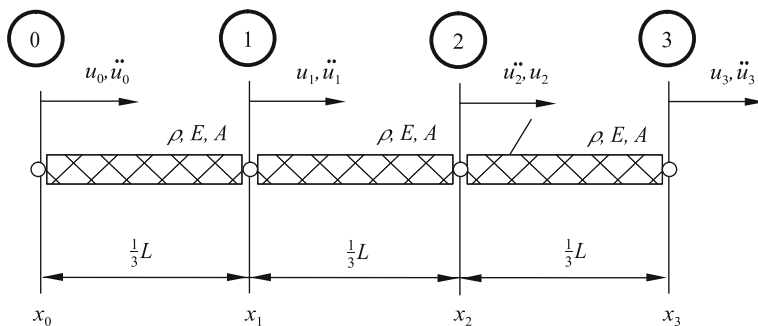
Fig. 13.13 Three elements with continuously distributed masses

with the abbreviations

$$\lambda^2 = \frac{1}{6}\frac{\rho(\frac{1}{3}L)^2}{E}\omega^2 = \frac{1}{6}\frac{1}{9}\frac{\rho L^2}{E}\omega^2 \tag{13.93}$$

can be gained. Three solutions result

$$\lambda_1^2 = \frac{2-\sqrt{3}}{4+\sqrt{3}}, \quad \lambda_2^2 = \frac{1}{2}, \quad \lambda_3^2 = \frac{2+\sqrt{3}}{4-\sqrt{3}}, \tag{13.94}$$

which appear as follows, written in detail

$$\omega_1 = \frac{54\left(2-\sqrt{3}\right)}{4+\sqrt{3}}\frac{E}{\rho L^2} \quad \Rightarrow \quad \omega_1 = 1.59\sqrt{\frac{\rho L^2}{E}}, \tag{13.95}$$

$$\omega_2 = 27\frac{E}{\rho L^2} \quad \Rightarrow \quad \omega_2 = 5.19\sqrt{\frac{\rho L^2}{E}}, \tag{13.96}$$

$$\omega_3 = \frac{54\left(2+\sqrt{3}\right)}{4-\sqrt{3}}\frac{E}{\rho L^2} \quad \Rightarrow \quad \omega_3 = 9.43\sqrt{\frac{\rho L^2}{E}}. \tag{13.97}$$

The deviation from the analytical solution will be considered later on.

Lumped Mass Method

Within this method discretizations with one, two and three finite elements will be introduced. First of all, a discretization with just one element will be considered (Fig. 13.14).
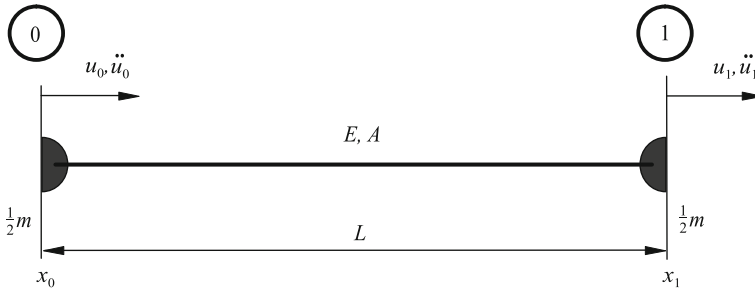
Fig. 13.14 One element with concentrated masses on the ends

From Eq. (13.78) one obtains directly

$$- \omega^2 \rho A L \times \frac{1}{2} + \frac{EA}{L} = 0 \tag{13.98}$$

and herefrom the solution

$$\omega = \sqrt{2}\sqrt{\frac{E}{\rho L^2}} \tag{13.99}$$

for the eigenfrequency. This result deviates significantly from the analytical solution.

Two Elements

Through a refining of the discretization with *two* elements a better solution can be achieved (Fig. 13.15). The system consists of two finite elements with linear shape functions and three nodes 0, 1, and 2 on the coordinates x_0, x_1 and x_2. With the mass and stiffness matrix

$$\boldsymbol{M} = \rho A \frac{1}{2} L \begin{bmatrix} 1 & 0 & 0 \\ 0 & 1 & 0 \\ 0 & 0 & \frac{1}{2} \end{bmatrix} \qquad \boldsymbol{K} = \frac{EA}{\frac{1}{2}L} \begin{bmatrix} 2 & -1 & 0 \\ -1 & 2 & -1 \\ 0 & -1 & 1 \end{bmatrix} \tag{13.100}$$

the equation of motion results in:

$$\begin{bmatrix} 1 & 0 & 0 \\ 0 & 1 & 0 \\ 0 & 0 & \frac{1}{2} \end{bmatrix} \begin{bmatrix} \ddot{u}_0 \\ \ddot{u}_1 \\ \ddot{u}_2 \end{bmatrix} + \frac{E}{\rho \frac{1}{4} L^2} \begin{bmatrix} 2 & -1 & 0 \\ -1 & 2 & -1 \\ 0 & -1 & 1 \end{bmatrix} \begin{bmatrix} u_0 \\ u_1 \\ u_2 \end{bmatrix} = \boldsymbol{0}. \tag{13.101}$$

No acceleration ($\ddot{u}_0 = 0$) and no displacement ($u_0 = 0$) occur on the fixing point.
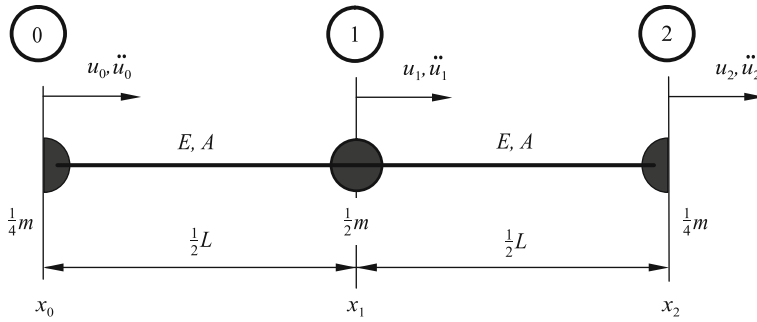
Fig. 13.15 Two elements with concentrated masses

The first row and the first column can be canceled from the system. From

$$\det\left(-\lambda^2 \begin{bmatrix} 1 & 0 \\ 0 & \frac{1}{2} \end{bmatrix} + \begin{bmatrix} 2 & -1 \\ -1 & 1 \end{bmatrix}\right) = 0 \tag{13.102}$$

with

$$\lambda^2 = \frac{1}{4}\frac{\rho L^2}{E}\omega^2 \tag{13.103}$$

one obtains via

$$\begin{vmatrix} -\lambda^2 + 2 & -1 \\ -1 & -\frac{1}{2}\lambda^2 + 1 \end{vmatrix} = 0 \quad \Rightarrow \quad \left(2 - \lambda^2\right)^2 = 2 \quad \Rightarrow \quad 2 - \lambda^2 = \pm\sqrt{2} \tag{13.104}$$

the solution $\lambda_1^2 = 2 - \sqrt{2}$ and $\lambda_2^2 = 2 + \sqrt{2}$. These can be written in detail as

$$\omega_1^2 = 4\left(2 - \sqrt{2}\right)\frac{E}{\rho L^2} \quad \Rightarrow \quad \omega_1 = 1.53\sqrt{\frac{E}{\rho L^2}} \tag{13.105}$$

and

$$\omega_2^2 = 4\left(2 + \sqrt{2}\right)\frac{E}{\rho L^2} \quad \Rightarrow \quad \omega_2 = 3.70\sqrt{\frac{E}{\rho L^2}}. \tag{13.106}$$

The solutions deviate significantly from the analytical solutions.

Three Elements

During the next refining the tension bar with three elements will be discretized. Therewith four nodes (0, 1, 2, 3) are on the coordinates x_0, x_1, x_2 and x_3 in the
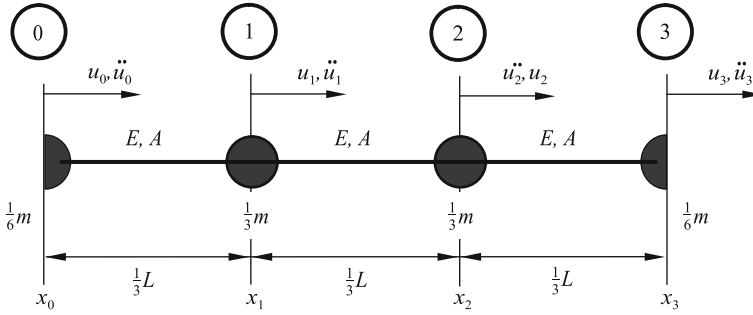
Fig. 13.16 Three elements with concentrated masses

system. The tension bar is fixed on the node 0 (Fig. 13.16). No acceleration ($\ddot{u}_0 = 0$) and no displacement $u_0 = 0$ occur on the fixing point. Therefore the respective first rows and columns can be canceled from the mass and stiffness matrix. The reduced matrices remain

$$\boldsymbol{M}^{\text{red}} = \rho A \frac{1}{3} L \begin{bmatrix} 1 & 0 & 0 \\ 0 & 1 & 0 \\ 0 & 0 & \frac{1}{2} \end{bmatrix} \quad \text{and} \quad \boldsymbol{K}^{\text{red}} = \frac{EA}{\frac{1}{3}L} \begin{bmatrix} 2 & -1 & 0 \\ -1 & 2 & -1 \\ 0 & -1 & 1 \end{bmatrix}. \tag{13.107}$$

With the abbreviation

$$\lambda^2 = \frac{1}{9} \frac{\rho L^2}{E} \omega^2 \tag{13.108}$$

one obtains the determinant and the characteristic equation

$$\begin{vmatrix} -\lambda^2 + 2 & -1 & 0 \\ -1 & -\lambda^2 + 2 & -1 \\ 0 & -1 & -\frac{1}{2}\lambda^2 + 1 \end{vmatrix} \stackrel{!}{=} 0 \quad \Rightarrow \quad \left(2 - \lambda^2\right)\left[\left(2 - \lambda^2\right)^2\right] = 0 \tag{13.109}$$

and herefrom the solutions

$$\lambda_1 = \sqrt{2 - \sqrt{3}}, \quad \lambda_2 = \sqrt{2}, \quad \lambda_3 = \sqrt{2 + \sqrt{3}} \;, \tag{13.110}$$

from which the eigenfrequency can be determined as follows

$$\omega_1 = 1.55\sqrt{\frac{\rho L^2}{E}}, \quad \omega_2 = 4.24\sqrt{\frac{\rho L^2}{E}}, \quad \omega_3 = 5.78\sqrt{\frac{\rho L^2}{E}}. \tag{13.111}$$

Table 13.1 summarizes all results. Therein are the relative errors in % for the FE solutions with continuously distributed and discretized masses (LMM). The errors relate to the analytical solution.

Table 13.1 Relative errors in % respective to the analytically determined eigenfrequency on the basis of elements with linear shape functions

Number of Elements	1	2		3		
Eigenfrequencies	1st	1st	2nd	1st	2nd	3rd
FEM	+10.27	+2.59	+19.5	+1.13	+8.23	+20.1
LMM	−9.97	−2.55	−21.5	−1.14	−9.96	−26.4

Table 13.2 Relative error in % respective to the analytically determined eigenfrequency on the basis of elements with quadratic shape functions

Number of elements	1		2			
Eigenfrequencies	1st	2nd	1st	2nd	3rd	4th
FEM	+0.38	+20.4	+0.03	+1.65	+11.77	+28.0
LMM	−0.8	−11.04	−0.17	−2.38	−5.52	−18.0

Remarks: From the comparison in Table 13.1 one can see that the lumped mass method (LMM) delivers values which are *too low*, while one obtains values which are too high from the finite element method (FEM). Through the concentration of the continuously mass on the nodal points, the inertia effects are enlarged, whereby the eigenfrequencies become smaller. In contrast, the inertia effects are reduced when making use of a mass matrix M according to the FEM, which is based on a linear form function matrix N. This leads to too high eigenfrequencies. Consequently a lower bound (LMM) and an upper bound (FEM) have been found for the limitation of the exact solution. If quadratic interpolation functions are used, the computing time of course increases. However a smaller number of elements is enough to achieve comparable results (Table 13.2).

13.6.2.2 The Tension Bar with Quadratic Shape Functions

The problem will be described similarly to the previous section (see Fig. 13.11). In contrast to a linear approach, the element with three nodes is described in a quadratic approach. First of all, the entire bar with only one element is presented. The system consists of one finite element with quadratic shape function and three nodes 0, 1 and 2 on the coordinates x_0, x_1 and x_2 (Fig. 13.17). With the mass and stiffness matrix for quadratic shape functions the following results for the equation of motion

$$\begin{bmatrix} 4 & 2 & -1 \\ 2 & 16 & 2 \\ -1 & 2 & 4 \end{bmatrix} \begin{bmatrix} \ddot{u}_0 \\ \ddot{u}_1 \\ \ddot{u}_2 \end{bmatrix} + \frac{10E}{\rho L^2} \begin{bmatrix} 7 & -8 & 1 \\ -8 & 16 & -8 \\ 1 & -8 & 7 \end{bmatrix} \begin{bmatrix} u_0 \\ u_1 \\ u_2 \end{bmatrix} = \begin{bmatrix} 0 \\ 0 \\ 0 \end{bmatrix}, \qquad (13.112)$$
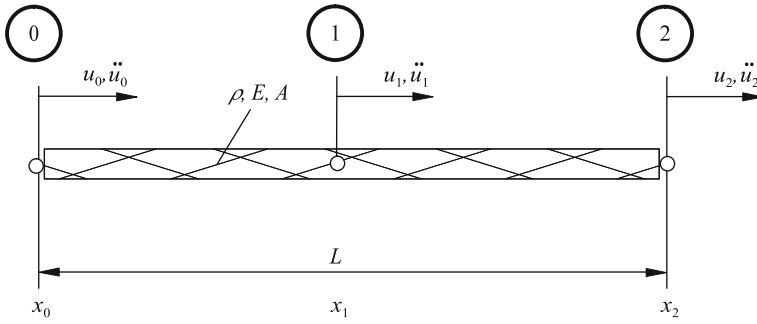
Fig. 13.17 One element with distributed mass and quadratic shape function

which can be simplified due to the boundary conditions on the fixing point $\ddot{u}_0 = 0, u_0 = 0$ to

$$
\begin{bmatrix} 16 & 2 \\ 2 & 4 \end{bmatrix} \begin{bmatrix} \ddot{u}_1 \\ \ddot{u}_2 \end{bmatrix} + \frac{10E}{\rho L^2} \begin{bmatrix} 16 & -8 \\ -8 & 7 \end{bmatrix} \begin{bmatrix} u_1 \\ u_2 \end{bmatrix} = \begin{bmatrix} 0 \\ 0 \end{bmatrix}. \tag{13.113}
$$

With the abbreviation

$$
\lambda^2 = \frac{\rho L^2}{10E} \omega^2 \tag{13.114}
$$

one obtains the characteristic equation

$$
\begin{vmatrix} -16\lambda^2 + 16 & -2\lambda^2 - 8 \\ -2\lambda^2 - 8 & -4\lambda^2 + 7 \end{vmatrix} \overset{!}{=} 0 \quad \Rightarrow \quad \lambda^4 - \frac{52}{15}\lambda^2 = -\frac{4}{5} \tag{13.115}
$$

with the solutions

$$
\lambda^2 = \frac{26}{15} \pm \frac{1}{15}\sqrt{496}, \tag{13.116}
$$

which can be written in detail as

$$
\omega_1^2 = 2.486 \frac{E}{\rho L^2} \quad \Rightarrow \quad \omega_1 = 1.57\sqrt{\frac{E}{\rho L^2}} \tag{13.117}
$$

and

$$
\omega_2^2 = 32.18 \frac{E}{\rho L^2} \quad \Rightarrow \quad \omega_2 = 5.67\sqrt{\frac{E}{\rho L^2}}. \tag{13.118}
$$

In contrast to the exact values ω_1 is affected by an error of $+0.38\%$ and ω_2 is affected by an error of $+20.4\%$. A slightly lower value for ω_1 with an error of

+1.13% was not achieved until a division of the bar into *three* finite elements on the basis of a linear displacement approach took place. For a single element, a value of $\omega_1 = 1.7321\sqrt{E/\rho L^2}$ has been achieved, which is affected by an error of 10.27 %. Therefore the value for ω_1 could be improved by +9.89 % through a quadratic displacement approach. To receive a comparable value for ω_2, two finite elements are required.

Two Elements

With this modeling, the bar is divided into two elements with quadratic shape functions. The system consists of five nodes in total 0, 1, 2, 3 and 4 on the coordinates x_0, x_1, x_2, x_3 and x_4 (Fig. 13.18).
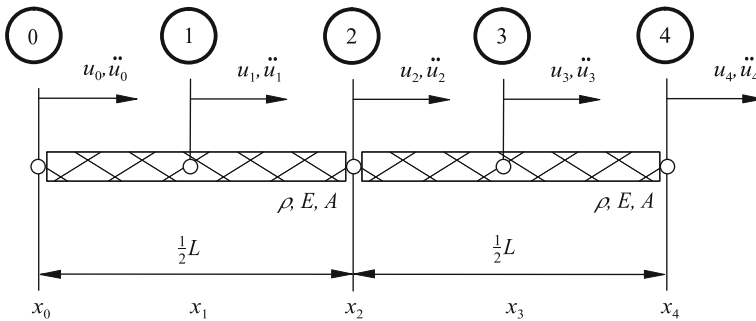
Fig. 13.18 Two elements with distributed masses and quadratic shape functions

The mass matrix

$$
M = \frac{\rho A \frac{1}{2} L}{30}
\begin{bmatrix}
4 & 2 & -1 & 0 & 0 \\
2 & 16 & 2 & 0 & 0 \\
-1 & 2 & 8 & 2 & -1 \\
0 & 0 & 2 & 16 & 2 \\
0 & 0 & -1 & 2 & 4
\end{bmatrix}
\tag{13.119}
$$

and the stiffness matrix

$$
K = \frac{E A}{3 \frac{1}{2} L}
\begin{bmatrix}
7 & -8 & 1 & 0 & 0 \\
-8 & 16 & -8 & 0 & 0 \\
1 & -8 & 14 & -8 & 1 \\
0 & 0 & -8 & 16 & -8 \\
0 & 0 & 1 & -8 & 7
\end{bmatrix}
\tag{13.120}
$$

have the dimension 5 × 5. No acceleration ($\ddot{u}_0 = 0$) and no displacement ($u_0 = 0$) occur on the fixing point. Therefore the first row and the corresponding first column

of the matrices can be canceled. From the equation of motion

$$
\begin{bmatrix} 16 & 2 & 0 & 0 \\ 2 & 8 & 2 & -1 \\ 0 & 2 & 16 & 2 \\ 0 & -1 & 2 & 4 \end{bmatrix} \begin{bmatrix} \ddot{u}_1 \\ \ddot{u}_2 \\ \ddot{u}_3 \\ \ddot{u}_4 \end{bmatrix} + \frac{40E}{\rho L^2} \begin{bmatrix} 16 & -8 & 0 & 0 \\ -8 & 14 & -8 & 1 \\ 0 & -8 & 16 & -8 \\ 0 & 1 & -8 & 7 \end{bmatrix} \begin{bmatrix} u_1 \\ u_2 \\ u_3 \\ u_4 \end{bmatrix} = \begin{bmatrix} 0 \\ 0 \\ 0 \\ 0 \end{bmatrix} \quad (13.121)
$$

the eigenvalue problem can be formulated

$$
\det\left(-\omega^2 \begin{bmatrix} 16 & 2 & 0 & 0 \\ 2 & 8 & 2 & -1 \\ 0 & 2 & 16 & 2 \\ 0 & -1 & 2 & 4 \end{bmatrix} + \frac{40E}{\rho L^2} \begin{bmatrix} 16 & -8 & 0 & 0 \\ -8 & 14 & -8 & 1 \\ 0 & -8 & 16 & -8 \\ 0 & 1 & -8 & 7 \end{bmatrix} \right) = 0 \quad (13.122)
$$

from which the solution for ω^2 or alternatively the eigenfrequency ω

$$
\omega_1^2 = 2.468664757 \frac{E}{\rho L^2} \quad \Rightarrow \quad \omega_1 = 1.5712 \sqrt{\frac{E}{\rho L^2}}, \quad (13.123)
$$

$$
\omega_2^2 = 22.94616601 \frac{E}{\rho L^2} \quad \Rightarrow \quad \omega_2 = 4.7902 \sqrt{\frac{E}{\rho L^2}}, \quad (13.124)
$$

$$
\omega_3^2 = 77.06313717 \frac{E}{\rho L^2} \quad \Rightarrow \quad \omega_3 = 8.7786 \sqrt{\frac{E}{\rho L^2}}, \quad (13.125)
$$

$$
\omega_4^2 = 198.6985027 \frac{E}{\rho L^2} \quad \Rightarrow \quad \omega_4 = 14.0961 \sqrt{\frac{E}{\rho L^2}} \quad (13.126)
$$

can be determined. The deviations from the analytical solutions are significantly lower in comparison with the approximations which were achieved with linear shape functions.

Method with Concentrated Masses (LMM)

In the first step of discretization the system consists of only one finite element with quadratic shape function and three nodes 0, 1 and 2 on the coordinates x_0, x_1 and x_2 (Fig. 13.19).
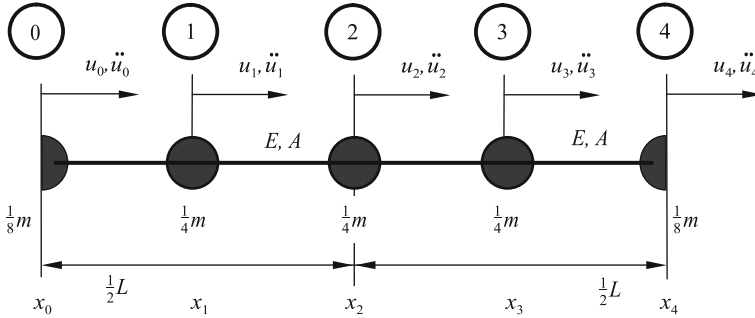With the mass and stiffness matrix

$$
M = \frac{\rho A L}{4} \begin{bmatrix} 1 & 0 & 0 \\ 0 & 2 & 0 \\ 0 & 0 & 1 \end{bmatrix} \quad \text{and} \quad K = \frac{EA}{3L} \begin{bmatrix} 7 & -8 & 1 \\ -8 & 16 & -8 \\ 1 & -8 & 7 \end{bmatrix} \quad (13.127)
$$
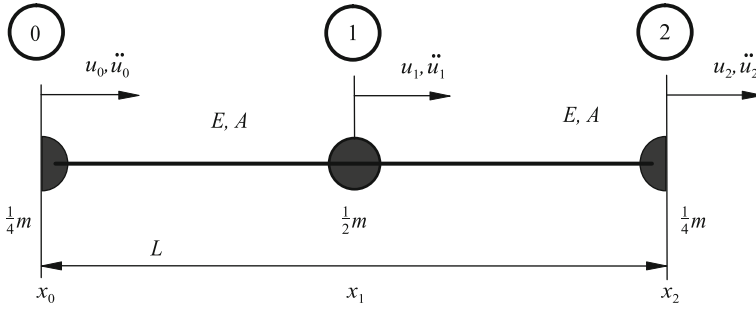
Fig. 13.19 One element with concentrated masses and quadratic shape function

the equation of motion appears as follows:

$$
\begin{bmatrix} 1 & 0 & 0 \\ 0 & 2 & 0 \\ 0 & 0 & 1 \end{bmatrix} \begin{bmatrix} \ddot{u}_0 \\ \ddot{u}_1 \\ \ddot{u}_2 \end{bmatrix} + \frac{4}{3} \frac{E}{\rho L^2} \begin{bmatrix} 7 & -8 & 1 \\ -8 & 16 & -8 \\ 1 & -8 & 7 \end{bmatrix} \begin{bmatrix} u_0 \\ u_1 \\ u_2 \end{bmatrix} = \begin{bmatrix} 0 \\ 0 \\ 0 \end{bmatrix}. \tag{13.128}
$$

No acceleration ($\ddot{u}_0 = 0$) and no displacement ($u_0 = 0$) occur on the fixing point. Therefore the first row and the respective first column of the matrices can be cancelled. With the abbreviation

$$
\lambda^2 = \frac{3}{4} \frac{\rho L^2}{E} \omega^2 \tag{13.129}
$$

one obtains the characteristic equation

$$
\begin{vmatrix} -2\lambda^2 + 16 & -8 \\ -8 & -\lambda^2 + 7 \end{vmatrix} \overset{!}{=} 0 \quad \Rightarrow \quad (\lambda^2 - 8)(\lambda^2 - 7) = 32 \tag{13.130}
$$

and therefore the solutions for λ_i

$$
\lambda_{2,1}^2 = \frac{15}{2} \pm \frac{1}{2} \sqrt{129} \tag{13.131}
$$

and therefrom the eigenfrequencies

$$
\omega_2 = 4.192 \sqrt{\frac{E}{\rho L^2}} \quad \text{and} \quad \omega_1 = 1.558 \sqrt{\frac{E}{\rho L^2}}. \tag{13.132}
$$

In comparison to the exact factor of 1.5708, the approximate value ω_1 is affected by an error of -8%, while ω_2 differs by -11.04%. One compares these results with the corresponding errors of $+0.38$ and $+20.4\%$ which result when using the equivalent mass matrix instead of the lumped-mass system.

Two Elements

In this step of discretization the system consists of two finite elements with quadratic shape functions and five nodes 0, 1, 2, 3 and 4 on the coordinates x_0, x_1, x_2, x_3 and x_4 (Fig. 13.20).

Fig. 13.20 Two elements with concentrated masses and quadratic shape functions

With the mass and stiffness matrix

$$M = \frac{\rho A \frac{1}{2} L}{4} \begin{bmatrix} 1 & 0 & 0 & 0 & 0 \\ 0 & 2 & 0 & 0 & 0 \\ 0 & 0 & 2 & 0 & 0 \\ 0 & 0 & 0 & 2 & 0 \\ 0 & 0 & 0 & 0 & 1 \end{bmatrix} \quad \text{and} \quad K = \frac{EA}{3\frac{1}{2}L} \begin{bmatrix} 7 & -8 & 1 & 0 & 0 \\ -8 & 16 & -8 & 0 & 0 \\ 1 & -8 & 14 & -8 & 1 \\ 0 & 0 & -8 & 16 & -8 \\ 0 & 0 & 1 & -8 & 7 \end{bmatrix} \quad (13.133)$$

one obtains, under consideration of the boundary conditions ($\ddot{x}_0 = 0$, $x_0 = 0$) the equation of motion:

$$\begin{bmatrix} 2 & 0 & 0 & 0 \\ 0 & 2 & 0 & 0 \\ 0 & 0 & 2 & 0 \\ 0 & 0 & 0 & 1 \end{bmatrix} \begin{bmatrix} \ddot{u}_1 \\ \ddot{u}_2 \\ \ddot{u}_3 \\ \ddot{u}_4 \end{bmatrix} + \frac{16}{3} \frac{E}{\rho L^2} \begin{bmatrix} 16 & -8 & 0 & 0 \\ -8 & 14 & -8 & 1 \\ 0 & -8 & 16 & -8 \\ 0 & 1 & -8 & 7 \end{bmatrix} \begin{bmatrix} u_1 \\ u_2 \\ u_3 \\ u_4 \end{bmatrix} = \begin{bmatrix} 0 \\ 0 \\ 0 \\ 0 \end{bmatrix}. \quad (13.134)$$

From the solution of the eigenvalue problem

$$\det\left(-\omega^2 \begin{bmatrix} 2 & 0 & 0 & 0 \\ 0 & 2 & 0 & 0 \\ 0 & 0 & 2 & 0 \\ 0 & 0 & 0 & 1 \end{bmatrix} + \frac{16}{3} \frac{E}{\rho L^2} \begin{bmatrix} 16 & -8 & 0 & 0 \\ -8 & 14 & -8 & 1 \\ 0 & -8 & 16 & -8 \\ 0 & 1 & -8 & 7 \end{bmatrix} \right) = 0 \quad (13.135)$$

one obtains the four real solutions

$$\omega_1^2 = 2.459021 \frac{E}{\rho L^2} \quad \Rightarrow \quad \omega_1 = 1.5681 \sqrt{\frac{E}{\rho L^2}}, \quad (13.136)$$

$$\omega_2^2 = 21.16383 \frac{E}{\rho L^2} \quad \Rightarrow \quad \omega_2 = 4.6004 \sqrt{\frac{E}{\rho L^2}}, \tag{13.137}$$

$$\omega_3^2 = 55.064934 \frac{E}{\rho L^2} \quad \Rightarrow \quad \omega_3 = 7.4206 \sqrt{\frac{E}{\rho L^2}}, \tag{13.138}$$

$$\omega_4^2 = 81.3122153 \frac{E}{\rho L^2} \quad \Rightarrow \quad \omega_4 = 9.0173 \sqrt{\frac{E}{\rho L^2}} \tag{13.139}$$

for ω_i^2 or alternatively the four eigenfrequencies ω_i.

Remark:
The eigenfrequencies approximated via the LMM are *smaller* as the analytically determined ones (*lower bound*). The following table summarizes all solutions. Given are the relative errors in % for the FE solutions with continuously distributed and discretized masses (LMM). The errors relate to the analytical solutions (Table 13.3).

Table 13.3 Relative error in % respective to the analytically determined eigenfrequency on the basis of elements with quadratic shape functions

Number of elements	1		2			
Eigenfrequencies	1st	2nd	1st	2nd	3rd	4th
FEM	+0.38	+20.4	+0.03	+1.65	+11.77	+28.0
LMM	−0.8	−11.04	−0.17	−2.38	−5.52	−18.0

13.7 Supplementary Problems

13.1. Analytical Solutions for Bending Vibrations
Determine the first four eigenfrequencies for the one-sided fixed mass loaded beam with length L with constant bending stiffness EI.
Given: ρ, L, EI

13.2 FE Solution for Bending Vibrations
Determine the first four eigenfrequencies for the one-sided fixed mass loaded beam with length L with constant bending stiffness EI.
Given: ρ, L, EI

References

1. Betten J (2004) Finite Elemente für Ingenieure 1: Grundlagen. Matrixmethoden. Elastisches Kontinuum, Springer, Berlin
2. Betten J (2004) Finite Elemente für Ingenieure 2: Variationsrechnung, Energiemethoden, Näherungsverfahren, Nichtlinearitäten. Numerische Integrationen, Springer, Berlin
3. Gross D, Hauger W, Schröder J, Werner EA (2008) Hydromechanik, Elemente der Höheren Mechanik. Numerische Methoden, Springer, Berlin
4. Gross D, Hauger W, Schröder J, Wall WA (2009) Technische Mechanik 2: Elastostatik. Springer, Berlin
5. Klein B (2000) FEM. Grundlagen und Anwendungen der Finite-Elemente-Methode, Vieweg-Verlag, Wiesbaden
6. Kwon YW, Bang H (2000) The finite element method using MATLAB. CRC Press, Boca Raton
7. Steinbuch R (1998) Finite Elemente–Ein Einstieg. Springer-Verlag, Berlin

Appendix A

A.1 Mathematics

A.1.1 The Greek Alphabet

Table A.1 The Greek Alphabet

Name	Lower case	Capital
Alpha	α	A
Beta	β	B
Gamma	γ	Γ
Delta	δ	Δ
Epsilon	ϵ	E
Zeta	ζ	Z
Eta	η	H
Theta	θ, ϑ	Θ
Iota	ι	I
Kappa	κ	K
Lambda	λ	Λ
My	μ	M
Ny	ν	N
Xi	ξ	Ξ
Omikron	o	O
Pi	π	Π
Rho	ρ, ϱ	P
Sigma	σ	Σ
Tau	τ	T
Ypsilon	υ	Υ
Phi	ϕ, φ	Φ
Chi	χ	X
Psi	ψ	Ψ
Omega	ω	Ω

A.1.2 Often Used Constants

$$\pi = 3.14159$$
$$e = 2.71828$$
$$\sqrt{2} = 1.41421$$
$$\sqrt{3} = 1.73205$$
$$\sqrt{5} = 2.23606$$
$$\sqrt{e} = 1.64872$$
$$\sqrt{\pi} = 1.77245$$

A.1.3 Special Products

$$(x+y)^2 = x^2 + 2xy + y^2, \tag{A.1}$$

$$(x-y)^2 = x^2 - 2xy + y^2, \tag{A.2}$$

$$(x+y)^3 = x^3 + 3x^2y + 3xy^2 + y^3, \tag{A.3}$$

$$(x-y)^3 = x^3 - 3x^2y + 3xy^2 - y^3, \tag{A.4}$$

$$(x+y)^4 = x^4 + 4x^3y + 6x^2y^2 + 4xy^3 + y^4, \tag{A.5}$$

$$(x-y)^4 = x^4 - 4x^3y + 6x^2y^2 - 4xy^3 + y^4. \tag{A.6}$$

A.1.4 Trigonometric Functions

Definition of the right-angled triangle
The triangle ABC has a right angle at C and the edge lengths a, b, c. The trigonometric functions of the angle α are defined in the following kind, see Fig. A.1 and (Table A.1):

Fig. A.1 Triangle with a
right angle at C
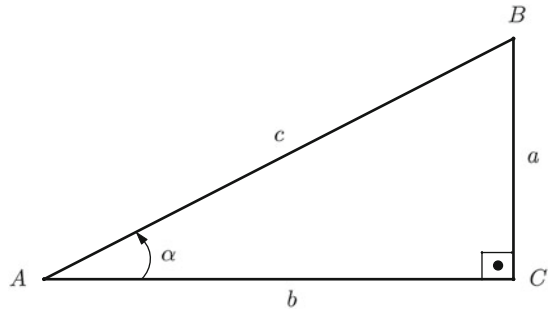
$$\text{Sine of } \alpha = \sin \alpha = \frac{a}{c} = \frac{\text{Opposite}}{\text{Hypotenuse}}, \tag{A.7}$$

$$\text{Cosine of } \alpha = \cos \alpha = \frac{b}{c} = \frac{\text{Adjacent}}{\text{Hypotenuse}}, \tag{A.8}$$

$$\text{Tangent of } \alpha = \tan \alpha = \frac{a}{b} = \frac{\text{Opposite}}{\text{Adjacent}}, \tag{A.9}$$

$$\text{Cotangent of } \alpha = \cot \alpha = \frac{b}{a} = \frac{\text{Adjacent}}{\text{Opposite}}, \tag{A.10}$$

$$\text{Secant of } \alpha = \sec \alpha = \frac{c}{b} = \frac{\text{Hypotenuse}}{\text{Adjacent}}, \tag{A.11}$$

$$\text{Cosecant of } \alpha = \csc \alpha = \frac{c}{a} = \frac{\text{Hypotenuse}}{\text{Opposite}}. \tag{A.12}$$

Addition Theorem

$$\sin(\alpha \pm \beta) = \sin \alpha \cos \beta \pm \cos \alpha \sin \beta, \tag{A.13}$$

$$\cos(\alpha \pm \beta) = \cos \alpha \cos \beta \mp \sin \alpha \sin \beta, \tag{A.14}$$

$$\tan(\alpha \pm \beta) = \frac{\tan \alpha \pm \tan \beta}{1 \mp \tan \alpha \tan \beta}, \tag{A.15}$$

$$\cot(\alpha \pm \beta) = \frac{\cot \alpha \cot \beta \mp 1}{\cot \beta \pm \cot \beta}. \tag{A.16}$$

Mutual Presentation

$$\sin^2 \alpha + \cos^2 \alpha = 1, \tag{A.17}$$

$$\tan \alpha = \frac{\sin \alpha}{\cos \alpha}. \tag{A.18}$$

Analytical Values for Different Angles

Table A.2 Analytical values of sine, cosine, tangent and cotangent for different angels

α in Degree	α in Radian	$\sin \alpha$	$\cos \alpha$	$\tan \alpha$	$\cot \alpha$
0	0	0	1	0	$\pm\infty$
30	$\frac{1}{6}\pi$	$\frac{1}{2}$	$\frac{\sqrt{3}}{2}$	$\frac{\sqrt{3}}{3}$	$\sqrt{3}$
45	$\frac{1}{4}\pi$	$\frac{\sqrt{2}}{2}$	$\frac{\sqrt{2}}{2}$	1	1
60	$\frac{1}{3}\pi$	$\frac{\sqrt{3}}{2}$	$\frac{1}{2}$	$\sqrt{3}$	$\frac{\sqrt{3}}{3}$
90	$\frac{1}{2}\pi$	1	0	$\pm\infty$	0
120	$\frac{2}{3}\pi$	$\frac{\sqrt{3}}{2}$	$-\frac{1}{2}$	$-\sqrt{3}$	$-\frac{\sqrt{3}}{3}$
135	$\frac{3}{4}\pi$	$\frac{\sqrt{2}}{2}$	$-\frac{\sqrt{2}}{2}$	1	1
150	$\frac{5}{6}\pi$	$\frac{1}{2}$	$-\frac{\sqrt{3}}{2}$	$-\frac{\sqrt{3}}{3}$	$-\sqrt{3}$
180	π	0	-1	0	$\pm\infty$
210	$\frac{7}{6}\pi$	$-\frac{1}{2}$	$-\frac{\sqrt{3}}{2}$	$\frac{\sqrt{3}}{3}$	$\sqrt{3}$
225	$\frac{5}{4}\pi$	$-\frac{\sqrt{2}}{2}$	$-\frac{\sqrt{2}}{2}$	1	1
240	$\frac{4}{3}\pi$	$-\frac{\sqrt{3}}{2}$	$-\frac{1}{2}$	$\sqrt{3}$	$\frac{\sqrt{3}}{3}$
270	$\frac{3}{2}\pi$	-1	0	$\pm\infty$	0
300	$\frac{5}{3}\pi$	$-\frac{\sqrt{3}}{2}$	$\frac{1}{2}$	$-\sqrt{3}$	$-\frac{\sqrt{3}}{3}$
315	$\frac{7}{4}\pi$	$-\frac{\sqrt{2}}{2}$	$\frac{\sqrt{2}}{2}$	-1	-1
330	$\frac{11}{6}\pi$	$-\frac{1}{2}$	$\frac{\sqrt{3}}{2}$	$-\frac{\sqrt{3}}{3}$	$-\sqrt{3}$
360	2π	0	1	0	$\pm\infty$

Double Angle Functions

$$\sin(2\alpha) = 2\sin\alpha \cdot \cos\alpha, \tag{A.19}$$

$$\cos(2\alpha) = \cos^2\alpha - \sin^2\alpha$$
$$= 2\cos^2\alpha - 1$$
$$= 1 - 2\sin^2\alpha, \tag{A.20}$$

$$\tan(2\alpha) = \frac{2\tan\alpha}{1 - \tan^2\alpha}. \tag{A.21}$$

Reduction Formulae

Table A.3 Reduction formulae for trigonometric functions

	$-\alpha$	$90° \pm \alpha$ $\frac{\pi}{2} \pm \alpha$	$180° \pm \alpha$ $\pi \pm \alpha$	$270° \pm \alpha$ $\frac{3\pi}{2} \pm \alpha$	$k(360°) \pm \alpha$ $2k\pi \pm \alpha$
sin	$-\sin\alpha$	$\cos\alpha$	$\mp\sin\alpha$	$-\cos\alpha$	$\pm\sin\alpha$
cos	$\cos\alpha$	$\mp\sin\alpha$	$-\cos\alpha$	$\pm\sin\alpha$	$\cos\alpha$
tan	$-\tan\alpha$	$\mp\cot\alpha$	$\pm\tan\alpha$	$\mp\cot\alpha$	$\pm\tan\alpha$
csc	$-\csc\alpha$	$\sec\alpha$	$\mp\csc\alpha$	$-\sec\alpha$	$\pm\csc\alpha$
sec	$\sec\alpha$	$\mp\csc\alpha$	$-\sec\alpha$	$\pm\csc\alpha$	$\sec\alpha$
cot	$-\cot\alpha$	$\mp\tan\alpha$	$\pm\cot\alpha$	$\mp\tan\alpha$	$\pm\cot\alpha$

A.1.5 Basics for Linear Algebra

Vectors

With

$$a = [a_1\ a_2\ a_i\ ...\ a_n] \tag{A.22}$$

a row vector and with

$$a = \begin{bmatrix} a_1 \\ a_2 \\ a_i \\ \vdots \\ a_n \end{bmatrix} \tag{A.23}$$

a column vector[1] of dimension n is defined, whereupon the following is valid for all components: $a_i \in \mathbb{R} = 1, 2, ..., n$ (Tables A.2 and A.3).

Matrices

The term matrix can be shown with the help of a simple example. The linear relation between a system of variables x_i and b_i

$$a_{11}x_1 + a_{12}x_2 + a_{13}x_3 + a_{14}x_4 = b_1 \tag{A.24}$$

$$a_{21}x_1 + a_{22}x_2 + a_{23}x_3 + a_{24}x_4 = b_2 \tag{A.25}$$

$$a_{31}x_1 + a_{32}x_2 + a_{33}x_3 + a_{34}x_4 = b_3 \tag{A.26}$$

can be summarized in a compact form as

$$Ax = b \tag{A.27}$$

or

$$\begin{bmatrix} a_{11} & a_{12} & a_{13} & a_{14} \\ a_{21} & a_{22} & a_{23} & a_{24} \\ a_{31} & a_{32} & a_{33} & a_{34} \end{bmatrix} \begin{bmatrix} x_1 \\ x_2 \\ x_3 \\ x_4 \end{bmatrix} = \begin{bmatrix} b_1 \\ b_2 \\ b_3 \end{bmatrix}. \tag{A.28}$$

---

[1] The expression vector is used differently in mathematics and physics. In physics, a vector represents a physical dimension such as, for example, a force. A direction as well as an absolute value can be assigned to this vector. In mathematics, the expression vector is used for a positioning of components. Also here values can be defined, which however are without any physical meaning. Therefore at times vectors are also referred to as row or column matrices.

Thereby the following is valid for all coefficients a_{ij} and all components b_i and x_i:
$a_{ij}, b_i, x_j \in \mathbb{R} = 1, 2, 3, j = 1, 2, 3, 4.$
Generally speaking a matrix A of the dimension $m \times n$

$$
A^{m \times n} = \begin{bmatrix} a_{11} & a_{12} & \dots & a_{1n} \\ a_{21} & a_{22} & \dots & a_{2n} \\ \vdots & \vdots & \dots & \vdots \\ a_{m1} & a_{m2} & \dots & a_{mn} \end{bmatrix} \tag{A.29}
$$

consists of m rows and n columns.
The **transpose** of a matrix results from interchanging of rows and columns:

$$
A^{\mathrm{T}} = \begin{bmatrix} a_{11} & a_{21} & \dots & a_{m1} \\ a_{12} & a_{22} & \dots & a_{m2} \\ \vdots & \vdots & \vdots & \vdots \\ \vdots & \vdots & \vdots & \vdots \\ a_{1n} & a_{2n} & \dots & a_{mn} \end{bmatrix}. \tag{A.30}
$$

Quadratic matrices have equivalent rows and columns:

$$
A^{n \times n} = \begin{bmatrix} a_{11} & a_{12} & \dots & a_{1n} \\ a_{21} & a_{22} & \dots & a_{2n} \\ \vdots & \vdots & \dots & \vdots \\ a_{n1} & a_{n2} & \dots & a_{nn} \end{bmatrix}. \tag{A.31}
$$

If the following is valid additionally for a quadratic matrix

$$
a_{ij} = a_{ji}, \tag{A.32}
$$

a symmetric matrix results. As an example, a symmetric (3×3) matrix has the form

$$
A^{3 \times 3} = \begin{bmatrix} a_{11} & a_{12} & a_{13} \\ a_{12} & a_{22} & a_{23} \\ a_{13} & a_{23} & a_{33} \end{bmatrix}. \tag{A.33}
$$

Matrix Operations
The multiplication of two matrices looks as follows in index notation

$$
c_{ij} = \sum_{k=1}^{m} a_{ik} b_{kj} \quad \begin{array}{l} i = 1, 2, ..., n \\ j = 1, 2, ..., r \end{array} \tag{A.34}
$$

or in matrix notation

$$
C = AB. \tag{A.35}
$$

Thereby the matrix $A^{n \times m}$ has n rows and m columns, matrix $B^{m \times r}$ m rows and r columns and the matrix product $C^{n \times r}$ n rows and r columns.

The multiplication of two matrices is not commutative, this means

$$AB \neq BA. \tag{A.36}$$

The product of two transposed matrices $A^{T}B^{T}$ results in

$$A^{T}B^{T} = (BA)^{T}. \tag{A.37}$$

The transpose of a matrix product can be split with the help of

$$(AB)^{T} = B^{T}A^{T} \tag{A.38}$$

into the product of the transposed matrices. When multiplying various matrices, the associative law

$$(A B)\, C = A\, (B C) = A B C \tag{A.39}$$

and the distributive law are valid

$$A\, (B + C) = A B + AC. \tag{A.40}$$

Determinant of a Matrix

The determinant of a quadratic matrix A of the dimension n can be determined recursively via

$$|A| = \sum_{i=1}^{n} (-1)^{i+1}\, a_{1i}\, |A_{1i}| \tag{A.41}$$

The submatrix A_{1i} of dimension $(n-1)(n-1)$ emerges due to canceling of the 1st row and the ith column of A.

Inverse of a Matrix

A is a quadratic matrix. The inverse A^{-1} is quadratic as well. The product of matrix and inverse matrix

$$A^{-1}A = I \tag{A.42}$$

yields the unit matrix.

The inverse of a matrices product results as a product of the inverses of the matrices:

$$(AB)^{-1} = B^{-1}A^{-1}. \tag{A.43}$$

The inverse of the transposed matrix results as the transpose of the inverse matrix:

$$[A^{T}]^{-1} = [A^{-1}]^{T}. \tag{A.44}$$

Formally, with the inverse of a matrix, the system of equations

$$\mathbf{A}\mathbf{x} = \mathbf{b} \tag{A.45}$$

can be solved. Thereby the quadratic matrix $\mathbf{A}$ and the vectors $\mathbf{x}$ and $\mathbf{b}$ have the same dimension. With the multiplication of the inverse from the left

$$\mathbf{A}^{-1}\mathbf{A}\mathbf{x} = \mathbf{A}^{-1}\mathbf{b} \tag{A.46}$$

one obtains the vector of the unknown to

$$\mathbf{x} = \mathbf{A}^{-1}\mathbf{b}. \tag{A.47}$$

For a (2×2)- and a (3×3)-matrix the inverses are given explicitly. For a quadratic (2×2)-matrix

$$\mathbf{A} = \begin{bmatrix} a_{11} & a_{12} \\ a_{21} & a_{22} \end{bmatrix} \tag{A.48}$$

the inverse results in

$$\mathbf{A}^{-1} = \frac{1}{|\mathbf{A}|} \begin{bmatrix} a_{11} & a_{12} \\ a_{21} & a_{22} \end{bmatrix} \tag{A.49}$$

with

$$|\mathbf{A}| = a_{11}a_{22} - a_{12}a_{21}. \tag{A.50}$$

For the quadratic (3×3)-matrix

$$\mathbf{A} = \begin{bmatrix} a_{11} & a_{12} & a_{13} \\ a_{21} & a_{22} & a_{23} \\ a_{31} & a_{32} & a_{33} \end{bmatrix} \tag{A.51}$$

the inverse results in

$$\mathbf{A}^{-1} = \frac{1}{|\mathbf{A}|} \begin{bmatrix} \tilde{a}_{11} & \tilde{a}_{12} & \tilde{a}_{13} \\ \tilde{a}_{21} & \tilde{a}_{22} & \tilde{a}_{23} \\ \tilde{a}_{31} & \tilde{a}_{32} & \tilde{a}_{33} \end{bmatrix} \tag{A.52}$$

with the coefficients of the inverses

$$\tilde{a}_{11} = +a_{22}a_{33} - a_{32}a_{23}$$
$$\tilde{a}_{12} = -(a_{12}a_{33} - a_{13}a_{32})$$
$$\tilde{a}_{13} = +a_{12}a_{23} - a_{22}a_{13}$$
$$\tilde{a}_{21} = -(a_{21}a_{33} - a_{31}a_{23})$$
$$\tilde{a}_{22} = +a_{11}a_{33} - a_{13}a_{31} \tag{A.53}$$
$$\tilde{a}_{23} = -(a_{11}a_{23} - a_{21}a_{13})$$
$$\tilde{a}_{31} = +a_{21}a_{32} - a_{31}a_{22}$$
$$\tilde{a}_{32} = -(a_{11}a_{32} - a_{31}a_{12})$$
$$\tilde{a}_{33} = +a_{11}a_{22} - a_{12}a_{21}$$

and with the determinant

$$|A| = a_{11}a_{22}a_{33} + a_{13}a_{21}a_{32} + a_{31}a_{12}a_{23}$$
$$-a_{31}a_{22}a_{13} - a_{33}a_{12}a_{21} - a_{11}a_{23}a_{32} . \tag{A.54}$$

Equation Solving

The initial point is the system of equations

$$A x = b \tag{A.55}$$

with the quadratic matrix A and the vectors x and b, which both have the same dimension. The matrix A and the vectors b are both assigned with known values. It is the goal to determine the vector of the unknowns x.

The central operation at the direct equations solving is the partition of the system matrix

$$A = LU \tag{A.56}$$

into a lower and a upper triangular matrix. In detail this operation looks as follows:

$$LU = \begin{bmatrix} 1 & 0 & \dots & 0 \\ L_{21} & 1 & \dots & 0 \\ \vdots & & \ddots & \vdots \\ L_{n1} & L_{n2} & \dots & 1 \end{bmatrix} \begin{bmatrix} U_{11} & U_{12} & \dots & U_{1n} \\ 0 & U_{22} & \dots & U_{2n} \\ \vdots & & \ddots & \vdots \\ 0 & 0 & \dots & U_{nn} \end{bmatrix} . \tag{A.57}$$

The triangular decomposition is quite computationally intensive. Variants of the GAUSS elimination are used as algorithms. Crucial is the structure of the system matrix A. If blocks with zero entries can be identified in advance in the system matrix the row and column operations can then be used for the blocks only with non-zero entries.

The equations solution is conducted with the paired solution of the two equations

$$Ly = b \tag{A.58}$$

and

$$\mathbf{Ux} = \mathbf{y} \tag{A.59}$$

whereupon $\mathbf{y}$ is solely an auxiliary vector. The single operations proceed as follows:

$$y_1 = b_1 \tag{A.60}$$

$$y_i = b_i - \sum_{j=1}^{i-1} L_{ij} y_j \quad i = 2, 3, ..., n \tag{A.61}$$

and

$$x_n = \frac{y_n}{U_{nn}} \tag{A.62}$$

$$x_i = \frac{1}{U_{ii}} \left(y_i - \sum_{j=i+1}^{n} U_{ij} x_j \right) \quad i = n - 1, n - 2, ..., 1. \tag{A.63}$$

The first two steps are referred to as forward partition and the last two steps as backward substitution.

In the last equation it is divided through the value of the diagonal of the upper triangular matrix. For very small and very large values this can lead to inaccuracies. An improvement can be achieved via a so-called pivoting, at which in the current row or column one has to search for the 'best' factor.

A.1.6 Derivatives

- $\frac{d}{dx}\left(\frac{1}{x}\right) = -\frac{1}{x^2}$
- $\frac{d}{dx} x^n = n \times x^{n-1}$
- $\frac{d}{dx} \sqrt[n]{x} = \frac{1}{n \times \sqrt[n]{x^{n-1}}}$
- $\frac{d}{dx} \sin(x) = \cos(x)$
- $\frac{d}{dx} \cos(x) = -\sin(x)$
- $\frac{d}{dx} \ln(x) = \frac{1}{x}$
- $\frac{d}{dx} |x| = \begin{cases} -1 & \text{if} \quad x < 0 \\ 1 & \text{if} \quad x > 0 \end{cases}$

A.1.7 Integration

A.1.7.1 Antiderivatives

- $\int e^x \, \mathrm{d}x = e^x$
- $\int \sqrt{x} \, \mathrm{d}x = \frac{2}{3} x^{\frac{3}{2}}$
- $\int \sin(x) \, \mathrm{d}x = -\cos(x)$
- $\int \cos(x) \, \mathrm{d}x = \sin(x)$
- $\int \sin(\alpha x) \cdot \cos(\alpha x) \, \mathrm{d}x = \frac{1}{2\alpha} \sin^2(\alpha x)$
- $\int \sin^2(\alpha x) \, \mathrm{d}x = \frac{1}{2} \left(x - \sin(\alpha x) \cos(\alpha x) \right) = \frac{1}{2} \left(x - \frac{1}{2\alpha} \sin(2\alpha x) \right)$
- $\int \cos^2(\alpha x) \, \mathrm{d}x = \frac{1}{2} \left(x + \sin(\alpha x) \cos(\alpha x) \right) = \frac{1}{2} \left(x + \frac{1}{2\alpha} \sin(2\alpha x) \right)$

A.1.7.2 Partial Integration

One-Dimensional Case:

$$\int_a^b f(x)g'(x)\mathrm{d}x = f(x)g(x)\big|_a^b - \int_a^b f'(x)g(x)\mathrm{d}x \tag{A.64}$$

$$= f(x)g(x)\big|_b - f(x)g(x)\big|_a - \int_a^b f'(x)g(x) \, \mathrm{d}x. \tag{A.65}$$

A.1.7.3 Integration and Coordinate Transformation

One-Dimensional Case:
$T : \mathbb{R} \to \mathbb{R}$ with $x = g(u)$ is a one-dimensional transformation of S to R. If g has a continuous partial derivative, so that the JACOBIAN matrix becomes nonzero, the following is valid

$$\int_R f(x) \, \mathrm{d}x = \int_S f(g(u)) \left| \frac{\mathrm{d}x}{\mathrm{d}u} \right| \mathrm{d}u, \tag{A.66}$$

whereupon the JACOBIAN matrix in the one-dimensional case is given through $J = \left| \frac{\mathrm{d}x}{\mathrm{d}u} \right| = x_u$.

A.1.7.4 One-Dimensional Integrals for the Calculation of the Stiffness Matrix

$$\int_{-1}^{1} (1-x)dx = 2 \qquad \int_{-1}^{1} (1-x)^2(1+x)dx = \frac{4}{3}$$

$$\int_{-1}^{1} (1+x)dx = 2 \qquad \int_{-1}^{1} (1-x^2)dx = \frac{4}{3}$$

$$\int_{-1}^{1} (1-x)(1+x)dx = \frac{4}{3} \qquad \int_{-1}^{1} (1+x^2)dx = \frac{8}{3}$$

$$\int_{-1}^{1} (1-x)^2 dx = \frac{8}{3} \qquad \int_{-1}^{1} (1-2x)xdx = -\frac{4}{3}$$

$$\int_{-1}^{1} (1+x)^2 dx = \frac{8}{3} \qquad \int_{-1}^{1} (1+2x)xdx = \frac{4}{3}$$

$$\int_{-1}^{1} (1-x)^3 dx = 4 \qquad \int_{-1}^{1} (1-2x)^2 dx = \frac{14}{3}$$

$$\int_{-1}^{1} (1+x)^3 dx = 4 \qquad \int_{-1}^{1} (1+2x)^2 dx = \frac{14}{3}$$

$$\int_{-1}^{1} (1-x)(1+x)^2 dx = \frac{4}{3} \qquad \int_{-1}^{1} (1-2x)(1+2x)dx = -\frac{2}{3}$$

A.1.8 Expansion of a Function in a Taylor's Series

The expansion of a function $f(x)$ in a TAYLOR's series at the position x_0 yields:

$$f(x) = f(x_0) + \left(\frac{df}{dx}\right)_{x_0} \cdot (x - x_0) + \frac{1}{2!}\left(\frac{d^2f}{dx^2}\right)_{x_0} \cdot (x - x_0)^2 + \cdots + \frac{1}{k!}\left(\frac{d^kf}{dx^k}\right)_{x_0} \cdot (x - x_0)^k .$$

$$(A.67)$$

An approximation of first order only takes into account the first derivative, and the approach for the function results in:

$$f(x) = f(x_0 + dx) \approx f(x_0) + \left(\frac{df}{dx}\right)_{x_0} \cdot (x - x_0) . \qquad (A.68)$$

If one considers from the analytical geometry that the first derivative of a function equals the slope of the tangent in the considered point and that the point-slope form of a straight line is given through $f(x) - f(x_0) = m \cdot (x - x_0)$, it results that the approximation of first order represents the equation of a straight line through the point $(x_0, f(x_0))$ with the slope $m = f'(x_0) = (df/dx)_{x_0}$, compare Fig. A.2.

Fig. A.2 Approximation of a function $f(x)$ via a TAYLOR's series of first order
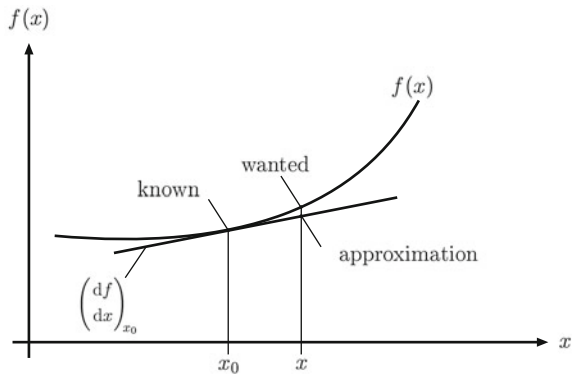
A.2 Units and Conversions

A.2.1 Consistent Units

In applying a finite element program usually there is no regulation on a specific physical mass or unit system. A finite element program retains *consistent* units throughout the analysis and requires the user to only enter absolute measure values without the information about a certain unit. Therewith the units, which are used by the user for the input, are also kept consistent in the output. The user therefore has to

ensure for himself that his/her chosen units are consistent, meaning compatible with each other. The following Table A.4 shows an example of consistent units.

Table A.4 Examples of consistent units

Size	Unit
Length	mm
Area	mm^2
Force	N
Stress	$MPa = \frac{N}{mm^2}$
Moment	Nmm
Moment of inertia	mm^4
Elastic modulus	$MPa = \frac{N}{mm^2}$
Density	$\frac{Ns^2}{mm^4}$
Time	s
Mass	$10^3 kg$

One can consider at this point the unit of the density. The following example shows the conversion of the density for steal:

$$\varrho_{St} = 7.8 \; \frac{kg}{dm^3} = 7.8 \times 10^3 \; \frac{kg}{m^3} = 7.8 \times 10^{-6} \; \frac{kg}{mm^3}. \tag{A.69}$$

With

$$1\,N = 1 \; \frac{m\,kg}{s^2} = 1 \times 10^3 \; \frac{mm\,kg}{s^2} \quad und \quad 1\,kg = 1 \times 10^{-3} \; \frac{Ns^2}{mm} \tag{A.70}$$

the consistent density results in:

$$\varrho_{St} = 7.8 \times 10^{-9} \; \frac{Ns^2}{mm^4}. \tag{A.71}$$

Since in the literature at one point or another also other units occur, the following Table A.5 shows an example of consistent English units:

Table A.5 Example of consistent English units

Size	Unit
Length	in
Area	in^2
Force	lbf
Stress	$psi = \frac{lbf}{in^2}$
Moment	lbf in
Moment of inertia	in^4
Elastic modulus	$psi = \frac{lbf}{in^2}$
Density	$\frac{lbf\,sec^2}{in^4}$
Time	sec

One also considers at this point the conversion of the density (Table A.6):

$$\varrho_{St} = 0.282 \; \frac{lb}{in^3} = 0.282 \; \frac{1}{in^3} \times 0.00259 \; \frac{lbf \; sec^2}{in}$$

$$= 0.73038 \times 10^{-3} \; \frac{lbf \; sec^2}{in^4} \; . \tag{A.72}$$

A.2.2 Conversion of Important English Units

Table A.6 Conversion of important English units

Type	English-speaking unit	Conversion
Length	Inch	1 in = 0.025400 m
	Foot	1 ft = 0.304800 m
	Yard	1 yd = 0.914400 m
	Mile (Statute)	1 mi = 1609.344 m
	Mile (Nautical)	1 nm = 1852.216 m
Area	Square inch	1 sq in = 1 in^2 = 6.45160 cm^2
	Square foot	1 sq ft = 1 ft^2 = 0.092903040 m^2
	Square yard	1 sq yd = 1 yd^2 = 0.836127360 m^2
	Square mile	1 sq mi = 1 mi^2 = 2589988.110336 m^2
	Acre	1 ac = 4046.856422400 m^2
Volume	Cubic inch	1 cu in = 1 in^3 = 0.000016387064 m^3
	Cubic foot	1 cu ft = 1 ft^3 = 0.028316846592 m^3
	Cubic yard	1 cu yd = 1 yd^3 = 0.764554857984 m^3
Mass	Ounce	1 oz = 28.349523125 g
	Pound (mass)	1 lb_m = 453.592370 g
	Short ton	1 sh to = 907184.74 g
	Long ton	1 lg to = 1016046.9088 g
Force	Pound-force	1 lbf = 1 lb_F = 4.448221615260500 N
	Poundal	1 pdl = 0.138254954376 N
Stress	Pound-force per square inch	1 psi = 1 $\frac{lbf}{in^2}$ = 6894.75729316837 $\frac{N}{m^2}$
	Pound-force per square foot	1 $\frac{lbf}{ft^2}$ = 47.880258980336 $\frac{N}{m^2}$
Energy	British thermal unit	1 Btu = 1055.056 J
	Calorie	1 cal = 4185.5 J
Power	Horsepower	1 hp = 745.699871582270 W

Short Solutions of the Exercises

Problems from Chap. 3

3.4 Short solution: Tension bar with quadratic approximation

Three nodes are being introduced in a quadratic approach. The three form functions are:

$$
\begin{aligned}
N_1(x) &= 1 - 3\frac{x}{L} + 2\left(\frac{x}{L}\right)^2, \\
N_2(x) &= 4\frac{x}{L}\left(1 - \frac{x}{L}\right), \\
N_3(x) &= \frac{x}{L}\left(-1 + 2\frac{x}{L}\right).
\end{aligned}
\tag{A.73}
$$

The derivatives of the three form functions result in:

$$
\begin{aligned}
\frac{dN_1(x)}{dx} &= N_1'(x) = -3 + 4\frac{x}{L}, \\
\frac{dN_2(x)}{dx} &= N_2'(x) = 4 - 8\frac{x}{L}, \\
\frac{dN_3(x)}{dx} &= N_3'(x) = -1 + 4\frac{x}{L}.
\end{aligned}
\tag{A.74}
$$

With the general calculation rule for the stiffness matrix

$$
\boldsymbol{k}^{\mathrm{e}} = \int_{\Omega} \boldsymbol{B}^{\mathrm{T}} \boldsymbol{D} \boldsymbol{B}\, \mathrm{d}\Omega = EA \int_0^L \boldsymbol{B}^{\mathrm{T}} \boldsymbol{B}\, \mathrm{d}x = EA \int_0^L \boldsymbol{N}'^{\mathrm{T}} \boldsymbol{N}'\, \mathrm{d}x
\tag{A.75}
$$

the following results for a three-nodal element

$$
\boldsymbol{k}^{\mathrm{e}} = EA \int_0^L \begin{bmatrix} N_1'^2 & N_1'N_2' & N_1'N_3' \\ & N_2'^2 & N_2'N_3' \\ \mathrm{sym.} & & N_3'^2 \end{bmatrix} \mathrm{d}x.
\tag{A.76}
$$

After the integration

$$
\int\limits_0^L
\begin{bmatrix}
(-3+4\tfrac{x}{L})^2 & (-3+4\tfrac{x}{L})(4-8\tfrac{x}{L}) & (-3+4\tfrac{x}{L})(-1+4\tfrac{x}{L}) \\
 & (4-8\tfrac{x}{L})^2 & (4-8\tfrac{x}{L})(-1+4\tfrac{x}{L}) \\
\text{sym.} & & (-1+4\tfrac{x}{L})^2
\end{bmatrix}
\mathrm{d}x \qquad (\mathrm{A.77})
$$

the stiffness matrix for a bar element with quadratic shape function results in:

$$
\boldsymbol{k}^{\mathrm{e}} = \frac{EA}{3L}
\begin{bmatrix}
7 & -8 & 1 \\
-8 & 16 & -8 \\
1 & -8 & 7
\end{bmatrix}. \qquad (\mathrm{A.78})
$$

A.6 Problems from Chap. 5

5.4 Equilibrium relation for infinitesimal beam element with changeable load
For the setup of the equilibrium relation the changeable load is evaluated in the
middle of the interval:

$$
-Q(x) + Q(x+\mathrm{d}x) + q_y\!\left(x+\tfrac{1}{2}\mathrm{d}x\right)\mathrm{d}x = 0. \qquad (\mathrm{A.79})
$$

$$
M_z(x+\mathrm{d}x) - M_z(x) + Q_y(x)\mathrm{d}x - \frac{1}{2}\,q_y\!\left(x+\tfrac{1}{2}\mathrm{d}x\right)\mathrm{d}x^2 = 0. \qquad (\mathrm{A.80})
$$

5.5 Weighted residual method with variable distributed load

$$
\int\limits_0^L \left(EI_z \frac{\mathrm{d}^4 u_y(x)}{\mathrm{d}x^4} - q_y(x) \right) W(x)\,\mathrm{d}x = 0 \qquad (\mathrm{A.81})
$$

$$
\int\limits_0^L EI_z \frac{\mathrm{d}^2 u_y}{\mathrm{d}x^2}\frac{\mathrm{d}^2 W}{\mathrm{d}x^2}\,\mathrm{d}x = \int\limits_0^L W q_y(x)\mathrm{d}x + \left[-W\frac{\mathrm{d}^3 u_y}{\mathrm{d}x^3} + \frac{\mathrm{d}W}{\mathrm{d}x}\frac{\mathrm{d}^2 u_y}{\mathrm{d}x^2} \right]_0^L \qquad (\mathrm{A.82})
$$

$$
\cdots = \delta\boldsymbol{u}_{\mathrm{p}}^{\mathrm{T}} \int\limits_0^L \boldsymbol{N}^{\mathrm{T}} q_y(x)\mathrm{d}x + \cdots \qquad (\mathrm{A.83})
$$

$$
\cdots = \int\limits_0^L
\begin{bmatrix}
N_{1u} \\
N_{1\varphi} \\
N_{2u} \\
N_{2\varphi}
\end{bmatrix}
q_y(x)\mathrm{d}x + \cdots \qquad (\mathrm{A.84})
$$

The additional expression on the right-hand side yields the equivalent nodal loads
for a load according to Eqs. (5.197) up to (5.200).

5.6 Stiffness matrix at bending in $x-z$ plane

Bending in the $x-z$ plane can be considered that the rotation is defined via $\varphi_y(x) = -\frac{\mathrm{d}u_z(x)}{\mathrm{d}x}$. Therefore, the following shape functions can be derived:

$$N_{1u}^{xz} = 1 - 3\left(\frac{x}{L}\right)^2 + 2\left(\frac{x}{L}\right)^3, \tag{A.85}$$

$$N_{1\varphi}^{xz} = -x + 2\frac{x^2}{L} - \frac{x^3}{L^2}, \tag{A.86}$$

$$N_{2u}^{xz} = 3\left(\frac{x}{L}\right)^2 - 2\left(\frac{x}{L}\right)^3, \tag{A.87}$$

$$N_{2\varphi}^{xz} = \frac{x^2}{L} - \frac{x^3}{L^2}. \tag{A.88}$$

A comparison with the shape functions in bending in the $x - y$ plane according to Eqs. (5.64) up to (5.67) yields that the shape functions for the rotation have been multiplied with (-1).

5.7 Bending beam with changeable cross-section

The axial second moments of area result in:

$$I_z(x) = \frac{\pi}{64}\left(d_1 + (d_2 - d_1)\frac{x}{L}\right)^4 \text{ (circle)}, \tag{A.89}$$

$$I_z(x) = \frac{b}{12}\left(d_1 + (d_2 - d_1)\frac{x}{L}\right)^3 \text{ (rectangle)}. \tag{A.90}$$

The following results for the circular and rectangular cross-section:

5.8 Equivalent nodal load for quadratic load

$q(x) = q_0 x^2$	$q(x) = q_0\left(\frac{x}{L}\right)^2$
$F_{1y} = -\dfrac{q_0 L^3}{15}$	$F_{1y} = -\dfrac{q_0 L}{15}$
$M_{1z} = -\dfrac{q_0 L^4}{60}$	$M_{1z} = -\dfrac{q_0 L^2}{60}$
$F_{2y} = -\dfrac{4q_0 L^3}{15}$	$F_{2y} = -\dfrac{4q_0 L}{15}$
$M_{1z} = \dfrac{q_0 L^4}{30}$	$M_{1z} = \dfrac{q_0 L^2}{30}$

$$
k^{\mathrm{e}} = \frac{\pi E}{64 L^{3}}
\begin{bmatrix}
\dfrac{12(11 d_2^4+11 d_1^4+5 d_2^3 d_1+3 d_2^2 d_1^2+5 d_2 d_1^3)}{35} & \dfrac{2(19 d_2^4+47 d_1^4+8 d_2^3 d_1+9 d_2^2 d_1^2+22 d_2 d_1^3)L}{35} & -\dfrac{12(11 d_2^4+11 d_1^4+5 d_2^3 d_1+3 d_2^2 d_1^2+5 d_2 d_1^3)}{35} & \dfrac{2(47 d_2^4+19 d_1^4+22 d_2^3 d_1+9 d_2^2 d_1^2+8 d_2 d_1^3)L}{35} \\[4mm]
\dfrac{2(19 d_2^4+47 d_1^4+8 d_2^3 d_1+9 d_2^2 d_1^2+22 d_2 d_1^3)L}{35} & \dfrac{4(3 d_2^4+17 d_1^4+2 d_2^3 d_1+4 d_2^2 d_1^2+9 d_2 d_1^3)L^2}{35} & -\dfrac{2(19 d_2^4+47 d_1^4+8 d_2^3 d_1+9 d_2^2 d_1^2+22 d_2 d_1^3)L}{35} & \dfrac{2(13 d_2^4+13 d_1^4+4 d_2^3 d_1+d_2^2 d_1^2+4 d_2 d_1^3)L^2}{35} \\[4mm]
-\dfrac{12(11 d_2^4+11 d_1^4+5 d_2^3 d_1+3 d_2^2 d_1^2+5 d_2 d_1^3)}{35} & -\dfrac{2(19 d_2^4+47 d_1^4+8 d_2^3 d_1+9 d_2^2 d_1^2+22 d_2 d_1^3)L}{35} & \dfrac{12(11 d_2^4+11 d_1^4+5 d_2^3 d_1+3 d_2^2 d_1^2+5 d_2 d_1^3)}{35} & -\dfrac{2(47 d_2^4+19 d_1^4+22 d_2^3 d_1+9 d_2^2 d_1^2+8 d_2 d_1^3)L}{35} \\[4mm]
\dfrac{2(47 d_2^4+19 d_1^4+22 d_2^3 d_1+9 d_2^2 d_1^2+8 d_2 d_1^3)L}{35} & \dfrac{2(13 d_2^4+13 d_1^4+4 d_2^3 d_1+d_2^2 d_1^2+4 d_2 d_1^3)L^2}{35} & -\dfrac{2(47 d_2^4+19 d_1^4+22 d_2^3 d_1+9 d_2^2 d_1^2+8 d_2 d_1^3)L}{35} & \dfrac{4(17 d_2^4+3 d_1^4+9 d_2^3 d_1+4 d_2^2 d_1^2+2 d_2 d_1^3)L^2}{35}
\end{bmatrix}
\tag{A.91}
$$

$$
k^{\mathrm{e}} = \frac{b E}{12 L^{3}}
\begin{bmatrix}
\dfrac{3(7 d_2^3+3 d_2^2 d_1+3 d_2 d_1^2+7 d_1^3)}{5} & \dfrac{3(2 d_2^3+d_2^2 d_1+2 d_2 d_1^2+5 d_1^3)L}{5} & -\dfrac{3(7 d_2^3+3 d_2^2 d_1+3 d_2 d_1^2+7 d_1^3)}{5} & \dfrac{3(5 d_2^3+2 d_2^2 d_1+d_2 d_1^2+2 d_1^3)L}{5} \\[4mm]
\dfrac{3(2 d_2^3+d_2^2 d_1+2 d_2 d_1^2+5 d_1^3)L}{5} & \dfrac{(2 d_2^3+2 d_2^2 d_1+5 d_2 d_1^2+11 d_1^3)L^2}{5} & -\dfrac{3(2 d_2^3+d_2^2 d_1+2 d_2 d_1^2+5 d_1^3)L}{5} & \dfrac{(4 d_2^3+d_2^2 d_1+d_2 d_1^2+4 d_1^3)L^2}{5} \\[4mm]
-\dfrac{3(7 d_2^3+3 d_2^2 d_1+3 d_2 d_1^2+7 d_1^3)}{5} & -\dfrac{3(2 d_2^3+d_2^2 d_1+2 d_2 d_1^2+5 d_1^3)L}{5} & \dfrac{3(7 d_2^3+3 d_2^2 d_1+3 d_2 d_1^2+7 d_1^3)}{5} & -\dfrac{3(5 d_2^3+2 d_2^2 d_1+d_2 d_1^2+2 d_1^3)L}{5} \\[4mm]
\dfrac{3(5 d_2^3+2 d_2^2 d_1+2 d_2 d_1^2+2 d_1^3)L}{5} & \dfrac{(4 d_2^3+d_2^2 d_1+d_2 d_1^2+4 d_1^3)L^2}{5} & -\dfrac{3(5 d_2^3+2 d_2^2 d_1+2 d_2 d_1^2+2 d_1^3)L}{5} & \dfrac{(11 d_2^3+5 d_2^2 d_1+2 d_2 d_1^2+2 d_1^3)L^2}{5}
\end{bmatrix}
\tag{A.92}
$$

5.9 Bending beam with changeable cross-section under point load
Analytical Solution:

$$EI_z(x) \frac{d^2 u_y(x)}{dx^2} = M_z(x), \tag{A.93}$$

$$\frac{E\pi h^4}{64} \left(2 - \frac{x}{L}\right)^4 \frac{d^2 u_y(x)}{dx^2} = -F(L - x). \tag{A.94}$$

$$u_y(x) = \frac{FL}{E\pi h^4} \left(\frac{64L^3}{2(-2L + x)} + \frac{64L^4}{6(-2L + x)}\right) + \frac{16L}{3} x + \frac{40L^2}{3}. \tag{A.95}$$

$$u_y(L) = -\frac{8}{3} \frac{FL^3}{E\pi h^4} \approx -2.666667 \frac{FL^3}{E\pi h^4}. \tag{A.96}$$

Finite Element Solution:

$$u_y(L) = -\frac{7{,}360}{2{,}817} \frac{FL^3}{E\pi h^4} \approx -2.612709 \frac{FL^3}{E\pi h^4}. \tag{A.97}$$

Problems from Chap. 6

6.1 Cubic displacement distribution in the tension bar
The natural coordinates of the four integration points are $\xi_1 = -1$, $\xi_2 = -1/3$, $\xi_3 = +1/3$ und $\xi_4 = +1$. The four shape functions

$$
\begin{aligned}
N_1 &= \frac{(\xi - \xi_2)(\xi - \xi_3)(\xi - \xi_4)}{(\xi_1 - \xi_2)(\xi_1 - \xi_3)(\xi_1 - \xi_4)} = +\frac{9}{19}\left(\xi^2 - \frac{1}{9}\right)(\xi - 1), \\
N_2 &= \frac{(\xi - \xi_1)(\xi - \xi_3)(\xi - \xi_4)}{(\xi_2 - \xi_1)(\xi_2 - \xi_3)(\xi_2 - \xi_4)} = -\frac{27}{16}\left(\xi - \frac{1}{3}\right)(\xi^2 - 1), \\
N_3 &= \frac{(\xi - \xi_1)(\xi - \xi_2)(\xi - \xi_4)}{(\xi_3 - \xi_1)(\xi_3 - \xi_2)(\xi_3 - \xi_4)} = -\frac{27}{16}\left(\xi + \frac{1}{3}\right)(\xi^2 - 1), \\
N_4 &= \frac{(\xi - \xi_1)(\xi - \xi_2)(\xi - \xi_3)}{(\xi_4 - \xi_1)(\xi_4 - \xi_2)(\xi_4 - \xi_3)} = +\frac{9}{19}\left(\xi^2 - \frac{1}{9}\right)(\xi + 1)
\end{aligned}
\tag{A.98}
$$

result via evaluation of Eq. (6.51) for $i = 1$ bis $i = n = 4$.

6.2 Coordinate transformation for tension bar in the plane
For the bar a normal force and a displacement in normal direction are defined on a node in local coordinates. In the plane the parameters each separate in the X- and Y-direction. Therefore, the transformation matrix has the dimension 4×4. In the transformation matrix according to Eq. (6.16) it is the task to define the following expressions

$$\sin(30°) = \frac{1}{2} \qquad \text{and} \qquad \cos(30°) = \frac{1}{2}\sqrt{3}. \tag{A.99}$$

With this, the transformation matrix results in

$$\boldsymbol{T} = \begin{bmatrix} \frac{1}{2}\sqrt{3} & \frac{1}{2} \\ -\frac{1}{2} & \frac{1}{2}\sqrt{3} \end{bmatrix}. \tag{A.100}$$

The single stiffness relation in global coordinates

$$\begin{bmatrix} F_{1X} \\ F_{1Y} \\ F_{2X} \\ F_{2Y} \end{bmatrix} = \frac{1}{4}\frac{EA}{L} \begin{bmatrix} 3 & \sqrt{3} & -3 & -\sqrt{3} \\ \sqrt{3} & 1 & -\sqrt{3} & -1 \\ -3 & -\sqrt{3} & 3 & \sqrt{3} \\ -\sqrt{3} & -1 & \sqrt{3} & 1 \end{bmatrix} \begin{bmatrix} u_{1X} \\ u_{1Y} \\ u_{2X} \\ u_{2Y} \end{bmatrix} \tag{A.101}$$

results via the evaluation of Eq. (6.20).

Problems from Chap. 7

7.1 Short solution: Structure of beams in the three-dimensional
Via integration the following solution vector results:

$$\begin{bmatrix} u_{2Z} \\ \varphi_{2X} \\ \varphi_{2Y} \\ u_{3Z} \\ \varphi_{3Y} \\ u_{4Z} \end{bmatrix} = \begin{bmatrix} +11.904 \\ +0.01785 \\ -0.05492 \\ +78.731 \\ -0.07277 \\ +78.732 \end{bmatrix}. \tag{A.102}$$

7.2 Structure of beams in the three-dimensional, alternative coordinate system
The column matrices of the state variables are the following in global coordinates:

$$[u_{1Z}, \varphi_{1X}, \varphi_{1Y}, u_{2Z}, \varphi_{2X}, \varphi_{2Y}, u_{3Z}, \varphi_{3X}, u_{4Z}]^{\mathrm{T}} \tag{A.103}$$

and

$$[F_{1Z}, M_{1X}, M_{1Y}, F_{2Z}, M_{2X}, M_{2Y}, F_{3Z}, M_{3X}, F_{4Z}]^{\mathrm{T}}. \tag{A.104}$$

The order of the entries on node 2 have changed in comparison to the original coordinate system. The angles for bending and torsion are exchanged:

$$
\begin{bmatrix} u_{2Z} \\ \varphi_{2X} \\ \varphi_{2Y} \\ u_{3Z} \\ \varphi_{3X} \\ u_{4Z} \end{bmatrix} = \begin{bmatrix} +\dfrac{F}{3\frac{EI_y}{L^3}} \\[2mm] +\dfrac{F}{2\frac{GI_t}{L}} \\[2mm] +\dfrac{F}{2\frac{EI_y}{L^2}} \\[2mm] +\dfrac{(2GI_t + 3EI_y)L^3 F}{3EI_y GI_t} \\[2mm] +\dfrac{L^2(GI_t + 2EI_y)F}{2EI_y GI_t} \\[2mm] +\dfrac{(3GI_t I_y + 2GI_t AL^2)LF}{3EI_y AGI_t} \end{bmatrix} .
\tag{A.105}
$$

The following solution vector results with the same numerical values as above

$$
\begin{bmatrix} u_{2Z} \\ \varphi_{2X} \\ \varphi_{2Y} \\ u_{3Z} \\ \varphi_{3X} \\ u_{4Z} \end{bmatrix} = \begin{bmatrix} +11.904 \\ +0.05492 \\ +0.01785 \\ +78.731 \\ +0.07277 \\ +78.732 \end{bmatrix}
\tag{A.106}
$$

with the same values. The algebraic signs as well as the order of the entries on node 2 have changed. The angle for torsion and bending have changed positions.

Problems from Chap. 8

8.3 Calculation of the shear correction factor for rectangular cross-section

$$
\int_{\Omega} \frac{1}{2G} \tau_{xy}^2 \, d\Omega \overset{!}{=} \int_{\Omega_s} \frac{1}{2G} \left(\frac{Q_y}{A_s} \right)^2 d\Omega_s,
\tag{A.107}
$$

$$
k_S = \frac{Q_y}{A \int_A \tau_{xy}^2 \, dA} = \frac{5}{6} .
\tag{A.108}
$$

8.4 Differential Equation under consideration of distributed moment

Shear force: no difference, meaning $\dfrac{dQ_y(x)}{dx} = -q_y(x)$.

Bending moment:

$$M_z(x + \mathrm{d}x) - M_z(x) + Q_y(x)\,\mathrm{d}x - \frac{1}{2}\,q_y\,\mathrm{d}x^2 + m_z\,\mathrm{d}x = 0\,. \tag{A.109}$$

$$\frac{\mathrm{d}M_z(x)}{\mathrm{d}x} = -Q_y(x) - m_z\,, \tag{A.110}$$

$$\frac{\mathrm{d}^2 M_z(x)}{\mathrm{d}x^2} + \frac{\mathrm{d}m_z(x)}{\mathrm{d}x} = q_y(x)\,. \tag{A.111}$$

Differential Equations:

$$\frac{\mathrm{d}}{\mathrm{d}x}\left(EI_z\frac{\mathrm{d}\phi_z}{\mathrm{d}x}\right) + k_\mathrm{S}AG\left(\frac{\mathrm{d}u_y}{\mathrm{d}x} - \phi_z\right) = -m_z(x)\,, \tag{A.112}$$

$$\frac{\mathrm{d}}{\mathrm{d}x}\left[k_\mathrm{S}AG\left(\frac{\mathrm{d}u_y}{\mathrm{d}x} - \phi_z\right)\right] = -q_y(x)\,. \tag{A.113}$$

8.5 Analytical calculation of the course of the bending and distortion for cantilever under point load

Boundary Conditions:

$$u_y(x = 0) = 0,\ \phi_z(x = 0) = 0, \tag{A.114}$$

$$M_z(x = 0) = FL,\ Q_y(x = 0) = F. \tag{A.115}$$

Integration Constants:

$$c_1 = -F;\ c_2 = FL;\ c_3 = \frac{EI_z}{k_\mathrm{S}AG}\,F;\ c_4 = 0\,. \tag{A.116}$$

Course of the Displacement:

$$u_y(x) = \frac{1}{EI_z}\left(-F\frac{x^3}{6} + FL\frac{x^2}{2} + \frac{EI_zF}{k_\mathrm{S}AG}\,x\right)\,. \tag{A.117}$$

Course of the Rotation:

$$\phi_z(x) = \frac{1}{EI_z}\left(-F\frac{x^2}{2} + FLx\right)\,. \tag{A.118}$$

Maximal Bending:

$$u_y(x = L) = \frac{1}{EI_z}\left(\frac{FL^3}{3} + \frac{EI_zFL}{k_\mathrm{S}AG}\right)\,. \tag{A.119}$$

Bending at the Loading Point:

$$\phi_z(x = L) = \frac{FL^2}{2EI_z}\,. \tag{A.120}$$

Limit Value:

$$u_y(x = L) = \frac{4F}{b}\left(\frac{L}{h}\right)^3 + \frac{F}{k_S bG}\left(\frac{L}{h}\right). \tag{A.121}$$

$$u_y(L)\big|_{h \ll L} \rightarrow \frac{4F}{b}\left(\frac{L}{h}\right)^3 = \frac{FL^3}{3EI_z}, \tag{A.122}$$

$$u_y(L)\big|_{h \gg L} \rightarrow \frac{F}{k_S bG}\left(\frac{L}{h}\right) = \frac{FL}{k_S AG}. \tag{A.123}$$

8.6 Analytical calculation of the normalized displacement for beams with shear

$$I_z = \frac{bh^3}{12}, \ A = hb, \ k_{\,s} = \frac{5}{6}, G = \frac{E}{2(1+v)}. \tag{A.124}$$

$$u_{y,\,\text{norm}} = \frac{1}{3} + \frac{1+v}{5}\left(\frac{h}{L}\right)^2, \tag{A.125}$$

$$u_{y,\,\text{norm}} = \frac{1}{8} + \frac{1+v}{10}\left(\frac{h}{L}\right)^2, \tag{A.126}$$

$$u_{y,\,\text{norm}} = \frac{1}{48} + \frac{1+v}{5}\left(\frac{h}{L}\right)^2. \tag{A.127}$$

8.7 Timoshenko bending element with quadratic shape functions for the displacement and linear shape functions for the rotation

The nodal point displacement on the middle node as a function of the other unknown results in:

$$u_{2y} = \frac{u_{1y} + u_{3y}}{2} + \frac{\phi_{1z} - \phi_{3z}}{8} L + \frac{1}{32}\frac{6L}{k_S AG} \int_0^L q_y(x)N_{2u}(x) \ dx. \tag{A.128}$$

The additional load vector on the right-hand side results in:

$$\cdots = \cdots + \begin{bmatrix} \int_0^L q_y(x)N_{1u} \ dx + \frac{1}{2}\int_0^L q_y(x)N_{2u} \ dx \\ + \frac{1}{8}L\int_0^L q_y(x)N_{2u} \ dx \\ \int_0^L q_y(x)N_{3u} \ dx + \frac{1}{2}\int_0^L q_y(x)N_{2u} \ dx \\ -\frac{1}{8}L\int_0^L q_y(x)N_{2u} \ dx \end{bmatrix}. \tag{A.129}$$

With $\int_0^L N_{1u}dx = \frac{L}{6}$, $\int_0^L N_{2u}dx = \frac{2L}{3}$ and $\int_0^L N_{3u}dx = \frac{L}{6}$ the following results for a constant line load q_y:

$$\cdots = \cdots + \begin{bmatrix} \frac{1}{2}\,q_y L \\ +\frac{1}{12}\,q_y L^2 \\ \frac{1}{2}\,q_y L \\ -\frac{1}{12}\,q_y L^2 \end{bmatrix}. \tag{A.130}$$

This result is identical with the equivalent line load for a BERNOULLI beam. For this see Table 5.8.

8.8 Timoshenko bending element with cubic shape functions for the displacement and quadratic shape functions for the rotation

The element is exact!

Deformation in the $x-y$ plane:

$$\frac{2EI_z}{L^3(1+12\Lambda)} \begin{bmatrix} 6 & 3L & -6 & 3L \\ 3L & 2L^2(1+3\Lambda) & -3L & L^2(1-6\Lambda) \\ -6 & -3L & 6 & -3L \\ 3L & L^2(1-6\Lambda) & -3L & 2L^2(1+3\Lambda) \end{bmatrix} \begin{bmatrix} u_{1y} \\ \phi_{1z} \\ u_{2y} \\ \phi_{2z} \end{bmatrix} = \begin{bmatrix} F_{1y} \\ M_{1z} \\ F_{2y} \\ M_{2z} \end{bmatrix}. \tag{A.131}$$

Deformation in the $x-z$ plane:

$$\frac{2EI_y}{L^3(1+12\Lambda)} \begin{bmatrix} 6 & -3L & -6 & -3L \\ -3L & 2L^2(1+3\Lambda) & 3L & L^2(1-6\Lambda) \\ -6 & 3L & 6 & 3L \\ -3L & L^2(1-6\Lambda) & 3L & 2L^2(1+3\Lambda) \end{bmatrix} \begin{bmatrix} u_{1z} \\ \phi_{1y} \\ u_{2z} \\ \phi_{2y} \end{bmatrix} = \begin{bmatrix} F_{1z} \\ M_{1y} \\ F_{2z} \\ M_{2y} \end{bmatrix}. \tag{A.132}$$

Problems from Chap. 9

9.1 Solution for 1: Determination of the stiffness matrix

The stiffness matrix can directly be taken on from the above derivation:

$$k^e = \frac{(EA)^V}{L} \begin{bmatrix} 1 & -1 \\ -1 & 1 \end{bmatrix}. \tag{A.133}$$

The expression $(EA)^V$ has to be determined for the composite. Since each layer is homogeneous and isotropic and additionally all layers have the same thickness, the generally valid relation in Eq. (9.122) simplifies to

$$(EA)^V = A_{11}\,b = b \sum_{k=1}^{3} Q_{11}^k\,h^k = b\,\frac{1}{3}\,h \sum_{k=1}^{3} E^{(k)} \tag{A.134}$$

and furtermore to

$$(EA)^V = \frac{1}{3} b h (E^{(1)} + E^{(2)} + E^{(3)}) = \frac{1}{3} b h (2 E^{(1)} + E^{(2)}) . \tag{A.135}$$

If one considers furthermore that $E^{(2)} = \frac{1}{10} E^{(1)}$ is valid, the relation simplifies to:

$$(EA)^V = \frac{1}{3} b h \, 2.1 \, E^{(1)} = 0.7 \, EA . \tag{A.136}$$

For the control of the result it can to be assumed that both moduli of elasticity are the same ($E^{(1)} = E^{(2)} = E^{(3)} = E$). Then the stiffness known for the homogeneous, isotropic tension bar with $(EA)^V = Ebh = EA$ results.

Solution for 2: Determination of the bending stiffness
The bending stiffness results according to Eq. (9.128) for three layers in the composite to

$$(EI)^V = b \frac{1}{3} \sum_{k=1}^{3} E^k \left((z^k)^3 - (z^{k-1})^3 \right) . \tag{A.137}$$

The z-coordinates result in $z^{(0)} = -3/2h$, $z^{(1)} = -1/2h$, $z^{(2)} = +1/2h$ and $z^{(3)} = +3/2h$ if the layer thickness h is equal and if the construction is symmetric to the ($z = 0$)-axis. Via integration one obtains:

$$(EI)^V = b \frac{1}{3} h^3 \left[E^{(1)} \left(\left(-\frac{1}{2} \right)^3 - \left(-\frac{3}{2} \right)^3 \right) \right. \tag{A.138}$$

$$\left. + E^{(2)} \left(\left(+\frac{1}{2} \right)^3 - \left(-\frac{1}{2} \right)^3 \right) + E^{(1)} \left(\left(+\frac{3}{2} \right)^3 - \left(+\frac{1}{2} \right)^3 \right) \right] \tag{A.139}$$

$$= \frac{1}{3} b h^3 \left[E^{(1)} \left(-\frac{1}{8} + \frac{27}{8} + \frac{27}{8} - \frac{1}{8} \right) + E^{(2)} \left(+\frac{1}{8} + \frac{1}{8} \right) \right] \tag{A.140}$$

and finally

$$(EI)^V = \frac{1}{3} b h^3 \left[\frac{26}{4} E^{(1)} + \frac{1}{4} E^{(2)} \right] . \tag{A.141}$$

For the control of the result it can be assumed that all moduli of elasticity are equal ($E^{(1)} = E^{(2)} = E^{(3)} = E$). Then the bending stiffness EI for a homogeneous beam with the cross-section b and $3h$ results in $\frac{9}{4} E b h^3$.

Fig. A.3 Stress–strain dia-
gram, based on quadratic
modulus of elasticity
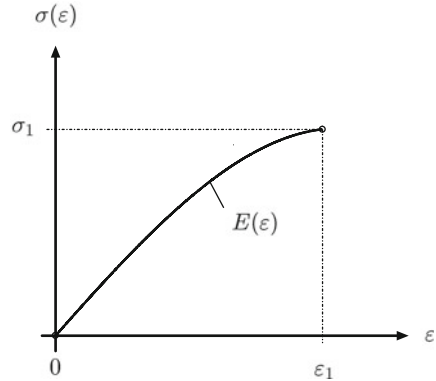
Problems from Chap. 10

10.5 Strain dependent modulus of elasticity with quadratic distribution

$$a = E_0, \ b = -\frac{E_0}{10\varepsilon_1}, \ c = -\frac{4E_0}{5\varepsilon_1^2}, \tag{A.142}$$

$$E(\varepsilon) = E_0 \left(1 - \underbrace{\frac{1}{10\varepsilon_1}}_{\alpha_1} \varepsilon - \underbrace{\frac{4}{5\varepsilon_1^2}}_{\alpha_2} \varepsilon^2 \right), \tag{A.143}$$

$$\sigma(\varepsilon) = E_0\varepsilon \left(1 - \frac{\varepsilon}{20\varepsilon_1} - \frac{4\varepsilon^2}{15\varepsilon_1^2} \right), \tag{A.144}$$

$$k^e = \frac{AE_0}{L^2} \left(L + \alpha_1 u_1 - \alpha_1 u_2 - \frac{\alpha_2}{L} u_1^2 + \frac{2\alpha_2}{L} u_1 u_2 - \frac{\alpha_2}{L} u_2^2 \right) \begin{bmatrix} 1 & -1 \\ -1 & 1 \end{bmatrix}, \tag{A.145}$$

$$K_T^e = \frac{AE_0}{L^2} \left(L + 2\alpha_1 u_1 - 2\alpha_1 u_2 - 3\frac{\alpha_2}{L} u_1^2 + 4\frac{\alpha_2}{L} u_1 u_2 - 3\frac{\alpha_2}{L} u_2^2 \right) \begin{bmatrix} 1 & -1 \\ -1 & 1 \end{bmatrix}. \tag{A.146}$$

10.6 Direct iteration with different initial values
10.7 Complete Newton-Raphson's scheme for a linear element with quadratic modulus of elasticity

Residual function:

$$r(u_2) = \frac{AE_0}{L^2} \left(L - \alpha_1 u_2 - \frac{\alpha_2}{L} u_2^2 \right) u_2 - F_2 = K(u_2)u_2 - F_2 = 0. \tag{A.147}$$

Table A.7 Numerical values for direct iteration at an external load of $F_2 = 800$ kN and different initial values

Iteration j	$u_2^{(j)}$	$\varepsilon_2^{(j)}$	$\sqrt{\frac{\left(u_2^{(j)}-u_2^{(j-1)}\right)^2}{\left(u_2^{(j)}\right)^2}}$
	mm	–	–
Initial value: $u_2^{(0)} = 0$ mm			
0	0	0	–
1	45.714286	0.114286	1.000000
2	59.259259	0.148148	0.228571
⋮	⋮	⋮	⋮
23	70.722968	0.176807	0.000000
⋮	⋮	⋮	⋮
31	70.722998	0.176807	0.000000
Initial value: $u_2^{(0)} = 30$ mm			
0	30.000000	0.075000	–
1	53.781513	0.134454	0.442187
2	62.528736	0.156322	0.139891
⋮	⋮	⋮	⋮
22	70.722956	0.176807	0.000000
⋮	⋮	⋮	⋮
31	70.722998	0.176807	0.000000
Initial value: $u_2^{(0)} = 220$ mm			
0	220.000000	0.550000	–
1	−457.142857	−1.142857	1.481250
2	13.913043	0.034783	33.857143
⋮	⋮	⋮	⋮
25	70.722971	0.176807	0.000000
⋮	⋮	⋮	⋮
33	70.722998	0.176807	0.000000

Geometry: $A = 100$ mm^2, $L = 400$ mm.   Material   properties: $E_0 = 70{,}000$ MPa, $E_1 = 49{,}000$ MPa, $\varepsilon_1 = 0.15$

Tangent stiffness:

$$K_{\mathrm{T}}(u_2) = \frac{AE_0}{L^2}\left(L - 2\alpha_1 u_2 - \frac{3\alpha_2}{L}\,u_2^2\right). \tag{A.148}$$

Iteration scheme:

$$u_2^{(j+1)} = u_2^{(j)} - \frac{\frac{AE_0}{L^2}\left(L - \alpha_1 u_2^{(j)} - \frac{\alpha_2}{L}\left(u_2^{(j)}\right)^2\right)u_2^{(j)} - F_2^{(j)}}{\frac{AE_0}{L^2}\left(L - 2\alpha_1 u_2^{(j)} - \frac{3\alpha_2}{L}\left(u_2^{(j)}\right)^2\right)}. \tag{A.149}$$

Table A.8 Numerical values for complete NEWTON-RAPHSON's method at an external load of $F_2 = 370$ kN. Geometry: $A = 100$ mm^2, $L = 400$ mm. Material properties: quadratic course with $E_0 = 70{,}000$ MPa and $\varepsilon_1 = 0.15$

Iteration j	$u_2^{(j)}$	$\varepsilon_2^{(j)}$	$\sqrt{\frac{\left(u_2^{(j)}-u_2^{(j-1)}\right)^2}{\left(u_2^{(j)}\right)^2}}$
	mm	–	–
0	0	0	–
1	21.142857	0.052857	1
2	25.648438	0.064121	0.175667
3	26.363431	0.065909	0.027121
4	26.384989	0.065962	0.000031
5	26.385009	0.065963	0.000001
6	26.385009	0.065963	0.000000
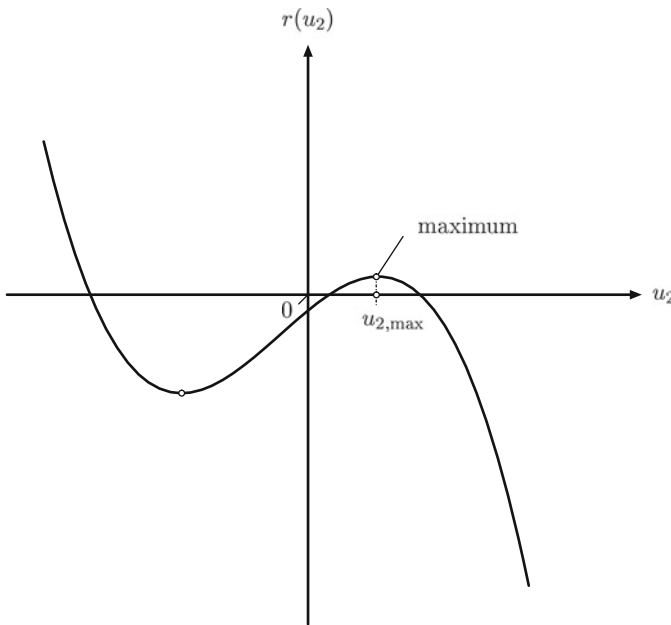
Fig. A.4 Illustration of the residual function according to Eq. (A.147)

Condition for convergence according to Eq. A.4:

$$r(u_{2,\text{max}}) \overset{!}{\geq} 0 \qquad\qquad (A.150)$$

or

$$F \leq \frac{AE_0}{27\alpha_2^2}\left(6\alpha_2 - \alpha_1\sqrt{\frac{\alpha_1^2 + 3\alpha_2}{\alpha_2^2}}\,\alpha_2 + \alpha_1^2\right)\left(\sqrt{\frac{\alpha_1^2 + 3\alpha_2}{\alpha_2^2}}\,\alpha_2 - \alpha_1\right). \qquad (A.151)$$

Table A.9 Numerical values of the back projection for a continuum bar in the case of linear hardening (10 increments; $\Delta\varepsilon = 0.001$)

Inc	ε	σ trial	σ	κ	$d\lambda$	E elpl
–	–	MPa	MPa	10^{-3}	10^{-3}	MPa
1	0.001	210.0	210.0	0.0	0.0	0.0
2	0.002	420.0	420.0	0.0	0.0	0.0
3	0.003	630.0	630.0	0.0	0.0	0.0
4	0.004	840.0	703.636	0.649	0.649	19090.909
5	0.005	913.636	722.727	1.558	0.909	19090.909
6	0.006	932.727	741.818	2.468	0.909	19090.909
7	0.007	951.818	760.909	3.377	0.909	19090.909
8	0.008	970.909	780.000	4.286	0.909	19090.909
9	0.009	990.000	799.091	5.195	0.909	19090.909
10	0.010	1009.091	818.182	6.104	0.909	19090.909

Table A.10 Numerical values of the back projection for a continuum bar in the case of linear hardening (20 increments; $\Delta\varepsilon = 0.0005$)

Inc	ε	σ trial	σ	κ	$d\lambda$	E elpl
–	–	MPa	MPa	10^{-3}	10^{-3}	MPa
1	0.0005	105.0	105.0	0.0	0.0	0.0
2	0.0010	210.0	210.0	0.0	0.0	0.0
3	0.0015	315.0	315.0	0.0	0.0	0.0
4	0.0020	420.0	420.0	0.0	0.0	0.0
5	0.0025	525.0	525.0	0.0	0.0	0.0
6	0.0030	630.0	630.0	0.0	0.0	0.0
7	0.0035	735.0	694.091	0.195	0.195	19090.909
8	0.0040	799.091	703.636	0.649	0.455	19090.909
9	0.0045	808.636	713.182	1.104	0.455	19090.909
10	0.0050	818.182	722.727	1.558	0.455	19090.909
11	0.0055	827.727	732.273	2.013	0.455	19090.909
12	0.0060	837.273	741.818	2.468	0.455	19090.909
13	0.0065	846.818	751.364	2.922	0.455	19090.909
14	0.0070	856.364	760.909	3.377	0.455	19090.909
15	0.0075	865.909	770.455	3.831	0.455	19090.909
16	0.0080	875.455	780.000	4.286	0.455	19090.909
17	0.0085	885.000	789.545	4.740	0.455	19090.909
18	0.0090	894.545	799.091	5.195	0.455	19090.909
19	0.0095	904.091	808.636	5.649	0.455	19090.909
20	0.0100	913.636	818.182	6.104	0.455	19090.909

The following results for the given numerical values, $F \leq 410.803$ kN so that the iteration scheme converges (Fig. A.3) and (Tables A.7 and A.8).

10.8 Strain dependant modulus of elasticity with general quadratic course

$$a = E_0\,, b = \frac{E_0}{\varepsilon_1}(4\beta_{05} - \beta_1 - 3)\,, c = -\frac{4E_0}{\varepsilon_1^2}\left(\beta_{05} - \frac{1}{2}\beta_1 - \frac{1}{2}\right). \qquad (A.152)$$

Table A.11 Numerical values of the back projection for continuum bar at linear hardening (20 increments; $\Delta\varepsilon = 0.001$)

Inc	ε	σ trial	σ	κ	$d\lambda$	E elpl
	–	MPa	MPa	10^{-3}	10^{-3}	MPa
1	0.001	210.0	210.0	0.0	0.0	0.0
2	0.002	420.0	420.0	0.0	0.0	0.0
3	0.003	630.0	630.0	0.0	0.0	0.0
4	0.004	840.0	703.636	0.649	0.649	19090.909
5	0.005	913.636	722.727	1.558	0.909	19090.909
6	0.006	932.727	741.818	2.468	0.909	19090.909
7	0.007	951.818	760.909	3.377	0.909	19090.909
8	0.008	970.909	780.000	4.286	0.909	19090.909
9	0.009	990.000	799.091	5.195	0.909	19090.909
10	0.010	1009.091	818.182	6.104	0.909	19090.909
11	0.011	1028.182	837.273	7.013	0.909	19090.909
12	0.012	1047.273	856.364	7.922	0.909	19090.909
13	0.013	1066.364	875.455	8.831	0.909	19090.909
14	0.014	1085.455	894.545	9.740	0.909	19090.909
15	0.015	1104.545	913.636	10.649	0.909	19090.909
16	0.016	1123.636	932.727	11.558	0.909	19090.909
17	0.017	1142.727	951.818	12.468	0.909	19090.909
18	0.018	1161.818	970.909	13.377	0.909	19090.909
19	0.019	1180.909	990.000	14.286	0.909	19090.909
20	0.020	1200.000	1009.091	15.195	0.909	19090.909

Table A.12 Numerical values of the back projection for a continuum bar in the case of nonlinear hardening (10 increments; $\varepsilon = 0.002$)

Inc	ε	σ^{trial}	σ	κ	$d\lambda$	E^{elpl}
–	–	MPa	MPa	10^{-3}	10^{-3}	MPa
1	0.002	140.0	140.0	0.0	0.0	0.0
2	0.004	280.0	280.0	0.0	0.0	0.0
3	0.006	420.0	360.817	0.845469	0.845469	10741.553
4	0.008	500.817	381.995	2.542923	1.697454	10435.865
5	0.010	521.995	402.557	4.249179	1.706256	10125.398
6	0.012	542.557	422.494	5.964375	1.715196	9810.025
7	0.014	562.494	441.794	7.688654	1.724279	9489.616
8	0.016	581.794	460.449	9.422161	1.733507	9164.034
9	0.018	600.449	478.447	11.165046	1.742885	8833.140
10	0.020	618.447	495.778	12.917462	1.752416	8496.787

Table A.13 Numerical values for bar with fixed support on both sides (3 increments; $\Delta F_2 = 2 \times 10^4$ N)

inc	u_2	ε^{I}	$\varepsilon^{\mathrm{II}}$	σ^{I}	σ^{II}	$\varepsilon^{\mathrm{pl,I}}$	$\varepsilon^{\mathrm{pl,II}}$
–	mm	10^{-3}	$2c10^{-3}$	MPa	MPa	10^{-3}	10^{-3}
1	0.0666667	0.666667	−1.33333	66.6667	−133.333	0.0	0.0
2	0.19806	1.9806	−3.9612	198.060	−201.938	0.0	−1.94182
3	6.88003	68.8003	−137.601	266.008	−333.992	66.1402	−134.261

$$E(\varepsilon) = E_0\left(1 - \underbrace{\frac{(3 + \beta_1 - 4\beta_{05})}{\varepsilon_1}}_{\alpha_1} \cdot \varepsilon - \underbrace{\frac{4(-\frac{1}{2} - \frac{1}{2}\beta_1 + \beta_{05})}{\varepsilon_1^2}}_{\alpha_2} \cdot \varepsilon^2\right). \tag{A.153}$$

With the introduced definitions *here* of α_1 and α_2 a course according to Eq. (A.143) results. Thus under consideration of the here introduced definitions of the stiffness matrix according to Eq. (A.145) as well as the tangent stiffness matrix according to Eq. (A.146) can be used for α_1 and α_2 (Fig. A.4).

Problems from Chap. 11

11.4 Plastic modulus and elasto-plastic modulus

a. $E^{\mathrm{elpl}} = \frac{E \times E^{\mathrm{pl}}}{E + E^{\mathrm{pl}}} = E \Rightarrow E = 0$.

Pure linear-plastic behavior without elastic part, meaning pure elastic behavior on macro-level.

b. $E^{\mathrm{pl}} = E :\Rightarrow E^{\mathrm{elpl}} = \frac{E \times E}{E + E} = \frac{1}{2} E$.

Linear hardening, whereupon the elasto-plastic modulus is half of the elastic modulus E.

11.5 Back projection at linear hardening
11.6 Back projection at nonlinear hardening
11.7 Back projection for bar with fixed support on both sides
The flow curve results in:

$$k(\kappa) = 200 \ \mathrm{MPa} + 1010.\overline{10} \ \mathrm{MPa} \times \kappa. \tag{A.154}$$

The iteration scheme of the NEWTON-RAPHSON method can be used as follows:

$$\Delta u_2^{(i+1)} = \frac{\Delta F^{(i)}}{A\left(\frac{\tilde{E}^{\mathrm{I}}}{L^{\mathrm{I}}} + \frac{\tilde{E}^{\mathrm{II}}}{L^{\mathrm{II}}}\right)}. \tag{A.155}$$

For the fulfillment of the convergence criteria nine cycles are necessary for the second increment and four cycles for the third increment (Table A.9).

11.7 Back projection for a finite element at ideal-plastic material behavior
In the elastic region, the calculation of the displacement on the node can take place. As soon as plastic material behavior occurs, no convergence can be achieved since no clear connection between load and strain exists. If the boundary force condition is being substituted by a boundary displacement condition, the stress in the bar is known and the stress can be calculated (Tables A.10, A.11, A.12 and A.13).

Problems from Chap. 12

12.2 Short solution for Euler's buckling loads II, III and IV, one element
The elastic and geometric stiffness matrix is obtained as in the description to EULER's buckling load I. Due to the boundary conditions two eigenvalues result for case II and one eigenvalue for case III. Case IV cannot be modeled with just one element. The eigenvalues result for the EULER's buckling load II:

$$\lambda_{1/2} = (36 \pm 24)\frac{EI}{L^2} \qquad\qquad (A.156)$$

and for the EULER' buckling load III:

$$\lambda = 30\frac{EI}{L^2} . \qquad\qquad (A.157)$$

For the definition of the critical load respectively the smallest eigenvalues are of interest. The deviations from the analytical solutions are significant.

12.3 Short solution for Euler's buckling loads, two elements
The entire stiffness matrix consists of elastic and geometric stiffness matrix. Load IV can also be modeled with two elements. The eigenvalues can only be determined numerically, only for load I can an analytical solution with reasonable expense be named. The eigenvalues for EULER's buckling load I:

$$\frac{16}{17}\frac{EI}{L^2}\begin{bmatrix} 80 + 19\sqrt{2} + \sqrt{5{,}847 + 3{,}550\sqrt{2}} \\ 80 + 19\sqrt{2} - \sqrt{5{,}847 + 3{,}550\sqrt{2}} \\ 80 - 19\sqrt{2} + \sqrt{5{,}847 + 3{,}550\sqrt{2}} \\ 80 - 19\sqrt{2} - \sqrt{5{,}847 + 3{,}550\sqrt{2}} \end{bmatrix} = \frac{EI}{L^2}\begin{bmatrix} 198.69 \\ 2.4686 \\ 77.063 \\ 22.946 \end{bmatrix}, \qquad (A.158)$$

for EULER's buckling load II:

$$\frac{EI}{L^2}\begin{bmatrix} 48.0 \\ 128.72 \\ 9.9438 \\ 240.0 \end{bmatrix}, \qquad\qquad (A.159)$$

for EULER's buckling load III:

$$\frac{EI}{L^2} \begin{bmatrix} 197.52 \\ 20.708 \\ 75.101 \end{bmatrix}, \tag{A.160}$$

for EULER's buckling load IV:

$$\frac{EI}{L^2} \begin{bmatrix} 120.0 \\ 40.0 \end{bmatrix}. \tag{A.161}$$

For the determination of the critical load respectively the smallest eigenvalues are of interest. The deviations from the analytical solutions are significant.

12.4 Euler's buckling loads, errors in regard to analytical solution

The following table shows the relative error of the solution of the critical buckling load, which was determined via the finite element method in regard to the analytical solution.

$$\text{error} = \frac{\text{FE solution} - \text{analytical solution}}{\text{analytical solution}} \tag{A.162}$$

The errors strongly differ for the different EULER's buckling loads. The error for the EULER's buckling load I is always the smallest, the one for the EULER's buckling load IV always the biggest. The difference in the single loads extends over two dimensions. At a cross-linking with four elements the error is already smaller 0.01 for all cases (Table A.14).

Table A.14 Relative error in relation to analytical buckling load

EULER case				
Number of elements	I	II	III	IV
1	7.52×10^{-3}	0.215854	0.485830	–
2	5.12×10^{-4}	7.52×10^{-3}	2.57×10^{-2}	1.32×10^{-2}
3	1.03×10^{-4}	1.58×10^{-3}	6.14×10^{-3}	2.19×10^{-2}
4	3.28×10^{-5}	5.12×10^{-4}	2.05×10^{-3}	7.52×10^{-3}
5	1.35×10^{-5}	2.12×10^{-4}	8.64×10^{-4}	3.21×10^{-3}
6	6.50×10^{-6}	1.03×10^{-4}	4.23×10^{-4}	1.58×10^{-3}
7	3.51×10^{-6}	5.58×10^{-5}	2.30×10^{-4}	8.66×10^{-4}
8	2.06×10^{-6}	3.28×10^{-5}	1.36×10^{-4}	5.12×10^{-4}
9	1.29×10^{-6}	2.05×10^{-5}	8.50×10^{-5}	3.22×10^{-4}
10	8.44×10^{-7}	1.35×10^{-5}	5.59×10^{-5}	2.12×10^{-4}

Index